Evaluation on the Effect of Mechanical Stress in Pericyclic Reactions: Mechanochemical Enabled 1,3-Dipolar Cycloaddition Between Nitrile Oxides and Alkynes

Rafael A. Hernandez R.

A Thesis

In

The Department

of

Chemistry and Biochemistry

Presented in Partial Fulfillment of the Requirements

For the Degree of

Doctor of Philosophy (Chemistry) at

Concordia University

Montreal, Quebec, Canada

November, 2023

CONCORDIA UNIVERSITY

SCHOOL OF GRADUATE STUDIES

This is to certify that the thesis prepared

By: Rafael Alberto Hernandez Rodriguez, Ph.D.

Entitled: Evaluation on the Effect of Mechanical Stress in Pericyclic Reactions: Mechanochemical Enabled 1,3-Dipolar Cycloaddition Between Nitrile oxides and Alkynes

and submitted in partial fulfillment of the requirements for the degree of

Doctor Of Philosophy (Chemistry)

complies with the regulations of the University and meets the accepted standards with respect to originality and quality.

Signed by the final examining committee:

_____ Chair

Dr. David H Kwang

_____ External Examiner

Dr. Thierry Ollevier

_____ External to Program

Dr. Melanie Hazlett

_____ Examiner

Dr. Rafik Naccache

_____ Examiner

Dr. Xavier Ottenwaelder

_____ Thesis Supervisor

Dr. Pat Forgione

Approved by   _____

_____   Dr. Louis Cuccia, Graduate Program Director

November 30th, 2023

_____

Dr. Pascale Sicotte, Dean Faculty and Science

Abstract

Evaluation on the Effect of Mechanical Stress in Pericyclic Reactions: Mechanochemical Enabled 1,3-Dipolar Cycloaddition Between Nitrile Oxides and Alkynes

Rafael A. Hernandez R., Ph.D.

Concordia University, 2023

The synthesis of heterocycles has constituted a proliferating and growing area in chemistry. Among these, isoxazole motifs are commonly found in many drug candidates, novel materials, and versatile intermediates used to synthesize complex natural products.

Isoxazoles are typically synthesized through a 1,3-dipolar cycloaddition between nitrile oxides (NOs) and terminal alkynes. However, this type of cycloaddition often results in low regioselectivity, forming complex mixtures of 3,5-isoxazoles and 3,4-isoxazoles. To improve regioselectivity, Cu-catalysts have been shown to enhance selectivity for the 3,5-isoxazoles, while Ru(II)-catalysts favour the formation of 3,4-isoxazoles. However, these solution-based protocols suffer significant drawbacks, such as long reaction times, low atom economy, and low energy efficiency.

A more promising alternative is mechanochemistry, which offers unprecedented modes of reactivity and selectivity with a lower environmental impact. Despite the diverse application of isoxazoles, very few reports have utilized mechanochemistry to synthesize these heterocycles. Herein, we discuss the impact of mechanochemistry in combination with catalysis in the regiospecific synthesis of 3,5-isoxazoles and 3,4-isoxazoles from terminal alkynes and NOs. Furthermore, we will highlight the applicability of the developed mechanocatalytic conditions in the synthesis of trisubstituted isoxazoles from internal alkynes and NOs.

Additionally, we explored the impact of mechanochemistry in desymmetrizations by cycloaddition-type reactions, specifically, in the desymmetrization of unbiased bis- and tris-alkynes to access unprecedented 3,5-isoxazoles-alkyne adducts selectively. This approach allows for the modular synthesis of unsymmetrical bis-3,5-isoxazoles.

Acknowledgements

Dedication

For My Mother,

You Always Have Believed That I Could Achieve More and That Nothing is Out of My Reach

Contribution of Authors

The experiments and concepts discussed in this thesis is based on the manuscripts previously published by the author of the thesis (Chapters 2 and 3) and one manuscript that has been submitted (Chapter 4).

Manuscript 1 (Chapter 2): Hernandez R., R. A.; Burchell-Reyes, K.; Braga, A. P. C. A.; Lopez, J. K.; Forgione, P. Solvent-free synthesis of 3,5-isoxazoles via 1,3- dipolar cycloaddition of terminal alkynes and hydroxyimidoyl chlorides over Cu/Al2O3 surface under ball-milling conditions *RSC Adv.* **2022**, *12*, 6396–6402.

Contributions from Arthur P. C. A. Bragaa and Jennifer Keough Lopez towards the optimization of Cu(II) catalysts and Kelly Burchell-Reyes in the time optimization of each substrate and the isolation of the 3,5-isoxazoles required for the reaction scope.

Manuscript 2 (Chapter 3): Hernandez, R. A.; Trakakis, I.; Do, J.; Cuccia, L. A.; Friščić, T.; Forgione, P. Mechanochemical Desymmetrization of Unbiased Bis- and Tris-alkynes to Access 3,5-Isoxazoles-Alkyne Adducts and Unsymmetrical Bis-3,5-isoxazoles *European J. Org. Chem.* **2023**, *19*, e202300374.

Additional contributions of Irini Trakakis and Jean-Louis Do in the reaction optimization conditions.

Manuscript 3 (Chapter 4): The current work has not been published and it is under current evaluation in the Journals of Royal Chemical Society.

Contributions of Stephanie Patterson in the optimization of Ru-catalysts and Negin Nabavi in the optimization of the uncatalyzed synthesis of 3,4,5-isoxazoles and the Ru(II) conditions for the umpolung synthesis of 3,4,5-isoxazoles.

Table of Contents

List of Figures

List of NMR Spectra

List of Tables

List of Abbreviations

SS   Solid-State

ss   stainless steel

LAG   Liquid Assisted Grinding

GAA   Grinding Auxiliary Agent

MM   Mixer Mill

TSE   Twin Screw Extrusion

RAM   Resonance Acoustic Mixing

DA   Diels-Alder

1,3-DC   1,3-Dipolar Cycloaddition

CuAAC   Copper Azide Alkyne

NOs   Nitrile Oxide

CuNOAC   Copper Nitrile Oxide Alkyne Cycloaddition

Chapter 1- Concepts on Mechanochemistry and Advances in Mechanochemical Cycloaddition

1. Introduction

The current focus of synthetic organic chemistry is the development of synthetic strategies to access novel chemical space in an environmentally friendly manner.[1] The high pressure placed on the chemical industry to supply chemical substances essential for society has inspired scientists to develop new synthetic protocols.[1–4] To minimize waste production and energy consumption required in chemical transformation, several alternative techniques are being slowly incorporated into the repertoire of the organic synthetic chemist.[1,2,5,6] These advances have led to dividing the energy inputs into thermal chemistry, electrochemistry, photochemistry, mechanochemistry, sonochemistry, and microwave; each process is characterized by a distinct sign (**Figure 1.1**). [7,8] However, except for mechanochemistry, electrochemistry, photochemistry, and sonochemistry processes commonly required bulk quantities of organic solvents as media for performing chemical reactions.[7]

Thermal   **Photochemistry**   **Mechanochemistry**

Sonochemistry   **Electrochemical**   **Microwave**
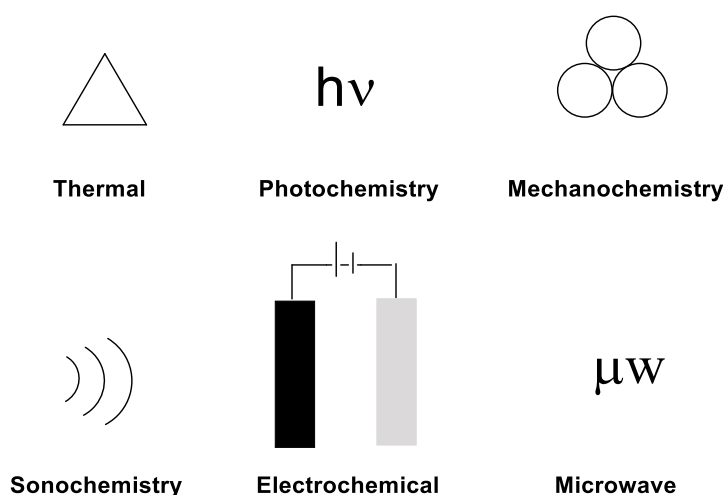
Figure 1.1. Schematic representation of signs used for chemical transformation depending on energy input.

1.1.   Solid-state reactions

Performing chemical transformation in the solid state (SS) differs from solution-based thermal reactions.[9] One clear difference is that in SS the reactions are conducted directly on the powder at ambient temperatures without the use of bulk amounts of solvent.[10] This challenges a concept first put forth by Aristotle: "No Coopora nisi Fluida", which means that no reaction occurs without a solvent.[10] However, scientific progress since the times of Aristotle has revealed that many biological processes such as food digestion in the stomach, interactions and reactions between spermatid and ovum, and cell multiplication, occur in SS rather than in solution.

Considering the complexity of biological processes in SS, organic reactions are expected to occur more selectively in the SS due to the low mobility and the even arrangement of the molecules in the crystal lattice.[11] In contrast, the presence of a solvent allows molecules to move more freely, resulting in a less restrictive arrangement.[10,11]

Many organic SS reactions are facilitated by grinding, melting or shaking to enhance mass-transfer of the substrates and supply energy to the reactants.[10,12]Additionally, the benefits of mechanical grinding is not

limited only to solids but also apply to gases and liquids, making it a versatile method across different physical states.[13] However, SS chemistry and synthesis primarily focus on studying solids-to-solid interactions, disregarding these other states. Furthermore, reactions enabled by mechanical force fall under the scope of mechanochemistry (**Figure 1.2**), which explores the effects and applications of mechanical stress on chemical transformations .[13]
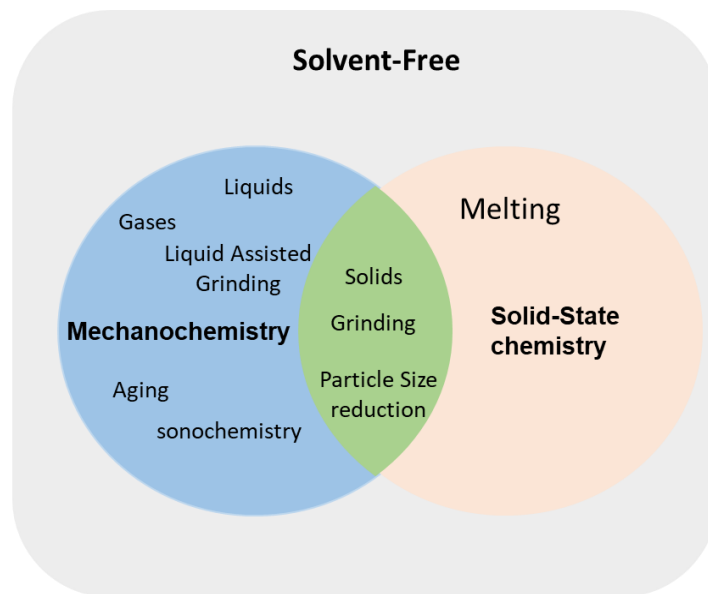
Figure 1.2. Properties and characteristics of mechanochemistry and SS chemistry.

1.2. Mechanochemistry and the Applications in Organic Reactions

The term mechanochemistry was first introduced by Oswald in 1891, and IUPAC has defined a mechanochemical reaction as a chemical transformation induced using mechanical energy.[13] The primary objective of mechanochemistry is to achieve chemical reactions without the need of the dissolution of the reagents.[11,14] Performing reactions in the absence of organic solvent significantly changes the environment in which the reagents or substrates are present, creating a heterogeneous environment where the substrates are in direct contact with the grinding medium and the surface of the material that is being used for the grinding, leading to potential changes in the reaction outcomes. This has significant benefits for chemical transformations in the solid state when compared to traditional solution-based thermal methods.

1.2.1. Increase in reaction rates

The main advantage of mechanochemistry in organic reactions is the enhancement in reaction rates. The absence of bulk amounts of solvents allows reagents to be present in maximal concentrations.[15] The increase in reaction kinetics significantly reduces the reaction time. It is essential to highlight that in most

3

cases, enhancing reaction rates in solution-thermal conditions is correlated to increasing the reaction temperature.[15] Mechanochemical reactions differ as the reactions can occur at ambient temperature.[16] Two main models explain the increase in reaction rate from a macromolecular perspective (**Figure 1.3**). The localized heating model describes that during mechanical shock, a localized high temperature is created in a concentrated environment that enhances the reaction rate (**Figure 1.3a**).[13,17] On the other hand, the particle size reduction model is particular for solids; it describes that constant milling reduces particle size and creates defects on the crystal lattice, facilitating the interaction between substrates (**Figure 1.3b**).[13,17] In either case, there is an increase in probability for substrates to encounter each other due to the high concentration in which reagents are present.

a. Localized heating Model

= subtrate 1

= substrate 2

= product

Jar Motion

Localized heat created during shock

b. Particle size reduction model

Jar Motion

Particle size reduction

Product formation

Jar Motion

= subtrate 1

= substrate 2

= product
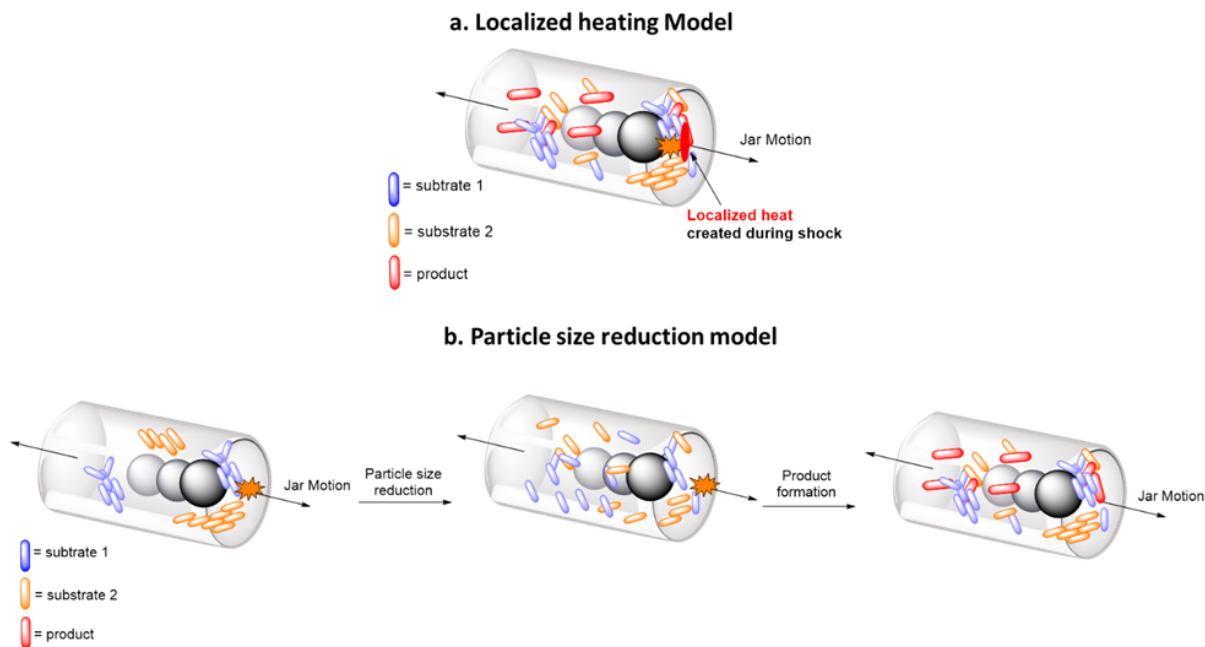
Figure 1.3. Mechanochemical and solid-state reaction models.

1.2.2. Sustainability and Accessibility

The sustainability of chemical processes has become a requirement for current and ongoing chemical processes. In the case of mechanochemistry, performing reactions and transformations in the absence of bulk-amounts of organic solvent have been a critical identifier for mechanochemical processes, thereby leading occasionally to not requiring a work-up and column chromatography for purifications from the protocol.[12,14,18 16,19]

The robust interaction created under mechanochemical conditions can also allow complex or expensive organometallic reagents to be replaced with less expensive, easily recoverable, and more eco-friendly alternatives with similar yields or new selectivity outcomes.[16,20,21] The high energy efficiency or low energy demand demonstrated by mechanochemical techniques compared to other techniques such as batch or microwave has also been a parameter to consider mechanochemistry techniques as more sustainable.[19,22] These aspects allow mechanochemistry to comply with all of the 12 principles outlined by the FDA for a sustainable process (**Figure 1.4**).[4]
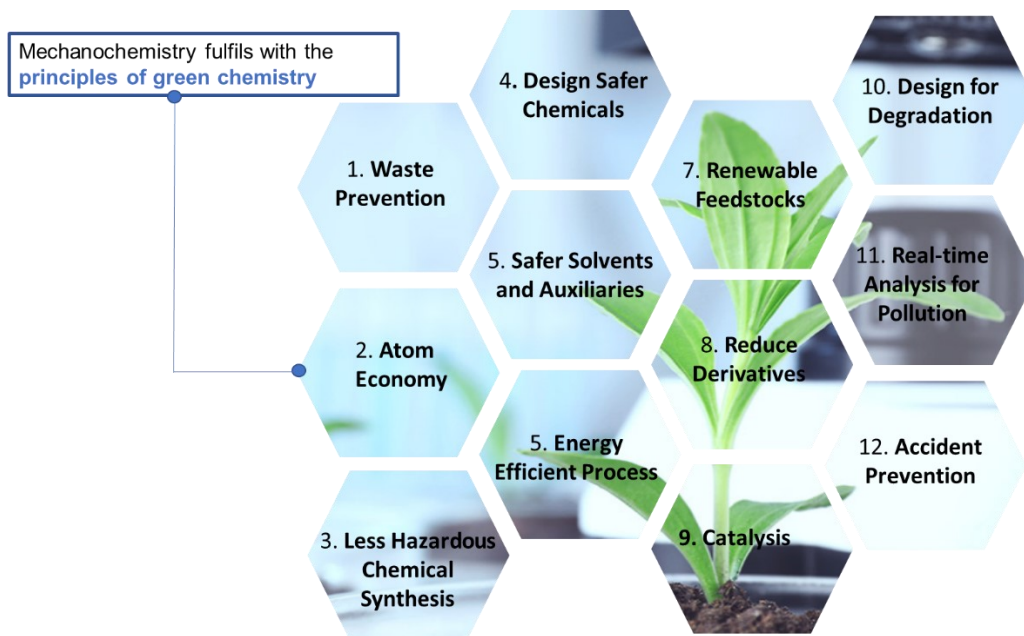
Figure 1.4. 12 principles of green chemistry.

1.2.3.   Selectivity Enhancement:

Mechanochemical reactions can increase selectively due to the even and tight arrangement of molecules in the solid-state. Physical state transitions like liquid substrate to solid product are more critical under mechanochemical conditions and open the door to unprecedented types of selectivity.[23] These state transitions are critical under mechanochemical reactions due to differences in mass transport between liquids and solid that can limit reactivity. [23] Additionally, mechanochemistry is able to alter the kinetic and thermodynamic nature of the reaction and toggle chemoselectivity or provide less complex reaction mixtures.[24–26]

1.3.   Assisting the Grinding

1.3.1.   Liquid Assisted Grinding

It is widely acknowledged that solvents play a crucial role in interacting with reaction substrates, leading to an increase in reactivity and stability.[27] In the field of mechanochemistry, the introduction of small amounts of liquid additives or small amounts of solvents can dramatically accelerate reactions and impact reaction selectivity.[28] Liquid-assisted grinding (LAG) is an extension of neat grinding or solvent-free grinding, and is empirically represented by the parameter "η", expressed in units of μL/mg.[29] This parameter indicates the volume of liquid in μL relative to the total weight of all reagents used in the reaction mixture. It is important to note that for liquid assisted grinding the **η** parameter must be within the range between $0 < η < 1$. This ensures that the aggregation state of the reagents remains unchanged (**Figure 1.5**).

The addition of small amounts of liquid additive can significantly improve mass transfer in the reaction mixture. It should be noted that liquid additives are not chemically innocent and can affect the reaction outcome through their coordinating ability, polarity, or molecular weight. Liquid additives can directly interact and stabilize catalysts, intermediates, or substrates leading to changes in kinetic and thermodynamic parameters compared to solution-based systems.[24,28–30]

The concept of LAG has expanded significantly, and other types of liquid reagents, such as ionic liquid additives for ionic liquid-assisted grinding (ILAG)[31], or polymers for polymers and liquid-assisted grinding (POLAG)[30,32] can also provide significant benefits to the reactions.[30]
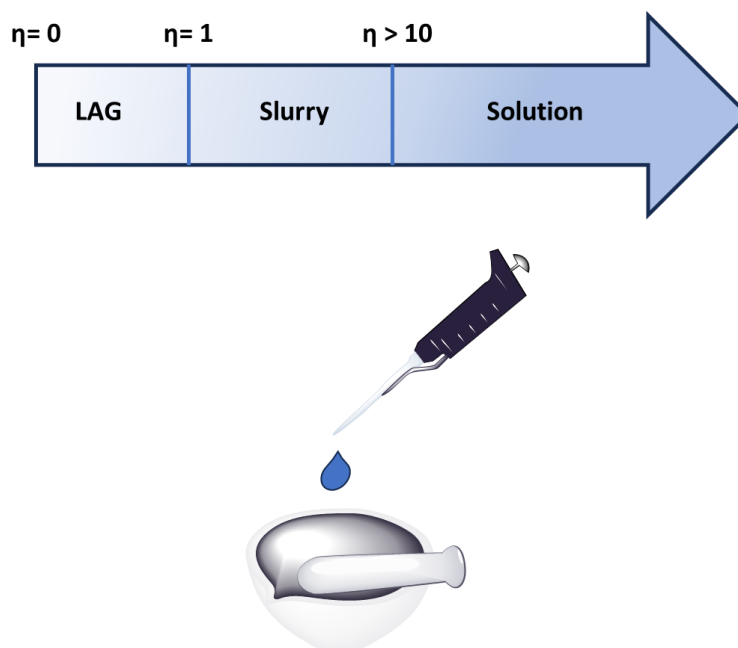
Figure 1.5. Liquid-assisted grinding η parameter.

1.3.2. Grinding Auxiliaries Agents (GAA)

While liquid additives are permitted in mechanochemical reactions, it must be taken into consideration that performing reactions in the solid-state are sensitive to differences in textures encountered in the reaction system. Grinding auxiliaries or solid additives can facilitate effective homogenization and provide a uniform texture in the reaction mixture.[33–36] Additionally, GAA can contribute to improvements in the rheology of the mixture, further improving mass transfer, behaving as an effective shock absorber, or increasing the internal temperature of the reaction mixture upon mechanical shock.[33]

1.4. Grinding and Milling Techniques

Performing mechanochemical reactions can be significantly different from conventional solution-based reactions. Solution reactions are commonly carried out using round-bottom flasks of inert material that can accommodate the required volume of solvent and using a heating source such as a heating mantel or silicon oil bath that can adequately heat the solution mixture. In the case of mechanochemistry, the round-bottom flasks and oil bath are replaced with jars and automated grinders that can provide the required reaction energy.[13–15] Current automated grinders and millers differ from each other in their design but most importantly in the major forces that dominate during the process.

1.4.1. Manual and Automated Grinder

The first type of grinding equipment to be used for chemical purposes was the mortar and pestle[37], and remarkably it continues to be used in most laboratory settings (**Figure 1.6a**). However, operating the mortar and pestle can lead to irreproducibility between operators.[15] To avoid challenges, automated alternatives to manual grinders or the traditional mortar pestle were developed (**Figure 1.6b**). In an automated grinder, the mixture is primarily pulverized and mixed by friction created during the shear between the mortar and the pestle.[10]

a. Mortar and Pestle   **b. Automatic Electric Grinder**
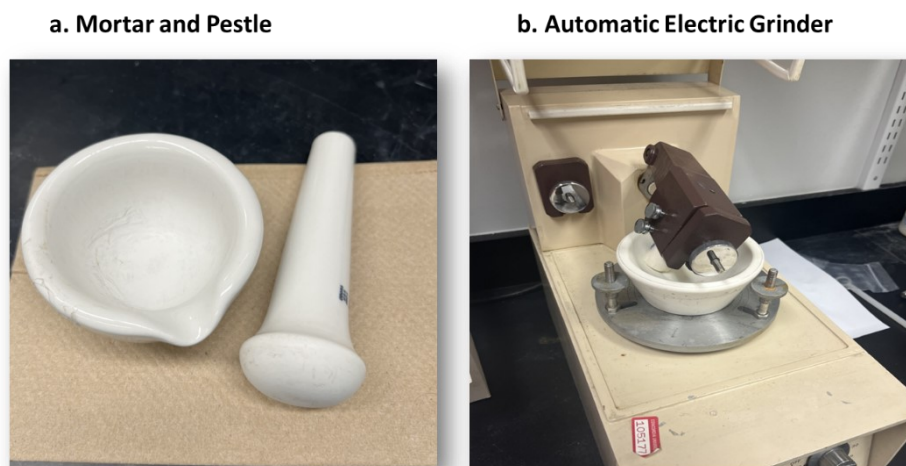
Figure 1.6. Mortar and Pestle and Automatic Grinder.

1.4.2. Planetary Ball-Milling

The planetary ball mill is the most common milling machine (**Figure 1.7**). In some instances, the reagents are added neatly into jars with a certain number of milling media (balls of certain dimensions and usually the same material as the milling jar) (**Figure 1.7b**). In this case, the jars spin in a central disc named the "sun wheel" (**Figure 1.7c**). The "sun wheel" rotation facilitates the milling media's motion inside the jar, which rotates counterclockwise to the direction to the sun wheel (**Figure 1.7c**). The motion of the milling media produces constant collisions with the walls of the jar, resulting in a shear force that mixes and pulverizes the mixture. Planetary ball mills have the advantage that they can be used on a laboratory scale and increased to be used as large size reactions, but the motion of the milling media changes with the increase in scale.[13–15]

a. Planetary Ball Mill

b. Planetary Ball Mill Jars and Milling Media

SS jars
(25 mL capacity)

PTFA jars
(25 mL capacity)
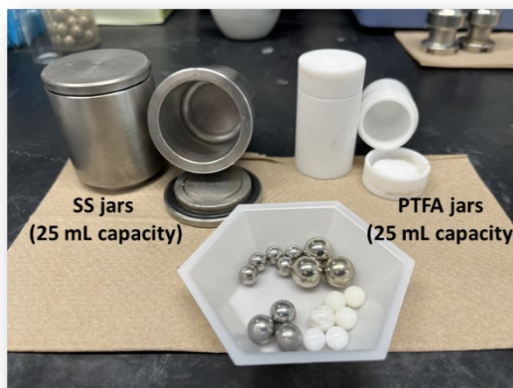
c. Planetary Ball Mill Motion

Milling media
direction

Sun Wheel

Jars

Sun Wheel
direction
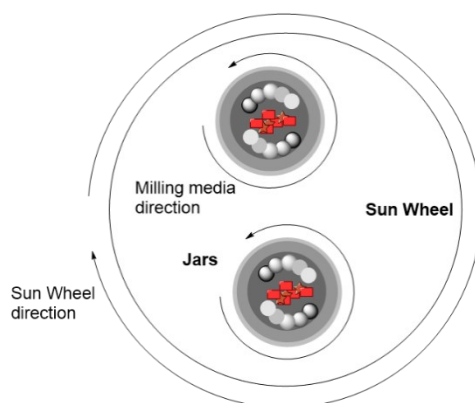
Figure 1.7. Planetary ball mill, jars, and a schematic representations of the motion of the "sun wheel".

1.4.3. Mixer Milling (MM)

Mixer mills (MMs) are excellent laboratory equipment, the procedures for performing reactions are identical to that used for the planetary mill previously described (section 1.3.2.) (**Figure 1.8a**). However, there are significant differences in the motion of the planetary ball mill to a MM. The MM moves relatively in a one-dimensional motion (**Figure 1.8b**), most commonly side to side horizontally. Consequently, the motion of the milling media does not result in shear but rather predominantly direct mechanical shock.[13–15,20] For the planetary milling and the MM the motion of the milling media is controlled by controlling the frequency of the grinding or milling, which serves as the primary source of energy, [38] this is analogous to increasing the temperature in solution-based thermal processes, with the difference that the type of method utilized can lead to different outcomes on the reaction.

a. Mixer Mill (MM)

b. Motion of the MM

Jar Motion

= subtrate 1

= substrate 2

=product
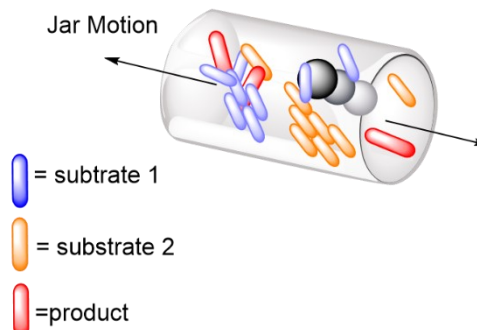
Figure 1.8. Mixer mill and a schematic representation of the motion of the milling media.

1.4.4. Milling Jars

Milling jar are commonly fabricated of stainless-steel, but other types of materials can be used. Other precious metals such as Cu, Ag, Pd, Ni, Al, or Au can also be used which have demonstrated to have catalytic activity (**Figure 1.9**).[21,39–42] This type catalysis is known as "direct mechanocatalysis" and the use of this concept is more a environmentally friendly alternative, as it does not require external ligands or transition metal catalysts, and the recovery of the metal is expeditious and quantitative.[21] In direct mechanochatalysis, surface of the jar or milling media catalyzes the reaction.[21] The vibrations generated during the grinding or milling process provide the necessary surface for catalysis, which is regenerated during the milling process.[21]

It must be understood that direct collisions over prolonged periods can cause severe contamination of the reaction mixture providing undesired products by leaching the metal into the surface of the mixture. [21] Other materials with more inert properties, such as ceramics can be used that contribute very little contamination to the reaction system. Additionally, Teflon (PTFA) jars have gained importance due to its inert nature and the low density of the Teflon jars, can be advantageous in improving reaction selectivity.[43]
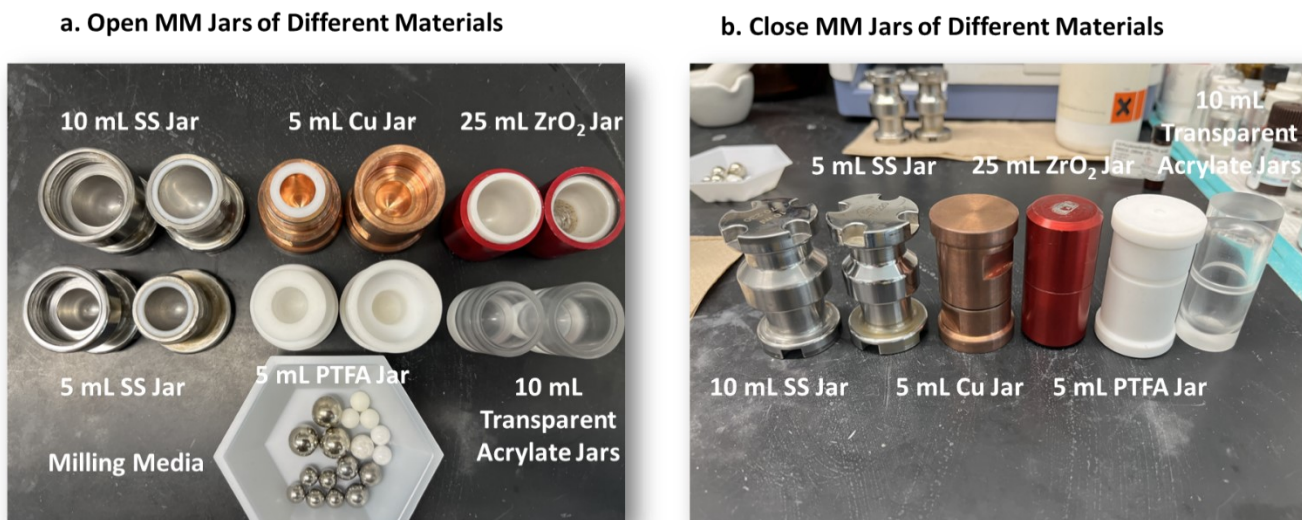
Figure 1.9. Examples of MM jars of different materials.

1.5.   Methods for Scaling-up

Among some of the benefits of milling is the ease in scalability by simply resizing the jar dimensions. However, after a certain capacity (about > 3.0 g), the scale can influence the outcome of the reaction. Taking the mechanical reaction to larger scales leave MM and planetary ball milling techniques to be replaced by other systems such as twin-screw extrusion (TSE) and Resonance acoustic Mixing (RAM).

1.5.1.   Twin Screw Extrusion (TSE) for continuous flow mechanochemistry

Despite the further progress achieved in "flow" mode reactors, they still require the use of large quantities of toxic solvents like DCM or DMF to solubilize molecules.[44] This represents a limitation for materials such as insoluble pigments that can cause clogging in the flow tubes. Additionally, the waste associated with the used of large amounts of solvents can result in a significant lowering of the sustainability metrics.[44,45] The use of extrusion reactors can extend solution flow chemistry by removing and significantly decreasing the use of organic solvents (**Figure 1.10**). TSE allows the mixing of the feeding materials in a confined space by the constant rotation of a pair of screws and with greater temperature control than the one achieved by small-scale milling methods.[44–47]

Depending on the direction of the motion of the screws, either counter-rotating (opposite direction) or co-rotating (same direction), can result in improvements in the shear and/or compression applied to the material.[45] Small-scale milling process can be complementary to the extrusion process. Ideally, a reaction will be optimized on a small scale (50 mg to 500 mg) using planetary milling of MM, and the conditions will be directly translated into the TSE process.[44] Different from small-scale milling reactions where all the substrates, liquid or solids, are directly added into the jar, TSE requires a pre-mixing of the material prior feeding the mixture into the extrude to ensure effective mixing. The development of TSE has allowed access to reactions in the absence of organic solvents and in a large scale (**Figure 1.10**).

Figure 1.10. Schematic representation of TSE reactors and a example of the twin-screw configuration. This images were taken with the permission of *Cowell (Nanjing) Extrusion Machinery Co.* Website.

1.5.2. *Resonance Acoustic Mixing (RAM) from the small scale to the large scale*

Small-scale milling methods and TSE require grinding media or screws to provide energy to the reaction system and guarantee efficient mass transport.[48] The strong mechanical shock, stress, or shear cause by the grinding media or the screws can damage the material, limit its reactivity, and create significant safety concerns when using materials that are shock sensitive.[49] Resonance acoustic mixing (RAM) (**Figure 1.11a-b**) represents an extension to grinding media-dependent processes by providing an environment that does not require grinding media (non-contact of material with milling media) that is dependent of ultrasonic or acoustic frequencies agitations. Generally, substrates will be directly added in a jar of inner material (in the absence of milling media), and the mixture will oscillate at a certain acceleration for a certain amount of time, thereby creating mixing zones that facilitate the contact of the substrates (**Figure 1.11c**).[50] Performing reactions in a grinding media-free environment facilitates the effective scaling as the necessity for screening for reaction parameters such as number of milling media, filling ratios, or milling frequencies is not required.[49,51] Despite being a relatively new technique, RAM demonstrated significant benefits and scalability for the synthesis of metal-organic frameworks (MOF),[48] co-crystals synthesis, mechanoredox catalysis,[49] and click-chemistry.[51]
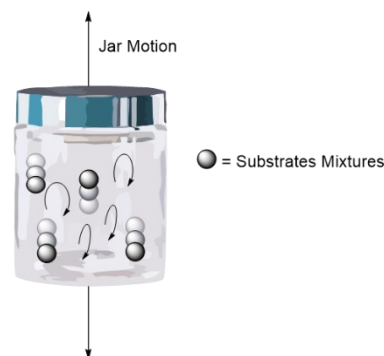
Figure 1.11. RAM reactors and their motion inside the reactor.

This images were taken with the permission of *Resodyn*.

1.6. Cycloaddition Reaction Enabled by Mechanochemistry:

Cycloaddition reactions have constituted essential and fundamental reactions in organic synthesis, allowing to add significant complexity and selectivity in a single reaction step. Interestingly, the utility of cycloaddition reactions has applications in the synthesis of complex natural products, biologically active molecules, and materials.[52–54] The investigation of cycloadditions has primarily focused for solution-based thermal- and photochemical reactions, where it has been established that the outcome of the reactions can be understood by the Woodward-Hoffmann rules (WH). [55,56] Mechanochemistry has provided advances and benefits to the field of transition metal catalysis (Ni[57,58], Pd[59–65], Cu[66–68], Ru[69–71], Rh[72–74], and Ir[75,76]) and metal-mediated chemistry (Mg[77–80], Mn[81,82], Zinc[83], Li[83], Ca[84]) for the functionalization of aromatic structures, however cycloadditions reactions have been overlooked and few examples evaluating the effect of mechanical stress or pressure in cycloaddition reactions have been reported.

1.6.1. Mechanochemical Diels-Alder reaction a [4+2] cycloadditions

Diels-Alder reactions (DA) are among the most fundamental type of cycloadditions and it has been extensively investigated in diverse conditions, providing the corresponding products in excellent yields and selectivity. DA occurs by reacting a diene (4π electron system) **1** and a dienophile (2π electron system) **2** to form a 6-member ring adduct **3** *via* simultaneous formation of 2 C-C bonds. This reaction is generally in equilibrium but the cyclic adduct **4** is generally favoured (**Figure 1.12**).[85] The importance of DA reactions has led to this concept being expanded beyond traditional solution-based chemistry and several research groups have exploited the effects of mechanical stress in this type of pericyclic reactions.[26]
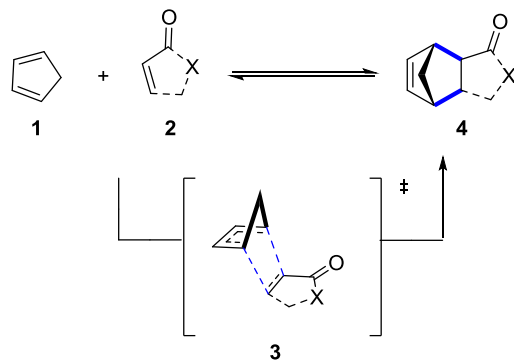
Figure 1.12. Schematic representation of a Diels-Alder a [4+2] cycloaddition.

Investigations from the Gao group for the synthesis of norbornene **7** from cyclopentadiene **5** and maleimides **6** has demonstrated that the high pressure achieved by milling significantly accelerates the reaction thereby obtaining norbornene **7** in higher yield and conversion than under the solution-based thermal conditions. Additionally, the absence of organic solvent simplifies the purifications to a simple recrystallization, eliminating the use of column chromatography and decreasing waste-production (**Figure 1.13a**).[86]

Performing reactions in a solvent-free environment allows insoluble substrates to effectively undergo a chemical reaction without jeopardizing the selectivity or disfavouring the formation cyclic adduct. The Swager group demonstrated the benefits of mechanochemical cycloadditions for insoluble and unreactive substrates by solution-based conditions. Mechanochemical-enabled DA facilitated the synthesis of Iptycenes **11** from anthracene **8** and 1,4-anthraquinones **9**, which could under further DA to form extended Iptycenes (**Figure 1.13b**).[87] It is essential to highlight that the synthesis Iptycene **11** and extended Iptycenes by DA is only allowed by mechanochemical means, the reported conditions in a solution-based thermal conditions does not allow access to **11** due to the poor solubility of the substrates **8** and **9** that limits their reactivity at ambient temperatures while increasing temperature only promotes the retro-DA.[87]

a) Zhang *et al. Mechanochemical Synthesis of Norbornene.*

(1.0 equiv.)
5

(1.0 equiv.)
6

MM
30 min
$n_{ss}=1$, 30 Hz

7
Yield = 94 %

b) Zhao *et al. Mechanochemical Synthesis of Extended Iptycenes.*

ZnCl$_2$ (8.3 equiv.)
C$_8$F$_{17}$CO$_2$H (3.7 equiv.)
MM
4.5 h
$n_{ss}=1$, 30 Hz
Yield= 88 %
exo:endo= 86:14

10

(1.0 equiv.)
8

(1.0 equiv.)
9

Aromatization

Yield= 85 %

11
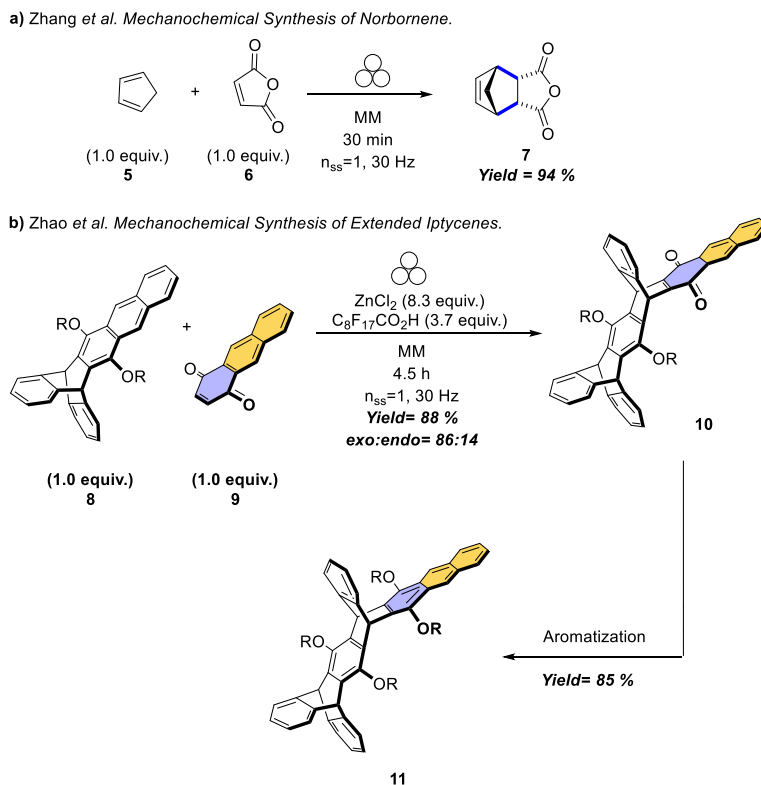
Figure 1.13. Examples of mechanochemical allowed Diels-Alder.

Several research groups have systematically investigated the effects of the reaction conditions and the impact mechanical stress on the cycloaddition outcome. Kinetic investigations determined that mechanical shock allows a small increases in the temperature of the jar, depending on the material density.[26,38] However, other reagents such as grinding auxiliaries provide the necessary surface for the formation of the product and accelerate the DA reaction.[88] In addition, the mechanical stress and shock achieved during the milling causes molecular distortion between the diene and dienophile, lowering the activation energy.[89]

1.6.2. Mechanochemical Enabled [2+2] Cycloaddition

commonly employed types

2+2 cycloaddition

12   **13**

hv

15

14

‡

14
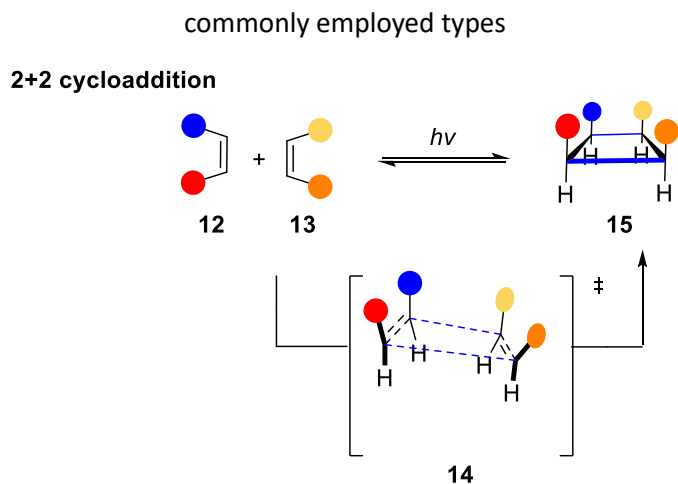
Figure 1.14. Schematic representation of a [2+2] cycloaddition between olefins.

[2+2] or [2π +2π] photochemical cycloadditions between olefins (**12** and **13**) is generally used in the synthesis of cyclobutanes **15** (**Figure 1.14**).[90] The inherited angular strain of the cyclobutanes **15** allows facile bond reorganizations and fragmentations.[90] In mechanochemistry, cyclobutanes rings have found numerous applications due to their high response to mechanical stress.[91–94] In terms of mechanochemistry, the [2+2] cycloadditions have been reported to occur directly by milling, direct UV-irradiation, or a combination of milling and UV-irradiation.

One clear application of mechanochemical [2+2] cycloadditions is in the dimerization of fullerenes **16**. Fullerenes **16** are chemical entities that have gained significant attention due to their empty spherical architecture and potential applications as a superconductor, photoconductor, and ferromagnet.[95] Dimerization of fullerenes **17** for the formation of cyclobutanes by photochemical solution-based approach is remarkably limited due to the poor solubility of the fullerenes.[96] Studies from Murata *et al.* demonstrated that performing reactions under mechanochemical conditions and using KCN as a promoter allowed selective access to the dimerized fullerene.[94,97,98] The synthesis of **17** by protocols optimized by Murata *et al.* highlights significant differences to a photochemically allowed process.[99,100] Mechanistically, the mechanochemical reactions do not proceed by a concerted photochemical cycloaddition but rather the nucleophilic reactivity of cyanide facilitates the increase in nucleophilicity in a step-wise formation of the cyclobutane ring (**Figure 1.15b**).[98]

Fullerene
16

Mechanochemically Allowed [2+2]   **[2+2] Forbidden**

KCN
MM
30 Hz, 30 min
Yield = 18 %

17   **16**   KCN   **17**

b) Mechanistic Hyphothesis

:C≡N

16   **18**   **19**   **20**

17

Figure 1.15. Mechanochemical dimerization of fullerenes by a mechanochemical-allowed [2+2] cycloadditions.

Mechanochemical solid-state transformations enhance supramolecular interactions that are weak or limited under solution-based thermal conditions.[101] Significant gains in selectivity can be achieved by providing a template that organizes the molecular arrangements to guarantee high degree of reactivity and selectivity. The MacGillivray group demonstrated a crystal-to-crystal [2+2] cycloaddition to form cyclobutene **24** by direct UV-irradiation on a template of 4,4'-bpe•2(resorcinol) **23** over a period of 72 h (**Figure 1.16a**).[102] H-bonding in **23** between the hydroxy moieties of the resorcinol **21** and the $N(sp^2)$ heteroatom and the π-π stacking between the aromatics of the pyridine, directly positions the alkene moieties facing each other (**Figure 1.16a**).[102] This pre-organization provided by the template guarantees the trans stereochemical outcome achieved for the cyclobutene **24** upon UV-irradiation. Additionally, the MacGillivray group demonstrated that by repeatedly grinding and exposing the mixture to UV irradiation enable **21** to be used in sub-stoichiometric amounts (~50 mol %) (**Figure 1.16c**), supposedly due to improvements in bulk mass transfer of the substrates.[101] This methods allowed the formation of **25** in 90 % yield and without the presence of the template **21**. This study represents the solid-state's first mechano-photochemical organocatalytic [2+2] cycloaddition approach. The impact of this protocol has expanded and has become the basis for other studies that describe the impact of supramolecular reactions

mechano-photochemical [2+2] cycloaddition with new templates or transitions metals complexes to unlock further reactivity.[103,104]
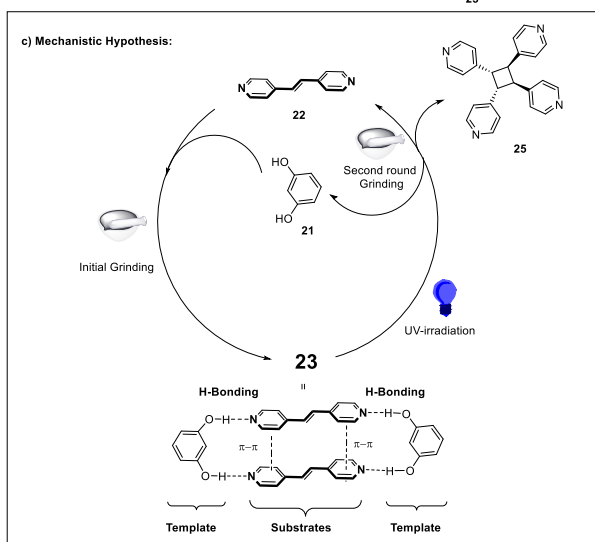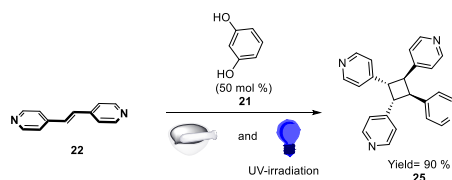
Figure 1.16. Mechanophotochemical [2+2]cycloaddition.

1.6.3.   Mechanochemical Enabled 1,3-dipolar [3+2] Cycloadditions

In the 1960's, Rolf Huisgens introduced the concept of 1,3-dipolar cycloadditions (1,3-DC) that emulates the DA (**section 1.6.1**).[105,106] Huisgens described a 1,3-DC to occur between a 1,3-dipoles **26** and a dipolarophile **27** to obtain a 5-membered product **29**. 1,3-dipoles are defined as a a-b-c system where atom "a" possesses an electron sextet that is incomplete combined with a "b" atom with a +1 formal charge, and a "c" atom of incomplete sextet and a formal charge of "-1" (**Figure 1.17**).[105] It is a requirement for 1,3-dipoles **26** that cannot have a neutral formula and they must have unpaired electrons, while the dipolarophile **29** is a "d-e" multiple bond system (double or triple) of neutral formal charge. Through

17

extensive and comprehensive work, Huisgens classified 1,3-dipoles in two groups, allyl anions and propargyl anions (**Figure 1.17**).[106]
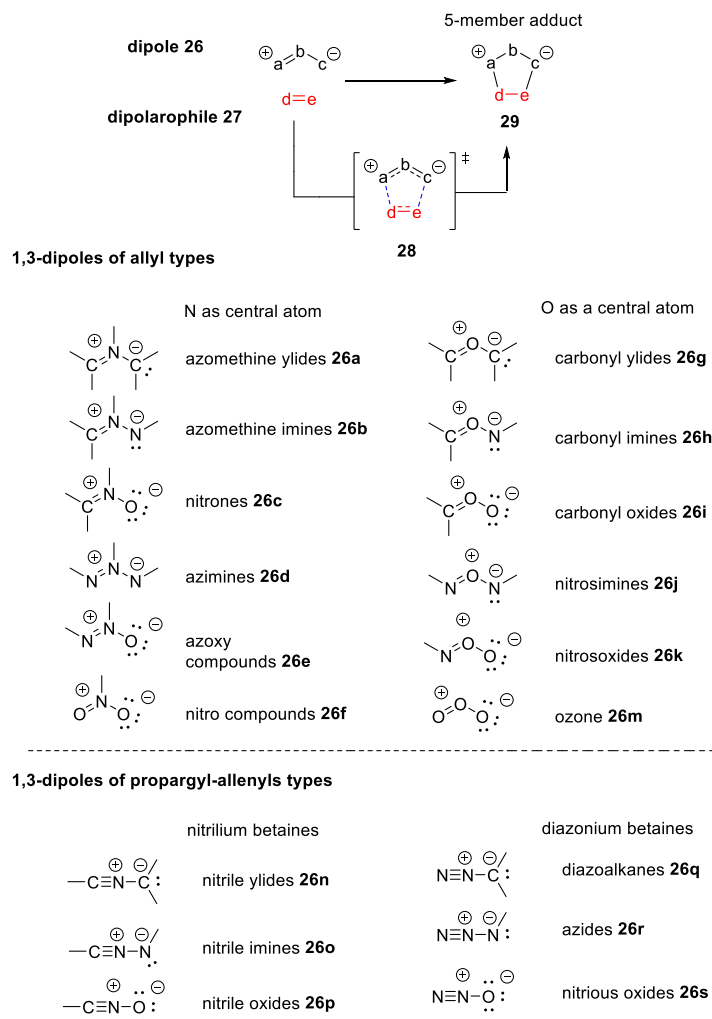
Figure 1.17. Representation 1,3-dipolar cycloaddition and classifications of 1,3-dipoles.

1.6.4. Mechanochemical Cu catalyze Azide Alkyne Cycloadditions (CuAAC)

Cu catalyzed Azide-Alkyne cycloadditions (CuAAC) is among the most notable transformation, demonstrating a high degree of selectivity, fast kinetics, and diverse scope. In part due to these developments, Mendal, Sharpless, and Bertozzi shared the 2022 Nobel Prize in chemistry.[107] The extension of this concept has evolved from traditional solution-based thermal conditions to where several groups have studied its impact under mechanochemical conditions.

Thorwith *et al* were the first to demonstrate the benefits of mechanochemistry and CuAAC for the synthesis of 1,4-triazoles **32** (**Figure 1.19**).[108] They identified that by using traditional catalytic conditions such as Cu(OAc)$_2$•H$_2$O and Na-Ascorbate, similar conditions as developed by Sharpless *et al,* 1,4-triazoles can be synthesized in short reactions times and with high regioselectivity (**Appendix A** for reaction conditions and mechanism)(**Figures 1.19a**).[109] The mechanochemistry method was successfully extended to the synthesis of high molecular weight polymers **35** with just 20 minutes of milling time (**Figure 1.19b**).[108]
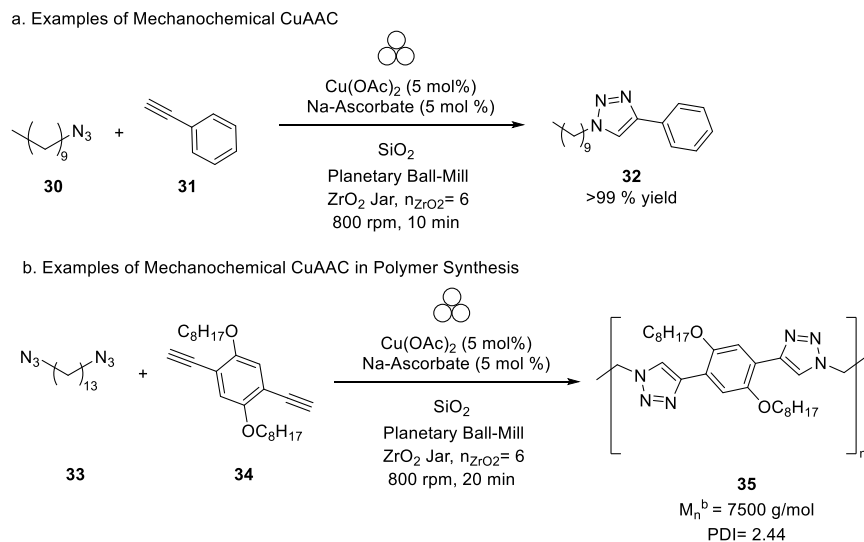
Figure 1.19. Examples of mechanochemistry in CuAAC for small molecules and in polymer synthesis.

Further investigations of the mechanochemical CuAAC for the synthesis of 1,4-triazoles, demonstrated that $Cu(OAc)_2 \bullet H_2O$ and Na ascorbate can be completely replaced with a jar and milling media made of Cu material. The Mack group demonstrated the effect of direct mechanocatalysis (**section 1.4.4**) for the synthesis of 1,4-triazoles **38** (**Figure 1.20a**). They demonstrated that equimolar mixtures of benzylbromide **36**, terminal alkyne **37**, excess sodium azide and using a copper jar and copper made milling media, resulted in the 1,4-triazole **38** in excellent yields after 16 hours of milling.[110] The sustainability of the CuAAC by direct mechanocatalysis is exemplified by the high atom economy achieved in the transformation and the simple protocol that eliminates the use of column chromatography as a purification alternative. Further investigation by the RAM technique demonstrated that copper-based milling media is not required and it can be replaced by a Cu^0 wire to form the 1,4-triazole **41** in excellent yields after 60 minutes of milling (**Figure 1.20b**).[111]

a. Mack *et al.* Direct Mechanocatalysis for the synthesis of 1,4-triazoles.
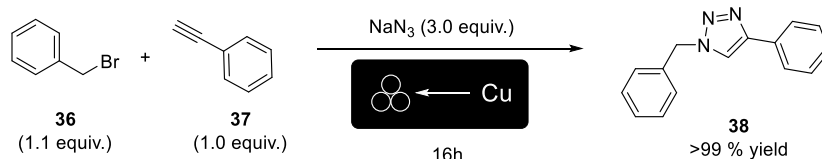
b. Lenox *et al.* Direct Mechanocatalysis by Resonance Acoustic Mixing (RAM) for the synthesis of 1,4-triazoles.
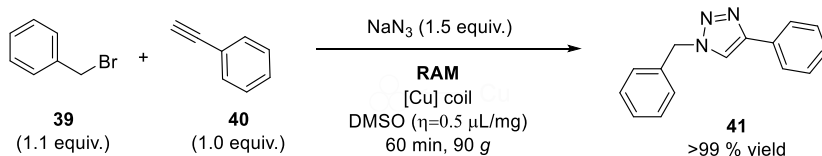
Figure 1.20. Examples of Direct Mechanocatalysis on CuAAC.

Other groups have evaluated the effect of Cu based nanocomposites and Cu nanoparticles as alternatives to using jars or milling media made of copper. Although external Cu source is introduced to the reaction mixture, the use of Cu based nanocomposites and Cu nanoparticles are a sustainable alternative to replace inert grinding auxiliaries (GAA) with auxiliaries with catalytic activity that can be easily recovered and re-used. The Ranu group demonstrated the use of Cu/Al_2O_3 nanocomposite for the multicomponent synthesis of 1,4-triazole **43** from alkyl halides **41**, sodium azide, and terminal alkynes **42** (**Figure 1.21 aI**).[112] Additionally, the use of Cu/Al_2O_3 demonstrated to be an effective catalyst in the synthesis of aryl azides from aryl boronic acids **44**, a reaction that was not developed employing *direct mechanocatalysis* (**Figure 1.21aII**). The Praveen group also demonstrated the use of commercially available copper oxide nanoparticles (CuONP of < 50 nm) and DABCO for the formation of oxindole-triazole **50** from N-methylmaleimide **48**, benzyl azide **49** and N-propargyl isatin **47** in excellent yields and short reaction times (**Figure 1.21b**).[113]
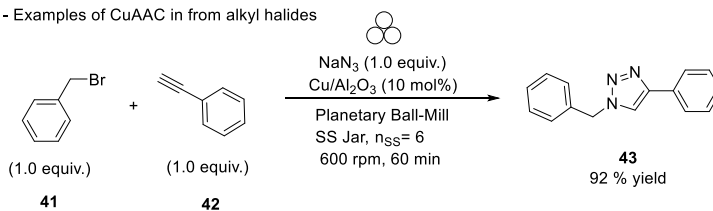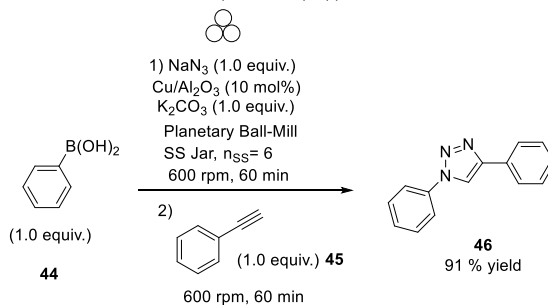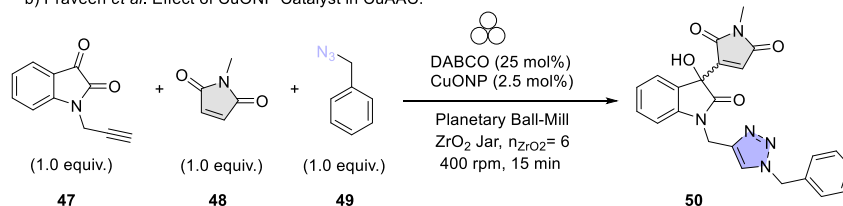
Figure 1.21. Cu nanoparticles used on CuAAC.

While most of the examples have focused on 1,4-triazoles using CuAAC, the Praveen group, demonstrated the regioselective organo-mechano catalytic synthesis of trisubtituted 1,4,5-triazoles **53** and **56** (**Figure 1.22a**).[114] The reaction proceeded in the presence of aryl of alkyl azides **51** or **54** but it is limited to trans olefins bearing electron-withdrawing groups such as nitro **52** or ketone **55** substituents. In their work, cetyltrimethylammonium bromide (CTAB) proved to be an efficient, easily recoverable organocatalyst, that through coordination with the electron-withdrawing groups on the olefin **57** facilitated the 1,3-dipolar cycloaddition and the oxidation adducts **58** to form the trisubstituted triazine **53** (**Figure 1.22b**).

Figure 1.22. Examples of organocatalytic mechanochemical synthesis of trisubtituted triazoles.

1.6.5. Mechanochemical 1,3-DC with Other Propargyl-Allenyl Dipoles

Beyond reports on CuAAC, there is limited reports of 1,3-DC using other types of 1,3-dipoles. The Bolm group recently reported the mechanochemical van Leusen pyrrole synthesis of 3,4-disubstituted pyrroles **61** from chalcones **60** and toluenesulfonylmethyl isocyanide (TosMIC) **59** (**Figure 1.23**).[115] The reaction proceeds only when enabled by mechanochemistry and without the need of a catalysts that is promoted by DBU for *in-situ* formation of the nitrile ylide (**25n**). The reaction demonstrated tolerability to several chalcones with diverse types of electronics and produced the desired product after just 60 minutes of milling (**Figure 1.23**).
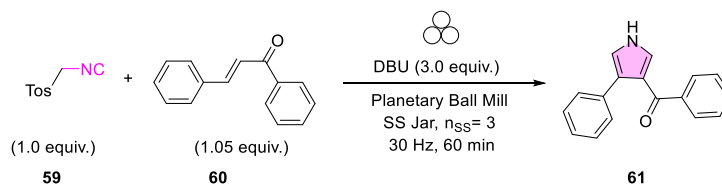
Figure 1.23. Mechanochemical van Lausen cycloaddition to obtain 3,4-pyrroles.

1.6.5.1. Nitrile Oxides for the synthesis of Isoxazoles

Mechanochemistry can provide significant advantages for pericyclic reactions, such as the removal of transition metal catalysts, short reaction times, improving the reactivity of insoluble substrates, and decrease in waste-production. The previously presented section demonstrates the number of studies on 1,3-DC using azides **25c** in mechanochemistry, but there are limited studies that evaluate the effect of mechanochemistry for other types of dipoles that do not show the same selectivity and reactivity as the azide **25c**.

Nitrile Oxides **25p** (NOs), as demonstrated in **Figure 1.17**, are analogous 1,3-dipoles to azides **25c**. However, NOs **25p** are more unstable and rapidly dimerize to form furoxans **63** by a 1,3-DC, even at room temperature.[116] Due to the high reactivity, NOs are generated *in-situ* from the bench stable hydroxyimidoyl chloride **62** when treated with organic amine bases (**Figure 1.24**).
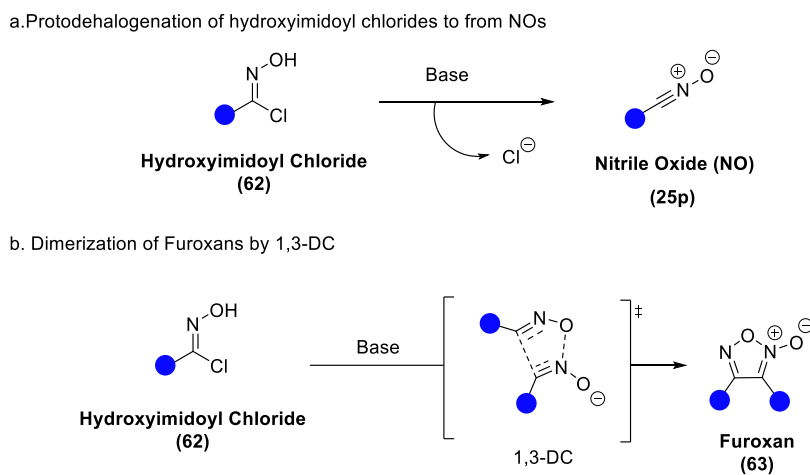
Figure 1.24. Synthesis of NOs and Furoxans

NOs have found numerous applications in the synthesis of isoxazoles and isoxazolines heterocycles.[116–118] Reaction between NOs (**25p**) with terminal alkynes provide direct access to the synthesis of disubstituted isoxazoles, specifically 3,5-isoxazoles **65** and 3,4-isoxazoles **66** (**Figure 1.25a**). The first 1,3-DC between NOs and terminal alkynes was reported by Quilico *et al*. with the preferential formation of the 3,5-isoxazoles in good yields.[105,119] A trivial feature of 1,3-DC of NOs with terminal alkynes is the regioselective formation of a C-C and a C-O bond. The impact of this 1,3-DC using NOs dipoles allows access to diverse types of isoxazole motifs in molecules that have demonstrated biological activity (**Figure 1.25b**) [117,120–123] or in the synthesis of molecules with innovative photochemical properties (**Figure 1.25c**).[124–127] Additionally, the regioselective formation of the C-C bond enables isoxazole heterocycles to be employed as versatile

intermediates in the synthesis of complex natural products (**Figure 1.25d**).[120,128–133134] Selected examples have been included in **Figure 1.25**.
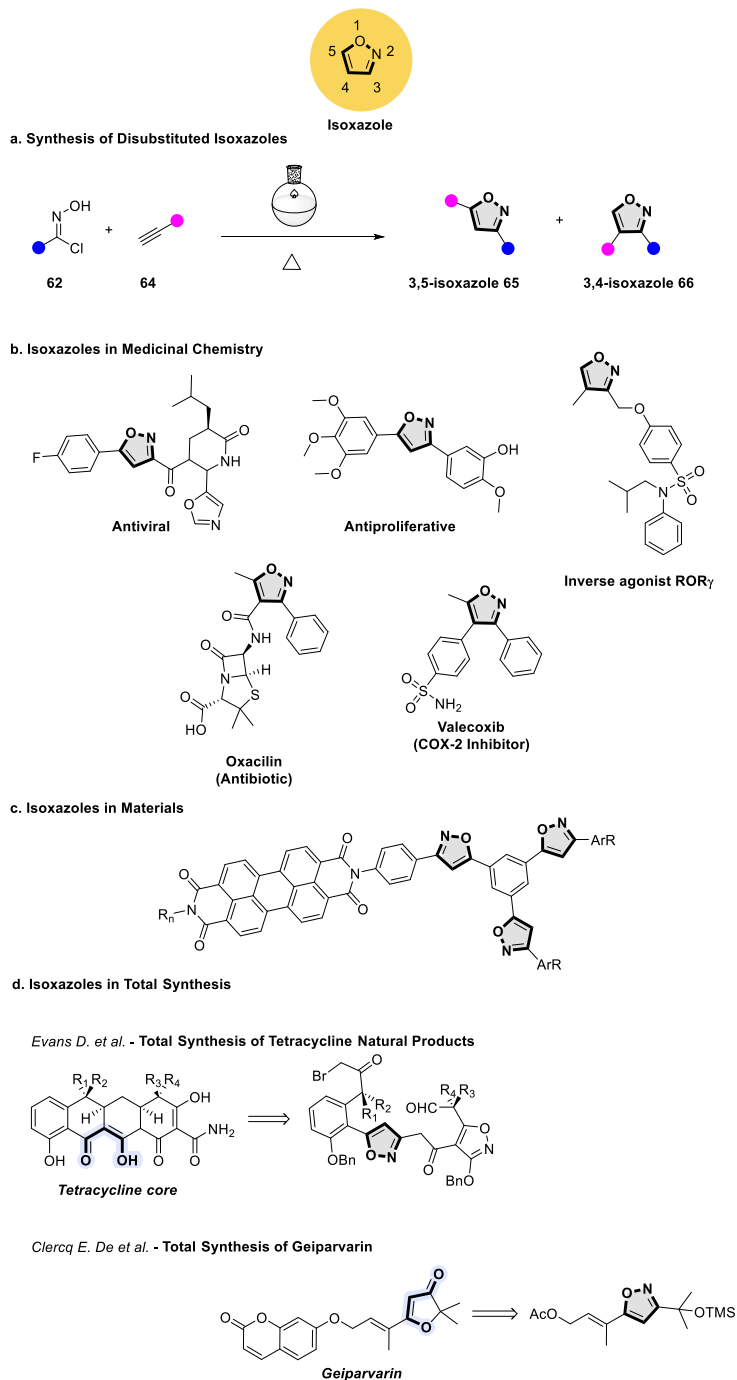
Figure 1.25. Application of Isoxazole Heterocycles in Various Fields of Chemistry.

1.6.5.2. Regioselectivity of 1,3-DC between Isoxazoles and Terminal Alkynes

1,3-DC between NOs and terminal alkynes generally forms mixtures of disubstituted isoxazole isomers, the poor regioselectivity of the 1,3-DC is attributed to the small difference in energy of about 2.8 kcal/mol between the transitions states **TSa** and **TSb** (**Figure 1.26**).[109] The lower energy of **TSa** leading for the preferential formation of 3,5-isoxazoles **65** is explained by the steric repulsions in **TSb**. Other factors such as interactions of the frontier molecular orbital interactions (FMO) of the dipole and the dipolarophile **64** and solvation effects can also have an impact in modulating the energies of the transition states.[105,135–137]
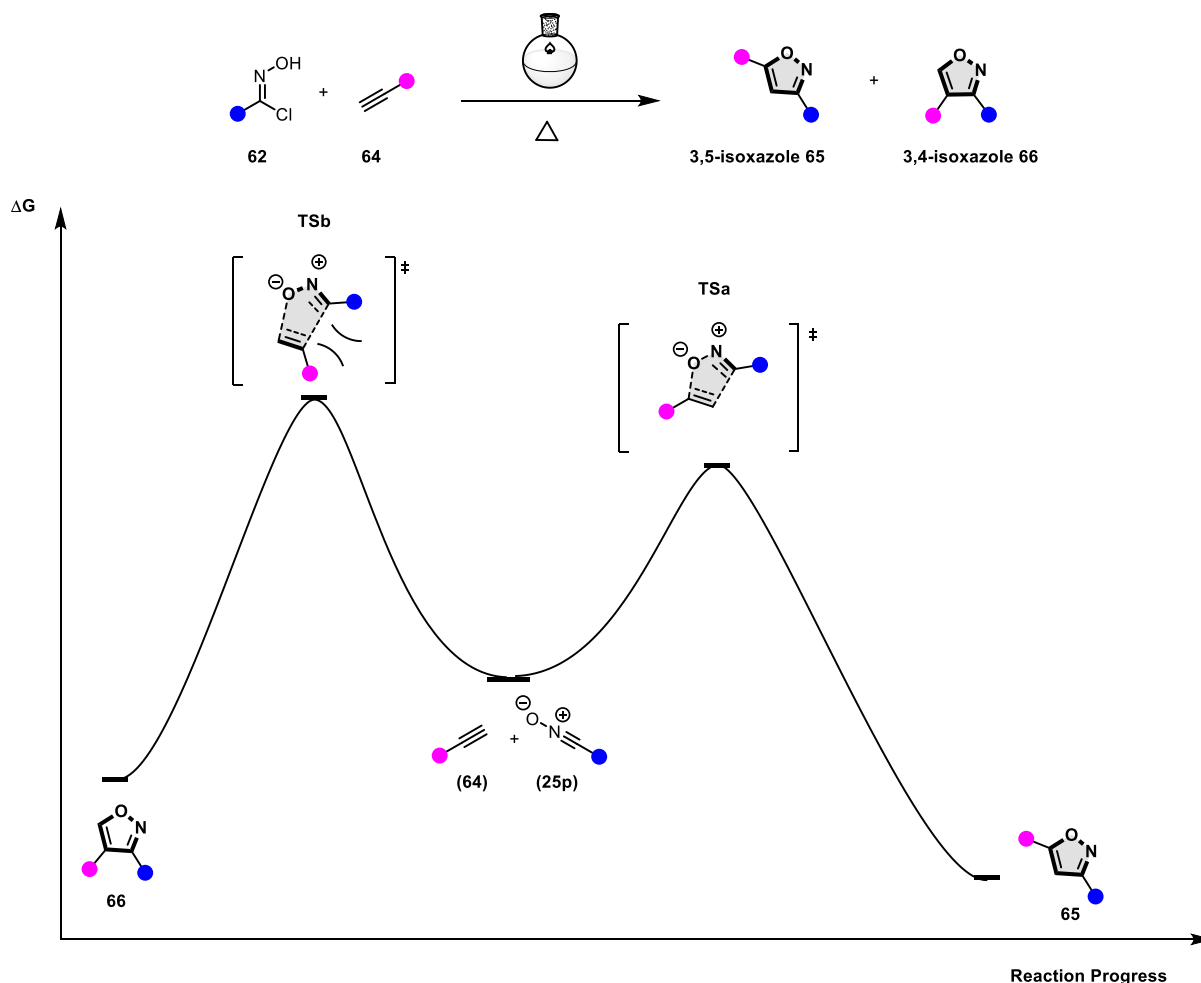
Figure 1.26. Generic reaction diagram for termal 1,3-DC between NOs and terminal alkynes.

1.6.5.3. Effect of Cu Catalysis in the Synthesis of 3,5-Isoxazoles

Improvements in the selectivity to access selectively 3,5-isoxazole **65** isomer were pioneered by Sharpless and Fokin.[109] It was envisaged that since azides and analogous 1,3-dipoles to NOs **25p,** the use of Cu catalysis could be further extended to NOs.[109] Cycloaddition between NOs and terminal alkynes catalyzed by Cu complexes (CuNOAC) improved the regioselectivity to form exclusively the 3,5-isoxazole **65** isomer (**Figure 1.27**).[109,121,138] Extensive computational studies demonstrated that the presence of copper deviates the mechanism from concerted to stepwise.[109] From a mechanistic perspective, the Fokin group

24

demonstrated that Cu(I)-alkyne complexation **67** is essential for the formation of copper acetylide **68**, followed by a coordination of the nitrile carbon of the NO to Cu(I) and subsequent attack on the O of the NO to the substituted carbon of the copper acetylide to form intermediate complex **69**, ring contraction of **69** and proteolysis of **70** forms the 3,5-isoxazole **65** (**Figure 1.27**).[109] The presented Cu(I)/Cu(II) catalytic process demonstrated excellent compatibility with a large number of alkyne and NOs substrates.[109,121,138]
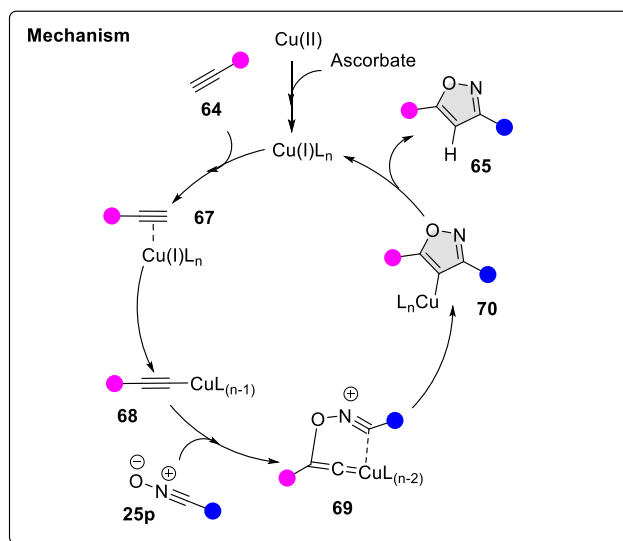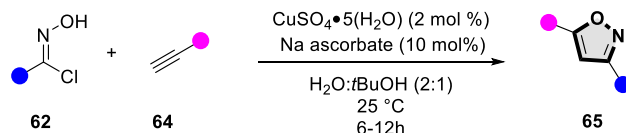
Figure 1.27. Cu(I) catalyze 1,3-DC between NOs and terminal alkyne

1.6.5.4. Effect of Ru Catalysis for the Synthesis of 3,4-isoxazoles

As an extension of Cu catalysis, the Fokin group pioneered in 2008 using [Cp*Ru] complexes **70** to provide regioselective access to 3,4-isoxazole **66** (**Figure 1.28a**).[139] The key feature of the [Cp*Ru] complexes **71** is that the Ru complex can reverse the polarity of the NO **25p** while the bulky Cp* ligand is able to position the substituent of the terminal alkyne under the ring such that the O and terminal C are oriented facing each other (**72**). Oxidative coupling leads to forming a 6-membered ruthenacycle **74** (**Figure 1.28b**). A highlight of this protocol is that it is not limited to terminal alkynes but can be extended to internal alkyne systems such as ynones **75** and ynols **76** (**Figure 1.28c**).
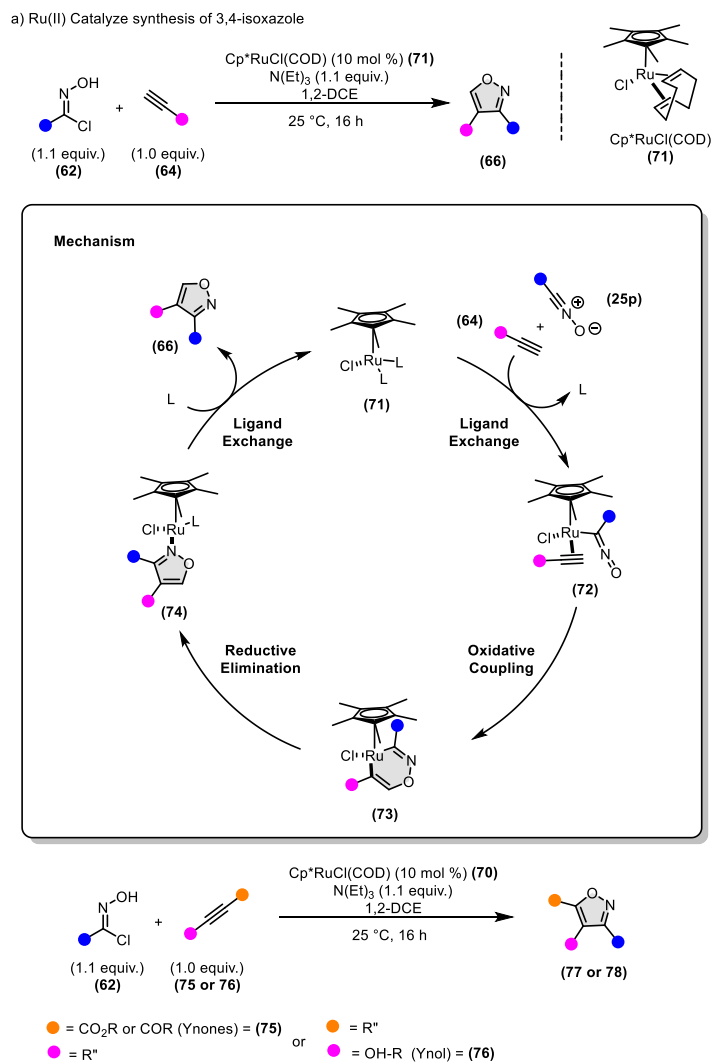
Figure 1.28. Ru(II) catalyze synthesis of 3,4- and 3,4,5-isoxazoles.

1.7. Research Goals and Thesis Organization

While the capabilities and benefits of mechanochemistry to access and facilitate cycloaddition reactions have been previously reported, the main thesis objective is the investigation on the effect of mechanical stress generated by mechanochemical techniques and specifically planetary ball milling in the control in regioselectivity of 1,3-DC between NOs (obtained from their precursors **62**) and terminal alkynes **64** to access all potential substitution patterns around the isoxazole heterocycles while focusing on the highest green chemistry standards, where possible.

Chapter 1 introduces the critical concepts in the field of solid-state chemistry and mechanochemistry and its applications in cycloadditions reactions and aims to highlight essential differences and benefits of performing cycloadditions under mechanochemical means. Following the recent advances in the field of mechanochemical cycloadditions, the chapter highlights the necessity to evaluate the effect of mechanochemistry to control cycloadditions.

After having established the concepts in mechanochemistry and its impact in 1,3-DC, Chapter 2 demonstrates the effects of mechanochemistry in a Cu(II)-catalyzed 1,3-DC to access 3,5-isoxazoles by

planetary ball milling. This work was published as an article in *RSC Advances* (DOI: 10.1039/D1RA08443G) and was completed primarily by the author of this thesis. Contributions from Arthur P. C. A. Bragaa and Jennifer Keough Lopez towards the optimization of Cu(II) catalysts and Kelly Burchell-Reyes in the time optimization of each substrates and the isolation of the 3,5-isoxazoles required for the reaction scope.

Chapter 3 evaluates the effect of mechanochemistry to control selectivity of 1,3-DC to control desymmetrization of unbiased symmetrical bis-/ or tris-alkyne substrates. This work was published as an article in the *European Journal of Organic Chemistry - Chemistry Europe* (doi.org/10.1002/ejoc.202300374). This work was done primarily by the author of this thesis with additional contributions of Irini Trakakis and Jean-Louis Do in the reaction optimization conditions.

Chapter 2 and 3, primarily focuses on the synthesis of 3,5-isoxazoles. Chapter 4 describes the effect of mechanochemistry by Ru(II) catalysis in the solid-state under solvent-free conditions to access 3,4- and 3,4,5-isoxazoles regioselectively. The current work has not been published but is under current evaluation in the Journals of the Royal Chemical Society. This work was done primarily by the author of this document. Contributions of Stephanie Patterson in the optimization of Ru-catalysts and Negin Nabavi in the optimization of the uncatalyzed synthesis of 3,4,5-isoxazoles and the Ru(II) conditions for the umpolung synthesis of 3,4,5-isoxazoles.

Chapter 5 is a highlights the essential aspects related to a health and safety at work when related to organic mechanochemistry that differs from what is normally required in a solution based organic chemistry laboratory.

Chapter 6 Discusses the general conclusions of all projects and potential future directions.

1.8. References

[1] Erythropel, H. C.; Zimmerman, J. B.; De Winter, T. M.; Petitjean, L.; Melnikov, F.; Lam, C. H.; Lounsbury, A. W.; Mellor, K. E.; Janković, N. Z.; Tu, Q.; Pincus, L. N.; Falinski, M. M.; Shi, W.; Coish, P.; Plata, D. L.; Anastas, P. T. *Green Chem.* **2018**, *20*, 1929–1961.

[2] DeVito, S. C.; Keenan, C.; Lazarus, D. *Green Chem.* **2015**, *17*, 2679–2692.

[3] Colberg, J.; Hii, K. K.; Koenig, S. G. *ACS Sustain. Chem. Eng.* **2022**, *10*, 8239–8241.

[4] Anastas, P.; Eghbali, N. *Chem. Soc. Rev.* **2010**, *39*, 301–312.

[5] Gu, Y.; Jérôme, F. *Chem. Soc. Rev.* **2013**, *42*, 9550–9570.

[6] Chemat, F.; Abert Vian, M.; Fabiano-Tixier, A. S.; Nutrizio, M.; Režek Jambrak, A.; Munekata, P. E. S.; Lorenzo, J. M.; Barba, F. J.; Binello, A.; Cravotto, G. *Green Chem.* **2020**, *22*, 2325–2353.

[7] Baig, R. B. N.; Varma, R. S. *Chem. Soc. Rev.* **2012**, *41*, 1559–1584.

[8] Liu, X.; Li, Y.; Zeng, L.; Li, X.; Chen, N.; Bai, S.; He, H.; Wang, Q.; Zhang, C. *Adv. Mater.* **2022**, *34*, 1–30.

[9] Matsumoto, A. *Top. Curr. Chem.* **2005**, *254*, 263–305.

[10] Toda, F. *Acc. Chem. Res.* **1995**, *28*, 480–486.

[11] Bartalucci, E.; Schumacher, C.; Hendrickx, L.; Puccetti, F.; d'Anciães Almeida Silva, I.; Dervişoğlu, R.; Puttreddy, R.; Bolm, C.; Wiegand, T. *Chem. - A Eur. J.* **2023**, *29*.

[12] Muñoz-Batista, M. J.; Rodriguez-Padron, D.; Puente-Santiago, A. R.; Luque, R. *ACS Sustain. Chem. Eng.* **2018**, *6*, 9530–9544.

[13] Boldyreva, E. *Chem. Soc. Rev.* **2013**, *42*, 7719–7738.

[14] Do, J. L.; Friščić, T. *ACS Cent. Sci.* **2017**, *3*, 13–19.

[15] Howard, J. L.; Cao, Q.; Browne, D. L. *Chem. Sci.* **2018**, *9*, 3080–3094.

[16] Hernández, J. G. *Chem. - A Eur. J.* **2017**, *23*, 17157–17165.

[17] Michalchuk, A. A. L.; Boldyreva, E. V.; Belenguer, A. M.; Emmerling, F.; Boldyrev, V. V. *Front. Chem.* **2021**, *9*, 1–29.

[18] Juaristi, E.; Avila-Ortiz, C. G. *Synth.* **2023**.

[19] Ardila-Fierro, K. J.; Hernández, J. G. *ChemSusChem* **2021**, *14*, 2145–2162.

[20] Friščić, T.; Mottillo, C.; Titi, H. M. *Angew. Chemie - Int. Ed.* **2020**, *59*, 1018–1029.

[21] Hwang, S.; Grätz, S.; Borchardt, L. *Chem. Commun.* **2022**, *58*, 1661–1671.

[22] Schneider, F.; Szuppa, T.; Stolle, A.; Ondruschka, B.; Hopf, H. *Green Chem.* **2009**, *11*, 1894–1899.

[23] Seo, T.; Kubota, K.; Ito, H. *J. Am. Chem. Soc.* **2020**, *142*, 9884–9889.

[24] Chen, L.; Regan, M.; Mack, J. *ACS Catal.* **2016**, *6*, 868–872.

[25] Howard, J. L.; Brand, M. C.; Browne, D. L. *Angew. Chemie - Int. Ed.* **2018**, *57*, 16104–16108.

[26] Hernández, J. G.; Bolm, C. *J. Org. Chem.* **2017**, *82*, 4007–4019.

[27] Sherwood, J.; Clark, J. H.; Fairlamb, I. J. S.; Slattery, J. M. *Green Chem.* **2019**, *21*, 2164–2213.

[28] Howard, J. L.; Sagatov, Y.; Repusseau, L.; Schotten, C.; Browne, D. L. *Green Chem.* **2017**, *19*, 2798–2802.

[29] Ying, P.; Yu, J.; Su, W. *Adv. Synth. Catal.* **2021**, *363*, 1246–1271.

[30] Kubota, K.; Seo, T.; Ito, H. *Faraday Discuss.* **2022**, *241*, 104–113.

[31] Mukherjee, A.; Rogers, R. D.; Myerson, A. S. *CrystEngComm* **2018**, *20*, 3817–3821.

[32] Hasa, D.; Schneider, G.; Voinovich, D.; Jones, W. *Angew. Chemie - Int. Ed.* **2015**, *54*, 7371–7375.

[33] Wang, C.; Yue, C.; Smith, A.; Mack, J. *J. Organomet. Chem.* **2022**, *976*, 122430.

[34] Martina, K.; Rinaldi, L.; Baricco, F.; Boffa, L.; Cravotto, G. *Synlett* **2015**, *26*, 2789–2794.

[35] Szuppa, T.; Stolle, A.; Ondruschka, B.; Hopfe, W. *Green Chem.* **2010**, *12*, 1288–1294.

[36] Andersen, J.; Brunemann, J.; Mack, J. *React. Chem. Eng.* **2019**, *4*, 1229–1236.

[37] Takacs, L. *J. Therm. Anal. Calorim.* **2007**, *90*, 81–84.

[38] McKissic, K. S.; Caruso, J. T.; Blair, R. G.; Mack, J. *Green Chem.* **2014**, *16*, 1628–1632.

[39] Yoo, K.; Fabig, S.; Grätz, S.; Borchardt, L. *Faraday Discuss.* **2022**, *241*, 206–216.

[40] Chen, L.; Leslie, D.; Coleman, M. G.; Mack, J. *Chem. Sci.* **2018**, *9*, 4650–4661.

[41] Pickhardt, W.; Grätz, S.; Borchardt, L. *Chem. - A Eur. J.* **2020**, *26*, 12903–12911.

[42] Haley, R. A.; Mack, J.; Guan, H. *Inorg. Chem. Front.* **2017**, *4*, 52–55.

[43] Andersen, J. M.; Mack, J. *Chem. Sci.* **2017**, *8*, 5447–5453.

[44] Bolt, R. R. A.; Leitch, J. A.; Jones, A. C.; Nicholson, W. I.; Browne, D. L. *Chem. Soc. Rev.* **2022**, *51*, 4243–4260.

[45] Crawford, D. E.; Wright, L. A.; James, S. L.; Abbott, A. P. *Chem. Commun.* **2016**, *52*, 4215–4218.

[46] Andersen, J.; Starbuck, H.; Current, T.; Martin, S.; Mack, J. *Green Chem.* **2021**, *23*, 8501–8509.

[47] Crawford, D. E.; Miskimmin, C. K. G.; Albadarin, A. B.; Walker, G.; James, S. L. *Green Chem.* **2017**, *19*, 1507–1518.

[48] Titi, H. M.; Do, J. L.; Howarth, A. J.; Nagapudi, K.; Friščić, T. *Chem. Sci.* **2020**, *11*, 7578–7584.

[49] Effaty, F.; Gonnet, L.; Koenig, S. G.; Nagapudi, K.; Ottenwaelder, X.; Friščić, T. *Chem. Commun.* **2022**, *59*, 1010–1013.

[50] Michalchuk, A. A. L.; Hope, K. S.; Kennedy, S. R.; Blanco, M. V.; Boldyreva, E. V.; Pulham, C. R. *Chem. Commun.* **2018**, *54*, 4033–4036.

[51] Lennox, C. B.; Borchers, T. H.; Gonnet, L.; Barrett, C. J.; Koenig, S. G.; Nagapudi, K.; Friščić, T.

Chem. Sci. **2023**, *14*, 7475–7481.

[52]   Ylijoki, K. E. O.; Stryker, J. M. *Chem. Rev.* **2013**, *113*, 2244–2266.

[53]   Bilodeau, D. A.; Margison, K. D.; Serhan, M.; Pezacki, J. P. *Chem. Rev.* **2021**, *121*, 6699–6717.

[54]   Wang, J.; Blaszczyk, S. A.; Li, X.; Tang, W. *Chem. Rev.* **2021**, *121*, 110–139.

[55]   Wollenhaupt, M.; Krupička, M.; Marx, D. *ChemPhysChem* **2015**, *16*, 1593–1597.

[56]   Woodward, R. B.; Hoffmann, R. *Angew. Chemie Int. Ed. English* **1969**, *8*, 781–853.

[57]   Williams, M. T. J.; Morrill, L. C.; Browne, D. L. *Adv. Synth. Catal.* **2023**, *365*, 1477–1484.

[58]   Bolt, R. R. A.; Raby-Buck, S. E.; Ingram, K.; Leitch, J. A.; Browne, D. L. *Angew. Chemie* **2022**, *134*.

[59]   Zhang, J.; Zhang, P.; Ma, Y.; Szostak, M. *Org. Lett.* **2022**, *24*, 2338–2343.

[60]   Seo, T.; Ishiyama, T.; Kubota, K.; Ito, H. *Chem. Sci.* **2019**, *10*, 8202–8210.

[61]   Kubota, K.; Takahashi, R.; Ito, H. *Chem. Sci.* **2019**, *10*, 5837–5842.

[62]   Kubota, K.; Seo, T.; Ito, H. *Faraday Discuss.* **2022**, *241*, 104–113.

[63]   Declerck, V.; Colacino, E.; Bantreil, X.; Martinez, J.; Lamaty, F. *Chem. Commun.* **2012**, *48*, 11778–11780.

[64]   Kubota, K.; Endo, T.; Uesugi, M.; Hayashi, Y.; Ito, H. *ChemSusChem* **2022**, *15*.

[65]   van Bonn, P.; Bolm, C.; Hernández, J. G. *Chem. - A Eur. J.* **2020**, *26*, 2576–2580.

[66]   Staleva, P.; Hernández, J. G.; Bolm, C. *Chem. – A Eur. J.* **2019**, *25*, 9202–9205.

[67]   Schumacher, C.; Hernández, J. G.; Bolm, C. *Angew. Chemie - Int. Ed.* **2020**, *59*, 16357–16360.

[68]   Puccetti, F.; Schumacher, C.; Wotruba, H.; Hernández, J. G.; Bolm, C. *ACS Sustain. Chem. Eng.* **2020**, *8*, 7262–7266.

[69]   Cheng, H.; Hernández, J. G.; Bolm, C. *Org. Lett.* **2017**, *19*, 6284–6287.

[70]   Do, J.; Mottillo, C.; Tan, D.; Štrukil, V.; Friščić, T. *J. Am. Chem. Soc.* **2015**, *137*, 2476–2479.

[71]   Bhawani; Shinde, V. N.; Sonam; Rangan, K.; Kumar, A. *J. Org. Chem.* **2022**, *87*, 5994–6005.

[72]   Schumacher, C.; Crawford, D. E.; Raguž, B.; Glaum, R.; James, S. L.; Bolm, C.; Hernández, J. G. *Chem. Commun.* **2018**, *54*, 8355–8358.

[73]   Hernandez, J. G.; Bolm, C. *Chem. Commun.* **2015**, No. 51, 12582–12584.

[74]   Hermann, G. N.; Becker, P.; Bolm, C. *Angew. Chemie - Int. Ed.* **2015**, *54*, 7414–7417.

[75]   Kondo, K.; Ishiyama, T.; Kubota, K.; Ito, H. *Chem. Lett.* **2023**, *52*, 333–336.

[76]   Pang, Y.; Ishiyama, T.; Kubota, K.; Ito, H. *Chem. - A Eur. J.* **2019**, *25*, 4654–4659.

[77]   Wu, C.; Ying, T.; Yang, X.; Su, W.; Dushkin, A. V; Yu, J. *Org. Lett.* **2021**, *23*, 6423–6428.

[78]   Nallaparaju, J. V.; Nikonovich, T.; Jarg, T.; Merzhyievskyi, D.; Aav, R.; Kananovich, D. G. *Angew. Chemie Int. Ed.* **2023**, *202305775*.

[79] Pfennig, V. S.; Villella, R. C.; Nikodemus, J.; Bolm, C. *Angew. Chemie - Int. Ed.* **2022**, *61*, 1–6.

[80] Takahashi, R.; Hu, A.; Gao, P.; Gao, Y.; Pang, Y.; Seo, T.; Jiang, J.; Maeda, S.; Takaya, H.; Kubota, K.; Ito, H. *Nat. Commun.* **2021**, *12*, 1–10.

[81] Das, D.; Bhosle, A. A.; Panjikar, P. C.; Chatterjee, A.; Banerjee, M. *ACS Sustain. Chem. Eng.* **2020**, *8*, 19105–19116.

[82] Takahashi, R.; Gao, P.; Kubota, K.; Ito, H. *Chem. Sci.* **2022**, *14*, 499–505.

[83] Cao, Q.; Howard, J. L.; Wheatley, E.; Browne, D. L. *Angew. Chemie* **2018**, *130*, 11509–11513.

[84] Gao, P.; Jiang, J.; Maeda, S.; Kubota, K.; Ito, H. *Angew. Chemie - Int. Ed.* **2022**, *61*.

[85] Funel, J. A.; Abele, S. *Angew. Chemie - Int. Ed.* **2013**, *52*, 3822–3863.

[86] Zhang, Z.; Peng, Z. W.; Hao, M. F.; Gao, J. G. *Synlett* **2010**, *2010*, 2895–2898.

[87] Zhao, Y.; Rocha, S. V; Swager, T. M. *J. Am. Chem. Soc.* **2016**, *138*, 13834–13837.

[88] Gonnet, L.; Chamayou, A.; André-Barrès, C.; Micheau, J. C.; Guidetti, B.; Sato, T.; Baron, M.; Baltas, M.; Calvet, R. *ACS Sustain. Chem. Eng.* **2021**, *9*, 4453–4462.

[89] Zholdassov, Y. S.; Yuan, L.; Garcia, S. R.; Kwok, R. W.; Boscoboinik, A.; Valles, D. J.; Marianski, M.; Martini, A.; Carpick, R. W.; Braunschweig, A. B. *Science.* **2023**, *380*, 1053–1058.

[90] Sarkar, D.; Bera, N.; Ghosh, S. *European J. Org. Chem.* **2020**, *2020*, 1310–1326.

[91] Overholts, A. C.; Robb, M. J. *ACS Macro Lett.* **2022**, *11*, 733–738.

[92] Kean, Z. S.; Niu, Z.; Hewage, G. B.; Rheingold, A. L.; Craig, S. L. *J. Am. Chem. Soc.* **2013**, *135*, 13598–13604.

[93] Izak-Nau, E.; Campagna, D.; Baumann, C.; Göstl, R. *Polym. Chem.* **2020**, *11*, 2274–2299.

[94] Ribas-Arino, J.; Shiga, M.; Marx, D. *Angew. Chemie - Int. Ed.* **2009**, *48*, 4190–4193.

[95] Zhu, S. E.; Li, F.; Wang, G. W. *Chem. Soc. Rev.* **2013**, *42*, 7535–7570.

[96] Wang, G. W.; Komatsu, K.; Murata, Y.; Shiro, M. *Nature* **1997**, *387*, 583–586.

[97] Komatsu, K.; Fujiwara, K.; Murata, Y. *Chem. Lett.* **2000**, No. 9, 1016–1017.

[98] Guan-Wu, W.; Koichi, K.; Yasujiro, M.; Motoo, S. *Nature* **1997**, *387*, 583–586.

[99] Ong, M. T.; Leiding, J.; Tao, H.; Virshup, A. M.; Martínez, T. J. *J. Am. Chem. Soc.* **2009**, *131*, 6377–6379.

[100] Hickenboth, C. R.; Moore, J. S.; White, S. R.; Sottos, N. R.; Baudry, J.; Wilson, S. R. *Nature* **2007**, *446*, 423–427.

[101] Sokolov, A. N.; Bučar, D. K.; Baltrusaitis, J.; Gu, S. X.; MacGillivray, L. R. *Angew. Chemie - Int. Ed.* **2010**, *49*, 4273–4277.

[102] MacGillivray, L. R.; Reid, J. L.; Ripmeester, J. A. *J. Am. Chem. Soc.* **2000**, *122*, 7817–7818.

[103] Santra, R.; Garai, M.; Mondal, D.; Biradha, K. *Chem. - A Eur. J.* **2013**, *19*, 489–493.

[104] Briceño, A.; Leal, D.; Ortega, G.; De Delgado, G. D.; Ocando, E.; Cubillan, L. *CrystEngComm* **2013**, *15*, 2795–2799.

[105] Huisgen, R. *Angew. Chemie Int. Ed.* **1963**, *2*, 633–696.

[106] Huigens, R. *Angew. Chemie Int. Ed.* **1963**, *2*, 5-565–563.

[107] AIP. *Nobel Prize 2022 Resources*. American Institute of Physics (Retrived August 16,2023 from https://www.nobelprize.org/prizes/medicine/2012/prize-announcement/).

[108] Thorwirth, R.; Stolle, A.; Ondruschka, B.; Wild, A.; Schubert, U. S. *Chem. Commun.* **2011**, *47*, 4370–4372.

[109] Himo, F.; Lovell, T.; Hilgraf, R.; Rostovtsev, V. V.; Noodleman, L.; Sharpless, K. B.; Fokin, V. V. *J. Am. Chem. Soc.* **2005**, *127*, 210–216.

[110] Cook, T. L.; Walker, J. A.; Mack, J. *Green Chem.* **2013**, *15*, 617–619.

[111] Lennox, C. B.; Borchers, T. H.; Gonnet, L.; Barrett, C. J.; Koenig, S. G.; Nagapudi, K.; Friščić, T. *Chem. Sci.* **2023**, No. d, 7475–7481.

[112] Mukherjee, N.; Ahammed, S.; Bhadra, S.; Ranu, B. C. *Green Chem.* **2013**, *15*, 389–397.

[113] Vadivelu, M.; Sugirdha, S.; Dheenkumar, P.; Arun, Y.; Karthikeyan, K.; Praveen, C. *Green Chem.* **2017**, *19*, 3601–3610.

[114] Vadivelu, M.; Raheem, A. A.; Raj, J. P.; Elangovan, J.; Karthikeyan, K.; Praveen, C. *Org. Lett.* **2022**, *24*, 2798–2803.

[115] Schumacher, C.; Molitor, C.; Smid, S.; Truong, K. N.; Rissanen, K.; Bolm, C. *J. Org. Chem.* **2021**, *86*, 14213–14222.

[116] Hashimoto, T.; Maruoka, K. *Chem. Rev.* **2015**, *115*, 5366–5412.

[117] Zhu, J.; Mo, J.; Lin, H.; Chen, Y.; Sun, H. *Bioorganic Med. Chem.* **2018**, *26*, 3065–3075.

[118] Deb, T.; Tu, J.; Franzini, R. M. *Chem. Rev.* **2021**, *121*, 6850–6914.

[119] Quilico, A.; Stango D'Alcontres, G.; Grunanger, P. *Nature* **1950**, *166*, 226.

[120] Klenc, J.; Raux, E.; Barnes, S.; Sullivan, S.; Duszynska, B.; Bojarski, A. J.; Strekowski, L. *J. Heterocycl. Chem.* **2009**, *46*, 1259–1265.

[121] Hu, F.; Szostak, M. *Adv. Synth. Catal.* **2015**, *357*, 2583–2614.

[122] Sysak, A.; Obmińska-Mrukowicz, B. *Eur. J. Med. Chem.* **2017**, *137*, 292–309.

[123] Pairas, G. N.; Perperopoulou, F.; Tsoungas, P. G.; Varvounis, G. *ChemMedChem* **2017**, *12*, 408–419.

[124] Ikeda, T.; Masuda, T.; Hirao, T.; Yuasa, J.; Tsumatori, H.; Kawai, T.; Haino, T. *Chem. Commun.* **2012**, *48*, 6025–6027.

[125] Haino, T.; Saito, H. *Synth. Met.* **2009**, *159*, 821–826.

[126] Hirano, K.; Ikeda, T.; Fujii, N.; Hirao, T.; Nakamura, M.; Adachi, Y.; Ohshita, J.; Haino, T. *Chem. Commun.* **2019**, *55*, 10607–10610.

[127] Jin, Q.; Li, J.; Zhang, L.; Fang, S.; Liu, M. *CrystEngComm* **2015**, *17*, 8058–8063.

[128] Kaiser, T. M.; Huang, J.; Yang, J. *J. Org. Chem.* **2013**, *78*, 10572.

[129] Akagawa, K.; Kudo, K. *J. Org. Chem.* **2018**, *83*, 4279–4285.

[130] Bode, J. W.; Uesuka, H.; Suzuki, K. *Org. Lett.* **2003**, *5*, 395–398.

[131] Paciorek, J.; Höfler, D.; Sokol, K. R.; Wurst, K.; Magauer, T. *J. Am. Chem. Soc.* **2022**, *144*, 19704–19708.

[132] Baraldi, P. G.; Guarneri, M.; Manfredini, S.; Simoni, D.; Balzarini, J.; de Clercq, E. *J. Med. Chem.* **1989**, *32*, 284–288.

[133] Nicolaou, K. C.; Hale, C. R. H.; Nilewski, C.; Ioannidou, H. A.; Elmarrouni, A.; Nilewski, L. G.; Beabout, K.; Wang, T. T.; Shamoo, Y. *J. Am. Chem. Soc.* **2014**, *136*, 12137–12160.

[134] Wzorek, J. S.; Knöpfel, T. F.; Sapountzis, I.; Evans, D. A. *Org. Lett.* **2012**, *14*, 5840–5843.

[135] Ess, D. H.; Houk, K. N. *J. Am. Chem. Soc.* **2008**, *130*, 10187–10198.

[136] Ess, D. H.; Houk, K. N. *J. Am. Chem. Soc.* **2007**, *129*, 10646–10647.

[137] Lin, B.; Yu, P.; He, C. Q.; Houk, K. N. *Bioorganic Med. Chem.* **2016**, *24*, 4787–4790.

[138] Hansen, T. V.; Wu, P.; Fokin, V. V. *J. Org. Chem.* **2005**, *70*, 7761–7764.

[139] Grecian, S.; Fokin, V. V. *Angew. Chemie - Int. Ed.* **2008**, *47*, 8285–8287.

Chapter 2- Solvent-Free Synthesis of 3,5-Isoxazoles via 1,3-Dipolar Cycloaddition of Terminal Alkynes and Hydroxyimidoyl Chlorides over Cu/Al$_2$O$_3$ Surface under Ball-Milling Conditions.

2.1. Abstract

Scalable, solvent-free synthesis of 3,5-isoxazoles under ball-milling has been developed. the proposed methodology allows to synthesize 3,5-isoxazoles in moderate to excellent yields from terminal alkynes and hydroxyimidoyl chlorides, using a recyclable Cu/Al_2O_3 nanocomposite catalyst. Furthermore, the proposed conditions are reproducible to a 1.0-gram scale without further milling time variations.

2.2. Introduction

The addition of oxygen or nitrogen-containing heterocycles in drug candidates has become a common feature of the recently approved drugs by the FDA.[1,2] In particular, isoxazoles are common molecular scaffolds employed in medicinal chemistry due to the non-covalent interactions such as hydrogen bonding (through the N) and π-π stacking (by the unsaturated 5-member ring).[3–6] Within the isoxazoles family, 3,5-isoxazoles **78** are regularly utilized as pharmacophores in medicinal chemistry.[2,5,6] Selected examples include Muscimol (GABAa agonist), Isocarboxazib (antidepressant), Isoxicam (anti-inflammatory), Berzosertib (ATR Kinase Inhibitor), and Sulfamethoxazole (Antibiotic) are highlighted in **Figure 2.1**.[7–10]
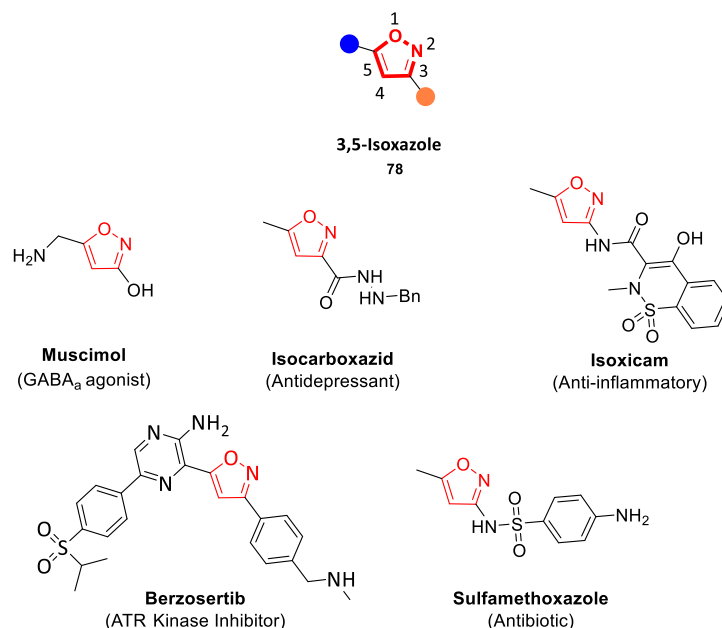
Figure 2.1. Examples of isoxazoles with pharmacological activity.

Various methodologies to synthesize 3,5-isoxazoles have been developed over the years.[7,9,11–13] Specifically, 1,3-dipolar cycloaddition between terminal alkynes **79** and nitrile oxides **81** formed in situ by deprotonation of hydroxyimidoyl chlorides **80** is a standard route to access 3,5-isoxazoles **78** (**Figure 2.2**).[7,9,14] Recent reports have sought to mitigate the environmental impact of this reaction by performing 1,3-dipolar cycloaddition under solvent-free conditions, using green solvents such as water or ionic liquids, under metal-free conditions, or using mild oxidants.[14–28] However, these methodologies have a low atom economy, have a higher hazardous waste production, and are less energy efficient. Therefore, developing a greener methodology that enables rapid and efficient access to these scaffolds is highly desirable.

1,3-Dipolar Cycloaddition
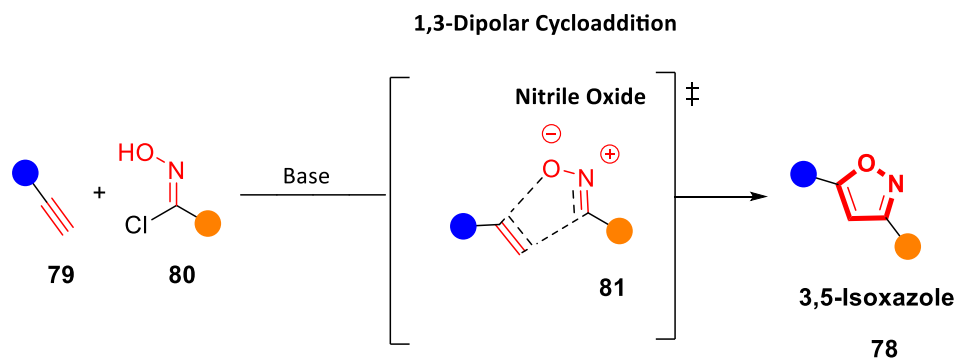
Figure 2.2. 1,3-Dipolar cycloaddition of terminal alkynes and nitrile oxides

Mechanochemistry has been recognized as an environmentally friendly technique as reactions can be performed under solvent-free conditions. Additionally, in some instances, work-up and purification are simplified or absent from procedures, and the process consumes less energy than other solution-based techniques. [29–33] The use of mechanochemical techniques to synthesize isoxazoles is limited. Sherin *et al.* reported a synthesis of 3,5-isoxazoles **84** by grinding in a mortar and pestle curcumin derivatives **82**, hydroxylamine **83**, and sub-stoichiometric amounts of acetic acid to form the 3,5-isoxazole **84** in short times and excellent yields (**Figure 2.3a**).[34] Likewise, Xu *et al.* studied the synthesis of trisubstituted isoxazoles **87** *via* 1,3-dipolar cycloaddition of N-hydroxybenzimidoyl chlorides **85** and N-substituted b-enamino carbonyl **86** compounds by ball-milling (**Figure 2.3b**) in high yields, short reaction times, in the absence of catalyst and liquid additives.[35] To our knowledge, mechanochemical synthesis of 3,5-isoxazoles **78** from terminal alkynes **79** and hydroxyimidoyl chloride **80** has not been reported (**Figure 2.3c**). The proposed methodology employs a planetary ball-milling technique that provides a route to access in large scale, short reaction times, and high atom economy the corresponding 3,5-isoxazoles **78**. Additionally, it utilizes synthetically accessible or commercially available motifs such as terminal alkynes **79** and hydroxyimidoyl chlorides **80** that are recurrent or easily installed in many substrates. Herein, we report a mechanochemical 1,3-dipolar cycloaddition using the planetary ball-mill to synthesize a wide range 3,5-isoxazoles from a broad library of alkynes and (E,Z)-N-hydroxy-4-nitrobenzimidoyl chloride **80a**, ethyl (E,Z)-2-chloro-2-(hydroxyimino)acetate **80b**, hydroxycarbonimidic dibromide **80c**, or (E,Z)-N-hydroxy-4-methoxybenzimidoyl chloride **80d** in moderate to excellent yields, in short reaction time, and with less waste production than in solution based reactions (**Figure 2.3c**).

a) Mechanochemical synthesis of 3,5-isoxazoles from Curcumin derivative (1,3-diketone) and hydroxylamine. (Ref 34.)
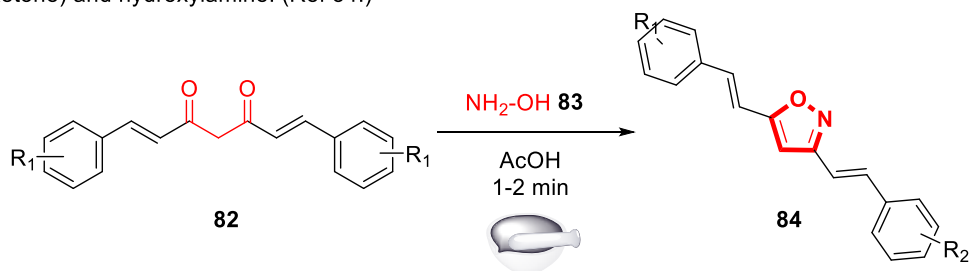
b) Mechanochemical synthesis of isoxazoles from N-hydroxybenzimidoyl chlorides and enamino carbonyl. (Ref 35.)
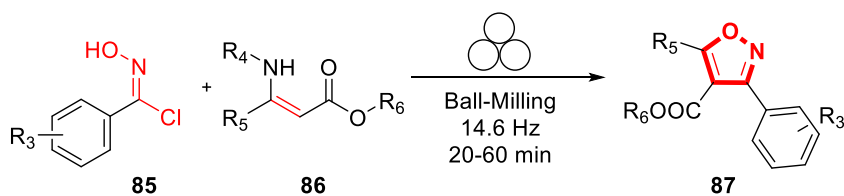
c) This work: Mechanochemical synthesis of 3,5-isoxazole from alkynes and a-chlorooximes.
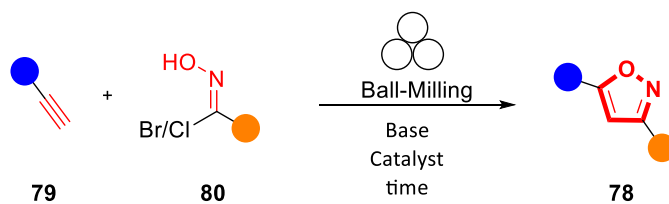
Figure 2.3: Previously reported synthesis of Isoxazoles

2.3. Results and Discussion

2.3.1. Reaction optimization

We began our investigation by performing an optimisation of the 1,3-dipolar cycloaddition reaction between alkyne **79a** and hydroxyimidoyl chlorides **80a** by milling the selected substrates in a stainless-steel (SS) jar in the planetary ball-mill to obtain 3,5-isoxazole **78a** (**Table 2.1**). During the optimization, the effect of milling time, amount of milling media, base, and equivalents of hydroxyimidoyl chlorides were

studied to obtain the highest yield of 3,5-isoxazole **78a** (**Table 2.1**). Optimization revealed the combination of 1.0 equivalent of alkyne **79a**, 1.5 equivalents of hydroxyimidoyl chlorides **80a**, and 2.0 equivalents of Na_2CO_3 while milling for 20 minutes with 8 SS balls provided the most effective conditions (**Table 2.1**, entry 1). Our first control experiments focused on optimizing the milling time (**Table 2.1**, entry 2-5). Milling the reagents for less than 20 minutes affords lower product yields (**Table 2.1**, entries 2 and 3). Conversely, milling the reagents longer than 20 minutes leads to a decrease in yield to about 60 % (**Table 2.1**, entries 4 and 5). The strong abrasion of the SS milling media for extended periods could lead to a ring-opening by a reduction of the N-O to yield β-keto-enamine.[36,37]

Table 2.1 *Optimization of reaction conditions* [a]

Entry	Changes from optimized conditions	Yield (%)[b] of 78a
1	none	72
2	Milling for 10 min, 7 SS balls.	59
3	Milling for 15 min 7 SS balls.	64
4	Milling for 30 min.	58
5	Milling for 40 min.	60
6	Using 1.0 equiv. of 80a.	65
7	Using 2.0 equiv. of 80a.	57
8	Using K_2CO_3	71
9	Using Cs_2CO_3	71
10	Using $CaCO_3$	44
11	Using Ag_2CO_3	18
12	Using NEt_3	N.R.

Reaction Conditions: 0.166 mmol of **79a**, 0.250 mmol of **80a**, 0.332 mmol of Na_2CO_3, SS beaker (50 mL capacity), 8 x SS milling balls (10 mm diameter), 20 min milling, 60 Hz. (b) ^{1}H-NMR yields were measured using 1,3,5-trimethoxybenzene as an internal standard.

Having optimized the milling time, we next attempted to improve the yield by varying the equivalents of hydroxyimidoyl chlorides **80a** since reaction stoichiometry has been shown to impact the product formed during mechanochemical reactions.[38,39] 3,5-isoxazole **78a** was obtained in lower yields when using

equimolar amounts alkyne **79a** to hydroxyimidoyl chlorides **80a** (entry 6, **Table 2.1**). Because nitrile oxides rapidly dimerize to form furoxans by a competing 1,3-dipolar cycloaddition.[40–45] Likewise, increasing the equivalents of **80a** from 1.0 to 2.0 equivalents lowered the yield of the reaction (entry 7, **Table 2.1**). We obtained the highest yield with 1.5 equivalents of the hydroxyimidoyl chlorides of **80a**, and these conditions were used for further experiments (entry 1, **Table 2.1**). We next studied the effect of diverse carbonated bases in the reaction. We observed that changing the base did not improve the yield of the reaction, and Ag_2CO_3 was most detrimental to the reaction as it promoted furoxan formation (entry 8-11, **Table 2.1**).[46,47] Using triethylamine (NEt_3) proved impractical as the addition of NEt_3 to hydroxyimidoyl chlorides was highly exothermic in the absence of solvent (entry 12, **Table 2.1**).

During the screening, we observed that milling time influences the reaction yield.[35,48] Therefore, a milling time optimization for other alkyne and hydroxyimidoyl chloride combinations revealed that the most optimal milling time was determined to be between 10 and 30 minutes (see experimental **section 2.8** for detailed milling time optimizations).
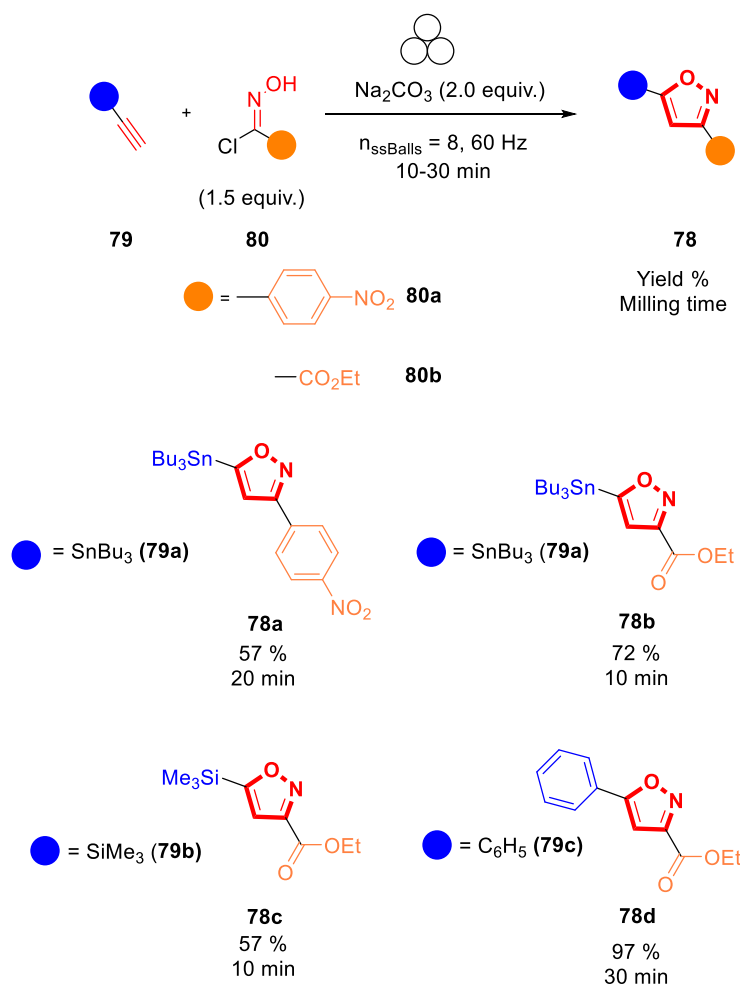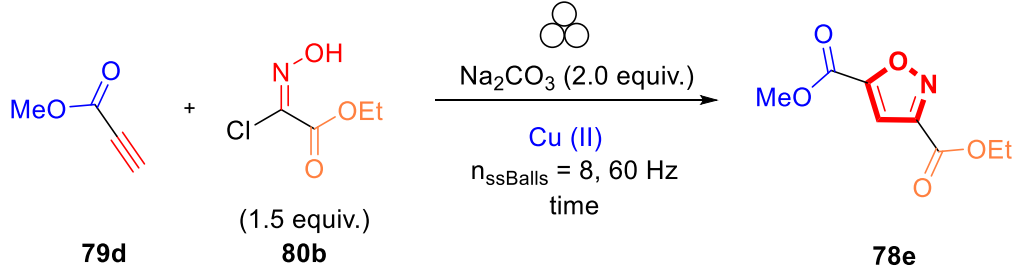
Figure 2.4. Catalyst-free mechanochemical synthesis of 3,5-isoxazoles.

As shown in **Figure 2.4**, stannanyl isoxazole **78a** and **78b**, silyl isoxazole **78c**, and phenyl isoxazole **78d** were synthesized with satisfactory yields under the proposed conditions. To explain these results, we suggest an electronic argument. The electron-withdrawing character of the metal substituents, stannyl or silyl of

alkyne **79a** and **79b**, respectively, accelerates the reaction by deactivating the alkyne moiety.[49–51] It is observed that alkyne **79a** bearing the alkylstannane substituent has a more pronounced effect than the alkyne with the silyl substituent **79b**. Therefore, alkyne **79a** was the most reactive as it reacted with hydroxyimidoyl chlorides **80a** and **80b** to synthesize 3,5-isoxazole **78a** and **78b** respectively, in short times and excellent yields (**Figure 2.4**). On the other hand, ethynyltrimethylsilane **78b** was less reactive as it could only react with a more labile hydroxyimidoyl chlorides **80b** to form 3,5-isoxazole **78c** (**Figure 2.4**). Comparably, we suggest that the phenyl substituent of alkyne **79c** increases the polarizability of the molecule, resulting in deactivating the alkyne moiety. As a result, phenylacetylene **78c** reacted in excellent yields with hydroxyimidoyl chlorides **80b**.[42] In addition, we observed that the electronic nature of the hydroxyimidoyl chloride substituent affects the reactivity of the nitrile oxide dipole. Hydroxyimidoyl chlorides **80a** containing an aromatic substituent with strong electron-withdrawing groups decreased the reactivity of the nitrile oxide.[52,53] Consequently, the nitrile oxide synthesized in situ from hydroxyimidoyl chlorides **80a** could only react with tributyl(ethynyl)stannane **79a**. On the other hand, hydroxyimidoyl chlorides **80b** was the most reactive due to the bearing of a weaker electron-withdrawing group such as the ester functional group.[43,52] Unfortunately, other alkynes containing substituents such as esters, pyridines, or substituted arenes were not tolerated under these conditions. Previous reports demonstrated the effect of copper catalyst or copper additives to accelerate the reaction and obtain the 3,5-isoxazoles in a regioselective manner. [15,53–59] Therefore, we aimed to investigate the effect of copper additives or catalysts on this reaction.

2.3.2. Investigations of Cu(II) catalysis in the synthesis of 3,5-isoxazole:

Table 2.2. *Effect of Copper(II) in the synthesis of 3,5-Isoxazoles*

Entry	Cu (II)	Equivalents	Time (min)	Yield (%)[b] 19e
1	Cu/Al$_2$O$_3$	0.14 of Cu(II)	10	73
			20	76
			30	79
			40	64
			50	56
2	Cu(NO$_3$)$_2$2.5•H$_2$O	0.1	30	78
3	Cu(NO$_3$)$_2$ 2.5•H$_2$O	1.0	30	84
4	Cu(OAc)$_2$•H$_2$O	1.0	30	88
5	Cu(OTf)$_2$	1.0	30	76
6	CuCl$_2$ •H$_2$O	1.0	30	76
7	Cu$_2$CO$_3$(OH)$_2$	2.0	30	36

Reaction Conditions: 0.220 mmol of 79d, 0.330 mmol of 80b, 0.220 mmol of Na$_2$CO$_3$, 0.440 mmol (14 mol %) of Cu/Al$_2$O$_3$, SS beaker (50 mL capacity), 8 x SS milling balls (10 mm diameter), 60 Hz. b) ^{1}H NMR yields

were measured using 1,3,5-trimethoxybenzene as an internal standard. c) See experimental section 2.9. for solid-state characterization by FT-IR and MALDI-TOF-MS of reaction crude 1e.

Although the mechanochemical synthesis of 3,5-isoxazoles using copper(II) catalyst is unprecedented, 1,2,3-triazoles have been synthesized in this way with copper(II) salts and copper(II) ions in alumina nanocomposites (Cu/Al$_2$O$_3$).[60,61] We investigated the effect of Cu/Al$_2$O$_3$ (see experimental **section 2.8.7.** for XPS spectrum) and copper salts using methyl propiolate **79d** and (E,Z)-2-chloro-2-(hydroxyimino)acetate **80b** as model substrates (**Table 2.2**).

We observed a significant increase in yield and regioselective control when using sub-stoichiometric amounts of copper (0.14 equivalents or 14 mol %) of Cu/Al$_2$O$_3$ or 10 mol % of Cu(NO$_3$)$_2$ 2.5•H$_2$O while milling the reagents for 30 minutes (entries 1 and 2, **Table 2.2**). Irreproducible yields were obtained by decreasing the catalytic loading to 7 mol % of Cu/Al$_2$O$_3$. In contrast, when the equivalents of Cu(NO$_3$)$_2$ 2.5•H$_2$O were increased to 1.0 equivalent, we observed no significant increase in yield (entry 3, **Table 2.2**). Additionally, when investigating the effect of the counter anion on the copper(II), it was observed that Cu(OAc)$_2$•H$_2$O performs similarly to Cu(NO3)$_2$ 2.5•H$_2$O (entry 4, **Table 2.2**), while Cu(OTf)$_2$ and CuCl$_2$ •H$_2$O produced lower yields (entries 5 and 6, **Table 2.2**). Substituting Na$_2$CO$_3$ with Cu$_2$CO$_3$(OH)$_2$ lowered the yield drastically (entry 7, **Table 2.2**). Interestingly, the addition of copper salts did not lead to homocoupling of the alkyne moiety by the Glaser reaction.[62–64]

We decided to continue our investigations using Cu/Al$_2$O$_3$ as the catalyst can be filtered and washed with solvent, thereby facilitating catalyst recovery and recycling (**Figure 2.5**).[60]

a   **b**
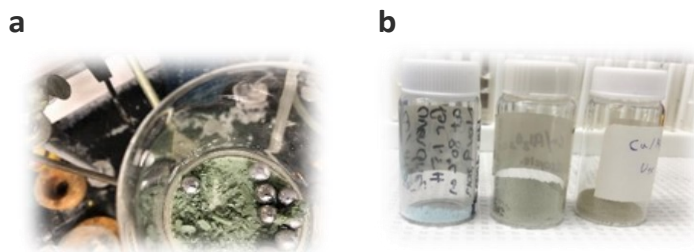
Figure 2.5. a) Filtration of the Cu/Al$_2$O$_3$ catalyst after the first run. b) Colour change of the Cu/Al$_2$O$_3$ catalyst after recycling. From left to right. (Left) Fresh catalyst: blue. (Middle) First recycle: Green. (Right) Second recycle: Brown
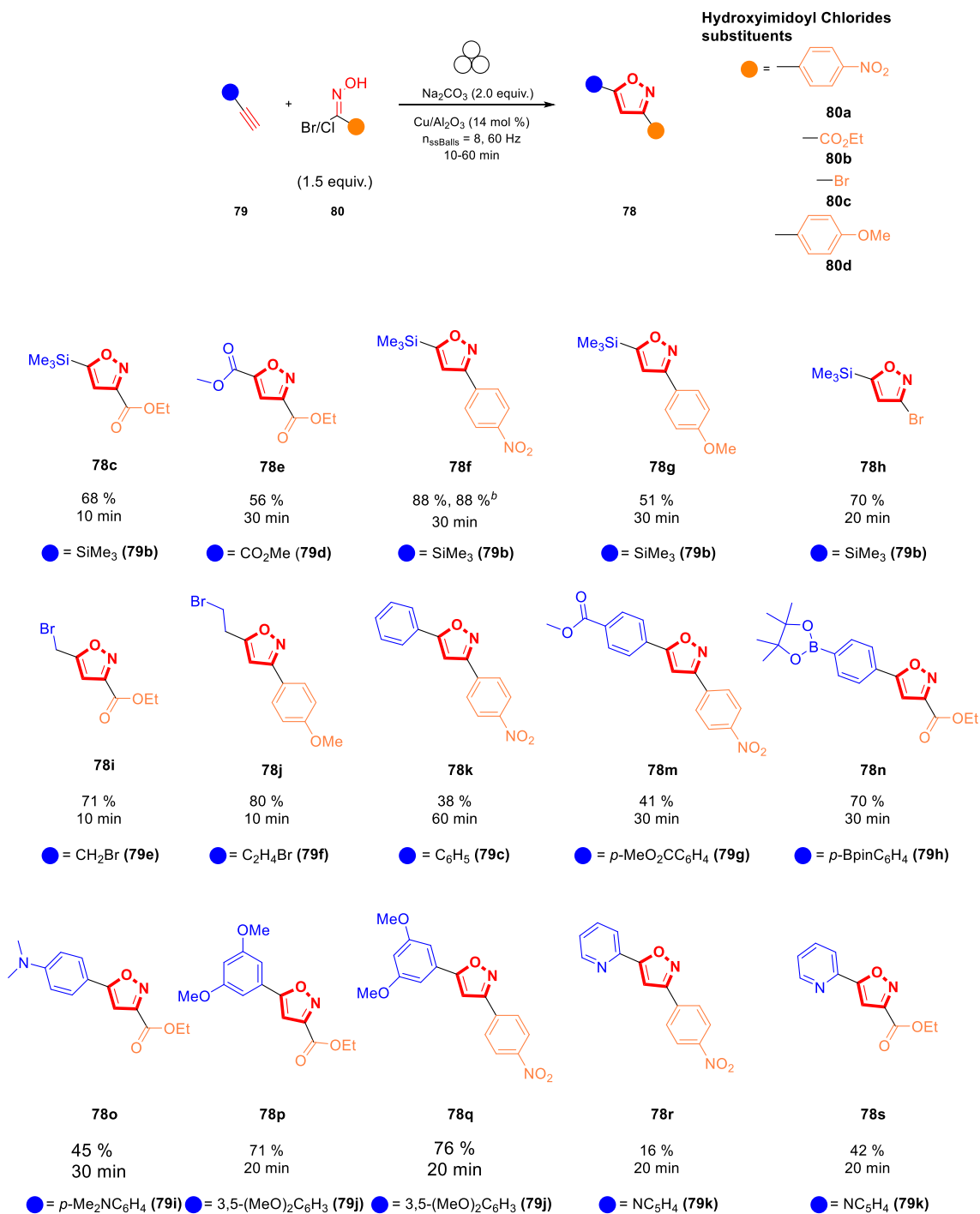
Figure 2.6. Mechanochemical synthesis of 3,5-isoxazoles reaction scope.

a All shown yields are isolated yields. *b* Reaction performed in 1.0-gram scale

The Cu/Al$_2$O$_3$ catalyst effect was not exclusively beneficial for the cycloaddition with methyl propiolate **79d** (3,5-isoxazole **78e**, **Figure 2.6**). This system improves the reactivity of hydroxyimidoyl chlorides **80a**, **80b**, **80c**, and **80d** and other alkynes inaccessible under copper-free conditions, thus allowing access to a

broader library of 3,5-isoxazoles (**Figure 2.6**). Moreover, the presence of Cu/Al$_2$O$_3$ nanocomposite as part of the reaction conditions is not impaired by the presence of labile substituents such as silanes (**78c,f-h**), alkyl halides (**78i-j**), and boronic esters (**78n**) (**Figure 2.6**). However, the presence of alkyl stannane substituents in the dipolarophile **79a** was not tolerated with Cu/Al$_2$O$_3$ catalyst, and no product was observed. Furthermore, Cu/Al$_2$O$_3$ enhances the reactivity of dipolarophiles bearing arenes with electron-donating substituents (EDG) **78o-q** and electron-withdrawing groups (EWG) **78n-r** when coupled with hydroxyimidoyl chlorides **80a** and **80b**. Additionally, pyridine substituents were more reactive towards the more reactive hydroxyimidoyl chlorides **80b** (3,5-isoxazole **80s**, **Figure 2.6**). Ethynyltrimethylsilane **78c** reacted efficiently with hydroxyimidoyl chlorides bearing EWG **80a**, **80b**, and **80c** to form the respective isoxazoles **80c**, **80f**, and **80h**, where silyl isoxazole 80c is obtained in higher yields compared to copper-free conditions (**80c**, **Figure 2.4**). Hydroxyimidoil chloride bearing EDG **80d**; resulted incompatible with terminal alkyne **79b** and silyl isoxazole **78g** was obtained in lower yields than with EWG in the hydroxyimidoyl chloride. However, terminal alkynes having an aliphatic substituent (**79e** and **79f**) showed greater reactivity towards hydroxyimidoil chloride **80d** bearing EDG; consequently, aliphatic isoxazole **78j** was obtained in higher yields than **78i**. Then, we evaluated the impact of our conditions in the synthesis of 3,5-isoxazole **78f** on a 1.0-gram scale (10.18 mmol). We were pleased to observe that the optimized Cu/Al$_2$O$_3$ conditions can be translated with excellent reproducibility from a 100 mg scale to a 1.0-gram scale without extending the milling time of the reagents (**Figure 2.6**).

2.3.3. Investigations on the recyclability of Cu/Al$_2$O$_3$

The practicality of the proposed methodology allows the recovery of Cu/Al$_2$O$_3$ nanocomposite catalyst directly after the milling of the reagents. In addition, the catalyst recovery allowed investigating the reusability of the recovered catalyst. The Cu/Al$_2$O$_3$ was reused on four occasions, and it was observed that 3,5-isoxazole **78f** was obtained successfully with only a minimal drop in yield with each subsequent use for the first two recycling cycles (**Figure 2.7**). The decrease in yield is explained by the decrease in the concentration of active Cu species in the Cu/Al$_2$O$_3$ nanocomposite (see **experimental section 2.8.6**). ICP-MS analysis demonstrates that the Cu concentration of the first recycling represents a decrease of 1.24-fold (with respect to the fresh catalyst); thus, similar yields are obtained compared to the fresh catalyst (**Figure 2.7**). However, the decrease in Cu concentration becomes more substantial for the second and third reuse with a decrease of 2.42 and 6.48-fold, respectively. Therefore, a considerable decrease in the yield of isoxazole **78f** is observed. Furthermore, a change in the oxidation state and the bonding of the supported Cu(II) ions. X-ray Photoelectron Spectroscopy (XPS) analysis of the first and second recycled catalyst reveals that the characteristic satellite signals of Cu(II) found at about 942.8 eV are weak while the satellite signal at 963.2 eV is absent. Additionally, the 2p3/2 signal at about 933-934 eV is wider than in the fresh sample (see **experimental section 2.8.7** for XPS spectra of the fresh, **Figure S2.3** for first recycling and **Figure S2.4** for second recycling). These observations suggest that the supported Cu(II) is reduced to Cu(0) and CuO is formed with each subsequent recycling.[65–67]

43
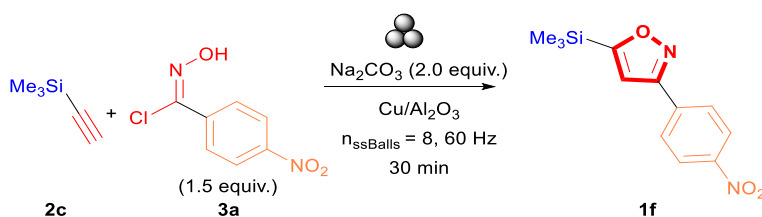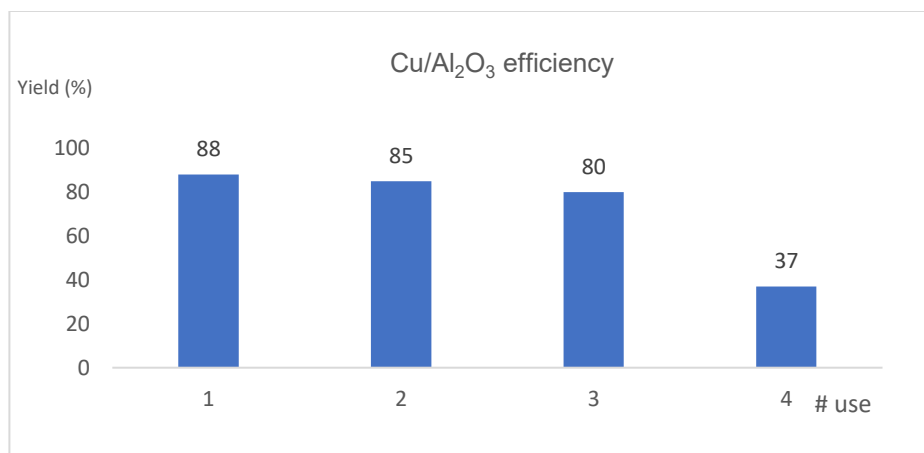
Figure 2.7. Cu/Al$_2$O$_3$ efficiency study in the synthesis of 3,5-isoxazole **78f**

Lastly, we evaluated the sustainability of the proposed mechanochemical 1,3-dipolar cycloaddition conditions by comparing E-factor for the synthesis of 3,5 isoxazoles **78d** and **78f** to previously reported solution-based conditions (**Figure 2.8**). [54,68] Using E-factor, the values calculated for the planetary ball milling conditions (pathway a and c, **Figure 2.8**) demonstrate the sustainability of this methodology compared to solution-based reactions (pathway b and d) (see **experimental section 2.8.3 and 2.8.9** for calculations). With our conditions, the absence of organic solvent is the most significant factor contributing to lowering the E-factor.[69] Time differences were also another factor of comparison with previously reported solution-based conditions. Our mechanochemical conditions did not surpass 60 minutes, contrary to the reported solution-based conditions that require at least two hours to synthesize the desired 3,5-isoxazoles. Furthermore, our conditions did not show any sensitivity to oxygen or moisture present in the air as all reactions were performed in an open atmosphere.
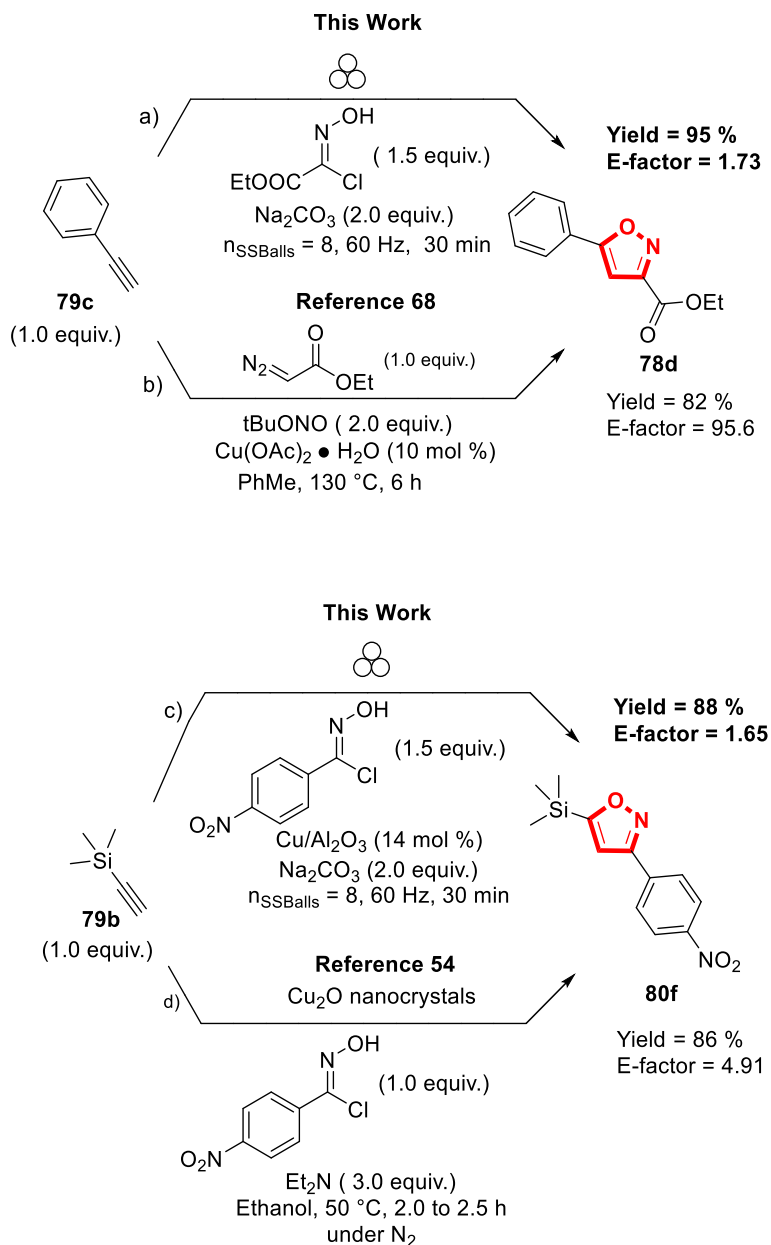
Figure 2.8. Comparative green metrics of the proposed methodology to previously reported solution-based methodologies.

2.4. Conclusion

In conclusion, we have developed a scalable, solvent-free, and efficient mechanochemical synthesis of 3,5-isoxazoles via 1,3-dipolar cycloaddition from terminal alkynes and hydroxyimidoyl chlorides. We presented two methodologies; a catalyst-free methodology which scopes extended to dipolarophiles bearing alkyl stannane substituent. Under catalyst-fee conditions, ethynyltrimethylsilane **79c** and phenylacetylene **79d** reacted satisfactorily with (E,Z)-2-chloro-2-(hydroxyimino)acetate **80b**. Additionally, a Cu/Al$_2$O$_3$ mediated methodology allowed to react a broader range of dipolarophiles bearing electron-donating or electron-

withdrawing substituents with any hydroxyimidoyl chloride. The reported methodology was scalable to a 1.0-gram scale without additional milling time variations. The Cu/Al$_2$O$_3$ catalyst was demonstrated to easily be recycled and reused three times with only a slight reduction in yield. The reported conditions require shorter reaction times, they had a lower E-factor, and no prevention was taken to air or moisture, making these methodologies less environmentally harmful and more practical than previously reported solution-based methodologies.

2.5. Acknowledgements

2.7. References

[1]. E. Vitaku, D. T. Smith and J. T. Njardarson, *J. Med. Chem.*, **2014**, *57*, 10257–10274.

[2]. M. D. Delost, D. T. Smith, B. J. Anderson and J. T. Njardarson, *J. Med. Chem.*, **2018**, *61*, 10996–11020.

[3]. K. P. Rakesh, C. S. Shantharam, M. B. Sridhara, H. M. Manukumar and H. L. Qin, *Med. Chem. Commun.*, **2017**, *8*, 2023–2039.

[4]. P. P. Sharp, J. M. Garnier, D. C. S. Huang and C. J. Burns, *Med. Chem. Commun.*, **2014**, *5*, 1834–1842.

[5]. A. Sysak and B. Obmińska-Mrukowicz, *Eur. J. Med. Chem.*, **2017**, *137*, 292–309.

[6]. J. Zhu, J. Mo, H. Lin, Y. Chen and H. Sun, *Bioorganic Med. Chem.*, **2018**, *26*, 3065–3075.

[7]. M. Kim, Y. S. Hwang, W. Cho and S. B. Park, *ACS Comb. Sci.*, **2017**, *19*, 407–413.

[8]. L. Gorecki, M. Andrs, M. Rezacova and J. Korabecny, *Pharmacol. Ther.*, **2020**, *210*, 107518.

[9]. F. Hu and M. Szostak, *Adv. Synth. Catal.*, **2015**, *357*, 2583–2614.

[10]. H. Zinnes, J. C. Sircar, N. Lindo, M. L. Schwartz, A. C. Fabian, J. Shavel, C. F. Kasulanis, J. D. Genzer, C. Lutomski and G. DiPasquale, *J. Med. Chem*, **1982**, *25*, 12–18.

[11]. S. Roscales and J. Plumet, *Org. Biomol. Chem.*, **2018**, *16*, 8446–8461.

[12]. L. Claisen and O. Lowman, *Berichte der Dtsch. Chem. Gesellschaft*, **1888**, *21*, 1149–1157.

[13]. J. Li, Z. Lin, W. Wu and H. Jiang, *Org. Chem. Front.*, **2020**, *7*, 2325–2348.

[14]. F. Himo, T. Lovell, R. Hilgraf, V. V. Rostovtsev, L. Noodleman, K. B. Sharpless and V. V. Fokin, *J. Am. Chem. Soc.*, **2005**, *127*, 210–216.

[15]. T. V. Hansen, P. Wu and V. V. Fokin, *J. Org. Chem.*, **2005**, *70*, 7761–7764.

[16]. J. Li, J. Yu, W. Xiong, H. Tang, M. Hu, W. Wu and H. Jiang, *Green Chem.*, **2020**, *22*, 465–470.

[17]. D. Wang, F. Zhang, F. Xiao and G. J. Deng, *Org. Biomol. Chem.*, **2019**, *17*, 9163–9168.

[18]. D. R. Meena, B. Maiti and K. Chanda, *Tetrahedron Lett.*, **2016**, *57*, 5514–5517.

[19]. S. B. Bharate, A. K. Padala, B. A. Dar, R. R. Yadav, B. Singh and R. A. Vishwakarma, *Tetrahedron Lett.*, **2013**, *54*, 3558–3561.

[20]. J. M. Pérez and D. J. Ramón, *ACS Sustain. Chem. Eng.*, **2015**, *3*, 2343–2349.

[21]. A. M. Jawalekar, E. Reubsaet, F. Rutjes and F. van Delft, *Chem. Commun.*, **2011**, *47*, 3198–3200.

[22]. M. Vadivelu, S. Sampath, K. Muthu, K. Karthikeyan and C. Praveen, *J. Org. Chem.*, **2019**, *84*, 13636–13645.

[23]. A. Yoshimura, K. R. Middleton, A. D. Todora, B. J. Kastern, S. R. Koski, A. V. Maskaev and V. V. Zhdankin, *Org. Lett.*, **2013**, *15*, 4010–4013.

[24]. L. Lin, J. Zhang and R. Wang, *Asian J. Org. Chem.*, **2012**, *1*, 222–225.

[25]. S. Mohammed, R. A. Vishwakarma and S. B. Bharate, *RSC Adv.*, **2015**, *5*, 3470–3473.

[26]. C. Kesornpun, T. Aree, C. Mahidol, S. Ruchirawat and P. Kittakoop, *Angew. Chemie - Int. Ed.*, **2016**, *55*, 3997–4001.

[27]. B. Touaux, F. Texier-Boullet and J. Hamelin, *Heteroat. Chem.*, **1998**, *9*, 351–354.

[28]. M. Hu, Z. Lin, J. Li, W. Wu and H. Jiang, *Green Chem.*, **2020**, *22*, 5584–5588.

[29]. F. Schneider, T. Szuppa, A. Stolle, B. Ondruschka and H. Hopf, *Green Chem.*, **2009**, *11*, 1894–1899.

[30]. D. Tan, L. Loots and T. Friščić, *Chem. Commun.*, **2016**, *52*, 7760–7781.

[31]. S. L. James, C. J. Adams, C. Bolm, D. Braga, P. Collier, T. Friščić, F. Grepioni, K. D. Harris, G. Hyett, W. Jones, A. Krebs, J. Mack, L. Maini, A. G. Orpen, I. P. Parkin, W. C. Shearouse, J. W. Steed, W. Shearouse, J. W. Steed and D. C. Waddell, *Chem. Soc. Rev.*, **2012**, *41*, 413–447.

[32]. J. L. Howard, Q. Cao and D. L. Browne, *Chem. Sci.*, **2018**, *9*, 3080–3094.

[33]. K. J. Ardila-Fierro and J. G. Hernández, ChemSusChem, **2021**, *14*, 2145–2162.

[34]. Daisy R. Sherin and Kallikat N. Rajasekharan, *Arch. Pharm. Chem. Life Sci.*, **2015**, 908–914.

[35]. H. Xu, G. P. Fan, Z. Liu and G. W. Wang, *Tetrahedron*, **2018**, *74*, 6607–6611.

[36]. S. Auricchio, A. Bini, E. Pastormerlo and A. M. Truscello, *Tetrahedron*, **1997**, *53*, 10911–10920.

[37]. M. J. Rak, N. K. Saadé, T. Friščić and A. Moores, *Green Chem.*, **2014**, *16*, 86–89.

[38]. V. Štrukil, D. Margetic, M. D. Igrc, M. Eckert-Maksic and T. Friščic, *Chem. Commun.*, **2012**, *48*, 9705–9707.

[39]. J. L. Do and T. Friščić, *ACS Cent. Sci.*, **2017**, *3*, 13–19.

[40]. J. W. Bode, Y. Hachisu, T. Matsuura and K. Suzuki, *Tetrahedron Lett.*, **2003**, *44*, 3555–3558.

[41]. C. Grundmann and J. M. Dean, *J. Org. Chem.*, **1965**, *30*, 2809–2812.

[42]. R. Huigens, *Angew. Chemie - Int. Ed.*, **1963**, *2*, 633–696.

[43]. C. Grundmann and R. Richter, *J. Org. Chem.*, **1967**, *32*, 2308–2312.

[44]. T. Hashimoto and K. Maruoka, *Chem. Rev.*, **2015**, *115*, 5366–5412.

[45]. C. Grundmann and S. K. Datta, *J. Org. Chem.*, **1968**, *34*, 2016–2018.

[46]. P. F. Pagoria, M. X. Zhang, N. B. Zuckerman, A. J. DeHope and D. A. Parrish, *Chem Heterocycl Comp*, **2017**, *53*, 760–778.

[47]. M. X. Zhang, A. J. Dehope and P. F. Pagoria, *Org. Process Res. Dev.*, **2019**, *23*, 2527–2531.

[48]. F. Schneider, A. Stolle, B. Ondruschka and H. Hopf, *Org. Process Res. Dev.*, **2009**, *13*, 44–48.

[49]. T. Deb, J. Tu and R. M. Franzini, *Chem. Rev.*, **2021**, *121*, 6850–6914.

[50]. E. Lukevics and P. Arsenyan, *Chem Heterocycl Comp*, **1998**, *34*, 1155–1169.

[51]. D. K. Heldmann and J. Sauer, *Tetrahedron Lett.*, **1997**, *38*, 5791–5794.

[52]. M. S. Chiang and J. U. Lowe, *J. Org. Chem.*, **1967**, *32*, 1577–1579.

[53]. F. Himo, T. Lovell, R. Hilgraf, V. V. Rostovtsev, L. Noodleman, K. B. Sharpless and V. V. Fokin, *J. Am. Chem. Soc.*, **2005**, *127*, 210–216.

[54]. K. Chanda, S. Rej and M. H. Huang, *Nanoscale*, **2013**, *5*, 12494–12501.

[55]. X. Di Wang, L. H. Zhu, P. Liu, X. Y. Wang, H. Y. Yuan and Y. L. Zhao, *J. Org. Chem.*, **2019**, *84*, 16214–16221.

[56]. V. V. S. T.M. Vishwanatha, *J. Heterocycl. Chem.*, **2015**, *52*, 1823–1833.

[57]. C. Chen and S. Cui, *J. Org. Chem.*, **2019**, *84*, 12157–12164.

[58]. Y. Sun, A. Abdukader, H. Zhang, W. Yang and C. Liu, *RSC Adv.*, **2017**, *7*, 55786–55789.

[59]. Y. Li, M. Gao, B. Liu and B. Xu, *Org. Chem. Front.*, **2017**, *4*, 445–449.

[60]. N. Mukherjee, S. Ahammed, S. Bhadra and B. C. Ranu, *Green Chem.*, **2013**, *15*, 389–397.

[61]. R. Thorwirth, A. Stolle, B. Ondruschka, A. Wild and U. S. Schubert, *Chem. Commun.*, **2011**, *47*, 4370–4372.

[62]. K. S. Sindhu and G. Anilkumar, *RSC Adv.,* **2014**, *4*, 27867–27887.

[63]. R. Schmidt, R. Thorwirth, T. Szuppa and A. Stolle, *Chem. - A Eur. J.*, **2011**, *17*, 8129–8138.

[64]. L. Chen, B. E. Lemma, J. S. Rich and J. Mack, *Green Chem.*, **2014**, *16*, 1101–1103.

[65]. Y. Wen, W. Huang and B. Wang, *Appl. Surf. Sci.*, **2012**, *258*, 2935–2938.

[66]. F. E. López-Suárez, A. Bueno-López, M. J. Illán-Gómez, A. Adamski, B. Ura and J. Trawczynski, *Environ. Sci. Technol.*, **2008**, *42*, 7670–7675.

[67]. J. B. Reitz and E. I. Solomon, *J. Am. Chem. Soc.*, **1998**, *120*, 11467–11478.

[68]. X. Di Wang, L. H. Zhu, P. Liu, X. Y. Wang, H. Y. Yuan and Y. L. Zhao, *J. Org. Chem.*, **2019**, *84*, 16214–16221.

[69]. R. A. Sheldon, *ACS Sustain. Chem. Eng.*, **2018**, *6*, 32–48.

2.8. Experimental Section for chapter 2

2.8.1. General Considerations, Materials, and Instrumentations

General Considerations: Solids were directly weighed open-air and added directly into the reaction vial. Liquids were directly transferred from the vial containing the reagent using an automatic pipette with a plastic tip of appropriate size or a plastic syringe with a stainless-steel needle. Flash chromatography was carried out using 40-63µm silica gel (Silicycle).

Materials: Distilled water was obtained from an in-house water distillery. All other reagents and chemicals were purchased from Sigma-Aldrich or AK Scientics and used without further purification.

Instrumentation: ^{1}H (500MHz) and ^{13}C (125MHz) NMR spectra were recorded in $CDCl_3$ or DMSO-d^6 using a Varian Inova 500MHz spectrometer. Spectra were referenced to the residual solvent signal or the TMS signal. Spectral features are tabulated in the following order (Note: Spectral features are reported in the following format): chemical shift (δ, ppm); multiplicity (s-singlet, d-doublet, t-triplet, q-quartet, dd-doublet of doublets, m-multiplet), dt-double of triplets, ddd-doublet of doublets of doublets; coupling constants (J, Hz); number of protons. High resolution mass spectra (HRMS) were obtained using a LTQ Orbitrap Velos ETD (positive and negative mode) mass spectrometer. Liquid Chromatography-Inductively Coupled Plasma Mass Spectrometry (LC-ICP-MS) was obtained using an Agilent 7500ce with a MicroMist glass concentric nebulizer and a Quadrupole MS with a sensitivity range of 10^{-12}-10^{-3} g/mL. The reactions were performed using a Fritsch Planetary Micro Mill model ''Pulverisette 7'' housing two stainless-steel (**SS**) cups containing eight stainless-steel (**SS**) balls each and sealed by a stainless-steel (**SS**) lid fitted with a Teflon gasket. The reported melting points are uncorrected and were measured using a Stuart SMP3 melting point apparatus. Fourier transform infrared (FT-IR) were acquired using a Thermo Scientific^{TM} Nicolet^{TM} iS5 FTIR Spectrometer, ranging from 4000 to 400 cm^{-1}. Spectra were collected using 64 scans, and the data was processed using the Spectrum One software. X-ray photoelectron microscopy (XPS) measurements were carried out at the McGill Institute for Advance Materials with a Thermo-Scientific K-Alpha equipped with a 180° double focusing hemispherical analyzer with a 128-channel detector. MALDITOF-MS was obtained using an Autoflex III Smart Beam (from BRUKER) equipped with a laser Nd-YAG UV at 355 nm and an acceleration voltage at 20 KV

Abbreviations: Hexanes (Hex), Ethyl Acetate (EtOAc), Dichloromethane (DCM), 1,3,5-trimethoxybenzene (TMB), Dimethylsulfoxide (DMSO), Stainless Steel (SS), Melting point (MP), Ratio to front (R_f).

2.8.2. Procedure S1 (PS1): Solvent-Free and catalyst-free synthesis of 3,5-isoxazoles *via* 1,3-dipolar cycloaddition from terminal alkynes and hydroxyimidoil chlorides under ball-milling conditions

Procedure Example:

79c + 80b (1.5 equiv.) → 78d

Na₂CO₃ (2.0 equiv.)
$n_{ssBalls}$ = 8, 60 Hz
30 min
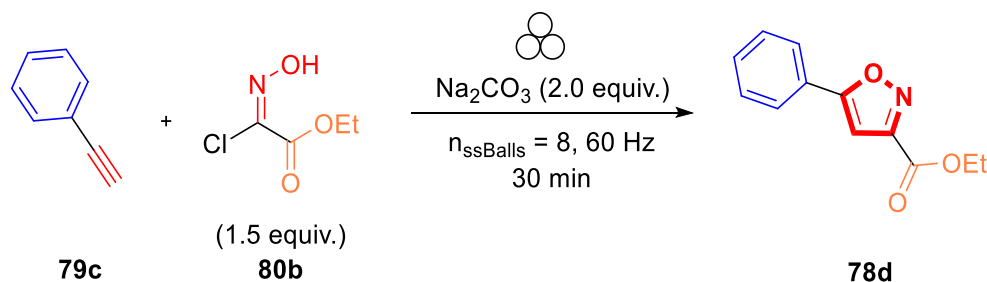
Synthesis of ethyl 5-phenylisoxazole-3-carboxylate (78b): To a clean and dried stainless-steel (**SS**) planetary milling jar (approximately 50 mL capacity) with 8 **SS** balls (10 mm of diameter), it was weighed **80b** (0.222 g, 1.47 mmol, 1.5 equivalents.) and Na₂CO₃ (0.207 g, 1.95 mmol, 2.0 equivalents.). Then, phenylacetylene **79c** (108 μL, 0.979 mmol, 1.0 equivalents.) was added *via* micropipette. Once all reagents were introduced on the planetary milling jar, the milling jar was tightly sealed, and the mixture was milled for 30 minutes at 60 Hz. After 30 min, the jar was cooled at room temperature, and the reaction mixture was carefully transferred to a separatory funnel, washed with EtOAc (2x10mL) and a saturated aqueous solution of NaCl (2x10mL). The organic layer was collected, dried over Na₂SO₄, and the solvent was evaporated under reduced pressure. **78d** was isolated from the crude mixture in a silica column using Hex: EtOAc (9:1) as eluent. Compound **78d** was isolated in 97 % yield (207.2 mg) as a white solid. **MP**: 54-57 °C, **R$_f$**: 0.38 **¹H NMR** (500 MHz, DMSO-d^6) δ 7.99 – 7.95 (m, 1H), 7.59 – 7.54 (m, 1H), 7.50 (s, 1H), 4.40 (q, J = 7.11 Hz, 1H), 1.35 (t, J = 7.12 Hz, 2H). **¹³C NMR** (125 MHz, DMSO-d^6) δ 171.5, 159.8, 157.3, 131.5, 129.8, 126.5, 126.3, 101.2, 62.4, 14.4. **HRMS:** m/z calculated for C₁₂H₁₁NO₃ [M+H]⁺: 218.0817 found 218.0813.

2.8.3 Atom Economy and E-Factor Calculations for the synthesis of 3,5-isoxazole 78d

79c (100 mg) + 80b (1.5 equiv.) (222 mg) → 78d (212 mg - 97%)

Na₂CO₃ (2.0 equiv.)
207 mg
$n_{ssBalls}$ = 8, 60 Hz
30 min

<center>**E-Factor**</center>

Total mass of reactants: 100 mg+ 222 mg + 207 mg= 529 mg

Product mass: 212 mg

Waste: 529 mg – 212 mg = 317 mg

E-Factor= $Waste/Product\ mass$= $317\ mg/212\ mg$ = **1.49**

E-factor calculation for previous report: X. Di Wang, L. H. Zhu, P. Liu, X. Y. Wang, H. Y. Yuan and Y. L. Zhao, *J. Org. Chem.*, 2019, **84**, 16214.

Cu(OAc)$_2$• H$_2$O (10 mol %)
tBuONO (**41.2 mg**)
DABCO (**22.4 mg**)

Toluene (**134** mg)
130 °C
6-10 h

(20.4 mg)   (27.4 mg)   43.44 mg (82 %)
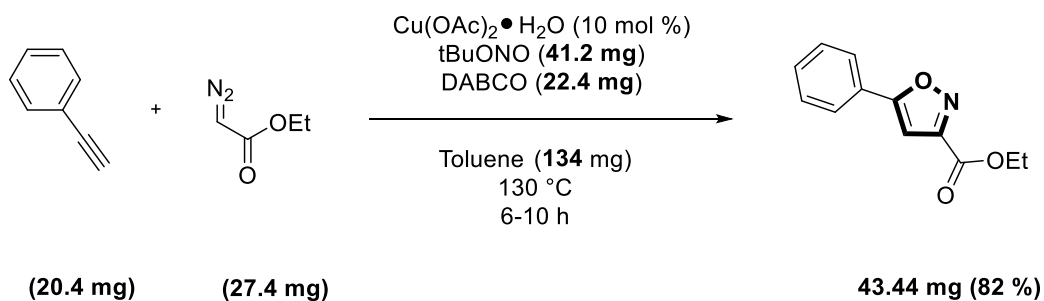
<center>**E-Factor**</center>

Total mass of reactants: 20.4 mg+ 27.4 mg + 41.2 mg + 22.4 mg + 134mg = 245.4 mg (Assuming 90 % recovery of toluene from distillation).

Product mass: 43.44 mg

Waste: 245.4 mg – 43.44 mg = 201.96 mg

E-Factor= $Waste/Product\ mass$= $201.96\ mg/43.44\ mg$ = **4.65**

Bu₃Sn + OH / N / Cl / NO₂ (1.5 equiv.)

Na₂CO₃ (2.0 equiv.)
n_ssB = 8, 60 Hz
20 min

Bu₃Sn—O—N / NO₂

79a **80a** **78a**
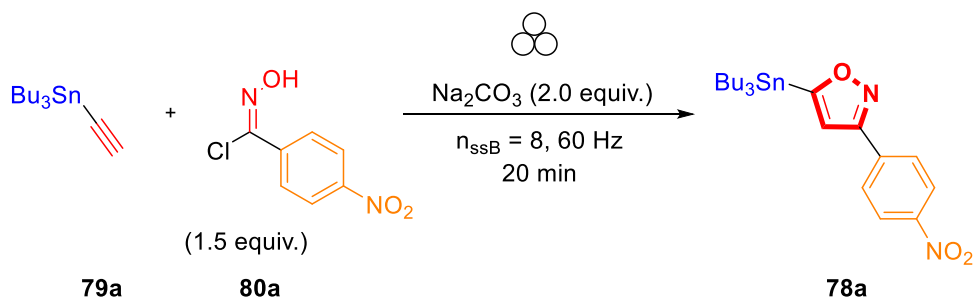
Synthesis of 3-(4-nitrophenyl)-5-(tributylstannyl)isoxazole (78a): Isoxazole **78a** was synthesized according to procedure (**PS1**), but the reagents were milled for 20 minutes rather than 60 minutes: Compound **78a** was isolated in a silica column using CHCl₃:Hexanes (9:1) as eluent. **78a** was isolated in 57 % yield (86.55 mg) as a colourless oil. R_f: 0.72 **¹H NMR** (500 MHz, CDCl₃) δ 8.30 (d, *J* = 8.82 Hz, 2H), 8.01 (d, *J* = 8.83 Hz, 2H), 6.75 (s, 1H), 1.65 – 1.54 (m, 6H), 1.36 (sextet, *J* = 7.33 Hz, 6H), 1.25 – 1.19 (m, 5H), 0.91 (t, *J* = 7.33 Hz, 9H). **¹³C NMR** (125 MHz, CDCl₃) δ 181.9, 158.5, 148.4, 135.9, 127.9, 124.1, 112.0, 28.8, 27.1, 13.6, 10.6. **HRMS:** *m/z* calculated for C₂₁H₃₂N₂O₃Sn [M+H]⁺: 481.1513 found 481.1509.

Bu₃Sn + OH / N / Cl / OEt / O (1.5 equiv.)

Na₂CO₃ (2.0 equiv.)
n_ssB = 8, 60 Hz
10 min

Bu₃Sn—O—N / OEt / O

79a **80b** **78b**
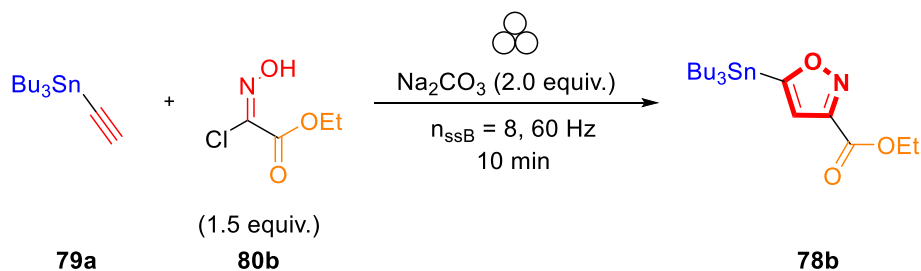
Synthesis of ethyl 5-(tributylstannyl)isoxazole-3-carboxylate (78b): Isoxazole **78b** was synthesized according to procedure (**PS1**), but the reagents were milled for 10 minutes rather than 60 minutes: Compound **78b** was isolated in a silica column using Hex:EtOAc (9:1) as eluent. **78b** was isolated in 72 % yield (98.18 mg) as a colourless oil. R_f: 0.40 **¹H NMR** (500 MHz, CDCl₃) δ 6.80 (s, 1H), 4.44 (q, *J* = 7.14 Hz, 2H), 1.60 – 1.52 (m, 6H), 1.42 (t, *J* = 7.15 Hz, 3H), 1.33 (sextet, 7.3 Hz, 6H), 1.22 – 1.15 (m, 6H), 0.89 (t, *J* = 7.33 Hz, 9H). **¹³C NMR** (125 MHz, CDCl₃) δ 182.4, 160.9, 154.4, 114.9, 61.9, 28.7, 27.1, 14.1, 13.5, 10.6 . **HRMS:** *m/z* calculated for C₁₈H₃₃NO₃Sn [M+H]⁺: 432.1561 found 432.1564.

Me₃Si + OH / N / Cl / OEt / O (1.5 equiv.)

Na₂CO₃ (2.0 equiv.)
n_ssB = 8, 60 Hz
Milling Time

Me₃Si—O—N / OEt / O

79b **80b** **78c**
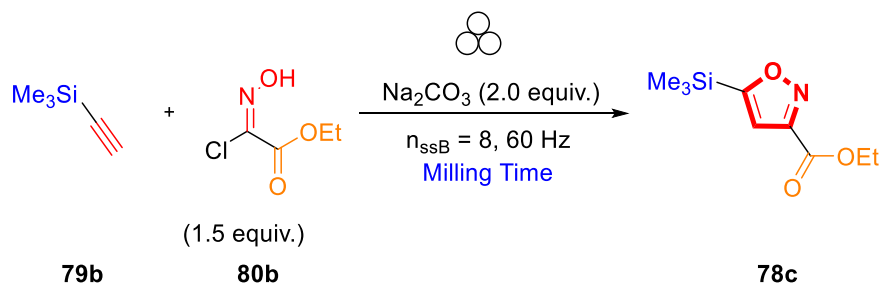
Synthesis of ethyl 5-(trimethylsilyl)isoxazole-3-carboxylate (78c): Isoxazole **1c** was synthesized according to procedure (**PS1**), but the reagents were milled for 10 minutes rather than 60 minutes: Compound **78c**

53

was isolated in a silica column using Hex:EtOAc (9:1) as eluent. **78c** was isolated in 57 % (121.6 mg) yield as a white solid. **R$_f$**: 0.56 **^{1}H NMR** (500 MHz, DMSO-d^6) δ 7.12 (s, 1H), 4.36 (q, J = 7.1 Hz, 2H), 1.31 (t, J = 7.1 Hz, 3H), 0.34 (s, 9H). **^{13}C NMR** (125 MHz, DMSO-d^6) δ 180.9, 160.1, 155.1, 113.9, 62.1, 14.4, -1.9. **HRMS:** m/z calculated for C$_9$H$_{15}$NO$_3$Si [M+H]$^+$: 214.0899 found 214.0896.

2.8.4. Milling Time Optimization: Solvent-Free and catalyst-free synthesis of 3,5-isoxazoles via 1,3-dipolar cycloaddition from terminal alkynes and hydroxyimidoil chlorides under ball-milling conditions

Prior to isolation of 3,5-isoxazoles (**78a-d**) the reactions between the corresponding terminal alkyne (**79a-c**) and hydroxyimidoil chloride (**80a-b**) were optimized in a 20 mg scale reaction to determine the proper milling time. The yield of the 3,5-isoxazoles was quantified by ^{1}H NMR and using TMB as an internal standard.

Procedure example for yield determination:
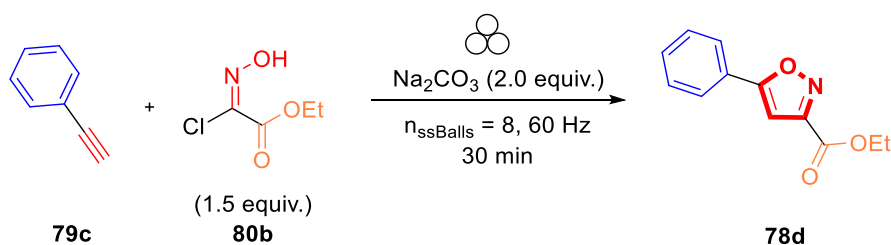
Milling time optimization for the synthesis of ethyl 5-phenylisoxazole-3-carboxylate (78d): To a clean and dried stainless-steel (**SS**) planetary milling jar (approximately 50 mL capacity) with 8 **SS** balls (10 mm of diameter), it was weighed **80b** (0.050 g, 0.330 mmol, 1.5 equivalents.) and Na$_2$CO$_3$ (0.047 g, 0.440 mmol, 2.0 equivalents.). Then, ethynylbenzene (**79c**) (24 μL, 0.220 mmol, 1.0 equivalents.) was added *via* an automated pipette. Once all reagents were introduced on the planetary milling jar, the mixture was milled at a corresponding time at 60 Hz. After the reaction time was accomplished, the jar was cooled at room temperature, and it was added 10-12 mg of TMB to the reaction crude. The reaction mixture was carefully transferred to a separatory funnel, washed with EtOAc (2x10mL) and a saturated aqueous solution of NaCl (2x10mL). The organic layer was collected, dried over Na$_2$SO$_4$, and the solvent was evaporated under reduced pressure. The yield of **78d** was obtained by ^{1}H NMR.

Time (min)	Yield (%)[a]
10	82
20	89
30	95 *97*[b]
40	79
50	84
60	37
70	25

[a]^{1}H NMR Yields. [b]Isolated yield according to **PS1**
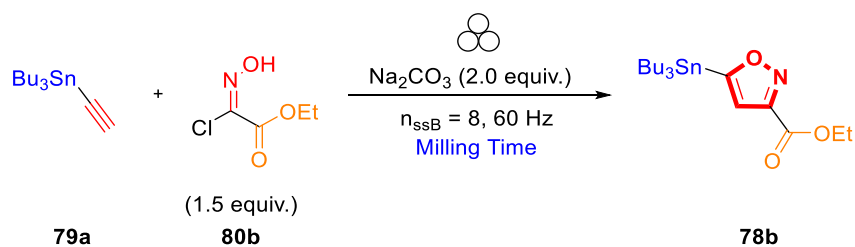
Milling Time (min)	Yield (%)[a]
10	95 72[b]
15	81
20	73

Reaction Conditions: 0.166 mmol of **79a**, 0.250 mmol of **80b**, 0.332 mmol of Na$_2$CO$_3$, SS beaker (50 mL capacity), 8 x SS milling balls (10 mm diameter), milling at 60 Hz. [a] ^{1}H-NMR yields were measured using TMB as an internal standard. [b] *Isolated yield according to PS1*
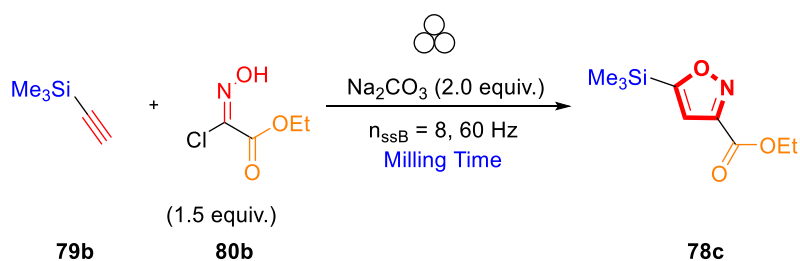
Milling Time (min)	Yield (%)[a]
10	66 57[b]
20	65
30	50

Reaction Conditions: 0.204 mmol of **79b**, 0.306 mmol of **80b**, 0.408 mmol of Na$_2$CO$_3$, SS beaker (50 mL capacity), 8 x SS milling balls (10 mm diameter), milling at 60 Hz. [a] ^{1}H-NMR yields were measured using TMB as an internal standard. [b] *Isolated yield according to PS1*

2.8.5. Procedure S2 (PS2): Preparation of Cu/Al₂O₃ nanocomposites catalyst.

Cu/Al$_2$O$_3$ nanocomposite catalyst was synthesized according to the method described by Mukherjee *et al.*[112] with a slight modification. Briefly, in a 1 L round bottom flask equipped with a magnetic stir bar, it was weighted 15 g of neutral alumina and 1 g of CuSO$_4$ •5H$_2$O. The reagents were suspended in 30 mL of H$_2$O, and the mixture was stirred overnight at room temperature. Then, excess water was removed under reduced pressure, and the obtained solid was further dried in a vacuum oven at 100 °C overnight to obtain a light blue solid. ICP-MS analysis determined that the concentration of copper present in the alumina is 21.91 mg/g.

2.8.6. Recycled Cu/Al₂O₃ nanocomposites catalyst

ICP-MS analysis determined that the concentration of copper present in the alumina is 17.75 mg/g (first recycled), 9.02 mg/g (second recycled), and 3.38 mg/g (third recycled).

2.8.7. XPS analysis of Cu/Al₂O₃

XPS results agree with those reported by Mukherjee *et al.*[1] Below is portrayed the XPS analysis obtained for Cu/Al$_2$O$_3$.
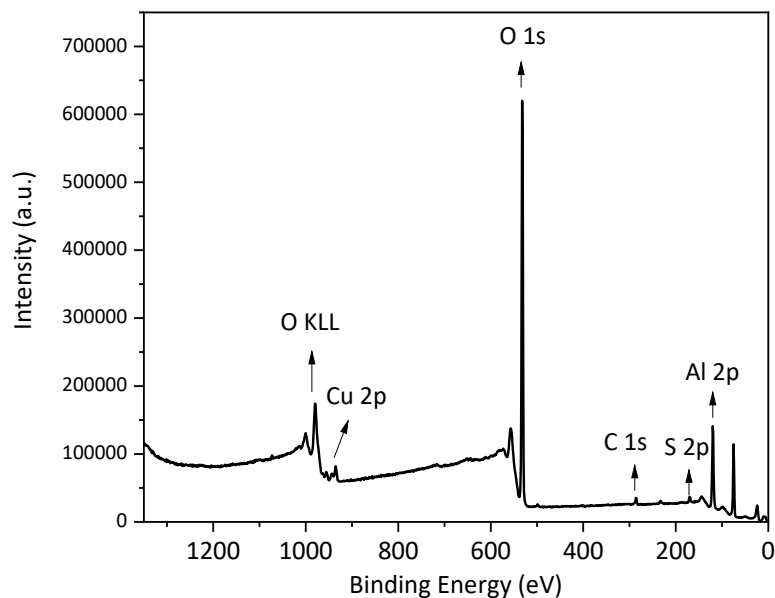
Figure S2.1: XPS survey spectrum of Cu/Al$_2$O$_3$ nanocomposite.
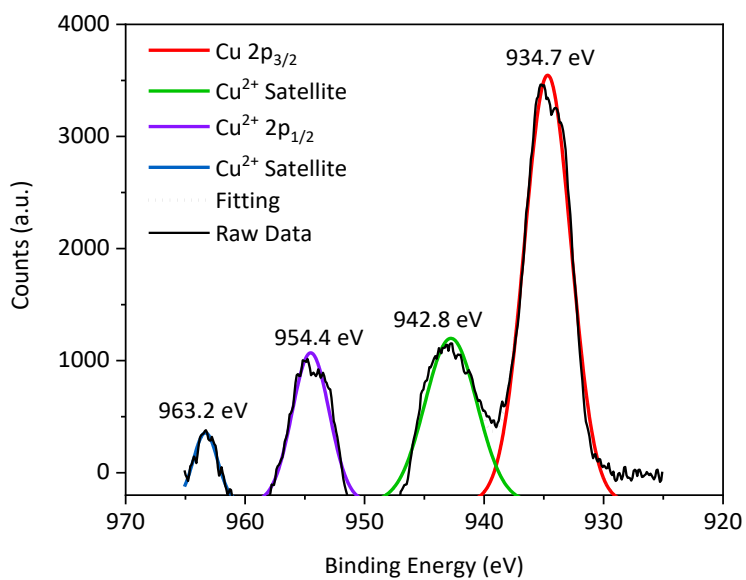
Figure S2.2: XPS pattern for a fresh sample of Cu/Al_2O_3 catalyst[1]
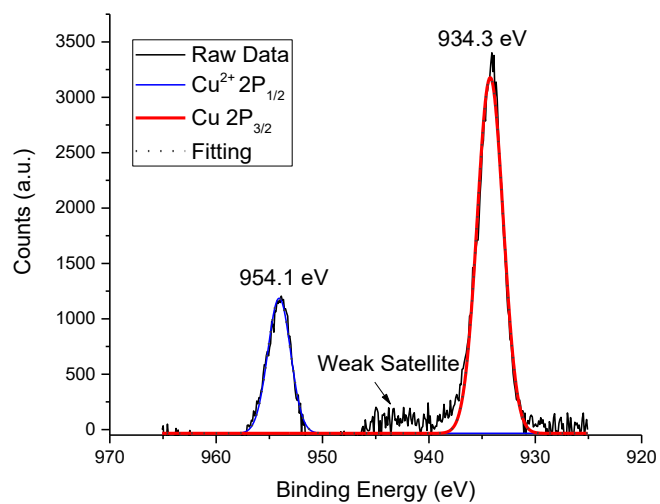
Figure S2.3: XPS pattern for first recycled of Cu/Al_2O_3 catalyst

[1] 1   N. Mukherjee, S. Ahammed, S. Bhadra and B. C. Ranu, *Green Chem.*, 2013, **15**, 389–397.
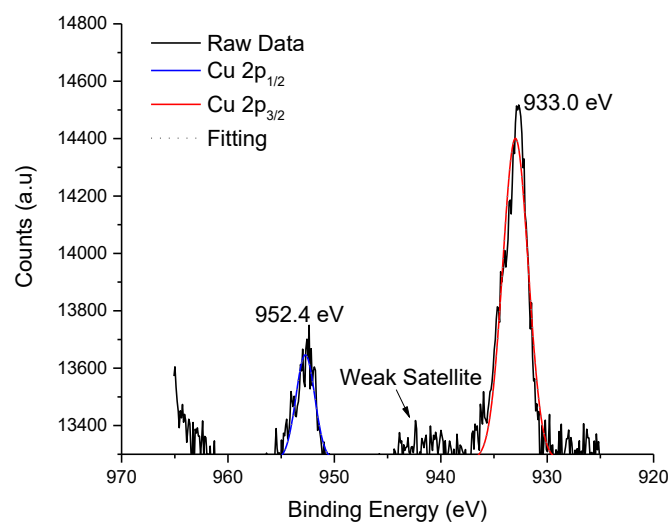
Figure S2.4: XPS pattern for second recycled of Cu/Al$_2$O$_3$ catalyst

2.8.8. Synthesis of (E,Z)-N-hydroxy-4-methoxybenzimidoyl chloride (80d)
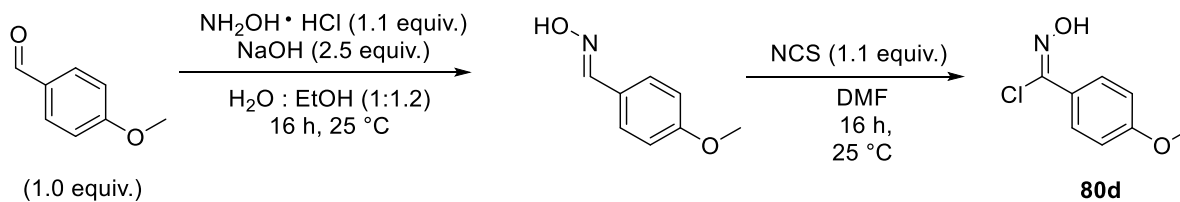
Hydroxyimidoyl chloride **80d** was synthesize according to the procedure outline by F. Himo *et al.*[2] **80d** was obtained in 74 % yield (10.0 g) as a pale yellow solid. **^{1}H NMR** (500 MHz, CDCl$_3$) δ 8.30 (br s, 1H), 7.77 (d, *J* = 9.0 Hz, 1H), 6.92 (d, *J* = 9.0 Hz, 1H), 3.85 (s, 1H).[2]

The reported analytical data is in agreement with the reported by E. Azzali *et al.* [3]

---

[2] F. Himo, T. Lovell, R. Hilgraf, V. V. Rostovtsev, L. Noodleman, K. B. Sharpless and V. V. Fokin, *J. Am. Chem. Soc.*, 2005, **127**, 210–216.

[3] E. Azzali, D. Machado, A. Kaushik, F. Vacondio, S. Flisi, C. S. Cabassi, G. Lamichhane, M. Viveiros, G. Costantino and M. Pieroni, *J. Med. Chem.*, 2017, **60**, 7108–7122.
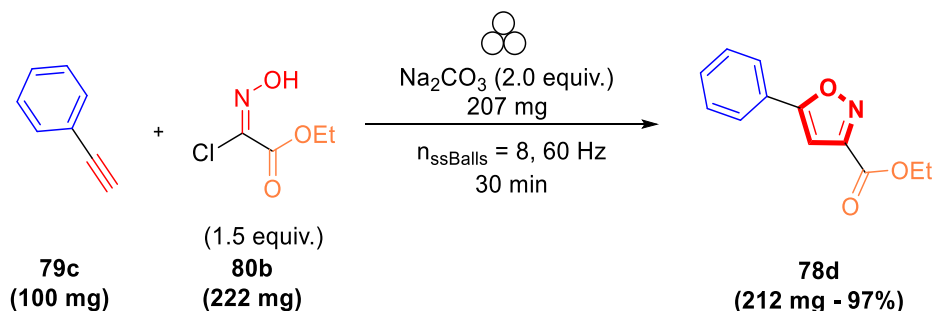
2.8.9. Procedure S3 (PS3): Solvent-Free synthesis of 3,5-isoxazoles via 1,3-dipolar cycloaddition from terminal alkynes and hydroxyimidoil chlorides under Cu/Al$_2$O$_3$ surface under ball-milling conditions.

Example:
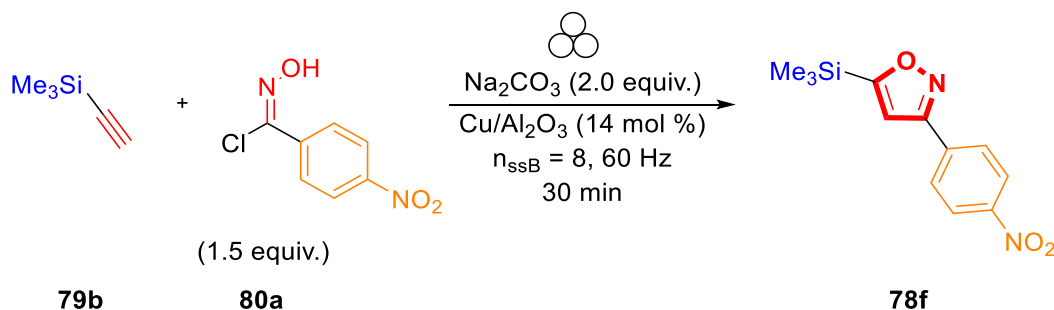
(1.5 equiv.)

79b   **80a**   **78f**

Synthesis of 3-(4-nitrophenyl)-5-(trimethylsilyl)isoxazole (78f): To a clean and dried stainless-steel (**SS**) planetary milling jar (approximately 50 mL capacity) with 8 **SS** balls (10 mm of diameter), it was weighed **80a** (0.300 g, 1.5 mmol, 1.5 equivalents.), Na$_2$CO$_3$ (0.211 g, 2.0 mmol, 2.0 equivalents.), and Cu/Al$_2$O$_3$ (0.405 g, 0.14 mmol, 14 mol %) . Then, ethynyltrimethylsilane **79b** (141 µL, 1.0 mmol, 1.0 equivalents.) was added via an automated pipette. Once all reagents were introduced on the planetary milling jar, the mixture was milled for 30 minutes at 60 Hz. After 30 min, the milling jar was cooled to room temperature, and the Cu/Al$_2$O$_3$ was filtered through a sintered funnel and washed with EtOH [4]. The filtrated was collected, and the excess EtOH was removed under reduced pressure. Compound **78f** was isolated in a silica column using CHCl$_3$:Hex (99:1) as eluent. Compound **78f** was obtained in 88 % yield (231.2 mg) as a white solid. **MP**: 158-161 °C, **R$_f$:** 0.86 **^{1}H NMR** (500 MHz, DMSO-d^6) δ 8.36 (d, *J* = 8.9 Hz, 2H), 8.18 (d, *J* = 8.9 Hz, 2H), 7.50 (s, 1H), 0.38 (s, 9H). **^{13}C NMR** (125 MHz, DMSO-d^6) δ 180.1, 159.4, 148.8, 135.2, 128.5, 124.8, 112.5, -1.6. **HRMS:** *m/z* calculated for C$_{12}$H$_{14}$N$_2$O$_3$Si [M+H]$^+$: 263.0852 found 263.0848.

---

[4] **Cu/Al$_2$O$_3$ recycling**: The green coloured solid filter (Cu/Al$_2$O$_3$) can be recycled by washing with another 20mL portion of EtOH and let to dry under vacuum. The solid is collected and dried in high vacuum at room temperature for another 16 hours.

2.8.11. Atom Economy and E-Factor Calculations for the synthesis of 3,5-isoxazole 78f

79b
100 mg

80a
300 mg

(1.5 equiv.)

78f
230 mg (88 %)

Na$_2$CO$_3$ (2.0 equiv.)
211 mg

Cu/Al$_2$O$_3$ (14 mol %)
n$_{ssB}$ = 8, 60 Hz
30 min
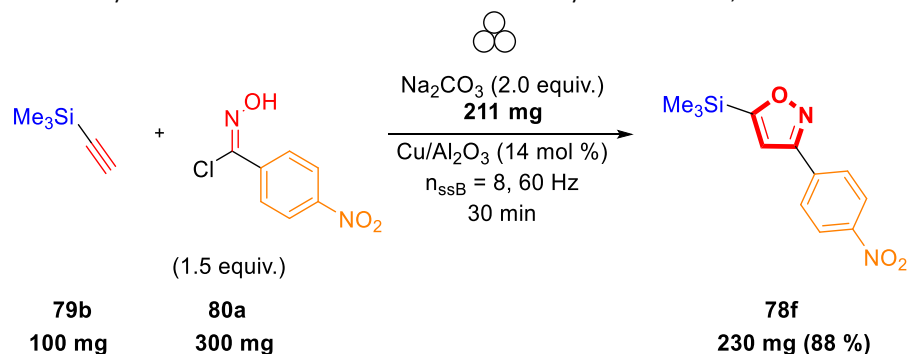
E-Factor

Total mass of reactants: 100 mg+ 300 mg + 211 mg= 611 mg (Cu/Al$_2$O$_3$ mass is not included in the calculations as the nanocomposite was recycled).

Product mass: 230 mg

Waste: 611 mg – 230 mg = 381 mg

E-Factor= $Waste/Product\ mass$= 381 mg/230 mg = **1.65**

E-factor calculation for previous report: K. Chanda, S. Rej and M. H. Huang, *Nanoscale*, 2013, **5**, 12494–12501.

(0. 25 mmol, 24.5 mg)   (0.25 mmol, 50.14 mg)

NEt$_3$
(**0.75 mmol, 75.8 mg**)
Cu$_2$O rhombic dodecahedra

EtOH
(**3.0 mL, ~236.7 mg**)
50 °C, 2.0 h to 2.5 h
under N$_2$ atm

65.5 mg (86 %)
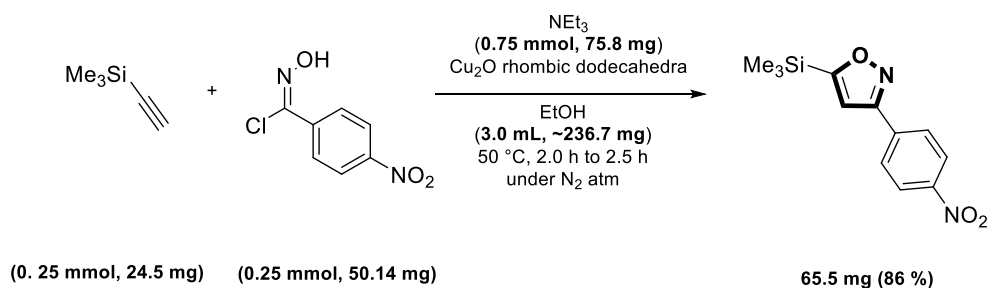
E-Factor

Total mass of reactants: 24.5 mg+ 50.14 mg + 75.8 mg + 236.7 mg= 387.14 mg (Assuming 90 % recovery of EtOH from distillation, and Cu$_2$O mass was not included in the calculations as this was recycled).

Product mass: 65.5 mg

Waste: 387.14 mg – 65.5 mg = 321.64 mg

**E-Factor**= $Waste/Product\ mass$= 321.64 mg/65.5 mg = **4.91**
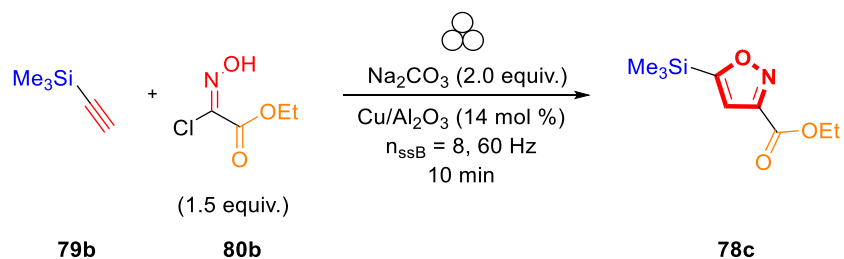
Synthesis of ethyl 5-(trimethylsilyl)isoxazole-3-carboxylate (78c): Isoxazole **78c** was synthesized according to procedure (**PS3**), but the reagents were milled for 10 minutes rather than 30 minutes. Compound **78c** was isolated in a silica column using Hex:EtOAc (9:1) as eluent. **78c** was isolated in 68 % yield (145.9 mg) as a colourless oil. **R$_f$**: 0.56 **^{1}H NMR** (500 MHz, DMSO-d^6) δ 7.12 (s, 1H), 4.36 (q, J = 7.1 Hz, 2H), 1.31 (t, J = 7.1 Hz, 3H), 0.34 (s, 9H). **^{13}C NMR** (126 MHz, DMSO-d^6) δ 180.9, 160.1, 155.1, 113.9, 62.1, 14.4, -1.9. **HRMS:** m/z calculated for C$_9$H$_{15}$NO$_3$Si [M+H]$^+$: 214.0899 found 214.0896.
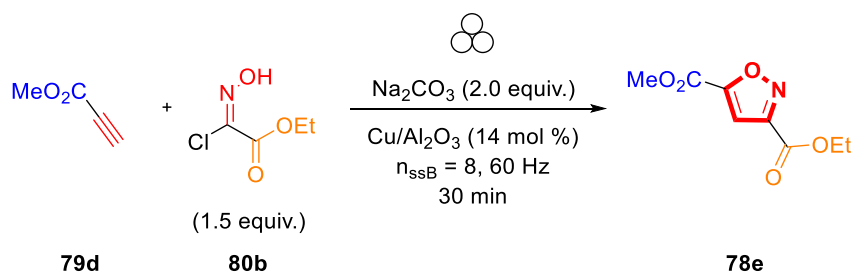
Synthesis of 3-ethyl 5-methyl isoxazole-3,5-dicarboxylate (78e): Isoxazole **78e** was synthesized according to procedure (**PS3**). Compound **78e** was isolated in a silica column using Hex: EtOAc:DCM (7:2:1) as eluent. **78e** was isolated in 56 % yield (132.4 mg) as a white solid. **MP**: 55-59 °C, **R$_f$**: 0.54, **^{1}H NMR** (500 MHz, DMSO-d^6) δ 7.57 (s, 1H), 4.39 (q, J = 7.07 Hz, 2H), 3.92 (s, 3H), 1.33 (t, J = 7.12 Hz, 3H). **^{13}C NMR** (126 MHz, DMSO-d^6) δ 161.8, 158.9, 157.4, 156.5, 109.9, 62.7, 53.6, 14.3. **HRMS:** m/z calculated for C$_8$H$_9$NO$_5$ [M+H]$^+$: 200.0559 found 200.0555.
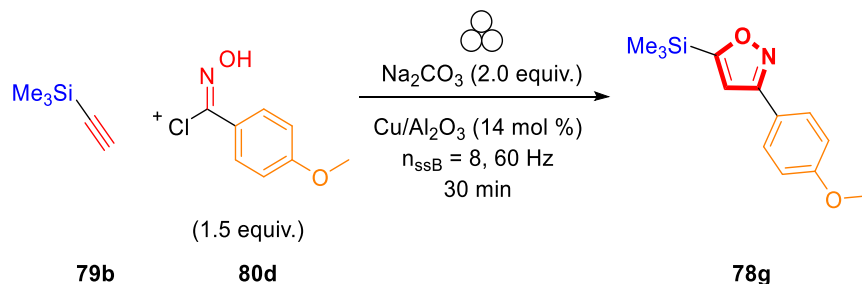
Synthesis of 3-(4-methoxyphenyl)-5-(trimethylsilyl)isoxazole (78g): Isoxazole **78g** was synthesized according to procedure (**PS3**), but the reagents were milled for 10 minutes rather than 30 minutes. Compound **78g** was isolated in a silica column using Hex:EtOAc: Tol (8:1.6:0.4) as eluent. **78g** was isolated in 51 % yield (127 mg) as a colourless oil. **R$_f$**: 0.51 **^{1}H NMR** (500 MHz, DMSO-d^6) δ 7.12 (s, 1H), 4.36 (q, J = 7.1 Hz, 2H), 1.31 (t, J = 7.1 Hz, 3H), 0.34 (s, 9H). **^{13}C NMR** (125 MHz, DMSO-d^6) δ 178.4, 160.7, 160.4, 128.4, 121.7, 114.2, 110.5, 55.3, -1.8. **HRMS:** m/z calculated for C$_{13}$H$_{17}$NO$_2$Si [M+H]$^+$: 248.1101 found 248.1101.

Me3Si + (Br)(Br)C=N-OH → [Na2CO3 (2.0 equiv.), Cu/Al2O3 (14 mol %), n_ssB = 8, 60 Hz, 20 min] → Me3Si-isoxazole-Br

79b   **80c** (1.5 equiv.)   **78h**

Synthesis of 3-bromo-5-(trimethylsilyl)isoxazole (78h): Isoxazole **78h** was synthesized according to procedure (**PS3**), but the reagents were milled for 20 minutes rather than 30 minutes. Compound **78h** was isolated in a silica column using Hex: EtOAc (100% Hexanes to 100% EtOAc) as eluent. **78h** was isolated in 70 % yield (149.7 mg) as a yellow solid. R_f: 0.37 **^{1}H NMR** (500 MHz, CDCl$_3$) δ 6.47 (s, 1H), 0.33 (s, 9H). **^{13}C NMR** (125 MHz, CDCl$_3$) δ 180.9, 139.1 115.9, -2.2. **HRMS:** m/z calculated for C6H10BrNOSi [M+H]$^+$: 219.9788 found 219.9792.

79e   **80b** (1.5 equiv.)   **78i**

[Br-CH2-C≡CH] + [Cl-C(=N-OH)-C(=O)-OEt] → [Na2CO3 (2.0 equiv.), Cu/Al2O3 (14 mol %), n_ssB = 8, 60 Hz, 10 min] → BrCH2-isoxazole-C(=O)OEt
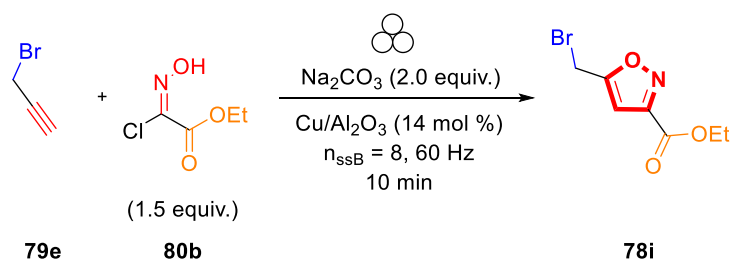
Synthesis of ethyl 5-(bromomethyl)isoxazole-3-carboxylate (78i): Isoxazole **78i** was synthesized according to procedure (**PS3**), but the reagents were milled for 10 minutes rather than 30 minutes. Compound **1i** was isolated in a silica column using Hex:DCM:EtOAc:Acetone (7:2:0.8:0.2) as eluent. **78i** was isolated in 71 % yield (139.6 mg) as a yellow solid. **MP**: 106-108 °C, R_f: 0.55 **^{1}H NMR** (500 MHz, DMSO-d^6) δ 6.97 (s, 1H), 4.87 (s, 1H), 4.35 (q, J = 7.11 Hz, 1H), 1.29 (t, J = 7.11 Hz, 1H). **^{13}C NMR** (125 MHz, DMSO-d^6) δ 170.6, 159.4, 156.9, 104.9, 62.4, 19.7, 14.4. **HRMS:** m/z calculated for C$_7$H$_8$BrNO$_3$ [M+H]$^+$: 233.976 found 233.9762.

79f   **80d** (1.5 equiv.)   **78j**

[Br-CH2CH2-C≡CH] + [Cl-C(=N-OH)-C6H4-OCH3] → [Na2CO3 (2.0 equiv.), Cu/Al2O3 (14 mol %), n_ssB = 8, 60 Hz, 10 min] → BrCH2CH2-isoxazole-C6H4-OCH3
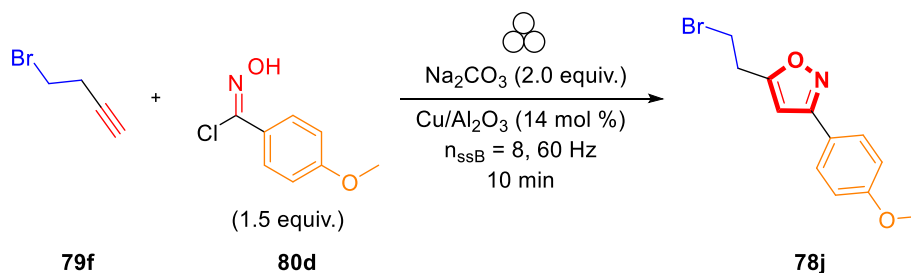
Synthesis of 5-(2-bromoethyl)-3-(4-methoxyphenyl)isoxazole (78j): Isoxazole **78j** was synthesized according to procedure (**PS3**), but the reagents were milled for 10 minutes rather than 30 minutes.

Compound **78j** was isolated in a silica column using Hex:Et$_2$O:tol (8:1.6:0.4) as eluent. **78j** was isolated in 80 % yield (169 mg) as a white solid. **MP**: 75.2-76.4 °C, **R**$_f$: 0.150 ^{1}H NMR (500 MHz, CDCl$_3$) δ 7.73 (d, J = 8.9 Hz, 2H), 6.97 (d, J = 8.9 Hz, 2H), 6.41 (s, 1H), 3.85 (s, 2H), 3.67 (t, J = 7.0 Hz, 2H), 3.37 (t, J = 7.0 Hz, 2H).^{13}C NMR (125 MHz, CDCl$_3$) δ 169.71, 162.09, 160.98, 128.16, 121.47, 114.28, 100.16, 55.34, 30.40, 27.93 **HRMS:** m/z calculated for C$_{12}$H$_{12}$BrNO$_2$ [M+H]$^+$: 282.0124found 282.0127.

79c   **80a**   **78k**
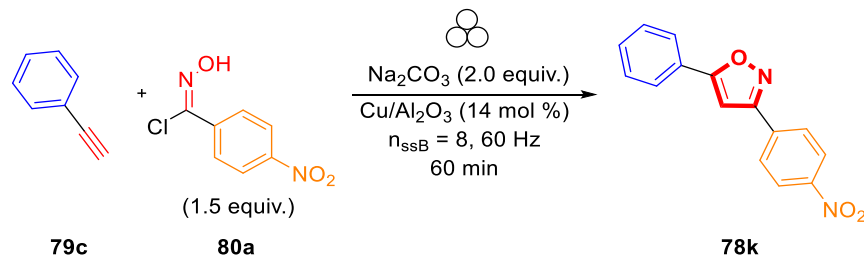
Synthesis of 3-(4-nitrophenyl)-5-phenylisoxazole (78k): Isoxazole **78k** was synthesized according to procedure (**PS3**), but the reagents were milled for 60 minutes rather than 30 minutes. Compound **78k** was isolated by recrystallizing the reaction crude in EtOH. **78k** was isolated in 38 % yield (98.6 mg) as a yellow solid. **MP**: 218-220 °C, **R**$_f$ 0.93 **^{1}H-NMR** (500 MHz, DMSO-d^6) δ 8.40 (d, J = 8.77 Hz, 2H), 8.20 (d, J = 8.78 Hz, 2H), 7.96 – 7.89 (m, 2H), 7.79 (s, 1H), 7.61 – 7.54 (m, 3H). ^{13}**C NMR** (125 MHz, DMSO-d^6) δ 170.9, 161.7, 148.9, 135.0, 131.3, 129.9, 128.3, 126.9, 126.1, 124.9, 99.6. **HRMS:** m/z calculated for C$_{15}$H$_{10}$N$_2$O$_3$ [M+H]$^+$: 267.0770 found 267.0765.

79g   **80a**   **78m**
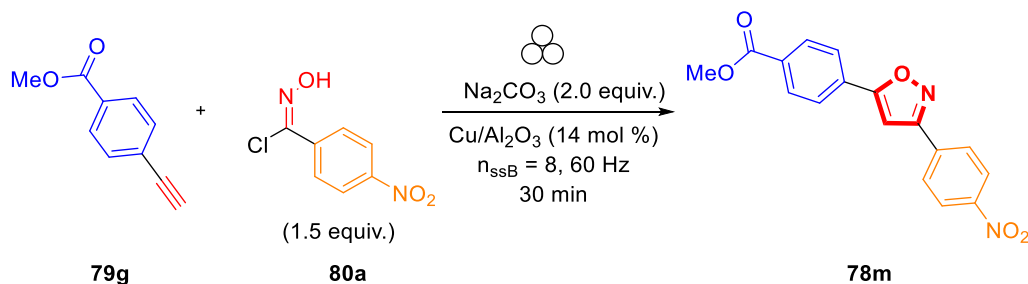
Synthesis of methyl 4-(3-(4-nitrophenyl)isoxazol-5-yl)benzoate (78m): Isoxazole **78m** was synthesized according to procedure (**PS3**). Compound **78m** was isolated in a silica column using DCM:Hex (9:1) as eluent. **78m** was isolated in 41 % yield (83.2 mg) as a white solid. **MP**: 229-230 °C, **R**$_f$: 0.93 **^{1}H NMR** (500 MHz, DMSO-d^6) δ 8.42 (d, J = 8.92 Hz, 1H), 8.22 (d, J = 8.92 Hz, 1H), 8.15 (d, J = 8.55 Hz, 1H), 8.09 (d, J = 8.59 Hz, 1H), 7.98 (s, 1H), 3.90 (s, 1H). ^{13}**C NMR** (125 MHz, DMSO-d^6) δ 169.8, 165.9, 161.9, 148.9, 134.8, 131.6, 130.8, 130.6, 128.4, 126.3, 124.9, 101.3, 52.9. **HRMS:** m/z calculated for C$_{17}$H$_{12}$N$_2$O$_5$ [M+H]$^+$: 325.0824 found 325.0819.
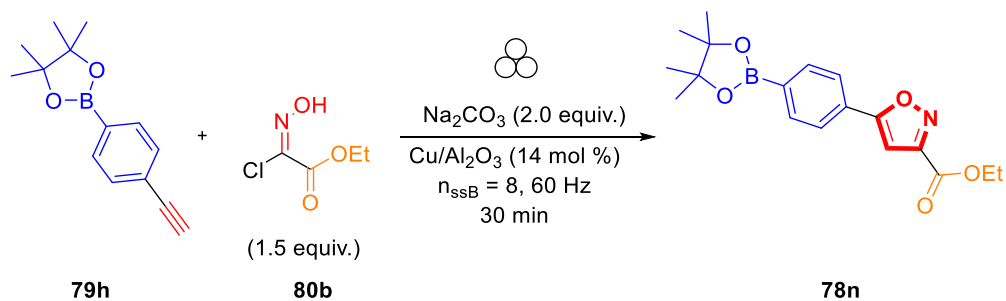
Synthesis of 3-(4-nitrophenyl)-5-(4-(4,4,5,5-tetramethyl-1,3,2-dioxaborolan-2-yl)phenyl)isoxazole (78n): Isoxazole **78n** was synthesized according to procedure (**PS3**). Compound **78n** was isolated in a by recrystallizing the reaction crude in Hexanes. **78n** was isolated in 70 % yield (107.6 mg) as a yellow solid. **MP**: 116-118 °C, **R**$_f$: 0.57 ^{1}**H NMR** (500 MHz, CDCl$_3$) δ 7.91 (d, J = 7.90 Hz, 2H), 7.80 (d, J = 7.75 Hz, 2H), 6.97 (s, 1H), 4.47 (q, J = 7.13 Hz, 2H), 1.44 (t, J = 7.15 Hz, 3H), 1.36 (s, 12H). ^{13}**C NMR** (125 MHz, CDCl$_3$) δ 171.6, 159.9, 156.9, 135.4, 128.7, 124.9, 100.5, 84.2, 62.2, 24.9, 14.2. **HRMS:** m/z calculated for C$_{18}$H$_{22}$BNO$_5$ [M+H]$^+$: 343.1700 found 343.1705.
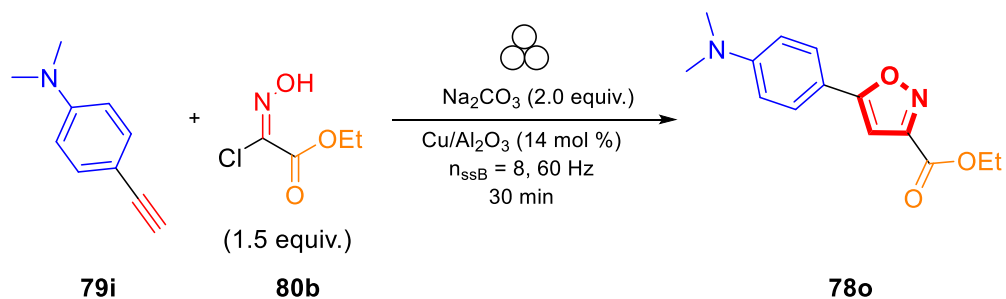
Synthesis of ethyl 5-(4-(dimethylamino)phenyl)isoxazole-3-carboxylate (78o): Isoxazole **78o** was synthesized according to procedure (**PS3**). Compound **78o** was isolated in a silica column using Hex: EtOAc: DCM (7:2:1) as eluent. **78o** was isolated in 45 % yield (81.4 mg) as a brown solid. **MP**: 108-111 °C, **R**$_f$: 0.91 ^{1}**H-NMR** (500 MHz, CDCl$_3$) δ 7.65 (d, J = 8.85 Hz, 2H), 6.72 (d, J = 8.87 Hz, 2H), 6.69 (s, 1H), 4.45 (q, J = 7.12 Hz, 2H), 3.03 (s, 6H), 1.43 (t, J = 7.13 Hz, 3H). ^{13}**C NMR** (125 MHz, CDCl$_3$) δ 172.5, 160.4, 156.7, 151.6, 127.2, 114.5, 111.9 , 97.0, 62.0, 40.1, 14.1. **HRMS:** m/z calculated for C$_{11}$H$_{10}$N$_2$O$_3$ [M+H]$^+$: 219.0764 found 219.0768.
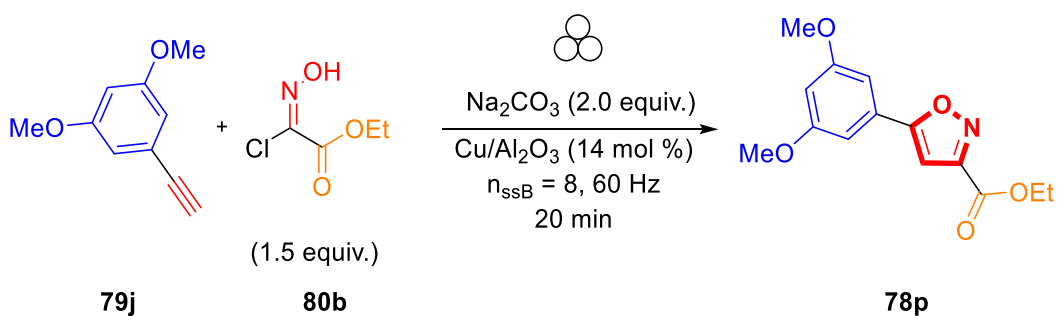
Synthesis of ethyl 5-(3,5-dimethoxyphenyl)isoxazole-3-carboxylate (78p): Isoxazole **78p** was synthesized according to procedure (**PS3**), but the reagents were milled for 20 minutes rather than 30 minutes. Compound **78p** was isolated by recrystallizing the reaction crude in Hexanes. **78p** was isolated in 71 % (121 mg) yield as a yellow solid. **MP**: 95.4-96.8 °C, R_f: 0.15 **^{1}H NMR** (500 MHz, DMSO-d^6) δ δ 7.56 (s, 1H), 7.09 (d, J = 2.3 Hz, 2H), 6.64 (t, J = 2.2 Hz, 1H), 4.38 (q, J = 7.1 Hz, 2H), 3.81 (s, 6H), 1.33 (t, J = 7.1 Hz, 3H).**^{13}C NMR** (125 MHz, DMSO-d^6) δ 171.4, 161.5, 159.8, 157.3, 128.1, 104.1, 103.6, 101.8, 62.35, 56.05, 14.4. **HRMS:** m/z calculated for $C_{14}H_{15}NO_5$ [M+H]$^+$: 278.1023 found 278.1024.
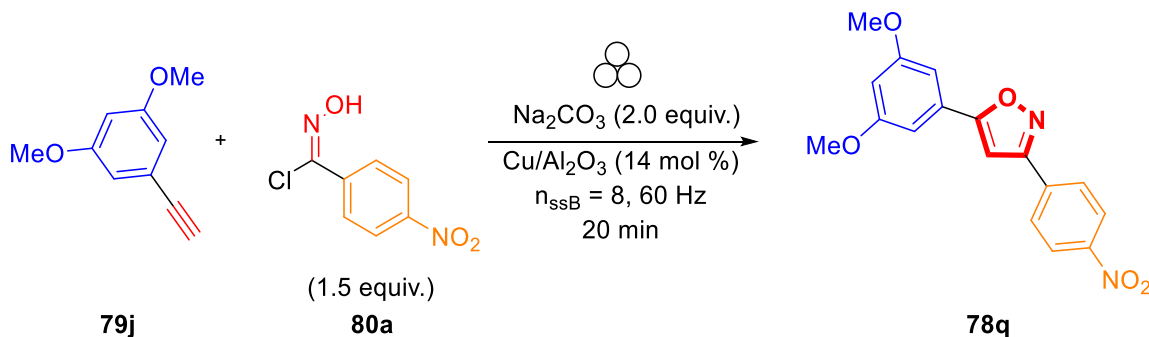
Synthesis of 5-(3,5-dimethoxyphenyl)-3-(4-nitrophenyl)isoxazole (78q): Isoxazole **78q** was synthesized according to procedure (**PS3**), but the reagents were milled for 20 minutes rather than 30 minutes. Compound **78q** was isolated by recrystallizing the reaction crude in Acetone:H$_2$O. **78q** was isolated in 76 % (152 mg) yield as a white solid. **MP**: 191-194 °C, R_f: 0.86 **^{1}H NMR** (500 MHz, DMSO-d^6) δ 8.40 (d, J = 8.84 Hz, 2H), 8.17 (d, J = 8.87 Hz, 2H), 7.82 (s, 1H), 7.06 (d, J = 2.23 Hz, 2H), 6.66 (t, J = 2.21 Hz, 1H), 3.83 (s, 6H). **^{13}C NMR** (125 MHz, DMSO-d^6) δ 170.8, 161.6, 161.5, 148.9, 135.0, 128.6, 128.3, 124.9, 104.0, 103.2, 100.1, 56.0. **HRMS:** m/z calculated for $C_{17}H_{14}N_2O_5$ [M+H]$^+$: 327.0975 found 327.0975.
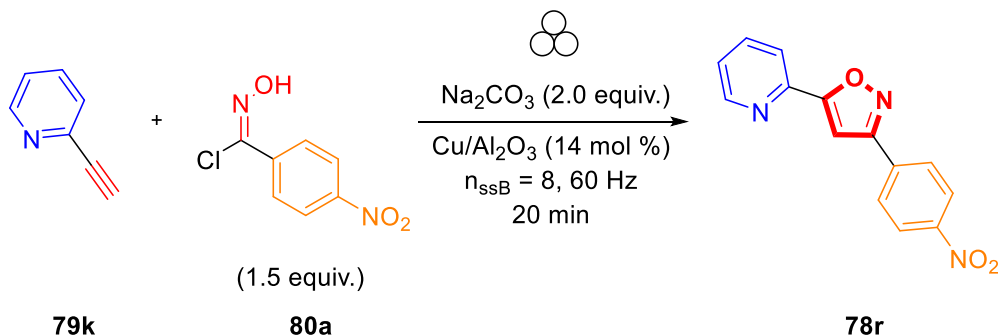
Synthesis of 3-(4-nitrophenyl)-5-(pyridin-2-yl)isoxazole (78r): Isoxazole **78r** was synthesized according to procedure (**PS3**), but the reagents were milled for 20 minutes rather than 30 minutes. Compound **78r** was isolated in a silica column using CHCl$_3$ as eluent. **78r** was isolated in 16 % yield (43.8 mg) as a yellow solid. **MP:** 225-228 °C, R_f: 0.34 **^{1}H NMR** (500 MHz, DMSO-d^6) δ 8.78 − 8.75 (m, 1H), 8.39 (d, J = 8.89 Hz, 2H), 8.27 (d, J = 8.89 Hz, 2H), 8.06 − 7.99 (m, 2H), 7.88 (s, 1H), 7.58 − 7.53 (m, 1H). **^{13}C NMR** (125 MHz, DMSO-d^6) δ 170.6, 161.8, 150.8, 149.0, 145.8, 138., 134.8, 128.5, 125.9, 124.8, 121.6, 101.8. **HRMS:** m/z calculated for $C_{14}H_9N_3O_3$ [M+H]$^+$: 268.0722 found 268.0719.

79k   **80b**   **78s**

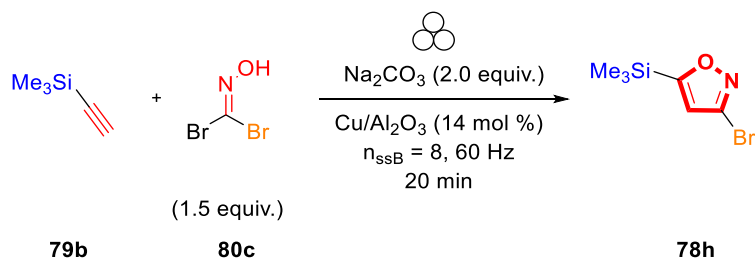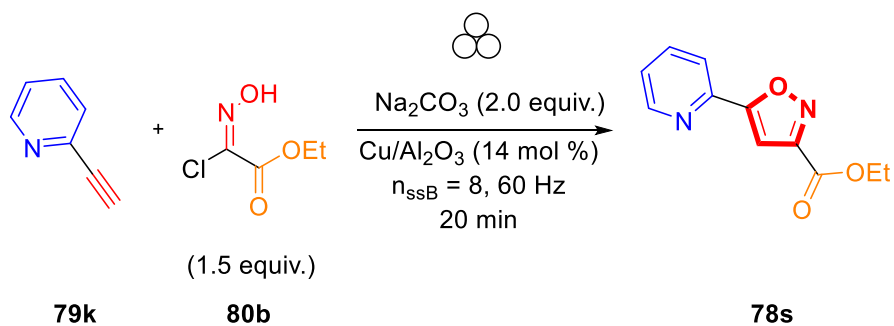**Synthesis of ethyl 5-(pyridin-2-yl)isoxazole-3-carboxylate (78s):** Isoxazole **78s** was synthesized according to procedure (**PS3**), but the reagents were milled for 20 minutes rather than 30 minutes. Compound **78s** was isolated in silica column using EtOAc:DCM:Hex (5:2:1) as eluent. **78s** was isolated in 42 % yield (88.3 mg) as a brown oil. R_f: 0.82 **^{1}H NMR** ^{1}H NMR (500 MHz, DMSO-d^6) δ 8.75 (d, J = 4.7 Hz, 1H), 8.08 (d, J = 7.9 Hz, 1H), 8.03 (td, J = 7.7, 1.7 Hz, 1H), 7.56 (ddd, J = 7.4, 4.8, 1.1 Hz, 1H), 7.47 (s, 1H), 4.41 (q, J = 7.1 Hz, 2H), 1.35 (t, J = 7.1 Hz, 3H). **^{13}C NMR** (125 MHz, DMSO-d^6) δ 170.9, 159.6, 157.3, 150.8, 145.3, 138.3, 126.0, 122.0, 103.2, 62.5, 14.4. **HRMS:** m/z calculated for $C_{14}H_{16}N_2O_3$ [M+H]$^+$: 261.1234 found 261.1233.

2.8.12. Milling Time Optimization for the Solvent-Free synthesis of 3,5-isoxazoles *via* 1,3-dipolar cycloaddition from terminal alkynes and hydroxyimidoil chlorides under Cu/Al_2O_3 surface under ball-milling conditions

Before isolation of 3,5-isoxazoles (**78c, 78e-s**), the corresponding terminal alkyne and hydroxyimidoil chloride reactions were optimized in a 20 mg scale reaction to determine the proper milling time. The yield of the 3,5-isoxazoles was quantified by ^{1}H NMR and using TMB as an internal standard.

Example:

79b   80a   78f
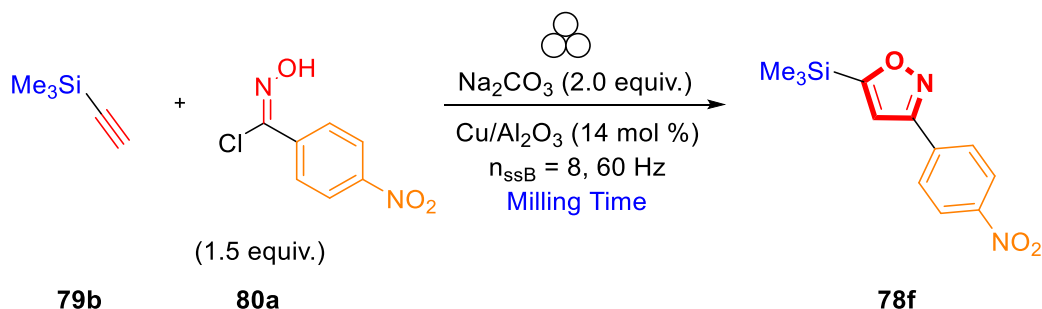
Milling time optimization for the synthesis of 3-(4-nitrophenyl)-5-(trimethylsilyl)isoxazole (78f): To a clean and dried stainless-steel (**SS**) planetary milling jar (approximately 50 mL capacity) with 8 **SS** balls (10 mm of diameter), it was weighed **80a** (0.050 g, 0.330 mmol, 1.5 equivalents.), Na_2CO_3 (0.047 g, 0.440 mmol, 2.0 equivalents.), and Cu/Al2O3 (89.1 mg, 0.031 mmol, 14 mol %). Then, ethynylbenzene **79c** (24 µL, 0.220 mmol, 1.0 equivalents.) was added *via* micropipette. Once all reagents were introduced on the planetary milling jar, the mixture was milled at a corresponding time at 60 Hz. After the reaction time was accomplished, the jar was cooled at room temperature, and it was added 10-12 mg of TMB to the reaction crude. Then the Cu/Al_2O_3 was filtered through a sintered funnel and washed with EtOH. The filtrated was collected, and the excess EtOH was removed under reduced pressure. The yield of **78f** was calculated by ^{1}H NMR using the signal at 7.50 ppm as a reference signal.

Milling Time (min)	Yield (%)[a]
10	38
20	32
30	92 *88*[b]

[a]^{1}H NMR Yields, [b] Isolated yield according to **PS3**

68
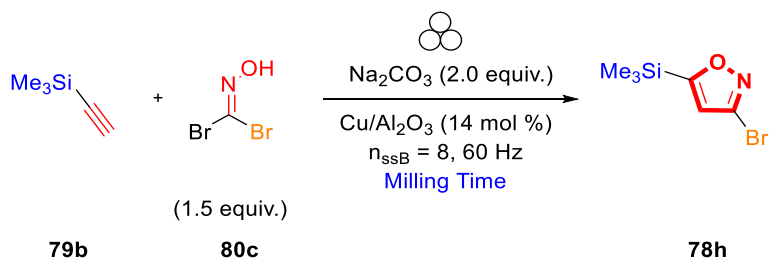
Milling Time (min)	Yield (%)[a]
20	20
30	73 70[b]

Reaction Conditions: 0.204 mmol of **79b**, 0.305 mmol of **80c**, 0.406 mmol of Na$_2$CO$_3$, 0.0285 mmol of Cu/Al$_2$O$_3$, SS beaker (50 mL capacity), 8 x SS milling balls (10 mm diameter), and milling at 60 Hz. [a] ^{1}H-NMR yields were measured using TMB as an internal standard. [b] *Isolated yield according to PS3*
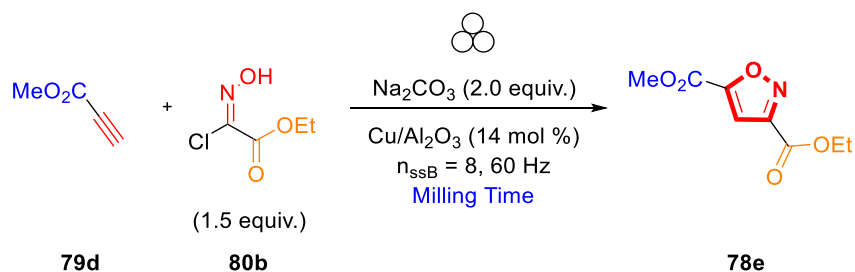
Milling Time (min)	Yield (%)[a]
10	70 *68[b]*
20	60
30	59

Reaction Conditions: 0.204 mmol of **80b**, 0.306 mmol of **79d**, 0.408 mmol of Na$_2$CO$_3$, 0.029 mmol of Cu/Al$_2$O$_3$, SS beaker (50 mL capacity), 8 x SS milling balls (10 mm diameter), milling at 60 Hz. [a] ^{1}H-NMR yields were measured using TMB as an internal standard. [b] *Isolated yield according to PS3*
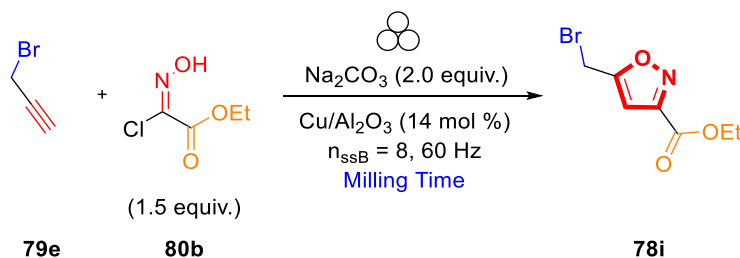
Time (min)	Yield (%)[a]
10	81 *71*[b]
20	70
30	70

40	65

Reaction Conditions: 0.168 mmol of **79e**, 0.252 mmol of **80b**, 0.336 mmol of Na_2CO_3, 0.024 mmol of Cu/Al_2O_3 , SS beaker (50 mL capacity), 8 x SS milling balls (10 mm diameter), milling at 60 Hz. [a] ^{1}H-NMR yields were measured using TMB as an internal standard. [b] *Isolated yield according to* **PS3**

79c + 80a → 78k

Na$_2$CO$_3$ (2.0 equiv.)
Cu/Al$_2$O$_3$ (14 mol %)
n_{ssB} = 8, 60 Hz
Milling Time

(1.5 equiv.)
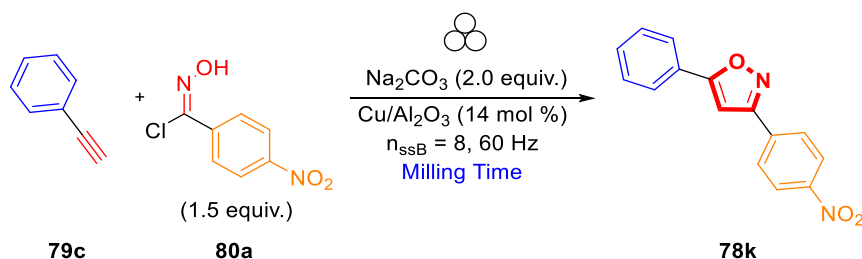
Milling Time (min)	Yield (%)[a]
10	N.R.
20	17
30	15
40	13
50	25
60	36 38[b]

Reaction Conditions: 0.220 mmol of **79c**, 0.330 mmol of **80a**, 0.440 mmol of Na_2CO_3, 0.031 mmol of Cu/Al_2O_3 , SS beaker (50 mL capacity), 8 x SS milling balls (10 mm diameter), milling at 60 Hz. [a] ^{1}H-NMR yields were measured using TMB as an internal standard. [b] *Isolated yield according to* **PS3**

79g + 80a → 78m

Na$_2$CO$_3$ (2.0 equiv.)
Cu/Al$_2$O$_3$ (14 mol %)
n_{ssB} = 8, 60 Hz
Milling Time

(1.5 equiv.)
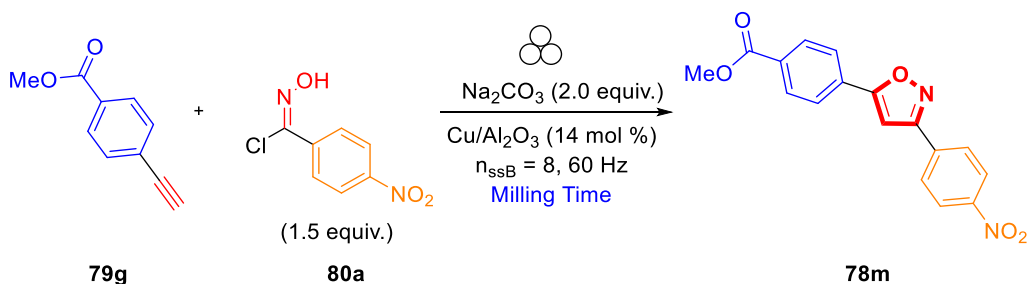
Milling Time (min)	Yield (%)[a]
10	33
20	24
30	45 41[b]
40	13

Reaction Conditions: 0.166 mmol of **79g**, 0.249 mmol of **80a**, 0.332 mmol of Na_2CO_3, 0.023 mmol of Cu/Al_2O_3 , SS beaker (50 mL capacity), 8 x SS milling balls (10 mm diameter), milling at 60 Hz. [a] ^{1}H-NMR yields were measured using TMB as an internal standard. [b] *Isolated yield according to* **PS3**
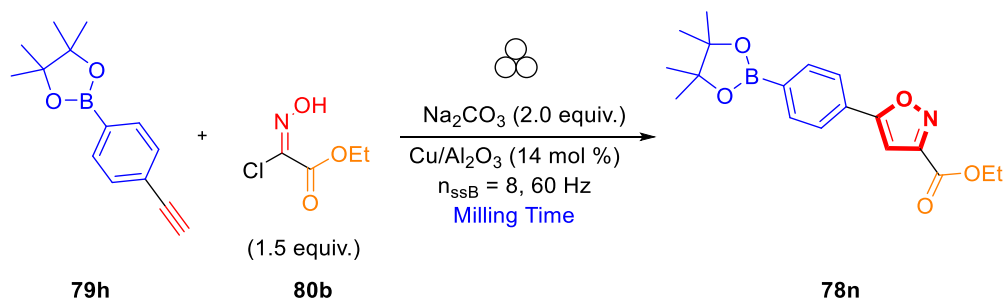
Milling Time (min)	Yield (%)[a]
20	50
30	75 70[b]
40	52

Reaction Conditions: 0.088 mmol of **79h**, 0.123 mmol of **80b**, 0.176 mmol of Na$_2$CO$_3$, 0.012 mmol of Cu/Al$_2$O$_3$, SS beaker (50 mL capacity), 8 x SS milling balls (10 mm diameter), milling at 60 Hz. [a] ^{1}H-NMR yields were measured using TMB as an internal standard. [b] *Isolated yield according to **PS3***
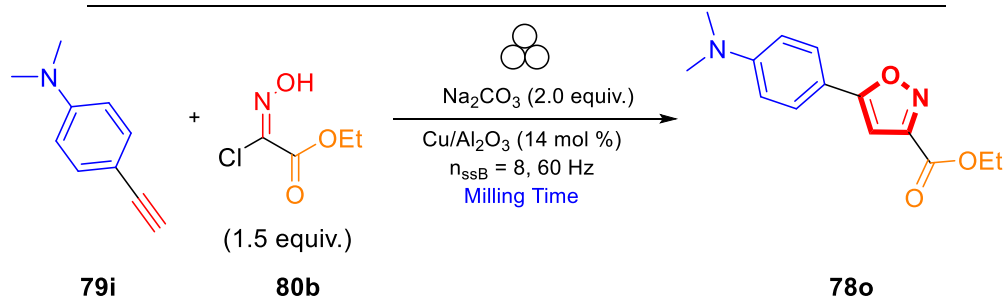
Milling Time (min)	Yield (%)[a]
20	61
30	70 45[b]

Reaction Conditions: 0.140 mmol of **79i**, 0.210 mmol of **80b**, 0.280 mmol of Na$_2$CO$_3$, 0.020 mmol of Cu/Al$_2$O$_3$, SS beaker (50 mL capacity), 8 x SS milling balls (10 mm diameter), milling at 60 Hz. [a] ^{1}H-NMR yields were measured using TMB as an internal standard. [b] *Isolated yield according to **PS3***
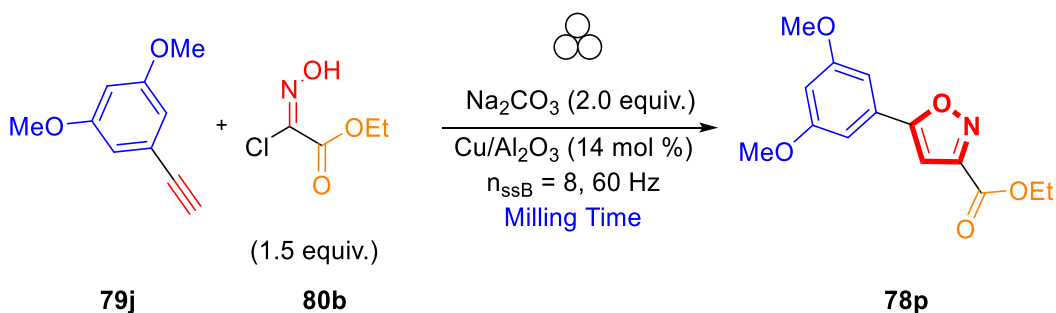
Milling Time (min)	Yield (%)^a
20	50
30	75 70^b
40	52

Reaction Conditions: 0.123 mmol of **79j**, 0.185 mmol of **80b**, 0.246 mmol of Na$_2$CO$_3$, 0.017 mmol of Cu/Al$_2$O$_3$, SS beaker (50 mL capacity), 8 x SS milling balls (10 mm diameter), milling at 60 Hz. ^{a} ^{1}H-NMR yields were measured using TMB as an internal standard. ^{b} *Isolated yield according to* **PS3**

2.8.12. ^{1}H NMR and ^{13}C spectra

3-(4-nitrophenyl)-5-(tributylstannyl)isoxazole (78a)
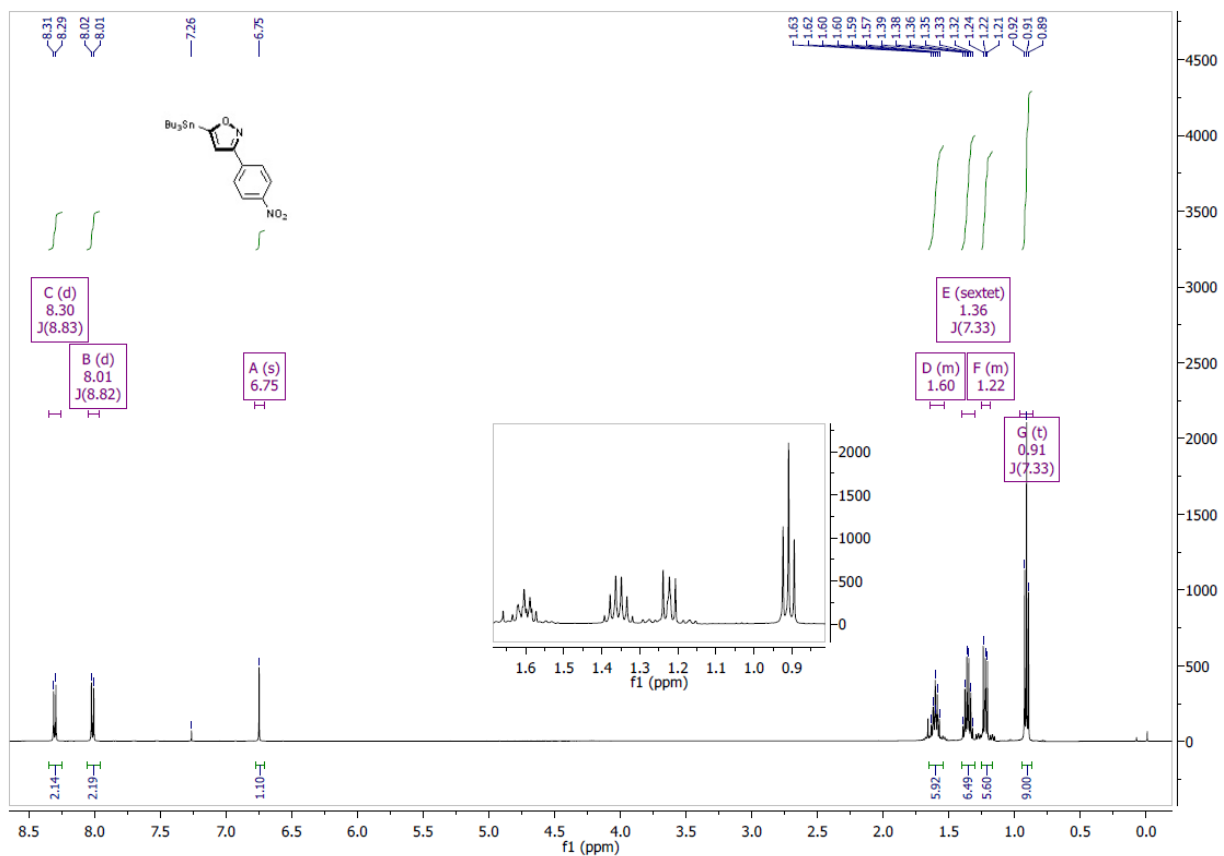
Figure S2.5: ^{1}H NMR spectrum of 3,5-isoxazole **78a**
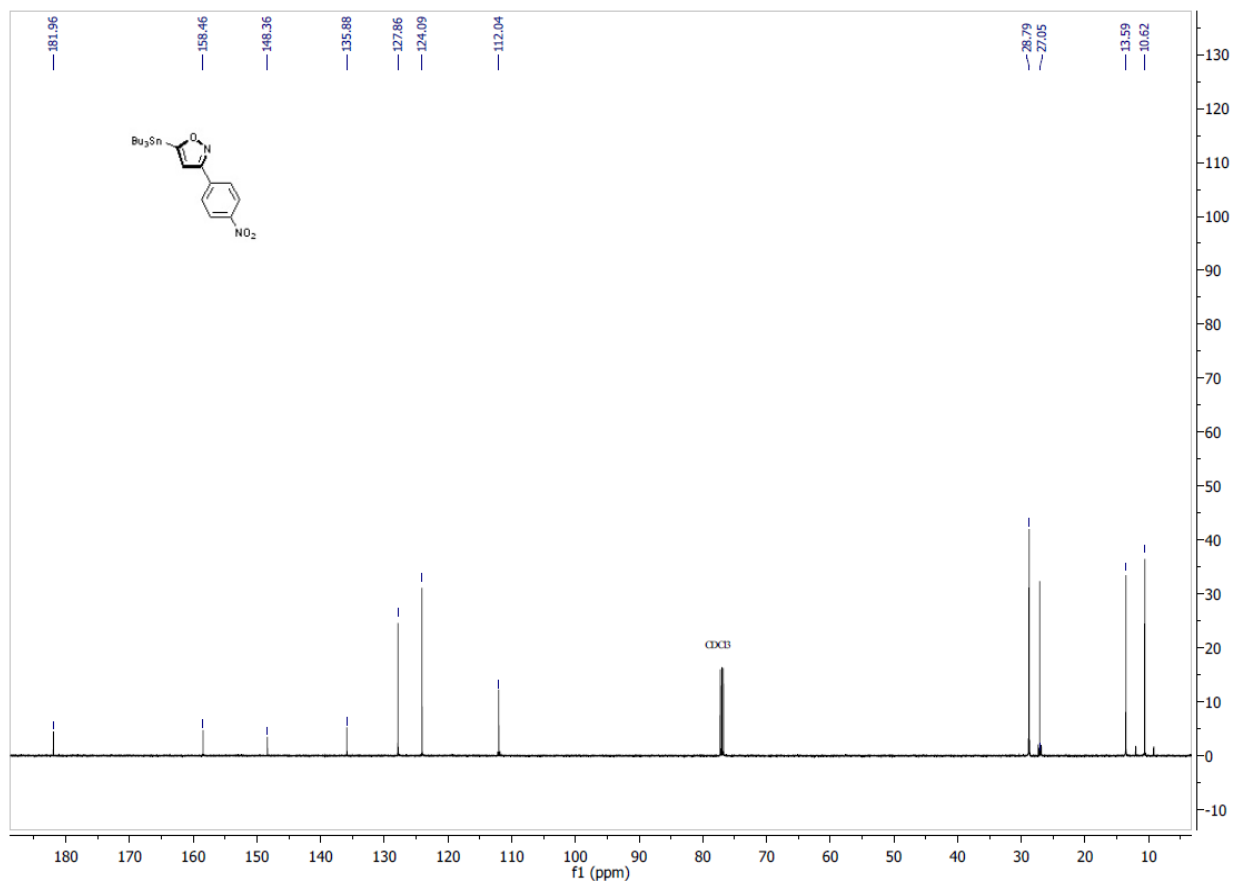
Figure S2.6: ^{13}C NMR spectrum of 3,5-isoxazole **78a**

Ethyl 5-(tributylstannyl)isoxazole-3-carboxylate (78b):
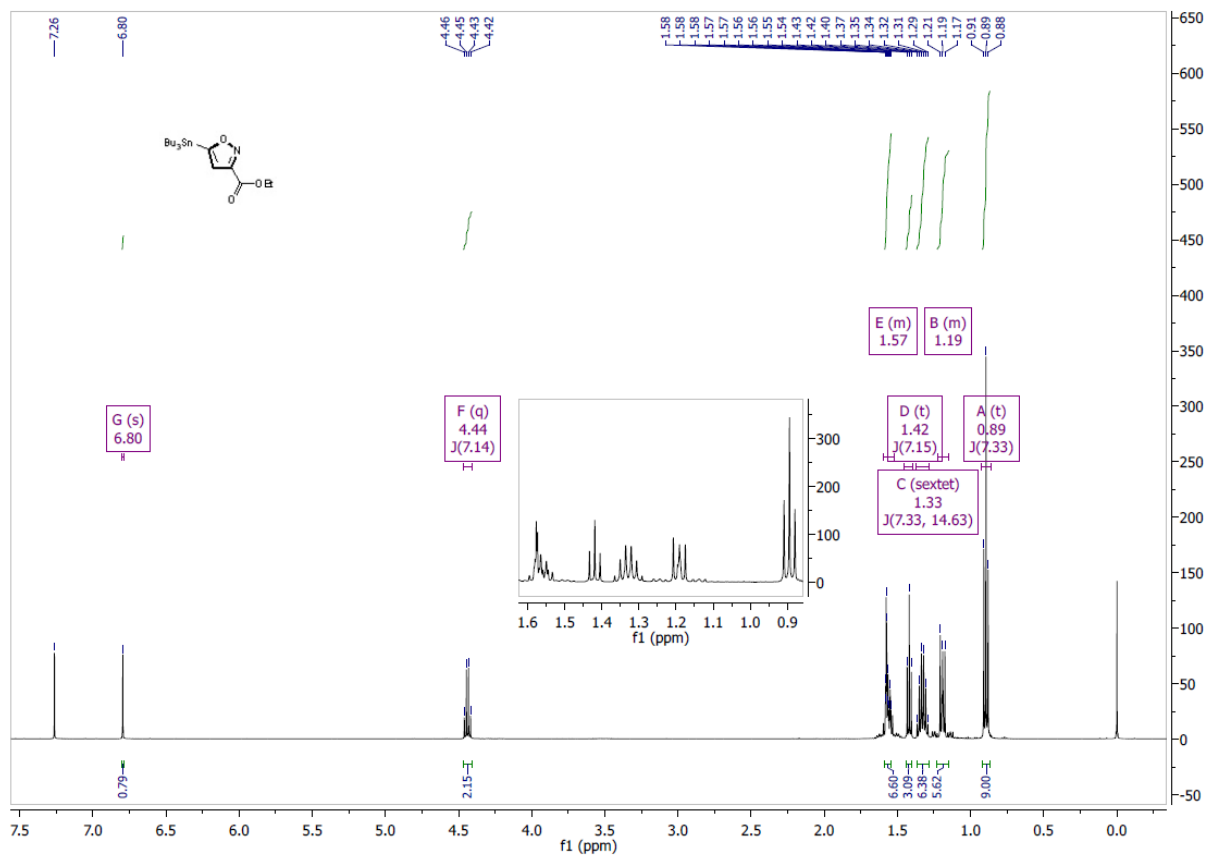
Figure S2.7: ^{1}H NMR spectrum of 3,5-isoxazole **78b**
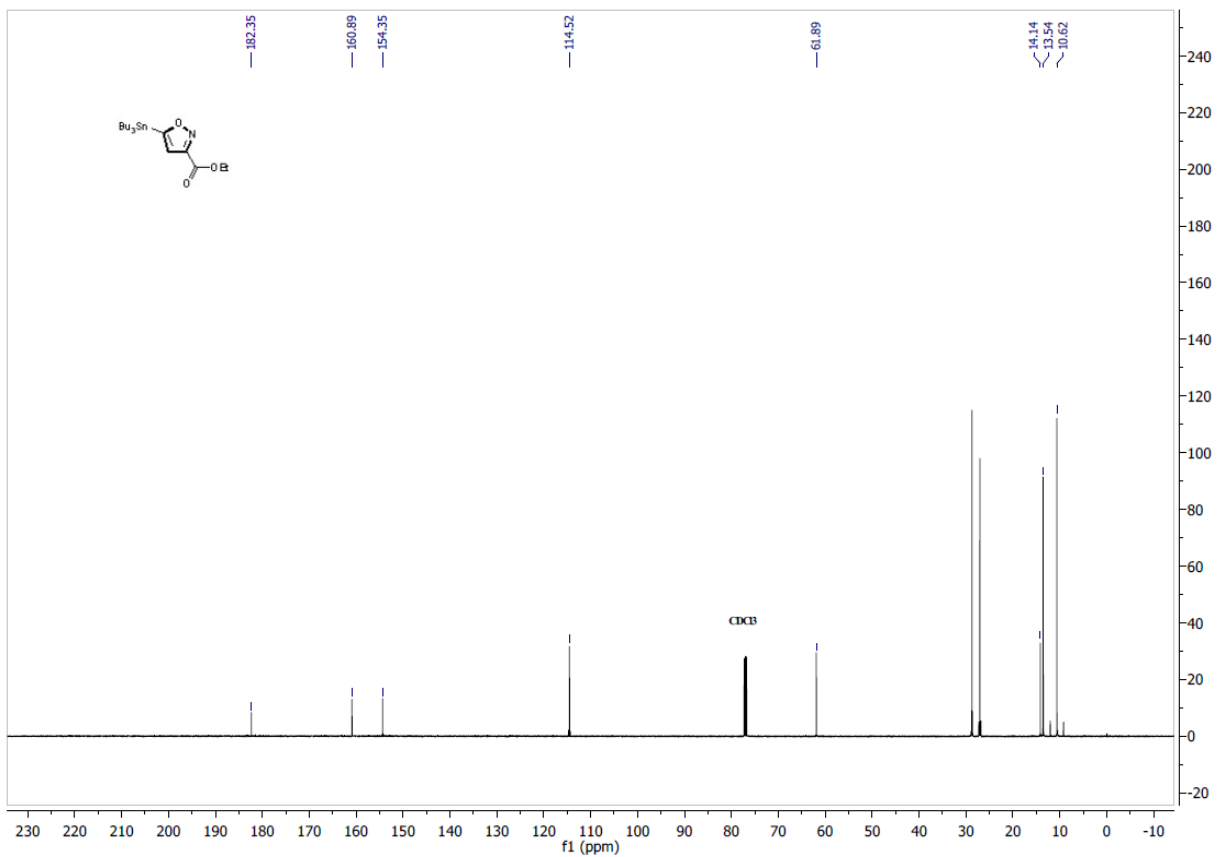
Figure S2.8: ^{13}C NMR spectrum of 3,5-isoxazole **78b**

Ethyl 5-(trimethylsilyl)isoxazole-3-carboxylate (78c)
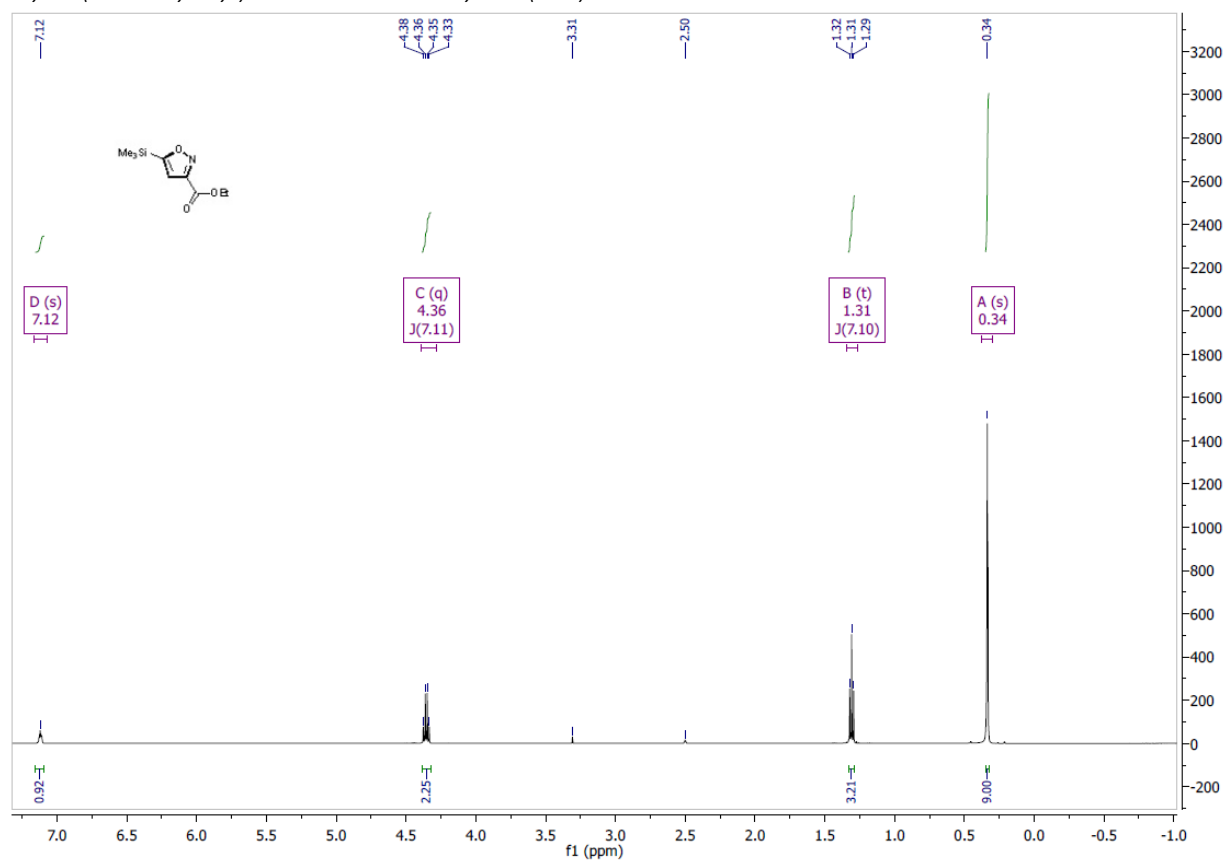
Figure S2.9: ^{1}H NMR spectrum of 3,5-isoxazole **78c**
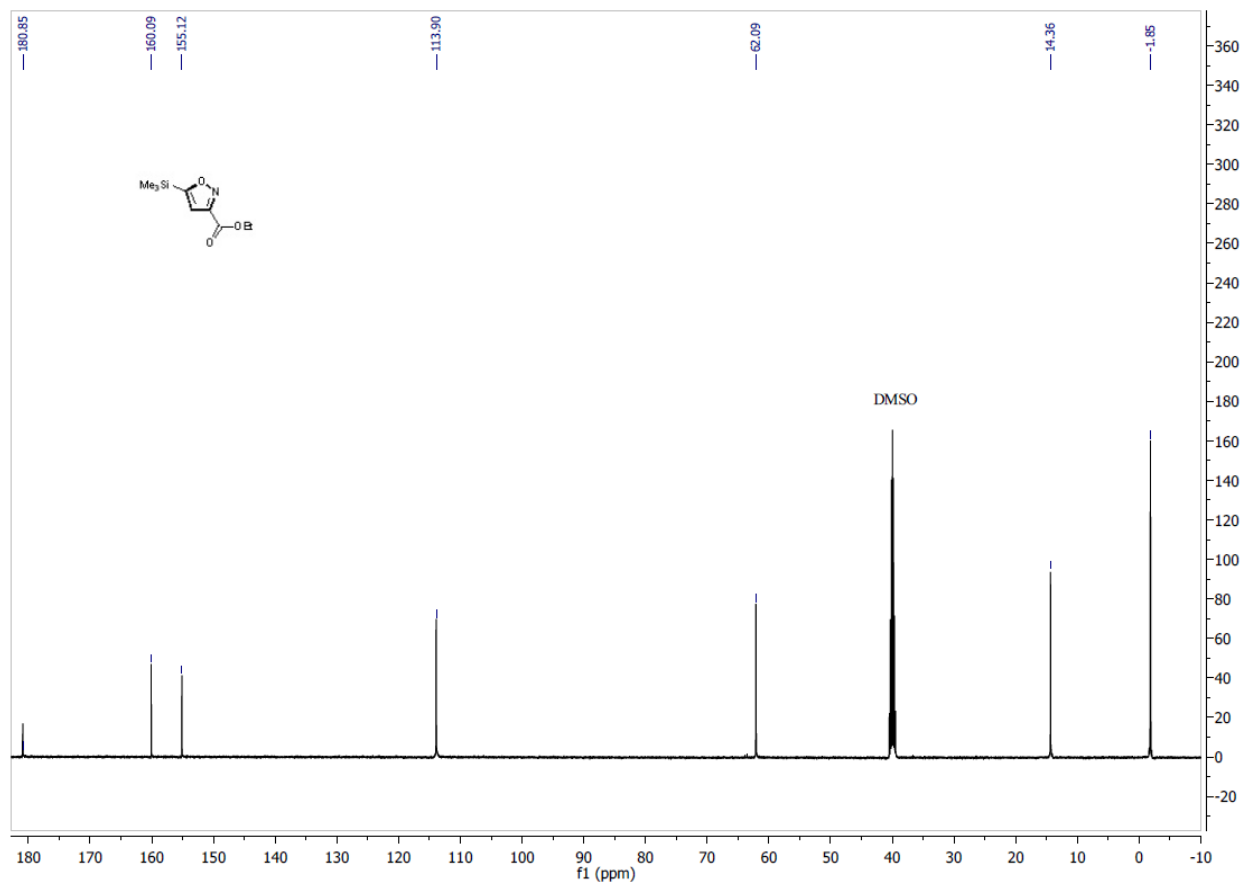
Figure S2.10: ^{13}C NMR spectrum of 3,5-isoxazole **78c**

Ethyl 5-phenylisoxazole-3-carboxylate (78d)
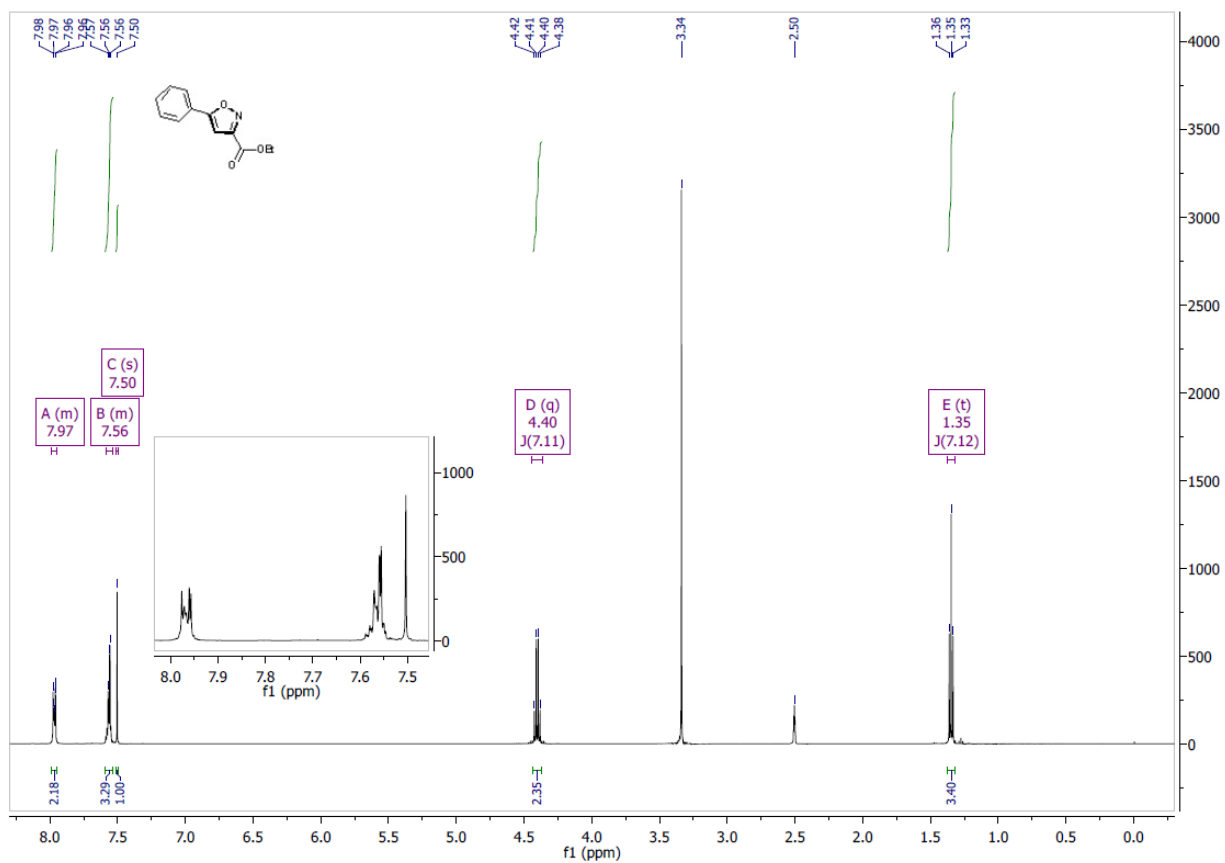
Figure S2.11: ^{1}H NMR spectrum of 3,5-isoxazole **78d**
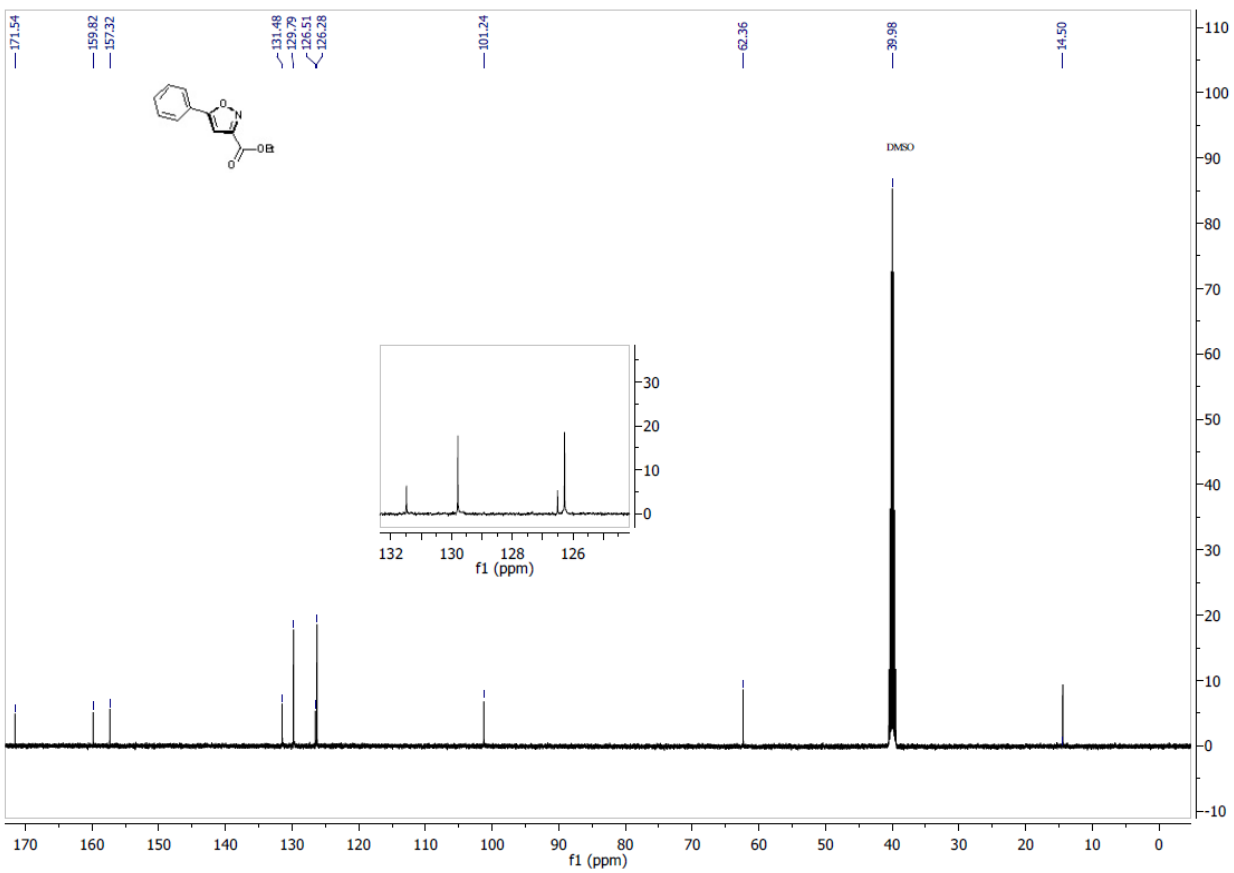
Figure S2.12: ^{13}C NMR spectrum of 3,5-isoxazole **78d**

3-ethyl 5-methyl isoxazole-3,5-dicarboxylate (78e)
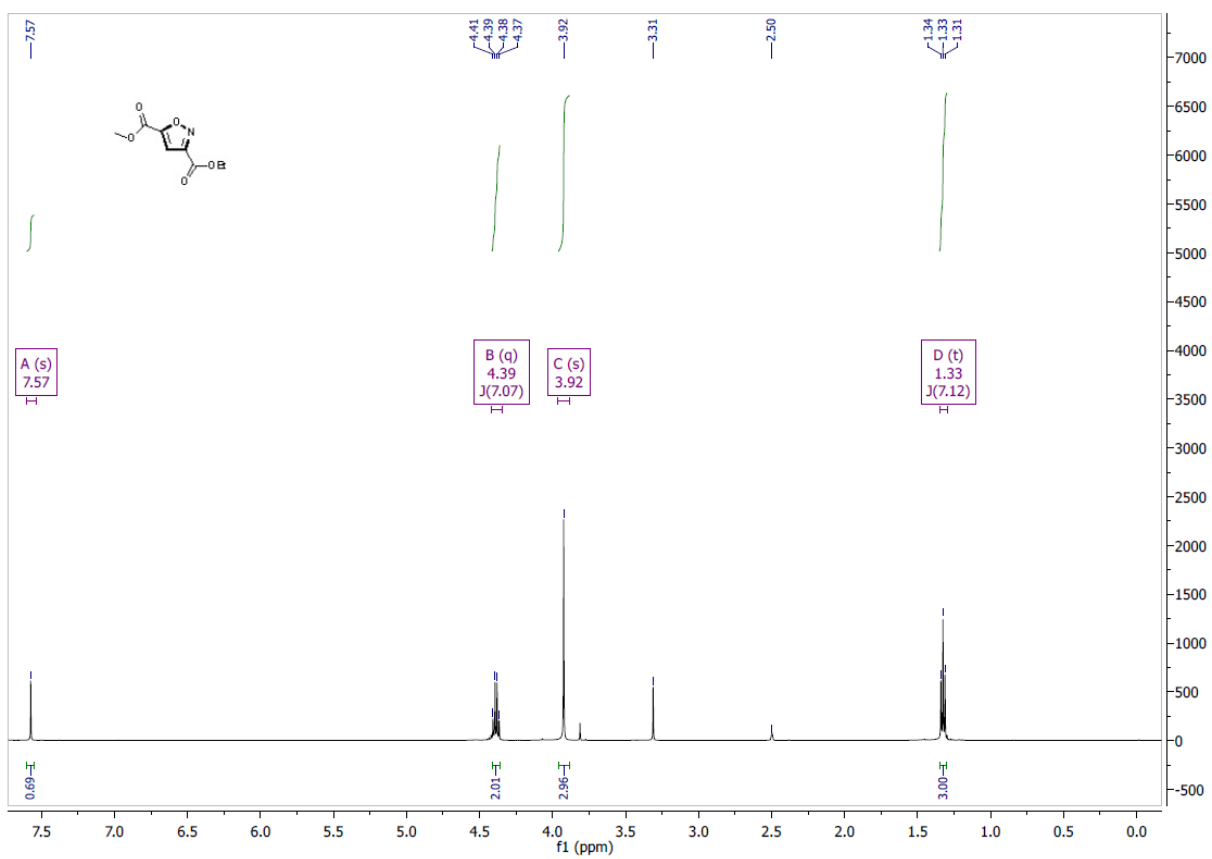
Figure S2.13: ^{1}H NMR spectrum of 3,5-isoxazole **78e**
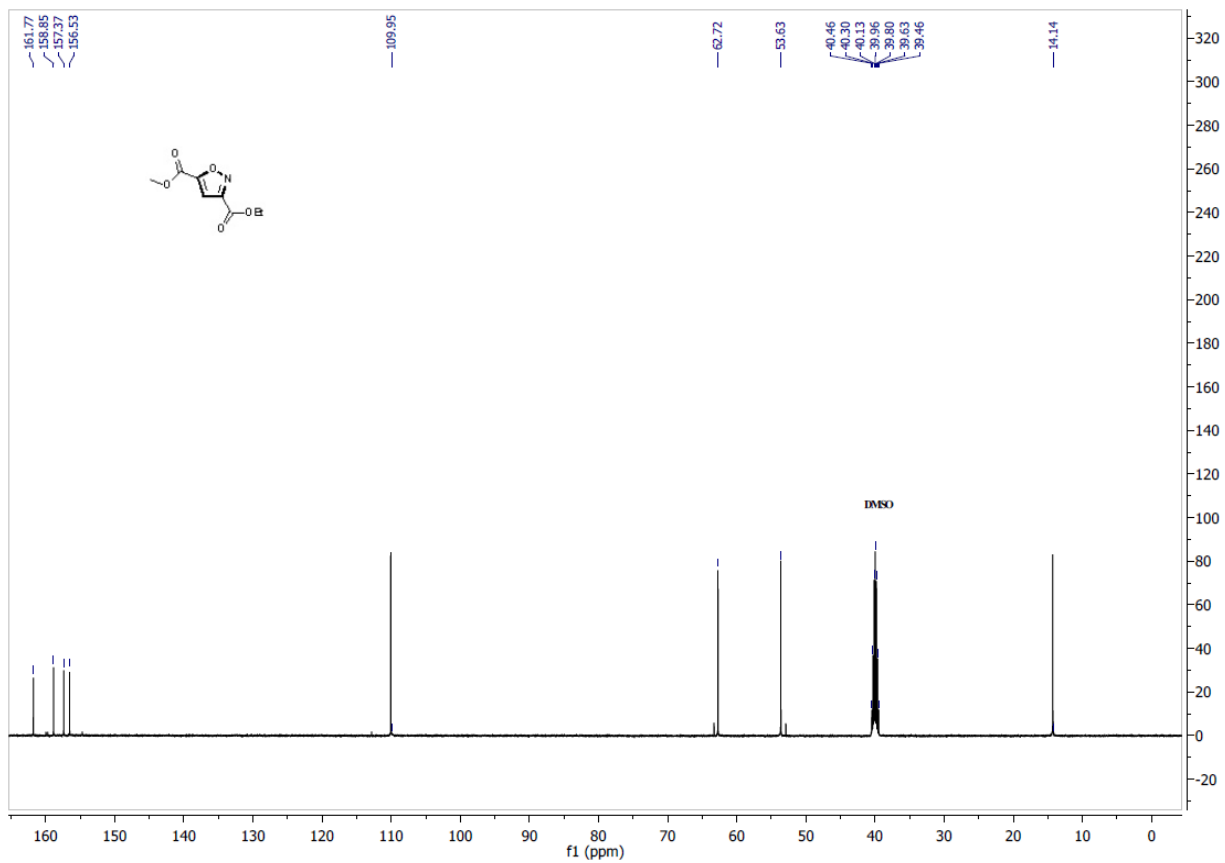
Figure S2.14: ^{13}C NMR spectrum of 3,5-isoxazole **78e**

3-(4-nitrophenyl)-5-(trimethylsilyl)isoxazole (78f)
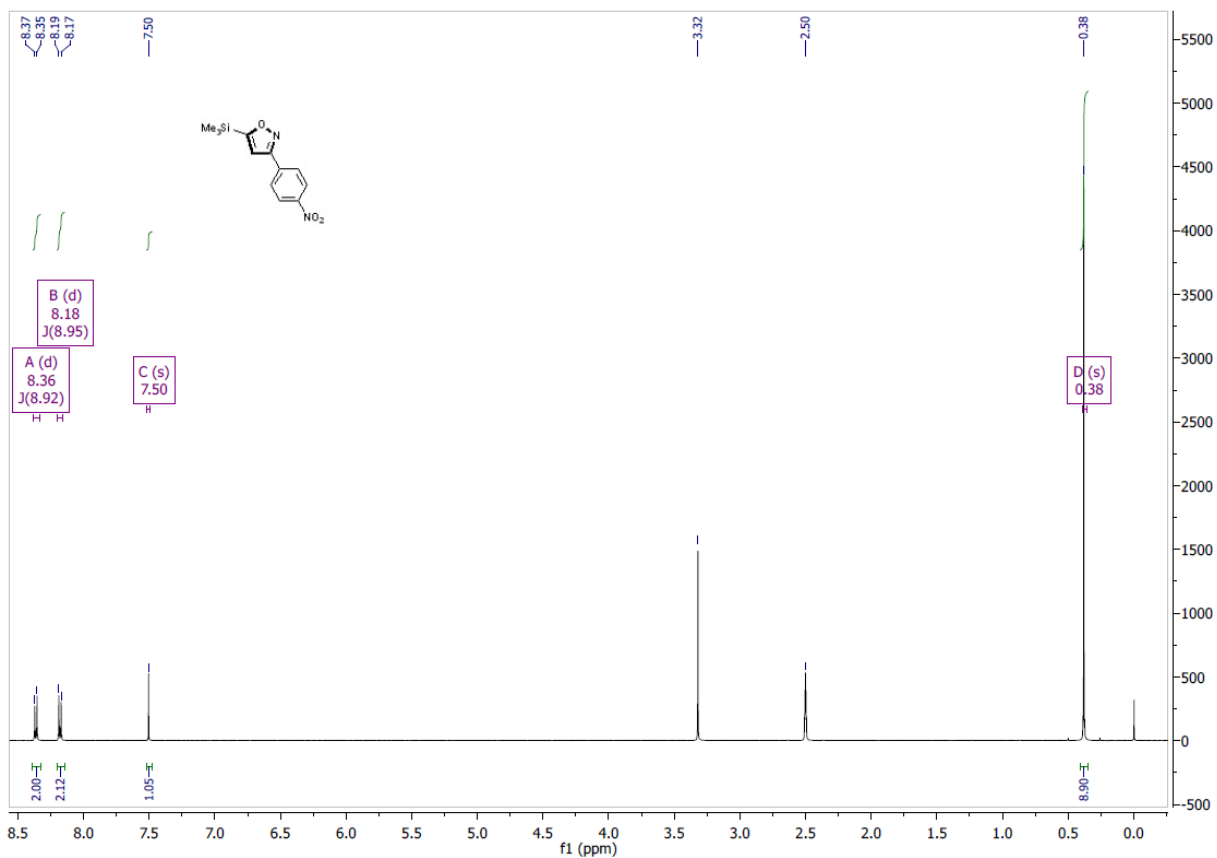
Figure S2.15: ^{1}H NMR spectrum of 3,5-isoxazole **78f**
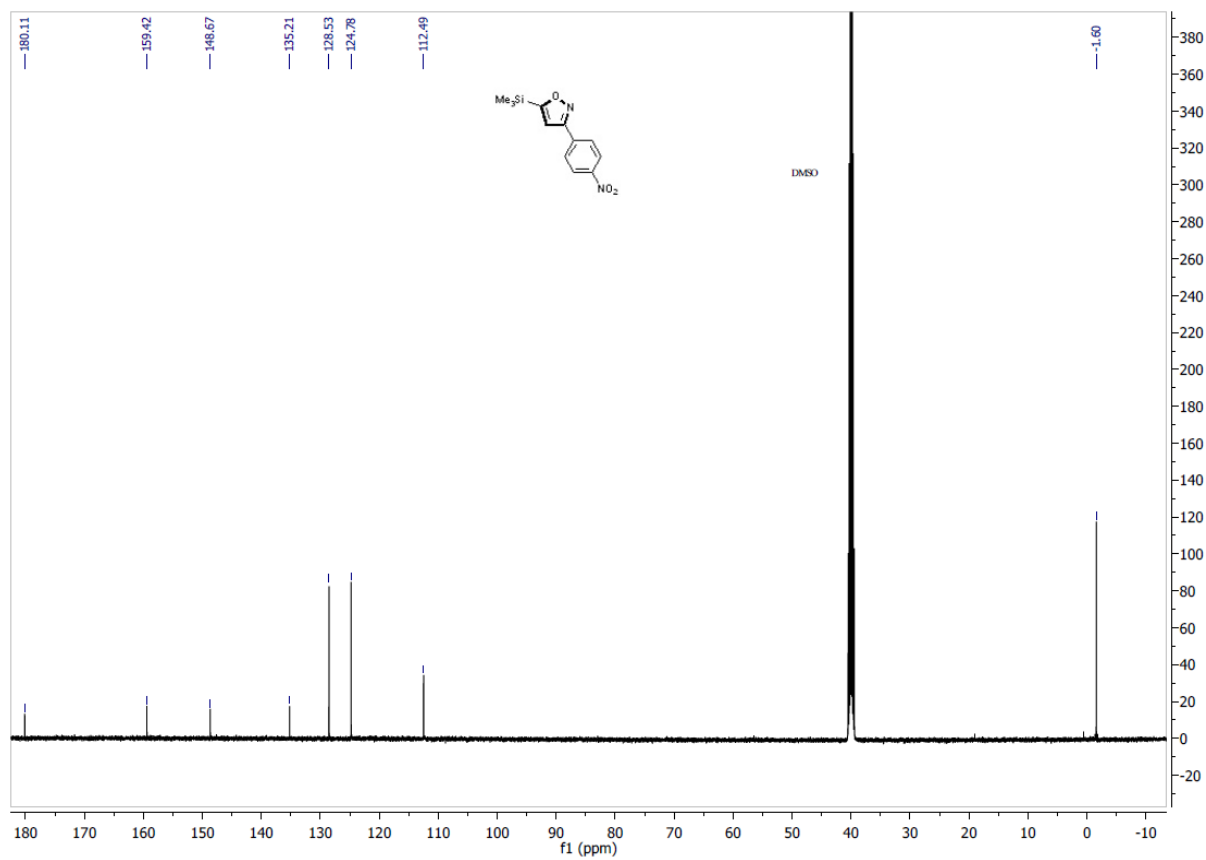
Figure S2.16: ^{13}C NMR spectrum of 3,5-isoxazole **78f**

3-(4-methoxyphenyl)-5-(trimethylsilyl)isoxazole (78g)
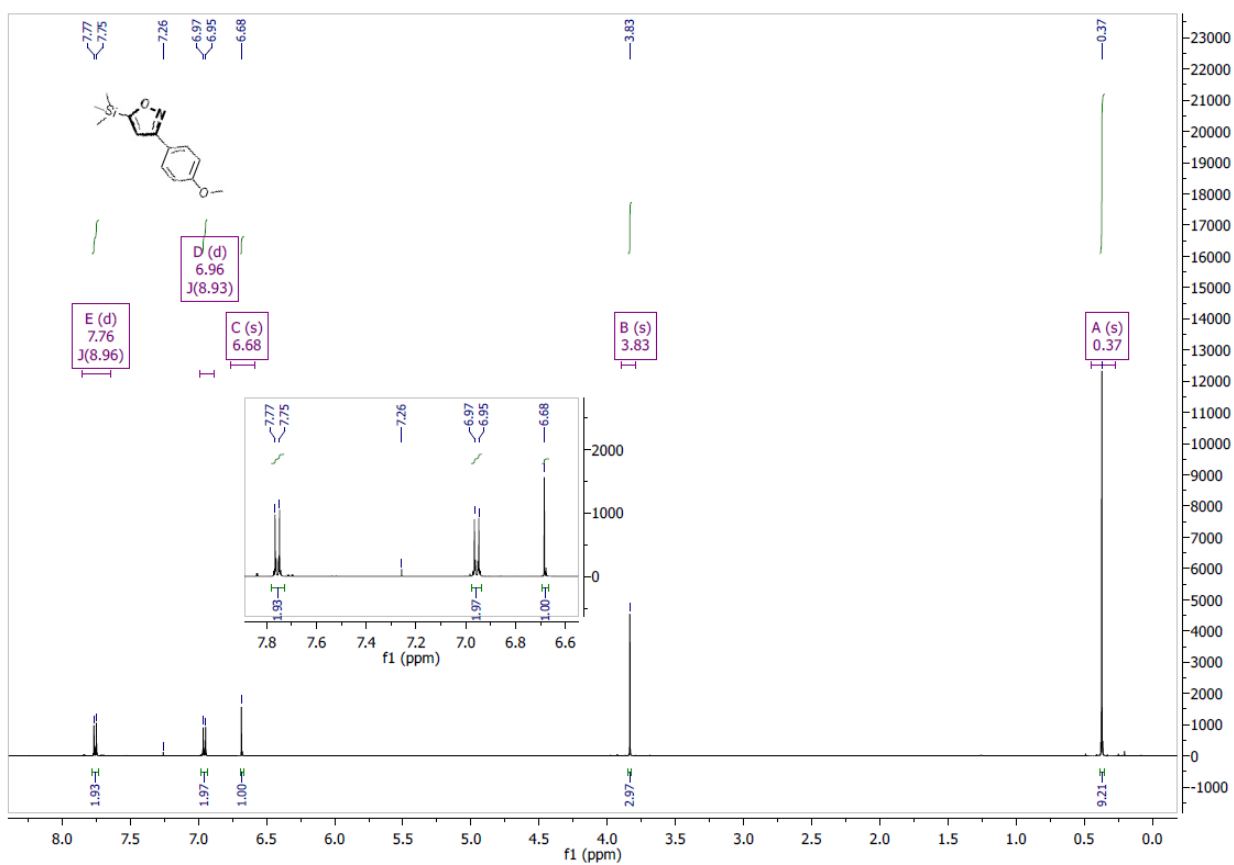
Figure S2.17: ¹H NMR spectrum of 3,5-isoxazole **78g**
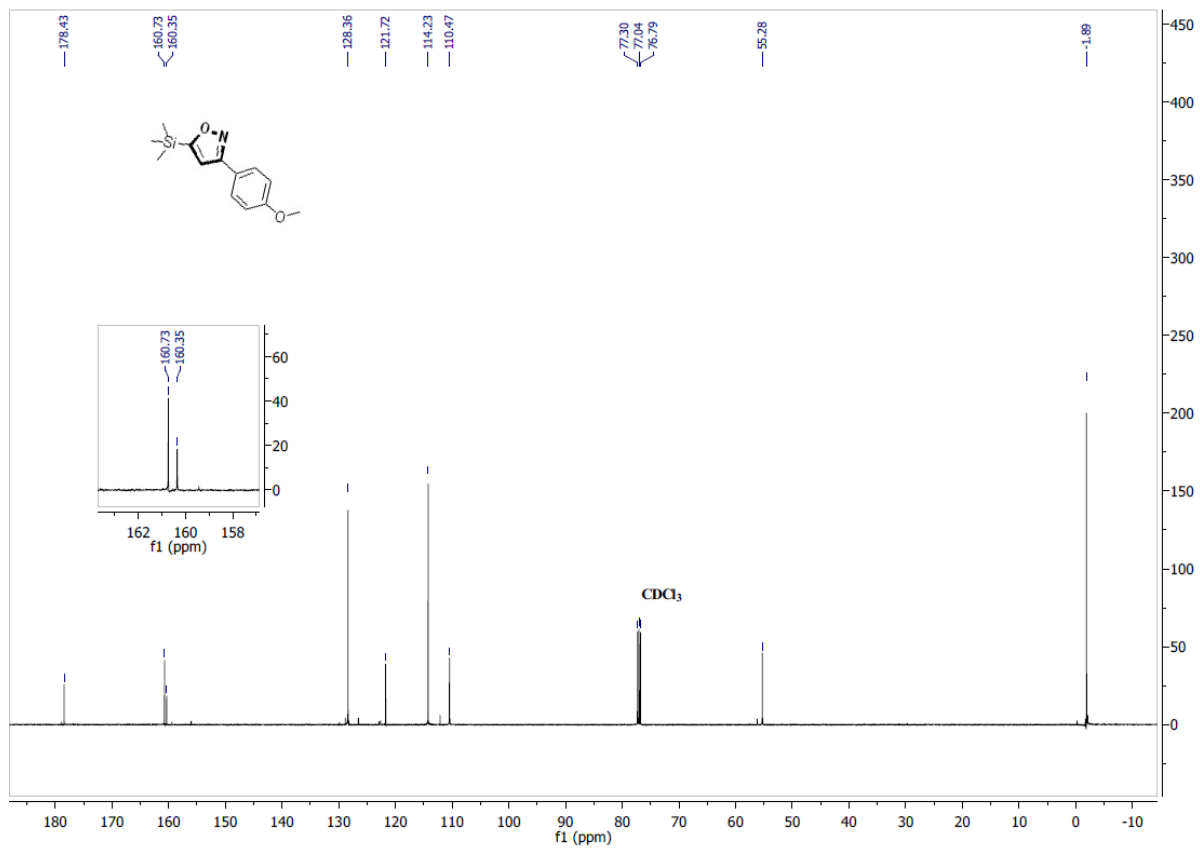
Figure S2.18: ^{13}C NMR spectrum of 3,5-isoxazole **78g**

3-bromo-5-(trimethylsilyl)isoxazole (78h)
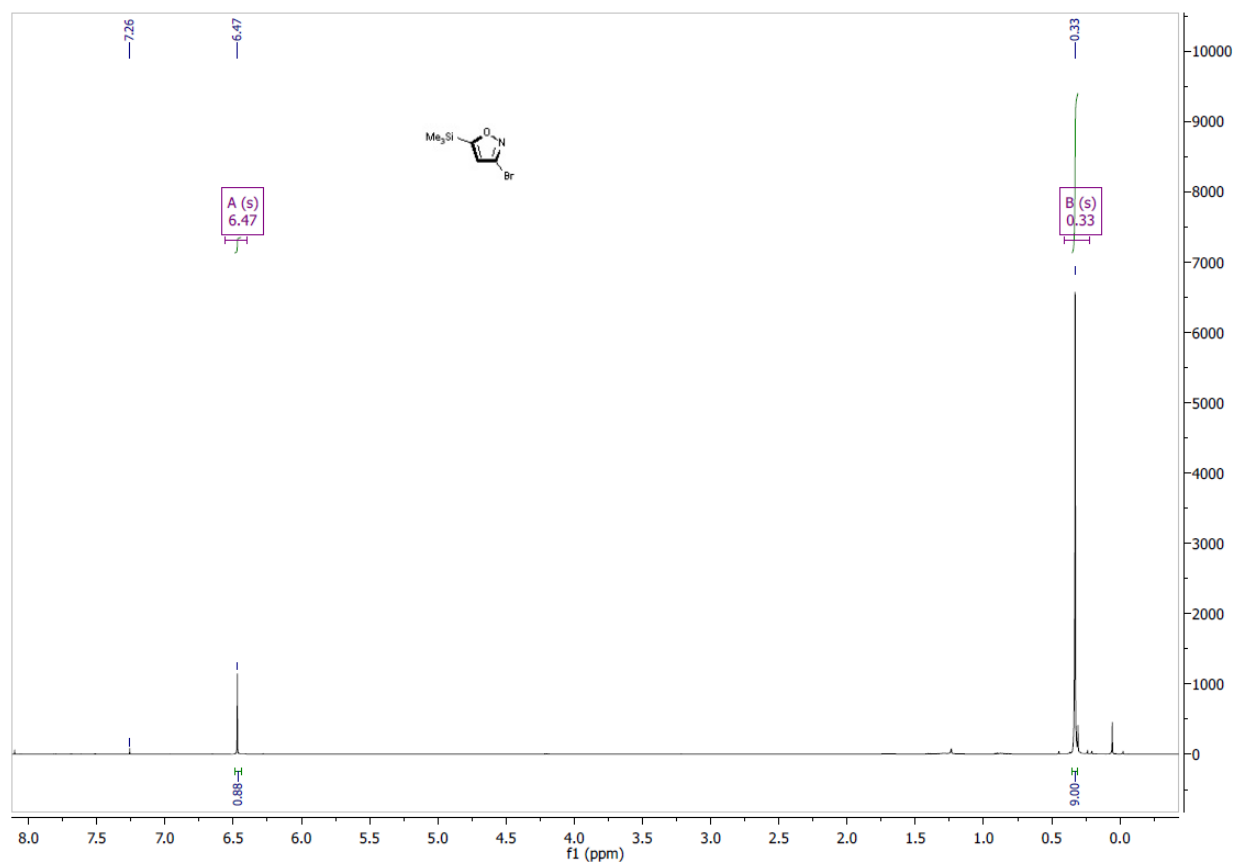
Figure S2.19: ^{1}H NMR spectrum of 3,5-isoxazole **78h**
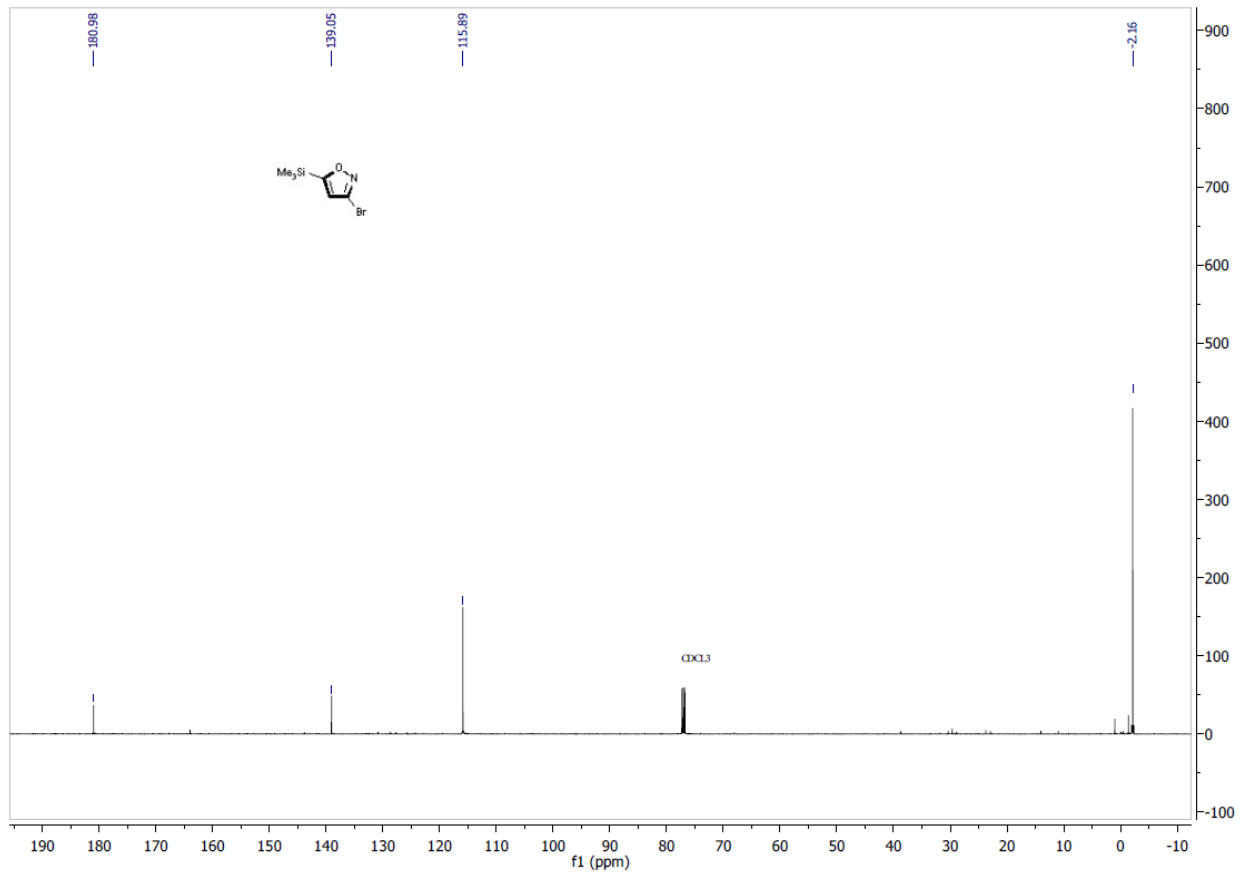
Figure S2.20: ^{13}C NMR spectrum of 3,5-isoxazole **78h**

ethyl 5-(bromomethyl)isoxazole-3-carboxylate (78i)
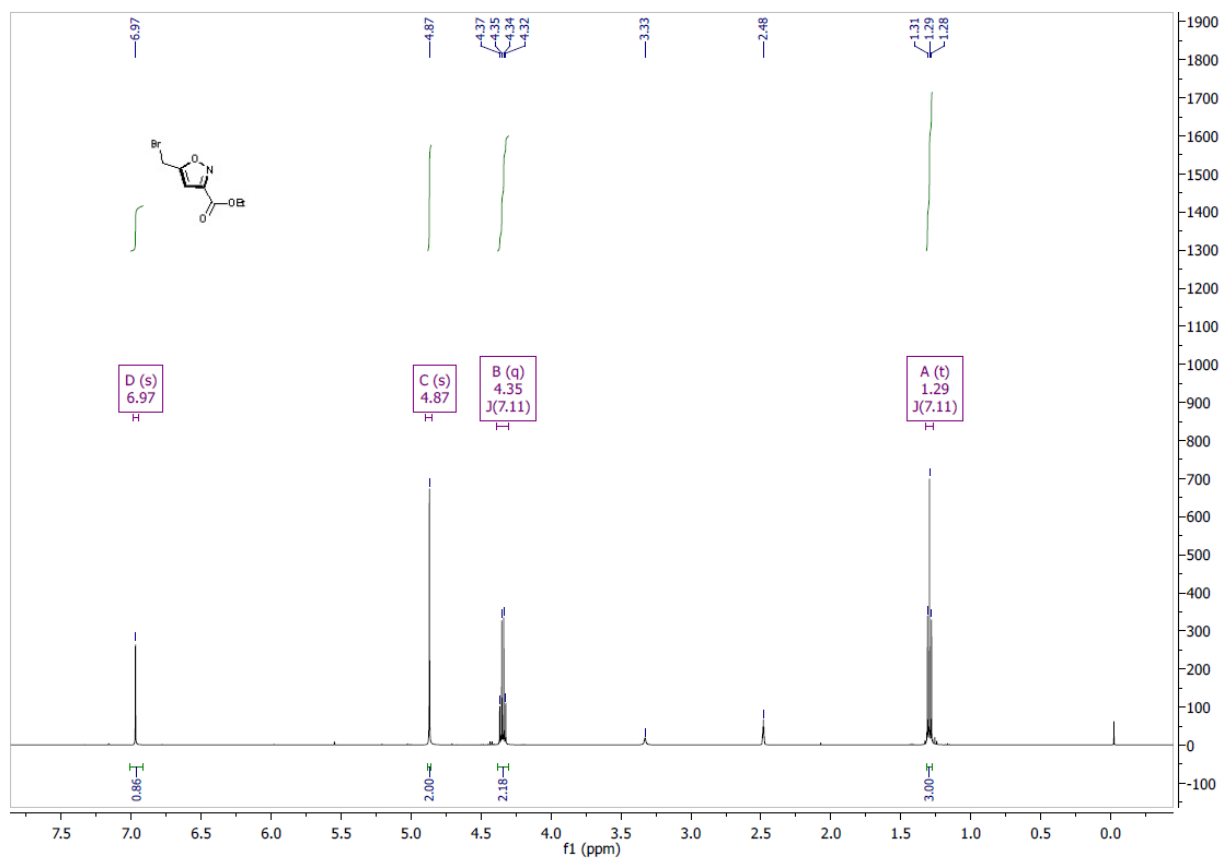
Figure S2.22: ^{1}H NMR spectrum of 3,5-isoxazole **78i**
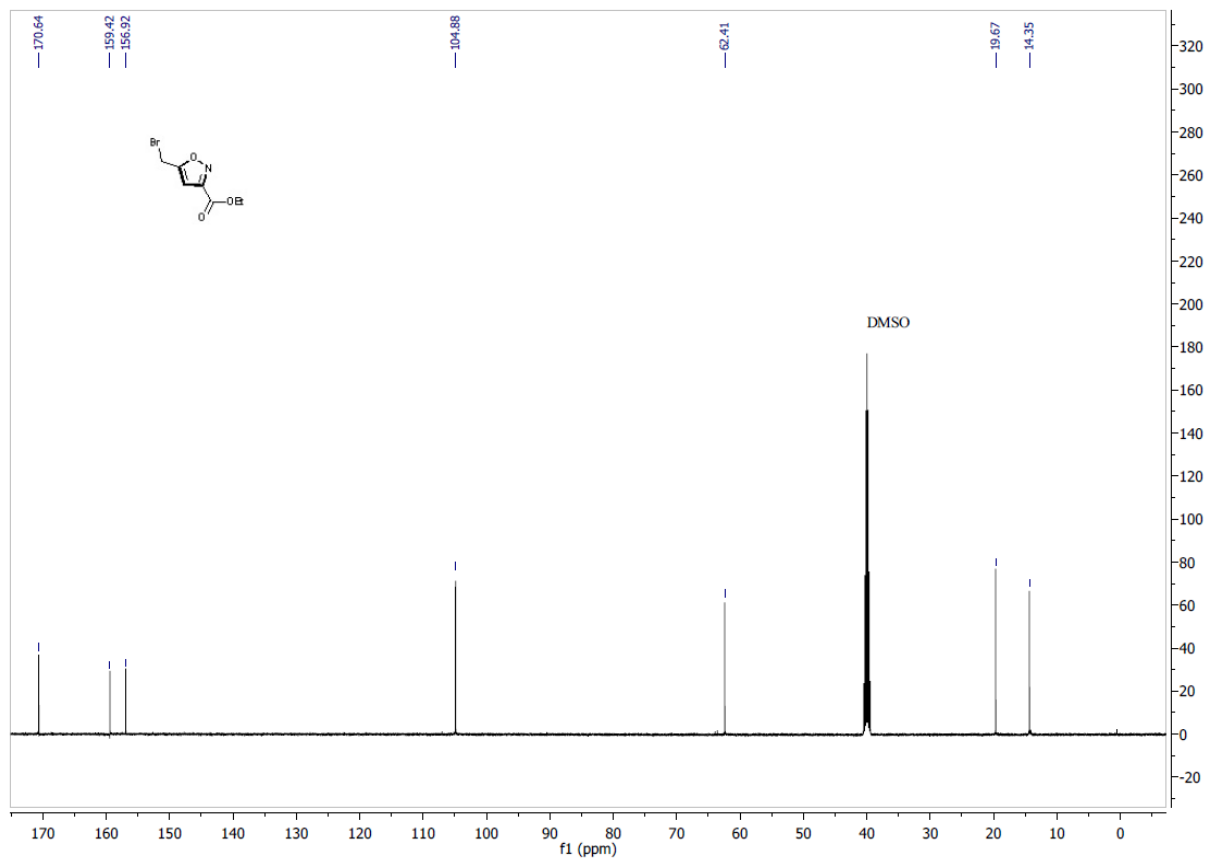
Figure S2.23: ^{13}C NMR spectrum of 3,5-isoxazole **78i**

5-(2-bromoethyl)-3-(4-methoxyphenyl)isoxazole (78j)
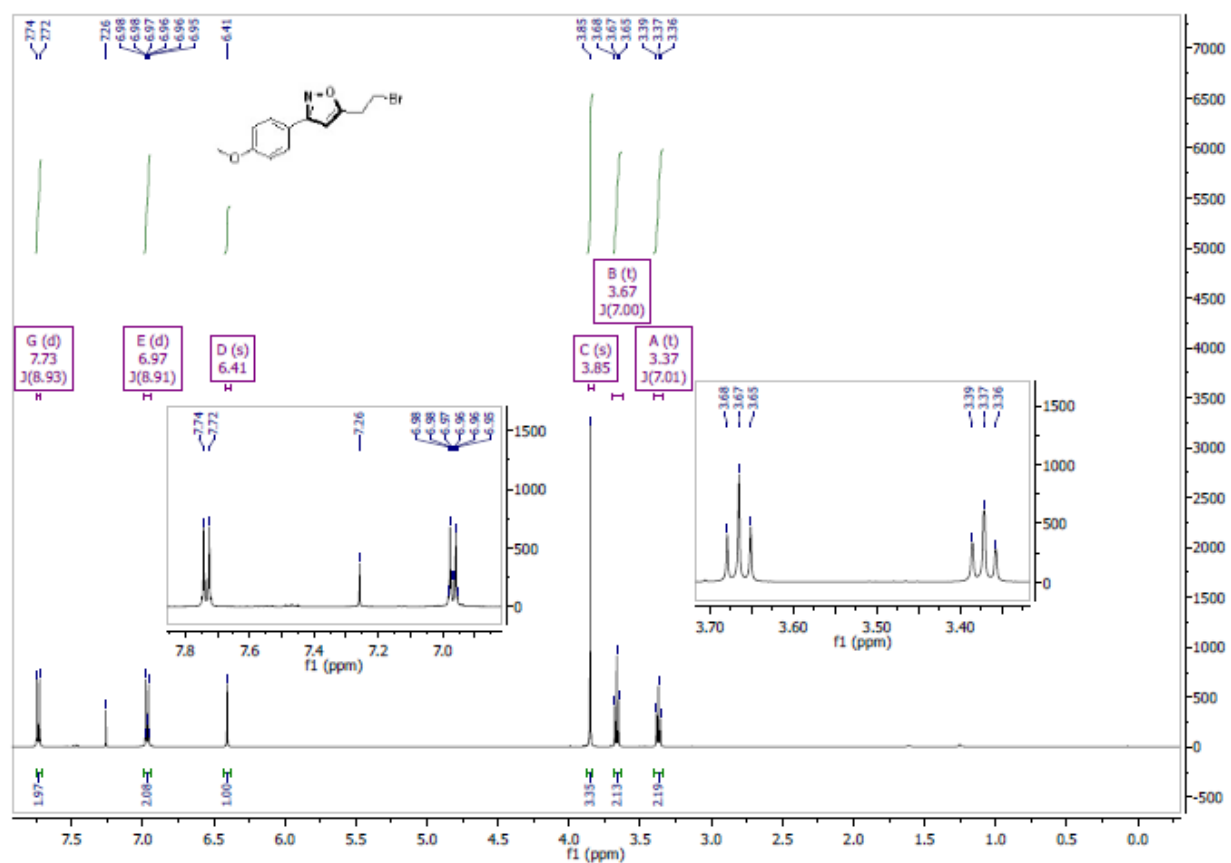
Figure S2.24: ^{1}H NMR spectrum of 3,5-isoxazole **78j**
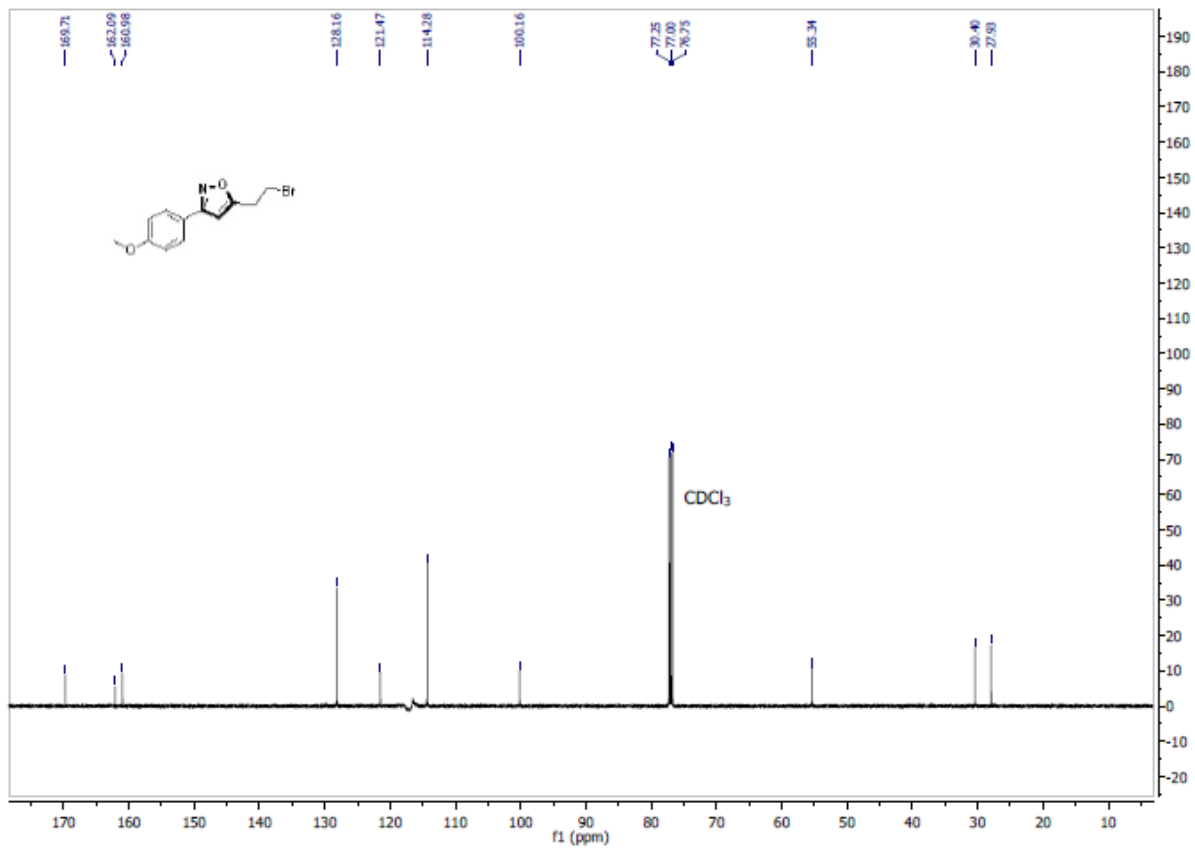
Figure S2.25: ^{13}C NMR spectrum of 3,5-isoxazole **78j**

3-(4-nitrophenyl)-5-phenylisoxazole (78k)
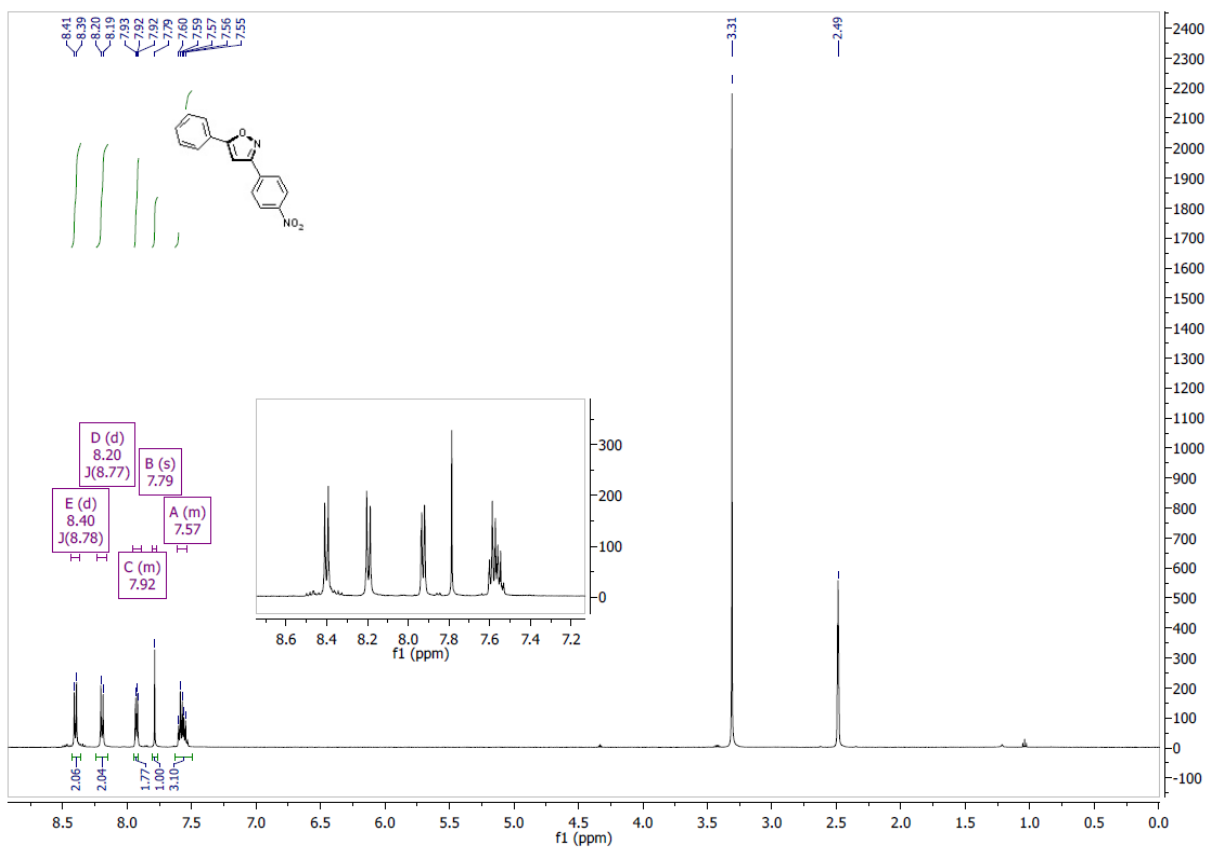
Figure S2.26: ^{1}H NMR spectrum of 3,5-isoxazole **78k**
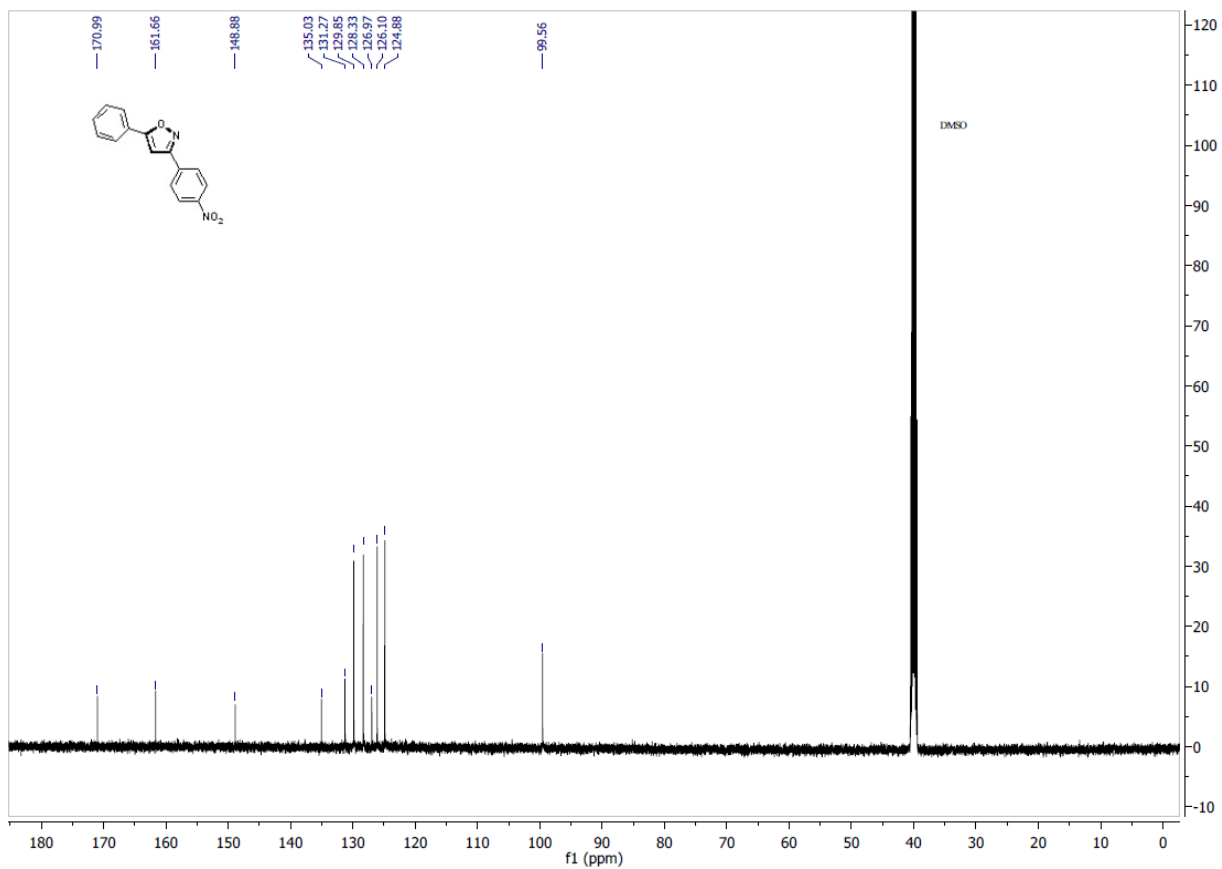
Figure S2.27. ^{13}C NMR spectrum of 3,5-isoxazole **78k**

Methyl 4-(3-(4-nitrophenyl)isoxazol-5-yl)benzoate (78m)
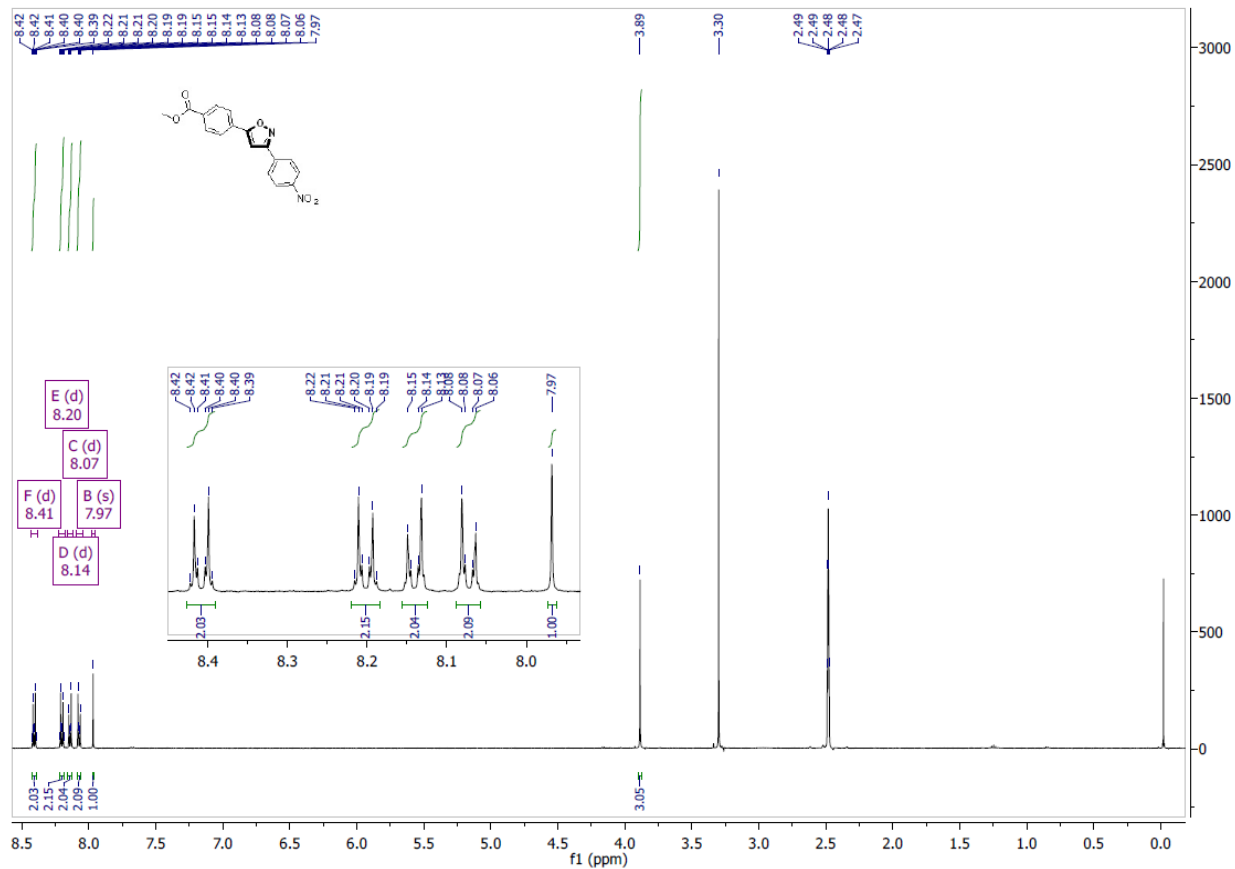
Figure S2.28: ^{1}H NMR spectrum of 3,5-isoxazole **78m**
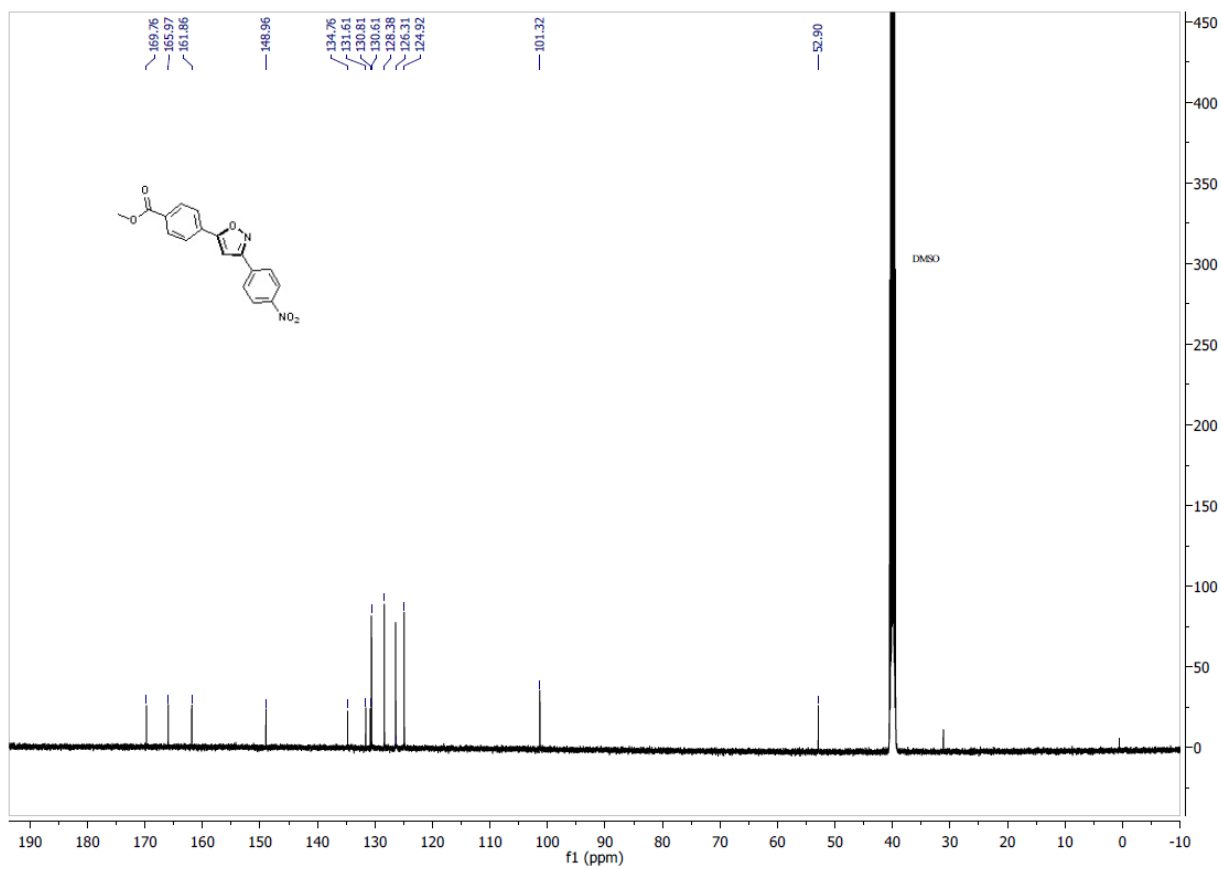
Figure S2.29. ^{13}C NMR spectrum of 3,5-isoxazole **78m**

3-(4-nitrophenyl)-5-(4-(4,4,5,5-tetramethyl-1,3,2-dioxaborolan-2-yl)phenyl)isoxazole (78n)
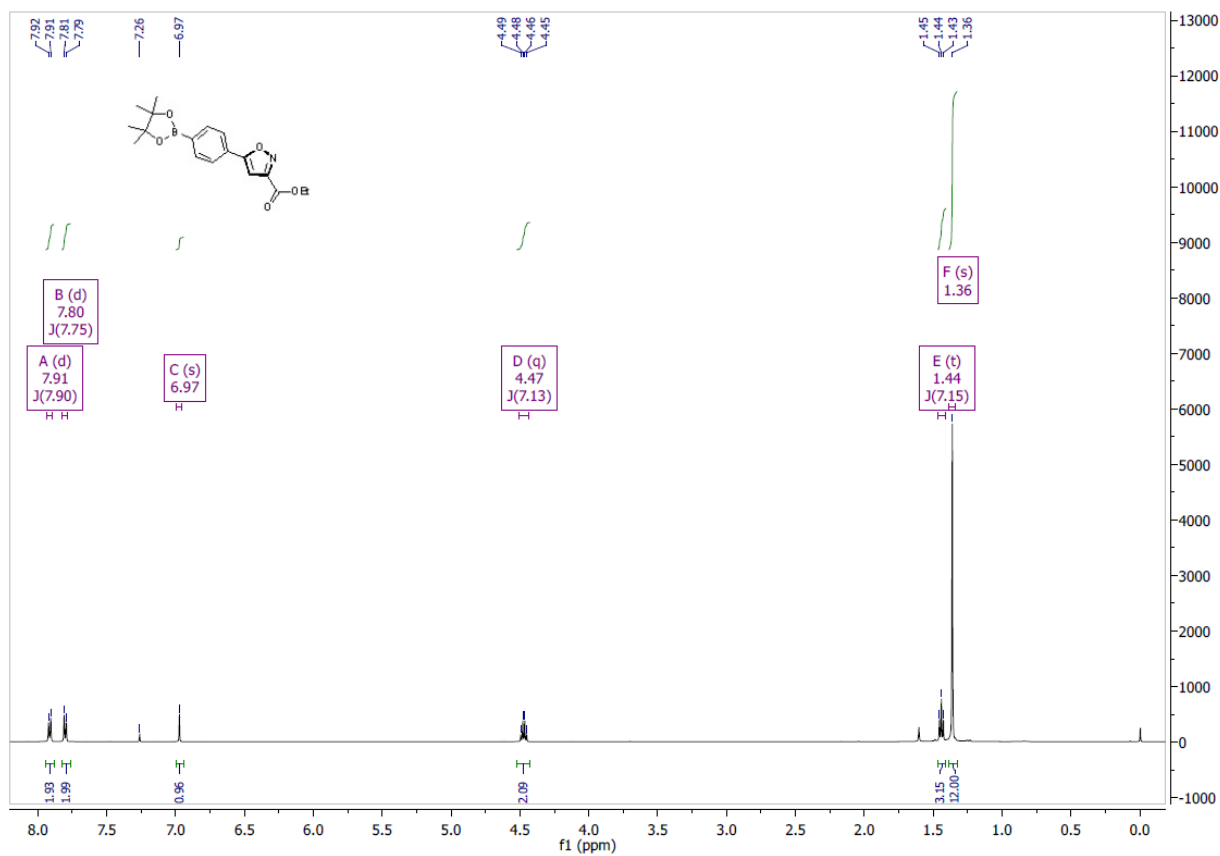
Figure S2.30. ^{1}H NMR spectrum of 3,5-isoxazole **78n**
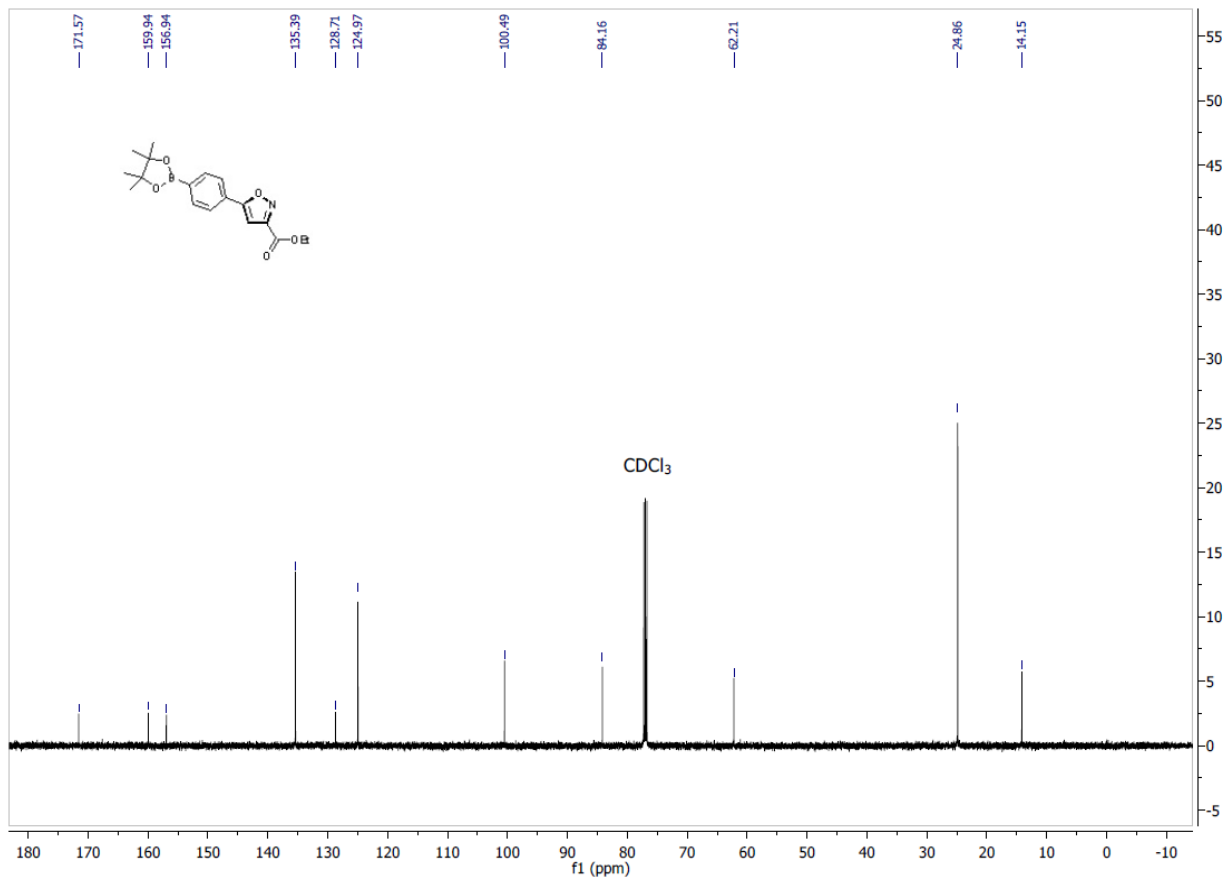
Figure S2.31: ^{13}C NMR spectrum of 3,5-isoxazole **78n**

Ethyl 5-(4-(dimethylamino)phenyl)isoxazole-3-carboxylate (78o)
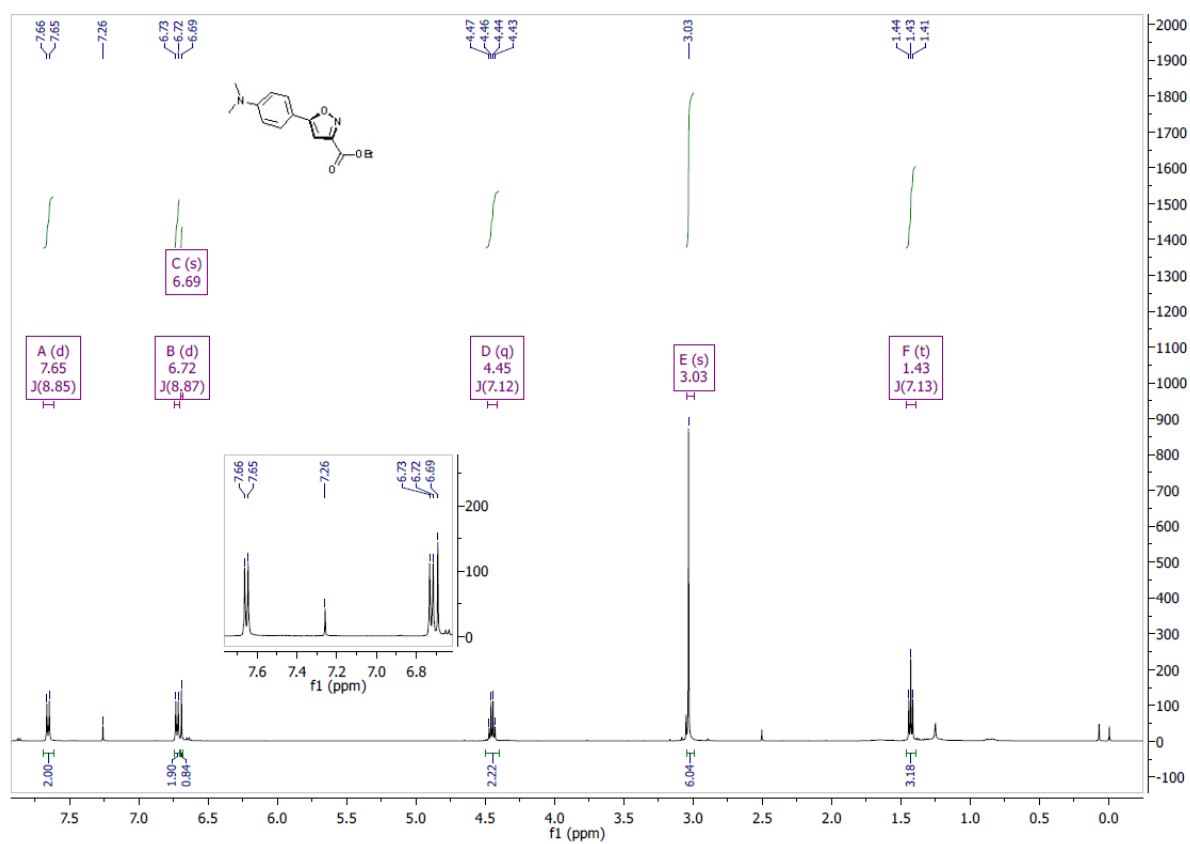
Figure S2.32: ^{1}H NMR spectrum of 3,5-isoxazole **78o**
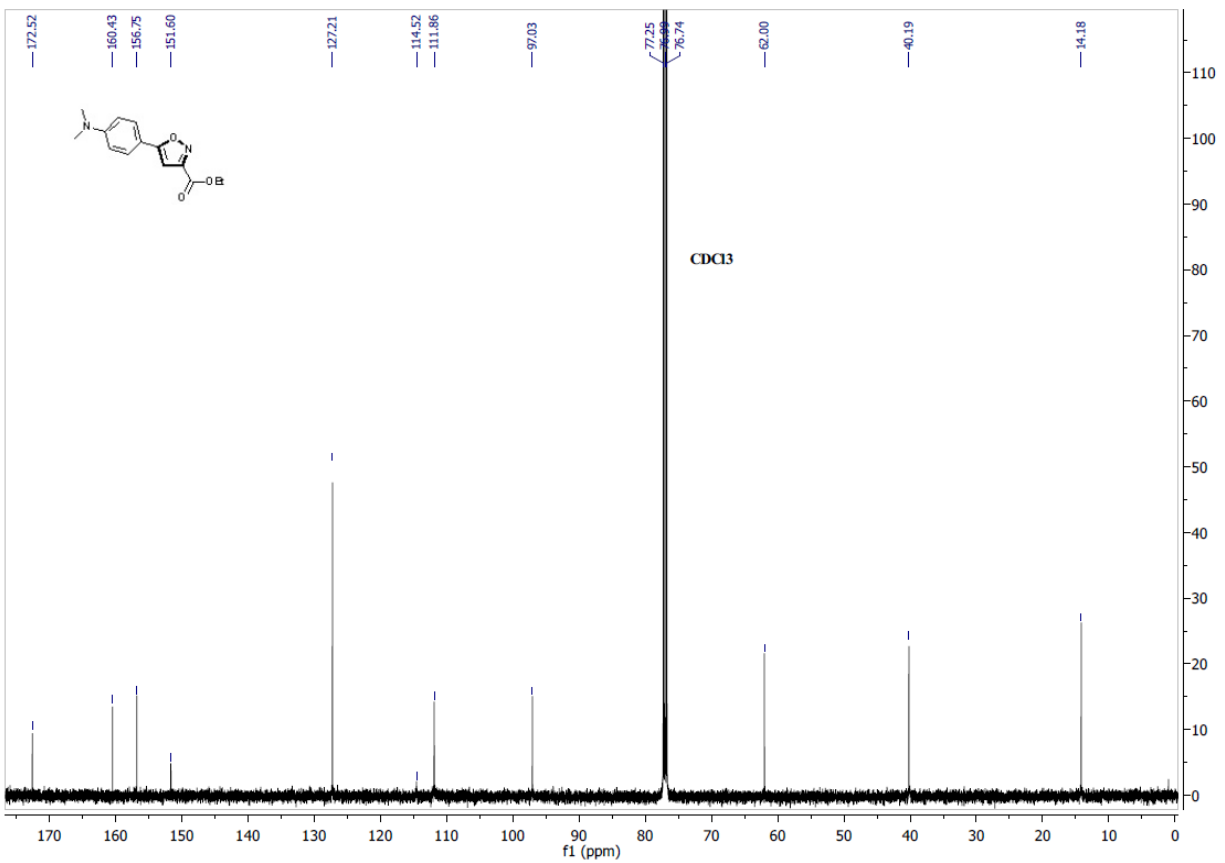
Figure S2.33. ^{13}C NMR spectrum of 3,5-isoxazole **78o**

ethyl 5-(3,5-dimethoxyphenyl)isoxazole-3-carboxylate (78p)
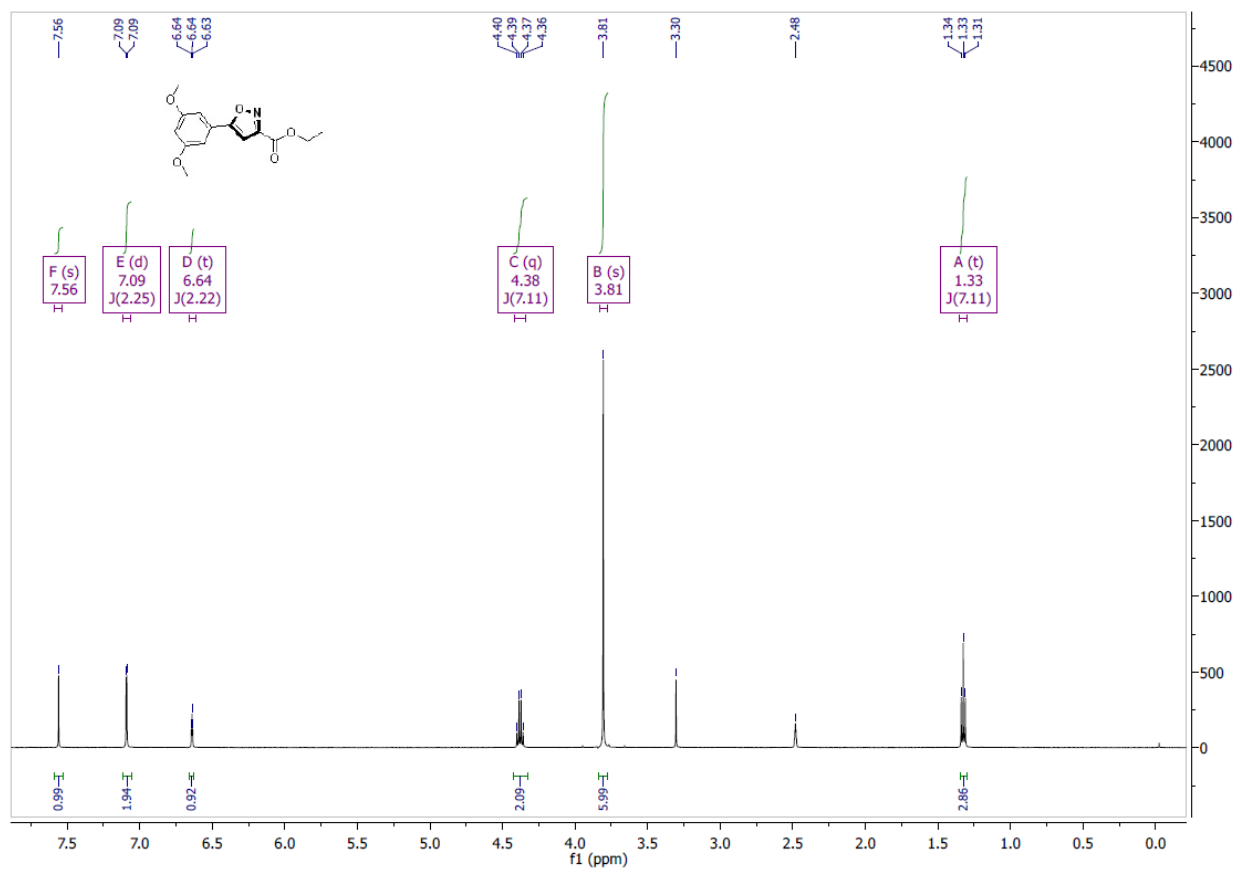
Figure S2.34. ^{1}H NMR spectrum of 3,5-isoxazole **78p**
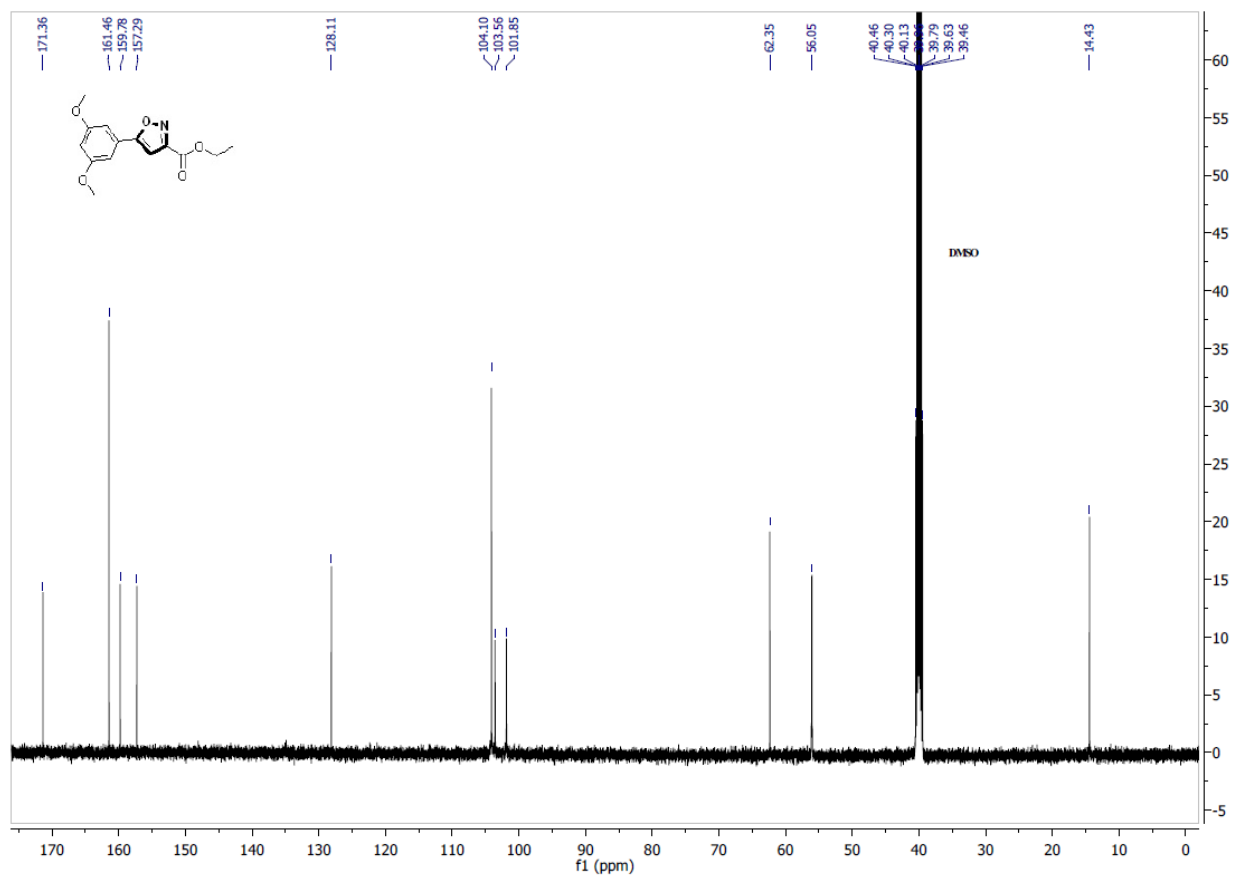
Figure S1.35: ^{13}C NMR spectrum of 3,5-isoxazole **78p**

5-(3,5-dimethoxyphenyl)-3-(4-nitrophenyl)isoxazole (78q)
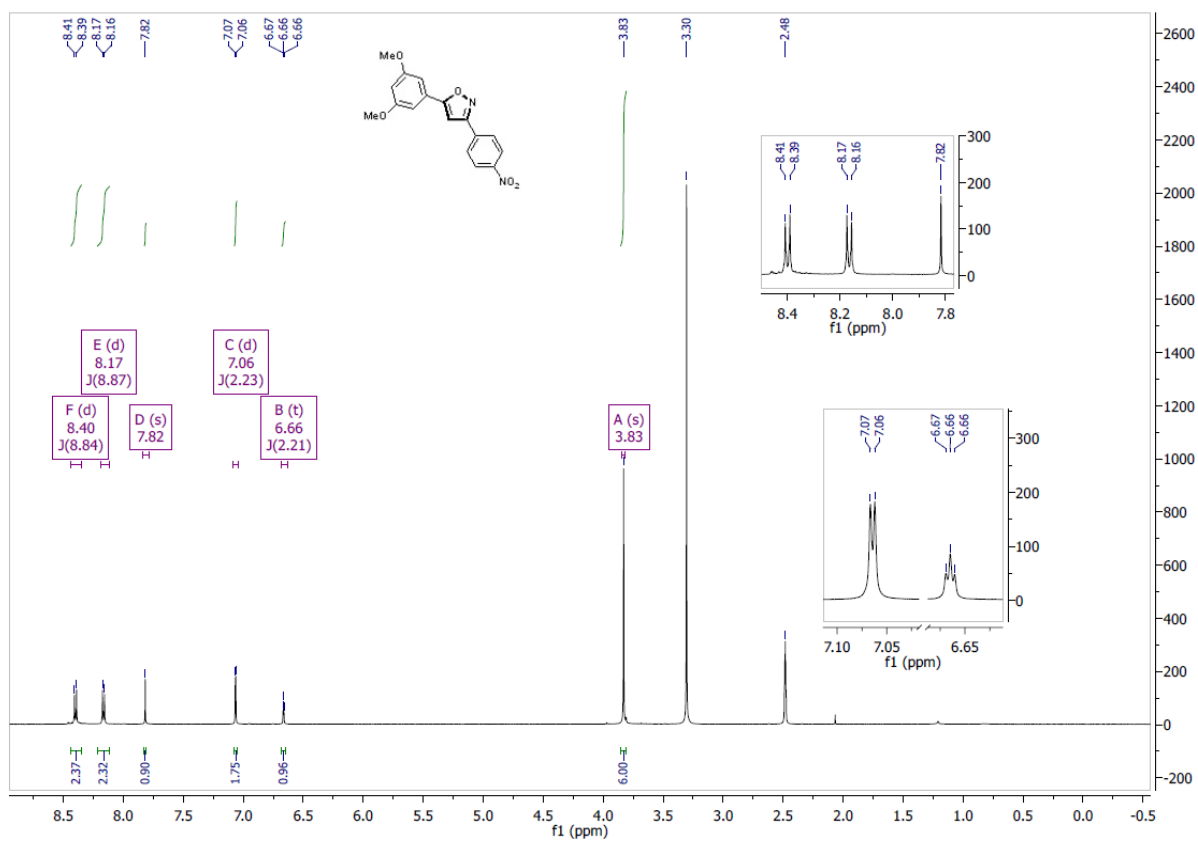
Figure S2.36: ¹H NMR spectrum of 3,5-isoxazole **78q**
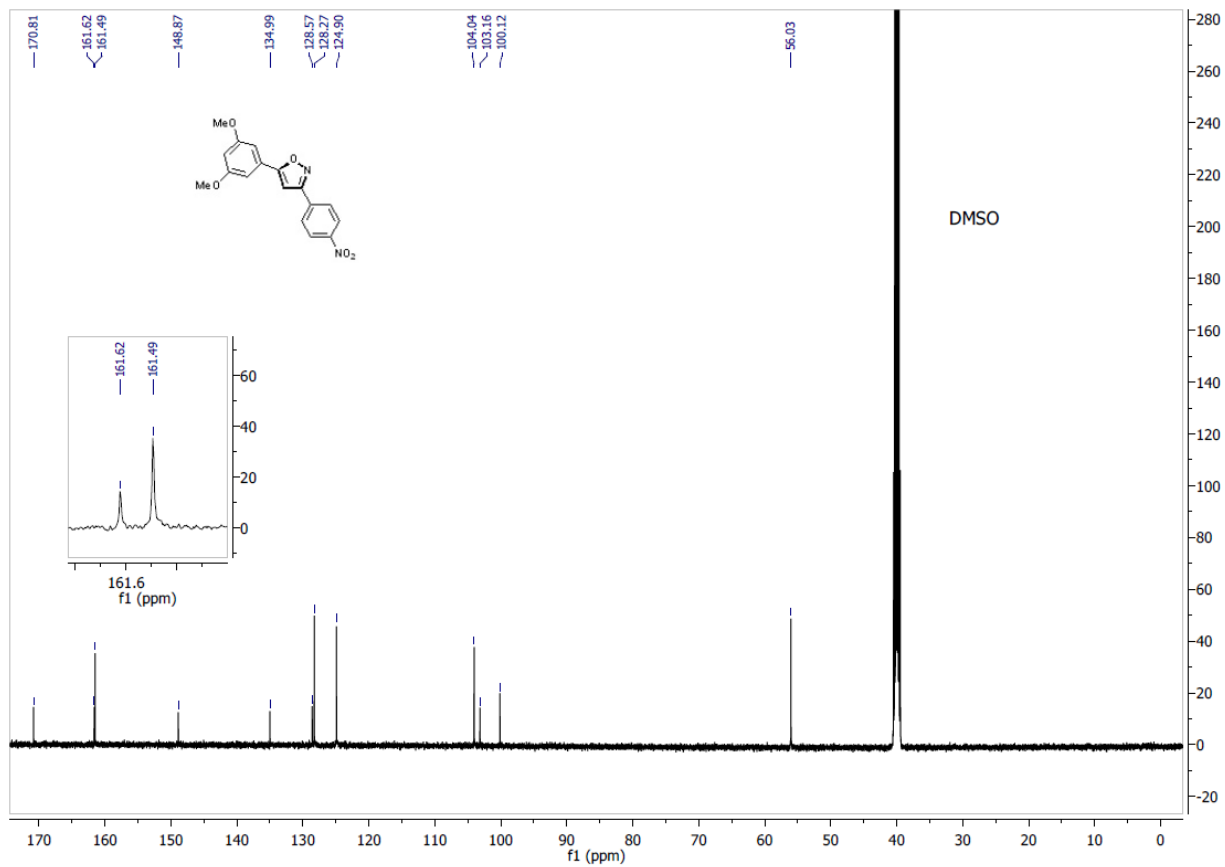
Figure S2.37: ^{13}C NMR spectrum of 3,5-isoxazole **78q**

3-(4-nitrophenyl)-5-(pyridin-2-yl)isoxazole (78r)
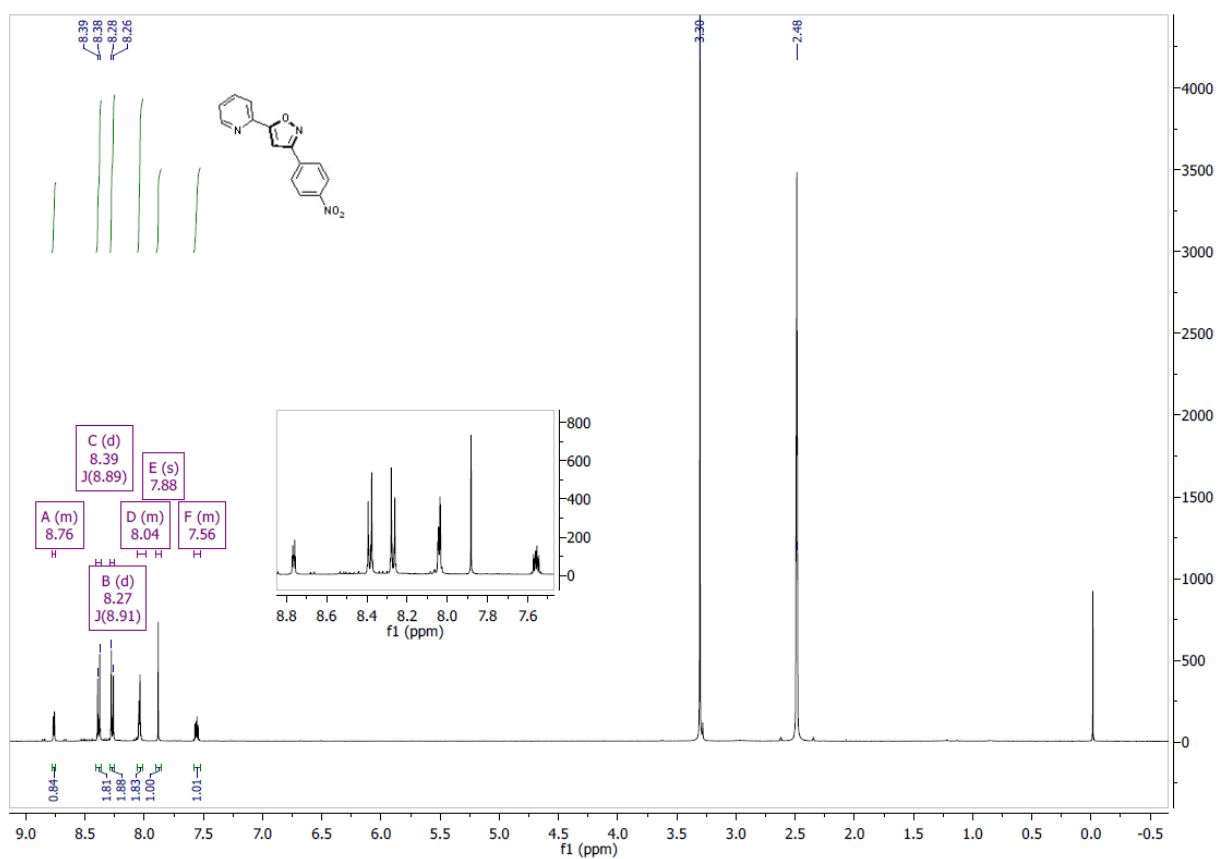
Figure S2.38: ^{1}H NMR spectrum of 3,5-isoxazole **78r**
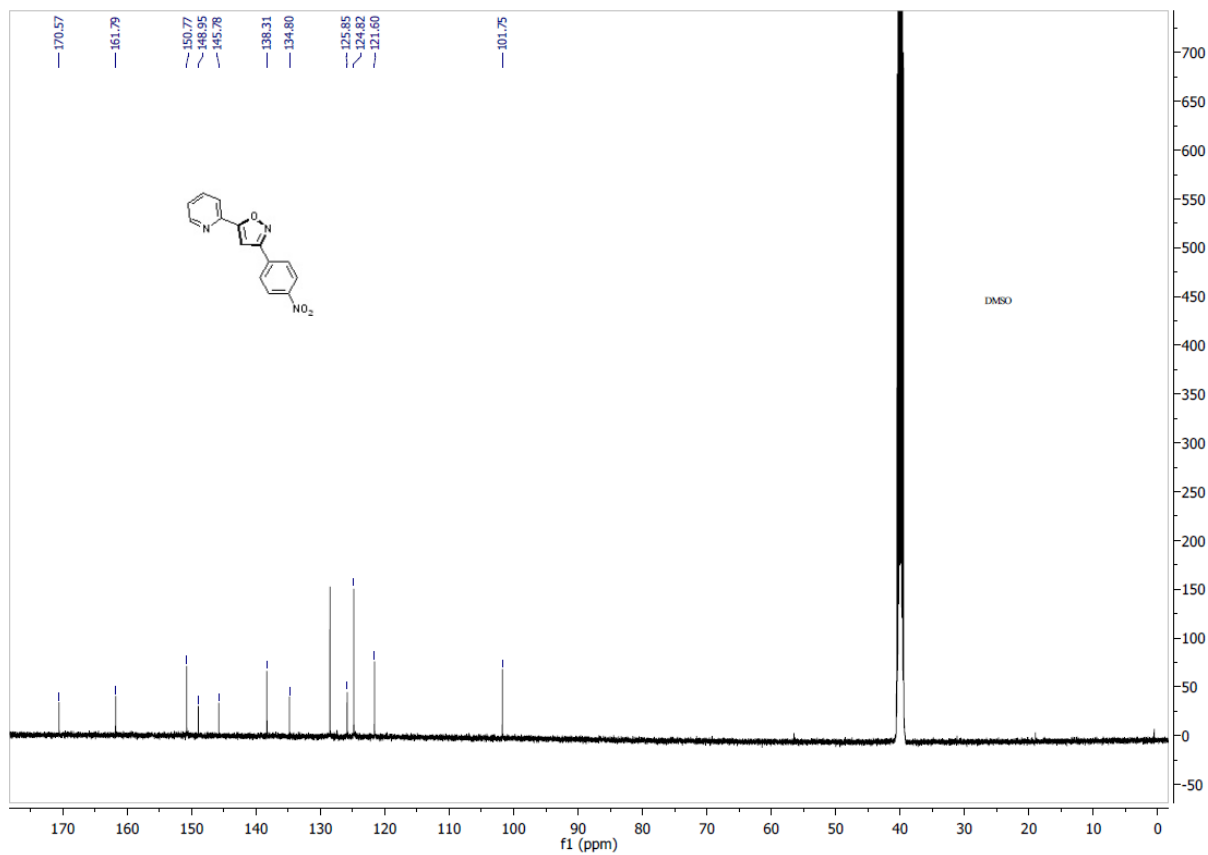
Figure S2.39: ^{13}C NMR spectrum of 3,5-isoxazole **78r**

Ethyl 5-(pyridin-2-yl)isoxazole-3-carboxylate (78s)
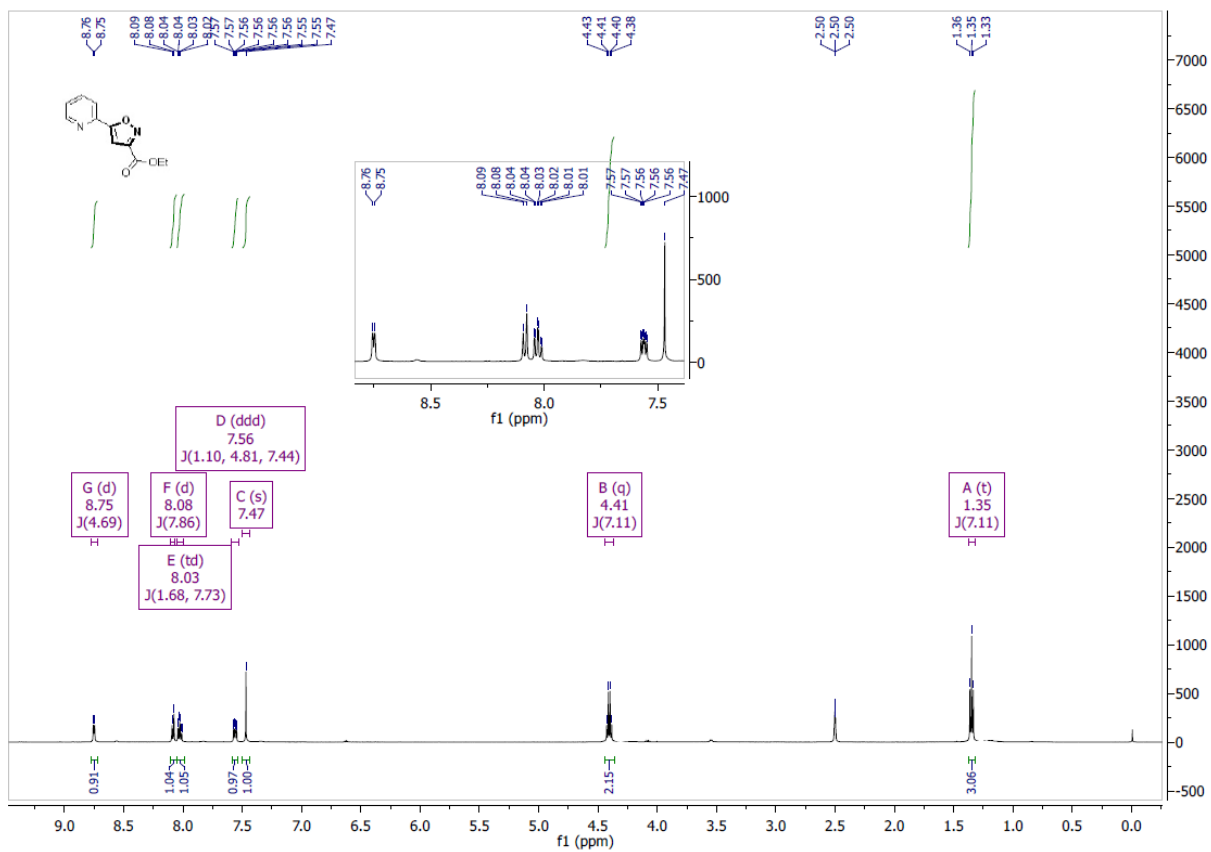
Figure S2.40. ^{1}H NMR spectrum of 3,5-isoxazole **78s**
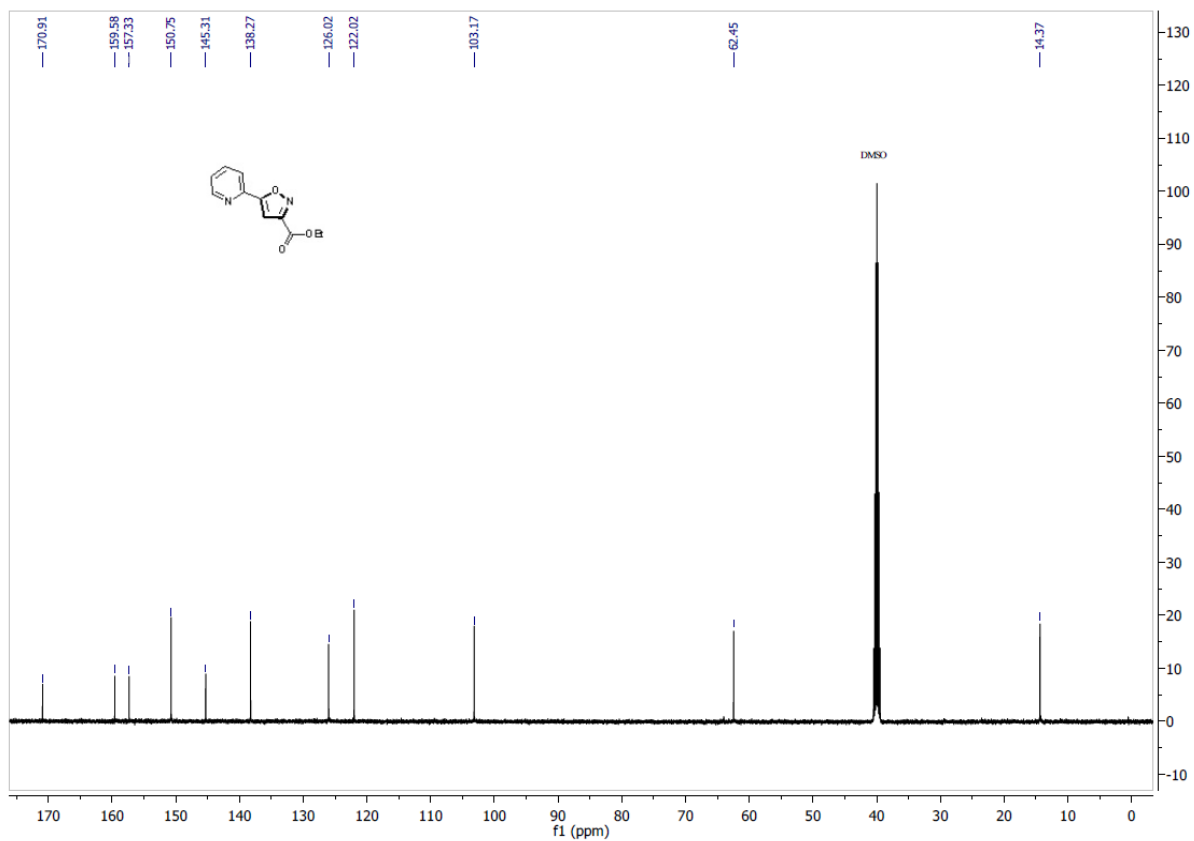
Figure S2.41. ^{13}C NMR spectrum of 3,5-isoxazole **78s**

2.8.13. Solid-state characterization of the reaction crude

| 79d | 80b | | 78e |
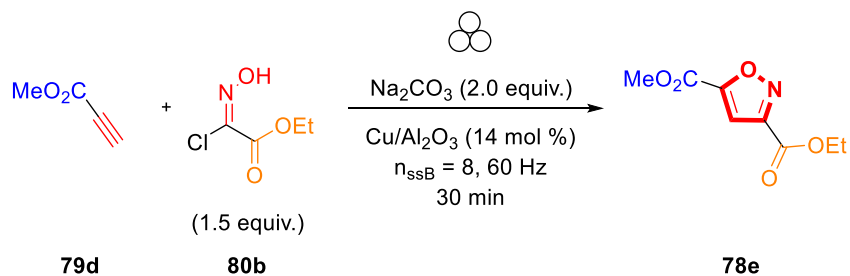
The solid crude for the synthesis of 3,5-Isoxazole **78e** was analyse by FT-IR spectroscopy and MALDI-TOF MS to determine that **78e** was synthesized by the effect of mechanical energy. As a result, 3,5-Isoxazole **78e** was synthesized according to **PS3,** but no isolation was attempted and the solid crude was analyse by FT-IR and MALDI-TOF MS with no addition of solvent .

2.8.13.1. FT-IR Spectra comparison.
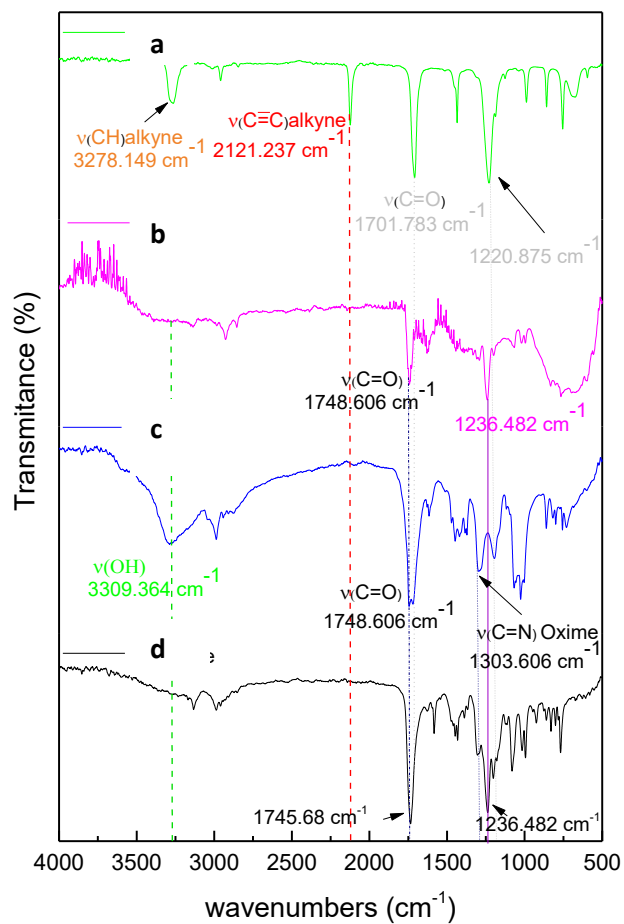
Figure S2.42: FT-IR spectra of the 3,5-isoxazole **78e** crude.

From top to bottom a) Methyl propiolate **79d**. b) **78e** crude isoxazole sample. c) (E,Z)-2-chloro-2-(hydroxyimino)acetate **80b** d) Isolates sample of isoxazole **78e**

2.8.13.2. MOLDI-TOF MS
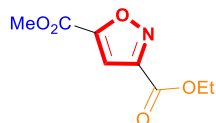
78e

Calculated m/z for (C8H9O5N). m/z=199.048 found 199.051
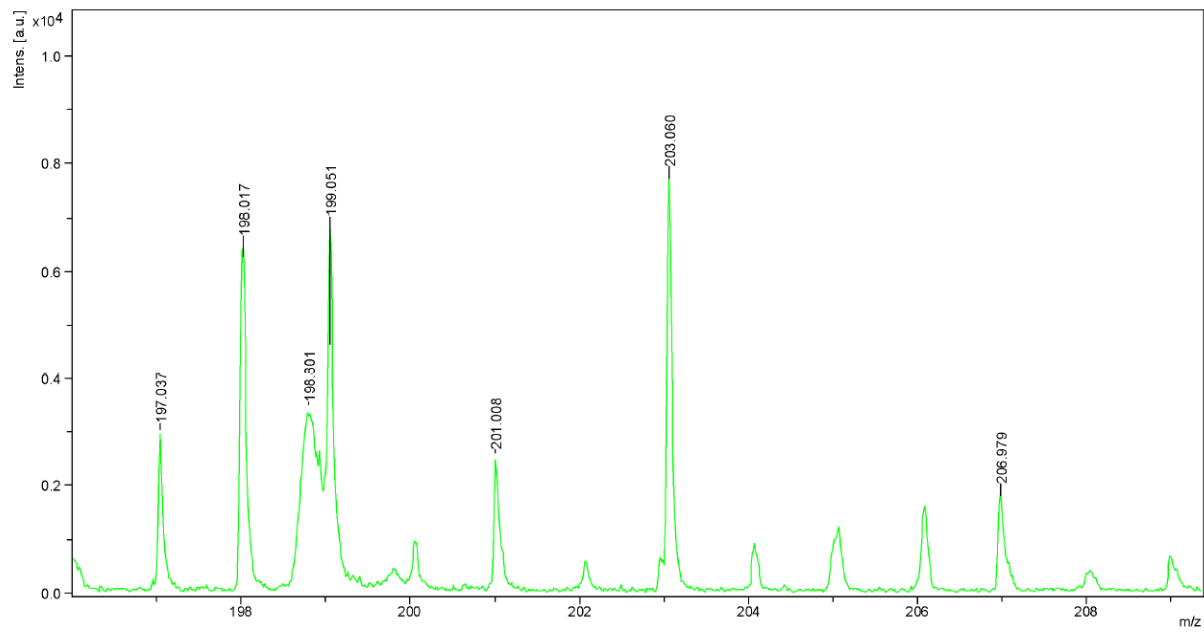
Figure S2.43: MALDI-TOF MS spectra of solid crude product 78e

Chapter 3- Mechanochemical Desymmetrization of Unbiased Bis- and Tris-alkyne to Access 3,5-Isoxazoles-alkyne Adducts and Unsymmetrical Bis-3,5-isoxazoles

3.1. Abstract

A mechanochemical desymmetrization of symmetrical bis- and tris-alkynes by a controlled 1,3-dipolar cycloaddition reaction using nitrile oxide dipoles (NOs). This operationally simple protocol allows access to 3,5-isoxazole-alkyne adducts from easily prepared or commercially available symmetrical bis- and tris-alkynes in moderate to excellent yield. In addition, we have highlighted the synthetic utility of 3,5-isoxazole-alkyne by developing a route to access, for the first time, β-ketoenamine-alkyne derivatives and unsymmetrical bis-3,5-isoxazoles.

3.2. Introduction

Desymmetrizations are synthetic strategies frequently employed in the synthesis of natural products, biologically active substances, and novel organic materials.[1,2] This modification results in the loss of symmetry elements within a molecule, such as a mirror plane, an axis of rotation, or a center of inversion.[3]

A limited number of synthetic methodologies demonstrate access to 3,5-isoxazole-alkyne adducts **91** by controlled 1,3-dipolar cycloaddition from unbiased bis- and tris-alkyne **88** and nitrile oxide dipoles (NOs) **90*** (**Figure 3.1a**).[4-8] To date, desymmetrization of bis- and tris-alkyne has focused primarily on CuAAC (Copper Azide-Alkyne Cycloaddition) to form 1,4-triazole-alkyne adducts **94** (**Figure 3.1b**).[3,9-14] In this regard, the Fokin, Zhou, and Stephenson groups demonstrated that in a 1:1 mixture of bis-alkyne and azide, there is the preferential formation of symmetrical bis-1,4-triazoles **95** over mono-1,4-triazoles **96** (**Figure 3.1b**).[15-18] These investigations highlight the limited selectivity achieved by cycloaddition reactions in solution-based methods. Common synthetic strategies to desymmetrize symmetrical substrates rely on using an excess of one of the substrates or using protecting groups, which decreases the synthesis's atom efficiency.[5, 9-13] Consequently, developing sustainable, efficient, and practical methodologies to improve atom economy and access novel chemical space from ubiquitous symmetrical substrates is desirable.[20-25]

a) **Control Desymmetrization of Unbiased Symmetrical bis- or tris-alkyne**
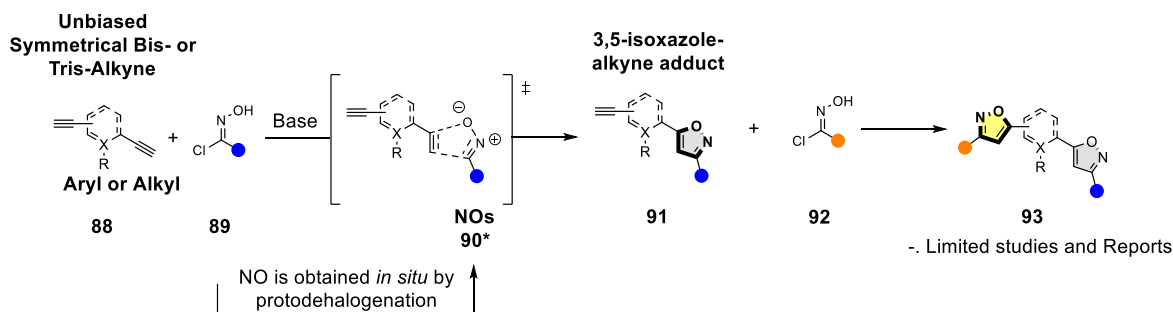
b) **CuAAC Kinetic Investigations (Fokin, Zhour and Stephenson Group)**

Figure 3.1: Limitation of solution-based desymmetrization of bis-and tris-alkynes by cycloaddition reactions.

Mechanochemical desymmetrization represents a concrete extension to previous desymmetrizations developed by solution-based methods.[26-27] For example, Štrukil *et al.* reported a mechanochemical click desymmetrization of aromatic diamines **97** to form unsymmetrical bis-thioureas **98** in quantitative yields (**Figure 3.2a**).[28-30] Similarly, Lanzillotto *et al*. demonstrated a mechanochemical desymmetrization of CDI (1,1'-carbonyldiimidazole) **100** to form carbamates **99** (**Figure 3.2b**).[31] Seo *et al*. reported a stepwise arylation of symmetrical dibromo arenes **101** by a mechanochemical Suzuki-Miyaura cross-coupling to obtain unsymmetrical arylated systems **102** (**Figure 3.2c**).[32] Our group previously reported the mechanochemical synthesis of 3,5-disubstituted isoxazoles by 1,3-dipolar cycloadditions.[33] However, mechanochemical desymmetrizations by a selective 1,3-dipolar cycloaddition reaction to desymmetrize symmetrical bis- or tris-alkynes **103** remains unstudied (**Figure 3.2d**). Herein, we report a selective, scalable, protecting-group-free, and atom-efficient mechanochemical desymmetrization of bis- and tris-alkynes **103** to access 3,5-isoxazole-alkyne adducts **105**. This protocol demonstrates compatibility for diverse bis- and tris-alkynes **103** and does not require protecting groups, excess bis- or tris-alkyne substrate **103**, or excess hydroxyimidoyl chloride **104**. Additionally, we demonstrate the utility of this methodology for the first modular synthesis of unsymmetrical bis-3,5-isoxazoles derivatives **107** (**Figure 3.2d**).

a) Štrukil *et al. -* **Desymmetrisation of Aromatic Diamines and**
Synthesis of Non-symmetrical Thiourea Derivatives by Click-mechanochemistry
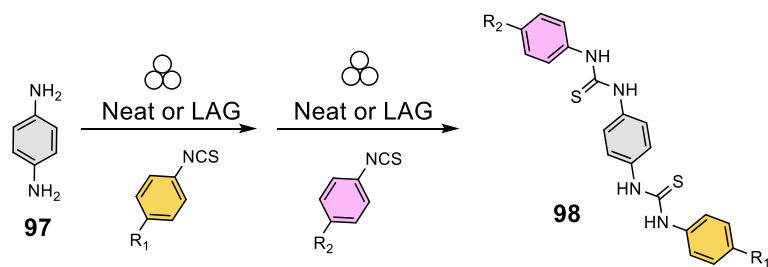
b) Lanzillotto *et al.-* **Mechanochemical 1,1′-Carbonyldiimidazole-Mediated Synthesis of Carbamates**
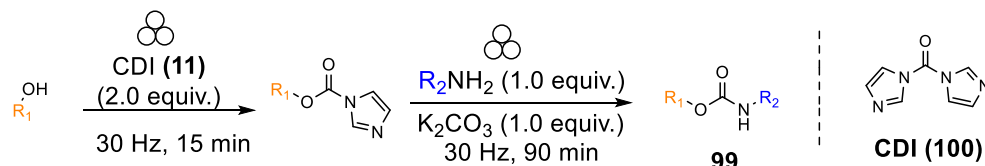
c) Seo *et al.-* **Selective Mechanochemical Monoarylation of Unbiased Dibromoarenes by in Situ Crystallization**
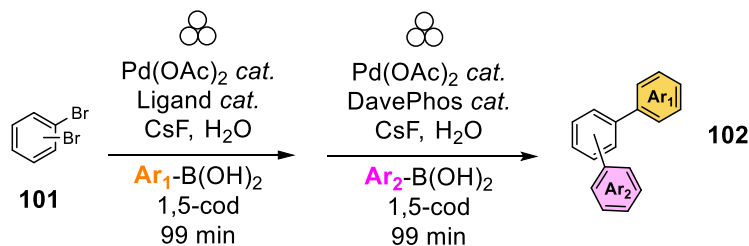
d) ***This work*** *-* **Mechanochemical Desymmetrization of Unbiased Bis- and Tris-alkynes**
to Access 3,5-Isoxazoles-alkyne Adducts and Unsymmetrical Bis-3,5-isoxazoles
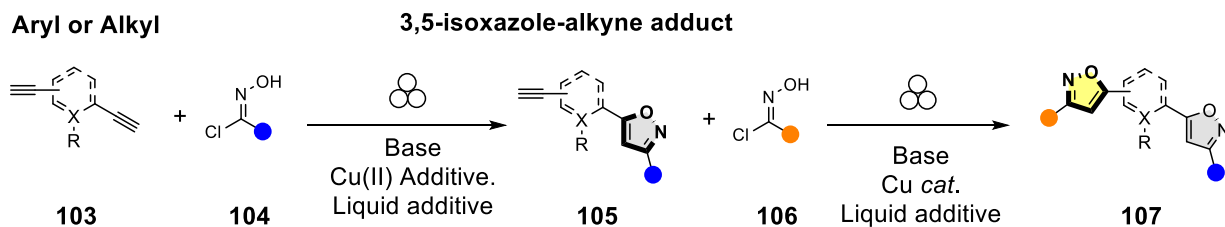
Figure 3.2. Mechanochemistry in the desymmetrization of symmetric organic molecules.

3.3. Results and Discussion

3.3.1. Mechanochemical desymmetrization optimization and optimization

Our investigations began by optimizing the desymmetrization of the symmetrical solid aromatic bis-alkyne **103a** with ester hydroxyimidoil chloride **104a** to form the 3,5-isoxazole-alkyne adduct **105a** (**Table 3.1**). All reactions were performed in a Pulverisette 7 mill, with reactants in a stainless-steel (SS) jar and eight SS balls (~32 g) of 1 cm diameter for 60 min at 60 Hz. We first evaluated the effect of stoichiometry in the reaction conditions; the desired product **105a** can be obtained selectively without the need to use an excess of either the aromatic bis-alkyne **103a** or ester hydroxyimidoyl chloride (**104a, Table 3.1,** entries 2-4). We attempted to improve the performance of the reaction by screening different additives with Lewis acid character (entries 5-9**, Table 3.1**). These additives can accelerate the cycloaddition *via* π-complexation with the alkyne moiety.[33,34-37] Using 1.0 equivalent of $Cu(NO_3)_2 \cdot 2.5\ H_2O$ improves the selectivity favoring the formation of the desired 3,5-isoxazole-alkyne adduct **105a** over the undesired symmetrical bis-3,5-isoxazole **108** (entry 7**, Table 3.1**). Other nanocomposites and metal additives such as Cu/Al_2O_3, $ZnCl_2$, and $IrCl_3 \cdot xH_2O$ were detrimental to the desymmetrization, promoted the formation of symmetrical bis-3,5-isoxazole **108a,** or the dimerization of the NOs to obtain undesired furoxans (entries 6-9). In addition to the plausible complexation between Cu(II) and the alkyne moiety, $Cu(NO_3)_2 \cdot 2.5\ H_2O$ may serve as a solid-state diluting agent that homogenizes the mixture, promoting the desymmetrization and the formation of the 3,5-isoxazole-alkyne adduct **105a**.[38-42] Increasing substrate dilution by using grinding auxiliary agents (GAAs) such as NaCl, KCl, or Al_2O_3 in combination with $Cu(NO_3)_2 \cdot 2.5\ H_2O$ were ineffective, and the 3,5-isoxazole-alkyne adduct **105a** was obtained in lower yields (entries 10-12).[39-44]

We investigated the effect of liquid-assisted grinding (LAG) in terms of the η parameter (defined as the ratio of the volume of liquid additive μL to the total mass of reactants in mg). LAG has been reported to accelerate mechanochemical reactions by facilitating mass-transport,[39,42,43,45] and enhancing reaction selectivity.[41,42,44-46] An increase in the reaction yield and selectivity for 3,5-isoxazole-alkyne adduct **105a** was achieved when using aromatic liquid additives (entries 1,15-16), where mesitylene was found to be the most effective additive (**Table 3.1**, entry 1). Only 0.25 μL/mg of mesitylene was required, and increasing the amount beyond this did not improve the yield and selectivity for the desired adduct **105a**. Other liquid additives having polar and protic properties, such as the case of methanol, ethyl acetate, or 2-methyl tetrahydrofuran, did not improve the yield or selectivity for **105a** (entries 13-14**,** and see experimental for full LAG screening in section PS1 **Table S3.4**). These observations suggest that mesitylene has the suitable polarity to accelerate the dehydrohalogenation of the hydroxyimidoyl chloride to form the corresponding NO.[47] The low polarity of the liquid additive accelerates cycloadditions by polarizing the NO and stabilizing the concerted transition state.[48] Additionally, π-π stacking between the mesitylene additive and bis-alkyne **103a** could promote the activation of the dipolarophile, making it more reactive toward NOs.[49,51,52]

Several reports utilized Cu(I) catalysis to accelerate 1,3-dipolar cycloaddition reactions.[51-58] In our case, *in situ* formation of Cu(I) by reduction of Cu(II) salts with sodium ascorbate or addition of Cu(I) complexes in sub-stoichiometric amounts were ineffective and lower selectivity and/or yields for the desired 3,5-isoxazole-alkyne **105a** were obtained (see experimental information for screening of Cu(I) catalyst in section PS1 **Table S3.7**).

Optimizations demonstrated that using equimolar amounts of bis-alkyne **103a** and hydroxyimidoyl chloride **104a** in combination with 2.0 equivalents of Na_2CO_3, 1.0 equivalent $Cu(NO_3)_2 \cdot 2.5\ H_2O$ and using mesitylene as a liquid additive were the optimal conditions to desymmetrize aromatic bis-alkyne.

Table 3.1. Optimization conditions for the mechanochemical desymmetrization of the bis-alkyne 103a

Entry	Condition	Yield [d] (105a)	Yield [d] (108a)	105a:108a [e]
1	No changes [a]	50	1	50:1
Effect of the stoichiometry of 1a and 2a				
2	1.5 equiv. of 104a	30	10	3:1
3	1.1 equiv. of 104a	30	10	3:1
4	2.0 equiv. of 103a	50	1	50:1
Effect of π-type Lewis Acid Additives				
5	No additive	34	4	8.5:1
6	Cu/Al$_2$O$_3$ (14 mol %)	33	10	3.3:1
7	Cu(NO$_3$)$_2$·2.5 H$_2$O (1.0 equiv)	30	2	15:1
8	IrCl$_3$·xH$_2$O	25	3	8.3:1
9	ZnCl$_2$ (1.0 equiv.)	9	4	2.3:1
Effect of GAA				
10	Al$_2$O$_3$ (150 wt %)	9	4	2.3:1
11	NaCl (150 wt%)	23	2	11.5:1
12	KCl (150 wt%)	17	2	8.5:1
Effect of LAG				
13	EtOAc [b]	36	3	12:1
14	EtOH [b]	30	2	15:1
15	Toluene [b], [c]	45	2	22.5:1
16	Xylenes [c]	45	2	22.5:1

[a] **Reaction conditions: 103a** (50 mg, 0.396 mmol, 1.0 equiv.), **104a** (60 mg, 0.396 mmol, 1.0 equiv.), Cu(NO$_3$)$_2$·2.5 H$_2$O (92.1 mg, 0.396, 1.0 equiv.), Na$_2$CO$_3$ (84 mg, 0.796 mmol, 2.0 equiv.), mesitylene (η = 0.25 µL/mg, ~72 µL) [b] (η = 0.5 µL/mg, ~144 µL) [c] (η = 0.25 µL/mg, ~72 µL) [d] Yield determined by 1H-NMR using 1,3,5-trimetoxybenzene (TMB) as an internal standard [e] **105a:108a** were determined by the integration of the crude ^{1}H-NMR signals. Complete optimization is reported in the experimental information **PS1**

We evaluated the effect of the optimized conditions on aromatic and alkyl bis- and tris-alkynes and hydroxyimidoyl chlorides with varied electronic profiles (**Figure 3.3**). It was observed that aromatic bis– or tris-alkynes (**103a-e**) displayed higher reactivity towards hydroxyimidoyl chlorides of opposite electronic nature; the highest yields are obtained when electron-neutral or deficient aromatic bis- and tris-alkynes **103a**, **103b**, **103e**, and **103f** were reacted with electron-rich hydroxyimidoyl chlorides **104e**. While electron-deficient aromatic **103c** and **103d** bis-alkynes best reacted with electron-deficient hydroxyimidoyl chlorides **104a**, **104b**, or **104c** (**Figure 3.3**). The electronic selectivity observed in aromatic bis-alkyne is explained by the increase in the polarizability of the 3,5-isoxazole-alkyne adduct compared to that of the symmetrical bis-alkyne substrate.[55,59,60]

Alkyl bis- or tris-alkyne have been investigated for CuAAC reactions due to their high degree of flexibility, stabilizing the Cu catalysts, accelerating intramolecular cycloadditions, and favoring the formation of symmetrical products.[16,61,62] In the case of mechanochemistry, the optimized conditions allowed to effectively desymmetrize alkyl bis- or tris-alkyne, and all 3,5-isoxazoles-alkyne adducts (**105p-s**) were obtained in good yields and with excellent selectivity (**Figure 3.3**, **103g-i**). However, the mesitylene liquid can be removed from the reaction conditions for alkyl systems **103g** and **103i,** as we observed lower yields and selectivity when the additive was used.

We compared the effect of the optimized mechanochemical conditions to reported solution-based approaches for the synthesis of adducts **105d** and **105o**, to observe the benefits of this mechanochemical methods in the synthesis of commonly found intermediates (In **Figure 3.3** we have highlighted the reported yields from the literature). Bonifazi's group reported the synthesis of 3,5-isoxazole adduct **105d** with an isolated yield of 18 % after using approximately 8 equivalents of their NO and after 16 h of reaction time.[5] In our case, we can obtain **105d** in 50 % yield, with less than 5 % of undesired symmetrical bis-3,5-isoxazole, with only a single equivalent of hydroxyimidoyl chloride **104d** and bis-alkyne **105a**, and in only 60 min. Saito's group reported the synthesis of adduct **105o** in 75 % after reacting about 10 equivalents of aromatic tris-alkyne **105f** with a single equivalent of **104e,** and after 72 h of reaction time.[7] Our mechanochemical conditions allow the synthesis of **105o** in 50 % yield, after 60 min, with only one equivalent of aromatic tris-alkyne **103f**. This comparison highlights the efficiency and convenience of our mechanochemical protocol to access 3,5-isoxazole-adducts, a valuable intermediate, in an atom-economical manner, with higher selectivity and shorter reaction times than those achieved by reports using solution-based thermal methods.

The scalability of the reaction was investigated for the aromatic bis-alkyne **103a** and alkyl bis-alkyne **103i**. The 1.0 g scale mechanochemical synthesis of 3,5-isoxazole-alkyne adduct **105e** from solid aromatic bis-alkyne **103a** showed a modest decrease in yield. In contrast, the 1.0 g scale synthesis of 3,5-isoxazole-alkyne adduct **105t** from liquid alkyl bis-alkyne **103i** showed no decrease in yield (**Figure 3.3**)**.**

We explain the formation of a single isoxazole moiety by considering the changes in physical state from liquid substrates to solid 3,5-isoxazole adducts and their differences in mass transfer. Liquid substrates are more reactive than solids because solid reagents have a limited mass transfer.[32,33,42,64-69] The risk for forming undesired symmetrical bis-isoxazoles or tris-isoxazoles products is limited under mechanochemical conditions due to phase transitions occurring during the reaction, specifically from a reactive liquid state of the bis-/tris-alkyne substrates to a less reactive solid-phase observed in the 3,5-isoxazole product. The selectivity achieved by changes in the physical state is observed for liquid substrates **103b**, **103c**, **103i**, and **103g** in which solid 3,5-isoxazole-alkyne products **105g**, **105h**, **105i**, **105p**, **105r**, and **105u** are always favored over the undesired symmetrical bis-3,5-isoxazole.

For solid bis-alkyne, the risk to form undesired symmetrical bis-isoxazoles is lowered due to the increased hardness of the 3,5-isoxazole-alkyne product compared to that of the substrates. The increase in hardness of the product limits mass and energy transfer as the reaction progresses, reducing the possibilities for subsequent cycloaddition in the free terminal alkyne.[67] This is observed for solid bis-alkyne systems **103a**, **103d**, **103e**,**103f,** and **103h**, in which the corresponding 3,5-isoxazole-alkyne adducts are always obtained with excellent selectivity.
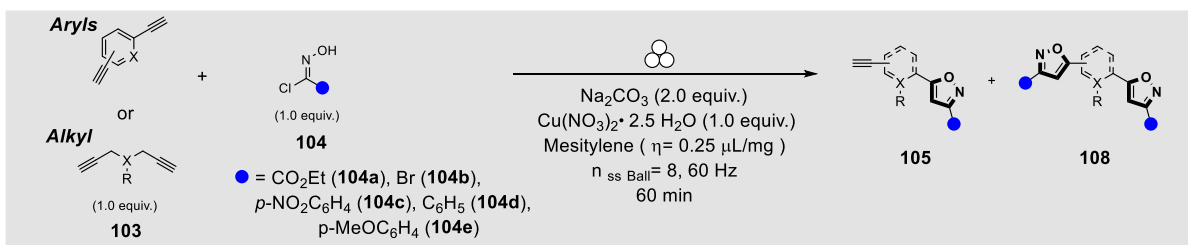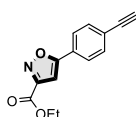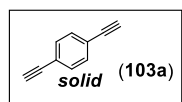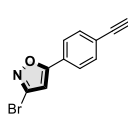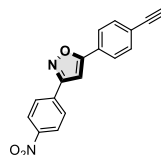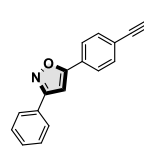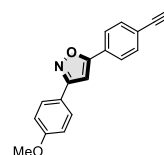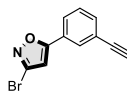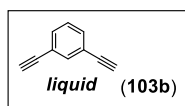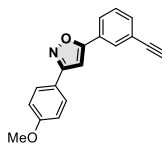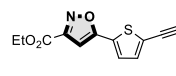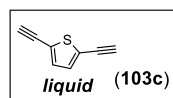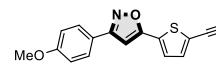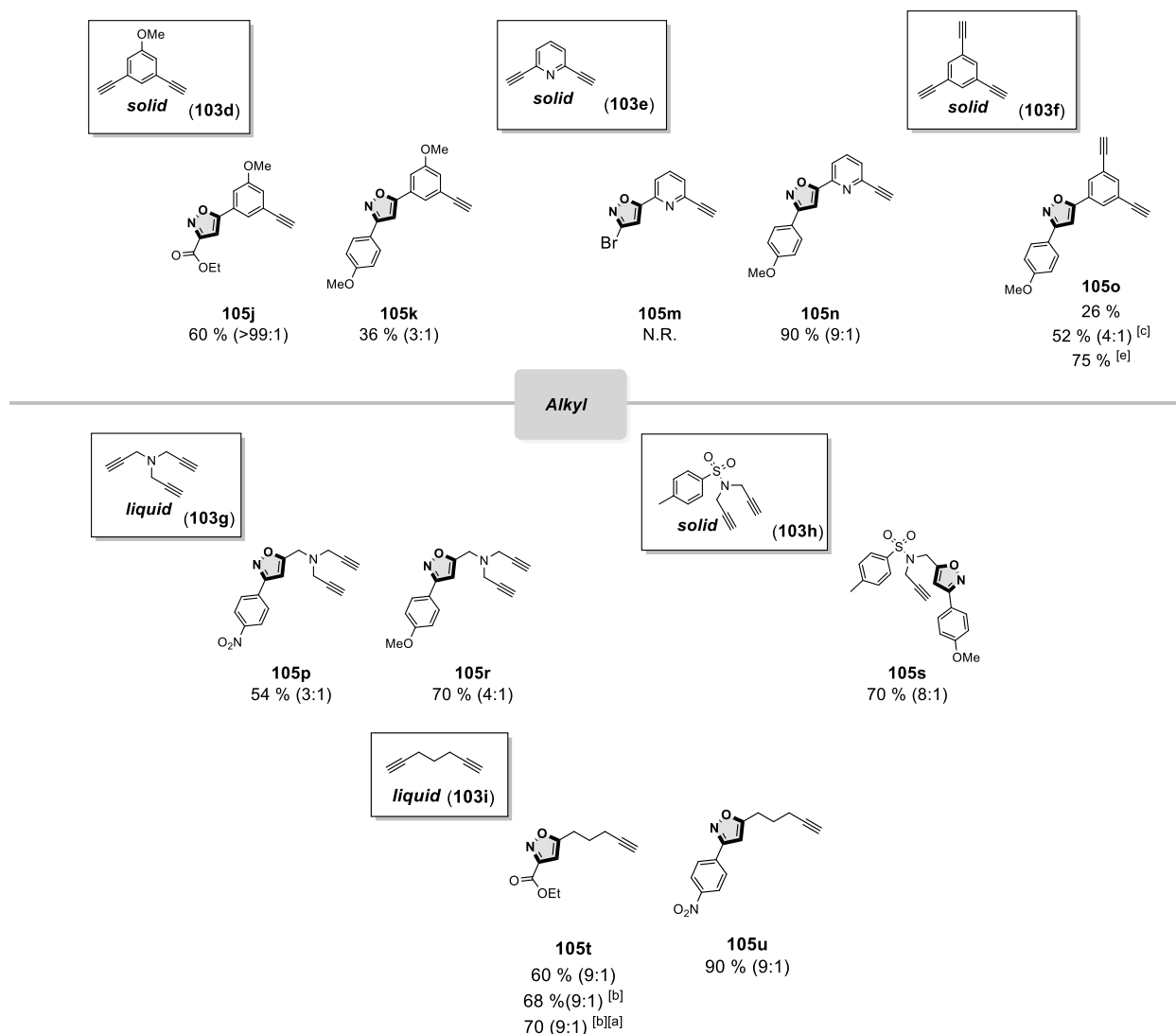
Figure 3.3. Scope for the mechanochemical desymmetrization of bis-alkynes and tris-alkynes to form 3,5-isoxazole-alkyne adducts.

All reported yields are isolated yields followed by ratios of **105**:**108** (mono 3,5-isoxazole (**105**): bis-3,5-isoxazole (**108**) were determined by ^{1}H-NMR of the crude product. *a* Reaction performed in a 1.0-gram scale of bis-alkyne. *b* Reaction performed in the absence of mesitylene liquid additive. *c* Results taken reported solution-based protocols for comparison (for **105d** ref: 5 and **105o** ref: 8).

To further highlight the selectivity obtained by mechanochemistry, we evaluated the effect of our optimized mechanochemical conditions and compared them to optimized solution-based conditions (see **experimental section** for reaction optimization in **section PS2**). In our solution-based optimization, we observed that solvents do not have an influence in selectivity (see **Table S4.8** in the experimental section for more details). Therefore, we proceeded with mesitylene as a solvent to best compare its effect when used as a liquid additive (η = 0.25 µL/mg) and as a solvent (η =45 µL/mg, 7 mL). Therefore, we first compare the desymmetrization of alkyl bis-alkyne **103h** to the corresponding 3,5-isoxazole-alkyne product **105s** by mechanochemical and solution-based conditions. Desymmetrization of the bis-alkyne **103h** was achieved

120

selectively by the optimized mechanochemical conditions, obtaining the 3,5-isoxazole-alkyne product **105s** in 70 % yield and with a selectivity of 8:1 favoring the 3,5-isoxazole adduct **105** after 60 minutes of milling (**Figure 3.4a**). In contrast, desymmetrization of alkyl bis-alkyne **103h** with bulk amounts of mesitylene solvent (η =45 µL/mg, 7 mL) produced the desired product **105s** in 32 % yield by ^{1}H NMR, with lower ratio of 2:1 favouring **105s** after 16 h at room temperature. While desymmetrization seems plausible with equimolar mixtures of bis-alkyne **103h** and **104e** by a solution-based approach, **105s** is obtained in low yields and poor selectivity (**Figure 3.4a**). From these results it can be stated that an excess amount of bis-alkyne substrate, large solvent volumes, and/or prolonged reactions times are required for solution-based conditions to obtain high yields, conversion, and selectivity for the desymmetrize product. The eviromental limitations imposed by solution-based methods becomes evident when comparing the E-factors for the developed mechanochemical process to the optimized solution-based process. The lower E-factor achieved by the mechanochemical process demonstrates the environmentally benign nature of the reported mechanochemical protocols compared to the solution-based approach (**Figure 3.4a**). The removal of the bulk amount of solvent and the low stoichiometry used is a crucial feature of mechanochemical reactions and is critical to reducing waste-production and enhancing the atom economy of the reaction without hampering selectivity.

To further elucidate the differences in selectivity achieved by mechanochemistry in contrast to solution-based conditions, we performed competition experiments between the symmetrical bis-alkyne **103b**, 3,5-isoxazole adduct **105g**, and electron-rich hydroxyimidoyl chloride **104e** (**Figure 3.4b**). Under mechanochemical conditions, it was observed that 3,5-isoxazole-alkyne adduct **105g** was obtained selectively over **108g** with ratios of about 4.7:1. The optimized solution-based method demonstrated the preferential formation of the symmetrical bis-3,5-isoxazole **108g**. These results confirm that by using mechanochemistry; higher selectivity and yields are achieved over the corresponding solution-based conditions for a variety of substrates. The selectivity observed stems from the differences in mixing ability between the more reactive liquid substrate to that of the less reactive solid product. The described competition experiments emphasizes mechanochemistry's impact in achieving unique reactivity modes to access unexplored chemical space with low waste-production.

A) Selectivity comparision using optimized conditions
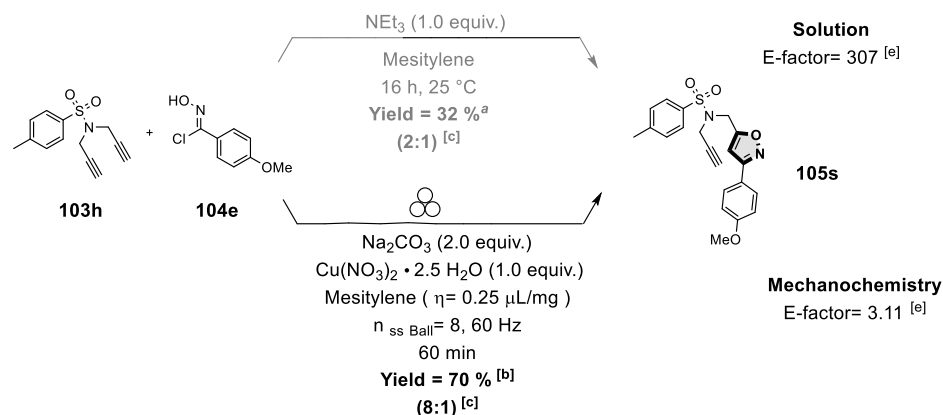
B) Kinetic comparision
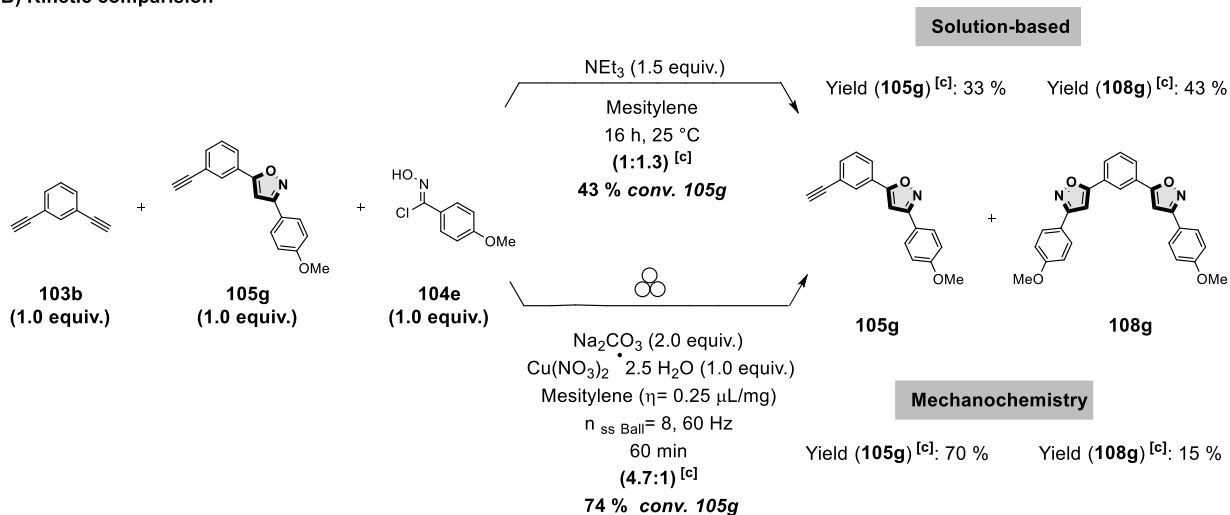
Figure 3.4. Comparative effect of mechanochemical to solution-based conditions for the desymmetrization of bis-alkynes and tris-alkynes

a ^{1}H-NMR Yield of **105s** when the reaction is performed by η= 45 µL/mg, 7 mL of mesitylene, for a detailed procedure, see experimental section. *b* Isolated yield of product **105s** *c* Ratios of **105g:108g** (mono to bis-3,5-isoxazole) determined by the integration of the signals in the crude ^{1}H-NMR. *d* E-factor calculations are confirmed in **the experimental section PS4**.

To exploit the formation of a new carbon-carbon bond (C_1-C_2) resulting from the cycloaddition, we investigated the N-O bond reduction of the isoxazole to access a β-ketoenamine-alkyne derivative (**Figure 3.5**). Although β-ketoenamine motifs are encountered in natural products, materials, and are versatile intermediates, there are no reports on the synthesis of β-ketoenamine-alkynes.[70-80] We studied the reduction of 3,5-isoxazole-alkyne **105e** using Mo(CO)₆, a conventional reducing agent for isoxazoles.[81-83] We found that N-O reduction to obtain β-ketoenamine **109** occurs in excellent yields when performing the reduction at 90 °C and using 1.5 equivalents of Mo(CO)₆ (**Figure 3.5**). This route achieves a convenient method to access β-ketoenamines with an alkyne handle that can be further modified.

122
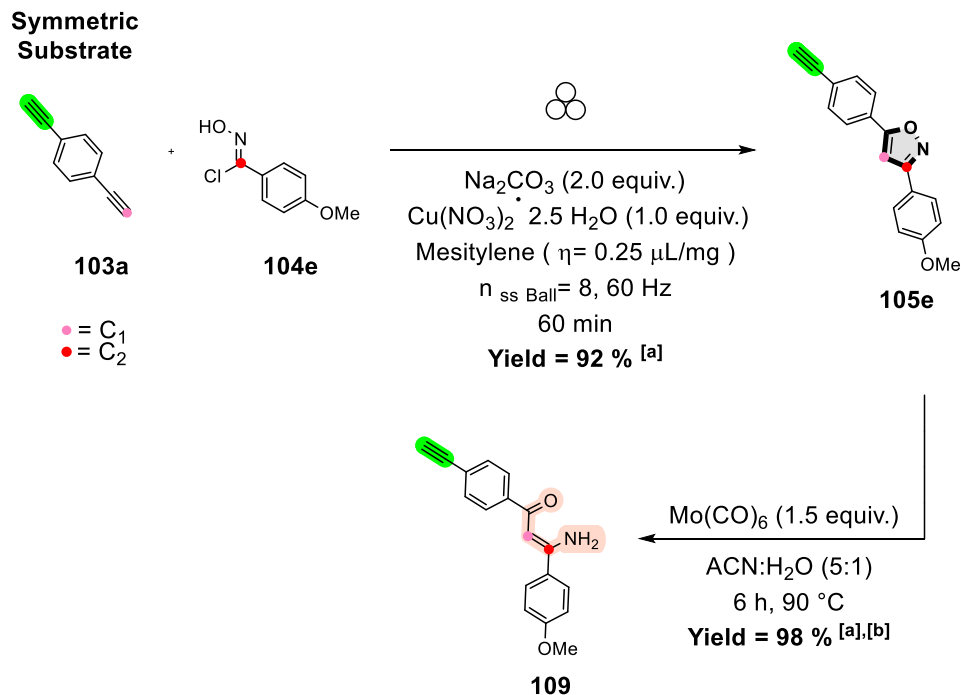
Figure 3.5. Synthesis of β-ketoenamines-alkyne from symmetrical bis-alkyne systems.

---

a Reported yields are isolated yields. *b* Reaction conditions for reduction: **105e** (0.18 mmol, 1.0 equiv.), Mo(CO)$_6$ (0.27 mmol, 1.5 equiv.), Acetonitrile:H$_2$O (5.0 mL: 1.0 mL) and heating the mixture at 90 °C for 6 h.

3.3.2. Mechanochemical synthesis of unsymmetrical bis-3,5,-isoxazoles

The proposed desymmetrization provides the template to synthesize, in a modular manner, unsymmetrical bis-3,5-isoxazoles **110** under solvent-free conditions. We observed that the optimized conditions for desymmetrization of **103** and previously reported conditions were ineffective for adding a second 3,5-isoxazole moiety (see experimental section for optimization conditions in section PS7). [33] The reaction was insensitive to electronic properties of reactants as coupling of solid 3,5-isoxazole-alkynes with EWG **105a** or EDG **105e** with either hydroxyimidoyl chlorides bearing EWG **109a** or EDG **109e** did not yield the corresponding product and only starting material was recovered.

A) Synthesis of unsymmetrical aromatic bis-3,5-isoxazole
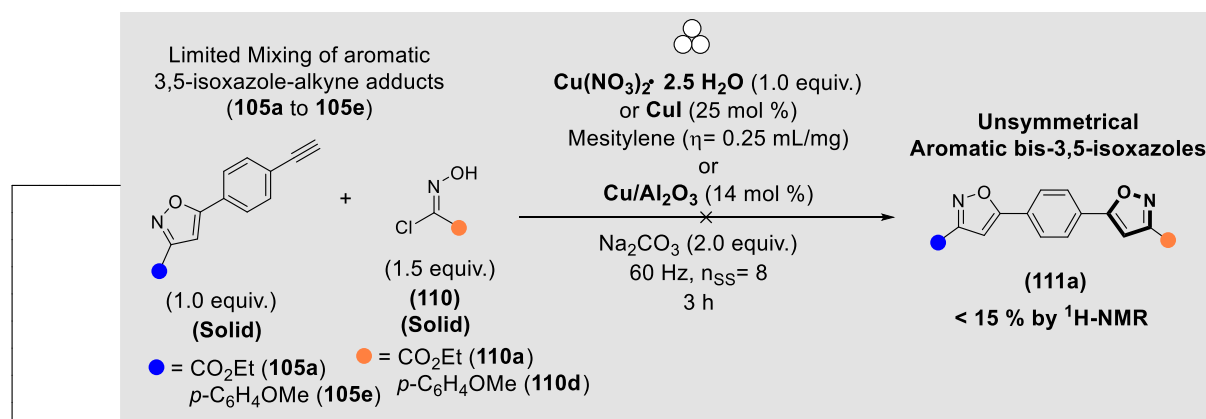
B) Synthesis of unsymmetrical alkyl bis-3,5-isoxazole
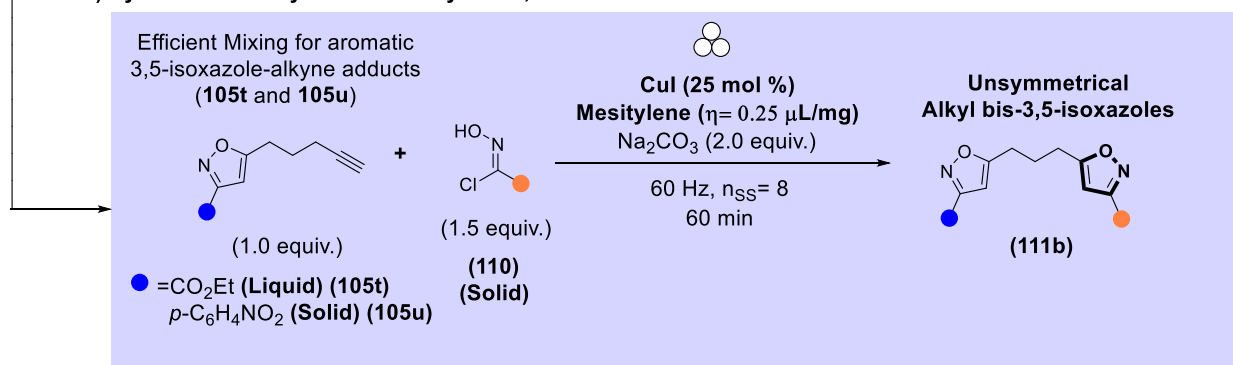
Figure 3.6: Reactivity difference between aromatic and alkyl 3,5-isoxazole-alkyne adducts under mechanochemical conditions.

Using alkyl 3,5-isoxazole-alkyne adduct **105t** and **105u** demonstrated an improvement in the reaction performance, presumably due to more efficient mixing of the alkyl 3,5-isoxazole-alkyne adduct over the aromatic adduct (**Figure 3.6**).[32,64,68-69] Liquid 3,5-isoxazole-alkyne adduct **105t** and sterically bulky hydroxyimidoyl chlorides with catalytic amounts of CuI and mesitylene liquid additive did not form the desired unsymmetrical bis-3,5-isoxazole alkyne **111a** (**Figure 3.7**). Improvements in the yield were observed when using less bulky substituents. Synthesis of the unsymmetrical bis-3,5-isoxazole **111b** was obtained only in moderate yields due to the competing formation of furoxans.[84] Using aromatic hydroxyimidoyl chlorides improves the yield of the reaction and the synthesis of unsymmetrical bis-3,5-isoxazoles **111c-f** was obtained in excellent yields independent of the electronic character of the substituent and their physical state. This is likely due to an enhanced coupling between the aromatic hydroxyimidoyl chlorides and alkyl terminal alkyne **105t-u** compared with the dimerization to form furoxans (**Figure 3.7**).[84-87]
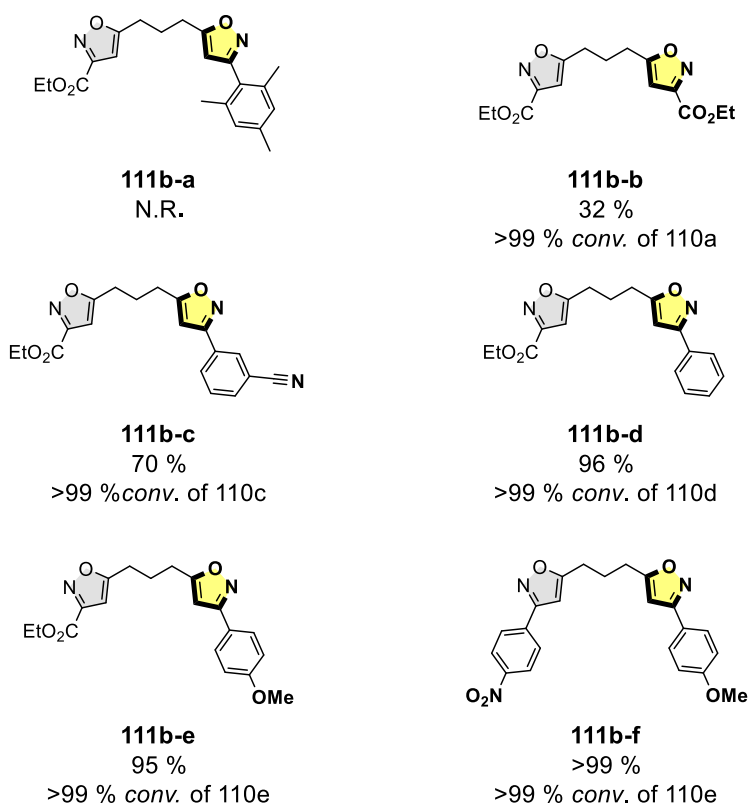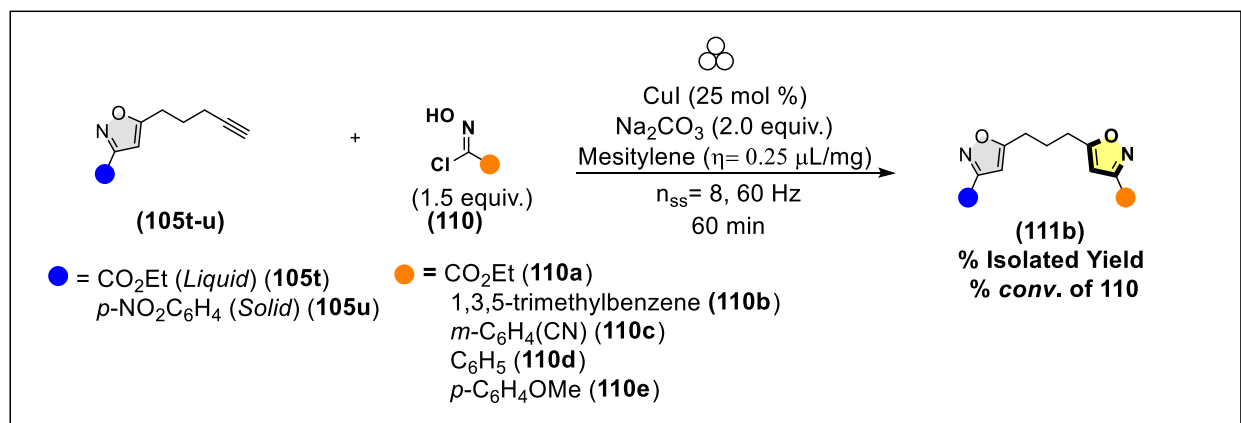
Figure 3.7: Synthesis of unsymmetrical bis-3,5-isoxazoles from alkyl 3,5-isoxazole-alkyne adducts.

a **Reaction Conditions: 105t-u** (0.517 mmol, 1.0 equiv.), hydroximidoyl chloride (0.755 mmol, 1.5 equiv.) **110**, Na_2CO_3 (1.03 mmol, 2.0 equiv.), CuI (0.130 mmol, 25 mol %), mesitylene (η = 0.25 μL/mg). *b* The reported yields are isolated yields of **111b** followed by the conversion of **110**

3.4. Conclusion

In conclusion, we developed the first mechanochemical desymmetrization strategy for bis- and tris-alkynes to form 3,5-isoxazole-alkyne adducts without using a large excess of either starting material and by a controlled 1,3-dipolar cycloaddition. The reported conditions were applicable for a range of aromatic and

alkyl bis- and tris-alkynes. The reduction of the 3,5-isoxazole moiety was achieved in high yield, allowing a concise route to β-ketoenamine-alkyne derivatives. Furthermore, the mechanochemical desymmetrization allowed access to unsymmetrical bis-3,5-isoxazole from alkyl 3,5-isoxazole-alkyne adducts (**105t-u**) in excellent yields. We believe this protocol can provide efficient access to more intricately functionalized poly-isoxazoles, boron-enaminoketonate, and facilitate the synthesis of natural products.

3.5. Acknowledgements

3.6. References

[1]   M. Yoshida, N. Sassa, T. Kato, S. Fujinami, T. Soeta, K. Inomata, Y. Ukaji, *Chem. - A Eur. J.* **2014**, *20*, 2058–2064.

[2]   J. Gajewy, M. Kwit, *Nat. Chem.* **2021**, *13*, 623–624.

[3]   W. D. G. Brittain, B. R. Buckley, J. S. Fossey, *ACS Catal*. **2016**, *6*, 3629–3636.

[4]   F. Xu, W. F. Kang, X. N. Wang, Y. Y. Zhu, S. X. Chen, Y. J. Kong, S. M. Fang, *Monatshefte fur Chemie* **2017**, *148*, 1109–1116.

[5]   L. E. Carloni, S. Mohnani, D. Bonifazi, European *J. Org. Chem*. **2019**, *44*, 7322–7334.

[6]   A. Ojosipe, *J. Am. Chem*. **1975**, *97,* 5940–5942.

[7]   T. Haino, H. Saito, *Synth. Met*. **2009**, *159*, 821–826.

[8]   Y. Ono, T. Hirao, T. Haino, *Org. Biomol. Chem*. **2021**, *19*, 7165–7171.

[9]   O. D. Montagnat, G. Lessene, A. B. Hughes, *J. Org. Chem*. **2010**, *75*, 390–398.

[10]   A. V. R. Murthy, V. Narendar, N. Sampath Kumar, P. Aparna, A. K. D. Bhavani, H. Solhi, R. Le Guevel, J. Roul, F. Gautier, P. Juin, C. R. Reddy, P. Mosset, N. Levoin, R. Grée, *Bioorganic Med. Chem. Lett*. **2021**, *52*, 3–7.

[11]   V. Fiandanese, S. Maurantonio, A. Punzi, G. G. Rafaschieri, *Org. Biomol. Chem*. **2012**, *10*, 1186–1195.

[12]   V. Aucagne, D. A. Leigh, *Org. Lett.* **2006**, *8*, 4505–4507.

[13]   J. M. Aizpurua, I. Azcune, R. M. Fratila, E. Balentova, M. Sagartzazu-Aizpurua, J. I. Miranda, *Org. Lett.* **2010**, *12*, 1584–1587.

[14]   N. G. Angelo, P. S. Arora, *J. Org. Chem*. **2007**, *72*, 7963–7967.

[15]   G. R. Stephenson, J. P. Buttress, D. Deschamps, M. Lancelot, J. P. Martin, I. G. Sheldon, C. Alayrac, A. Gaumont, C. B. Page*, Synlett* **2013**, *24*, 2723–2729.

[16]   V. O. Rodionov, V. V. Fokin, M. G. Finn, *Angew. Chemie* **2005**, *117*, 2250–2255.

[17]   F. Zhou, C. Tan, J. Tang, Y. Y. Zhang, W. M. Gao, H. H. Wu, Y. H. Yu, J. Zhou, *J. Am. Chem. Soc*. **2013**, *135*, 10994–10997.

[18]   T. Luu, R. McDonald, R. R. Tykwinski, *Org. Lett*. **2006**, *8,* 6035–6038.

[19]   R. A. Sheldon, *Chem. Soc. Rev*. **2012**, *41*, 1437–1451.

[20]   E. Boldyreva, *Chem. Soc. Rev*. **2013**, *42*, 7719–7738.

[21]   S. Mateti, M. Mathesh, Z. Liu, T. Tao, T. Ramireddy, A. M. Glushenkov, W. Yang, Y. I. Chen, *Chem. Commun*. **2021**, *57*, 1080–1092.

[22]   S. L. James, C. J. Adams, C. Bolm, D. Braga, P. Collier, T. Friščic, F. Grepioni, K. D. M. Harris, G. Hyett, W. Jones, A. Krebs, J. Mack, L. Maini, A. G. Orpen, I. P. Parkin, W. C. Shearouse, J. W. Steed, D. C. Waddell, *Chem. Soc. Rev.* **2012**, *41*, 413–447.

[23]   K. Kubota, Y. Pang, A. Miura, H. Ito, *Science* **2019**, *366*, 1500–1504.

[24]   E. Juaristi, C. G. Avila-Ortiz, Synthesis **2023**, *55*, 2439–2459

[25]   M. Pérez-Venegas, E. Juaristi, ChemSusChem **2021**, *14*, 2682–2688

[26]   J. L. Howard, Y. Sagatov, L. Repusseau, C. Schotten, D. L. Browne, *Green Chem.* **2017**, *19*, 2798–2802.

[27]   T. Friščić, C. Mottillo, H. M. Titi, *Angew. Chemie - Int. Ed.* **2020**, *59*, 1018–1029.

[28]   V. Štrukil, M. D. Igrc, M. Eckert-Maksić, T. Friščić, *Chem. - A Eur. J.* **2012**, *18*, 8464–8473. **[29]** V. Štrukil, Beilstein *J. Org. Chem.* **2017**, *13*, 1828–1849.

[30]   V. Štrukil, D. Margetic, M. D. Igrc, M. Eckert-Maksic, T. Frišcic, *Chem. Commun.* **2012**, *48*, 9705–9707.

[31]   M. Lanzillotto, L. Konnert, F. Lamaty, J. Martinez, E. Colacino, *ACS Sustain. Chem. Eng.* **2015**, *3*, 2882–2889.

[32]   T. Seo, K. Kubota, H. Ito, *J. Am. Chem. Soc.* **2020**, *142*, 9884–9889.

[33]   R. A. Hernandez R., K. Burchell-Reyes, A. P. C. A. Braga, J. K. Lopez, P. Forgione, *RSC Adv*. **2022**, *12*, 6396–6402.

[34]   S. R. Pathipati, A. Van Der Werf, N. Selander, *Synth.* **2017**, *49*, 4931–4941.

[35]   M. Gao, R. Ye, W. Shen, B. Xu, *Org. Biomol. Chem*. **2018**, *16*, 2602–2618.

[36]   Y. Yamamoto, *J. Org. Chem*. **2007**, *72*, 7817–7831.

[37]   A. T. McFarlin, R. B. Watson, T. E. Zehnder, C. S. Schindler, *Adv. Synth. Catal*. **2020**, **362**, 365–369.

[38]   J. L. Do, T. Friščić, *ACS Cent. Sci*. **2017**, *3*, 13–19.

[39]   S. Heimanns, *Rev. Prog. Color. Relat. Top.* **1981**, *11*, 1–8.

[40]   T. Friščić, D. G. Reid, I. Halasz, R. S. Stein, R. E. Dinnebier, M. J. Duer, *Angew. Chemie - Int. Ed*. **2010**, *49*, 712–715.

[41]   J. G. Hernández, C. Bolm, *J. Org. Chem*. **2017**, *82*, 4007–4019.

[42]   K. J. Ardila-Fierro, J. G. Hernández, *ChemSusChem* **2021**, *14*, 2145–2162.

[43]   J. L. Howard, M. C. Brand, D. L. Browne, Angew. Chemie - Int. Ed. **2018**, *57*, 16104–16108.

[44]   N. R. Rightmire, T. P. Hanusa*, Dalt. Trans*. **2016**, *45*, 2352–2362.

[45]   P. Ying, J. Yu, W. Su, *Adv. Synth. Catal*. **2021**, *363*, 1246–1271.

[46]   A. Delori, T. Frišić, W. Jones, *CrystEngComm* **2012**, *14*, 2350–2362.

[47]   F. Ono, Y. Ohta, M. Hasegawa, S. Kanemasa, *Tetrahedron Lett*. **2009**, *50*, 2111–2114.

[48]   T. Rispens, J. B. F. N. Engberts, *J. Phys. Org. Chem*. **2005**, *18*, 908–917.

[49]   W. Benchouk, S. M. Mekelleche, B. Silvi, M. J. Aurell, L. R. Domingo, *J. Phys. Org. Chem*. **2011**, *24*, 611–618.

[50]   F. P. Cossío, I. Morao, H. Jiao, P. Von Ragué Schleyer, *J. Am. Chem. Soc*. **1999**, *121*, 6737–6746.

[51]   Y. Hu, K. N. Houk, *Tetrahedron* **2000**, *56*, 8239–8243.

[52]   A. Qin, J. W. Y. Lam, B. Z. Tang, *Chem. Soc. Rev*. **2010**, *39*, 2522–2544.

[53]   J. E. Hein, V. V. Fokin, *Chem. Soc. Rev*. **2010**, *39*, 1302–1315.

[54]   F. Himo, T. Lovell, R. Hilgraf, V. V. Rostovtsev, L. Noodleman, K. B. Sharpless, V. V. Fokin, *J. Am. Chem. Soc.* **2005**, *127*, 210–216.

[55]   F. Sebest, J. J. Dunsford, M. Adams, J. Pivot, P. D. Newman, S. Díez-González, *ChemCatChem* **2018**, *10*, 2041–2045.

[56]   S. Hwang, S. Grätz, L. Borchardt, Chem. Commun. 2022, 58, 1661–1671.

[57]   W. Pickhardt, S. Grätz, L. Borchardt, *Chem. - A Eur. J*. **2020**, *26*, 12903–12911.

[58]   T. L. Cook, J. A. Walker, J. Mack, *Green Chem*. **2013**, *15*, 617–619.

[59]   A. Dondoni, G. Barbaro, *J. Chem. Soc. Perkin Trans*. **1973**, *13,* 1769-1773.

[60]   R. Huigens, *Angew. Chemie - Int. Ed*. **1963**, *2*, 633–696.

[61]   S. N. Semenov, L. Belding, B. J. Cafferty, M. P. S. Mousavi, A. M. Finogenova, R. S. Cruz, E. V. Skorb, G. M. Whitesides, *J. Am. Chem. Soc*. **2018**, *140*, 10221–10232.

[62]   D. Döhler, P. Michael, W. H. Binder, Macromolecules 2012, 45, 3335–3345.

[63]   T. R. Chan, R. Hilgraf, K. B. Sharpless, V. V. Fokin, *Org. Lett*. **2004**, *6*, 2853–2855.

[64]   F. Toda, *Acc. Chem. Res.* **1995**, *28*, 480–486.

[65]   B. Rodríguez, A. Bruckmann, T. Rantanen, C. Bolm, *Adv. Synth. Catal*. **2007**, *349*, 2213–2233.

[66]   K. Tanaka, F. Toda, 2000.

[67]   L. Vugrin, M. Carta, S. Lukin, *Faraday Discuss*. **2023**, *241,* 217–229.

[68]   R. Thorwirth, A. Stolle, B. Ondruschka, A. Wild, U. S. Schubert, *Chem. Commun.* **2011**, *47*, 4370–4372.

[69]   F. Schneider, B. Ondruschka, *ChemSusChem* **2008**, *1*, 622–625.

[70]   J. S. Wzorek, T. F. Knöpfel, I. Sapountzis, D. A. Evans, *Org. Lett*. **2012**, *14*, 5840–5843.

[71]   H. Choe, H. Cho, H. J. Ko, J. Lee, *Org. Lett*. **2017**, *19*, 6004–6007.

[72]   C. P. Felix, N. Khatimi, A. J. Laurent, *J. Org. Chem*. **1995**, *60*, 3907–3909.

[73]   T. Haino, H. Saito, *Synth. Met*. **2009**, *159*, 821–826.

[74]   Y. Ono, T. Hirao, T. Haino, Org. Biomol. Chem. **2021**, *19*, 7165–7171.

[75]   K. Hirano, T. Ikeda, N. Fujii, T. Hirao, M. Nakamura, Y. Adachi, J. Ohshita, T. Haino, *Chem. Commun*. **2019**, *55*, 10607–10610.

[76]   T. Matsumura, Y. Koyama, S. Uchida, M. Yonekawa, T. Yui, O. Ishitani, T. Takata, *Polym. J*. **2014**, *46*, 609–616.

[77]   X. Guo, G. Xu, L. Zhou, H. Yan, X. Q. Hao, Q. Wang, *Org. Chem. Front*. **2020**, *7*, 2467–2473.

[78]   P. Kumar, M. Kapur, Asian J. *Org. Chem*. **2020**, *9*, 1065–1069.

[79]   M. Lautens, A. Roy, *Org. Lett.* **2000**, *2*, 555–557.

[80]   J. Paternoga, T. Opatz, European *J. Org. Chem.* **2019**, *42*, 7067–7078.

[81]   of D. Donati, S. Ferrini, S. Fusi, F. Ponticelli, *J. Heterocycl. Chem*. **2004**, *41*, 761–766.

[82]   M. Nitta, T. Kobayashi, *J. Chem. Soc. Chem. Commun*. **1982**, *15*, 877.

[83]   J. M. Pérez, D. J. Ramón, *ACS Sustain. Chem. Eng*. **2015**, *3*, 2343–2349.

[84]   C. Grundmann and S. K. Datta, *J. Org. Chem*. **1968**, *34*, 2016–2018.

[85]   C. Grundmann, R. Richter, *J. Org. Chem*. **1967**, *32*, 2308–2312.

[86]   C. Grundmann, J. M. Dean, *J. Org. Chem*. **1965**, *30,* 2809–2812.

[87]   M. S. Chiang, J. U. Lowe, *J. Org. Chem*. **1967**, *32*, 1577–1579.

3.7. Experimental Section for chapter 3

3.7.1. General Considerations, Materials, and Instrumentations

General Considerations: Solids were directly weighed open-air and added directly into the reaction vial. Liquids were directly transferred from the vial containing the reagent using an automatic pipette with a plastic tip of appropriate size or a plastic syringe with a stainless-steel needle. Flash chromatography was carried out using 40-63μm silica gel (Silicycle).

Materials: Distilled water was obtained from an in-house water distillery. All other reagents and chemicals were purchased from Sigma-Aldrich or AK Scientifics and used without further purification.

Instrumentation: ^{1}H (500MHz) and ^{13}C (125MHz) NMR spectra were recorded in CDCl$_3$ or DMSO-d_6 using a Varian Inova 500 MHz spectrometer. Spectra were referenced to the residual solvent signal or the TMS signal. Spectral features are tabulated in the following order (Note: Spectral features are reported in the following format): chemical shift (δ, ppm); multiplicity (s-singlet, d-doublet, t-triplet, q-quartet, dd-doublet of doublets, m-multiplet), dt-double of triplets, ddd-doublet of doublets of doublets; coupling constants (J, Hz); number of protons. High resolution mass spectra (HRMS) were obtained using a LTQ Orbitrap Velos ETD (positive and negative mode) mass spectrometer. Liquid Chromatography-Inductively Coupled Plasma Mass Spectrometry (LC-ICP-MS) was obtained using an Agilent 7500ce with a MicroMist glass concentric nebulizer and a Quadrupole MS with a sensitivity range of 10-12-10-3 g/mL. The reactions were performed using a Fritsch Planetary Micro Mill model ''Pulverisette 7'' housing two stainless-steel (**SS**) cups containing eight stainless-steel (**SS**) balls each of 1 cm diameter and sealed by a stainless-steel (**SS**) lid fitted with a Teflon gasket. The reported melting points are uncorrected and were measured using a Stuart SMP3 melting point apparatus. Fourier transform infrared (FT-IR) were acquired using a Thermo ScientificTM NicoletTM iS5 FTIR Spectrometer, ranging from 4000 to 400 cm-1. Spectra were collected using 64 scans, and the data was processed using the Spectrum One software. MALDITOF-MS was obtained using an Autoflex III Smart Beam (from BRUKER) equipped with a laser Nd-YAG UV at 355 nm and an acceleration voltage at 20 KV

Abbreviations: Hexanes (Hex), Ethyl Acetate (EtOAc), Dichloromethane (DCM), 1,3,5-trimethoxybenzene (TMB), Dimethylsulfoxide (DMSO), Stainless Steel (SS), Melting point (MP), Ratio to front (R$_f$).

3.7.2. Procedure S1 (PS1): Optimization of Solvent-Free Desymmetrization of Aromatic(bis-alkyne) Systems

Prior to the isolation of 3,5-isoxazoles-alkyne adducts **105**, the cycloaddition reactions between the corresponding bis-alkyne **103a** and hydroxyimidoil chloride **104a** was used as a model reaction to optimize the synthesis of 3,5-isoxazoles-alkyne adduct **105a**. The reaction was optimized in a 50 mg of bis-alkyne **103a** reaction to determine the optimal parameters. The yield of the 3,5-isoxazoles-alkyne adduct was quantified by ^{1}H NMR and using TMB as an internal standard.

Example procedure for optimization:

Optimization for the synthesis of ethyl 5-(4-ethynylphenyl)isoxazole-3-carboxylate (105a): To a clean and dried stainless-steel (**SS**) planetary milling jar (approximately 50 mL capacity) with 8 **SS** balls (10 mm of diameter), it was weighed bis-alkyne **103a** (0.050 g, 0.396 mmol, 1.0 equivalents.), hydroxyimidoyl chloride **104a** (0.062 g, 0.396 mmol, 1.0 equivalents.), Cu(NO₃)₂•2.5(H₂O) (0.092 g, 0.396 mmol, 1.0 equivalents.), Na₂CO₃ (0.084 g, 0.792 mmol, 2.0 equivalents.). Once all the solids were introduced then it was added via an automated pipette mesitylene (η= 0.25 μL/mg, 72 μL). Then, the jar was closed, and the mixture was milled for 60 min at 60 Hz. After 60 min, the jar was cooled at room temperature, and it was added 10-12 mg of TMB to the reaction crude. The reaction mixture was carefully filtered over a celite plug using EtOAc as eluent. The filtrate was collected and reduced *in vacuo.* The yield of **105a** was obtained by ^{1}H NMR.

Initial or Starting Conditions:[4]
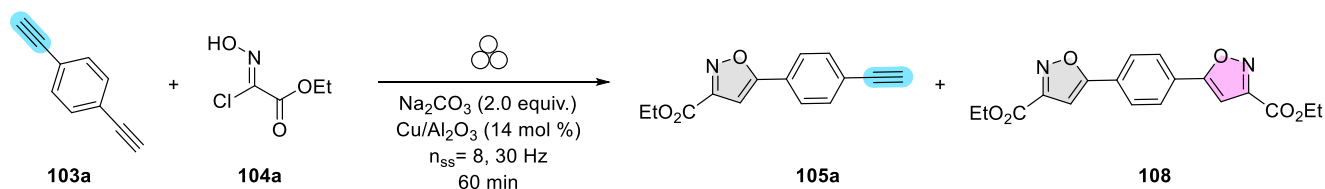
Table S3.1. *Effect of the stoichiometry of 104a*

Equiv. 104a	105a:108a	Yield % of 105a	Yield % of 108a
1.5	10:1	30	3
1.1	30:1	30	1
1.0	3.7:1	33	9

Table S3.2. *Effect of the additive in the desymmetrization of 103a*

Additives	Equiv.	105a:108a	Yield % of 105a	Yield % of 108a
N/A	-	8.5:1	34	4

---

[4] Initial conditions were taken from previously reported experiments [33]

132

Cu/Al$_2$O$_3$ (14 mol %)	0.14	3.7:1	33	9
Cu/Al$_2$O$_3$ (50 mol %)	0.50	3:1	3	1
Cu(NO$_3$)$_2$•2.5 H$_2$O	1.0	10:1	30	3
ZnCl$_2$	1.0	2.3:1	9	4
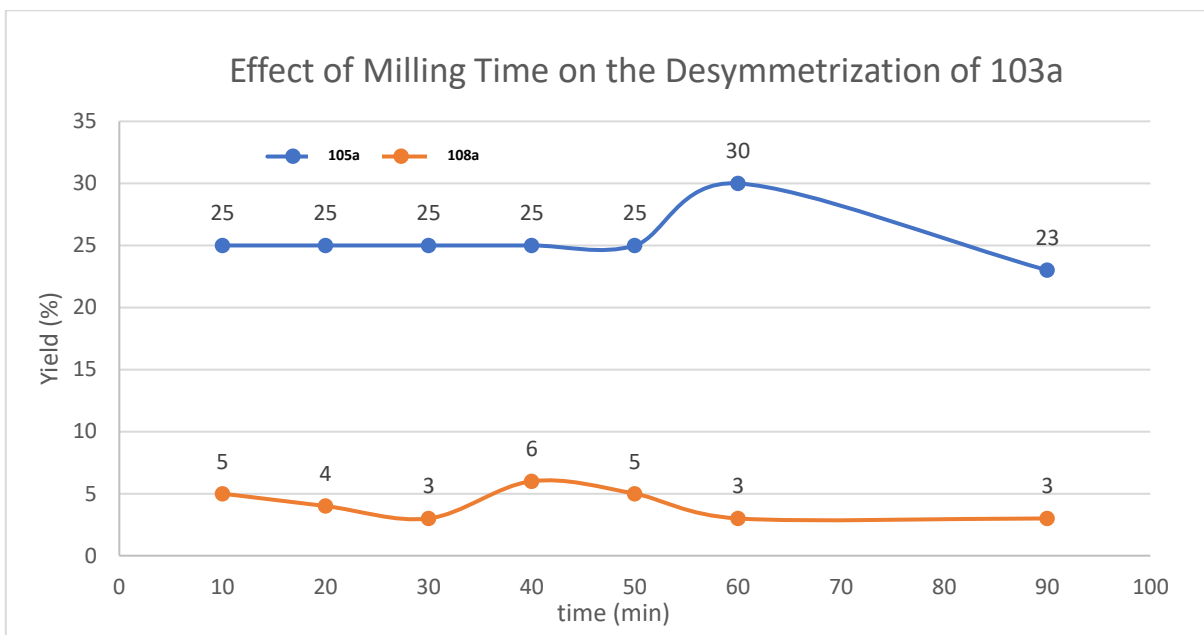
Figure S3.1. Effect of milling time in the desymmetrization of **103a**

Table S3.3. Effect of the GAA in the desymmetrization 103a

GAA	105a:108a	Yield % of 105a	Yield % of 103a
-	10:1	30	3
NaCl	11.5:1	23	2
KCl	8.5:1	17	2
Neutral Alumina	2.3:1	9	4

Table S3.4. Effect of the LAG in the desymmetrization 103a

LAG	η (μL/mg)	105a:108a	Yield % of 105a	Yield % of 108a
EtOAc		12:1	36	3
EtOH	0.5	15:1	30	2
2-MeTHF		5.6:1	28	5
Toluene		15:1	45	3
Toluene	0.25	15:1	45	3
Mesitylene		50:1	50	1

1,3,5-tri(isopropyl)benzene	5:1	41	8
Xylenes	22.5:1	45	2

Figure S3.2. Homogenization effect of the $Cu(NO_3)_2 \bullet 2.5\ H_2O$ in the dezymmetrization of symmetical bis-alkyne systems

Table S3.5. *Effect of the base in the desymmetrization 103a*

Base	Equiv.	105a:108a	Yield % of 103a	Yield % of 108a
Na_2CO_3	1.0	20:1	20	1
Na_2CO_3	3.0	10:1	40	2
DABCO	0.5	7:1	14	2
$Cu_2CO_3\ (OH)_2^{a}$	1.0	4.8:1	34	7
K_2CO_3	2.0	28:1	28	1
Cs_2CO_3	2.0	20:1	20	1
K_2PO_4H	2.0	18:1	36	2
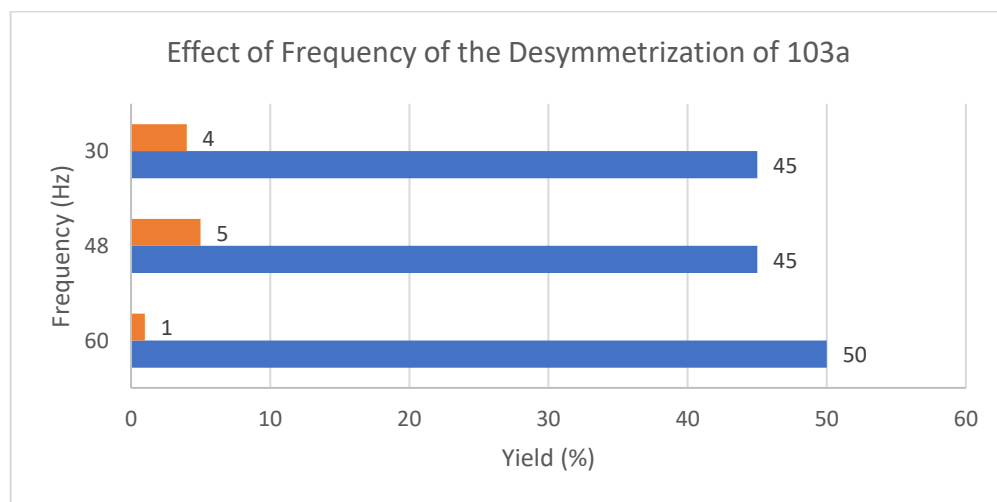
Figure S3.3. Effect of Frequency of the Desymmetrization of 103a

Table S3.6. *Effect stoichiometry on desymmetrization of 103a*

Equiv. 103a	105a:108a	Yield % of 105a	Yield % of 108a
2.0	51:1	51	1

| 1.5 | 49:1 | 49 | 1 |
| 1.0 | 50:1 | 50 | 1 |

Table S3.7. *Effect of Cu(I) catalysis in the desymmetrization of 103a*

Cu(I) System	mol %	105a:108a	Yield % of 105a	Yield % of 108a
Cu(NO₃)₂•2.5 H₂O	100 and 30 min of rest time	4.3:1	30	7
Cu(OAc)₂•H₂O Na Ascorbate	10 (each)	17.5:1	35	2
Cu(OAc)₂•H₂O Na Ascorbate	50 (each)	8:1	40	5
CuSO₄ •5 H₂O Na Ascorbate	50 (each)	8:1	39	5
Cu(SO₄)₂•5 H₂O Na Ascorbate	150 (each)	4.8:1	24	5
CuI	10	9.6:1	29	3
Cu₂O	50	17:1	33	2
[1,3-Bis(2,6-diisopropylphenyl)imidazol-2-ylidene]copper(I) chloride	25	16.5:1	37	2
[1,3-Bis(2,6-diisopropylphenyl)imidazol-2-ylidene]copper(I) chloride	25	6.8:1	34	5

Chloro(1,5-cyclooctadiene)copper(I) dimer	25	6.3:1	44	7
Chloro(1,5-cyclooctadiene)copper(I) dimer (No LAG)	25	8:1	8	1
Bromotris(triphenylphosphine)copper(I)	25	9:1	36	4

3.7.3. Procedure S2 (PS2): Optimization of Desymmetrization of Alkyl bis-alkyne **103h** by Solution-based method

The cycloaddition reactions between the corresponding bis-alkyne **103h** and hydroxyimidoil chloride **104e** was used as a model reaction to optimize the synthesis of 3,5-isoxazoles-alkyne adduct **105s**. The reaction was optimized in a 66 mg of bis-alkyne **103h** reaction to determine the optimal parameters. The yield of the 3,5-isoxazoles-alkyne adduct was quantified by ^{1}H NMR and using TMB as an internal standard.

103h   **104e**   Conditions   **105s**   **108s**
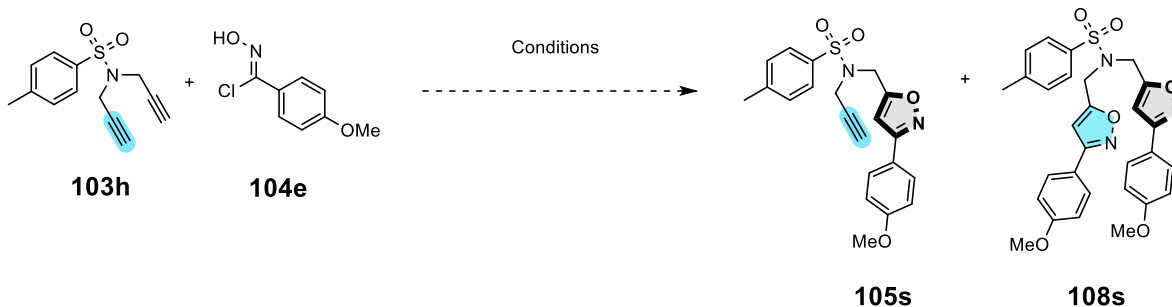
Example reaction procedure by solution-base conditions:

In a clean round-bottom flask of 10 mL capacity, it was weighted, it was weighed bis-alkyne **103h** (0.066 g, 0.266 mmol, 1.0 equivalents.) and hydroxyimidoyl chloride **104e** (0.050 g, 0.266 mmol, 1.0 equivalents.). The solids were dissolved in 7 mL of mesitylene (η= 45.2 µL/mg, 7 mL). Then triethylamine was added (38 µL, 0.266 mmol, 1.0 equivalents.). The reaction was left to stir for 1 to 6 h (see table S8). After 16 h, 12-15 mg of 1,3,5-trimetoxybenzene (TMB) was added as an internal standard. The reaction was diluted with EtOAc and washed with brine (2x10 mL) and water (2x 10 mL). The organic layer separated, dried over Na_2SO_4, filtered, and reduced *in vacuo*. The ratios of **103h**:**105s**:**108s** were calculated based on their integrations of ^{1}H-NMR.

Table S3.8. *Optimization for the desymmetrization of bis-alkyne* **103h**

Additive (1.0 equiv.)	Solvent (7 mL)	Base	Equiv. of base	Temperature (°C)	Yield 103h[a]	Yield 105s[a]	Yield 108s[a]	105s:108s
$Cu(NO_3)_2 \cdot 2.5(H_2O)$	Mesitylene	Na_2CO_3	2.0	25	-	-	-	-
		NEt$_3$	1.0		52 %	32 %	16 %	2:1
-					52 %	32 %	16 %	2:1
-				70	68 %	16 %	16 %	1:1
-	MeOH			25	55	30	15	2:1
-	DCM			25	52	33	17	1.9:1

[a] Yield determined by ^{1}H-NMR.

3.7.4. Procedure 3 (PS3): Solvent-Free Desymmetrization of Aromatic bis- and tris- alkyne (Isolation and Characterization)
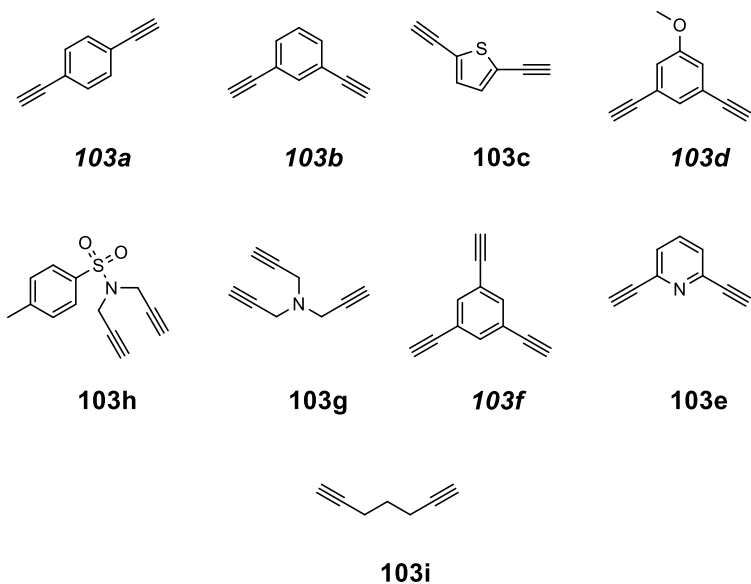
Figure S3.4. Bis- and tris-alkynes used

Bis-alkynes **103c**, **103d**, **103e** were synthesized according to the procedure reported by Beves, J.E. *et al.*[1]
[5]

---

[5] Beves, J. E.; Blanco, V.; Blight, B. A.; Carrillo, R.; D'Souza, D. M.; Howgego, D.; Leigh, D. A.; Slawin, A. M. Z.; Symes, M. D. *J. Am. Chem. Soc.* **2014**, *136*, 2094–2100.
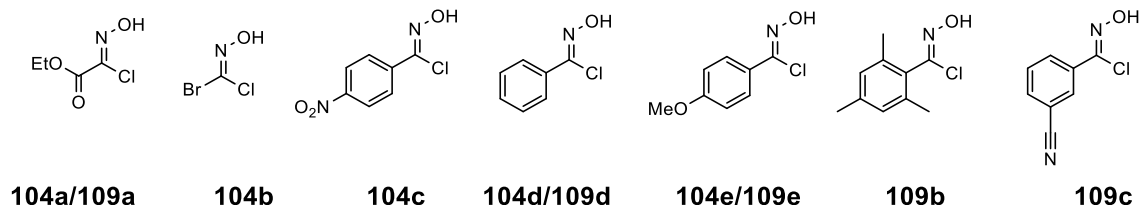
Figure S3.5. Hydroxyimidoyl chloride used in these experiments.

104a/109a   104b   104c   104d/109d   104e/109e   109b   109c

104c, 104d/109d, 104e/109e, 104b, 109c were synthesized according to the procedure developed by Himo, F. *et al.*[54]

The presented reaction was performed in 25 mg, 50 mg, 100 mg or 1.0g scale of bis-alkyne systems **103a-i.** Ratios of mono to bis-isoxazoles (**105a**:**108a**) were obtained by of the ^{1}H NMR reaction crude.
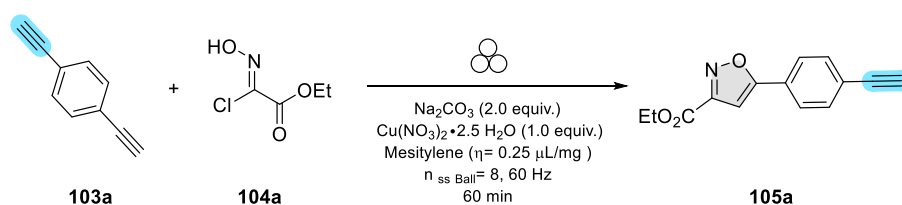
Synthesis of ethyl 5-(4-ethynylphenyl)isoxazole-3-carboxylate (105a): To a clean and dried stainless-steel (**SS**) planetary milling jar (approximately 50 mL capacity) with 8 **SS** balls (10 mm of diameter), it was weighed bis-alkyne **103a** (0.100 g, 0.792 mmol, 1.0 equivalents.), hydroxyimidoyl chloride **104a** (0.123 g, 0.792 mmol, 1.0 equivalents.), Cu(NO$_3$)$_2$•2.5 H$_2$O (0.184 g, 0.792 mmol, 1.0 equivalents.), Na$_2$CO$_3$ (0.168 g, 1.584 mmol, 2.0 equivalents.). Once all the solids were introduced, it was added *via* an automated pipette mesitylene (η= 0.25 µL/mg, 144 µL). The jar was closed, and the mixture was milled for 60 min at 60 Hz. After 60 min, the jar was cooled at room temperature, and the reaction mixture was carefully filtered over a celite plug using EtOAc as eluent. The filtrate was collected and reduced *in vacuo.* The obtained solid was washed with Et$_2$O and filtered for a second time using a Buchner funnel. The filtrate was reduced under pressure and recrystallized in EtOH: Water. The solid was filtered and washed with hot hexanes to obtain **105a** as a yellow powder. **105a** was obtained in 30 % yield (53.3 mg) in ratios of (98:2). R$_f$= 0.24 (9:1 Hex:EtOAc), MP= 101.9-103.9 °C. ^{1}**H NMR** (500 MHz, CDCl$_3$) δ 7.77 (d, *J* = 8.4 Hz, 2H), 7.60 (d, *J* = 8.4 Hz, 2H), 6.95 (s, 1H), 4.48 (q, *J* = 7.1 Hz, 2H), 3.22 (s, 1H), 1.45 (t, *J* = 7.1 Hz, 3H) ^{13}**C NMR** (125 MHz, CDCl$_3$) δ 170.75, 159.85, 157.02, 132.8, 126.57, 125.75, 124.62, 100.57, 82.69, 79.69, 62.31, 14.15. **HRMS** calculated for [C$_{14}$H$_{11}$NO$_3$] requires [M+H]$^+$ 242.0812, observed 242.0814.
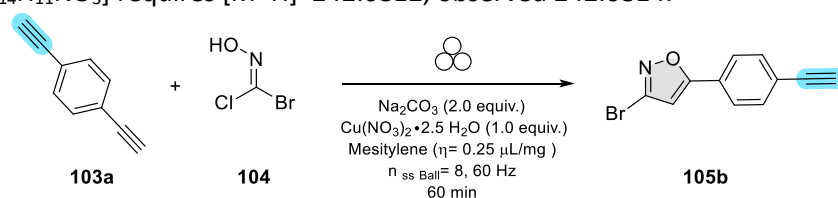
Synthesis of 3-bromo-5-(4-ethynylphenyl)isoxazole (105b): To a clean and dried stainless-steel (**SS**) planetary milling jar (approximately 50 mL capacity) with 8 **SS** balls (10 mm of diameter), it was weighed bis-alkyne **103a** (0.100 g, 0.792 mmol, 1.0 equivalents.), hydroxyimidoyl chloride **104b** (0.161 g, 0.792 mmol, 1.0 equivalents.), Cu(NO$_3$)$_2$•2.5 H$_2$O (0.184 g, 0.792 mmol, 1.0 equivalents.), Na$_2$CO$_3$ (0.168 g, 1.584 mmol, 2.0 equivalents.). Once all the solids were introduced, it was added *via* an automated pipette mesitylene (η= 0.25 µL/mg, 153 µL). The jar was closed, and the mixture was milled for 60 min at 60 Hz.

After 60 min, the jar was cooled at room temperature, and the reaction mixture was carefully filtered over a celite plug using EtOAc as eluent. The filtrate was collected and reduced *in vacuo.* **105b** was isolated in silica column using Hex:EtOAc in ratios of 9:1 as eluent. **105b** was obtained as a white solid in 26 % (52 mg) in ratios of (>99:1). R_f=0.45, MP=89.2-90.1 °C. **^{1}H NMR** (500 MHz, CDCl$_3$) δ 7.71 (d, *J* = 8.6 Hz, 2H), 7.59 (d, *J* = 8.5 Hz, 2H), 6.61 (s, 1H), 3.22 (s, 1H). **^{13}C NMR** (125 MHz, CDCl$_3$) δ 170.4, 140.9, 132.8, 126.3, 125.7, 124.8, 103.5, 82.6, 79.8. **HRMS** calculated for [C$_{11}$H$_6$NBrO] requires [M+H]$^+$ 247.9706, observed 247.9708.
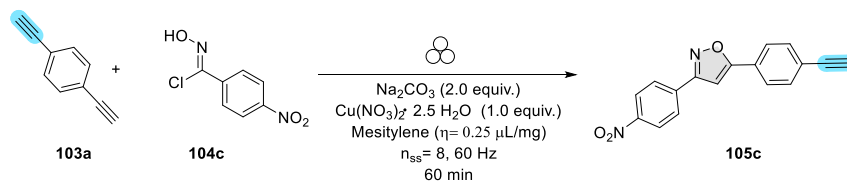
Synthesis of 5-(4-ethynylphenyl)-3-(4-nitrophenyl)isoxazole (105c): To a clean and dried stainless-steel (**SS**) planetary milling jar (approximately 50 mL capacity) with 8 **SS** balls (10 mm of diameter), it was weighed bis-alkyne **103a** (0.100 g, 0.792 mmol, 1.0 equivalents.), hydroxyimidoyl chloride **104c** (0.161 g, 0.792 mmol, 1.0 equivalents.), Cu(NO$_3$)$_2$•2.5 H$_2$O (0.184 g, 0.792 mmol, 1.0 equivalents.), Na$_2$CO$_3$ (0.168 g, 1.584 mmol, 2.0 equivalents.). Once all the solids were introduced, it was added *via* an automated pipette mesitylene (η= 0.25 µL/mg, 153 µL). Then, the jar was closed, and the mixture was milled for 60 min at 60 Hz. After 60 min, the jar was cooled at room temperature, and the reaction mixture was carefully filtered over a celite plug using EtOAc as eluent The filtrate was collected and reduced *in vacuo.* The obtained solid was washed with Et$_2$O and filtered for a second time using a Buchner funnel. The filtrate was reduced under pressure and recrystallized in Acetone:H$_2$O. The solid was filtered and washed with hot hexanes to obtain **105c** as a yellow solid. **105c** was obtained in 23 % yield (51.3 mg) in ratios of (>99:1). R_f=0.17 (9:1 Hex:EtOAc), MP=173-175.8 °C. **^{1}H NMR** (500 MHz, CDCl$_3$) δ 8.35 (d, *J* = 8.6 Hz, 2H), 8.05 (d, *J* = 8.6 Hz, 2H), 7.81 (d, *J* = 8.14), 7.63 (d, *J* = 8.2 Hz, 2H), 6.92 (s, 1H), 3.23 (s, 1H). **^{13}C NMR** (125 MHz, DMSO-*d^6*) δ 170.1, 161.7, 148.9, 134.9, 133.1, 128.3, 127.0, 126.3, 124.9, 124.3, 100.4, 83.6, 83.3. **HRMS** calculated for [C$_{17}$H$_{10}$N$_2$O$_3$] requires [M+H]$^+$ 291.0764, observed 291.0763.

Synthesis of   5-(4-ethynylphenyl)-3-phenylisoxazolethyl 5-(4-ethynylphenyl)isoxazole-3-carboxylate (105d): To a clean and dried stainless-steel (**SS**) planetary milling jar (approximately 50 mL capacity) with 8 **SS** balls (10 mm of diameter), it was weighed bis-alkyne **103a** (0.100 g, 0.792 mmol, 1.0 equivalents.), hydroxyimidoyl chloride **104d** (0.147 g, 0.792 mmol, 1.0 equivalents.), Cu(NO$_3$)$_2$•2.5 H$_2$O (0.184 g, 0.792 mmol, 1.0 equivalents.), Na$_2$CO$_3$ (0.168 g, 1.584 mmol, 2.0 equivalents.). Once all the solids were introduced then it was added *via* an automated pipette mesitylene (η= 0.25 µL/mg, 150 µL). Then, the jar was closed, and the mixture was milled for 60 min at 60 Hz. After 60 min, the jar was cooled at room temperature, and the reaction mixture was carefully filtered over a celite plug using EtOAc as eluent. The filtrate was collected and reduced *in vacuo.* The obtained solid was washed with Et$_2$O and filtered for a second time using a Buchner funnel. The filtrate was reduced under pressure and recrystallized in acetone-water. The solid was filtered and washed with hot hexanes to obtain **105d** as a yellow solid. **105d** was obtained in 50 % yield (200 mg) in ratios of (95:5). R_f=0.68 (7:3 Hex:EtOAc), MP= 67.9-70.1 °C. **^{1}H NMR** (500 MHz, CDCl$_3$) δ 7.89 – 7.82 (m, 2H), 7.80 (d, *J* = 8.6 Hz, 2H), 7.60 (d, *J* = 8.5 Hz, 2H), 7.54 – 7.41 (m, 3H),

140

6.85 (s, 1H), 3.21 (s, 1H). **^{13}C NMR** (125 MHz, CDCl3) δ 169.5, 163.1, 132.7, 130.1, 128.9, 128.9, 127.4, 126.8, 125.7, 1243.9, 98.2, 82.9, 79.3. **HRMS** calculated for [$C_{17}H_{11}NO$] requires [M+H]$^+$ 246.0913, observed 246.0914.

Optimization for the synthesis of 5-(4-ethynylphenyl)-3-(4-methoxyphenyl)isoxazole (105e): [6]To a clean and dried stainless-steel (**SS**) planetary milling jar (approximately 50 mL capacity) with 8 **SS** balls (10 mm of diameter), it was weighed bis-alkyne **103a** (0.100 g, 0.792 mmol, 1.0 equivalents.), hydroxyimidoyl chloride **104e** (0.147 g, 0.792 mmol, 1.0 equivalents.), Cu(NO$_3$)$_2$•2.5(H$_2$O) (0.184 g, 0.792 mmol, 1.0 equivalents.), Na$_2$CO$_3$ (0.168 g, 1.584 mmol, 2.0 equivalents.). Once all the solids were introduced then it was added *via* an automated pipette mesitylene (η= 0.25 μL/mg, 150 μL). Then, the jar was closed, and the mixture was milled for 60 min at 60 Hz. After 60 min, the jar was cooled at room temperature, and the reaction mixture was carefully filtered over a celite plug using EtOAc as eluent. The filtrate was collected and reduced *in vacuo.* The obtained solid was washed with Et$_2$O and filtered for a second time using a Buchner funnel. The filtrate was reduced under pressure and recrystallized in Acetone:H$_2$O. The solid was filtered and washed with hot hexanes to obtain **105e** as a yellow powder. **105e** was obtained in 92 % yield (200 mg) in ratios of (95:5). R$_f$=0.23 (9:1 Hex:EtOAc), MP= 178.2-181.3 °C. **^{1}H NMR** (500 MHz, CDCl$_3$) δ 7.84 – 7.71 (m, 4H), 7.60 (d, *J* = 8.6 Hz, 2H), 7.00 (d, *J* = 8.9 Hz, 2H), 6.80 (s, 1H), 3.87 (s, 3H), 3.20 (s, 1H). **^{13}C NMR** (125 MHz, CDCl$_3$) δ 169.2, 162.7, 161.1, 132.7, 128.2, 127.5, 125.6, 123.9, 121.4, 114.3, 97.9, 82.9, 79.2, 55.4. **HRMS** calculated for [$C_{18}H_{13}NO_2$] requires [M+H]$^+$ 276.1019, observed 276.1021.
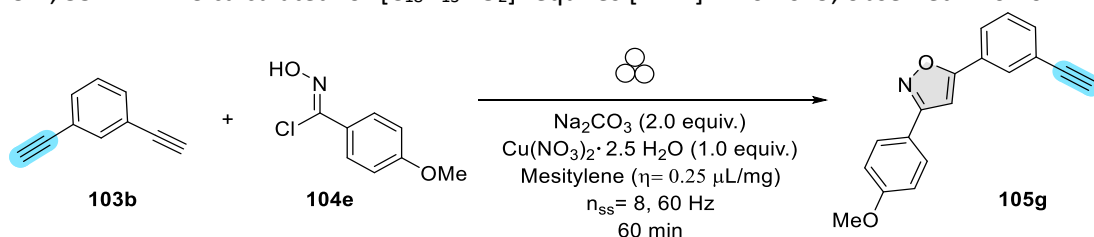
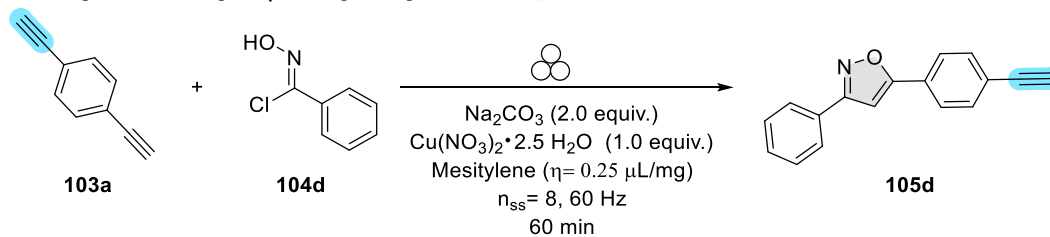**Synthesis of 5-(3-ethynylphenyl)-3-(4-methoxyphenyl)isoxazole (105g):** To a clean and dried stainless-steel (**SS**) planetary milling jar (approximately 50 mL capacity) with 8 **SS** balls (10 mm of diameter), hydroxyimidoyl chloride **104e** (148 mg, 0.792 mmol, 1.0 equivalents.), Cu(NO$_3$)$_2$•2.5(H$_2$O) (0.185 g, 0.792 mmol, 1.0 equivalents.), Na$_2$CO$_3$ (0.168 g, 1.584 mmol, 2.0 equivalents.). Once all the solids were introduced then it was added *via* an automated pipette liquid bis-alkyne **103b** (105 μL, 0.792 mmol, 1.0 equivalents.), and mesitylene (η= 0.25 μL/mg, 150 μL). The jar was closed, and the mixture was milled for 60 min at 60 Hz. After 60 min, the jar was cooled at room temperature, and the reaction mixture was carefully filtered over a celite plug using EtOAc as eluent. The filtrate was collected and reduced *in vacuo.* The obtained solid was washed with Et$_2$O and filtered for a second time using a Buchner funnel. The filtrate

---

[6] The same procedure was followed in a 1.0-g scale synthesis of **105e. 105e** was obtained in **80 %** in ratios of (95:5)

was reduced under pressure and recrystallized in Acetone:H$_2$O. The solid was filtered and washed with hot hexanes to obtain **105g** as a brown solid. **105g** was obtained in >99 % yield (318.9 mg) in ratios of (>99:1). R$_f$=0.25 (9:1 Hex:EtOAc), MP= 124.6-127.6 °C. **^{1}H NMR** (500 MHz, CDCl$_3$) δ 7.95 (t, *J* = 1.4 Hz, 1H), 7.83 – 7.82 (m, 1H), 7.80 (d, *J* = 8.9 Hz, 2H), 7.56 (dt, *J* = 7.7, 1.3 Hz, 1H), 7.45 (t, *J* = 7.8 Hz, 1H), 7.00 (d, *J* = 8.8 Hz, 2H), 6.80 (s, 1H), 3.87 (s, 3H), 3.16 (s, 1H). **^{13}C NMR** (125 MHz, CDCl$_3$) δ 169.05, 162.62, 161.06, 133.51, 129.37, 129.07, 128.19, 127.77 , 125.96, 123.07, 121.41, 114.34, 97.80, 82.63, 78.27, 55.36. **HRMS** calculated for [C$_{18}$H$_{13}$NO$_2$] requires [M+H]$^+$ 276.1019, observed 276.102.

Synthesis of ethyl 5-(5-ethynylthiophen-2-yl)isoxazole-3-carboxylate (105h): To a clean and dried stainless-steel (**SS**) planetary milling jar (approximately 50 mL capacity) with 8 **SS** balls (10 mm of diameter), it was weighed bis-alkyne **103c** (0.050 g, 0.378 mmol, 1.0 equivalents.), hydroxyimidoyl chloride **104a** (0.0572 g, 0.378 mmol, 1.0 equivalents.), Cu(NO$_3$)$_2$•2.5 H$_2$O (0.0879 g, 0.378 mmol, 1.0 equivalents.), Na$_2$CO$_3$ (0.0801 g, 0.756 mmol, 2.0 equivalents.). Once all the solids were introduced it was added *via* an automated pipette mesitylene (η= 0.25 µL/mg, 69 µL). The jar was closed, and the mixture was milled for 60 min at 60 Hz. After 60 min, the jar was cooled at room temperature, and the reaction mixture was carefully filtered over a celite plug using EtOAc as eluent. The filtrate was collected and reduced *in vacuo.* **105h** was isolated in silica column using Hex:EtOAc in ratios of 8:2 as eluent. **105h** was obtained as a white solid in >99% yield (92 mg) in ratios of (>99:1). R$_f$=0.45, MP=76.4-78.2 °C. **^{1}H NMR** (500 MHz, CDCl$_3$) δ 7.41 (d, *J* = 3.9 Hz, 2H), 7.27 (d, *J* = 3.9 Hz, 2H), 6.79 (s, 1H), 4.46 (q, *J* = 7.2 Hz, 2H), 3.50 (s, 1H), 1.43 (t, *J* = 7.2 Hz, 3H). **^{13}C NMR** (125 MHz, CDCl$_3$) δ 165.5, 159.6, 157.0, 133.9, 129.2, 127.3, 125.4, 100.2, 84.2, 75.8, 62.4, 14.1. **HRMS** calculated for [C$_{12}$H$_9$NO$_3$S] requires [M+H]$^+$ 248.0376, observed 248.0377.
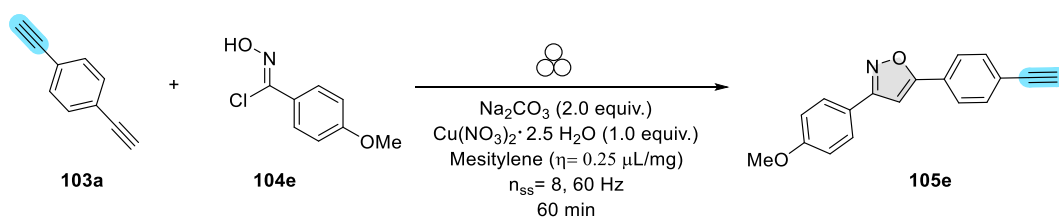

Synthesis of 5-(5-ethynylthiophen-2-yl)-3-(4-methoxyphenyl)isoxazole (105i): To a clean and dried stainless-steel (**SS**) planetary milling jar (approximately 50 mL capacity) with 8 **SS** balls (10 mm of diameter), it was weighed bis-alkyne **103c** (0.050 g, 0.378 mmol, 1.0 equivalents.), hydroxyimidoyl chloride **104a** (0.0572 g, 0.378 mmol, 1.0 equivalents.), Cu(NO$_3$)$_2$•2.5 H$_2$O (0.0879 g, 0.378 mmol, 1.0 equivalents.), Na$_2$CO$_3$ (0.0801 g, 0.756 mmol, 2.0 equivalents.). Once all the solids were introduced it was added *via* an automated pipette mesitylene (η= 0.25 µL/mg, 69 µL). The jar was closed, and the mixture was milled for 60 min at 60 Hz. After 60 min, the jar was cooled at room temperature, and the reaction mixture was carefully filtered over a celite plug using EtOAc as eluent. The filtrate was collected and reduced *in vacuo.* **105i** was isolated in silica column using Hex:EtOAc in ratios of 9:1 as eluent. **105i** was obtained as a white solid in 90% yield (95.8 mg) in ratios of (90:1). R*f*=0.14. **^{1}H NMR** (500 MHz, CDCl$_3$) δ 7.77 (d, *J* = 8.9 Hz, 2H), 7.40 (d, *J* = 3.8 Hz, 1H), 7.28 (d, *J* = 3.8 Hz, 1H), 6.99 (d, *J* = 8.9 Hz, 2H), 6.66 (s, 1H), 3.87 (s, 3H), 3.48 (s, 1H) **^{13}C NMR** (125 MHz, CDCl$_3$) δ 164.0, 162.6, 161.1, 133.8, 130.5, 128.2, 126.4, 124.4, 121.1, 114.3, 97.8, 83.7, 76.1, 55.4. **HRMS** calculated for [C$_{16}$H$_{11}$NO$_2$S] requires [M+H]$^+$ 282.0583, observed 282.0583.
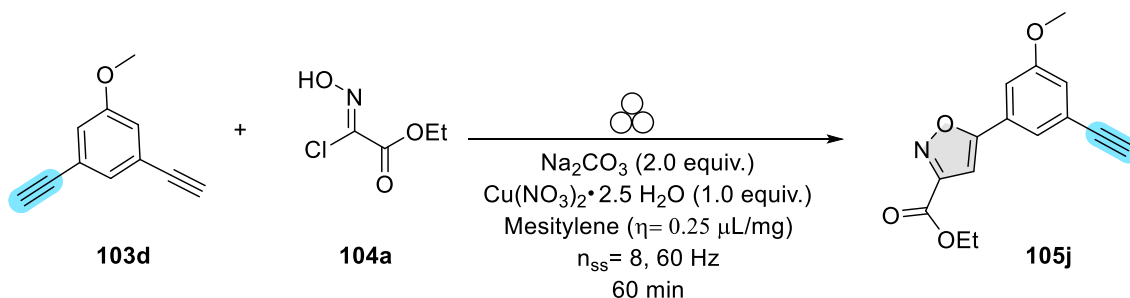
Synthesis of ethyl 5-(3-ethynyl-5-methoxyphenyl)isoxazole-3-carboxylate (105j): To a clean and dried stainless-steel (**SS**) planetary milling jar (approximately 50 mL capacity) with 8 **SS** balls (10 mm of diameter), it was weighed bis-alkyne **103d** (0.050g, 0.320 mmol, 1.0 equivalents.), hydroxyimidoyl chloride **104a** (0.0485 g, 0.320 mmol, 1.0 equivalents.), $Cu(NO_3)_2 \bullet 2.5\ H_2O$ (0.0744 g, 0.320 mmol, 1.0 equivalents.), Na_2CO_3 (0.0678 g, 0.640 mmol, 2.0 equivalents.). The jar was closed, and the mixture was milled for 60 min at 60 Hz. Once all the solids were introduced then it was added *via* an automated pipette mesitylene (η= 0.25 µL/mg, 60 µL). After 60 min, the jar was cooled at room temperature, and the reaction mixture was carefully filtered over a celite plug using EtOAc as eluent. The filtrate was collected and reduced *in vacuo.* **105j** was isolated in silica column using Hex:EtOAc in ratios of 7:3 as eluent. **105j** was obtained as a white solid in 60 % yield (54 mg) in ratios of (>99:1). R_f=0.63, MP=144.8-146.7 °C. **^{1}H NMR** (500 MHz, CDCl$_3$) δ 7.51 (t, *J* = 1.5 Hz, 1H), 7.32 (dd, *J* = 2.4, 1.5 Hz, 1H), 7.10 (dd, *J* = 2.4, 1.2 Hz, 1H), 6.93 (s, 1H), 4.47 (q, *J* = 7.1 Hz, 2H), 3.87 (s, 3H), 3.13 (s, 1H), 1.44 (t, *J* = 7.1 Hz, 3H). **^{13}C NMR** (125 MHz, CDCl$_3$) δ 170.5, 159.8, 127.9, 124.3, 122.0, 119.4, 112.2, 100.6, 82.3, 78.3, 63.6, 62.3, 55.6, 14.2. **HRMS** calculated for [C$_{20}$H$_{13}$NO$_2$] requires [M+H]$^+$ 300.1019, observed 300.1019. **HRMS** calculated for [C$_{15}$H$_{13}$NO$_4$] requires [M+H]$^+$ 272.0917, observed 272.0918.
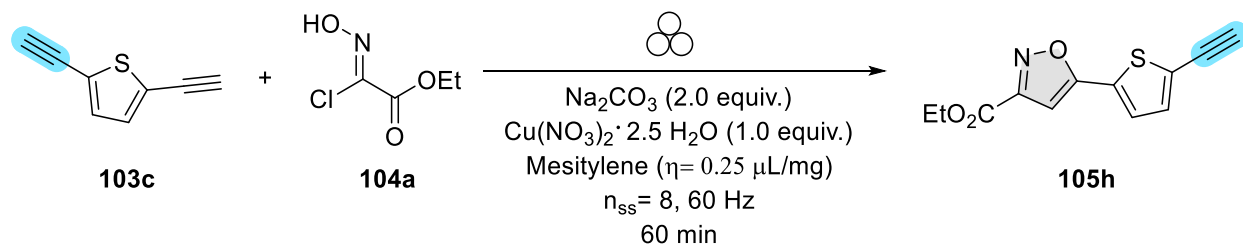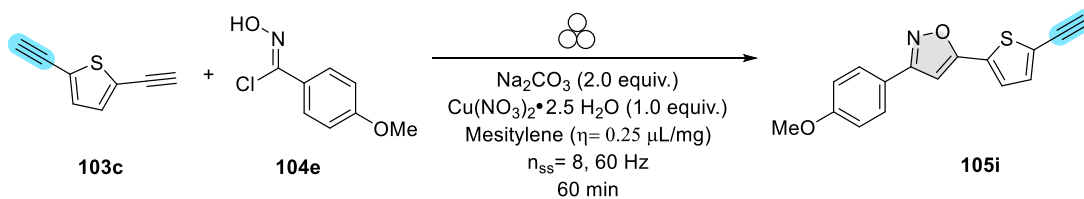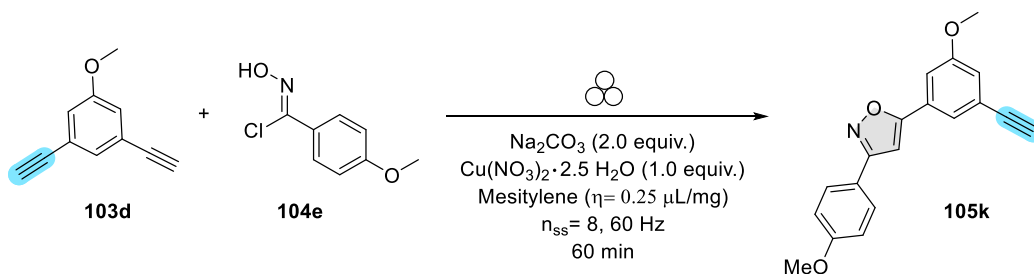

Synthesis of 5-(3-ethynyl-5-methoxyphenyl)-3-(4-methoxyphenyl)isoxazole (105k): To a clean and dried stainless-steel (**SS**) planetary milling jar (approximately 50 mL capacity) with 8 **SS** balls (10 mm of diameter), it was weighed bis-alkyne **103d** (0.050 g, 0.320 mmol, 1.0 equivalents.), hydroxyimidoyl chloride **104e** (0.060 g, 0.320 mmol, 1.0 equivalents.), $Cu(NO_3)_2 \bullet 2.5\ H_2O$ (0.0744 g, 0.320 mmol, 1.0 equivalents.), Na_2CO_3 (0.0678 g, 0.640 mmol, 2.0 equivalents.). The jar was closed, and the mixture was milled for 60 min at 60 Hz. Once all the solids were introduced then it was added *via* an automated pipette mesitylene (η= 0.25 µL/mg, 60 µL). After 60 min, the jar was cooled at room temperature, and the reaction mixture was carefully filtered over a celite plug using EtOAc as eluent. The filtrate was collected and reduced *in vacuo.* **105k** was isolated in silica column using Hex:EtOAc in ratios of 7:3 as eluent. **105k** was obtained as a white solid in 36 % yield (34.9 mg) in ratios of (3:1). R_f=0.53, MP= 100.0-103.0 °C. **^{1}H NMR** (500 MHz, CDCl$_3$) δ 7.79 (t, *J* = 8.4 Hz, 2H), 7.54 (t, *J* = 1.4 Hz, 1H), 7.37 (dd, *J* = 2.4, 1.5 Hz, 1H), 7.09 (dd, *J* = 2.5, 1.3 Hz, 1H), 7.00 (d, *J* = 8.9 Hz, 2H), 6.78 (s, 1H), 3.88 (s, 3H), 3.87 (s, 3H), 3.13 (s, 1H). **^{13}C NMR** (125 MHz, CDCl$_3$) δ 168.9, 162.6, 161.1, 159.8, 128.9, 128.2, 123.9, 122.0, 121.4, 118.9, 114.3, 112.1, 98.0, 82.6, 77.9, 55.6, 55.4. **HRMS** calculated for [C$_{19}$H$_{15}$NO$_3$] requires [M+H]$^+$ 306.1125, observed 306.1125.

Synthesis of 5-(6-ethynylpyridin-2-yl)-3-(4-methoxyphenyl)isoxazole (105n): To a clean and dried stainless-steel (**SS**) planetary milling jar (approximately 50 mL capacity) with 8 **SS** balls (10 mm of diameter), it was weighed bis-alkyne **103e** (0.025 g, 0.197, 1.0 equivalents.), hydroxyimidoyl chloride **104e** (0.037 g, 0.197, 1.0 equivalents.), $Cu(NO_3)_2 \cdot 2.5(H_2O)$ (0.0457 g, 0.197, 1.0 equivalents.), Na_2CO_3 (0.0416 g, 0.393 mmol, 2.0 equivalents.). The jar was closed, and the mixture was milled for 60 min at 60 Hz. Once all the solids were introduced then it was added *via* an automated pipette mesitylene (η= 0.25 μL/mg, 37 μL). After 60 min, the jar was cooled at room temperature, and the reaction mixture was carefully filtered over a celite plug using EtOAc as eluent. The obtained solid was washed with Et_2O and filtered for a second time using a Buchner funnel. The filtrate was reduced under pressure and recrystallized in Acetone:H_2O. The solid was filtered and washed with hot hexanes to obtain **105n** as a grey solid. **105n** was obtained in 90 % yield (50 mg) in ratios of (9:1). R_f=0.13 (9:1 Hex:EtOAc), MP=151.0-152.0 °C. **¹H NMR** (500 MHz, CDCl₃) δ 7.93 (dd, *J* = 7.9, 1.0 Hz, 1H), 7.86 – 7.79 (m, *J* = 8.3, 7.5 Hz, 3H), 7.52 (dd, *J* = 7.7, 1.0 Hz, 1H), 7.31 (s, 1H), 7.00 (d, *J* = 8.9 Hz, 2H), 3.87 (s, 3H), 3.24 (s, 1H). **¹³C NMR** (125 MHz, CDCl₃) δ 168.7, 162.9, 161.1, 147.0, 142.6, 137.3, 128.2 ,127.9, 121.3, 120.4, 114.4, 100.9, 82.3, 77.9, 55.4. **HRMS** calculated for [$C_{17}H_{12}N_2O_2$] requires [M+H]⁺ 277.0972, observed 277.0973.
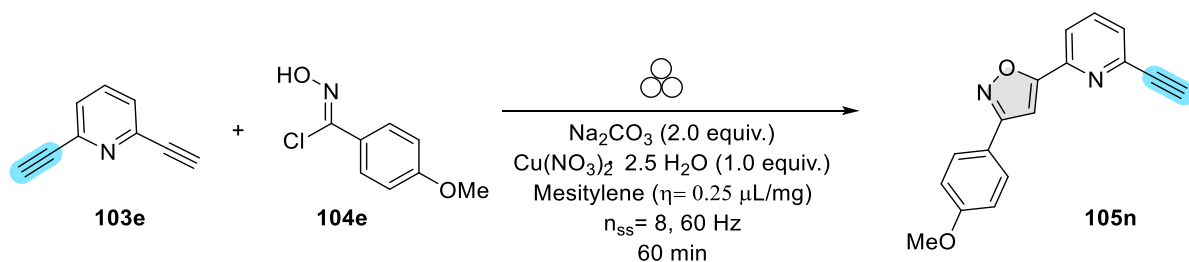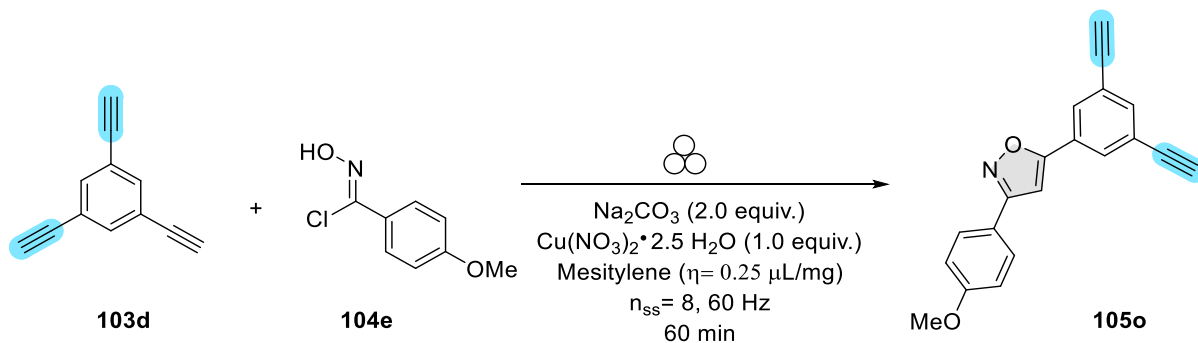

Synthesis of 5-(3,5-diethynylphenyl)-3-(4-methoxyphenyl)isoxazole (105o): [7]To a clean and dried stainless-steel (**SS**) planetary milling jar (approximately 50 mL capacity) with 8 **SS** balls (10 mm of diameter), it was weighed tris-alkyne **103d** (0.100 g, 0.666 mmol, 1.0 equivalents.), hydroxyimidoyl chloride **104e** (0.123 g, 0.792 mmol, 1.0 equivalents.), $Cu(NO_3)_2 \cdot 2.5 H_2O$ (0.153.5 g, 0.792 mmol, 1.0 equivalents.), Na_2CO_3 (0.141 g, 1.584 mmol, 2.0 equivalents.). The jar was closed, and the mixture was milled for 60 min at 60 Hz. After 60 min, the jar was cooled at room temperature, and the reaction mixture was carefully filtered over a celite plug using EtOAc as eluent. The filtrate was collected and reduced *in vacuo.* **105o** was isolated in silica column using Hex:EtOAc in ratios of 9:1 as eluent. **105o** was obtained as a white solid in 52 % yield (100 mg) in ratios of (4:1). R_f=0.17, MP= 168.7-170.1 °C. **¹H NMR** (500 MHz,

---

[7] Compound **105i** was also synthesized utilizing Mesitylene liquid additive (η= 0.25 μL/mg, 129 μL), but it was obtained in 26 % yield.

CDCl₃) 7.92 (d, *J* = 1.2 Hz, 2H), 7.79 (d, *J* = 8.8 Hz, 2H), 7.66 (s, 1H), 7.00 (d, *J* = 8.8 Hz, 2H), 6.82 (s, 1H), 3.87 (s, 3H), 3.17 (s, 2H). **^{13}C NMR** (125 MHz, CDCl₃) δ 168.9, 162.6, 161.1, 159.8, 128.9, 128.2, 123.9, 122.0, 121.4, 118.9, 114.3, 112.1, 98.0, 82.6, 77.9, 55.6, 55.4. **HRMS** calculated for [$C_{20}H_{13}NO_2$] requires [M+H]⁺ 300.1019, observed 300.1019.

Synthesis of N-((3-(4-nitrophenyl)isoxazol-5-yl)methyl)-N-(prop-2-yn-1-yl)prop-2-yn-1-amine (105p): To a clean and dried stainless-steel (**SS**) planetary milling jar (approximately 50 mL capacity) with 8 **SS** balls (10 mm of diameter), it was weighed tris-alkyne **103g** (0.107 µL, 0.762 mmol, 1.0 equivalents.), hydroxyimidoyl chloride **104c** (0.153 mg, 0.762 mmol, 1.0 equivalents.), Cu(NO₃)₂•2.5 H₂O (0.177 mg, 0.762 mmol, 1.0 equivalents.), Na₂CO₃ (0.161 mg, 1.524 mmol, 2.0 equivalents.). The jar was closed, and the mixture was milled for 60 min at 60 Hz. After 60 min, the jar was cooled at room temperature, and the reaction mixture was carefully filtered over a celite plug using EtOAc as eluent. The filtrate was collected and reduced *in vacuo.* **105p** was isolated in silica column using Hex:EtOAc in ratios of 8:2 as eluent. **105p** was obtained as a yellow solid in 59 % yield (121.3 mg) in ratios of (3:1). R*f*=0.26, MP=113.5-115.2 °C.**^{1}H NMR** (500 MHz, CDCl₃) δ 8.31 (d, *J* = 9.0 Hz, 2H), 7.98 (d, *J* = 8.9 Hz, 2H), 6.65 (s, 1H), 3.97 (s, 2H), 3.52 (d, *J* = 2.4 Hz, 3H), 2.32 (t, *J* = 2.4 Hz, 2H). **^{13}C NMR** (125 MHz, CDCl₃) δ 171.0, 160.6, 148.7, 135.1, 127.6, 124.2, 101.6, 77.8, 74.0, 48.00, 42.5. **HRMS** calculated for [$C_{16}H_{13}N_3O_3$] requires [M+H]⁺ 296.1030, observed 296.1028.
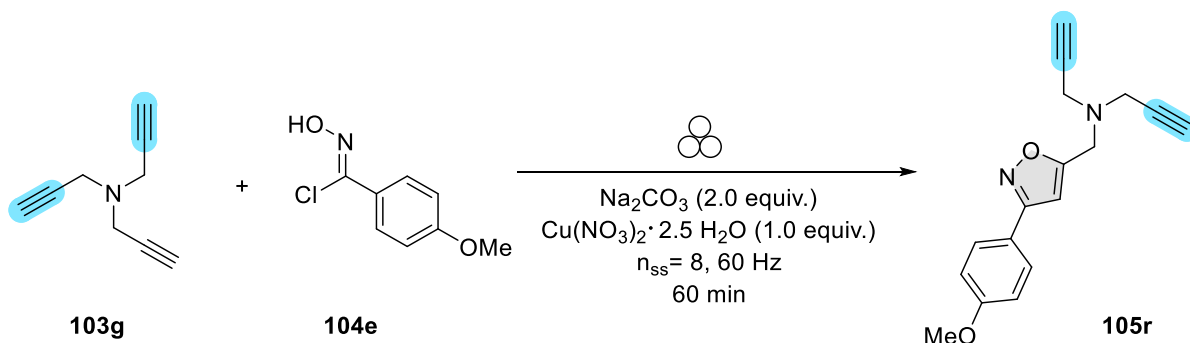
Synthesis of N-((3-(4-methoxyphenyl)isoxazol-5-yl)methyl)-N-(prop-2-yn-1-yl)prop-2-yn-1-amine (105r): To a clean and dried stainless-steel (**SS**) planetary milling jar (approximately 50 mL capacity) with 8 **SS** balls (10 mm of diameter), it was weighed tris-alkyne **103g** (0.107 µL, 0.762 mmol, 1.0 equivalents.), hydroxyimidoyl chloride **104e** (0.153 g, 0.762 mmol, 1.0 equivalents.), Cu(NO₃)₂•2.5 H₂O (0.177 g, 0.762 mmol, 1.0 equivalents.), Na₂CO₃ (0.161 g, 1.524 mmol, 2.0 equivalents.). The jar was closed, and the mixture was milled for 60 min at 60 Hz. After 60 min, the jar was cooled at room temperature, and the reaction mixture was carefully filtered over a celite plug using EtOAc as eluent. The filtrate was collected and reduced *in vacuo.* **105r** was isolated in silica column using Hex:EtOAc in ratios of 6:4 as eluent. **105r** was obtained as a yellow solid in 70 % yield (150 mg) in ratios of (8:1). R*f*= 0.58, MP: 53.9-56.0 °C.**^{1}H NMR** (500 MHz, CDCl₃) δ 7.74 (d, *J* = 8.90 Hz, 2H), 6.96 (d, *J* = 8.9 Hz, 2H), 6.51 (s, 1H), 3.92 (s, 2H), 3.82 (s, 3H),

3.52 (d, J = 2.4 Hz, 4H), 2.31 (t, J = 2.4 Hz, 2H). **^{13}C NMR** (125 MHz, CDCl$_3$) δ 171.0, 160.6, 148.7, 135.1, 127.6, 124.2, 101.6, 77.8, 74.0, 48.00, 42.5. **HRMS** calculated for [C$_{17}$H$_{16}$N$_2$O$_2$] requires [M+H]$^+$ 281.1285, observed 281.1285
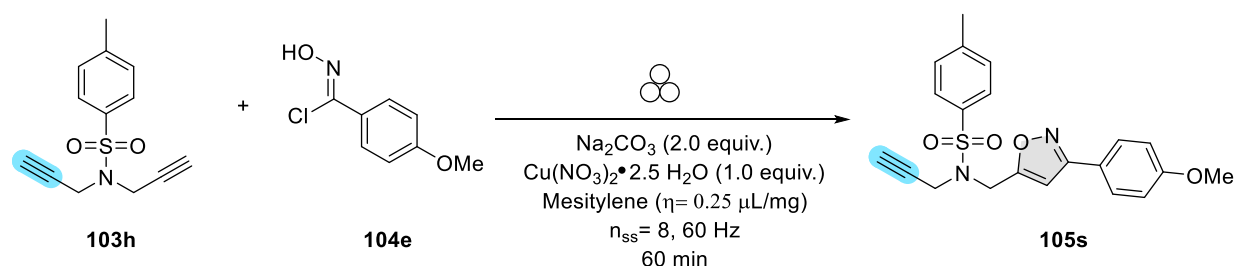
Synthesis of N-((3-(4-methoxyphenyl)isoxazol-5-yl)methyl)-4-methyl-N-(prop-2-yn-1-yl)benzenesulfonamide (105s): To a clean and dried stainless-steel (**SS**) planetary milling jar (approximately 50 mL capacity) with 8 **SS** balls (10 mm of diameter), it was weighed bis-alkyne **103h** (0.100 mg, 0.404 mmol, 1.0 equivalents.), hydroxyimidoyl chloride **104e** (0.075 g, 0.404 mmol, 1.0 equivalents.), Cu(NO₃)₂•2.5 H₂O (0.098 g, 0.404 mmol, 1.0 equivalents.), Na₂CO₃ (0.086 g, 0.808 mmol, 2.0 equivalents.). Once all the solids were introduced it was added *via* an automated pipette mesitylene (η= 0.25 μL/mg, 89 μL). The jar was closed, and the mixture was milled for 60 min at 60 Hz. After 60 min, the jar was cooled at room temperature, and the reaction mixture was carefully filtered over a celite plug using EtOAc as eluent. The filtrate was collected and reduced *in vacuo*. **105s** was isolated in silica column using Hex: DCM: EtOAc in ratios of 7:2:1 as eluent. **105s** was obtained as a white solid in 70 % yield (112.2 mg) in ratios of (8:1). R$_f$=0.14, MP= 122.0-124.3 °C.**^{1}H NMR** (500 MHz, CDCl$_3$) δ 7.76 (d, J = 8.2 Hz, 2H), 7.70 (d, J = 8.8 Hz, 2H), 7.32 (d, J = 8.0., 2H), 6.97 (d, J = 8.8, 2H), 6.49 (s, 1H), 4.60 (s, 2H), 4.17 (d, J = 2.30, 2H), 3.86 (s, 3H), 2.43 (s, 3H), 2.15 (t, J = 2.42, 1). **^{13}C NMR** (125 MHz, CDCl$_3$) δ 171.0, 160.6, 148.7, 135.1, 127.6, 124.2, 101.6, 77.8, 74.0, 48.00, 42.5. **HRMS** calculated for [C$_{21}$H$_{20}$N$_2$O$_4$] requires [M+H]$^+$ 397.1217, observed 397.1216.

Synthesis of ethyl 5-(pent-4-yn-1-yl)isoxazole-3-carboxylate (105t):[89] To a clean and dried stainless-steel (**SS**) planetary milling jar (approximately 50 mL capacity) with 8 **SS** balls (10 mm of diameter), it was weighed bis-alkyne **103i** (0.124 μL, 1.09 mmol, 1.0 equivalents.), hydroxyimidoyl chloride **104a** (0.165 mg, 1.09 mmol, 1.0 equivalents.), Cu(NO₃)₂•2.5 H₂O (0.253 mg, 1.09 mmol, 1.0 equivalents.), Na₂CO₃ (0.231 mg, 2.18 mmol, 2.0 equivalents.). The jar was closed, and the mixture was milled for 60 min at 60 Hz. After 60 min, the jar was cooled at room temperature, and the reaction mixture was carefully filtered over a celite plug using EtOAc as eluent. The filtrate was collected and reduced *in vacuo*. **105t** was isolated in silica column using Hex: EtOAc in ratios of 9:1 as eluent. **105t** was obtained as colourless oil in 68 % yield (153.4 mg). Rf= 0.25.**^{1}H NMR** (500 MHz, CDCl$_3$) δ 6.45 (s, 1H), 4.43 (d, J = 7.10 Hz, 2H), 2.95 (t, J = 7.58, 2H) ,2.28 (td, J = 2.63, 6.84, 2H), 2.01 (t, J = 2.61, 1H), 1.94 (m, 2H), 2.32 (t, J = 2.4 Hz, 2H), 1.40 (t, J = 7.11,

---

[8]Compound **104t** was also synthesized utilizing Mesitylene liquid additive (η= 0.25 μL/mg, 187 μL), but it was obtained in 54 % yield.

[9] A 1.0-g scale synthesis of 105t followed the same procedure. **105t** was obtained in 70 % (157.9 mg)

3H). ^{13}C NMR (125 MHz, CDCl$_3$) δ 171.0, 160.6, 148.7, 135.1, 127.6, 124.2, 101.6, 77.8, 74.0, 48.00, 42.5. HRMS calculated for [C$_{11}$H$_{13}$NO$_3$] requires [M+H]$^+$ 208.0968, observed 208.0969.

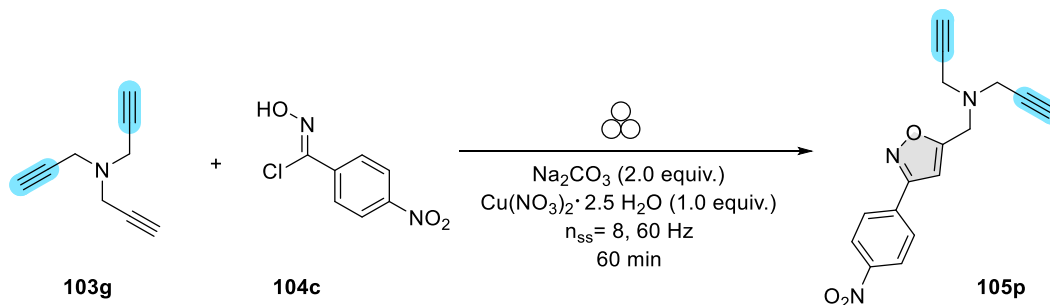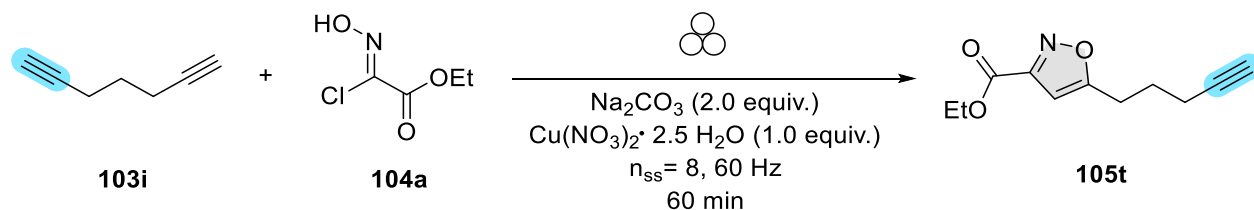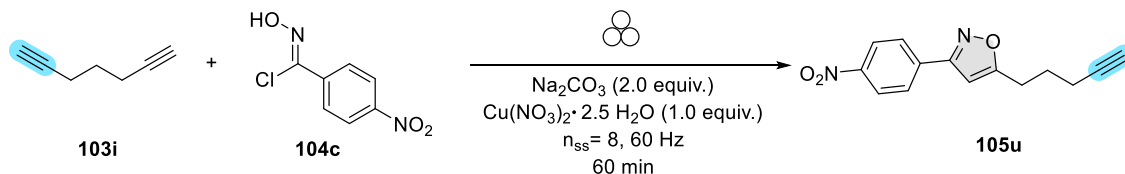

Synthesis of 3-(4-nitrophenyl)-5-(pent-4-yn-1-yl)isoxazole (105u): To a clean and dried stainless-steel (**SS**) planetary milling jar (approximately 50 mL capacity) with 8 **SS** balls (10 mm of diameter), it was weighed bis-alkyne **103i** (0.124 μL, 1.09 mmol, 1.0 equivalents.), hydroxyimidoyl chloride **104c** (217 mg, 1.09 mmol, 1.0 equivalents.), Cu(NO$_3$)$_2$•2.5 H$_2$O (217 mg, 1.09 mmol, 1.0 equivalents.), Na$_2$CO$_3$ (229 mg, 2.18 mmol, 2.0 equivalents.). Then, the jar was closed, and the mixture was milled for 60 min at 60 Hz. After 60 min, the jar was cooled at room temperature, and the reaction mixture was carefully filtered over a celite plug using EtOAc as eluent. The filtrate was collected and reduced *in vacuo.* The crude product was recrystallized in EtOAc:Hex. The solid was filtrated in a Buchner funnel, and the filtrate was collected and reduced *in vacuo* to obtain **105u**. **105u** was obtained as white solid in 90 % yield (216 mg). R*f*= 0.35, MP= 65.2-67.1 °C.^{1}**H NMR** (500 MHz, CDCl$_3$) δ ^{1}H NMR (500 MHz, CDCl$_3$) δ 8.32 (d, *J* = 9.0 Hz, 1H), 7.97 (d, *J* = 9.0 Hz, 2H), 6.42 (s, 1H), 3.00 (t, *J* = 7.5 Hz, 2H), 2.33 (td, *J* = 6.9, 2.7 Hz, 2H), 2.03 (t, *J* = 2.7 Hz, 1H), 2.00 (dt, *J* = 14.3, 7.0 Hz, 2H). ^{13}**C NMR** (125 MHz, CDCl3) δ 174.1, 160.6, 148.6, 135.4, 127.6, 124.2, 99.5, 82.7, 69.6, 25.8, 25.6, 17.8. **HRMS** calculated for [C$_{14}$H$_{12}$N$_2$O$_3$] requires [M+H]$^+$ 257.0921, observed 257.0921.

3.7.5. Procedure 4 (PS4): Comparative effects of solution-based conditions to mechanochemical conditions for the desymmetrizations alkyl bis-alkynes **103h**

The next set of experiments investigated and compared the effect of solution-based conditions to the developed mechanochemical conditions.
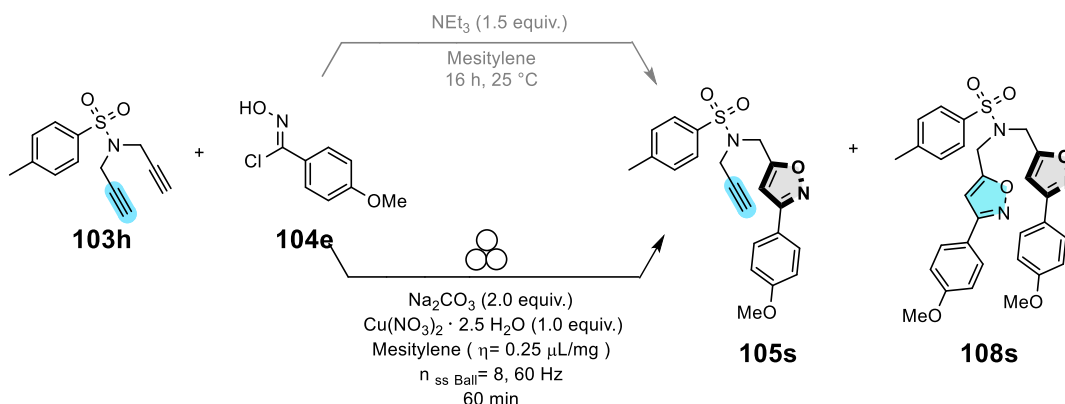
Solution-base conditions for the synthesis of N-((3-(4-methoxyphenyl)isoxazol-5-yl)methyl)-4-methyl-N-(prop-2-yn-1-yl)benzenesulfonamide (105s): In a clean round-bottom flask of 10 mL capacity, it was weighed bis-alkyne **103h** (0.066 g, 0.266 mmol, 1.0 equivalents.) and hydroxyimidoyl chloride **104e** (0.050 g, 0.266 mmol, 1.0 equivalents.). The solids were dissolved in 7 mL of mesitylene (η= 45.2 μL/mg). Then triethylamine was added (38 μL, 0.266 mmol, 1.0 equivalents.). The reaction was left to stir for 16 h. After 16 h, 12-15 mg of 1,3,5-trimetoxybenzene (TMB) was added as an internal standard. The reaction was diluted with EtOAc and washed with brine (2x10 mL) and water (2x 10 mL). The organic layer separated, dried over Na_2SO_4, filtered, and reduced *in vacuo*. The ratios of **103h**:**105s**:**108s** were calculated based on their integrations of ^{1}H-NMR.

Table S3.9. *Comparison of solution-based chemistry to mechanochemistry in the desymmetrization of bis-alkyne 103h*

Conditions	Yield 103h	Yield 105s	Yield 108s	105s:108s
Solution-based	66 %[a]	32 %[a]	16 %[a]	2:1
Mechanochemistry	20 %[b]	70 %[b]	9 %[b]	8:1

[a] Yield determined by ^{1}H-NMR. [b] Yield determined by isolation.

3.7.5.1. E-Factor Calculations

$$E_{factor} = \frac{Total\ mass\ of\ waste\ from\ process}{Total\ mass\ of\ product}$$

Mechanochemistry

Reaction yield = 112.2 mg (70 %)

Total mass of reactants: 75 mg + 100 mg + 103 mg + 98 mg + 86 mg= 462 mg

Waste formed by the reaction = 462 mg – 112 mg = 349.8 mg

E_{factor} = 349.8 mg / 112.2 mg = 3.11

Solution-based method: (Assuming 70 % of solvent recovery)

Reaction yield= 28 mg (32 % by 1H NMR) (calculated for a 50 mg scale reaction)

Total mass of reactants= 50 mg + 75 mg +2427.6 mg + 409 mg= 2961.6 mg

Waste formed by the reaction= 2961.6 mg – 28 mg = 2933.6

E_{factor} = 2933.6 mg / 28 mg = 104.7

3.7.6. Procedure 5 (PS5): Reaction Selectivity Comparison between Mechanochemistry and Solution-base

The next set of experiments investigated and compared the effect of solution-based conditions to the developed mechanochemical conditions for the selectivity and formation of the mono isoxazole product **105g**.
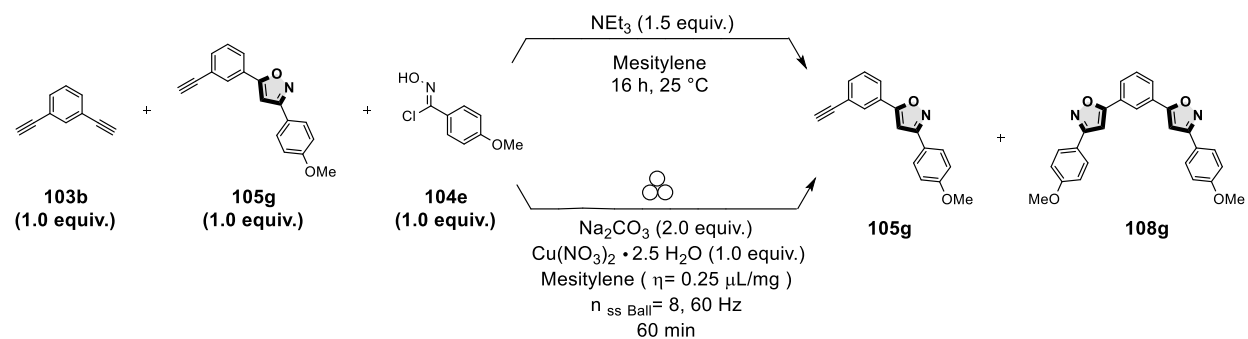
Kinetic competition experiment in **solution using optimized conditions**: In a clean round-bottom flask of 10 mL capacity, it was weighted , it was weighed bis-alkyne **103b** (24 μL , 0.181 mmol, 1.0 equivalents.), **105g** (0.050 g, 0.181 mmol, 1.0 equivalents.), and hydroxyimidoyl chloride **104e** (0.040 g, 0.266 mmol, 1.0 equivalents.). The solids were dissolved in 7 mL of mesitylene (η = 45.2 μL/mg). Then triethylamine was added (38 μL, 0.266 mmol, 1.0 equivalents.). The reaction was left to stir for 16 h. After 16 h, 12-15 mg of 1,3,5-trimetoxybenzene (TMB) was added as an internal standard. The reaction was diluted with EtOAc and washed with brine (2x10 mL) and water (2x 10 mL). The organic layer separated, dried over Na_2SO_4, filtered, and reduced *in vacuo*. The ratios of **103b**:**108g**:**105g** were calculated based on their integrations of ^{1}H-NMR. (Refer to Table)

Kinetic competition experiment in **solvent-free conditions**. To a clean and dried stainless-steel (**SS**) planetary milling jar (approximately 50 mL capacity) with 8 **SS** balls (10 mm of diameter), it was weighed bis-alkyne **103b** (24 μL, 0.181 mmol, 1.0 equivalents.), **105g** (0.050 g, 0.181 mmol, 1.0 equivalents.), hydroxyimidoyl chloride **16e** (0.040 g, 0.266 mmol, 1.0 equivalents.), Na_2CO_3 (40 mg, 0.362 mmol, 2.0 equivalents.), and 37 μL of mesitylene (η= 0.24 μL/mg). Then, the jar was closed, and the mixture was milled for 60 min at 60 Hz. After 60 min, the jar was cooled at room temperature, and 12-15 mg of 1,3,5-trimetoxybenzene (TMB) was added as an internal standard. The reaction mixture was carefully filtered over a celite plug using EtOAc as eluent. The filtrate was collected and reduced *in vacuo.* The ratios of **103b**:**105g**:**108g** were calculated based on their integrations by ^{1}H-NMR.

Table S3.10. *Kinetic Selectivity Comparison*

Conditions	103b conv.	Yield 105g	Yield 108g	105g:108g
Solution-based	*43 %*	33 %[a]	43 %[a]	1:1.3
Mechanochemistry	74 %[b]	70 %[b]	15 %[b]	4.7:1

[a] Yields determined by ^{1}H-NMR.

3.7.7. Selectivity on other Aromatic Bis-Alkyne Substrates by Mechanochemical Conditions

It was also demonstrated the selectivity of the reaction under mechanochemical conditions for substrate **103a**. Thus, it was reacted symmetrical bis-alkyne **103a** with equimolar amounts of 3,5-isoxazole-alkyne adduct **105a** and hydroxyimidoyl chloride **104a** under optimized conditions.
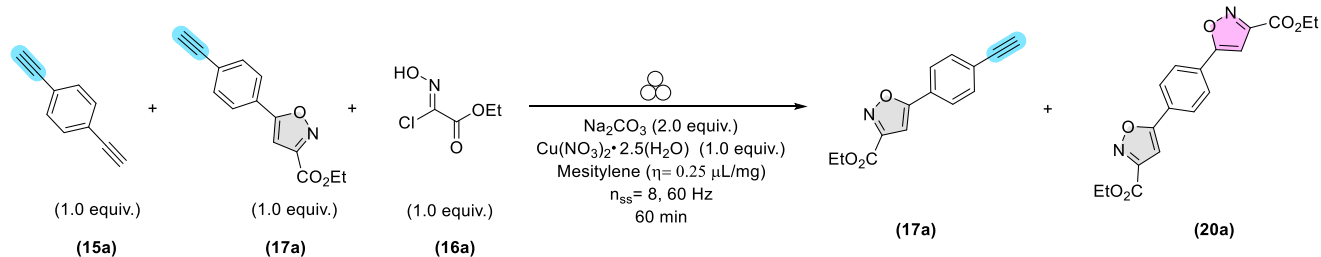
Procedure:

To a clean and dried stainless-steel (**SS**) planetary milling jar (approximately 50 mL capacity) with 8 **SS** balls (10 mm of diameter), it was weighed bis-alkyne **15a** (0.050 g, 0.396 mmol, 1.0 equivalents.), hydroxyimidoyl chloride **16a** (0.062 g, 0.396 mmol, 1.0 equivalents.), 3,5-isoxazole-alkyne adduct **117a** (0.142 g, 0.396 mmol, 1.0 equivalents.), $Cu(NO_3)_2 \cdot 2.5 H_2O$ (0.092 g, 0.396 mmol, 1.0 equivalents.), Na_2CO_3 (0.084 g, 0.792 mmol, 2.0 equivalents.). Once all the solids were introduced it was added *via* an automated pipette mesitylene liquid additive (η= 0.25 µL/mg, 72 µL). The jar was closed, and the mixture was milled for 60 min at 60 Hz. After 60 min, the jar was cooled at room temperature, and it was added 10-12 mg of TMB to the reaction crude. The reaction mixture was carefully filtered over a celite plug using EtOAc as eluent. The filtrate was collected and reduced *in vacuo.* The yield of **17a** and **17a:20a** ratios was obtained by ^{1}H NMR.

Table S3.11. *Reaction Selectivity Under Mechanochemical Conditions*

105a:108a	Yield % of 105a	Yield % of 108a
3:1	74	23

3.7.8. Procedure 6 (PS6): Synthesis of β-ketoenamine-alkyne

Synthesis of (Z)-3-amino-1-(4-ethynylphenyl)-3-(4-methoxyphenyl)prop-2-en-1-one (109) : In a clean ace pressure vial of 10 mL capacity, it was weighted 3,5-isoxazole-alkyne adduct (**105e**) (0.050 g, 0.181, 1.0 equiv.) and Mo(CO)$_6$ (0.072 g, 0.271, 1.5 equiv.) The solids were dissolved in 5 mL of ACN and 1 mL H$_2$O. The reaction was warmed to 90 °C (it was observed that **105e** dissolve) for 6 h. After 16 h, the crude product was let to cool to room temperature The crude solution was filtered through a silica plug using EtOAc as an eluent. The filtrate was collected and washed with HCl (1M) (2x 10 mL), brine (2x10 mL) and water (2x 10 mL). The organic layer collected, dried over Na$_2$SO$_4$, filtered, and reduced *in vacuo*. **109** was isolated in silica column using Hex: EtOAc in ratios of 7:3 as eluent. **109** was obtained as yellow solid in 98 % yield (49 mg). R$_f$=0.30 , MP= 131.3-133.3 °C. **^{1}H NMR** (500 MHz, CDCl$_3$) δ 10.51 (bs, 1H), 7.89 (d, *J* = 8.4 Hz, 2H), 7.58 (d, *J* = 8.8 Hz, 2H), 7.54 (d, *J* = 8.4 Hz, 2H), 6.97 (d, *J* = 8.8 Hz, 2H), 6.09 (s, 1H), 5.52 (s, 1H), 3.86 (s, 3H), 3.18 (bs, 1H).**^{13}C NMR** (125 MHz, CDCl$_3$) δ 188.5, 163.0, 161.8, 140.5, 132.0, 129.4, 127.8, 127.1, 124.5, 114.4, 91.1, 83.4, 78.9, 55.5. **HRMS** calculated for [C$_{18}$H$_{15}$NO$_2$] requires [M+H]$^+$ 278.1176, observed 278.1175

3.7.9. Procedure 7 (PS7): Optimization for the Synthesis of Unsymmetrical Bis-3,5-isoxazoles
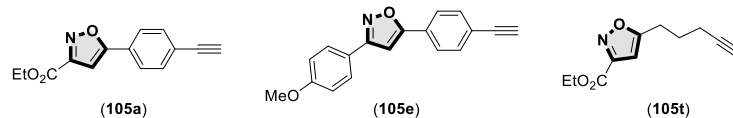
Figure S3.6. 3,5-Isoxazole-alkyne adduct substrates used in this optimization.

Prior to the isolation of unsymmetrical bis-3,5-isoxazoles **111**, the cycloaddition reactions between the corresponding 3,5-isoxazole-alkyne adduct **105a** and hydroxyimidoil chloride **110a** were used as a model reaction to optimize the synthesis of bis-3,5-isoxazoles. The reaction was optimized in a 50 mg using adduct **105a** to determine the optimal parameters. The yield of the unsymmetrical bis-3,5-isoxazole was quantified by ^{1}H NMR and using TMB as an internal standard.
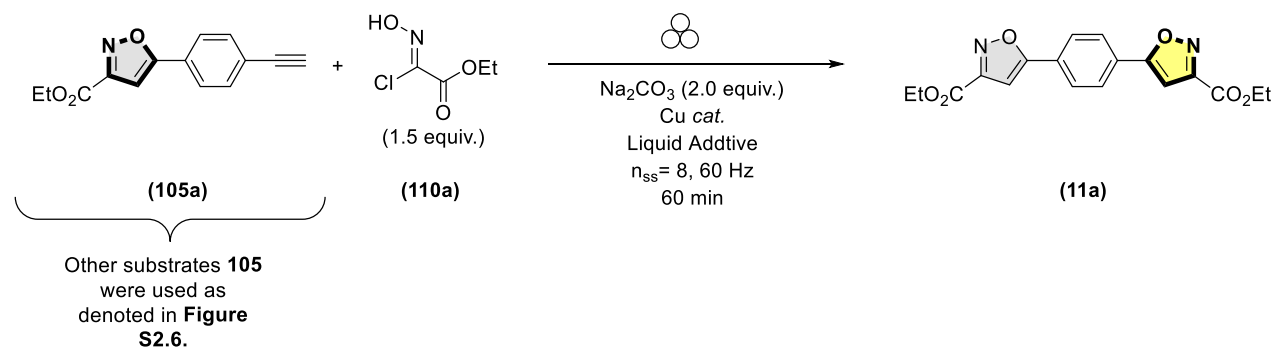
Table S3.12. *Effect of Cu catalyst and additive*

Cu complex	mol %	Yield of 111a %
Cu/Al$_2$O$_3$	14	N.R.
Cu(NO$_3$)$_2$•2.5 H$_2$O	100	N.R.
Cu(NO$_3$)$_2$•2.5 H$_2$O	10	N.R.
CuI	25	12
Chloro(1,5-cyclooctadiene)copper(I) dimer	25	8

Table S3.13. *Optimization of LAG*

LAG	η (μL/mg)	Yield of 111a %
	0.25	12
Mesitylene	0.5	12
	0.9	12
DCE	0.25	10
DMF	0.25	9

Table S3.14. *Effect of Substrate 105*

Substrate 105	Physical State	Equiv.	Yield %
105a	Solid		10
		1.00	
105e	Solid		5
105t	Liquid		45

3.7.10. Procedure 8 (PS8): Synthesis of Unsymmetrical Bis-3,5-isoxazoles

Example procedure for the synthesis of unsymmetrical bis-3,5-isoxazoles 111e

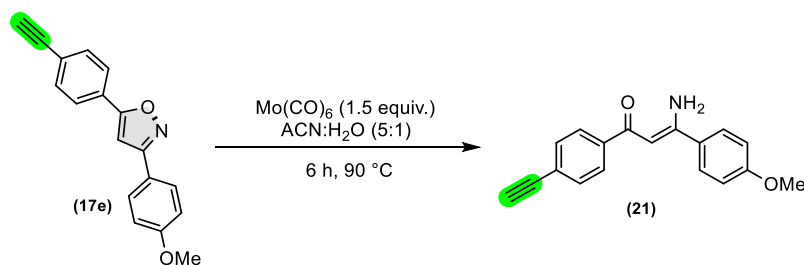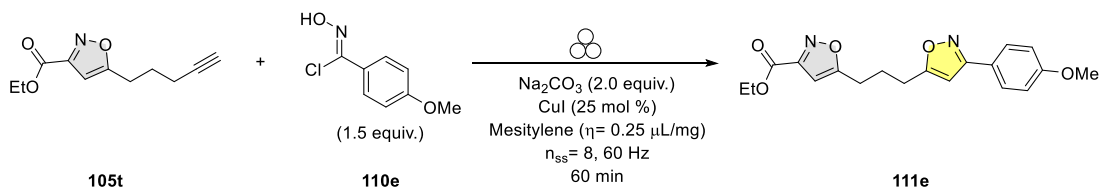**Synthesis of ethyl 5-(3-(3-(4-methoxyphenyl)isoxazol-5-yl)propyl)isoxazole-3-carboxylate (111e):** To a clean and dried stainless-steel (**SS**) planetary milling jar (approximately 50 mL capacity) with 8 **SS** balls (10 mm of diameter), it was weighed 3,5-isoxazole-alkyne adduct **105t** (92 μL, 0.482 mmol, 1.0 equivalents.), hydroxyimidoyl chloride **110e** (0.137 g, 0.722 mmol, 1.0 equivalents.), CuI (0.022 mg, 0.120 mmol, 25 mol %), Na$_2$CO$_3$ (0.102 mg, 0.964 mmol, 2.0 equivalents.), and mesitylene as liquid additive (η= 0.25 μL/mg, 64 μL). Then, the jar was closed, and the mixture was milled for 60 min at 60 Hz. After 60 min, the jar was cooled at room temperature, and the reaction mixture was carefully filtered over a silica plug using EtOAc as eluent. The filtrate was collected and reduced *in vacuo.* **111e** was isolated in silica column using Hex: EtOAc in ratios of 7:3 as eluent. **111e** was obtained as a white solid in 95 % yield (163.7 mg). R$_f$=0.30, MP=72.4-74.2 °C. **^{1}H NMR** (500 MHz, CDCl$_3$) δ 7.69 (d, *J* = 8.8 Hz, 2H), 6.94 (d, *J* = 8.8 Hz, 2H), 6.39 (s, 1H), 6.25 (s, 1H), 4.40 (q, *J* = 7.1 Hz, 2H), 3.82 (s, *J* = 5.9 Hz, 3H), 2.89 (t, *J* = 7.5 Hz, 2H), 2.84 (t, *J* = 7.4 Hz, 2H), 2.15 (p, *J* = 7.5 Hz, 2H), 1.38 (t, *J* = 7.1 Hz, 3H).**^{13}C NMR** (125 MHz, CDCl$_3$) δ 174.1, 171.9, 162.0, 161.0, 160.0, 156.4, 128.1, 121.6, 114.3, 102.0, 99.3, 62.1, 55.3, 25.9, 25.8, 25.3, 14.1. **HRMS** calculated for [C$_{19}$H$_{20}$N$_2$O$_5$] requires [M+H]$^+$ 357.1445, observed 357.1443
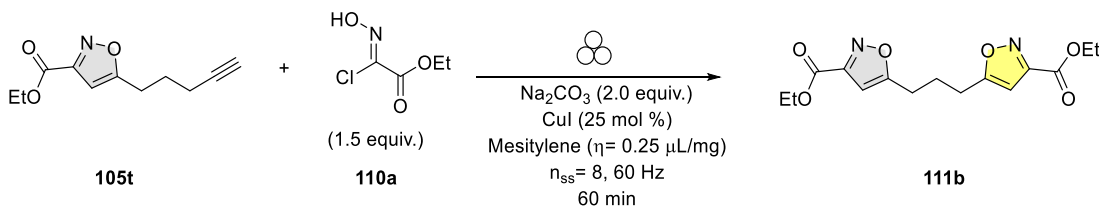
Synthesis of diethyl 5,5'-(propane-1,3-diyl)bis(isoxazole-3-carboxylate) (111b): Symmetrical bis-3,5-isoxazole **111b** was synthesize according to PS5. **111b** was recrystallized in EtOAC:Hex. **111b** was obtained as a white solid in 32 % yield (50 mg). R$_f$=0.11 (8:2 Hex:EtOAc), MP=91.5-93.5 °C. **^{1}H NMR** (500 MHz, CDCl$_3$) δ 6.44 (s, 2H), 4.41 (q, *J* = 7.1 Hz, 4H), 2.88 (t, *J* = 7.5 Hz, 4H), 2.16 (p, *J* = 7.5 Hz, 2H), 1.39 (t, *J* = 7.1 Hz, 6H). **^{13}C NMR** (125 MHz, CDCl$_3$) δ 173.6, 159.9, 156.5, 102.1, 62.1, 25.8, 25.2, 14.1. **HRMS** calculated for [C$_{15}$H$_{18}$N$_2$O$_6$] requires [M+H]$^+$ 323.1238, observed 323.1236.
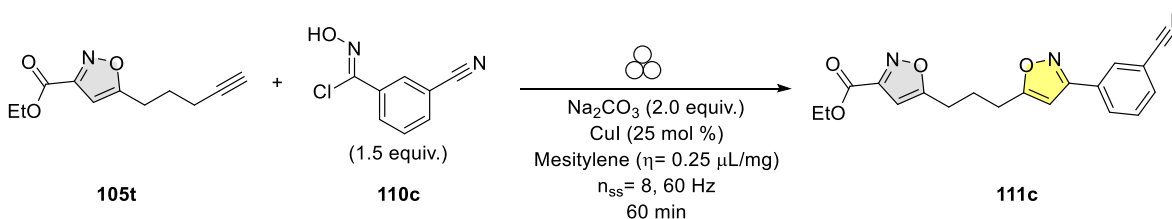
Synthesis of ethyl 5-(3-(3-(3-cyanophenyl)isoxazol-5-yl)propyl)isoxazole-3-carboxylate (111c): Unsymmetrical bis-3,5-isoxazole **111c** was synthesize according to PS5. **111c** was isolated in silica column using Hex: EtOAc in ratios of 8:2 as eluent. **111c** was obtained as a white solid in 70 % yield (118.5 mg).

R*f*=0.10, MP=80.2-83.1 °C. **¹H NMR** (500 MHz, CDCl₃) δ 8.03 (td, *J* = 1.7, 0.4 Hz, 1H), 8.01 (dt, *J* = 5.0, 1.5 Hz, 1H), 7.69 (dt, *J* = 10.0, 5.0 Hz, 1H), 7.56 (t, *J* = 7.8 Hz, 1H), 6.45 (s, 1H), 6.36 (s, 1H), 4.39 (q, *J* = 7.1 Hz, 2H), 2.91 (dd, *J* = 16.1, 7.6 Hz, 4H), 2.19 (p, *J* = 5.0 Hz, 2H), 1.37 (t, *J* = 7.1 Hz, 3H). **¹³C NMR** (125 MHz, CDCl₃) δ 173.8, 173.2, 160.6, 159.9, 156.5, 133.2, 130.8, 130.5, 130.2, 129.8, 118., 113.2, 102.0, 99.3, 62.1, 25.9, 25.9, 25.3, 14.1. **HRMS** calculated for [C₁₉H₁₇N₃O₄] requires [M+H]⁺ 352.1292, observed 352.129.
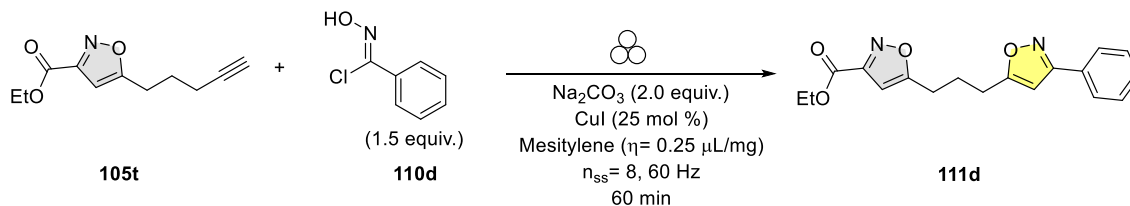
Synthesis of ethyl 5-(3-(3-phenylisoxazol-5-yl)propyl)isoxazole-3-carboxylate (111d): Unsymmetrical bis-3,5-isoxazole **105d** was synthesize according to PS5. **111d** was isolated in silica column using Hex: EtOAc in ratios of 8:2 as eluent. **111d** was obtained as a white solid in 96 % yield (118.5 mg). R*f*=0.68, MP=57.1-58.3 °C. **¹H NMR** (500 MHz, CDCl₃) δ 7.78 – 7.74 (m, 2H), 7.45 – 7.39 (m, 3H), 6.45 (s, 1H), 6.32 (s, 1H), 4.40 (q, *J* = 7.1 Hz, 2H), 2.90 (t, *J* = 7.5 Hz, 2H), 2.87 (t, *J* = 7.4 Hz, 2H), 2.17 (p, *J* = 7.5 Hz, 1H), 1.38 (t, *J* = 7.2 Hz, 3H). **¹³C NMR** (125 MHz, CDCl₃) δ 174.0, 172.2, 162.4, 160.0, 156.5, 129.9, 129.1, 128.9, 126.7, 102.0, 99.5, 62.1, 25.9, 25.3, 14.1. **HRMS** calculated for [C₁₈H₁₈N₂O₄] requires [M+H]⁺ 327.1339, observed 327.1343.
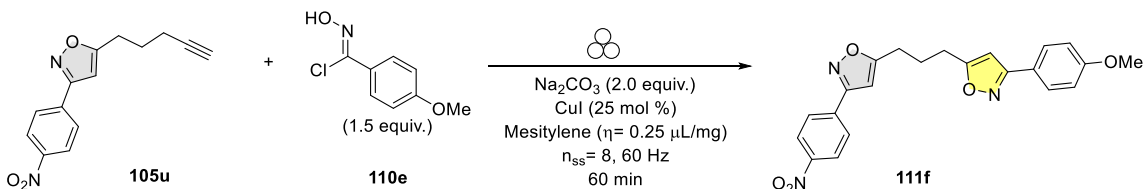
Synthesis of ethyl 5-(3-(3-phenylisoxazol-5-yl)propyl)isoxazole-3-carboxylate (111f): Unsymmetrical bis-3,5-isoxazole **111f** was synthesize according to PS5. **111f** by recrystallisation of the reaction crude in EtOAc:Hexanes. **111f** was obtained as a yellow solid in >99 % yield (79 mg). R*f*=0.21 (7:3 Hex:EtOAc), MP= 110.6-113.2 °C. **¹H NMR** (500 MHz, *d⁶*-DMSO) δ 8.35 (d, *J* = 8.7 Hz, 2H), 8.12 (d, *J* = 8.6 Hz, 2H), 7.76 (d, *J* = 8.7 Hz, 2H), 7.05 (d, *J* = 8.6 Hz, 2H), 7.03 (s, 1H), 6.80 (s, 1H), 3.81 (s, 3H), 2.96 (t, *J* = 7.6 Hz, 2H), 2.91 (t, *J* = 7.4 Hz, 2H), 2.13 (quint, *J* = 7.4 Hz, 2H).**¹³C NMR** (125 MHz, *d⁶*-DMSO) δ 174.6, 173.2, 161.8, 161.0, 160.9, 148.7, 135.3, 128.4, 128.2, 124.7, 121.6, 114.9, 100.6, 99.8, 55.7, 25.9, 25.8, 25.3. **HRMS** calculated for [C₂₂H₁₉N₃O₅] requires [M+H]⁺ 406.1397, observed 406.1396

3.7.11. Spectroscopic Data for the demonstrated compounds

Ethyl 5-(4-ethynylphenyl)isoxazole-3-carboxylate (105a)
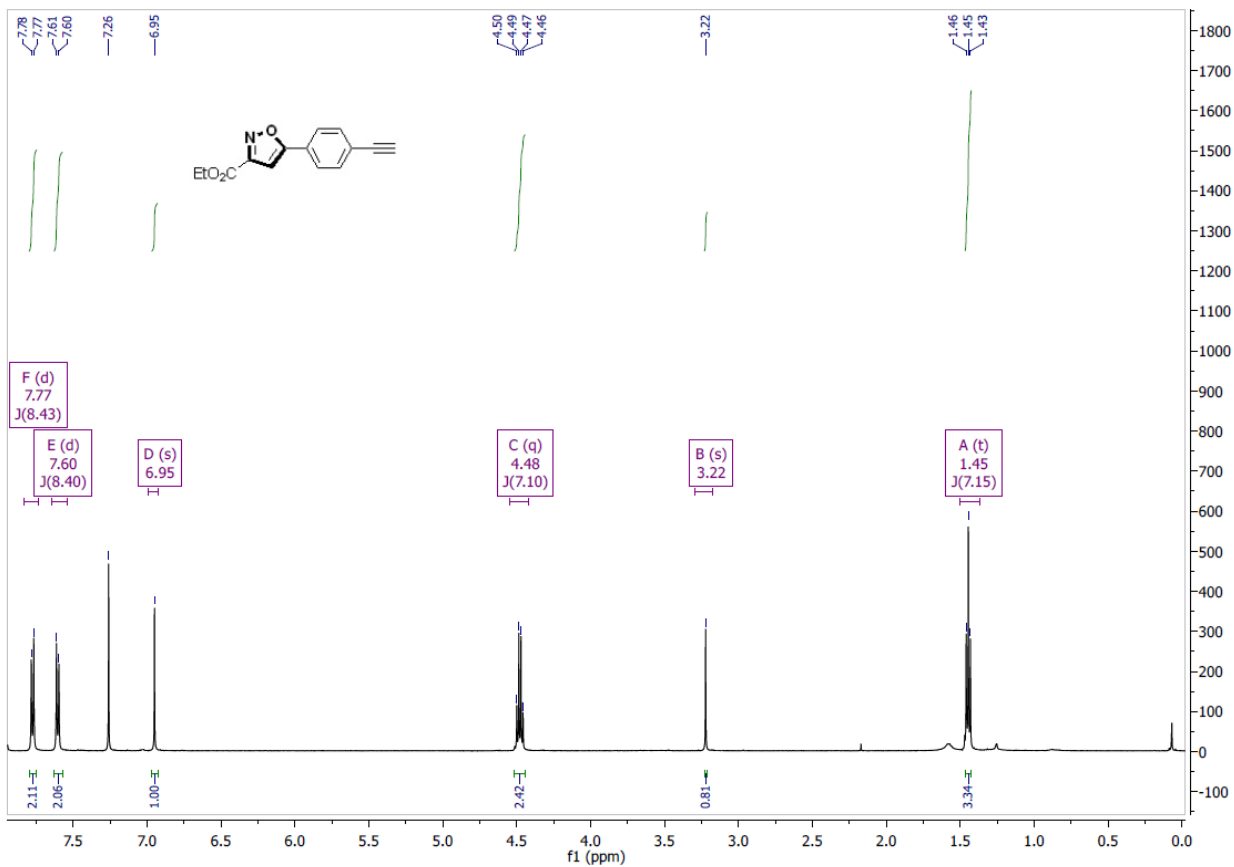
Figure S3.7. ¹H-NMR (500 MHz, CDCl₃) of ethyl 5-(4-ethynylphenyl)isoxazole-3-carboxylate (105a)
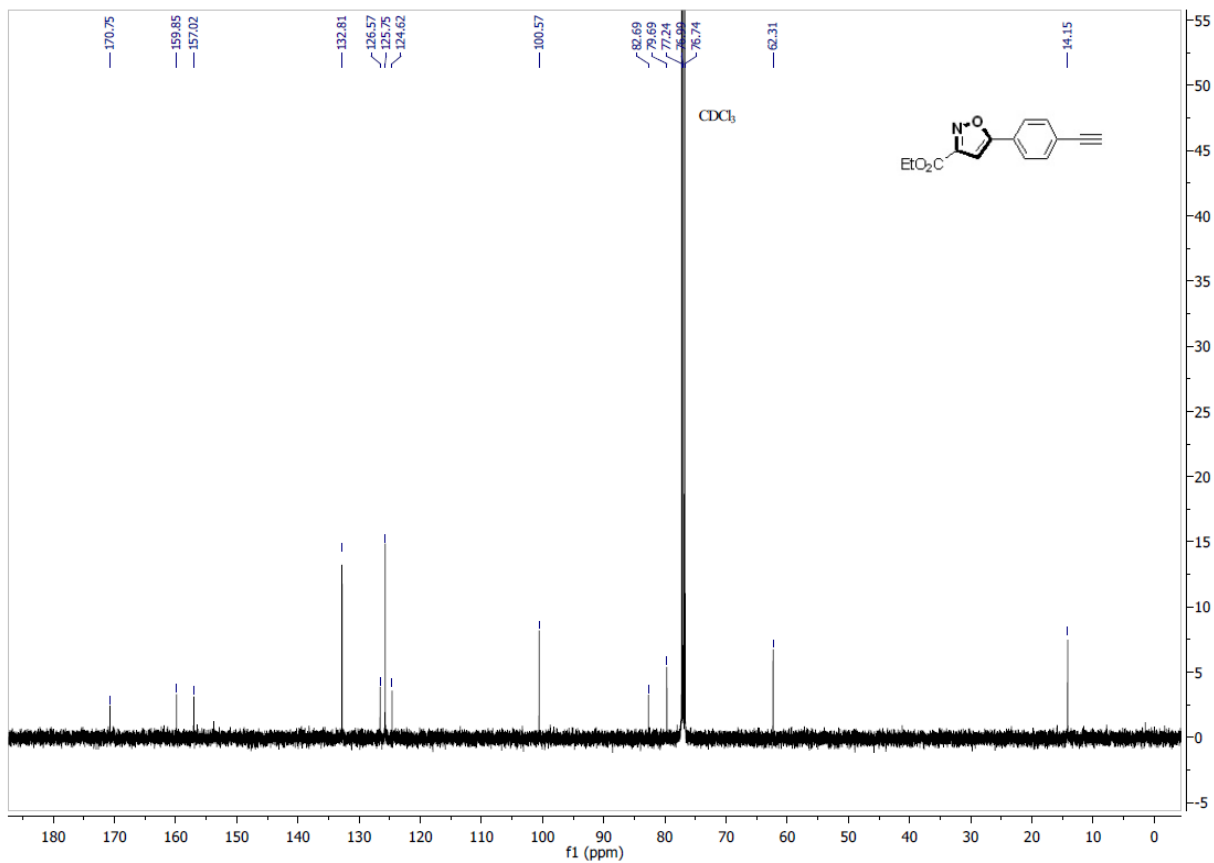
Figure S3.8. ^{13}C-NMR (125 MHz, CDCl$_3$) of ethyl 5-(4-ethynylphenyl)isoxazole-3-carboxylate (105a)

3-bromo-5-(4-ethynylphenyl)isoxazole (105b)
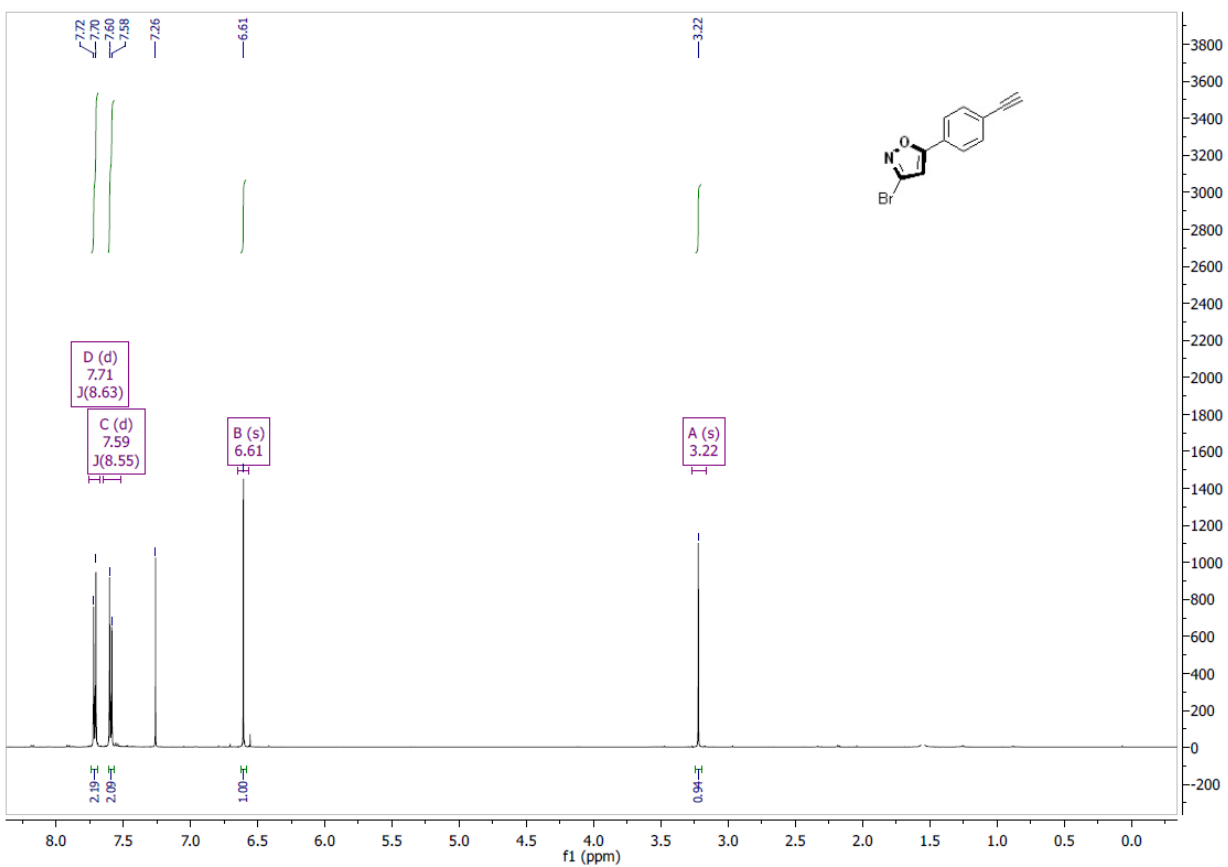
Figure S3.9. ^{1}H-NMR (500 MHz, CDCl$_3$) of 3-bromo-5-(4-ethynylphenyl)isoxazole (105b)
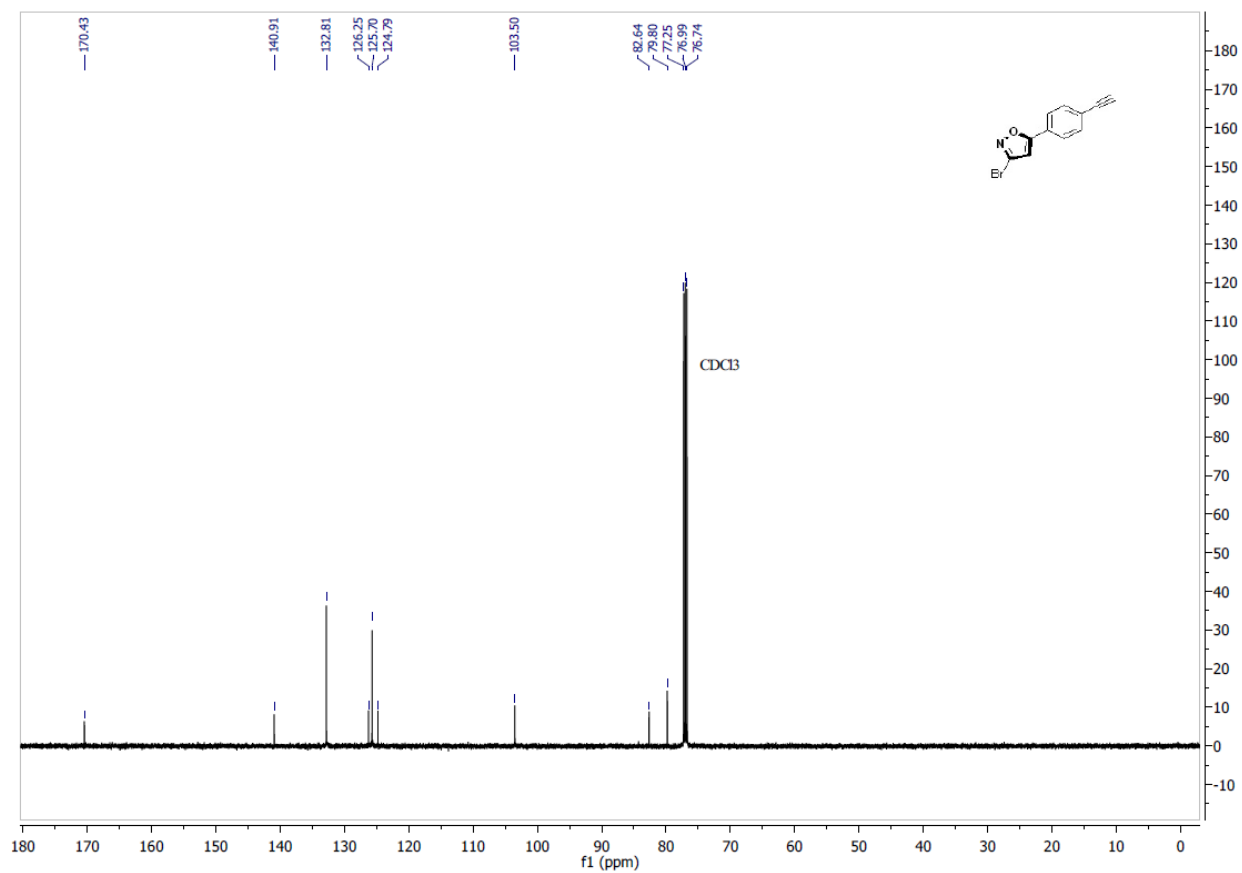
Figure S3.10. ^{13}C-NMR (125 MHz, CDCl$_3$) of 3-bromo-5-(4-ethynylphenyl)isoxazole (105b)

5-(4-ethynylphenyl)-3-(4-nitrophenyl)isoxazole (105c)
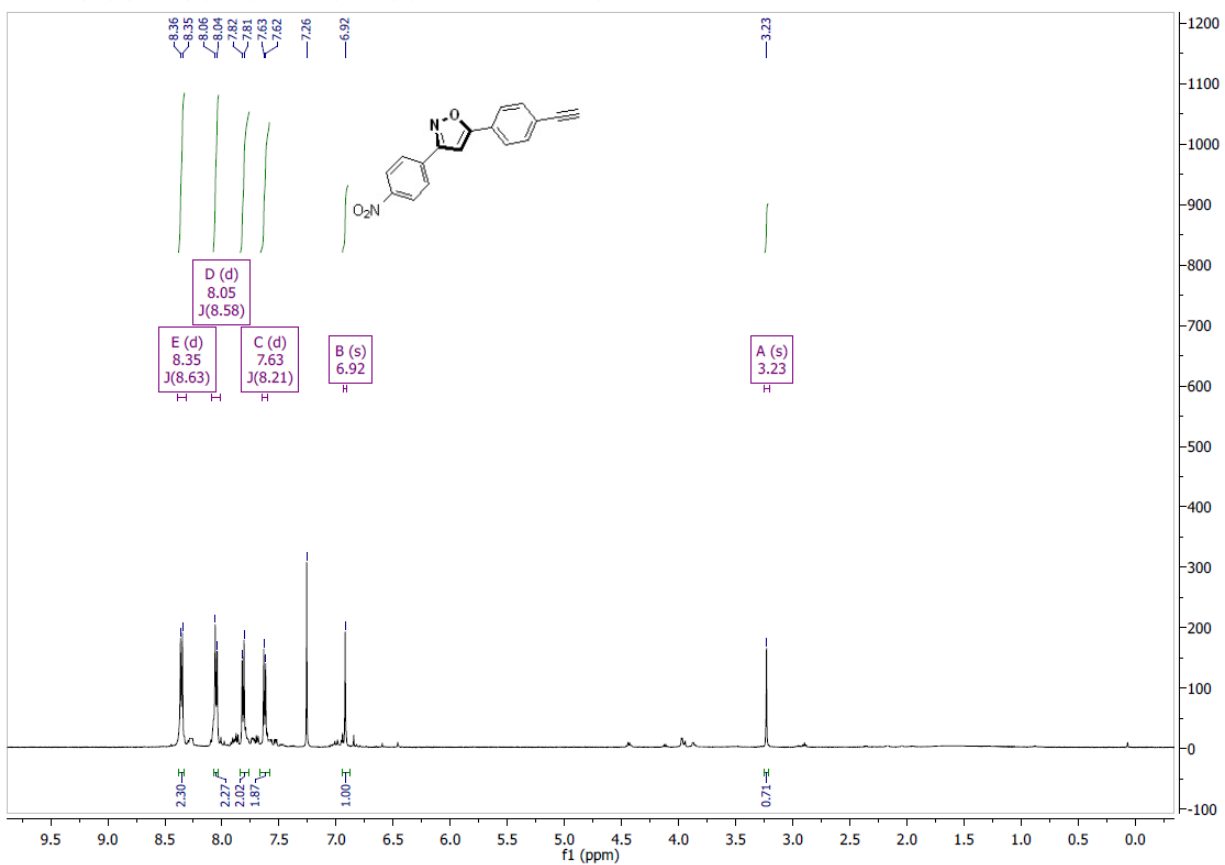
Figure S3.11. ^{1}H-NMR (500 MHz, CDCl$_3$) of 5-(4-ethynylphenyl)-3-(4-nitrophenyl)isoxazole (105c)
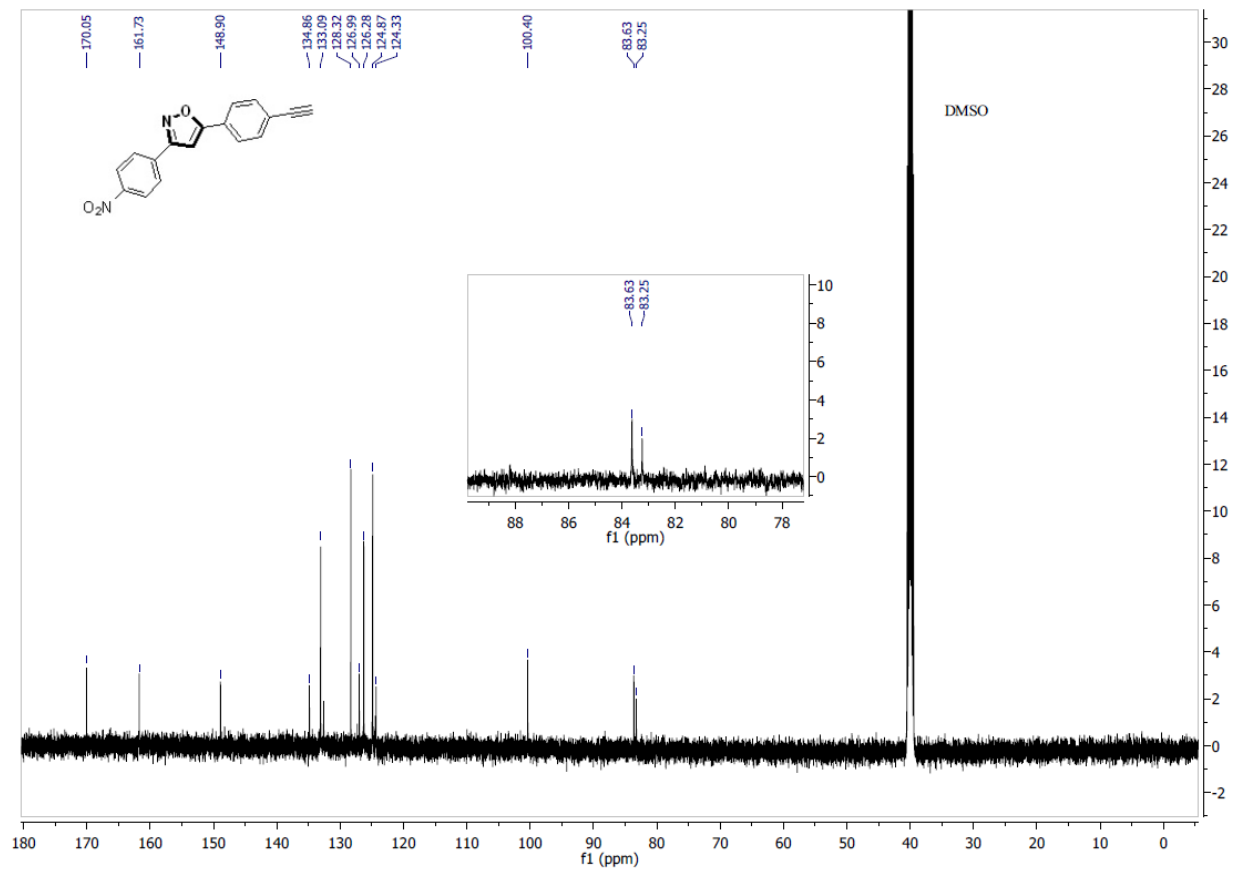
Figure S3.12. ^{13}C-NMR (125 MHz, DMSO-d^6) of 5-(4-ethynylphenyl)-3-(4-nitrophenyl)isoxazole (105c)

5-(4-ethynylphenyl)-3-phenylisoxazolethyl 5-(4-ethynylphenyl)isoxazole-3-carboxylate (105d)
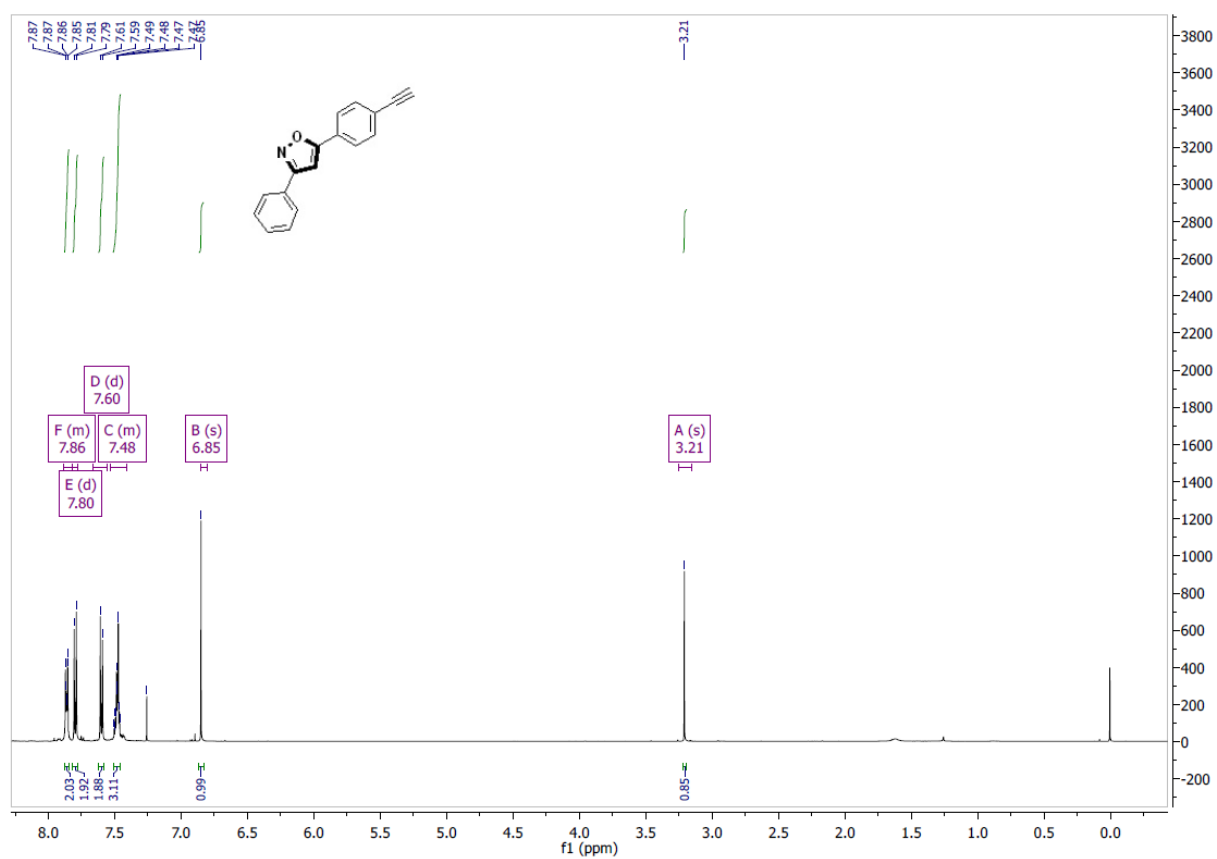
Figure S3.13. ^{1}H-NMR (500 MHz, CDCl$_3$) of 5-(4-ethynylphenyl)-3-phenylisoxazolethyl 5-(4-ethynylphenyl)isoxazole-3-carboxylate (105d)
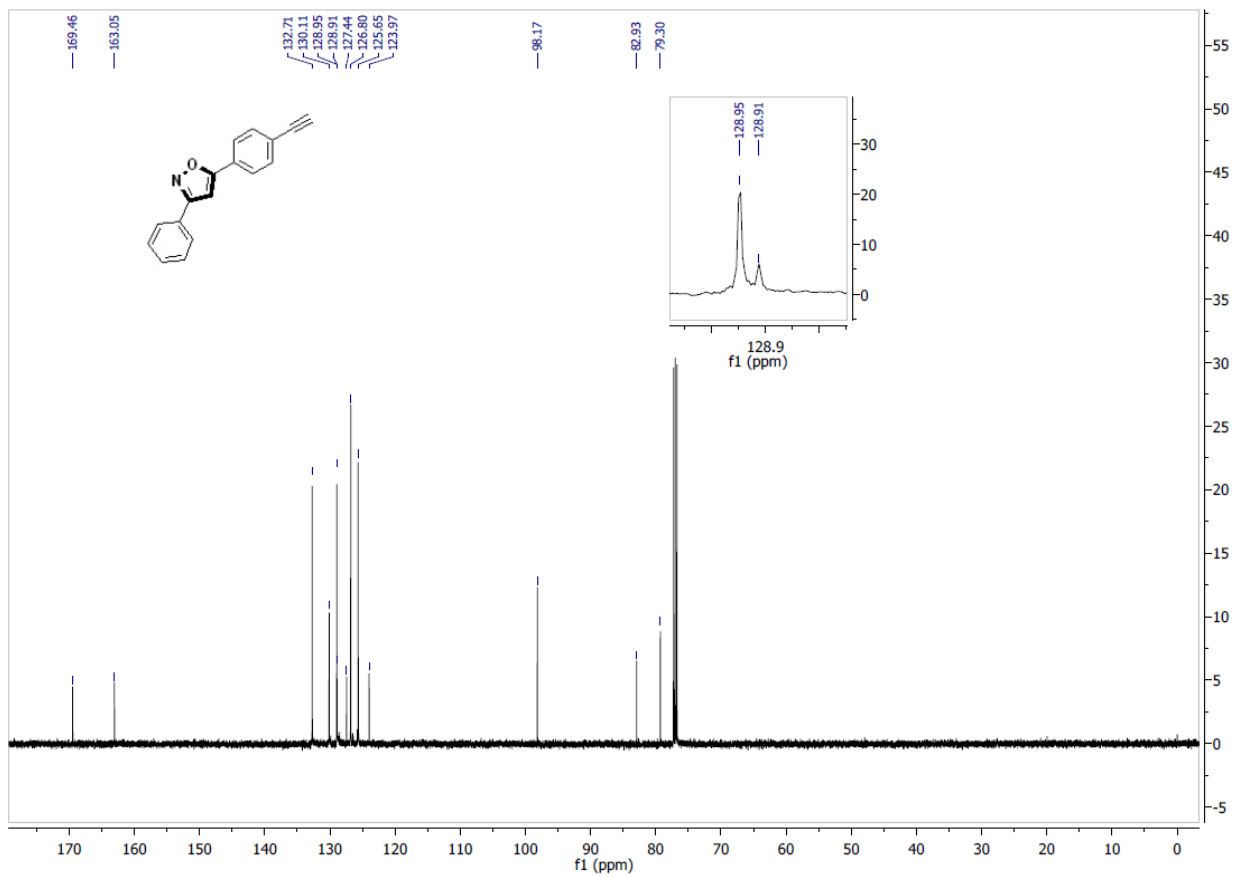
Figure S3.14. ^{13}C-NMR (125 MHz, CDCl$_3$) of 5-(4-ethynylphenyl)-3-phenylisoxazolethyl 5-(4-ethynylphenyl)isoxazole-3-carboxylate (105d)

5-(4-ethynylphenyl)-3-(4-methoxyphenyl)isoxazole (105e)
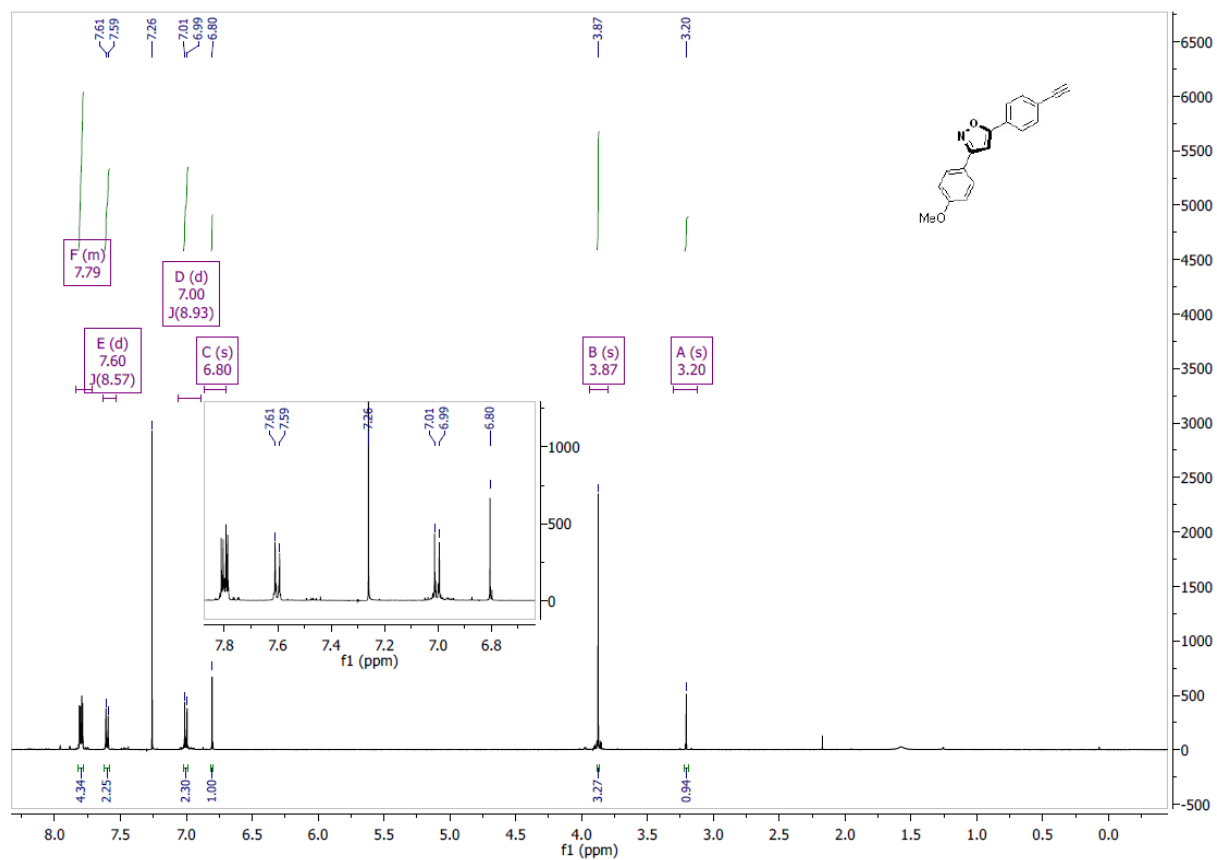
Figure S3.15. ^{1}H-NMR (500 MHz, CDCl₃) of 5-(4-ethynylphenyl)-3-(4-methoxyphenyl)isoxazole (105e)
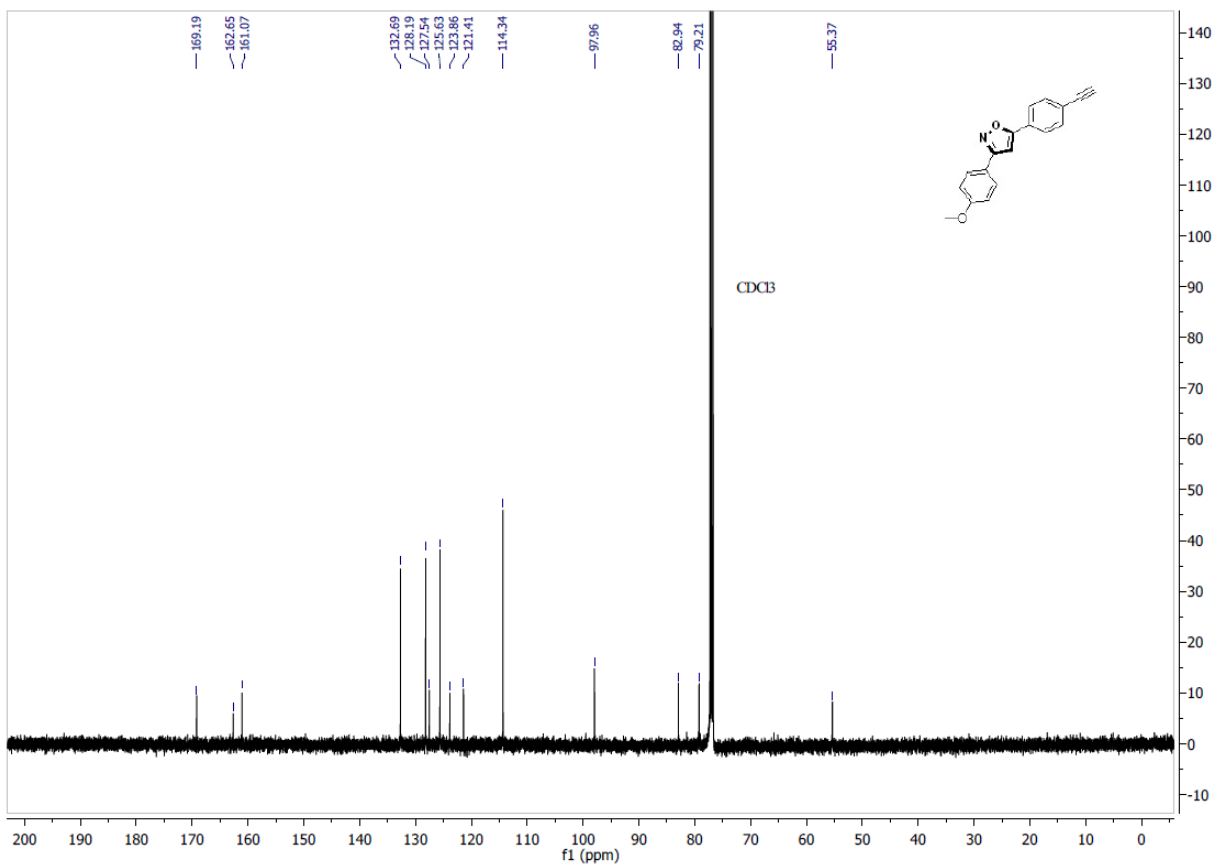
Figure S3.16. ^{13}C-NMR (125 MHz, CDCl$_3$) of 5-(4-ethynylphenyl)-3-(4-methoxyphenyl)isoxazole (105e)

5-(3-ethynylphenyl)-3-(4-methoxyphenyl)isoxazole (105g)
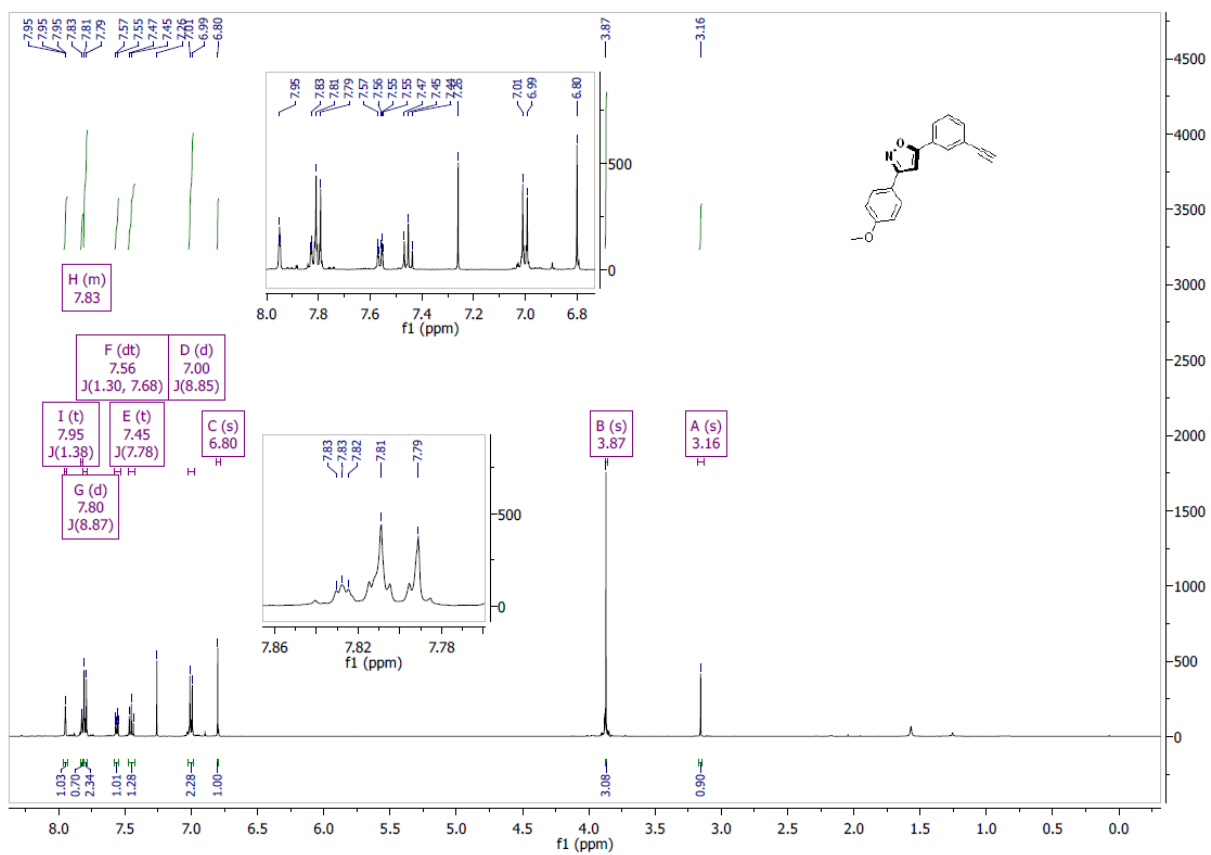
Figure S3.17. ^{1}H-NMR (500 MHz, CDCl$_3$) of 5-(3-ethynylphenyl)-3-(4-methoxyphenyl)isoxazole (105g)
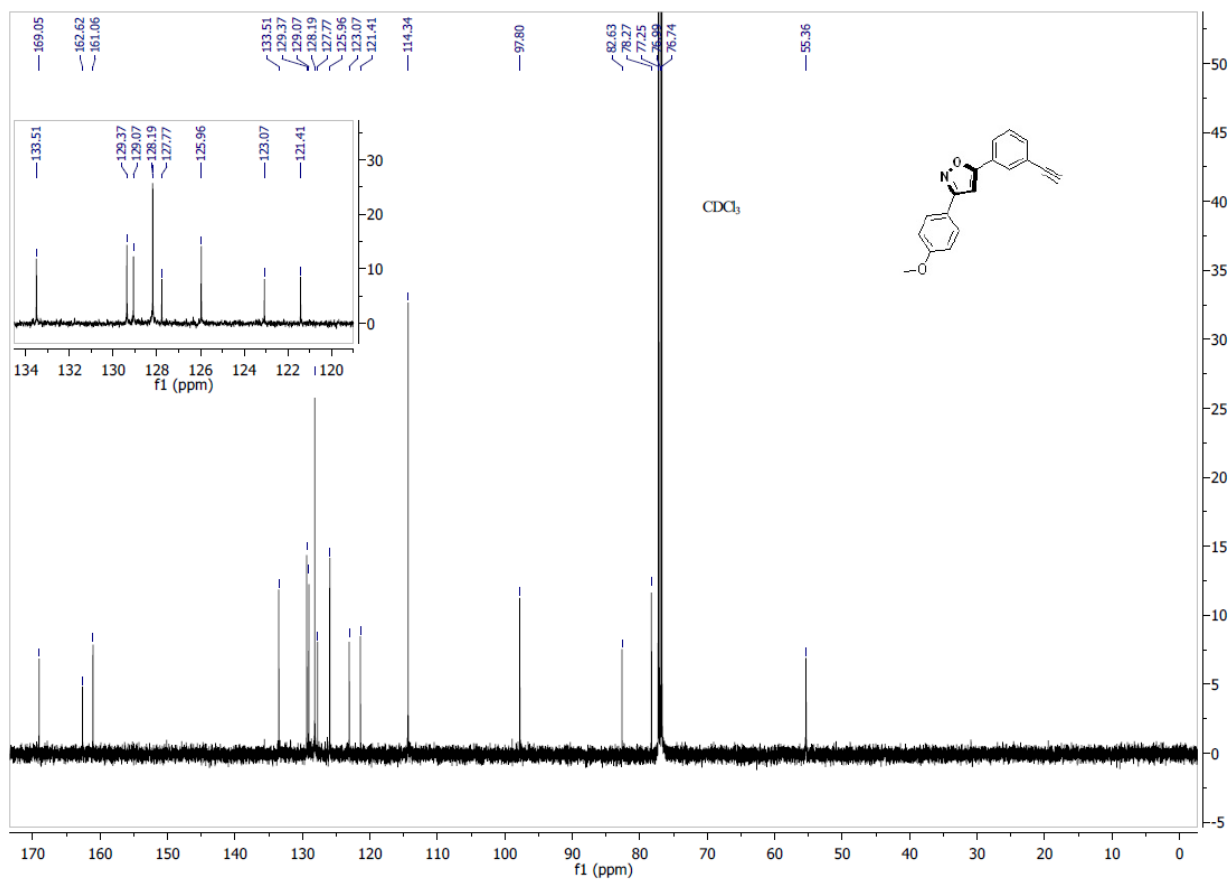
Figure S3.18. ^{13}C-NMR (125 MHz, CDCl$_3$) of 5-(3-ethynylphenyl)-3-(4-methoxyphenyl)isoxazole (105g)

Ethyl 5-(5-ethynylthiophen-2-yl)isoxazole-3-carboxylate (105h)
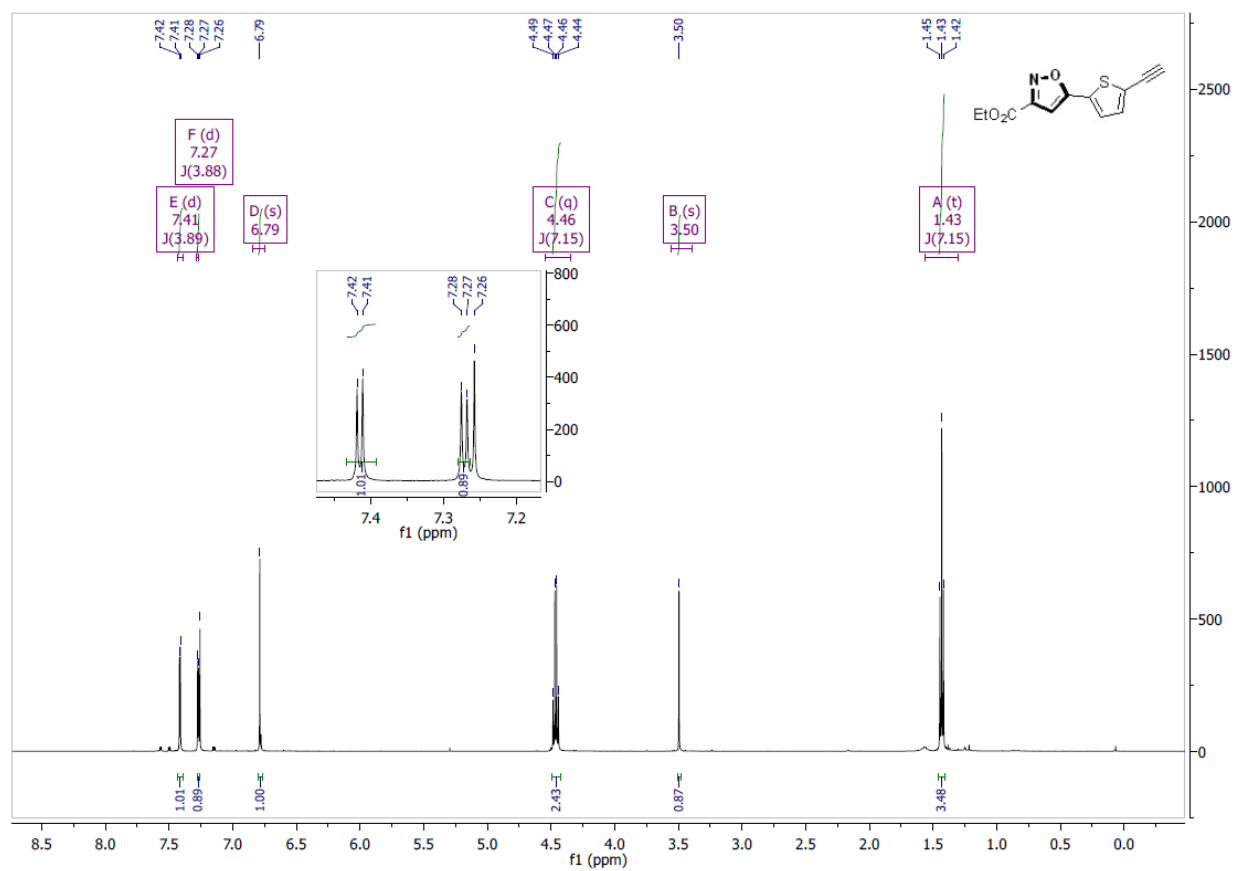
Figure S3.19. ^{1}H-NMR (500 MHz, CDCl$_3$) of ethyl 5-(5-ethynylthiophen-2-yl)isoxazole-3-carboxylate (105h)
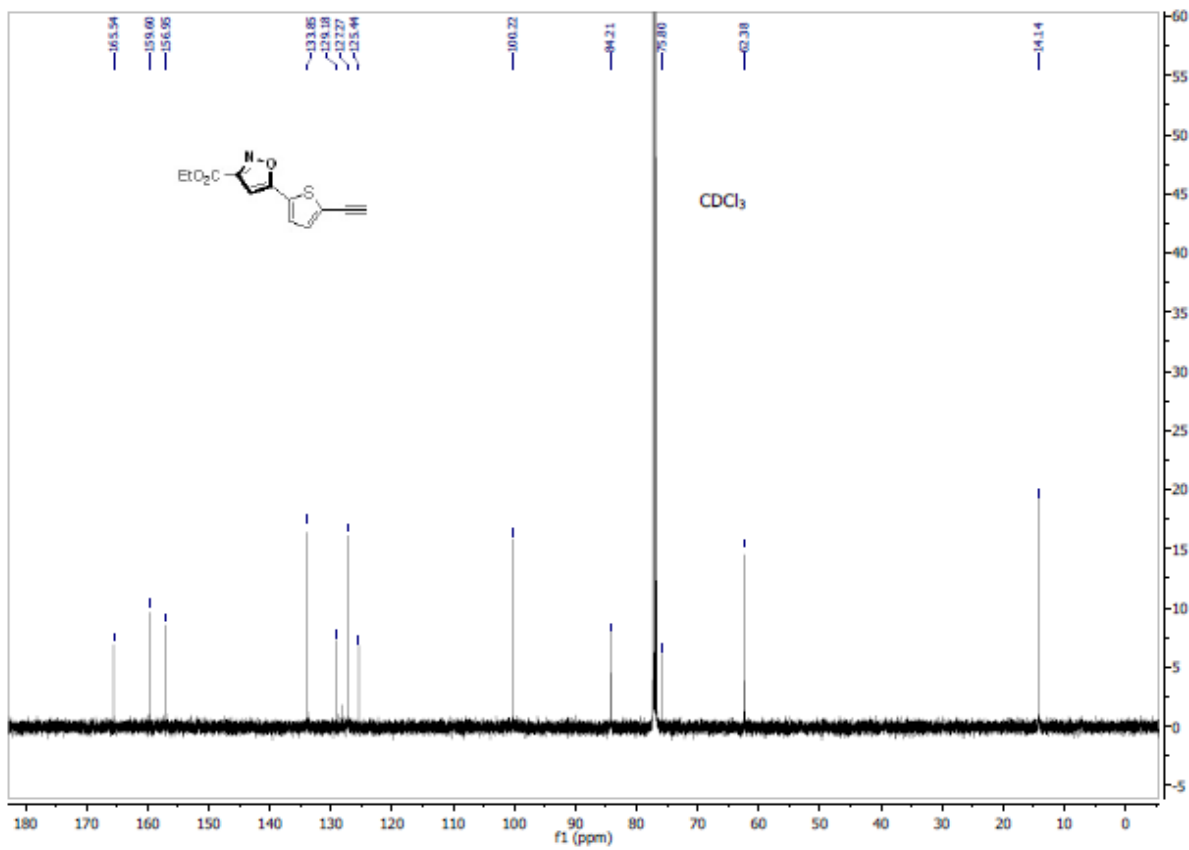
Figure S3.20. ^{13}C-NMR (125 MHz, CDCl$_3$) of ethyl 5-(5-ethynylthiophen-2-yl)isoxazole-3-carboxylate (105h)

5-(5-ethynylthiophen-2-yl)-3-(4-methoxyphenyl)isoxazole (105i)
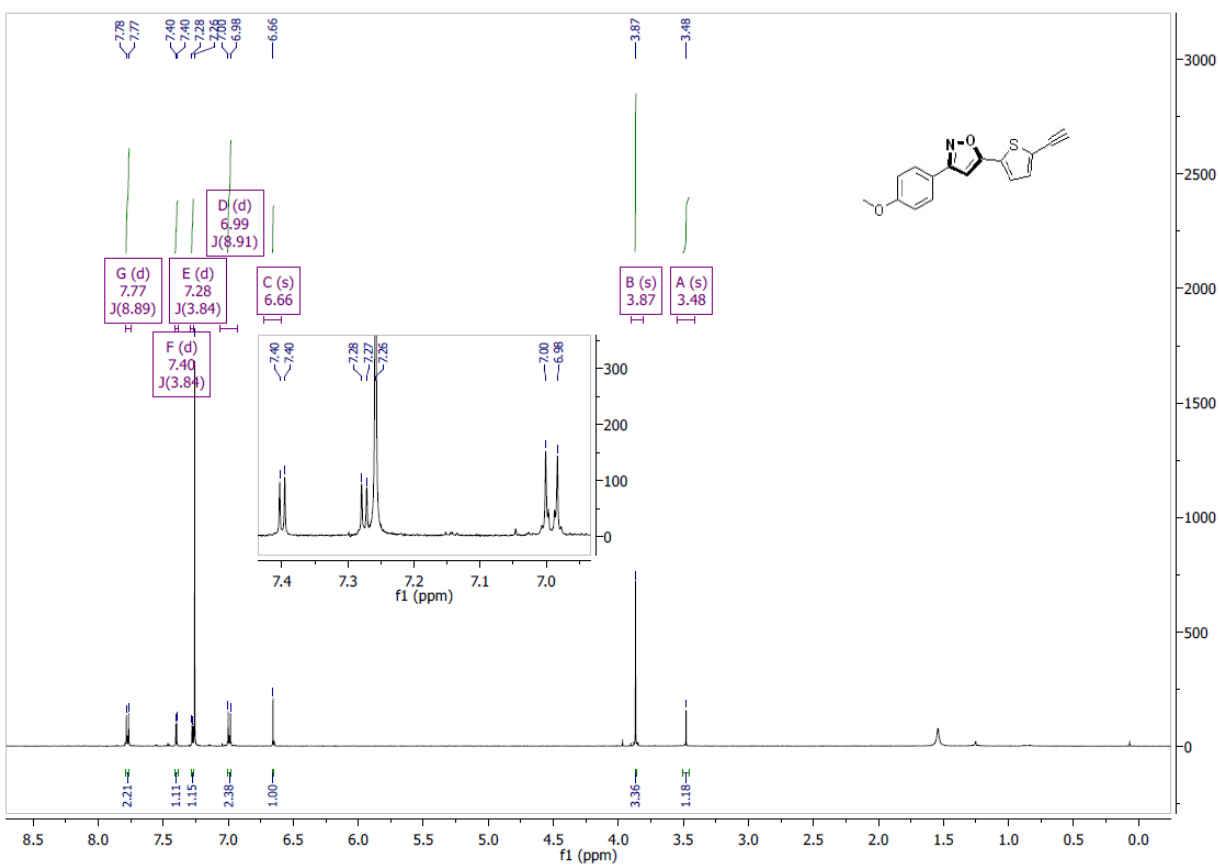
Figure S3.21. ^{1}H-NMR (500 MHz, CDCl$_3$) of 5-(5-ethynylthiophen-2-yl)-3-(4-methoxyphenyl)isoxazole (105i)
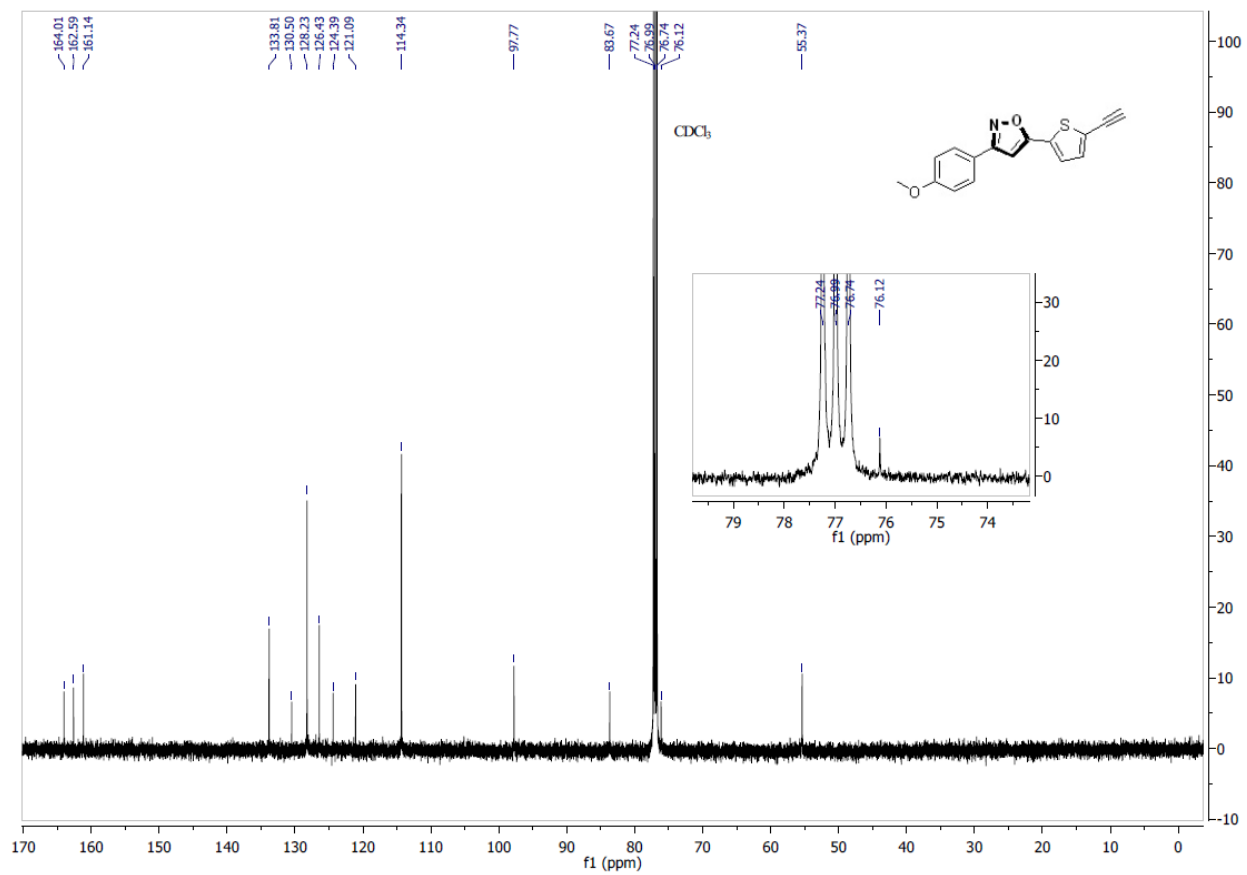
Figure S3.22. ^{13}C-NMR (125 MHz, CDCl$_3$) of 5-(5-ethynylthiophen-2-yl)-3-(4-methoxyphenyl)isoxazole (105i)

Ethyl 5-(3-ethynyl-5-methoxyphenyl)isoxazole-3-carboxylate (105j)
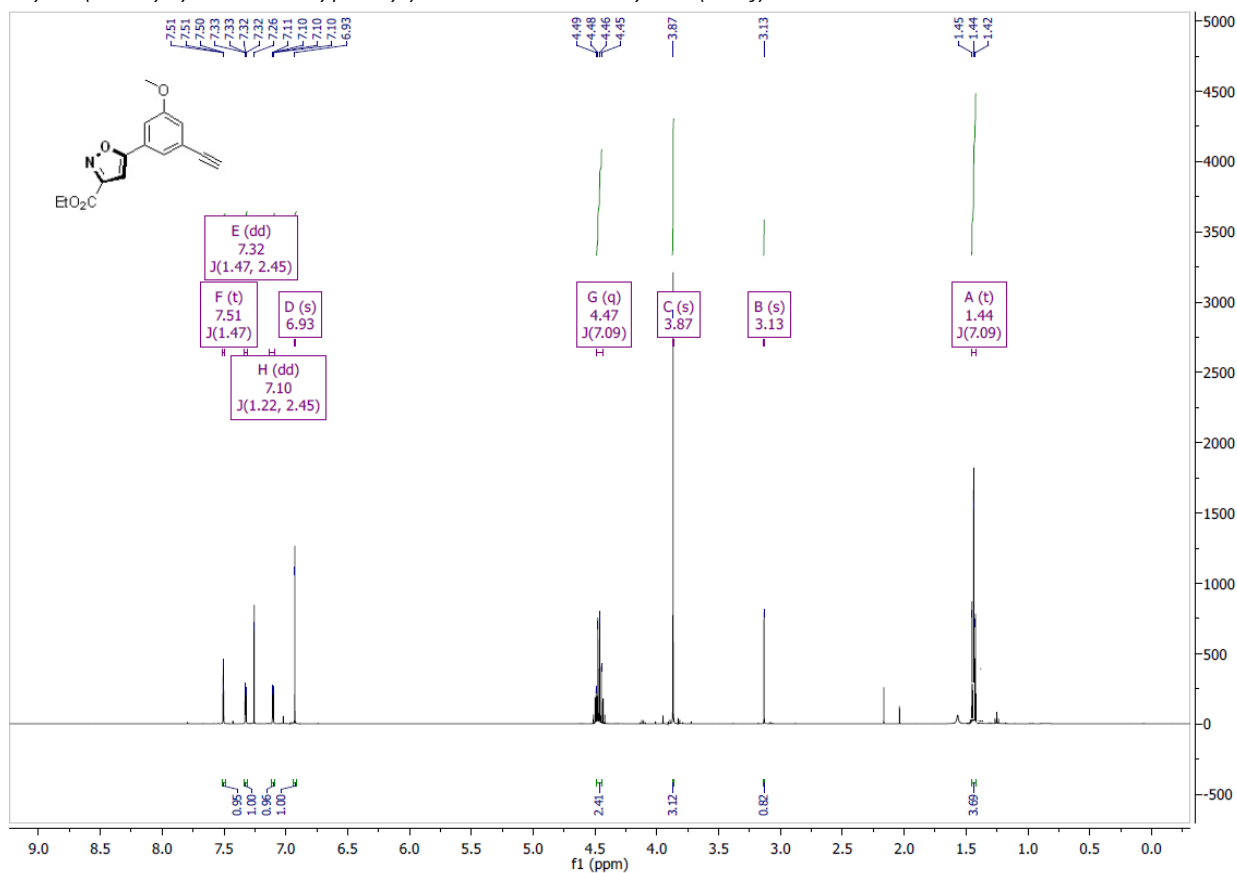
Figure S3.23. ^{1}H-NMR (500 MHz, CDCl₃) of ethyl 5-(3-ethynyl-5-methoxyphenyl)isoxazole-3-carboxylate (105j)
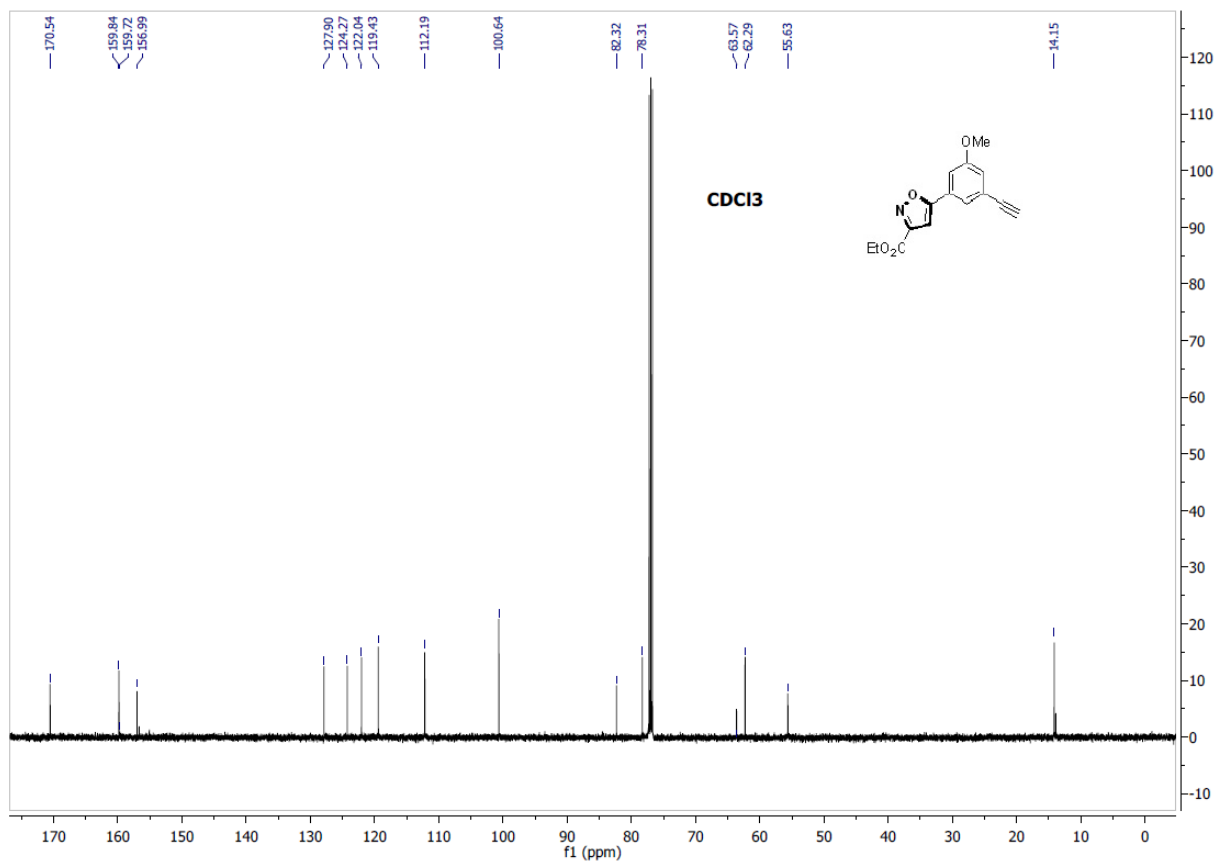
Figure S3.24. ^{13}C-NMR (125 MHz, CDCl$_3$) of ethyl 5-(3-ethynyl-5-methoxyphenyl)isoxazole-3-carboxylate (105j)

5-(3-ethynyl-5-methoxyphenyl)-3-(4-methoxyphenyl)isoxazole (105k)
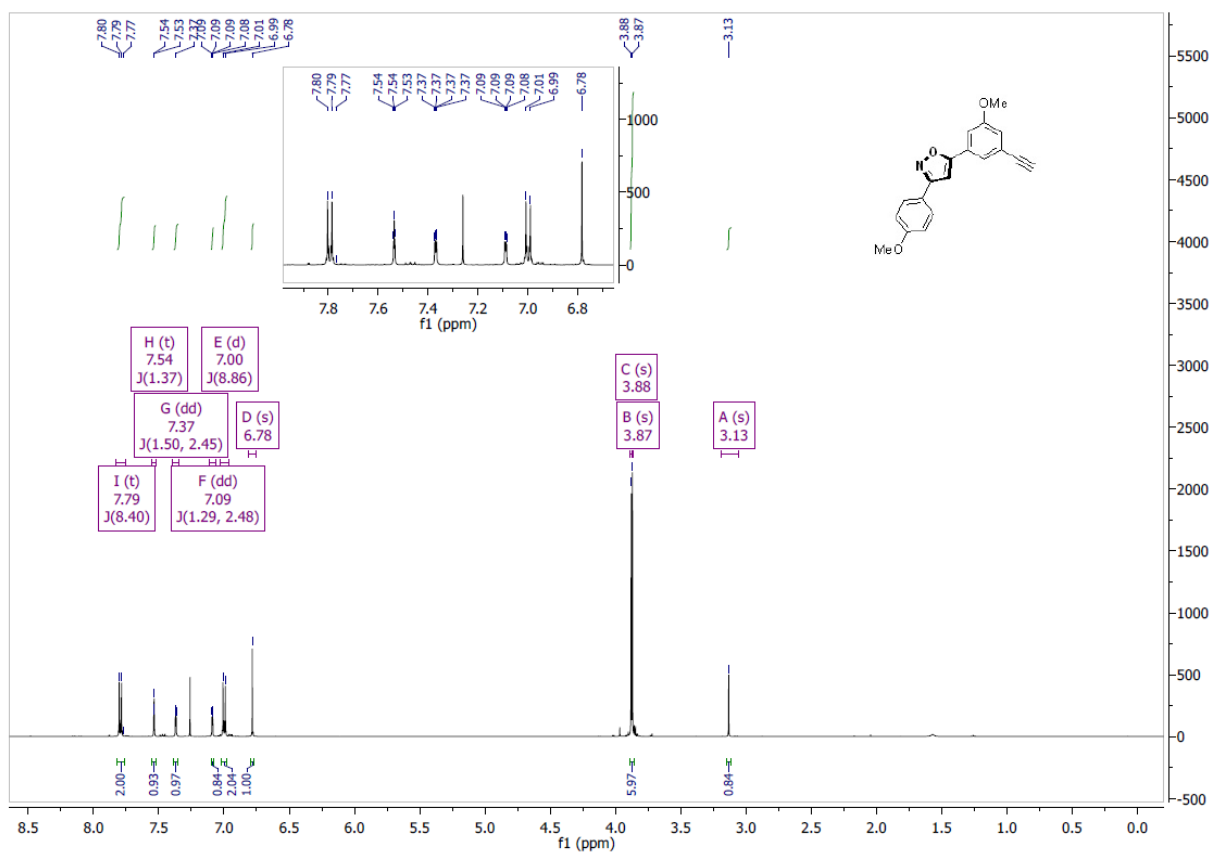
Figure S3.25. ^{1}H-NMR (500 MHz, CDCl$_3$) of 5-(3-ethynyl-5-methoxyphenyl)-3-(4-methoxyphenyl)isoxazole (105k)
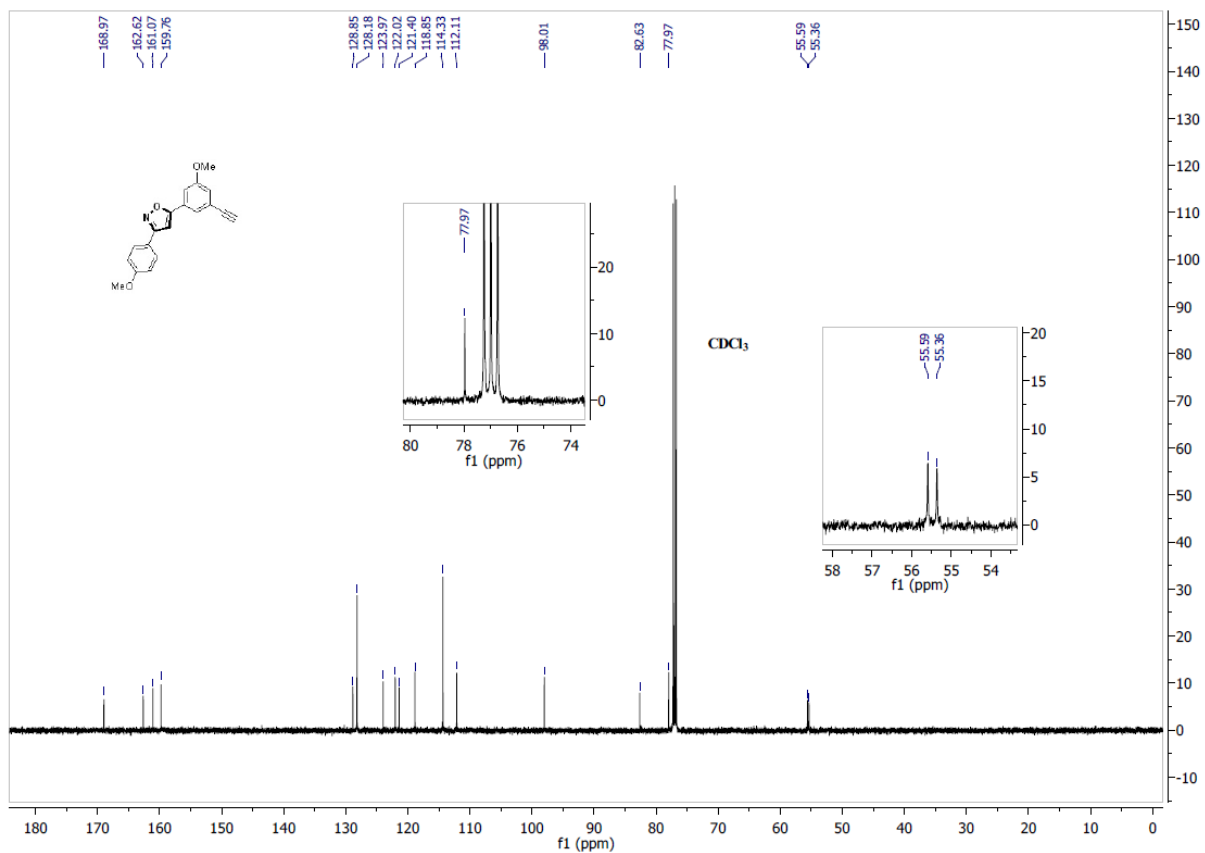
Figure S3.26. ^{13}C-NMR (125 MHz, CDCl$_3$) of 5-(3-ethynyl-5-methoxyphenyl)-3-(4-methoxyphenyl)isoxazole (105k)

5-(6-ethynylpyridin-2-yl)-3-(4-methoxyphenyl)isoxazole (105n)
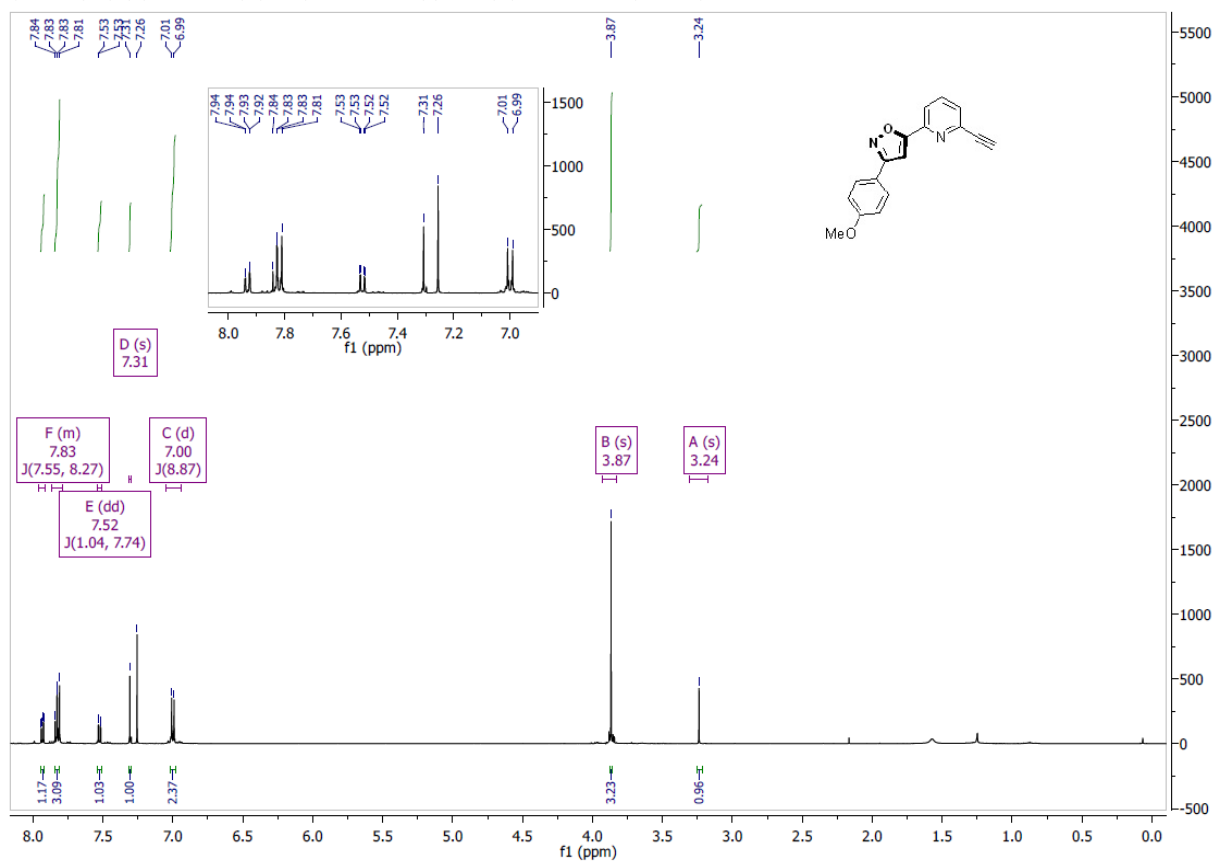
Figure S3.27. ^{1}H-NMR (500 MHz, CDCl$_3$) of 5-(6-ethynylpyridin-2-yl)-3-(4-methoxyphenyl)isoxazole (105n)
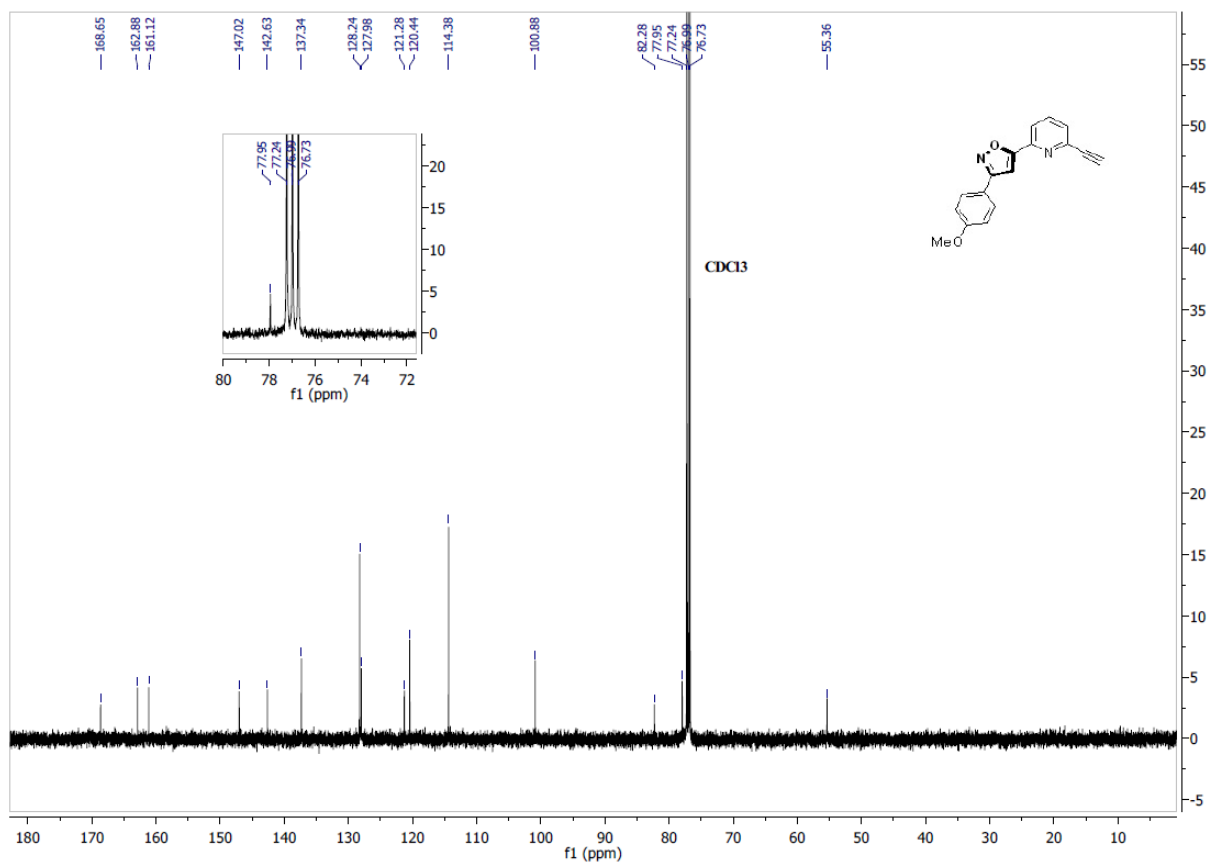
Figure S3.28. ^{13}C-NMR (125 MHz, CDCl$_3$) of 5-(6-ethynylpyridin-2-yl)-3-(4-methoxyphenyl)isoxazole (105n)

5-(3-ethynylphenyl)-3-(4-methoxyphenyl)isoxazole (105o)
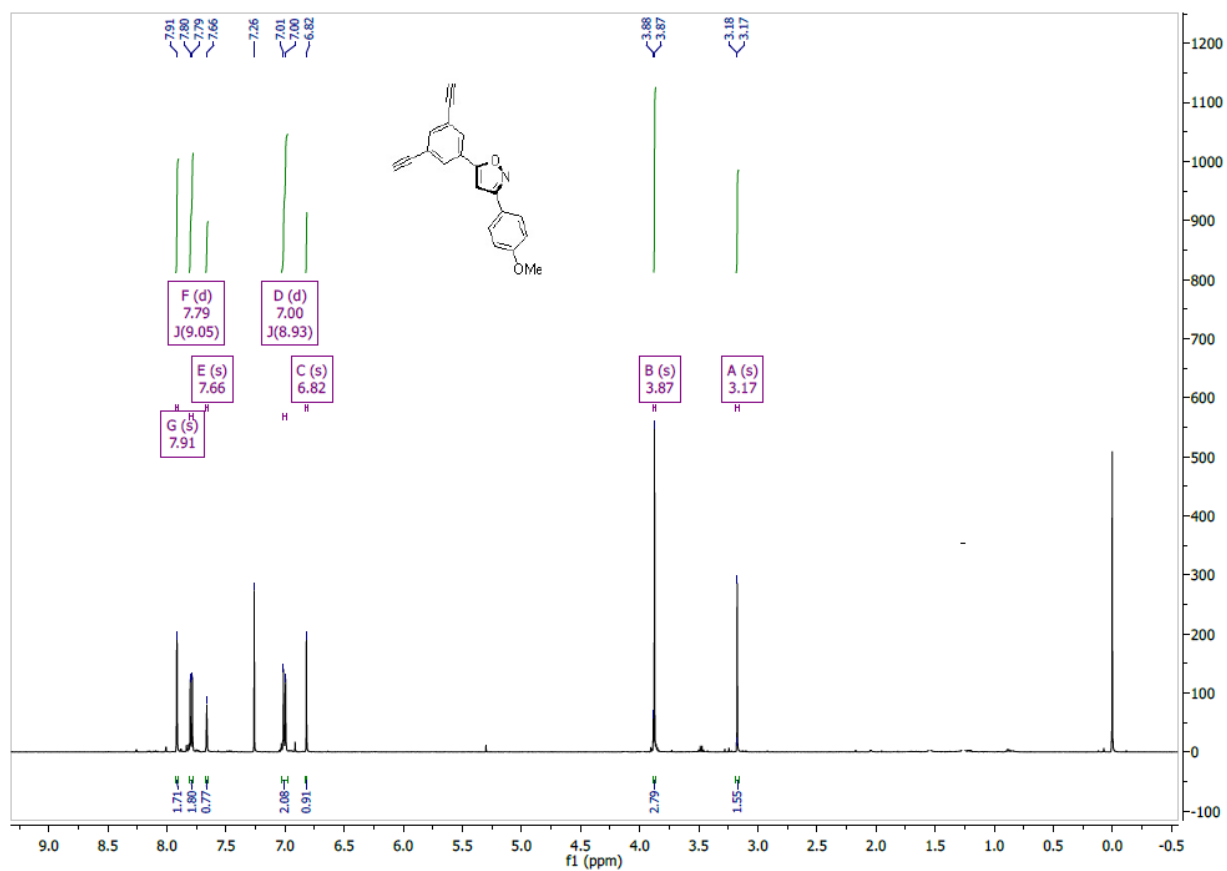
Figure S3.29. ^{1}H-NMR (500 MHz, CDCl$_3$) of 5-(3-ethynylphenyl)-3-(4-methoxyphenyl)isoxazole (105o)
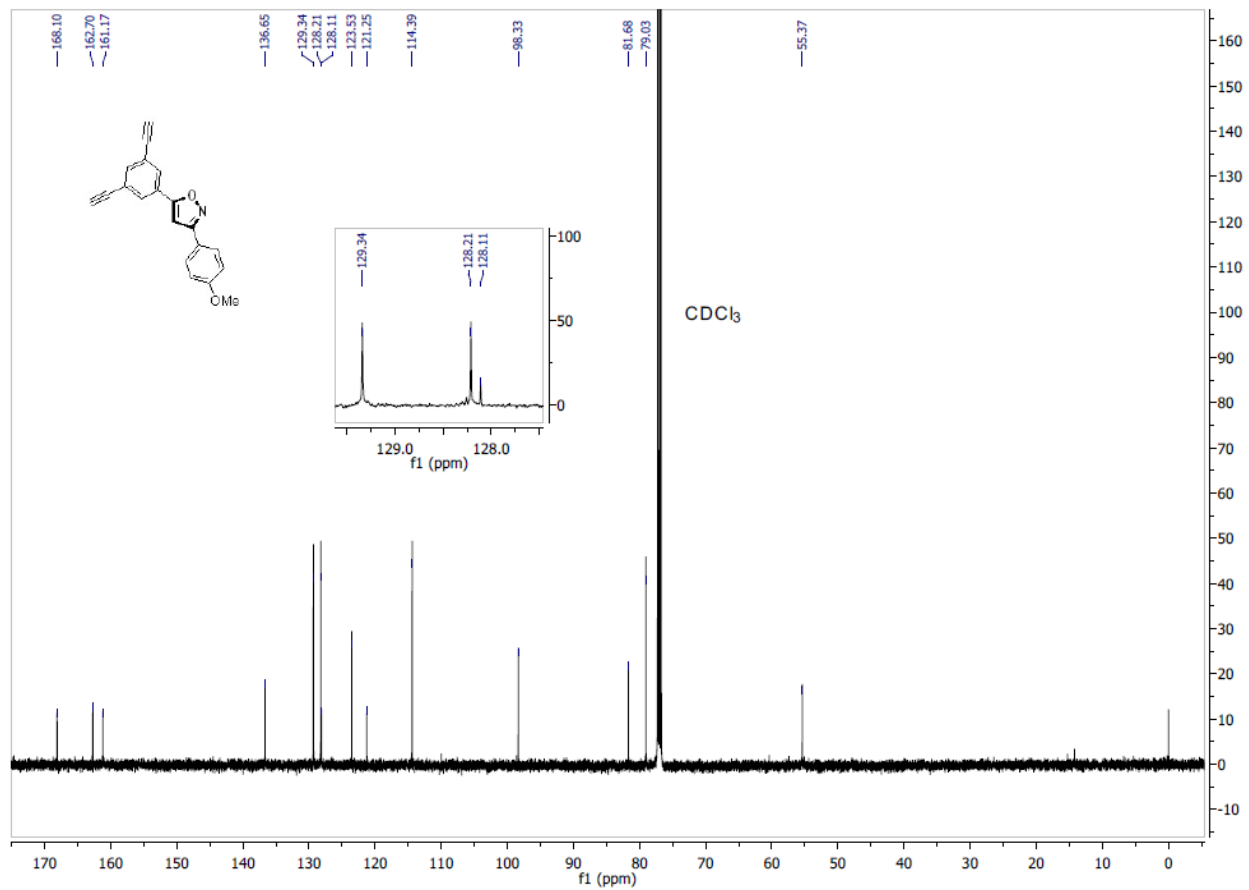
Figure S3.30. ^{13}C-NMR (125 MHz, CDCl$_3$) of 5-(3-ethynylphenyl)-3-(4-methoxyphenyl)isoxazole (105o)

N-((3-(4-nitrophenyl)isoxazol-5-yl)methyl)-N-(prop-2-yn-1-yl)prop-2-yn-1-amine (105p)
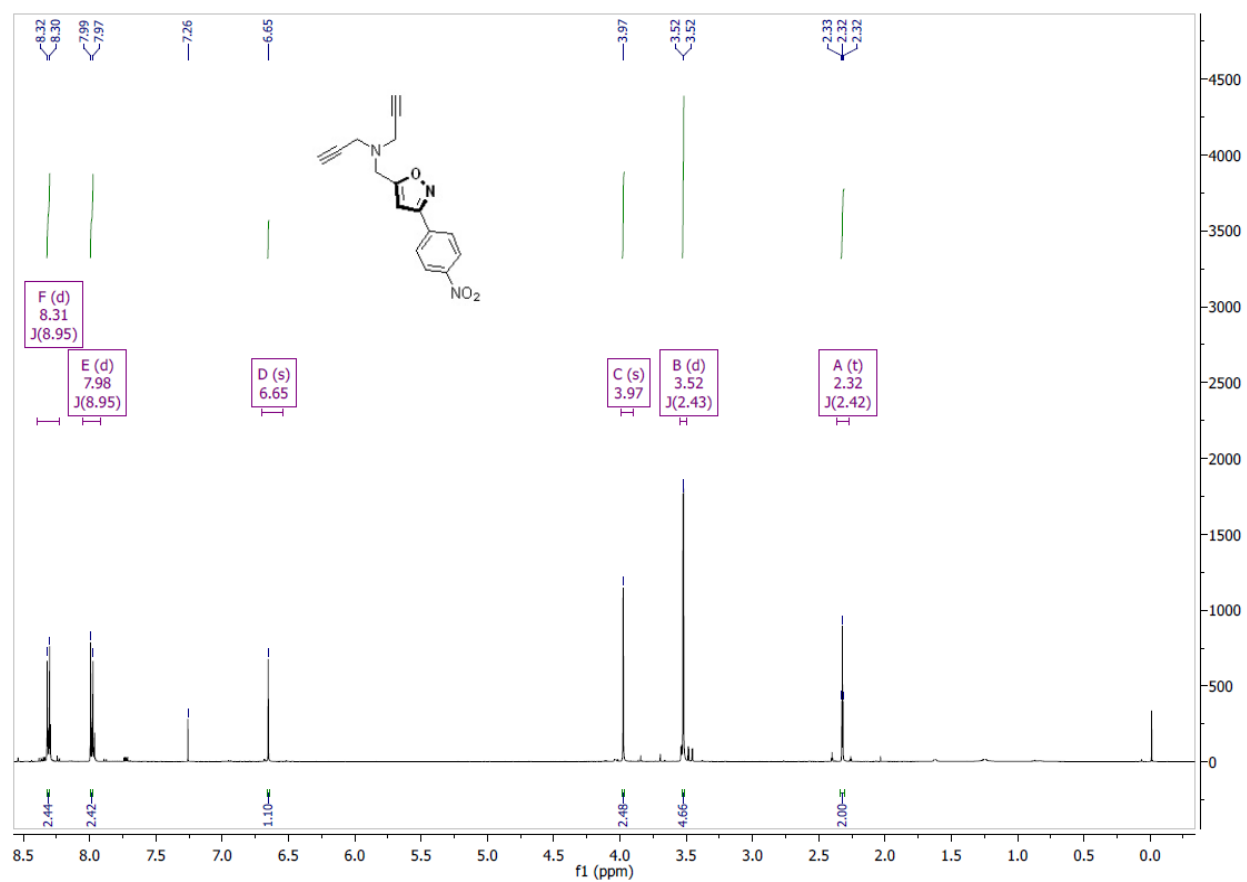
Figure S3.31. ^{1}H-NMR (500 MHz, CDCl$_3$) of N-((3-(4-nitrophenyl)isoxazol-5-yl)methyl)-N-(prop-2-yn-1-yl)prop-2-yn-1-amine (105p)
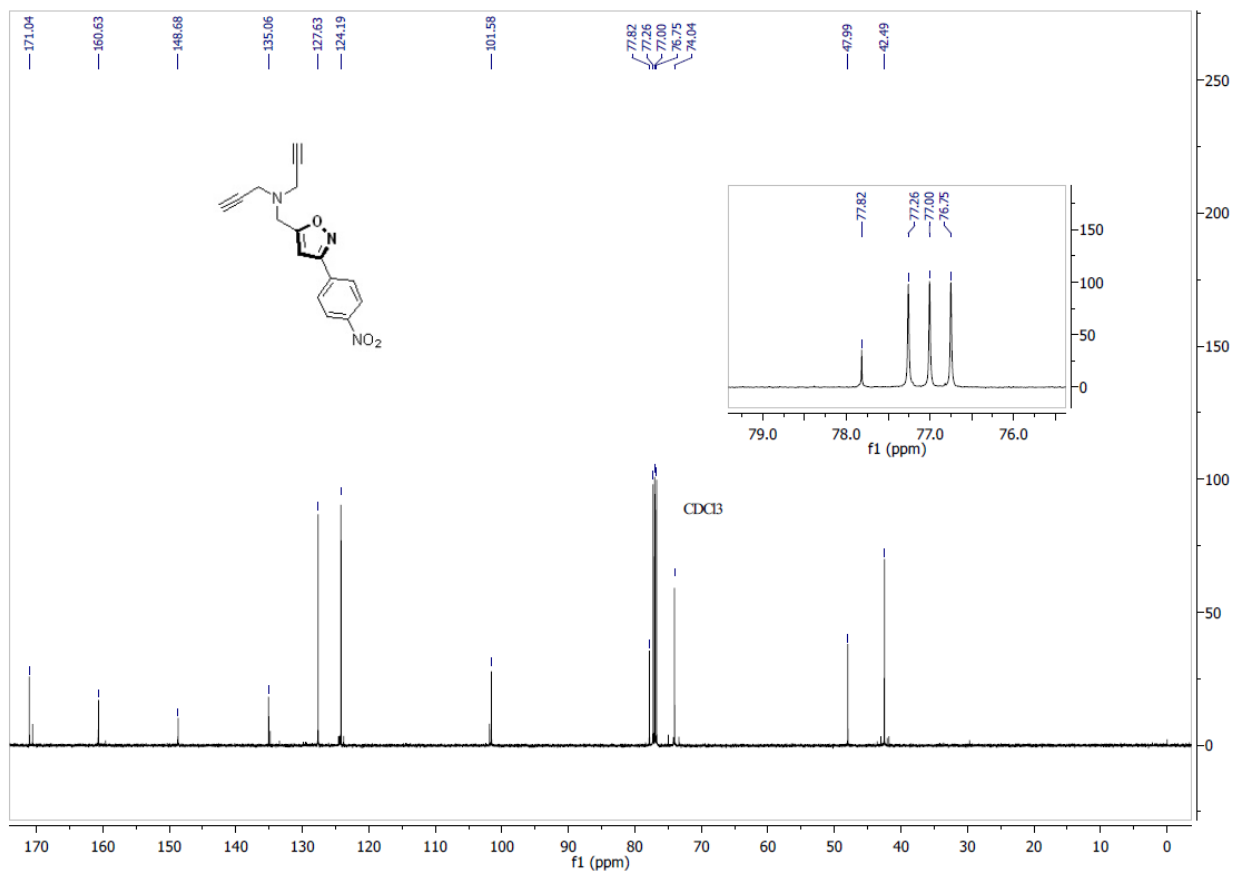
Figure S3.32. ^{13}C-NMR (125 MHz, CDCl$_3$) of N-((3-(4-nitrophenyl)isoxazol-5-yl)methyl)-N-(prop-2-yn-1-yl)prop-2-yn-1-amine (105p)

N-((3-(4-methoxyphenyl)isoxazol-5-yl)methyl)-N-(prop-2-yn-1-yl)prop-2-yn-1-amine (105r)
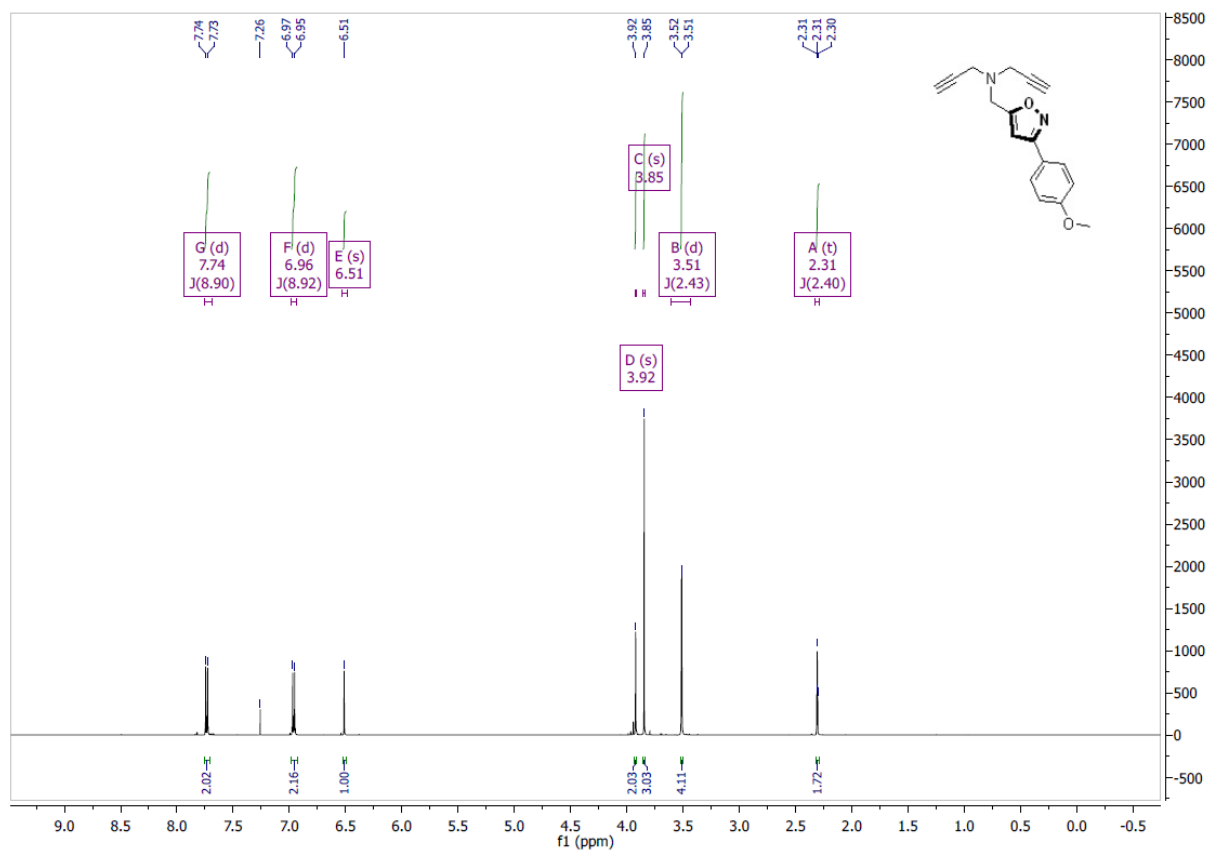
Figure S3.33. ^{1}H-NMR (500 MHz, CDCl$_3$) of N-((3-(4-methoxyphenyl)isoxazol-5-yl)methyl)-N-(prop-2-yn-1-yl)prop-2-yn-1-amine (105r)
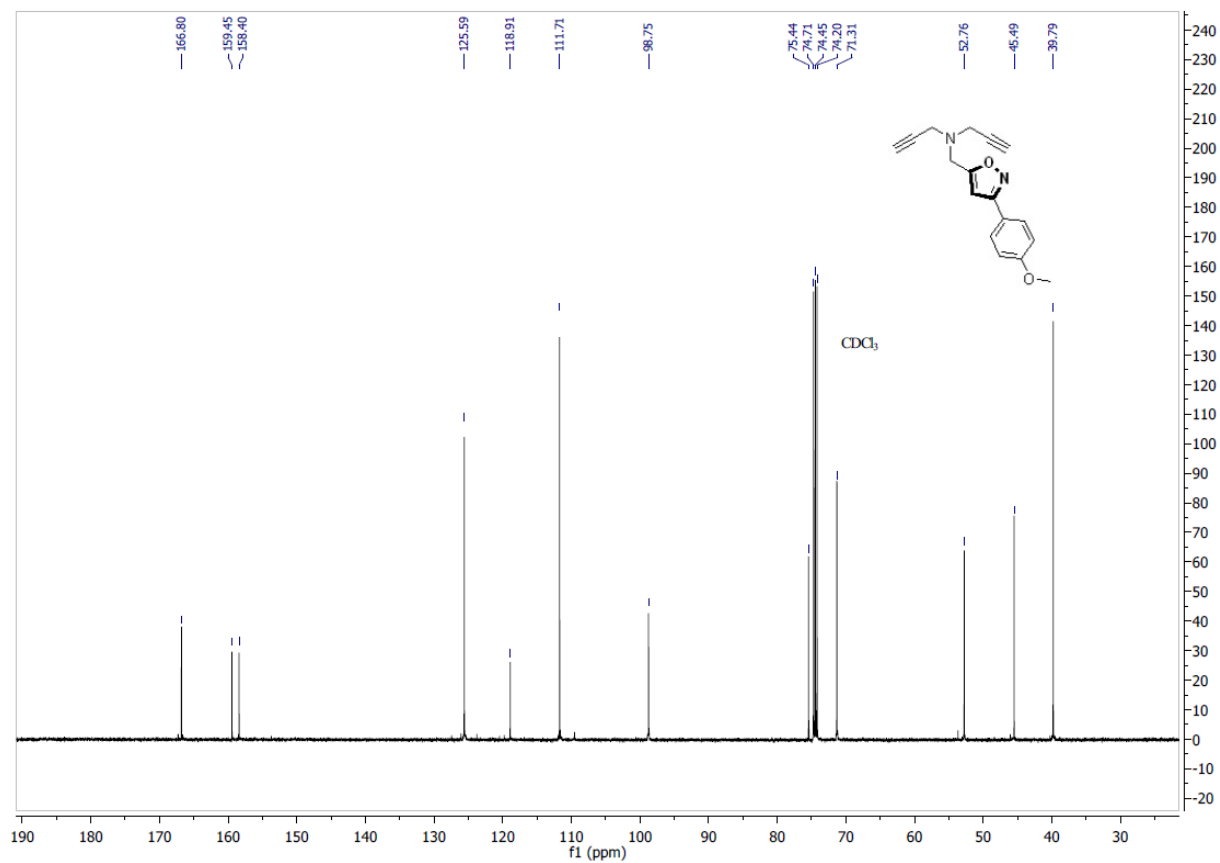
Figure S3.34. ^{13}C-NMR (125 MHz, CDCl$_3$) of N-((3-(4-methoxyphenyl)isoxazol-5-yl)methyl)-N-(prop-2-yn-1-yl)prop-2-yn-1-amine (105r)
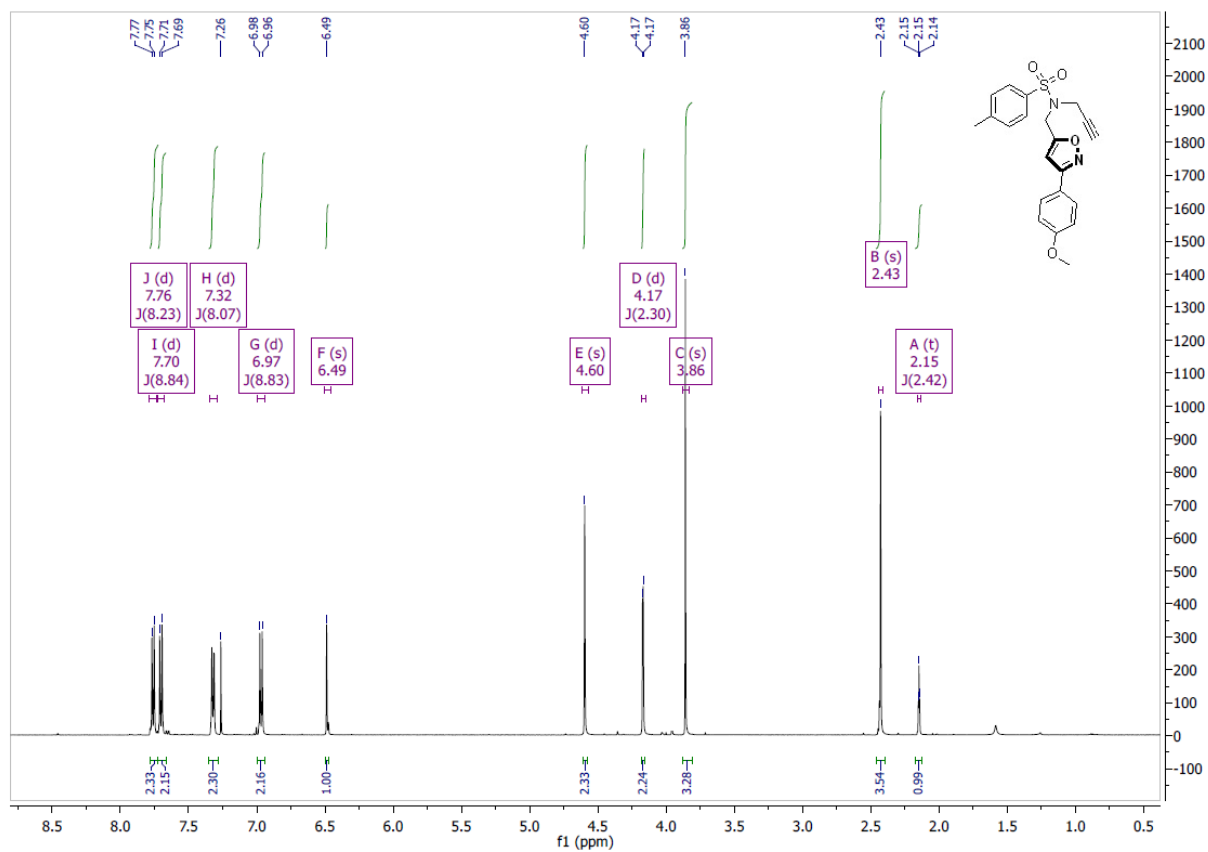
Figure S3.35. ^{1}H-NMR (500 MHz, CDCl$_3$) of N-((3-(4-methoxyphenyl)isoxazol-5-yl)methyl)-4-methyl-N-(prop-2-yn-1-yl)benzenesulfonamide (105s)
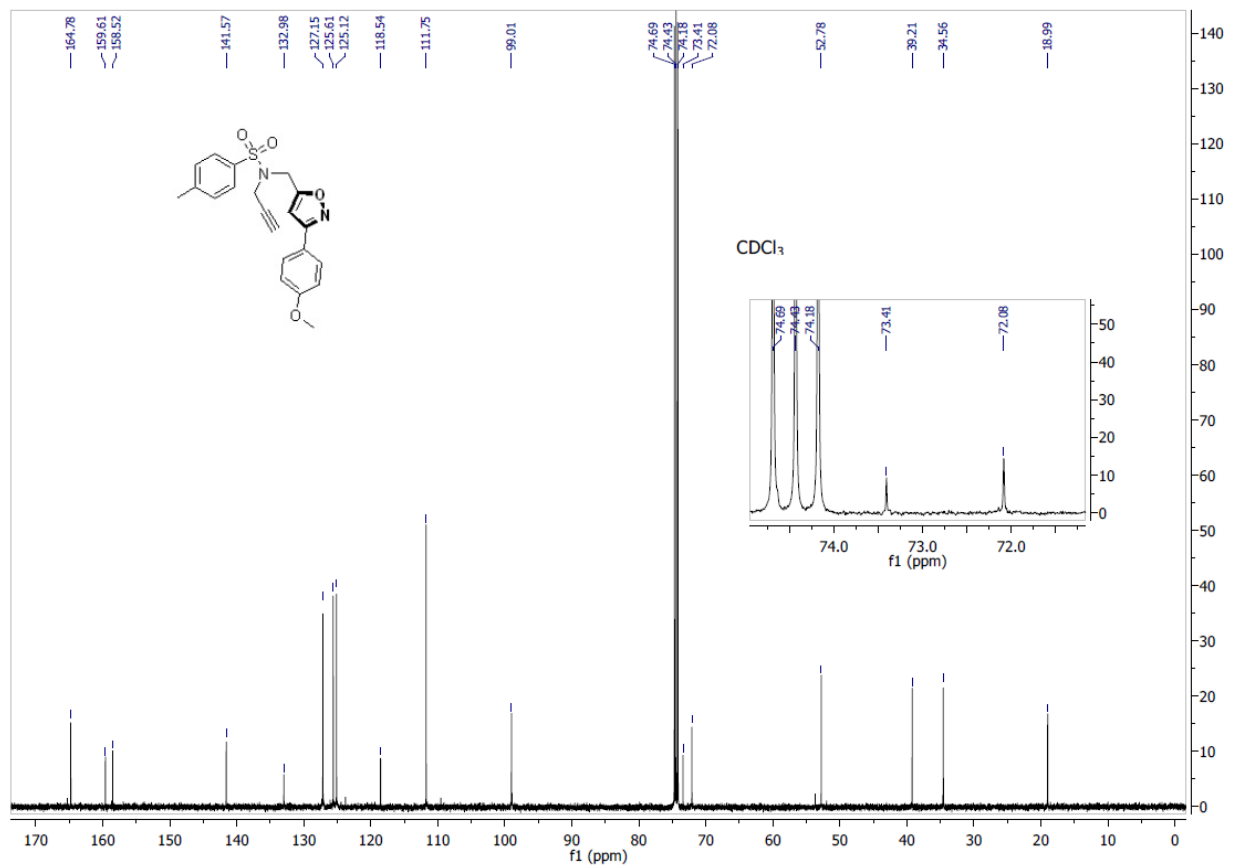
Figure S3.36. ^{13}C-NMR (125 MHz, CDCl$_3$) of N-((3-(4-methoxyphenyl)isoxazol-5-yl)methyl)-4-methyl-N-(prop-2-yn-1-yl)benzenesulfonamide (105s)

Ethyl 5-(pent-4-yn-1-yl)isoxazole-3-carboxylate (105t)
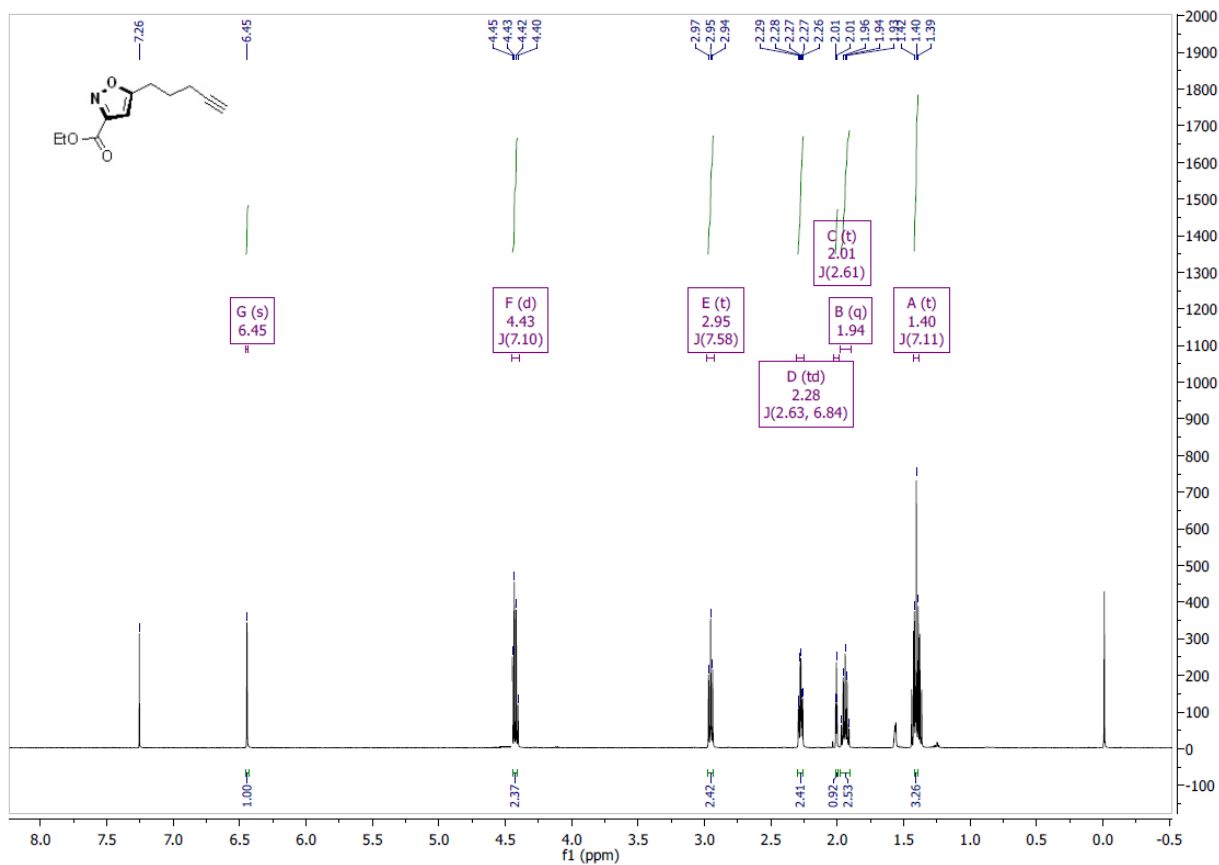
Figure S3.37. ^{1}H-NMR (500 MHz, CDCl₃) of ethyl 5-(pent-4-yn-1-yl)isoxazole-3-carboxylate (105t)
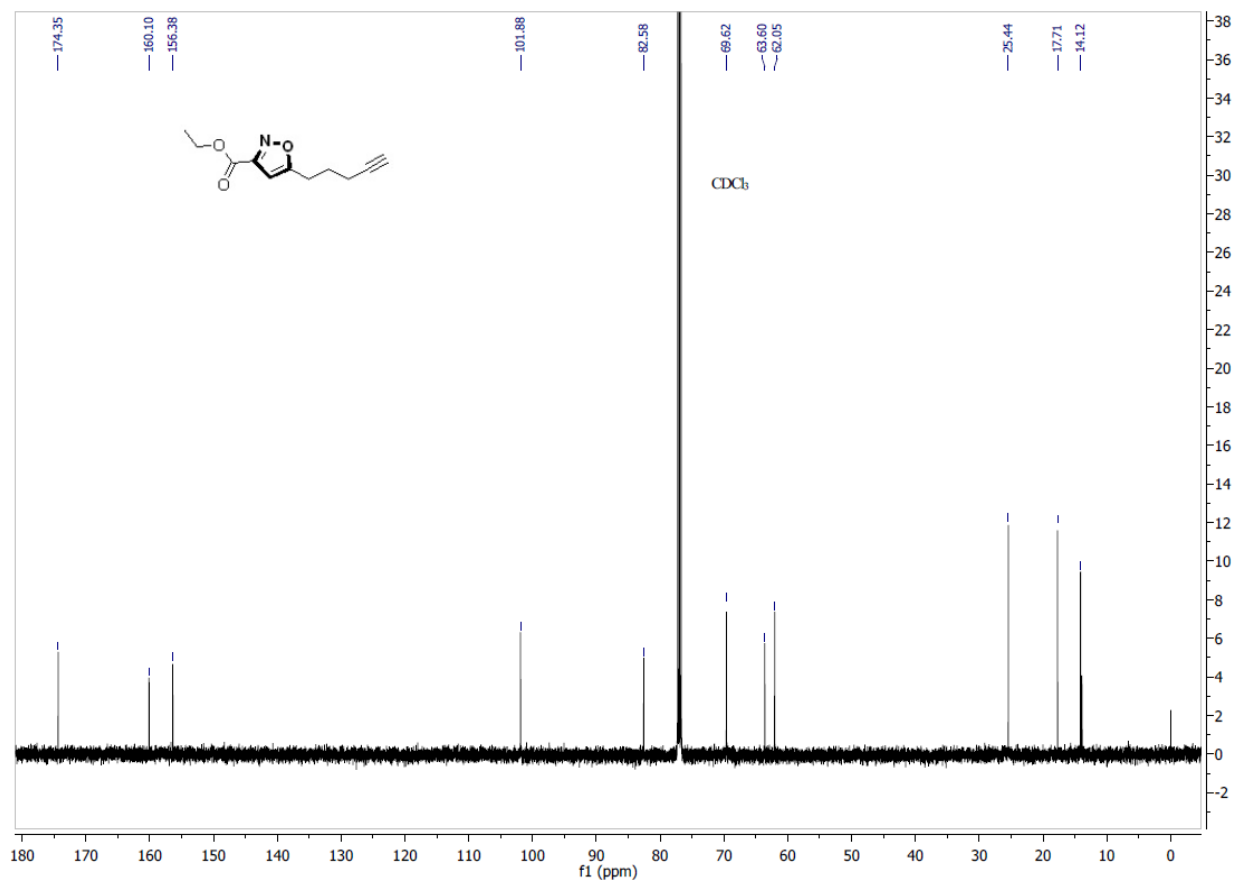
Figure S3.38. [13] C-NMR (125 MHz, CDCl₃) of ethyl 5-(pent-4-yn-1-yl)isoxazole-3-carboxylate (105t)

3-(4-nitrophenyl)-5-(pent-4-yn-1-yl)isoxazole (105u)
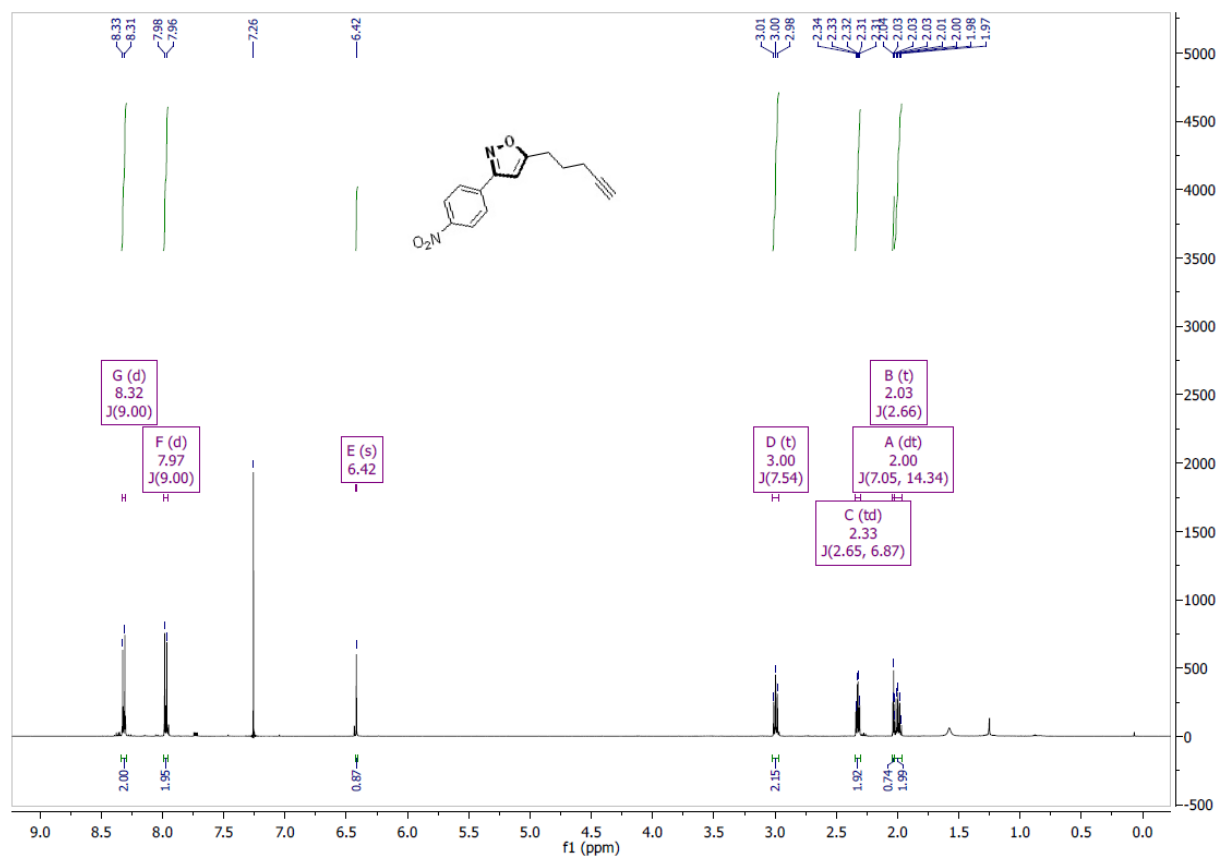
Figure S3.39. ^{1}H-NMR (500 MHz, CDCl$_3$) of 3-(4-nitrophenyl)-5-(pent-4-yn-1-yl)isoxazole (105u)
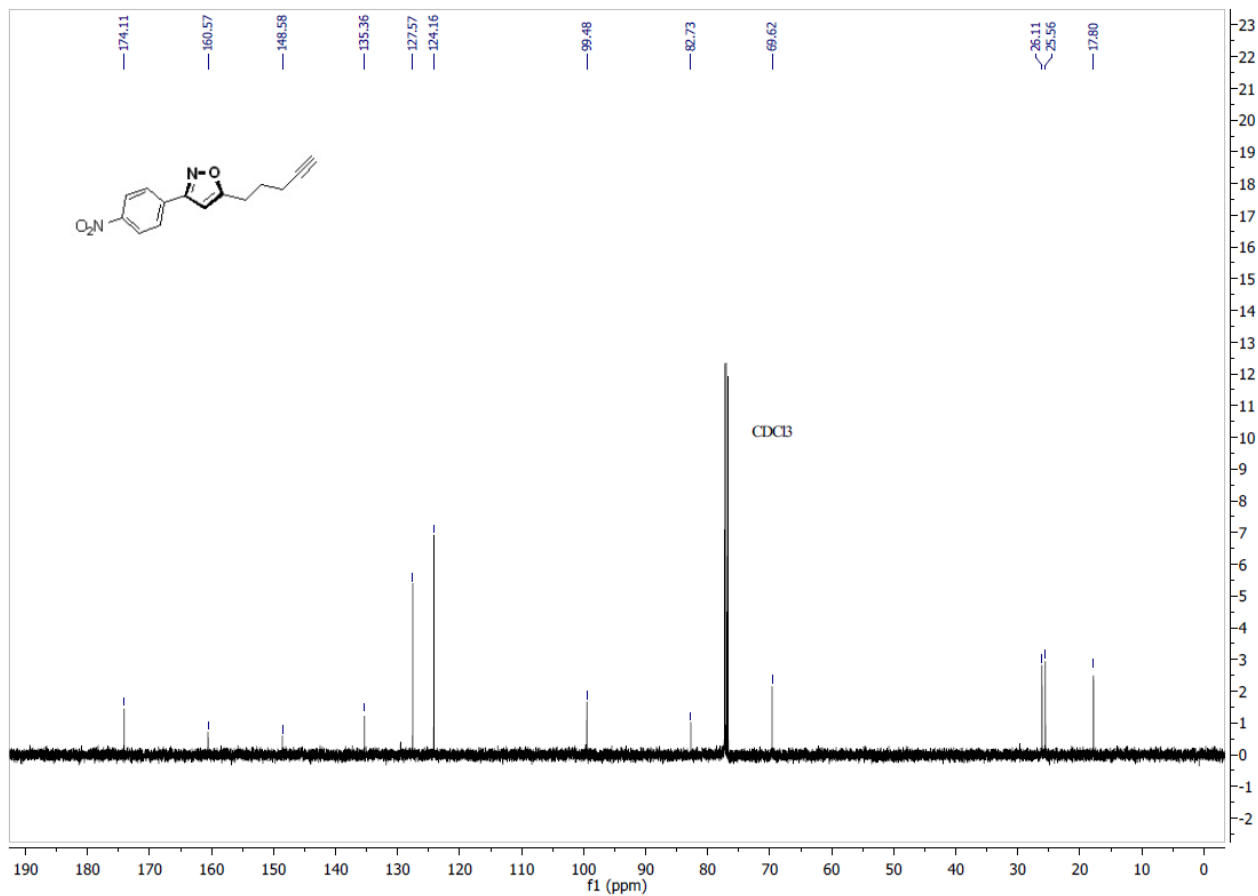
Figure S3.40. ^{13}C-NMR (500 MHz, CDCl$_3$) of 3-(4-nitrophenyl)-5-(pent-4-yn-1-yl)isoxazole (105u)

(Z)-3-amino-1-(4-ethynylphenyl)-3-(4-methoxyphenyl)prop-2-en-1-one (109)
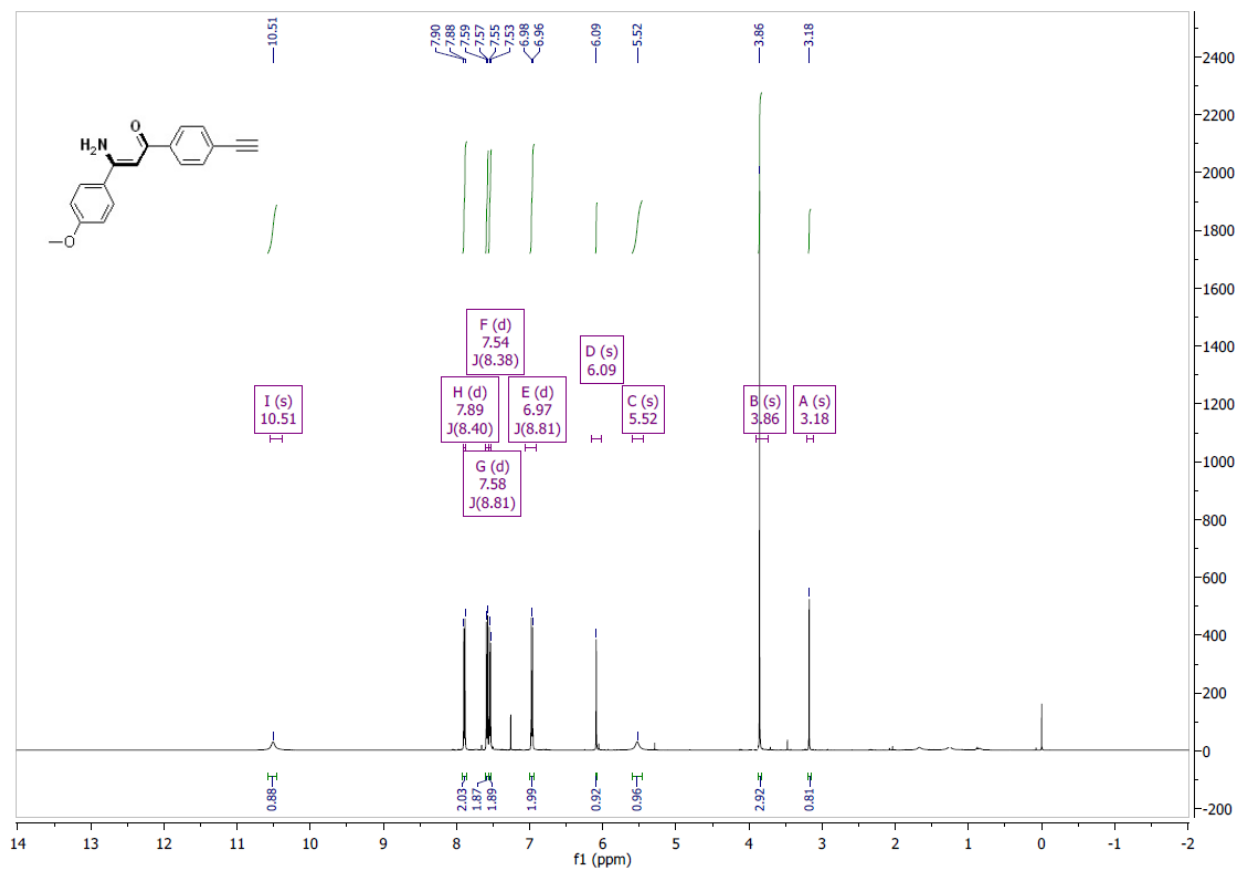
Figure S3.41. ^{1}H-NMR (500 MHz, CDCl$_3$) of (Z)-3-amino-1-(4-ethynylphenyl)-3-(4-methoxyphenyl)prop-2-en-1-one (109)
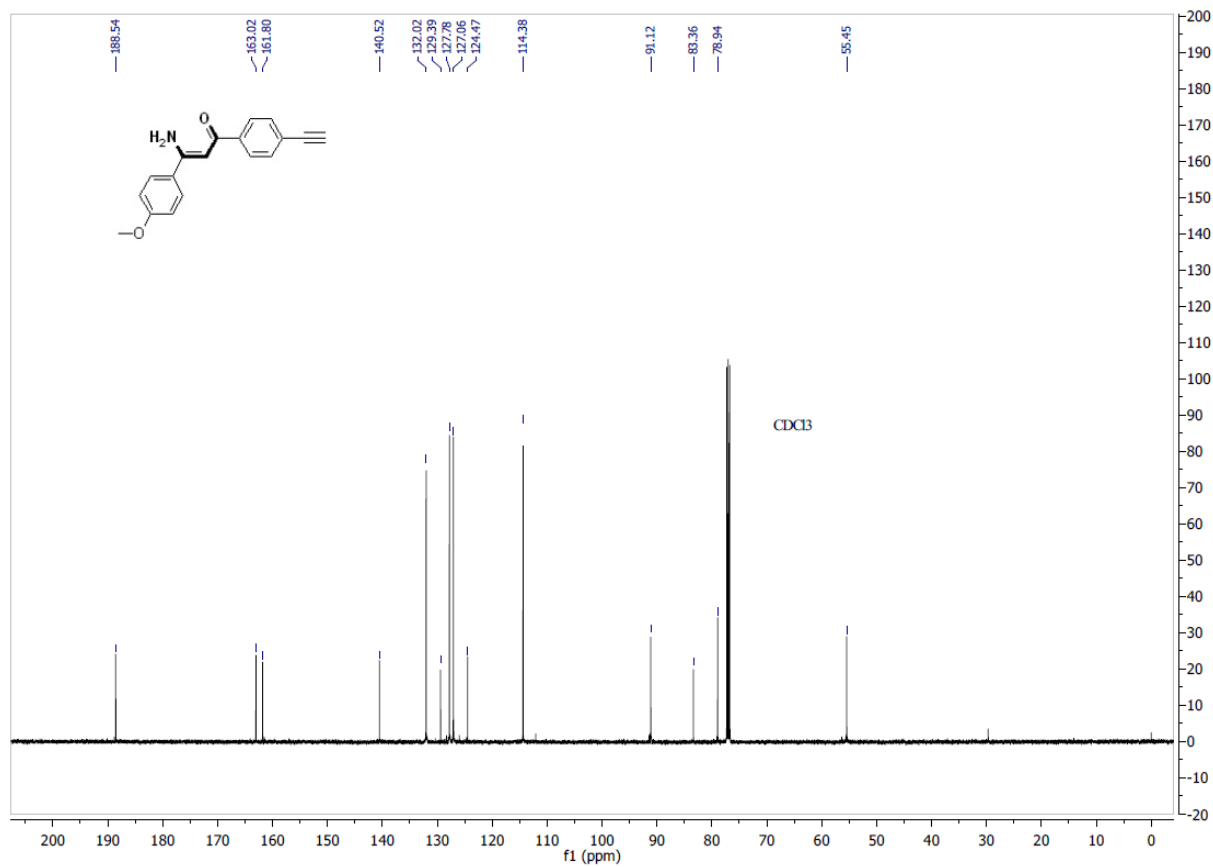
Figure S3.42. ^{13}C-NMR (125 MHz, CDCl$_3$) of (Z)-3-amino-1-(4-ethynylphenyl)-3-(4-methoxyphenyl)prop-2-en-1-one (109)

Diethyl 5,5'-(propane-1,3-diyl)bis(isoxazole-3-carboxylate) (111b)
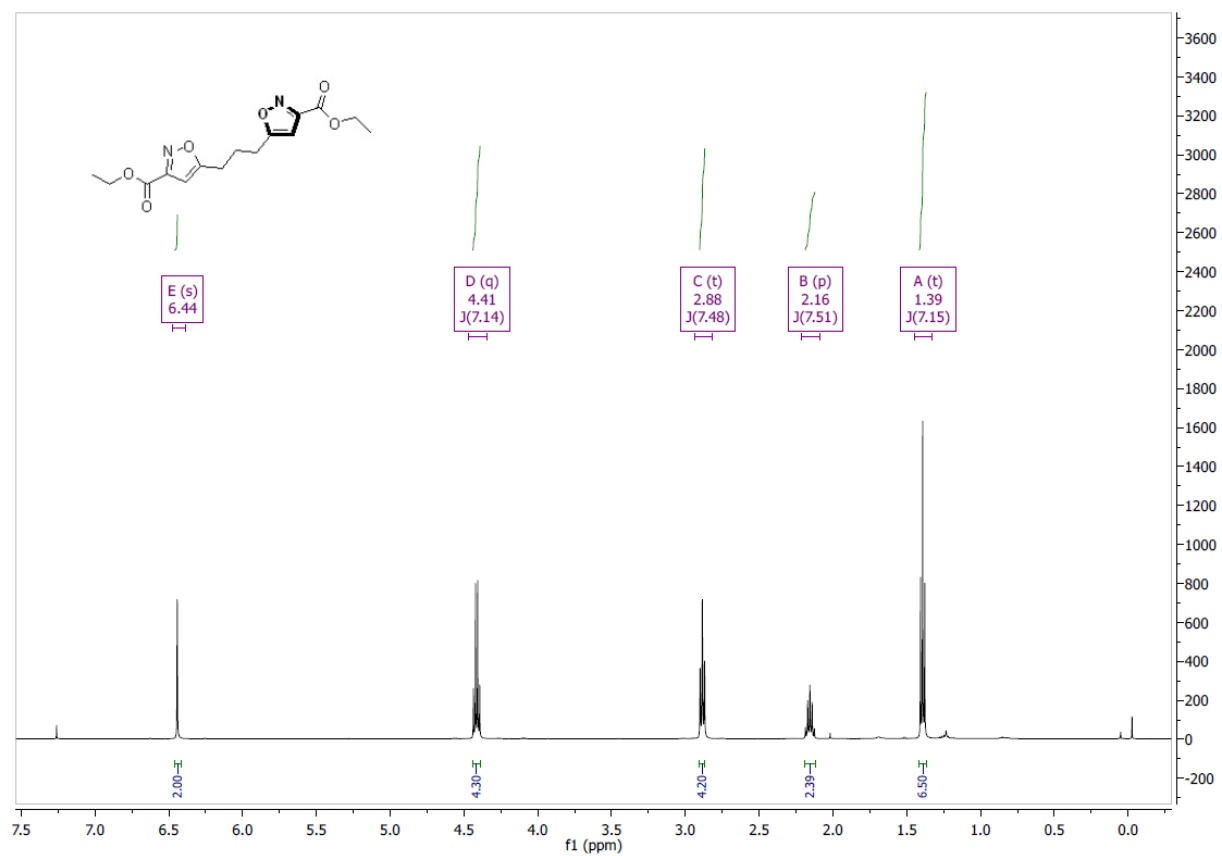
Figure S3.43. ^{1}H-NMR (500 MHz, CDCl$_3$) of diethyl 5,5'-(propane-1,3-diyl)bis(isoxazole-3-carboxylate) (111b)
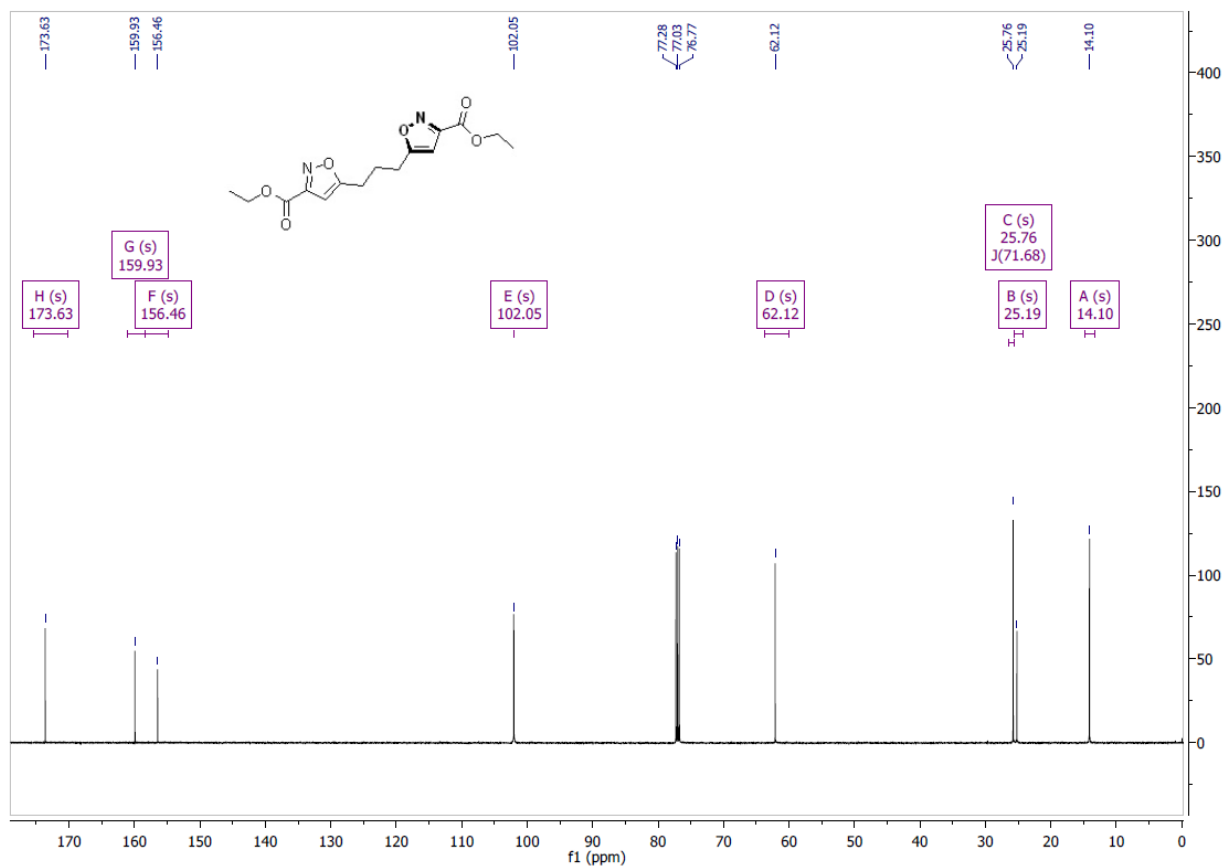
Figure S3.44. ^{13}C-NMR (125 MHz, CDCl$_3$) of diethyl 5,5'-(propane-1,3-diyl)bis(isoxazole-3-carboxylate) (111b)

Ethyl 5-(3-(3-(3-cyanophenyl)isoxazol-5-yl)propyl)isoxazole-3-carboxylate (111c)
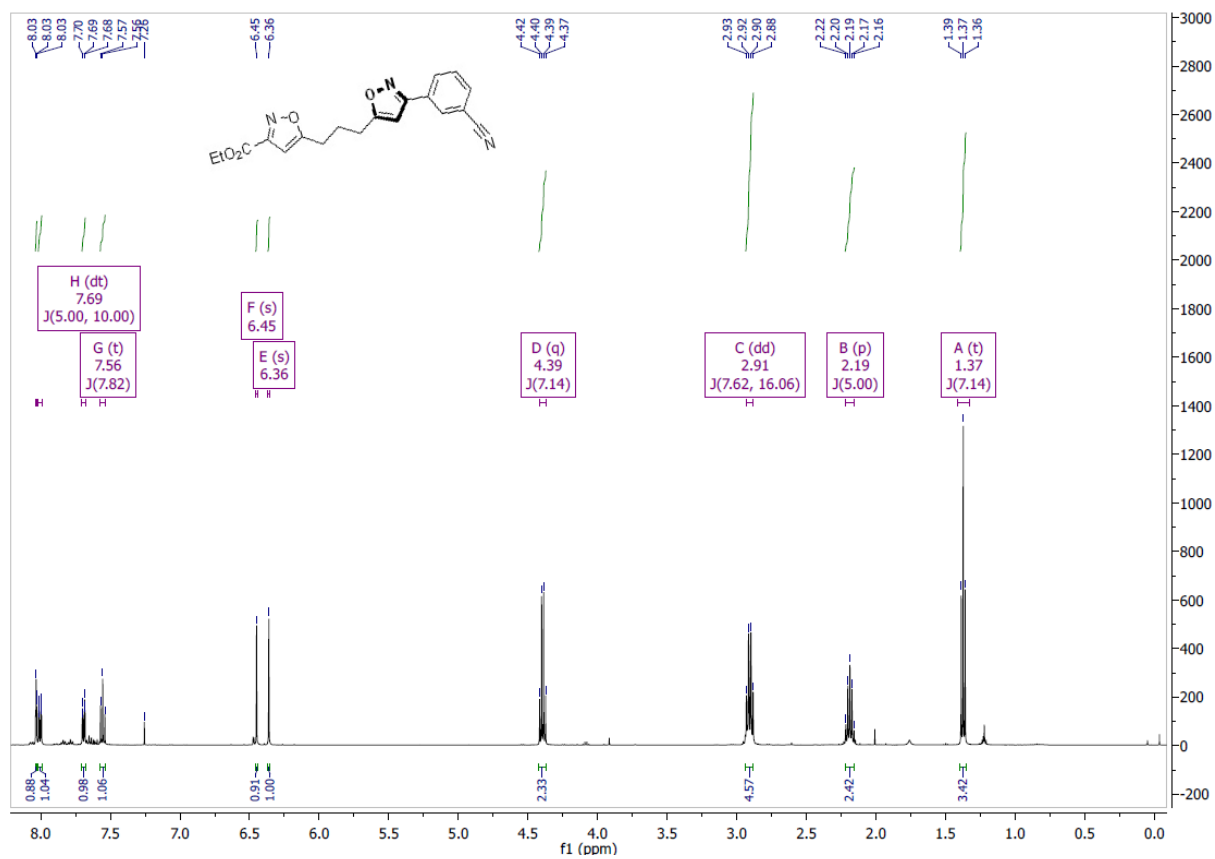
Figure S3.45. ¹H-NMR (500 MHz, CDCl3) of ethyl 5-(3-(3-(3-cyanophenyl)isoxazol-5-yl)propyl)isoxazole-3-carboxylate (111c)
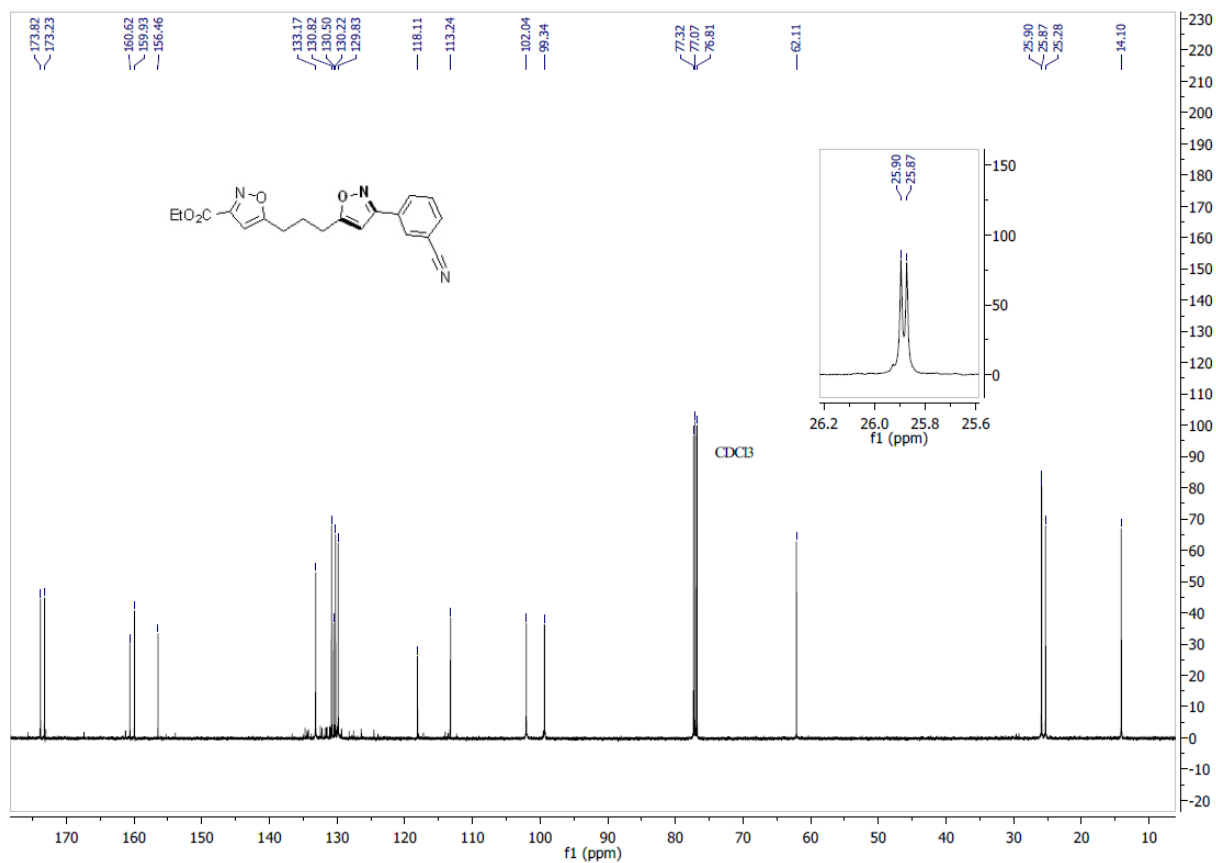
Figure S3.46. ^{13}C-NMR (125 MHz, CDCl$_3$) of ethyl 5-(3-(3-(3-cyanophenyl)isoxazol-5-yl)propyl)isoxazole-3-carboxylate (111c)

Ethyl 5-(3-(3-phenylisoxazol-5-yl)propyl)isoxazole-3-carboxylate (111d)
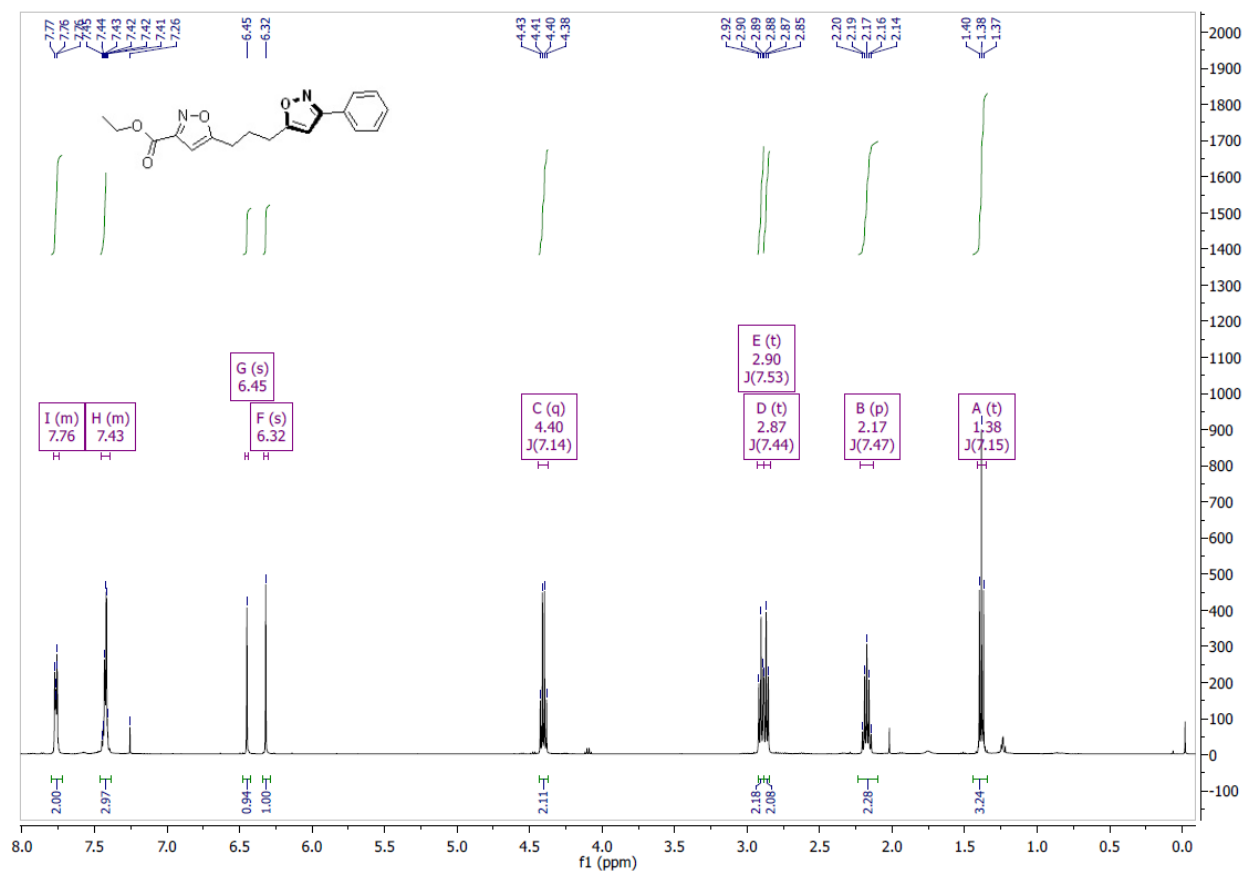
Figure S3.47. ^{1}H-NMR (500 MHz, CDCl₃) of ethyl 5-(3-(3-phenylisoxazol-5-yl)propyl)isoxazole-3-carboxylate (111d)
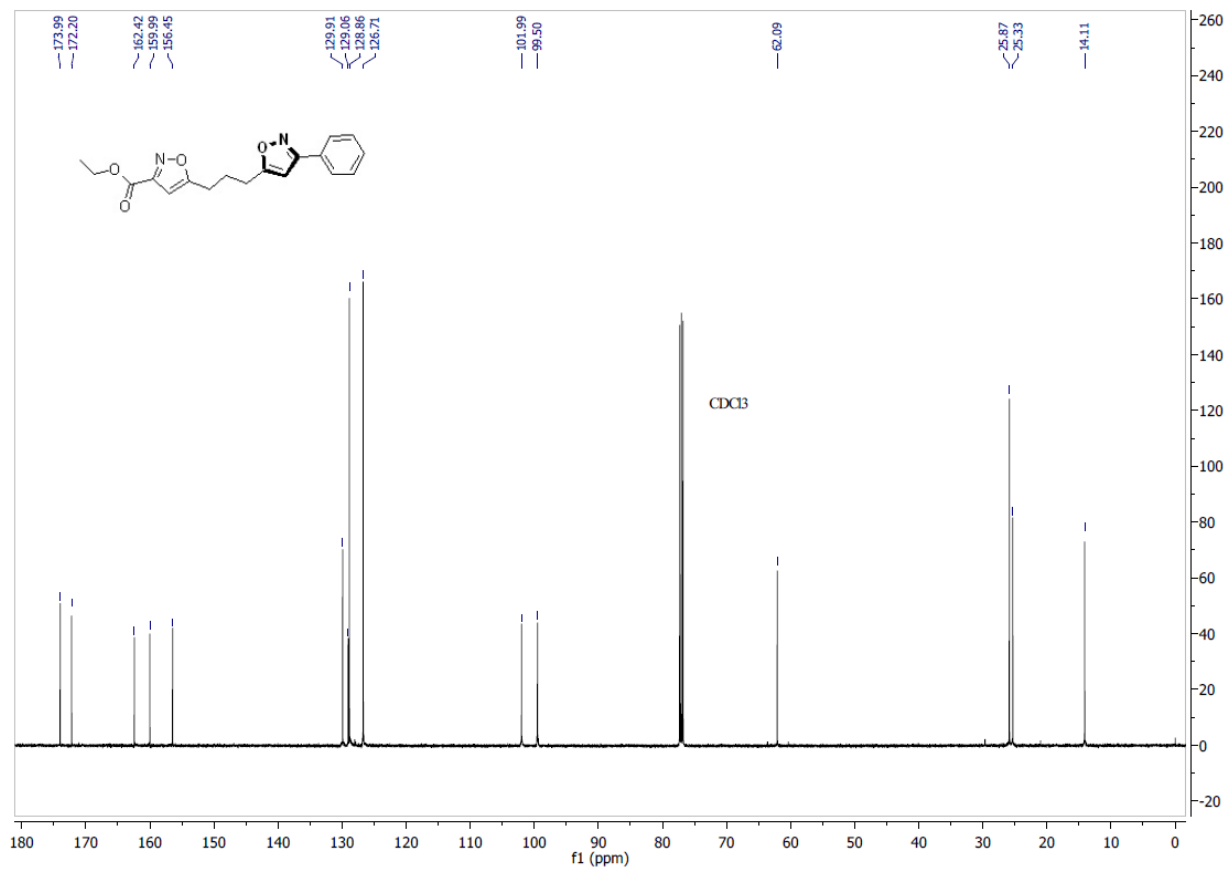
Figure S3.48. ^{13}C-NMR (125 MHz, CDCl$_3$) of ethyl 5-(3-(3-phenylisoxazol-5-yl)propyl)isoxazole-3-carboxylate (111d)

Ethyl 5-(3-(3-(4-methoxyphenyl)isoxazol-5-yl)propyl)isoxazole-3-carboxylate (111e)
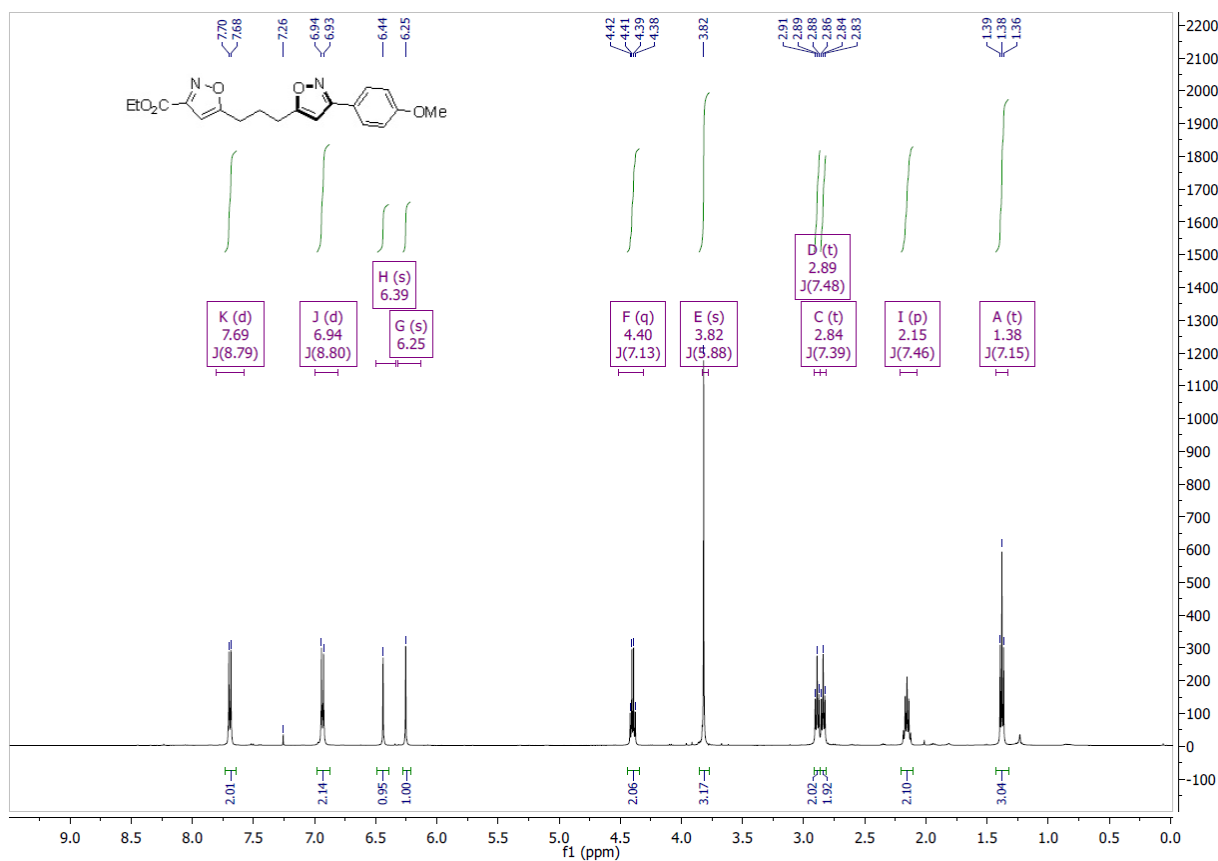
Figure S3.49. ^{1}H-NMR (500 MHz, CDCl$_3$) of ethyl 5-(3-(3-(4-methoxyphenyl)isoxazol-5-yl)propyl)isoxazole-3-carboxylate (111e)
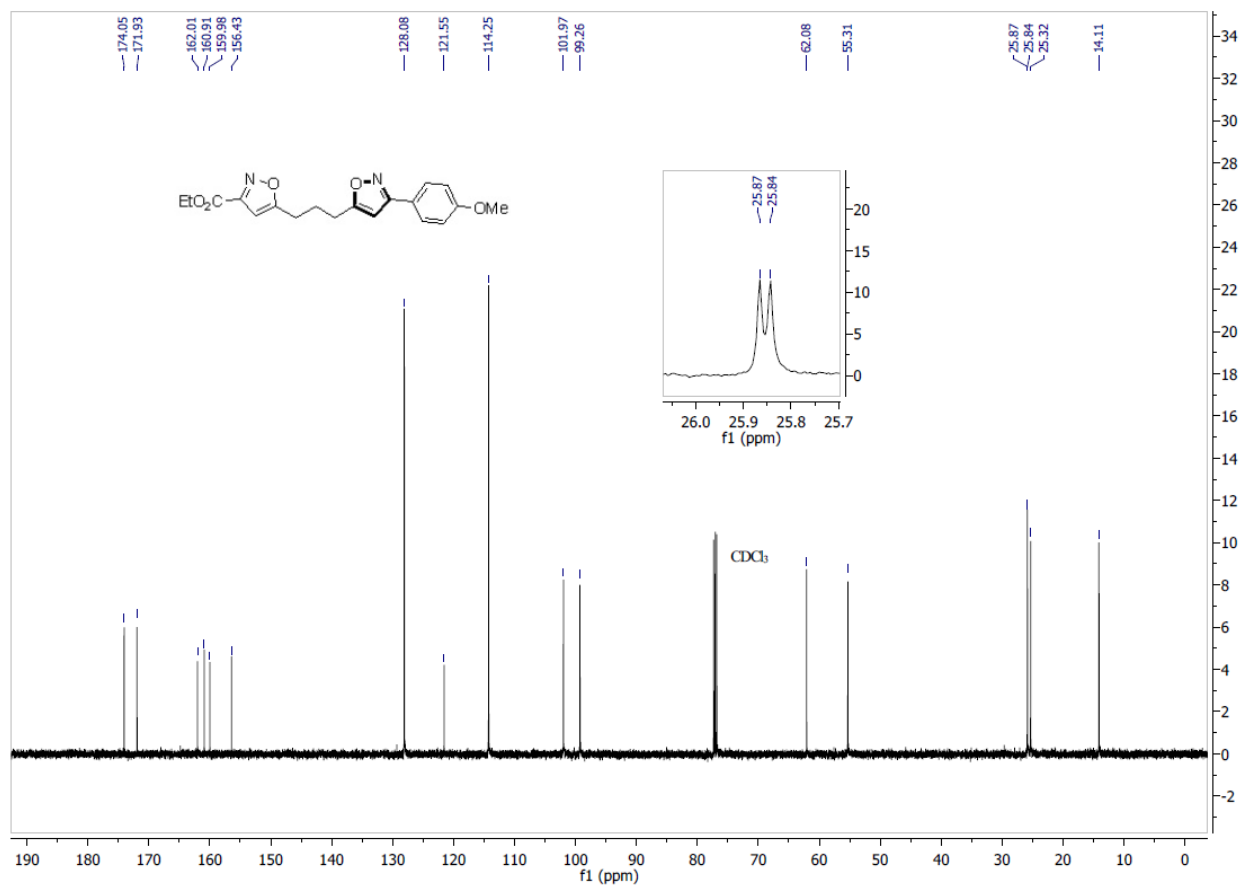
Figure S3.50. ^{13}C-NMR (125 MHz, CDCl$_3$) of ethyl 5-(3-(3-(4-methoxyphenyl)isoxazol-5-yl)propyl)isoxazole-3-carboxylate (111e)

3-(4-methoxyphenyl)-5-(3-(3-(4-nitrophenyl)isoxazol-5-yl)propyl)isoxazole (111f)
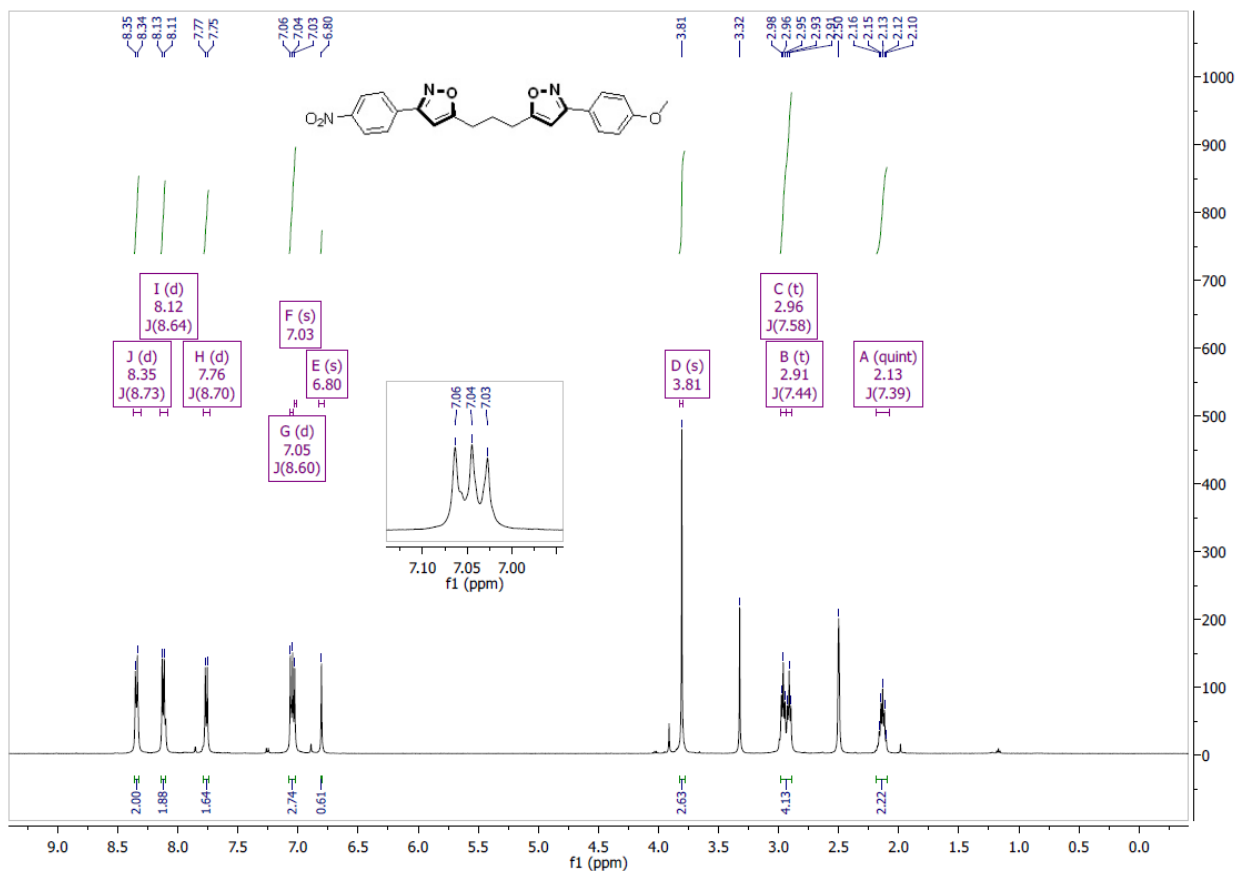
Figure S3.51. ^{1}H-NMR (500 MHz, *d[6]*-DMSO) of 3-(4-methoxyphenyl)-5-(3-(3-(4-nitrophenyl)isoxazol-5-yl)propyl)isoxazole (111f)
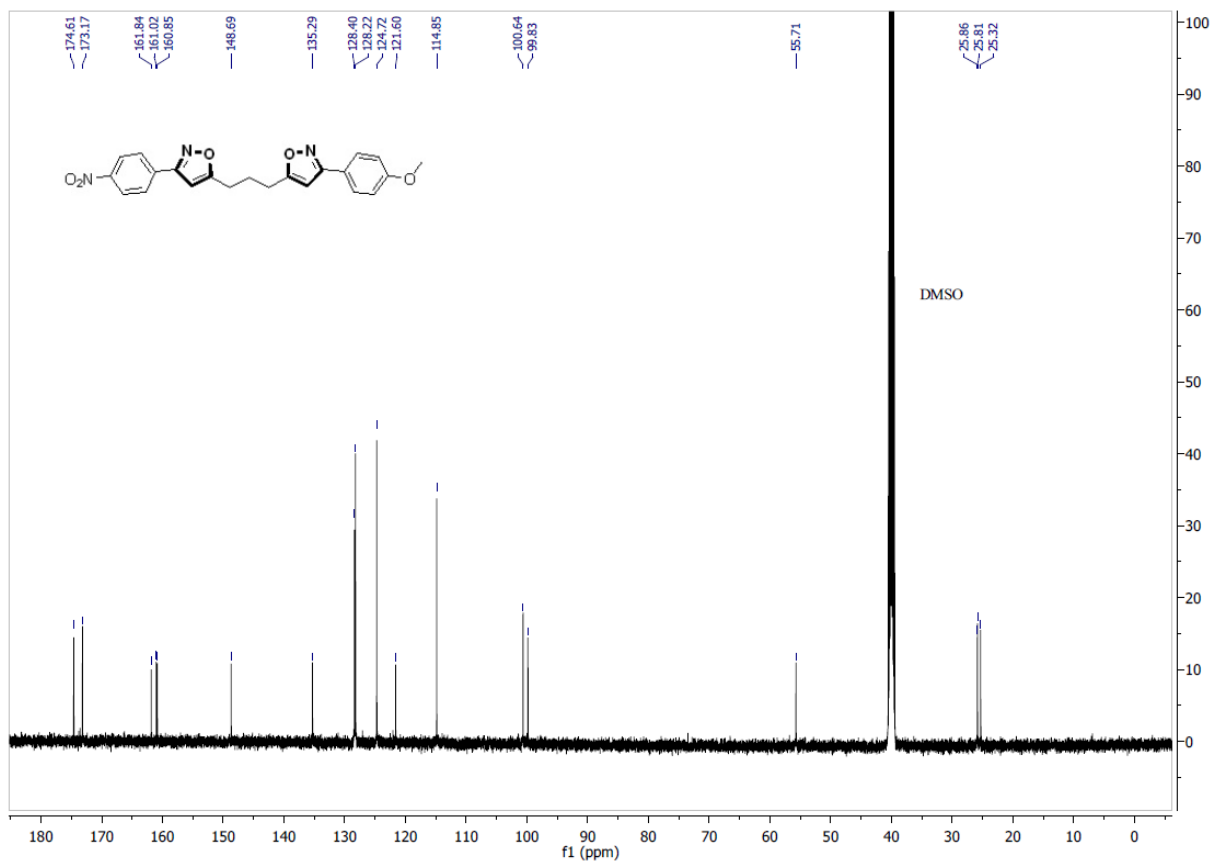
Figure S3.52. ^{13}C-NMR (500 MHz, d^6-DMSO) of 3-(4-methoxyphenyl)-5-(3-(3-(4-nitrophenyl)isoxazol-5-yl)propyl)isoxazole (111f)

3.7.12. Solid state characterization of desymmetrization product 103e

In the following set of results, it was determined the that the synthesis of 3,5-isoxazole-alkyne adduct **105e** as a model substrate occurred during the milling of the bis-alkyne **103a** hydroxyimidoyl chloride **104e** rather than during the isolation process. Consequently, the reaction to synthesize **105e** was carried as reported PS2 but the reaction crude was studied by FT-IR and MALDI-TOF-MS.

103a + **104e** → **105e**

Na$_2$CO$_3$ (2.0 equiv.)
Cu(NO$_3$)$_2$•2.5(H$_2$O) (1.0 equiv.)
Mesitylene (η= 0.25 µL/mg)
n$_{ss}$= 8, 60 Hz
60 min
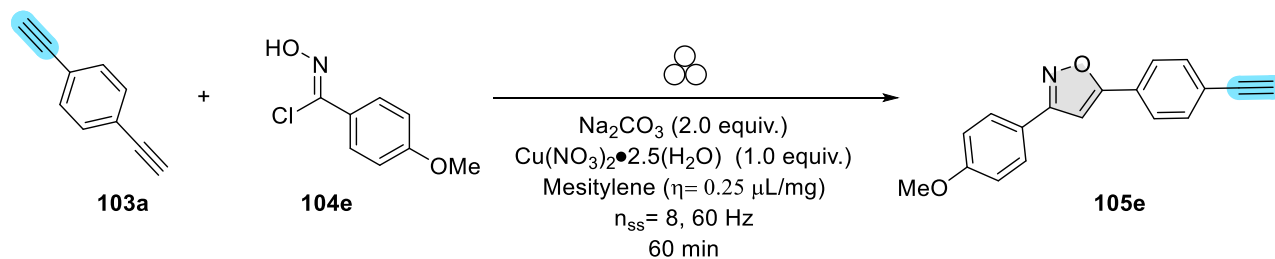
3.7.12.1. FT-IR:
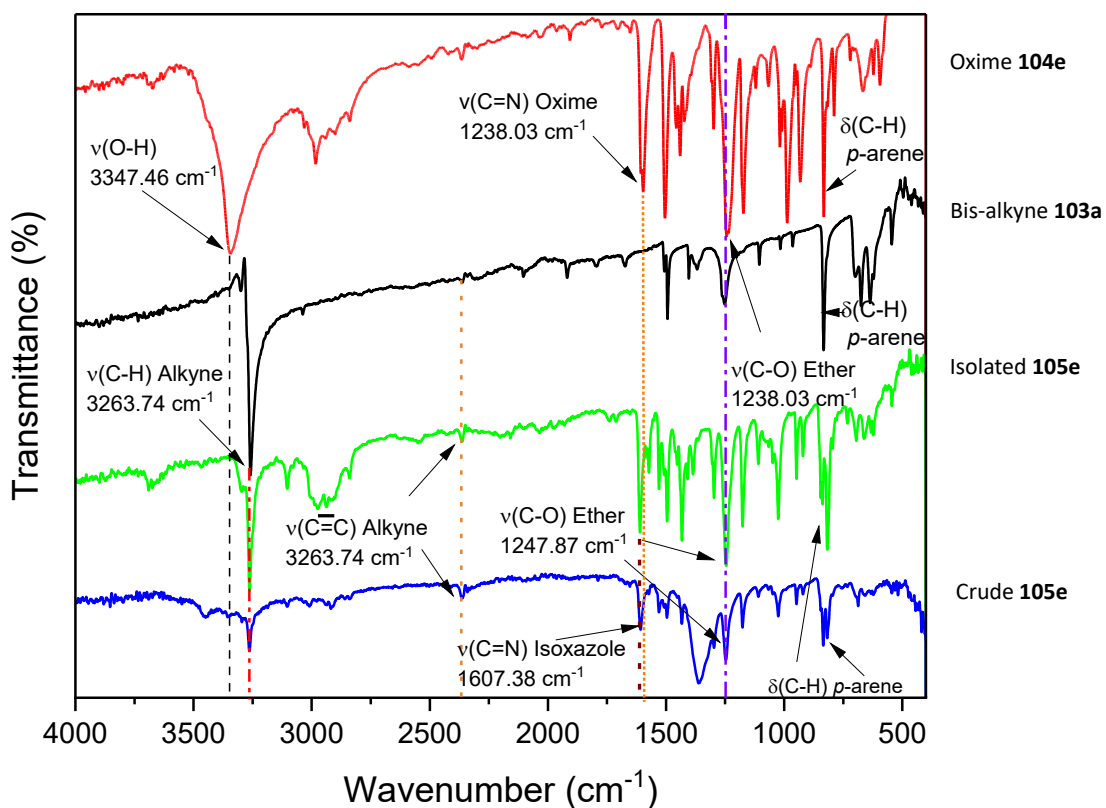
Figure S3.53. Comparative FT-IR of the reaction substrates to the crude product of **105e**

3.7.12.2. MALDI-TOF-MS:

(17e)
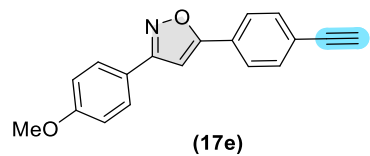
Mass calculated 275.31 found [M+H] 276.105
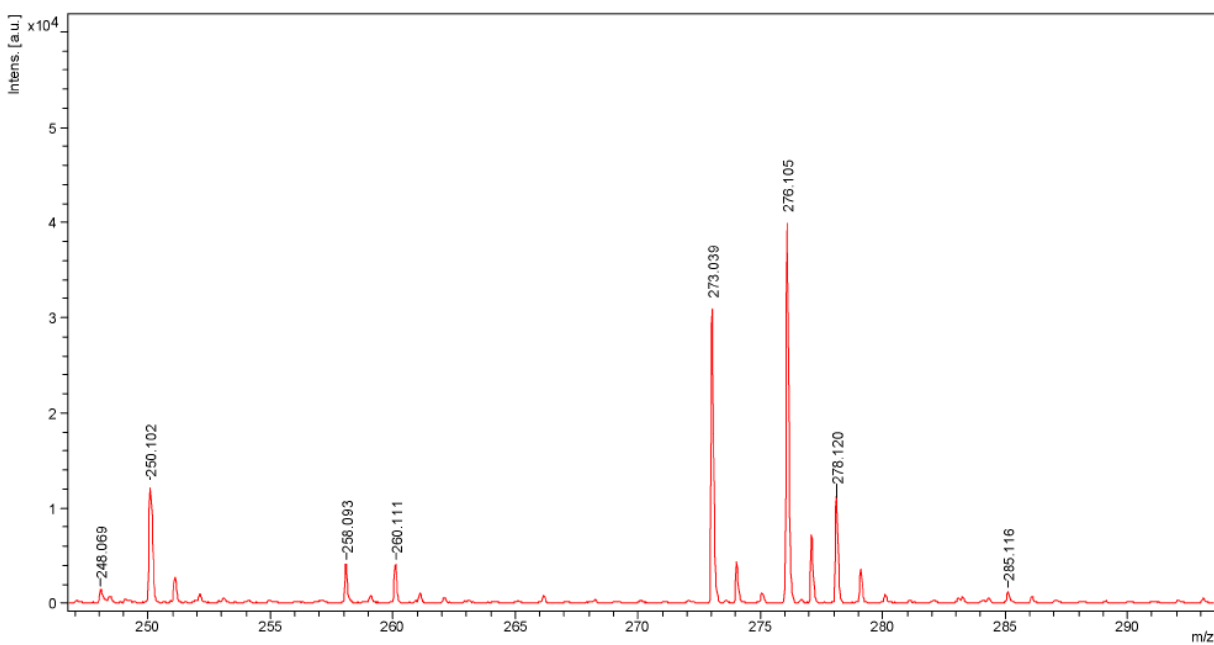
Figure S3.54. MALDI-TOF MS of the reaction crude

Chapter 4- Enabling Regioselective Control For Solvent-Free Reactions: A Mechanochemical Ru-Catalyzed Synthesis of 3,4- and 3,4,5-Isoxazoles by Planetary Ball-Milling Technique.

4.1. Abstract

A mechanochemical enabled Ru(II) catalyzed synthesis of 3,4-isoxazoles and 3,4,5-isoxazoles from terminal and internal alkynes and hydroxyimidoyl chlorides. This solid-state approach allows convenient access to a diverse library of 3,4- and 3,4,5-isoxazoles with excellent yields and regioselectivity. In-depth mechanistic investigations have determined that using liquid-assisted grinding (LAG) with coordinating liquid additives is critical in enhancing the catalytic activity of Ru(II) complexes. Notably, the regioselective control achieved over the solvent-free and solid-state Ru(II) catalyzed 1,3-dipolar cycloaddition reaction demonstrates the remarkable ability of mechanochemistry to tune kinetic and thermodynamic parameters in regio-divergent reactions.

4.2. Introduction

Cycloaddition reactions have become indispensable transformations for the synthesis of complex organic molecules.[1] Excellent examples that showcase the power of cycloadditions reactions in the synthesis of natural products and active pharmaceutical ingredients (APIs), includes the Diels-Alder reaction ([4+2] cycloaddition),[2-7] 1,3-dipolar cycloadditions ([3+2] cycloaddition),[8-13] and [2+1] cycloadditions.[14-18]

The use of 1,3-dipolar cycloadditions between alkynes and nitrile oxides (NOs) is an effective synthetic strategy for accessing isoxazole **112**. This heterocycle serves as a versatile intermediate in the synthesis of complex natural products (**Figure 4.1a**),[19-23] and an essential pharmacophore in various drug candidates (**Figure 4.1b**).[24-28]

Different types of substitutions can be observed in isoxazole heterocycles, as shown in **Figure 4.1b**. Di-substituted isoxazoles, including 3,4-isoxazoles **125** and 3,5-isoxazoles **124**, are synthesized through thermal 1,3-dipolar cycloadditions with low regioselectivity forming complex mixtures of regioisomers (**Figure 2**).[29]

Research conducted by the Houk and Fokin groups aimed to evaluate the regioselectivity of 1,3-dipolar cycloadditions between terminal alkynes **122** and NOs **123*,** obtained *in situ* by protodehalogenation of the hydroxyimidoyl chloride **123** (**Figure 4.2**). Both groups support that the energetic barriers between the transition states, **TSa** and **TSb**, are very small, resulting in poor regioselectivity and the formation of both regioisomers **124** and **125**.[29,38] However, on many occasions, a slight preference is observed for 3,5-isoxazoles **124**. This preference arises from the lower steric collisions encountered on **TSa** compared to **TSb** (**Figure 4.2**).[30] Other factors, such as the electronic properties of the terminal alkyne substituents **122** and the polarity of the solvent, can play a small role in promoting the formation of 3,4-isoxazoles **125** by minimizing energetic differences between the frontier molecular orbitals (FMO) of the terminal alkyne **122** and hydroxyimidoyl chloride **123**.[29-43]
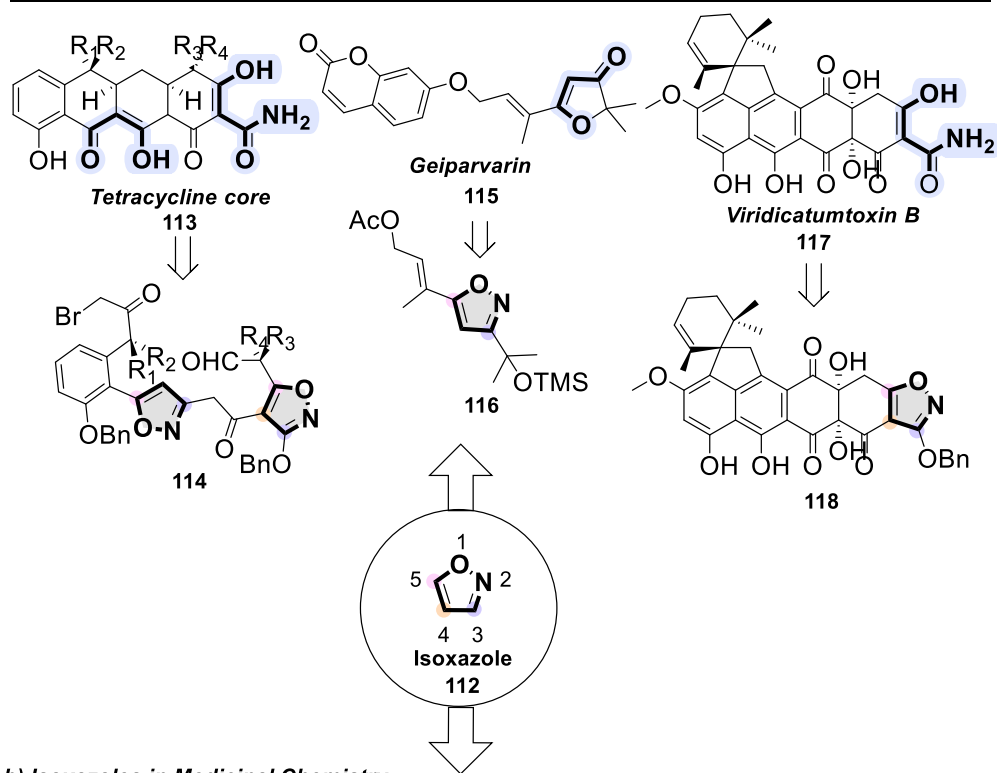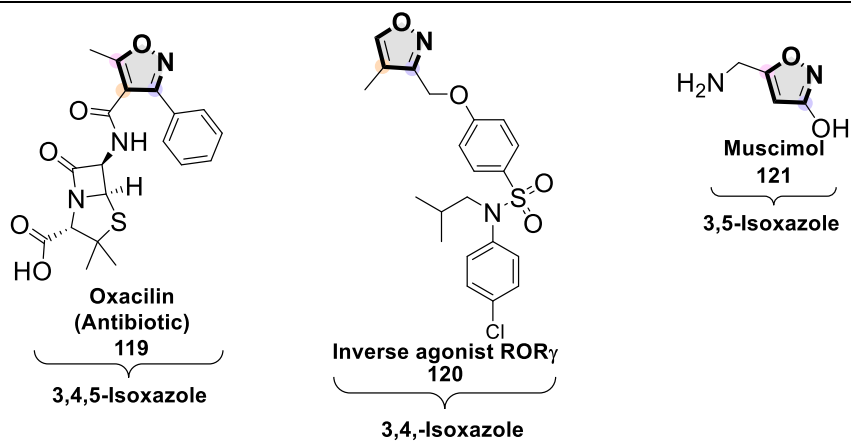
Figure 4.1: Application of isoxazoles scaffolds
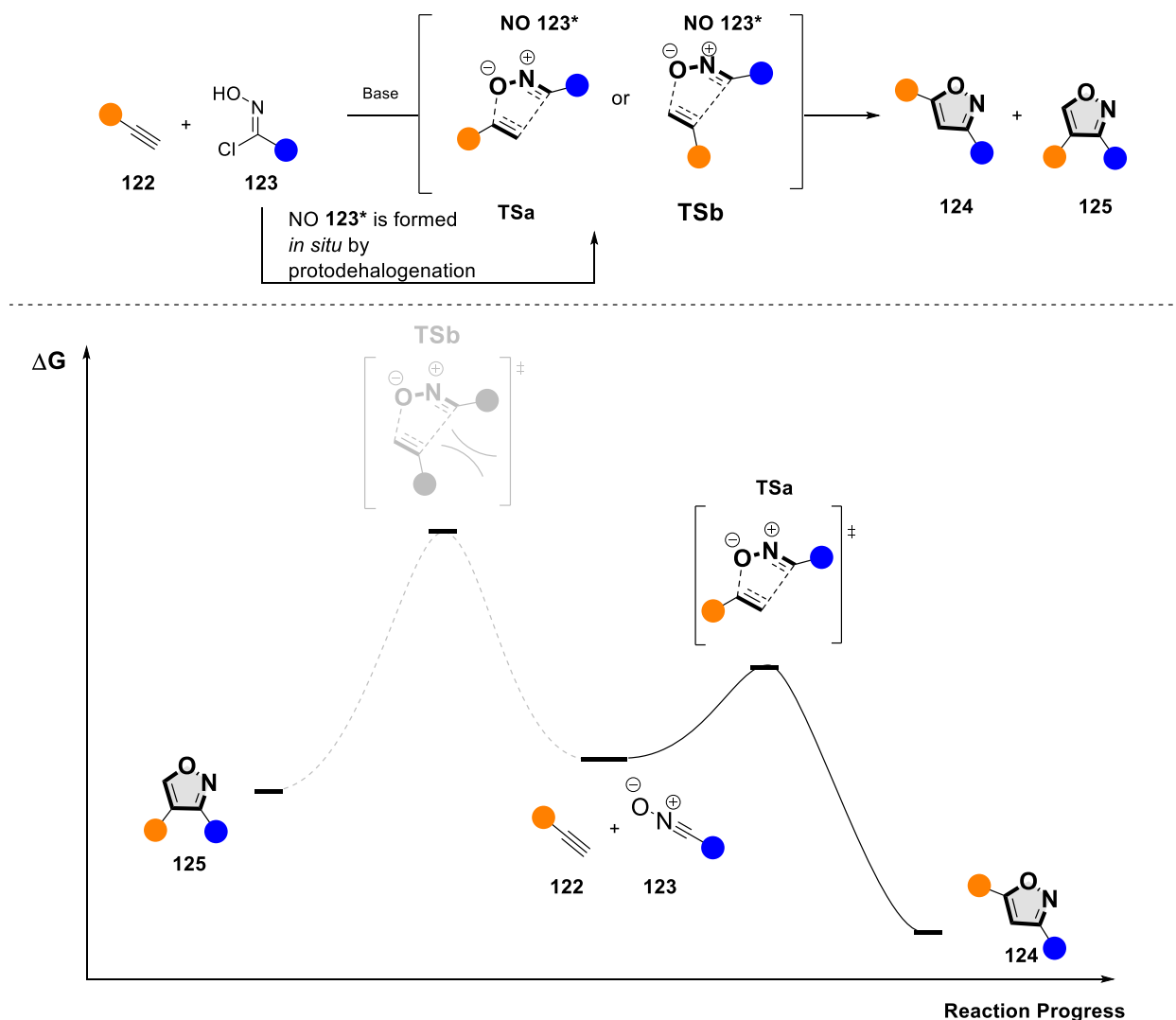
Figure 4.2. Generic energy diagram for 1,3-dipolar cycloadditions between NOs and terminal alkynes to obtain di-substituted isoxazoles

In 2008, the Fokin group introduced the use of [Cp*RuCl] catalysts to enabled a regioselective synthesis of 3,4-isoxazoles **125** from terminal alkynes **122** (**Figure 4.3b**).[44-49] The protocol has proven an effective strategy to access 3,4-isoxazoles with good regioselectivity and yields. The reported Ru(II) catalysis to obtain 3,4-isoxazoles **125** has only been explored by solution-thermal methods, leaving a tantalizing opportunity for exploration of this catalytic method by mechanochemical techniques.

Mechanochemistry is a sustainable technique to perform organic reactions by milling or grinding, reducing or eliminating the use of bulk amounts of organic solvent.[50-57] The absence of organic solvent has proven to be beneficial in increasing reaction rates because reagents are present at a maximal concentration and reaction conditions are not dependent on the solvation and desolvation of reagents.[9] In addition, new types of product selectivity and product distributions can be obtained from those commonly observed in solution-based reactions due to the fix and even arrangement of molecules in the crystal lattice.[58-63]

In relation to the 1,3-dipolar cycloadditions and mechanochemistry, our group previously demonstrated the advantages of mechanochemistry and planetary ball-milling in the synthesis of 3,5-isoxazoles **124** by

a Cu-catalyzed 1,3-dipolar cycloadditions from terminal alkynes **122** and hydroxyimidoyl chlorides **123** (**Figure 4.3a**).[64] We have further expanded this concept and demonstrated the ease with which symmetrical bis- and tris-alkynes can be desymmetrized by controlled 1,3-dipolar cycloadditions to obtain unsymmetrical bis-3,5-isoxazoles using mechanochemistry.[65]

a) **Cu-Catalyzed Cycloaddition of Nitrile Oxides and Alkynes**

b) **Ru-Catalyzed Cycloaddition of Nitrile Oxides and Alkynes**
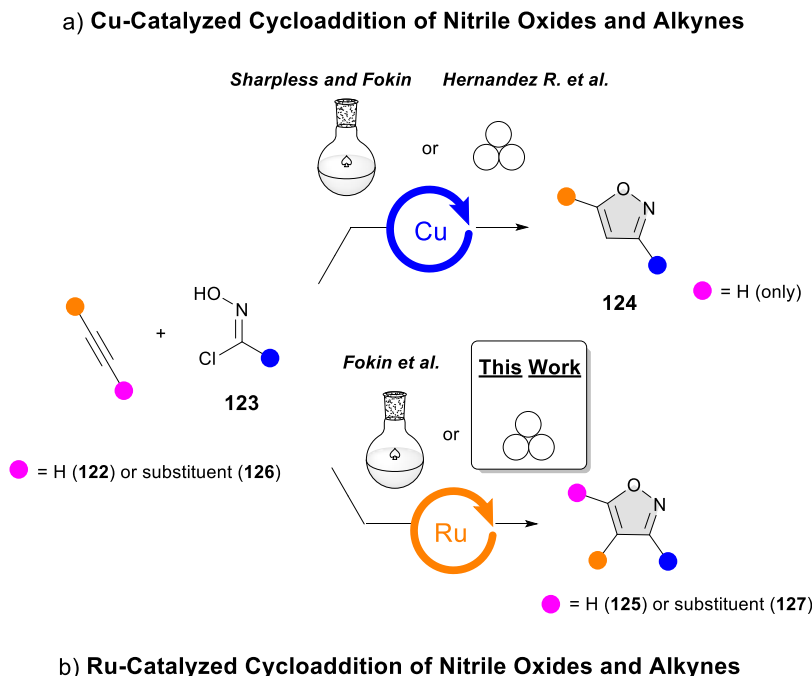
Figure 4.3. Development of synthetic methods by mechanochemistry and solution-based thermal methods to access substituted isoxazoles

While it has been established that kinetic and thermodynamic parameters can be altered through mechanochemistry,[66-70] the ability to control the regioisomer distribution obtained for cycloaddition reactions remains elusive. Therefore, enabling a mechanochemical Ru(II) catalytic system to access 3,4-isoxazoles **124** would contribute to a better understanding of the essential parameters necessary for controlling the outcome and product distribution for cycloaddition reactions (**Figure 4.3b**). Herein, we report the first mechanochemical Ru-catalyzed regioselective synthesis of 3,4-isoxazoles **124** and 3,4,5-isoxazoles **127** from terminal alkynes **122** and internal alkynes **126,** with hydroxyimidoyl chlorides **123** (**Figure 4.3b**). We have conducted mechanistic investigations to thoroughly evaluate the effects of mechanical stress on the catalytic activity of Ru complexes for these cycloaddition reactions.

4.2. Results and Discussion

As demonstrated by Houk's group, the regioselectivity of 1,3-dipolar cycloadditions under solution-based thermal uncatalyzed conditions is partly determined by the steric and electronic nature of the substituents in the terminal alkyne.[38] In order to determine if mechanical grinding influences the regioselectivity, we examined the selectivity outcome for liquid methyl propiolate **122a** and solid 1-ethynyl-3,5-dimethoxybenzene **122b** when reacted with ester hydroxyimidoyl chloride **123a** under mechanochemical conditions (**Figure 4.4**). These control experiments were carried out using a Fritsch 7 planetary ball mill with a stainless-steel (SS) jar and 8 SS milling media of 1 cm diameter (~32 g). When the reagents were mechanically ground, no formation of the desired 3,4-isoxazole (**125a** or **125b**) was observed by ^{1}H-NMR.

Instead, only 3,5-isoxazole **125b** was observed in 36% yield, suggesting the need of a catalyst to access the 3,4-isoxazole (**Figure 4.4**). Our investigation continued using a solid aromatic alkyne **122b** because the limited mass transfer of solid reagents provides more general conditions.[62]
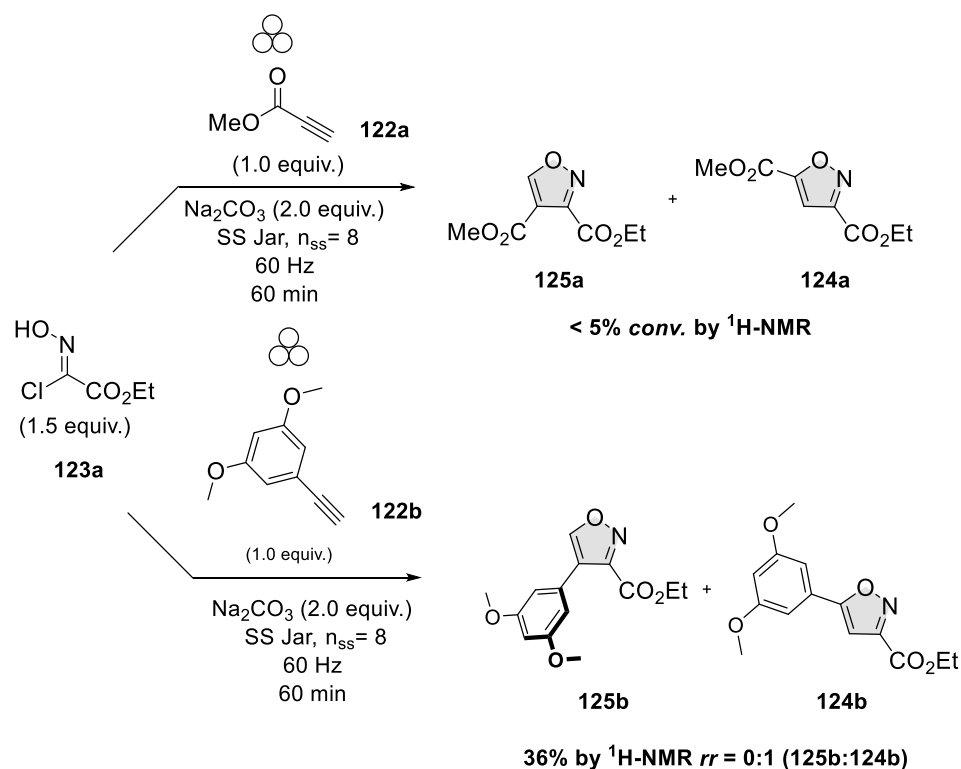
Figure 4.4. Effect of mechanical grinding in the regioselectivity in 1,3-dipolar cycloadditions to form di-substituted isoxazoles

Firstly, we screened **Ru-1** and **Ru-2** both Ru(II) complexes (**Figure 4.5**). Out of the two, only **Ru-1** complex bearing a Cp* ligand was able to form the desired 3,4-isoxazole **14b** (**Table 4.1**).
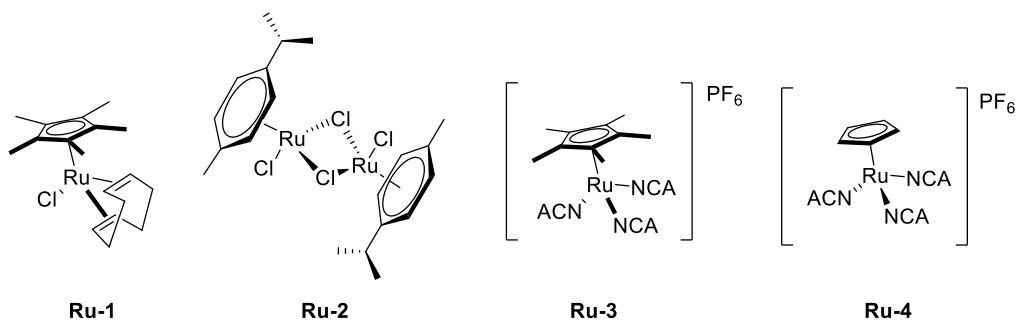
Figure 4.5. Ru(II) complexes screened.

In terms of the effective catalytic loading, **Ru-1** was able to catalyze the formation of the desire isoxazole isomer **125b**, even when using 5 mol % of the catalyst. However, **125b** was formed in low yields as the minor isomer (**entry 1**), presumably due to the catalyst decomposition caused by the strong abrasion. Increasing the loading of **Ru-1** also increased the yield of the desired isoxazole **125b**, reaching a yield of

14%, but still as the minor isomer (**entry 3**). Further increase of **Ru-1** loading above 25 mol% was detrimental, resulting in no product forming instead a sticky mixture that hindered the mixing of the reagents (**entry 4, Table 4.1**). Based on these control experiments, it was evident that 25 mol% was the most optimal loading, and it was used for subsequent control experiments.

Next, we assessed different grinding auxiliary agents (GAA) to enhance the rheology of the mixture (**Table 4.1**, **entries 5-11**).[71-75] In our study, utilizing 150 wt% of KBr demonstrated exceptional compatibility with the **Ru-1** catalyst, in contrast to other ionic salts such as NaCl, KCl, KI, and CsBr (**entries 5, 6, 9-10**). The compatibility between the **Ru-1** catalyst and KBr suggests that KBr behaves as a shock absorber that disperses the heat generated during milling and prevents the decomposition of the **Ru-1** catalyst. The heat dispersion effect of KBr becomes evident when comparing the specific heat capacities (C_p) of the ionic salts (**entry 5-11**), with KBr exhibiting the lowest heat capacity.[76-78]

Table 4.1. *Optimization conditions for the synthesis of 3,4-isoxazole using SS Jar.*

122b (1.0 equiv.) + 123a (1.5 equiv.) ● = CO₂Et → Ru *cat.* Na₂CO₃ (2.0 equiv.) GAA THF (η= 0.5 µL/mg) SS Jar, n$_{ss}$= 8 60 min, 60 Hz → 125b + 124b ● = 3,5-(CH₃O)₂C₆H₃
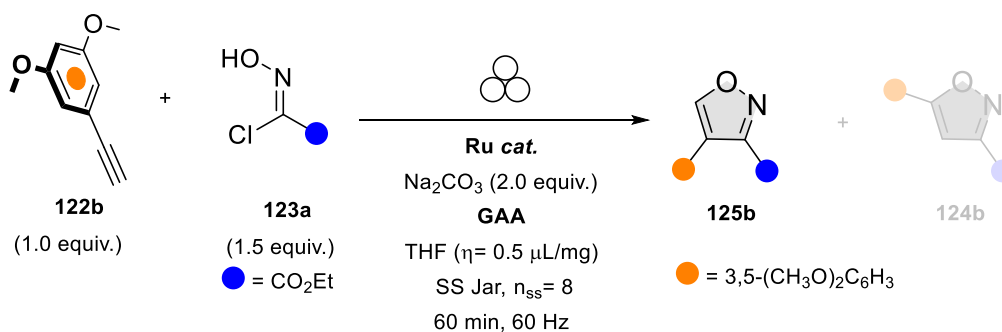
Ru(II) Complex [a]

Entry	Ru *cat.*	mol %	Yield (%) 125b [b]	Yield (%) 124b [b]	rr [c]
1	Ru-1	5	9	25	1:2.8
2	Ru-2	10	-	36	0:1
3	Ru-1	25	14	20	1:1.4
4	Ru-1	50	-	-	-

Grinding Auxiliary Agent (GAA) [d]

	GAA	wt %	C_p (J/KgK)	Yield (%) 125b [b]	Yield (%) 124b [b]	rr [c]
5	NaCl	150	880	8	12	1:1.5

6	KCl	150	690	8	8	1:1
7	KBr	150	460	20	10	2:1
8	KBr	300		17	12	1.4:1
9	KI	150	-	-	-	-
10	CsBr	150	270	6	10	1:1.7
11	Al_2O_3	150	880	-	-	-

[a] **Reaction conditions:** Alkyne **122b** (1.0 equiv., 0.308 mmol, 50 mg), hydroxyimidoyl chloride **123a** (1.5 equiv., 0.462 mmol, 20 mg), Na_2CO_3 (2.0 equiv., 0.612 mmol, 64.8 mg), **Ru-1** (25 mol %, 29 mg), THF (η=0.5 µL/mg, ~107 µL), reagents were milled in SS jar with 8 SS balls of 1 cm diameter for 60 min. [b] Yields were determined by ^{1}H NMR using 1,3,5-trimetoxybenzene as an internal standard. [c] rr represents the regio-ratios of 125b:124b, which were determined from the ^{1}H NMR of the crude product. [d] It was included 150 wt % of GAA ~320 mg.

Further improvements in the regioselectivity of the reaction were related to modulating the milling energy. Mack's group demonstrated that the milling material hardness and density as well as frequency parameters, can impact the reaction selectivity.[79,80] Inspired by these finding, we decided to systematically evaluate the effect of milling material and frequency on the regioselectivity of the reaction.

We evaluated the impact of using Teflon (PTFE) jars (ρ = 2.2 g/cm^3) a material with a lower density than SS (ρ = 7.9 g/cm^3) (**Table 4.2**). By milling the reagents in Teflon jars and with 1 SS ball (1 cm diameter), we were able to reduce the catalytic loading from 25 mol% to 15 mol% without compromising the regioselectivity for the desired 3,4-isoxazole **125b.** This also led to an increase in reaction yield to 35% as determined by ^{1}H-NMR (**entry 2, Table 4.2**). These results indicate that Ru-1 decomposes due to the strong abrasion when milled in the SS jar.[73,85-87] However, reducing the catalyst loading below 15 mol% severely diminished the regioselectivity and the yield for the desired isomer **125b,** thereby predominantly forming the undesired isomer **124b** (**entry 4**).

Table 4.2. *Effect of the jar material in the Ru(II)-catalyzed synthesis of 3,4-isoxazoles.*

Entry	Jar/MM[b]	mol %	P (g/cm³)	Yield % 125b[c]	Yield % 124b[c]	rr[d]

1	SS/SS	25	7.9	20	10	2:1
2	Teflon/SS	25	2.2	-	-	-
3	Teflon/SS	15	2.2	35	21	1.7:1
4	Teflon/SS	5	2.2	10	30	1:3

[a] **Reaction conditions**: Alkyne **122b** (1.0 equiv., 0.308 mmol, 50 mg), hydroxyimidoyl chloride **123a** (1.5 equiv., 0.462 mmol, 20 mg), Na$_2$CO$_3$ (2.0 equiv., 0.612 mmol, 64.8 mg), KBr (150 wt %, 320 mg) **Ru-1** (15 mol %, 17 mg), and THF (η=0.5 µL/mg, ~250 µL) were milled in a Teflon jar with 1 SS balls of 1 cm diameter for a period of 60 min. [b] MM refers to milling- media. [c] Yields were determined from ^{1}H NMR and using 1,3,5-trimetoxybenzene as an internal standard. [d] rr is regio-ratios of 125b:124b, which were determined from ^{1}H NMR of the crude product.

Further improvements in yield and regioselectivity were achieved by optimizing milling frequency.[79-84] Decreasing the milling frequency resulted in an improvement in the yield and regioselectivity (*rr*) for the desired 3,4-isoxazole **125b** (**Figure 4.6a**). The optimal frequency was found at 6 Hz (~360 rpm), which led to a 60% yield and a *rr* of 12:1 for the desired isomer **125b**. Performing the reaction at low frequency led us to question whether milling was required for the reaction. However, by simply stirring the mixture with a stir bar in a round-bottom flask at 6 Hz (360 rpm), the product was formed in less than 5% yield by ^{1}H-NMR, even after prolonged reaction times.

These results demonstrate that the Ru catalytic pathway for synthesizing 3,4-isoxazole **125b** requires less energy compared to the concerted pathway involved for the formation of 3,5-isoxazole **124b**.[29,40,41] The limited shear force obtained at 6 Hz in the planetary ball-milling provides sufficient energy for the reaction to proceed preferentially by the Ru-catalysed pathway. The low milling frequency reduces the chances for the alkyne **122** and NO **123*** substrates to undergo an uncatalyzed reaction that would lead to the undesired regioisomer.[70,79-84]
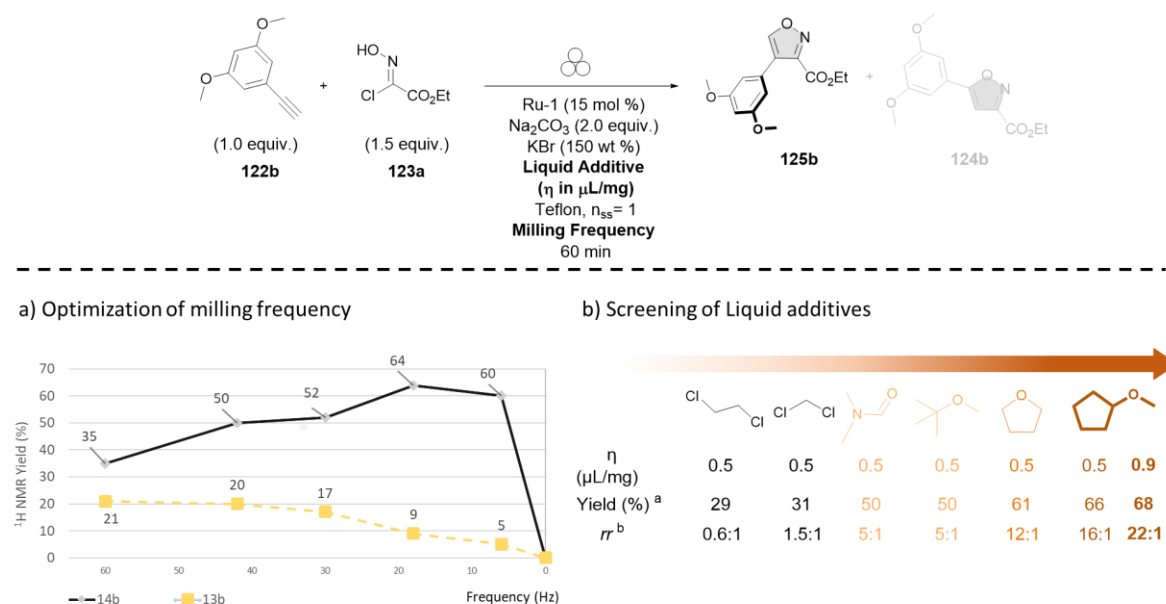
Figure 4.6. Effect of milling frequency in the yield and regioselectivity

Reaction conditions: Alkyne **122b** (1.0 equiv., 0.308 mmol, 50 mg), hydroxyimidoyl chloride **123a** (1.5 equiv., 0.462 mmol, 20 mg), Na_2CO_3 (2.0 equiv., 0.612 mmol, 64.8 mg), KBr (150 wt %, 320 mg) **Ru-1** (15 mol %, 17 mg), and the corresponding liquid additive were milled in a Teflon jar with 1 SS balls of 1cm diameter for 60 min.[a] ^{1}H-NMR were determined by using 1,3,5-trimetoxybenzene as an internal standard. [b] *rr* represents the regio-ratios of 125b:124b which were determined from the ^{1}H NMR of the crude product.

Our optimizations led us to evaluate the effect of liquid additives with different polarities and coordination strengths (**Figure 4.6b**). The use of small amounts of a liquid additive for liquid-assisted grinding (LAG) is known to increase reaction yield, control selectivity, and eliminate the formation of undesired side products.[88-102] For our case, ether additives such as THF and CPME improved the regioselectivity for the desired 3,4-isoxazole **125b**, compared to non-polar chlorinated additives such as 1,2-DCE or DCM, which decreased the regioselectivity. Further optimizations using CPME proved to be advantageous compared to THF due to the eco-friendly nature, stability, and safety profile.[101,102]

Other control experiments demonstrated that doubling the equivalents of hydroxyimidoyl chloride **123a** from 1.5 equivalents to 3.0 improved the yield and regioselectivity for the desired isoxazole isomer **125b**. However, other optimization experiments related to changes in the equivalence of carbonate base and changes to the milling time resulted in a decrease in either the yields or regioselectivity for the desired isomer **125b**. (See experimental information for optimizations in base and milling time PS1).

After extensive optimization, it was found that the optimal conditions were 1.0 equivalent of the terminal alkyne **122**, 3.0 equivalents of hydroxyimidoyl chloride **123**, 2.0 equivalents of Na_2CO_3, 150 wt% of KBr, 15 mol% of **Ru-1** catalyst, and milling the reagents in a Teflon jar with a single SS ball for 60 minutes.
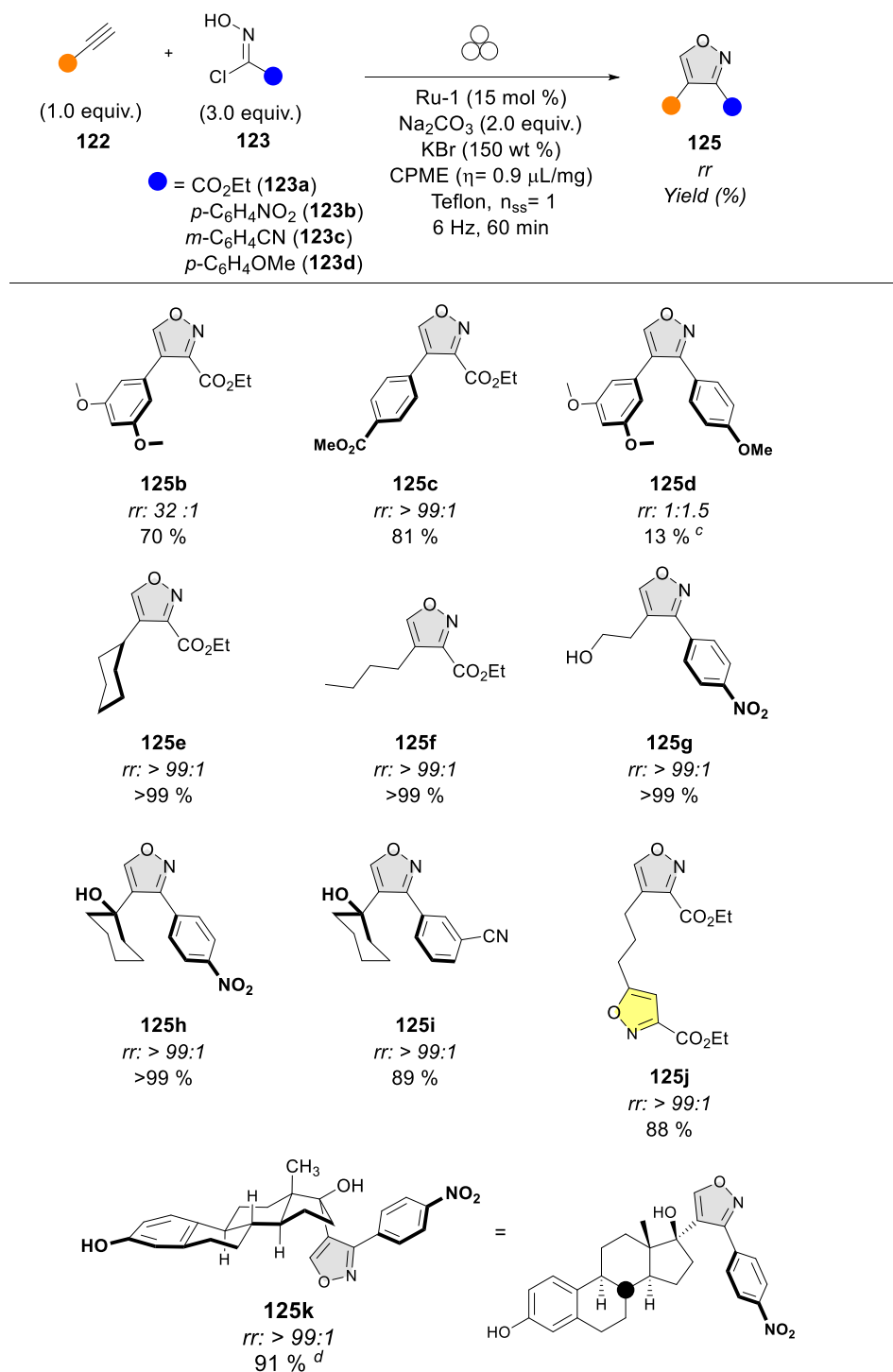
Figure 4.7. Reaction scope for mechanochemical Ru-catalyzed synthesis of 3,4-Isoxazole **125**.

[a] Reactions performed in a 50 mg scale. [b] *rr* is the ratios of **125:124** or 3,4-isoxazole to 3,5-isoxazole, determined from the ^{1}H-NMR of the crudes c) Yield was determined by ^{1}H-NMR. [d] Reaction performed at a milling frequency of 30 Hz (see supplementary information for details on the isolation).

We evaluated the generality of the optimized conditions with different terminal alkynes **122** and hydroxyimidoyl chlorides **123** with varied electronic and steric properties (**Figure 4.7**). The hydroxyimidoyl chlorides **123** were categorized based on the electronic nature of their substituents. Hydroxyimidoyl chlorides **123a**, **123b**, and **123c** were classified as electron-withdrawing groups (EWG) and **123d** as electron-donating groups (EDG). Using the optimized conditions, we successfully synthesized 3,4-isoxazoles **125b, 125c, 125e-k** with excellent regioselectivity and yields when using the electron-deficient (EWG) hydroxyimidoyl chlorides **123a**, **123b**, and **123c** (**Figure 4.7**). However, the electron-rich hydroxyimidoyl chlorides **123d** produced the corresponding 3,4-isoxazole **125d** as the minor isomer.

We observed no steric influence by substituents in the terminal alkyne, and tertiary propargyl alcohols were tolerated under mechanochemical conditions, leading to the formation of 3,4-isoxazoles **125h** and **125i** with excellent yields and regioselectivity. The high regioselectivity achieved with propargyl alcohols suggests that the hydroxyl moiety acts as an H-bonding directing group, like what has been observed in solution-thermal synthesis.[44,46] The optimized conditions were also compatible with more complex starting materials, enabling us to synthesize a novel estradiol-isoxazole derivative **125k** using hydroxyimidoyl chloride **123b** that is unreactive in solution-based thermal conditions due to the limited solubility of **123b**. The reaction demonstrated good compatibility with heterocycles, and we were able to synthesize the first unsymmetrical and regio-divergent bis-isoxazoles **125j** in excellent yield and regioselectivity.

After establishing the conditions for synthesizing 3,4-isoxazoles **125**, we focused on accessing 3,4,5-isoxazoles through mechanochemistry. The synthesis of tri-substituted 5-membered heterocycles by mechanochemistry is limited, and there are currently no mechanochemical methodologies available for accessing a fully substituted heterocycle *via* a controlled regioselective cycloaddition from unsymmetrical internal alkynes **126** (**Figure 4.8**).[103-106]
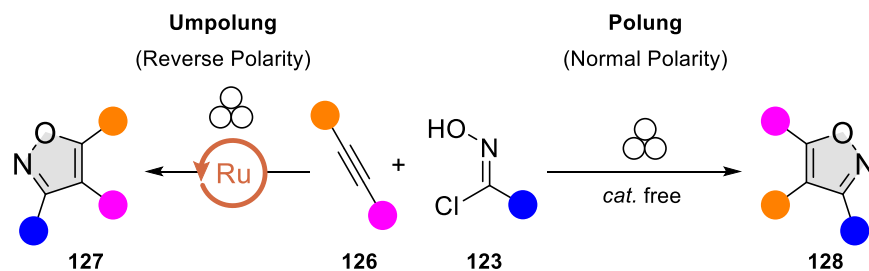
Figure 4.8. Effect of Ru catalysis in regioselectivity in the synthesis of 3,4,5-Isoxazoles

In contrast to the Cu catalysis, Ru(II) catalysis can be applied to internal alkynes **126** to effectively access trisubstituted isoxazoles **127** through polarity reversal or "umpolung" reactivity of the internal alkyne and NO (**Figure 4.8**).[44-49] Due to the scarcity in the literature on the synthesis of 3,4,5-isoxazoles, we first established the "polung" synthesis of 3,4,5-isoxazole by a Ru-free pathway.

In our study, we initially assessed the effect of mechanochemistry on symmetrical internal alkynes bearing an EWG (**126a**) that have been previously shown to enhance the rate of the 1,3-dipolar cycloaddition.[42]

Through our optimization efforts, it became apparent that internal alkynes require higher milling frequencies to synthesize the corresponding 3,4,5-isoxazole. Consequently, we increased the milling frequencies from 6 Hz to 30 Hz. This frequency increase suggested greater shear force was required to overcome the energetic barrier posed by more hindered internal alkynes.[40,107-108] Moving on to GAA, we found that solid NMe$_4$Br exhibited superior performance as compared to KBr. We inferred a potential

216

activation of the carbonyl groups by the NMe$_4$Br that accelerates the cycloadditions.[106] (see supplementary information section PS3 for complete details on the optimization).

The optimized conditions were applicable to a large range of internal alkynes and the corresponding "polung" 3,4,5-isoxazoles **128** were synthesized with high yields and with no electronic discrimination observed for hydroxyimidoyl chloride **123** (**Figure 4.9a**). The same optimized conditions were compatible for ynones **126b-e**, an unsymmetrical internal alkyne bearing a single EWG substituent, and 3,4,5-isoxazoles **16e-k** were obtained in good to excellent yields and with excellent regioselectivity (**Figure 4.9b**). However, ynols **126f** was unreactive and did not lead the formation of the desired tri-substituted isoxazole **128m** or **128n** under these conditions (**Figure 4.9c**).

In the case of the unsymmetrical ynones **126b-e**, the regioselectivity achieved was predictable, with the carbonyl substituent ending up in the C-4 position of the isoxazole. The regioselectivity is explained by considering the polarity of the ynones , where the β-C is electron-deficient, and α-C is an electron-rich, complementing the electron-rich O and electron-deficient C of the nitrile oxide **123*** (**Figure 4.9b**). This electronegative complementarity directs the positioning of the carbonyl substituent of the ynone to the C-4 position of the isoxazole.
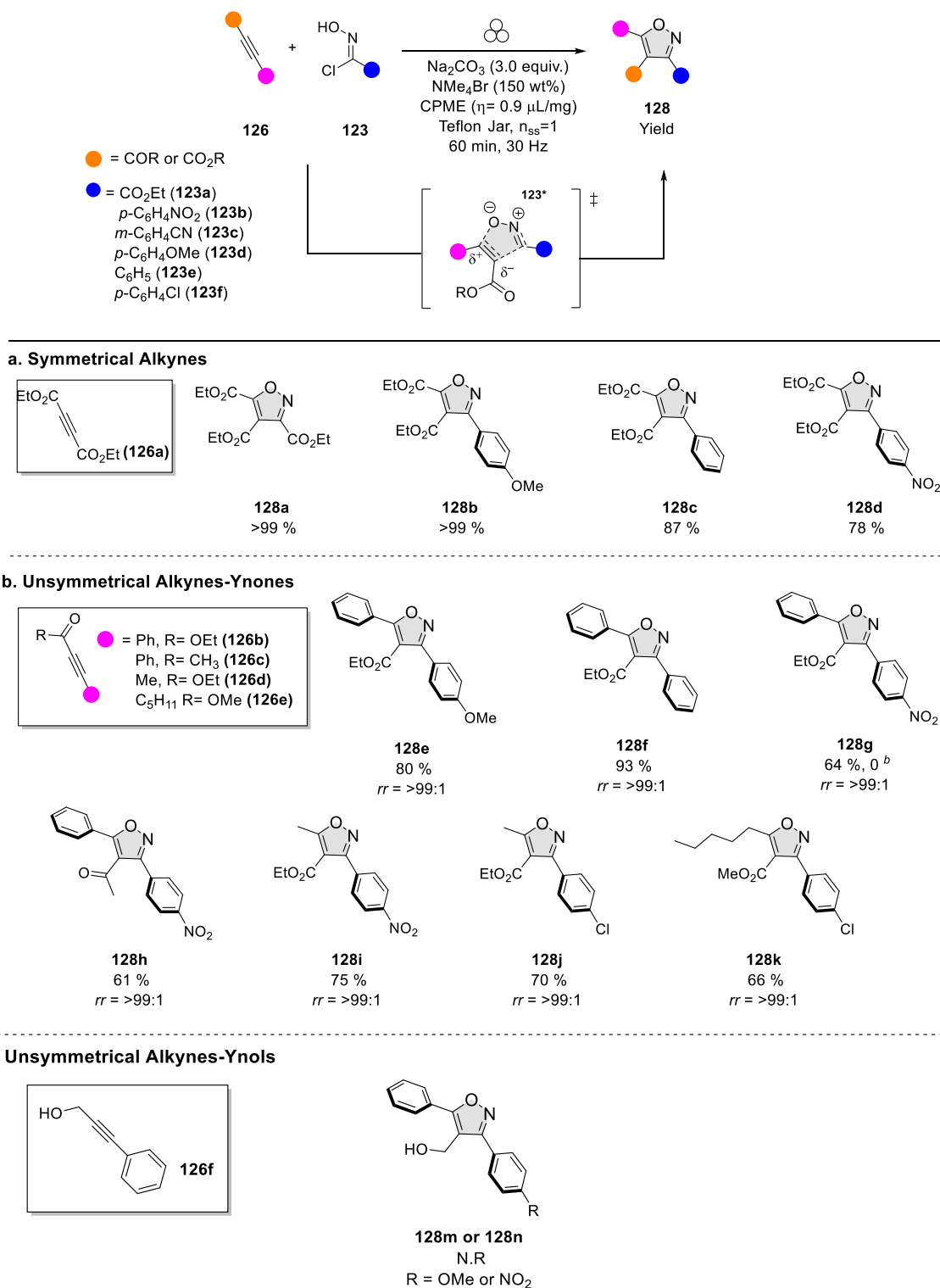
Figure 4.9. "Polung" Synthesis of 3,4,5-isoxazoles

[a] Reported yields are isolated yields and *rr* represents the ratios of **128:127** determined by ^{1}H NMR from the crude product. [b] Yield of the product obtained by solution-based conditions, for detail procedure please see supplementary information

Once established the conditions for the "polung'' synthesis of 3,4,5-isoxazole **128** from ynones, we investigated Ru(II) catalysis to access "umpolung" 3,4,5-isoxazoles **127** from ynones and ynols.

We initially sought to optimize the conditions for synthesizing of hydroxylisoxazoles **128n** from Ynols **126f** and hydroxyimidoyl chloride **123b** using a **Ru-1** catalyst (**Table 4.3**). Unfortunately, the established conditions for synthesizing 3,4-isoxazoles proved to be ineffective, yielding no product (**Table 4.3, entry 1**). To address this issue, increasing the milling frequency to 30 Hz proves critical in achieving the formation of isoxazole **128n** in about 40% by ^{1}H-NMR and with excellent regioselectivity (*rr*= >99%) (**entry 2**). The addition of 0.9 μL/mg of toluene liquid additive demonstrated higher effectiveness compared to the use of CPME. However, reducing the quantity of the toluene additive beyond this had a detrimental effect on the yield (**Table 4.3**, **entries 6 and 7**). Furthermore, we achieved a significant improvement in the yield by increasing the equivalents of base from 2.0 to 3.0. This adjustment resulted in an 83% yield of **128n** by ^{1}H-NMR (**Table 4.3, entry 10**). Once we successfully optimized the conditions for Ynols, we shifted our focus towards Ynones.

Table 4.3. *Optimization of Ru-catalyzed synthesis of 3,4,5-isoxazole from ynols.*

Entry	mol %	Frequency (Hz)	Yield (%) 128n[a]	rr[b]
1		6	N.R.	-
2	15	**30**	**40**	**>99:1**
3		60	N.R.	-

Effect of Liquid Additive

	mol %	Liquid Additive	η (μL/mg)	Yield (%)	rr
4		Mesitylene	0.9	48	>99:1
5		**Toluene**	**0.9**	**53**	**>99:1**
6	15	Toluene	0.5	42	>99:1
7		Toluene	0.25	25	>99:1
8		Benzene	0.9	48	>99:1
9		Cyclohexene	0.9	6	>99:1

Effect of Equivalents of Base

219

	mol %	Base	Equiv.	Yield (%)	rr
10	15	Na₂CO₃	3.0	83	>99:1

Reaction conditions: Ynol **126f** (1.0 equiv., 0.380 mmol, 47μL), hydroxyimidoyl chloride **123b** (3.0 equiv., 1.14 mmol, 80.56 mg), Na₂CO3 (3.0 equiv., 1.13 mmol, 120.2 mg), KBr (150 wt %, 628.85 mg), **Ru-1** (15 mol %, 0.057 mmol, 22 mg), Toluene liquid additive (η= 0.9 μL/mg, ~940 μL). [a] Yields were determined from the ^{1}H NMR and using 1,3,5-trimetoxybenzene as an internal standard. [b] rr represents the regio-ratios of **128n**:**127n**, which were determined by ^{1}H NMR of the crude product.

Ynones substrates were less reactive than ynols when using **Ru-1** catalyst (**Figure 4.10a**), and the umpolung 3,4,5-isoxazole **127a** was obtained in a moderate yield of 54% with a limited rr of 1.7:1. Screening of other half-sandwiched Ru(II) complexes revealed that **Ru-4** was the most effective catalyst, producing the desired 3,4,5-isoxazole isomer **127a** in rr of 3.6:1 and 76% yield (**Figure 4.10a**). These results indicate that the bulkiness of the Cp* ligand limits the reactivity on the Ru center and a more electron-deficient ligand such as Cp increases the Lewis acidity character of the Ru center and facilitates coordination with the alkyne bond.[48,49]

Liquid additive was essential for enhancing yields and regioselectivity for the desired isoxazole isomer **127a.** Acetone was identified as the optimal liquid additive when used with the **Ru-4** catalyst, resulting in an improve yield of 86% and rr to 6.6:1 (**Figure 4.10b**).

We evaluated the scope of the optimized conditions for diverse ynones and ynols (**Figure 4.11**). Alkyl and aryl ynones **126b-d** demonstrated compatibility with the **Ru-4** complex, forming the 3,4,5-isoxazole **127a-e** in low to excellent yields and with preferential selectivity. Ynols **126f-h** also demonstrate excellent compatibility with **Ru-1**, forming the hydroxyl isoxazoles **128n-q** in good to excellent yields and excellent regioselectivity, and always obtaining the hydroxyl moiety at the C-4 position of the corresponding heterocycle (**Figure 4.11,** see experimental information for control experiments to confirm regioselectivity section PS5b).

However, the proposed conditions exhibited limitations for electron-rich thio-ethers alkynes, which were unreactive towards the Ru(II) optimized system and no isoxazole product **127f** was obtained. This limitation may be due to the poor polarizability of the alkyne.[47] Additionally, tertiary ynols were also not tolerated, and no product was obtained for hydroxyl isoxazole **128r**, with either optimized Ru catalytic system, likely due to the large steric repulsions between the tertiary alcohol and the Cp* or Cp ligand.

Beyond the effectiveness of mechanochemistry to access the diverse library of 3,4 and 3,4,5-isoxazoles by Ru catalysis, we would like to highlight its practicality compared to the solution-based thermal approach. The proposed mechanochemical approached eliminates the need for anhydrous chlorinated solvents, a glove-box, and Schlenk lines. It was found that conducting the mechanochemical reaction under inert conditions did not result in improvements in the reaction yield or regioselectivity. Moreover, the proposed mechanochemical conditions significantly reduce the reaction times to just 60 min, as opposed to the 16 h required by the corresponding solution-based approach.
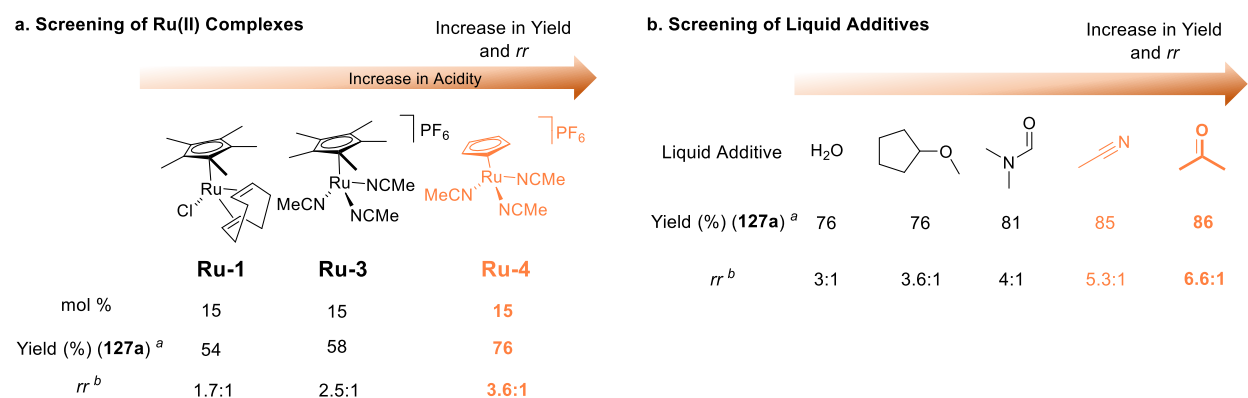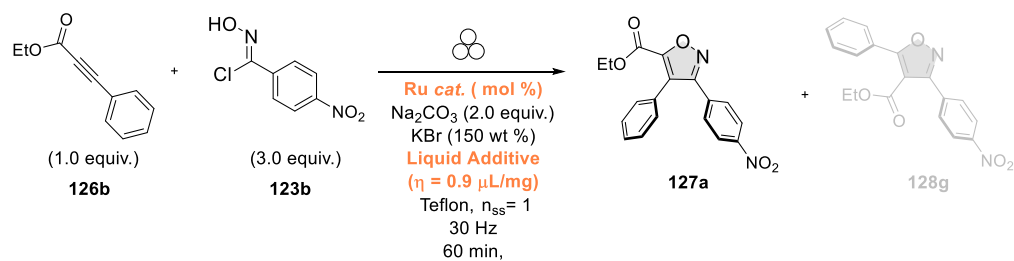
Figure 4.10. Screening of Ru catalysts and Liquid additives for the "umpolung" synthesis of 3,4,5-isoxazoles from Ynones.

Reaction conditions: [a] Yields were determined by ^{1}H NMR and using 1,3,5-trimetoxybenzene as an internal standard. [b] *rr* represents the regio-ratios express as ratio of **127a**:**128g**, which were determined by ^{1}H NMR of the crude product.
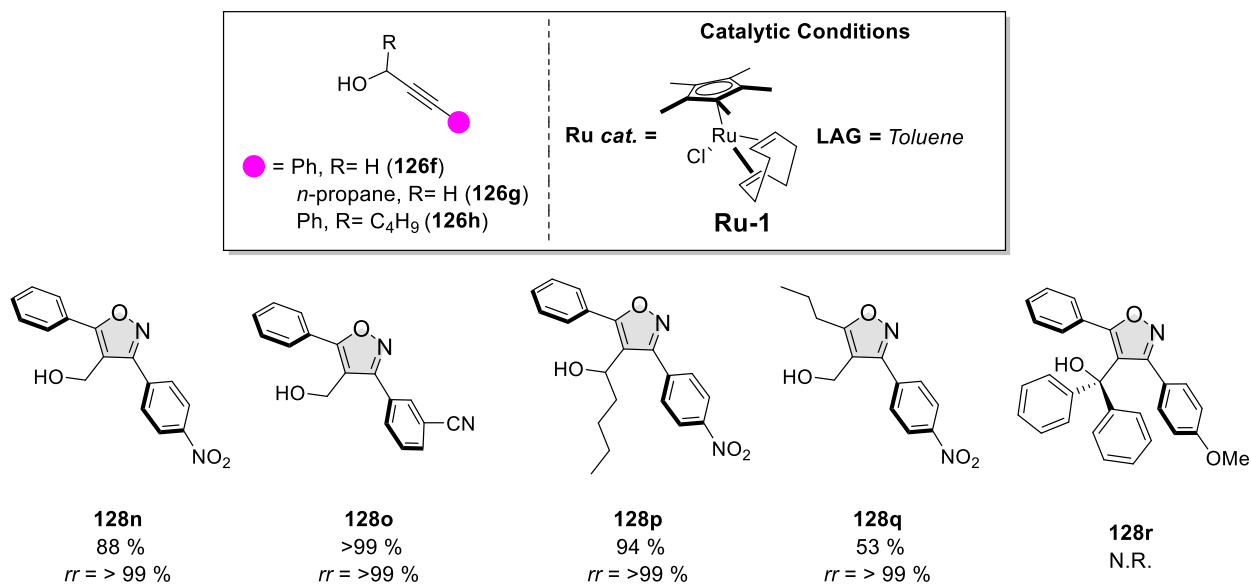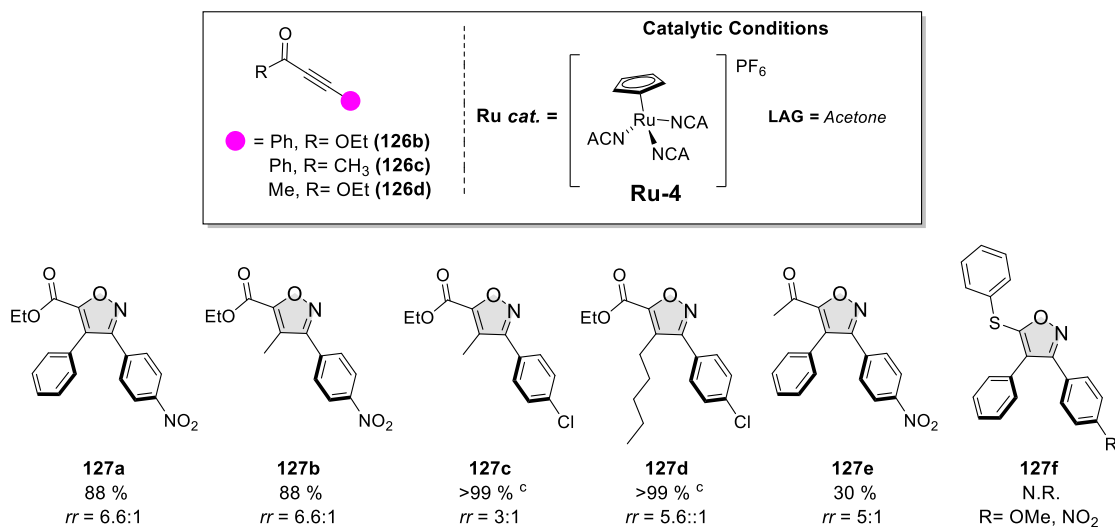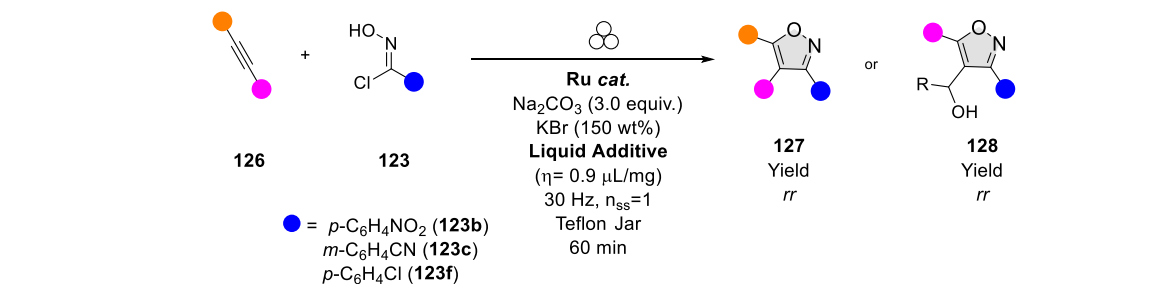
Figure 4.11. Umpolung Synthesis of 3,4,5-Isoxazoles from ynones and ynols.

[a] Yields were determined by ^{1}H NMR and using 1,3,5-trimetoxybenzene as an internal standard. [b] *rr* represents the regio-ratios expressed as a ratio of **127**:**128** or **128**:**127**, which were determined by ^{1}H NMR of the crude product. [c] Compounds were isolated as mixtures of regioisomer.

4.3. Mechanochemical Ru(II)-catalyzed mechanistic investigations

After having established conditions to access 3,4-isoxazoles **125**, and 3,4,5-isoxazoles **128**, we performed mechanistic investigation to gain an understanding on the influence of mechanical stress in the regioisomer outcome. Previous studies have shown that a select few 3,4-isoxazoles can undergo a retro-1,3-dipolar cycloadditions to isomerize into 3,5-isoxazole.[43] Considering the frequency dependence observed under mechanochemical conditions, we investigated a plausible Ru-catalyzed isomerization. However, subjecting 3,5-isoxazole **124b** and 3,4-isoxazole **125b** to the optimized conditions did not result in any isomerization of any of the isoxazole isomers (**Figure 4.12**). These finding suggests that the Ru catalysis and concerted pathways operate independently of each other and are irreversible.
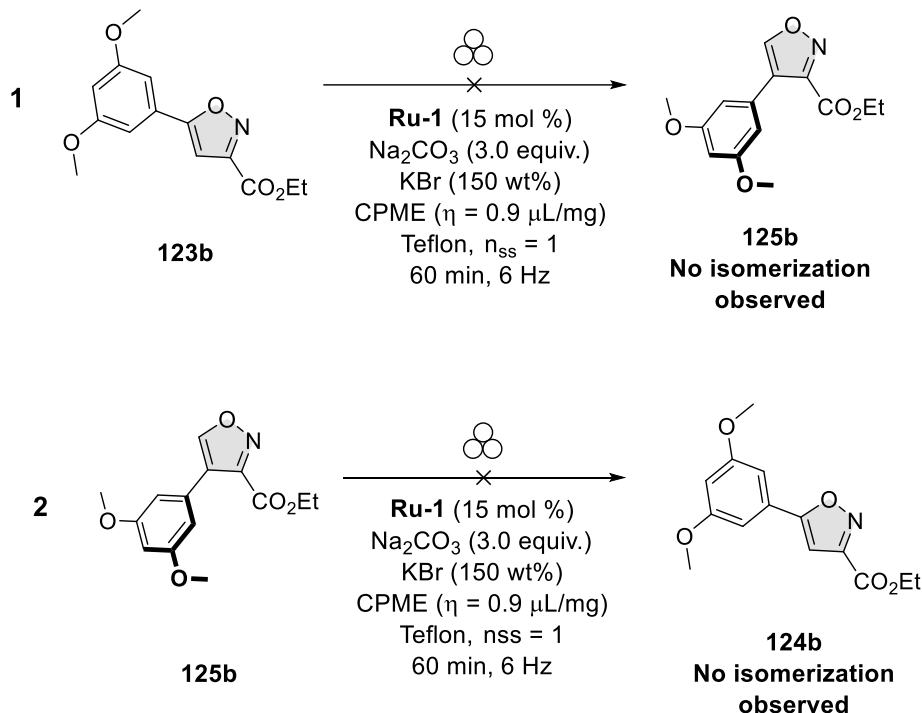
Figure 4.12. Isomerization studies of 3,4-isoxazoles to 3,5-isoxazoles.

Ru(II) complexes demonstrated selectivity toward hydroxyimidoyl chlorides with EWG, **123a**, **123b**, and **123c**. We assessed the selectivity of Ru complexes for hydroxyimidoyl chlorides with EDG or EWG by performing competition reactions with equimolar amounts of EWG and EDG hydroxyimidoyl chlorides with both Ru complexes (**Figure 4.13**). In the case of **Ru-1** (**Figure 4.13a**, reaction 1), terminal alkyne **122b** was reacted with equimolar quantities of hydroxyimidoyl chlorides **123a** EWG and **123d** EDG. The reaction exclusively forms the 3,4-isoxazole ester **125b** with EWG hydroxyimidoyl chloride **123a**, while EDG hydroxyimidoyl chloride **123d** formed the 3,5-isoxazole anisole **13d** exclusively in 35% yield.

In the case of **Ru-4** (**Figure 4.13a**, reaction 2), the internal alkyne **122d** was reacted with equimolar amounts of hydroxyimidoyl chloride **123a** and **123d**. **Ru-4** showed selectivity for the EWG hydroxyimidoyl chloride **123b** forming preferentially the "umpolung" 3,4,5-isoxazole nitro-arene **128b** in 52% yield. On the other hand, hydroxyimidoyl chloride **123d** formed the corresponding "umpolung" 3,4,5-isoxazole anisole **128h** in only 10% yield.

In both cases, the selectivity shown by Ru(II) complexes for electron-deficient hydroxyimidoyl chloride stems from the increase in softness and polarizability of the nitrile carbon (C_1) tuned by the presence of electron-withdrawing groups, facilitating stronger C_1-Ru interactions (**Figure 4.13b**).[109-110]
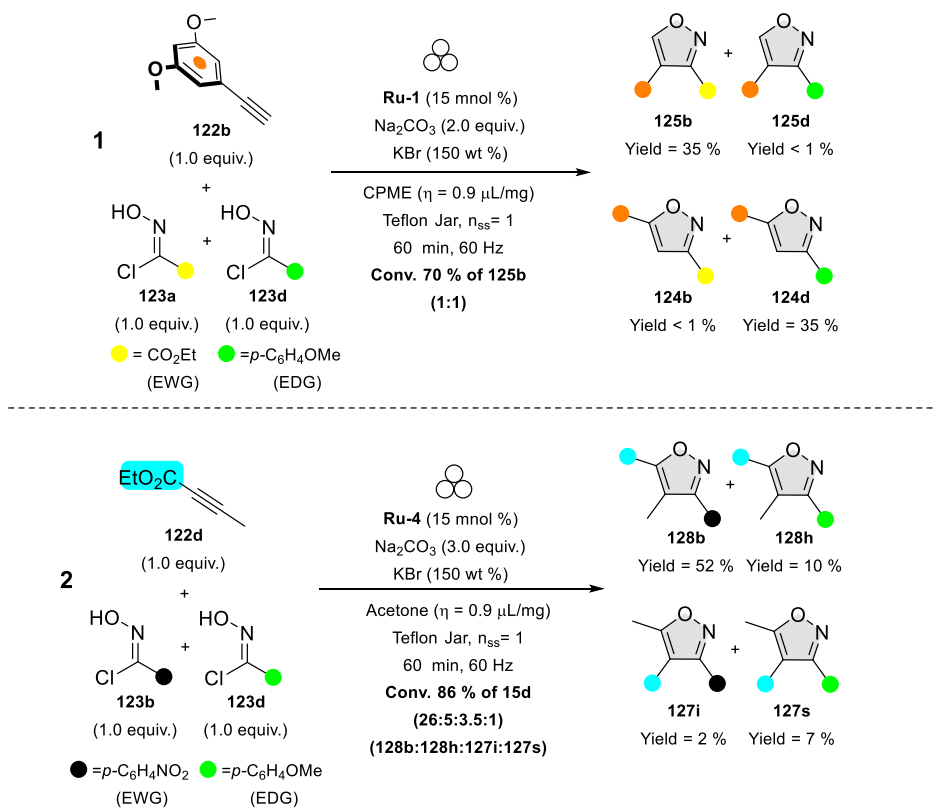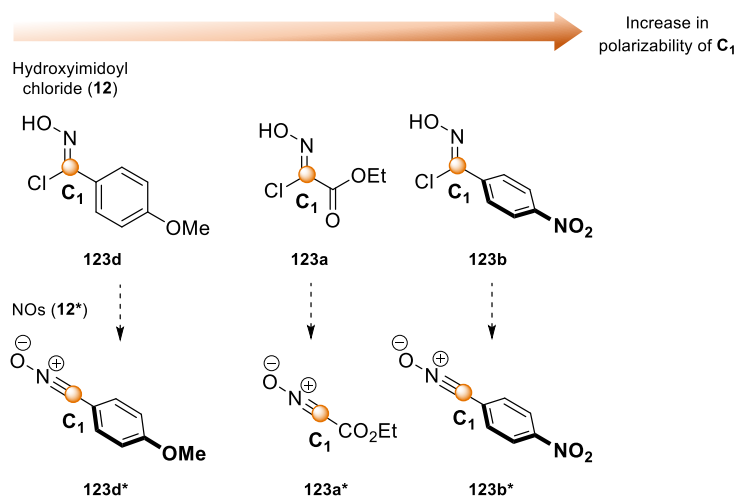
Figure 4.13. Selectivity studies of mechanochemical Ru(II) catalyze reactions for 3,4-isoxazoles and 3,4,5-isoxazoles.

The specificity of **Ru-1** and **Ru-4** for coordinating liquid additives must be considered due to the critical role of LAG in the regioselectivity. We compared the transmission electron microscope (TEM) images of the reaction crude when using polar and coordinating liquid additives like CPME **III** and acetone **IV**, as well as poorly coordinating additives such as 1,2-DCE and toluene (**Figure 4.14a**). TEM revealed the formation of Ru nanoparticles, where the presence of CPME and acetone suppress aggregation of the Ru nanoparticles (**Figure 4.14a III** and **IV**).[62,90,92] In contrast, non-polar and poorly coordinating additives caused the aggregation of the Ru nanoparticles (**Figure 4.14a I** and **V,** see supporting information section PS6 for EDS analysis of the nanoparticles).

The LAG concentration of 0.9 μL/mg was important in reducing the size of the Ru nanoparticles. At such quantities, the **Ru-1** and **Ru-4** nanoparticles were measured to be 172.4 nm and 5.3 nm, respectively. The reduced size of the Ru nanoparticles facilitates the dispersion and increases the catalytic activity of the **Ru-1** and **Ru-4** catalysts (**Figure 4.14b**).[85] This is more noticeable when comparing the selectivity achieved using 1,2-DCE, and CPME liquid additives for **Ru-1**. Where the combination between CPME and **Ru-1** results in excellent selectivity and yield of the 3,4-isoxazole (**Figure 4.6b**).

In the cases of ynols substrates **126f-h**, the use of toluene liquid additive demonstrated to be a more effective in enhancing H-bonding interactions between hydroxyl group and **Ru-1** complex.[111-112] This improvement is evident in the TEM, which showed that the liquid additive caused aggregation of the Ru nanoparticles (**Figure 4.14a-V**).

In addition, powder X-ray diffraction (PXRD) detected no changes in the crystallinity of the **Ru-1** and **Ru-4** catalysts, even in the presence of the liquid additives, confirming that the stabilization effect of the CPME and acetone additives on the Ru nanoparticles occurs *in situ* (see experimental section PS7).

225
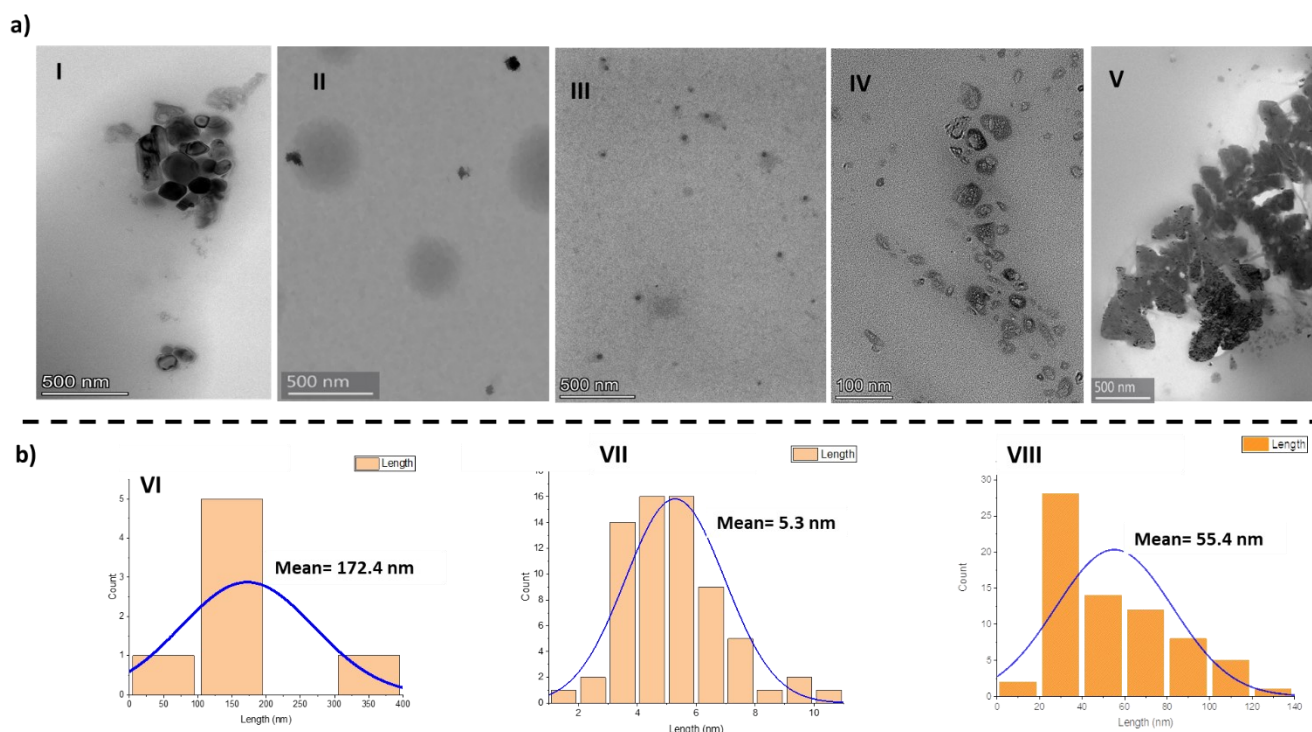
Figure 4.14. Ru-1 and Ru-4 nanoparticles characterization.

a) TEM image conditions: **I)** Ru-1 with 0.5 µL/mg of 1,2-DCE liquid additive, taken at 500 nm of magnification. **II)** Ru-1 with 0.5 µL/mg of CPME liquid additive, taken at 500 nm of magnification. **III)** Ru-1 with 0.9 µL/mg of CPME liquid additive, taken at 500 nm of magnification. **IV)** Ru-4 with 0.9 µL/mg of acetone liquid additive, taken at 100 nm of magnification. **V)** Ru-1 with 0.9 µL/mg of toluene liquid additive, taken at 500 nm of magnification. **b)** Histograms for particle size distribution: **VI)** Histogram for Ru-1 with 0.5 µL/mg of CPME liquid additive. **VII)** Histogram for Ru-1 with 0.9 µL/mg of CPME liquid additive. **VIII)** Histogram for Ru-1 with 0.9 µL/mg of acetone liquid additive.

Based on these experiments, we propose a potential catalytic cycle (**Figure 4.15**). The addition of CPME and acetone as additives is crucial for stabilizing the formation of catalytically active Ru nanoparticles (**Figure 4.15c**). Since COD and acetonitrile are labile spectator ligands [113-114], we proposed that the liquid additive (LAG) displaces the spectator ligands to form the active Ru complexes **IIa** and **IIb** (**Figure 4.15b**). The steric collisions between the LAG and the Cp or Cp* facilitates the ligand exchange with the alkyne substrates **III**. Additionally, the Lewis acidic nature of the cationic **Ru-4** facilitates the coordination with the internal alkynes. In the cases of ynols, the **Ru-1** catalyst positions the hydroxyl groups below the Cp* ligand through H-bonding (**Figure 4.15d**). Considering the selectivity for hydroxyimidoyl chlorides with EWG, the Ru centre binds strongly with the nitrile C_1, reversing the polarity of the nitrile oxide (**Figure 4.13**). From intermediate **III**, oxidative coupling forms the six-membered ruthenacycle **IV.** The desired 3,4-isoxazoles and 3,4,5-isoxazoles are formed by reductive elimination of **V** and ligand exchange to reform the catalytically active Ru complex.
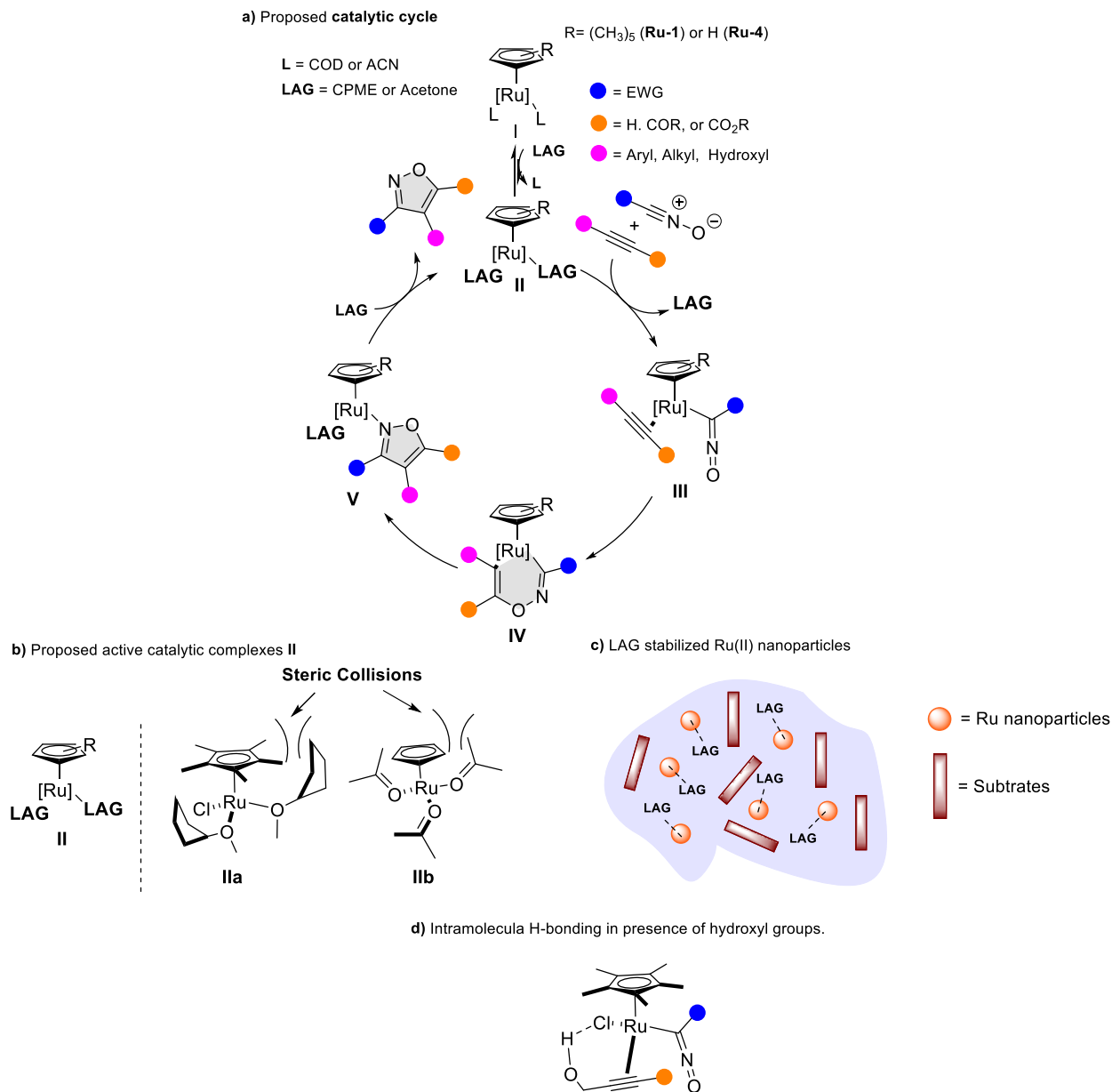
Figure 4.15. Proposed catalytic cycle under mechanochemical conditions.

4.4. Conclusions

In conclusion, we have demonstrated for the first-time the impact of mechanochemistry in controlling regioselectivity in regiodivergent cycloadditions, and particularly in the synthesis of 3,4-isoxazole and 3,4,5-isoxazoles by a Ru catalyze 1,3-dipolar cycloaddition. The mechanochemical Ru catalytic conditions prove to be highly effective in achieving excellent regioselectivity and yields for both terminal and internal alkynes and demonstrating significant benefits in operational simplicity.

Moreover, the mechanochemical Ru catalysis exhibits complementarity with previously reported Cu(II) mediated mechanochemical protocols, effectively expanding the existing chemical space. Considering the

high demand and importance for substituted isoxazoles in medicinal chemistry and natural product synthesis, this methodology will have an impact on the synthesis of APIs.

4.5. Acknowledgements

4.6.References

[1]. Ylijoki, K. E. O.; Stryker, J. M. *Chem. Rev.* **2013**, *113*, 2244–2266.

[2]. Eschenbrenner-Lux, V.; Kumar, K.; Waldmann, H. *Angew. Chemie - Int. Ed.* **2014**, *53,* 11146–11157.

[3]. Nicolaou, K. C.; Snyder, S. A.; Montagnon, T.; Vassilikogiannakis, G. *Angew. Chemie - Int. Ed.* **2002**, *41*, 1668–1698.

[4]. Kahlert, L.; Bassiony, E. F.; Cox, R. J.; Skellam, E. J. *Angew. Chemie - Int. Ed.* **2020**, *59,* 5816–5822.

[5]. Takao, K. I.; Munakata, R.; Tadano, K. I. *Chem. Rev.* **2005**, *105*, 4779–4807**.**

[6]. Cao, M. H.; Green, N. J.; Xu, S. Z. *Org. Biomol. Chem.* **2017**, *15*, 3105–3129.

[7]. Funel, J. A.; Abele, S. *Angew. Chemie - Int. Ed.* **2013**, *52*, 3822–3863.

[8]. Gothelf, K. V; Jørgensen, K. A. *Chem. Rev.* **1998**, *98*, 863–910.

[9]. Narayan, R.; Potowski, M.; Jia, Z. J.; Antonchick, A. P.; Waldmann, H. *Acc. Chem. Res.* **2014**, *47*, 1296–1310.

[10]. Breugst, M.; Reissig, H. U. *Angew. Chemie - Int. Ed.* **2020**, *59*, 12293–12307.

[11]. Pineiro, M.; Pinho E Melo, T. M. V. D. *European J. Org. Chem.* **2009**, No. 31, 5287–5307.

[12]. Mulzer, J. *Org. Synth. Set* **2008**, No. 2, 77–95.

[13]. Hashimoto, T.; Maruoka, K. *Chem. Rev.* **2015**, *115*, 5366–5412.

[14]. Ma, S.; Mandalapu, D.; Wang, S.; Zhang, Q. *Nat. Prod. Rep.* **2021**, *39*, 926–945.

[15]. Zhu, Z. Bin; Wei, Y.; Shi, M. *Chem. Soc. Rev.* **2011**, *40*, 5534–5563.

[16]. Lautens, M.; Klute, W.; Tam, W. *Chem. Rev.* **1996**, *96*, 49–92.

[17]. Reissig, H. U.; Zimmer, R. *Chem. Rev.* **2003**, *103*, 1151–1196.

[18]. Ebner, C.; Carreira, E. M. *Chem. Rev.* **2017**, *117*, 11651–11679.

[19]. Meijer, F. A.; Doveston, R. G.; De Vries, R. M. J. M.; Vos, G. M.; Vos, A. A. A.; Leysen, S.; Scheepstra, M.; Ottmann, C.; Milroy, L. G.; Brunsveld, L. *J. Med. Chem.* **2020**, *63*, 241–259.

[20]. Wzorek, J. S.; Knöpfel, T. F.; Sapountzis, I.; Evans, D. A. *Org. Lett.* **2012**, *14*, 5840–5843.

[21]. Nicolaou, K. C.; Hale, C. R. H.; Nilewski, C.; Ioannidou, H. A.; Elmarrouni, A.; Nilewski, L. G.; Beabout, K.; Wang, T. T.; Shamoo, Y. *J. Am. Chem. Soc.* **2014**, *136*, 12137–12160.

[22]. Baraldi, P. G.; Barco, A.; Benetti, S.; Pollini, G. P.; Simoni, D. *Synthesis.* **1987**, *10*, 857–869.

[23]. Baranczak, A.; Sulikowski, G. A. *Org. Lett.* **2012**, *14*, 1027–1029.

[24]. Pairas, G. N.; Perperopoulou, F.; Tsoungas, P. G.; Varvounis, G. *ChemMedChem* **2017**, *12*, 408–419.

[25]. Zhu, J.; Mo, J.; Lin, H. zhi; Chen, Y.; Sun, H. peng. *Bioorganic Med. Chem.* **2018**, *26*, 3065–3075.

[26]. Kim, M.; Hwang, Y. S.; Cho, W.; Park, S. B. *ACS Comb. Sci.* **2017**, *19*, 407–413.

[27].   Sysak, A.; Obmińska-Mrukowicz, B. *Eur. J. Med. Chem.* **2017**, *137*, 292–309.

[28].   Talley, J.; Brown, D. L.; Nagarajan, S.; Carter, J. S.; Weier, R. M.; Stealey, M. A.; Collins, P. W.; Rogers., R. S.; Seibert, K. SUBSTITUTED ISOXAZOLES FOR THE TREATMENT OF INFLAMMATION, 1997 (US patent).

[29].   Himo, F.; Lovell, T.; Hilgraf, R.; Rostovtsev, V. V.; Noodleman, L.; Sharpless, K. B.; Fokin, V. V. *J. Am. Chem. Soc.* **2005**, *127*, 210–216.

[30].   Houk, K. N.; Sims, J.; Watts, C. R.; Luskus, L. J. *J. Am. Chem. Soc.* **1973**, *95*, 7301–7315.

[31].   Clayden, J.; Greeves, N.; Warren, S. *Org. Chem. Front.* **2012**, *58*, 1261.

[32].   Van Mersbergen, D.; Wijnen, J. W.; Engberts, J. B. F. N. *J. Org. Chem.* **1998**, *63*, 8801–8805.

[33].   Ess, D. H.; Houk, K. N. *J. Am. Chem. Soc.* **2007**, *129*, 10646–10647.

[34].   Ess, D. H.; Houk, K. N. *J. Am. Chem. Soc.* **2008**, *130*, 10187–10198.

[35].   Toma, L.; Quadrelli, P.; Perrini, G.; Gandolfi, R.; Di Valentin, C.; Corsaro, A.; Caramella, P. *Tetrahedron* **2000**, *56*, 4299–4309.

[36].   Domingo, L. R.; Chamorro, E.; Pérez, P. *European J. Org. Chem.* **2009**, No. 18, 3036–3044.

[37].   Rahman, P.; Glanzer, A.; Singh, J.; Wachter, N. M.; Rhoad, J.; Denton, R. W. *World J. Org. Chem.* **2017**, *5*, 6–10.

[38].   Hu, Y.; Houk, K. N. *Tetrahedron* **2000**, *56*, 8239–8243.

[39].   Cossío, F. P.; Morao, I.; Jiao, H.; Von Ragué Schleyer, P. *J. Am. Chem. Soc.* **1999**, *121*, 6737–6746.

[40].   Johansson, J. R.; Beke-Somfai, T.; Said Stålsmeden, A.; Kann, N. *Chem. Rev.* **2016**, *116*, 14726–14768.

[41].   Boren, B. C.; Narayan, S.; Rasmussen, L. K.; Zhang, L.; Zhao, H.; Lin, Z.; Jia, G.; Fokin, V. V. *J. Am. Chem. Soc.* **2008**, *130*, 8923–8930.

[42].   Huisgen, R. *Angew. Chemie Int. Ed. English* **1963**, *2*, 633–645.

[43].   Kaiser, T. M.; Huang, J.; Yang, J. *J. Org. Chem.* **2013**, *78*, 10572.

[44].   Grecian, S.; Fokin, V. V. *Angew. Chemie - Int. Ed.* **2008**, *47*, 8285–8287.

[45].   Oakdale, J. S.; Sit, R. K.; Fokin, V. V. *Chem. - A Eur. J.* **2014**, *20*, 11101–11110.

[46].   Boren, B. C.; Narayan, S.; Rasmussen, L. K.; Zhang, L.; Zhao, H.; Lin, Z.; Jia, G.; Fokin, V. V. *J. Am. Chem. Soc.* **2008**, *130*, 8923–8930.

[47].   Feng, Q.; Huang, H.; Sun, J. *Org. Lett.* **2021**, *23*, 2431–2436.

[48].   Trost, B. M.; Papillon, J. P. N.; Nussbaumer, T. *J. Am. Chem. Soc.* **2005**, *127*, 17921–17937.

[49].   Hitt, D. M.; Holland, R. L.; Baldridge, K. K.; Cope, S. K.; O'Connor, J. M. *Organometallics* **2017**, *36*, 4256–4267.

[50].   Boldyreva, E. *Chem. Soc. Rev.* **2013**, *42*, 7719–7738.

[51].   Mateti, S.; Mathesh, M.; Liu, Z.; Tao, T.; Ramireddy, T.; Glushenkov, A. M.; Yang, W.; Chen, Y. I. *Chem. Commun.* **2021**, *57*, 1080–1092.

[52].   Hwang, S.; Grätz, S.; Borchardt, L. *Chem. Commun.* **2022**, *58*, 1661–1671.

[53].   Friščić, T.; Mottillo, C.; Titi, H. M. *Angew. Chemie - Int. Ed.* **2020**, *59*, 1018–1029.

[54].   Wohlgemuth, M.; Mayer, M.; Rappen, M.; Schmidt, F.; Saure, R.; Grätz, S.; Borchardt, L. *Angew. Chemie - Int. Ed.* **2022**, No. 61, e202212694.

[55].   Pickhardt, W.; Grätz, S.; Borchardt, L. *Chem. - A Eur. J.* **2020**, *26*, 12903–12911.

[56].   Vogt, C. G.; Oltermann, M.; Pickhardt, W.; Grätz, S.; Borchardt, L. *Adv. Energy Sustain. Res.* **2021**, *2*, 2100011.

[57].   Boyde, N. C.; Rightmire, N. R.; Bierschenk, E. J.; Steelman, G. W.; Hanusa, T. P.; Brennessel, W. W. *Dalt. Trans.* **2016**, *45*, 18635–18642.

[58].   Seo, T.; Kubota, K.; Ito, H. *J. Am. Chem. Soc.* **2020**, *142*, 9884–9889.

[59].   Toda, F. *Organic Solid-State Reactions*, 1st ed.; Toda, F., Ed.; Springer Netherlands: Dordrecht, 2002.

[60].   Andersen, J.; Mack, J. *Green Chem.* **2018**, *20*, 1435–1443.

[61].   James, S. L.; Adams, C. J.; Bolm, C.; Braga, D.; Collier, P.; Friščic, T.; Grepioni, F.; Harris, K. D. M.; Hyett, G.; Jones, W.; Krebs, A.; Mack, J.; Maini, L.; Orpen, A. G.; Parkin, I. P.; Shearouse, W. C.; Steed, J. W.; Waddell, D. C. *Chem. Soc. Rev.* **2012**, *41*, 413–447.

[62].   Seo, T.; Ishiyama, T.; Kubota, K.; Ito, H. *Chem. Sci.* **2019**, *10*, 8202–8210.

[63].   Bartalucci, E.; Schumacher, C.; Hendrickx, L.; Puccetti, F.; d'Anciães Almeida Silva, I.; Dervişoğlu, R.; Puttreddy, R.; Bolm, C.; Wiegand, T. *Chem. – A Eur. J.* **2023**, *29*, e202203466.

[64].   Hernandez R., R. A.; Burchell-Reyes, K.; Braga, A. P. C. A.; Lopez, J. K.; Forgione, P. *RSC Adv.* **2022**, *12*, 6396–6402.

[65].   Hernandez, R. A.; Trakakis, I.; Do, J.; Cuccia, L. A.; Friščić, T.; Forgione, P. *European J. Org. Chem.* **2023**, *26,*. e2023003

[66].   Hutchings, B. P.; Crawford, D. E.; Gao, L.; Hu, P.; James, S. L. Angew. Chemie - Int. Ed. **2017**, *56*, 15252–15256.

[67].   Shi, Y. X.; Xu, K.; Clegg, J. K.; Ganguly, R.; Hirao, H.; Friščić, T.; García, F. Angew. Chemie **2016**, *128*, 12928–12932.

[68].   Belenguer, A. M.; Friščić, T.; Day, G. M.; Sanders, J. K. M. Chem. Sci. **2011**, *2*, 696–700.

[69].   Howard, J. L.; Brand, M. C.; Browne, D. L. Angew. Chemie - Int. Ed. **2018**, *57*, 16104–16108.

[70].   Hernández, J. G.; Bolm, C. *J. Org. Chem.* **2017**, *82*, 4007–4019.

[71].   Yu, J.; Peng, G.; Jiang, Z.; Hong, Z.; Su, W. *European J. Org. Chem.* **2016**, No. 32, 5340–5344.

[72].   Yadav, C. S.; Suhasini, R.; Thiagarajan, V.; Velmurugan, D.; Kannadasan, S. *ChemistrySelect* **2018**, *3*, 12576–12581. **c)** Wang, C.; Yue, C.; Smith, A.; Mack, J. *J. Organomet. Chem.* **2022**, *976*, 122430.

[73]. Do, J. L.; Mottillo, C.; Tan, D.; Štrukil, V.; Friščić, T. *J. Am. Chem. Soc.* **2015**, *137*, 2476–2479.

[74]. Li, Z.; Jiang, Z.; Su, W. *Green Chem.* **2015**, *17*, 2330–2334.

[75]. Yu, J.; Hong, Z.; Yang, X.; Jiang, Y.; Jiang, Z.; Su, W. *Beilstein J. Org. Chem.* **2018**, *14*, 786–795.

[76]. Abdulagatov, I. M.; Abdulagatova, Z. Z.; Kallaev, S. N.; Bakmaev, A. G.; Ranjith, P. G. *Int. J. Thermophys.* **2015**, *36*, 658–691.

[77]. Parker, W. J.; Jenkins, R. J.; Butler, C. P.; Abbott, G. L. *J. Appl. Phys.* **1961**, *32*, 1679–1684.

[78]. Mottaghy, D.; Vosteen, H. D.; Schellschmidt, R. *Int. J. Earth Sci.* **2008**, *97*, 435–442.

[79]. McKissic, K. S.; Caruso, J. T.; Blair, R. G.; Mack, J. *Green Chem.* **2014**, *16*, 1628–1632.

[80]. Andersen, J. M.; Mack, J. *Chem. Sci.* **2017**, *8*, 5447–5453.

[81]. Gonnet, L.; Chamayou, A.; André-Barrès, C.; Micheau, J. C.; Guidetti, B.; Sato, T.; Baron, M.; Baltas, M.; Calvet, R. *ACS Sustain. Chem. Eng.* **2021**, *9*, 4453–4462.

[82]. Howard, J. L.; Brand, M. C.; Browne, D. L. *Angew. Chemie - Int. Ed.* **2018**, *57*, 16104–16108.

[83]. Andersen, J.; Brunemann, J.; Mack, J. *React. Chem. Eng.* **2019**, *4*, 1229–1236.

[84]. Zhang, Z.; Peng, Z. W.; Hao, M. F.; Gao, J. G. *Synlett* **2010**, *19*, 2895–2898.

[85]. Rak, M. J.; Saadé, N. K.; Friščić, T.; Moores, A. *Green Chem.* **2014**, *16*, 86–89.

[86]. Declerck, V.; Colacino, E.; Bantreil, X.; Martinez, J.; Lamaty, F. *Chem. Commun.* **2012**, *48*, 11778–11780.

[87]. Baláž, M.; Kudličková, Z.; Vilková, M.; Imrich, J.; Balážová, Ľ.; Daneu, N. *Molecules* **2019**, *24*, 3347.

[88]. Tan, D.; Loots, L.; Friščić, T. *Chem. Commun.* **2016**, *52*, 7760–7781.

[89]. Kubota, K.; Seo, T.; Ito, H. *Faraday Discuss.* **2022**, *241*, 104–113.

[90]. Kubota, K.; Seo, T.; Koide, K.; Hasegawa, Y.; Ito, H. *Nat. Commun.* **2019**, *10*, 1–11.

[91]. Sarmah, K. K.; Rajbongshi, T.; Bhuyan, A.; Thakuria, R. *Chem. Commun.* **2019**, *55*, 10900–10903.

[92]. Konnert, L.; Dimassi, M.; Gonnet, L.; Lamaty, F.; Martinez, J.; Colacino, E. *RSC Adv.* **2016**, *6*, 36978–36986.

[93]. Friščić, T.; Fábián, L.; Burley, J. C.; Jones, W.; Motherwell, W. D. S. *Chem. Commun.* **2006**, *48*, 5009–5011.

[94]. Brede, F. A.; Mühlbach, F.; Sextl, G.; Müller-Buschbaum, K. *Dalt. Trans.* **2016**, *45*, 10609–10619.

[95]. Mukherjee, A.; Rogers, R. D.; Myerson, A. S. *CrystEngComm* **2018**, *20*, 3817–3821.

[96]. Hasa, D.; Schneider, G.; Voinovich, D.; Jones, W. *Angew. Chemie - Int. Ed.* **2015**, *54*, 7371–7375.

[97]. Friščić, T.; Reid, D. G.; Halasz, I.; Stein, R. S.; Dinnebier, R. E.; Duer, M. J. *Angew. Chemie - Int. Ed.* **2010**, *49*, 712–715.

[98]. Yu, J.; Ying, P.; Wang, H.; Xiang, K.; Su, W. *Adv. Synth. Catal.* **2020**, *362*, 893–902.

[99].   Ying, P.; Yu, J.; Su, W. *Adv. Synth. Catal.* **2021**, *363*, 1246–1271.

[100].   Terban, M. W.; Madhau, L.; Cruz-Cabeza, A. J.; Okeyo, P. O.; Etter, M.; Schulz, A.; Rantanen, J.; Dinnebier, R. E.; Billinge, S. J. L.; Moneghini, M.; Hasa, D. *CrystEngComm* **2022**, *24*, 2306–2313.

[101].   Howard, J. L.; Brand, M. C.; Browne, D. L. **2018**, 16104–16108.

[102].   Watanabe, K. *Molecules* **2013**, *18*, 3183–3194.

[103].   Xu, H.; Fan, G. P.; Liu, Z.; Wang, G. W. *Tetrahedron* **2018**, *74*, 6607–6611.

[104].   Fang, R. K.; Yin, Z. C.; Chen, J. S.; Wang, G. W. *Green Chem. Lett. Rev.* **2022**, *15*, 519–528.

[105].   Thorwirth, R.; Stolle, A.; Ondruschka, B.; Wild, A.; Schubert, U. S. *Chem. Commun.* **2011**, *47*, 4370–4372.

[106].   Vadivelu, M.; Raheem, A. A.; Raj, J. P.; Elangovan, J.; Karthikeyan, K.; Praveen, C. *Org. Lett.* **2022**, *24*, 2798–2803.

[107].   Kuram, M. R.; Bhanuchandra, M.; Sahoo, A. K. *J. Org. Chem.* **2010**, *75*, 2247–2258.

[108].   Mizushima, E.; Sato, K.; Hayashi, T.; Tanaka, M. *Angew. Chem.* **2002**, *114*, 4745–4747.

[109].   Occhipinti, G.; Jensen, V. R. *Organometallics* **2011**, *30*, 3522–3529.

[110].   Nasrallah, D. J.; Zehnder, T. E.; Ludwig, J. R.; Steigerwald, D. C.; Kiernicki, J. J.; Szymczak, N. K.; Schindler, C. S. *Angew. Chemie - Int. Ed.* **2022**, *61*, 1–7.

[111].   Meredith, N. Y.; Borsley, S.; Smolyar, I. V.; Nichol, G. S.; Baker, C. M.; Ling, K. B.; Cockroft, S. L. *Angew. Chemie Int. Ed.* **2022**, *61*.

[112].   Meng, X.; Song, L.; Zhao, J.; Han, H.; Zheng, D. *J. Phys. Org. Chem.* **2022**, *35*, 1–10.

[113].   Vovard-Le Bray, C.; Dérien, S.; Dixneuf, P. H. *Comptes Rendus Chim.* **2010**, *13*, 292–303.

[114].   Luo, L.; Zhu, N.; Zhue, N.-J.; Steven, E. D.; Nolan, S. P. *Organometallics* **1994**, *13*, 669–675.

4.7. Experimental Section for Chapter 4:

4.7.1. General Considerations, Materials, and Instrumentations

General Considerations: Solids were directly weighed in the open-air atmosphere and added into the reaction vial. Liquids were directly transferred from the vial containing the reagent using an automatic pipette with a plastic tip of appropriate size or a plastic syringe with a stainless-steel needle. Flash chromatography was carried out using 40-63μm silica gel (Silicycle).

Materials: Distilled water was obtained from an in-house water distillery. All other reagents and chemicals were purchased from Sigma-Aldrich, AK Scientific, or Combie-Blocks and used without further purification.

Instrumentation: ^{1}H (500MHz) and ^{13}C (125MHz) NMR spectra were recorded in CDCl$_3$ or d^6-DMSO using a Varian Inova 500 MHz spectrometer. Spectra were referenced to the residual solvent signal or the TMS signal. Spectral features are tabulated in the following order (Note: Spectral features are reported in the following format): chemical shift (δ, ppm); multiplicity (s-singlet, d-doublet, t-triplet, q-quartet, dd-doublet of doublets, m-multiplet), dt-double of triplets, ddd-doublet of doublets of doublets; coupling constants (J, Hz); number of protons. High resolution mass spectra (HRMS) were obtained using a LTQ Orbitrap Velos ETD (positive and negative mode) mass spectrometer. The reactions were performed using a Fritsch Planetary Micro Mill model ''Pulverisette 7''. TEM (Transition Electron Microscope) images were taken at McGill University using in a Thermo Scientific Talos F200X G2, samples were directly mounted in a copper grid. PXRD (Powder X-Ray Diffraction) pattern was taken in a Rigaku MiniFlex 6G.

Jars: For this experiment, it was used jars of different materials:

1) Stainless-steel (SS) Jars of 25 mL capacity containing eight stainless-steel (SS) balls each of 1 cm diameter and sealed by a stainless-steel (SS) lid fitted with a Teflon gasket.
2) Teflon Reaction Vessel of 25 mL capacity from Alpha Nanotech Inc. was adapted to perform mechanochemical reactions. The jars are commercially available and can be bought from Amazon Canada.

Abbreviations: Hexanes (Hex), Ethyl Acetate (EtOAc), Dichloromethane (DCM), 1,3,5-trimethoxybenzene (TMB), Dimethylsulfoxide (DMSO), Stainless Steel (SS), Melting point (MP), Ratio to front (R$_f$).
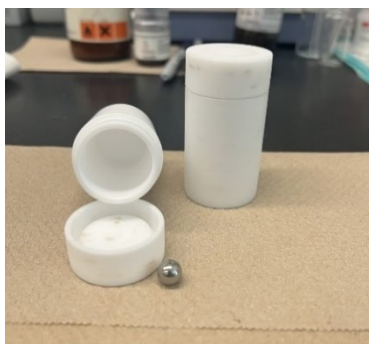
Figure S4.1. Teflon Jars of 25 mL capacity used in this protocol.

Figure S4.2. Planetary Ball Mill with adapted Teflon Jar.

4.7.2. Procedure S1 (PS1): Optimization results for Ru(II) catalyzed synthesis of 3,4-isoxazoles from terminal alkynes and hydroxyimidoyl chlorides

Note: Prior to every reaction demonstrated in this section, the Teflon Jars were carefully washed with aqua regia, to remove leftovers of Ru(II) complex and avoid potential memory effects.

In this section, it is presented the optimizations performed for the stoichiometry of alkyne and hydroxyimidoyl chloride, the effect of the base, and the effect of milling time in the yield and regioselectivity of the reaction to obtain 3,4-isoxazoles **125b**. All reported yields are ^{1}H-NMR yields obtained from the spectrum of the crude product.

Table S4.1. *Effect of Stoichiometry in reaction yield and selectivity.*

122b equiv.	123a equiv.	125b:124b	125b Yield (%)	124b Yield (%)
1.0	3.0	34:1	68	2
1.0	1.5	22:1	68	4
1.0	1.0	15:1	60	4
2.0	1.0	9:1	70	8

Table S4.2. *Effect of Base in reaction yield and regioselectivity.*

Base	equiv.	125b:124b	125b Yield (%)	124b Yield (%)
Na$_2$CO$_3$	2.0	34:1	68	2
Na$_2$CO$_3$	1.0	43:1	43	1
Na$_2$CO$_3$	3.0	20:1	60	3
K$_2$CO$_3$	2.0	6:1	60	10
Cs$_2$CO$_3$	2.0	1:5.7	6	34

Table S4.3. *Effect of milling time in reaction yield and regioselectivity.*

Time (min)	125b:124b	125b Yield (%)	124b Yield (%)
15	33:1	61	2
30	30:1	60	2
60	34:1	68	2
120	30:1	60	2

4.7.3. Procedure S2 (PS2): Synthesis and isolation of 3,4-isoxazoles.

Note: Prior to every reaction demonstrated in this section, the Teflon Jars were carefully washed with aqua regia, to remove leftovers of Ru(II) complex and avoid potential memory effects.
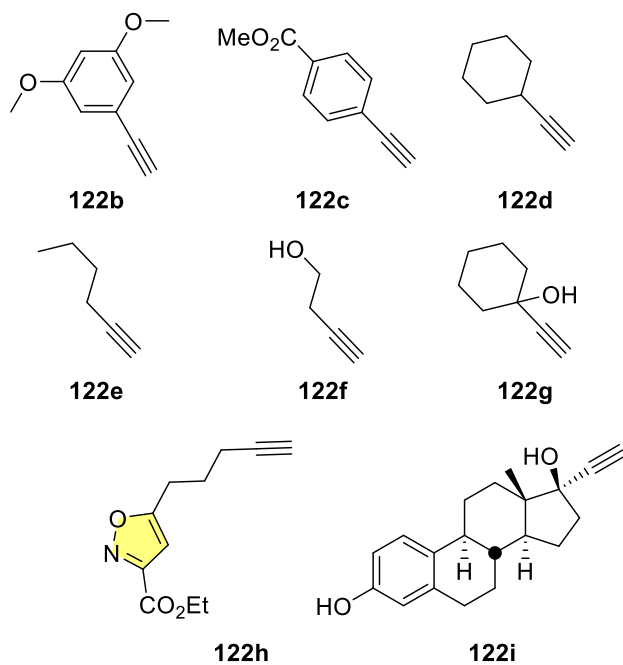
Figure S4.3. Terminal alkynes used for the synthesis of 3,4-isoxazoles.
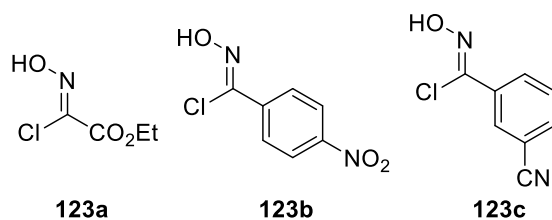
Figure S4.4. Hydroxyimidoyl chlorides used for the synthesis of 3,4-isoxazoles.

Terminal alkyne **122h** was synthesized according to the procedure reported in the literature.[10]

All hydroxyimidoyl chlorides were synthesized according the the reported procedure by Himo, F. *et al.*[11]

---

[10] R. A. Hernandez, I. Trakakis, J. Do, L. A. Cuccia, T. Friščić, P. Forgione, *European J. Org. Chem.* **2023**, *19*, DOI 10.1002/ejoc.202300374.

[11] F. Himo, T. Lovell, R. Hilgraf, V. V. Rostovtsev, L. Noodleman, K. B. Sharpless, V. V. Fokin, *J. Am. Chem. Soc.* **2005**, *127*, 210–216.

Example procedure:
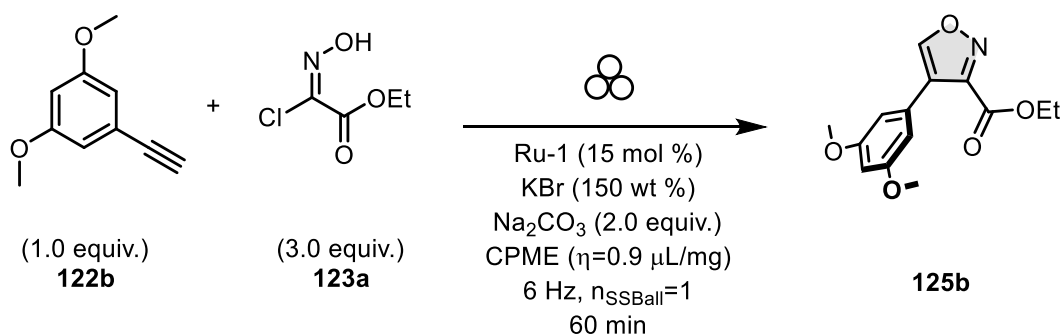
Synthesis of ethyl 4-(3,5-dimethoxyphenyl)isoxazole-3-carboxylate (125b): In a clear and dry Teflon Jar of 25 mL capacity and 1 SS ball of 1 cm diameter, it was directly weight **122b** (1.0 equiv., 0.308 mmol, 50 mg), hydroxyimidoyl chloride **123a** (3.0 equiv., 0.924 mmol, 140 mg), Na_2CO_3 (2.0 equiv., 0.612 mmol, 65 mg), KBr (150 wt%, 409 mg), CPME (η= 0.9 μL/mg, 612 μL), and **Ru-1** catalyst (15 mol %, 0.0467 mmol, 18 mg). The mixture was closed with the Teflon lit and recovered with parafilm. Then the reagents were milled for 60 minutes at 6 Hz. After 60 minutes, the jar was opened, and the mixture was passed over an activated charcoal and silica plug, using diethyl ether as eluent. The desired isoxazole **125b** was isolated by silica gel column chromatography using 8:2 Hex: EtOAc mixture as a white solid in 70 % yield (60 mg). R_f= 0.34, **^{1}H NMR** (500 MHz, CDCl$_3$) δ 8.56 (s, 1H), 6.60 (d, J = 2.3 Hz, 2H), 6.49 (t, J = 2.3 Hz, 1H), 4.41 (q, J = 7.1 Hz, 2H), 3.81 (s, 6H), 1.36 (t, J = 7.1 Hz, 3H). **^{13}C NMR** (125 MHz, CDCl$_3$) δ 160.7, 160.1, 157.3, 153.2, 129.0, 122.0, 107.4, 100.5, 62.3, 55.4, 14.0. **HRMS** Calculated for $C_{14}H_{15}NO_5$ [M+H] 278.1023, found 278.1023.
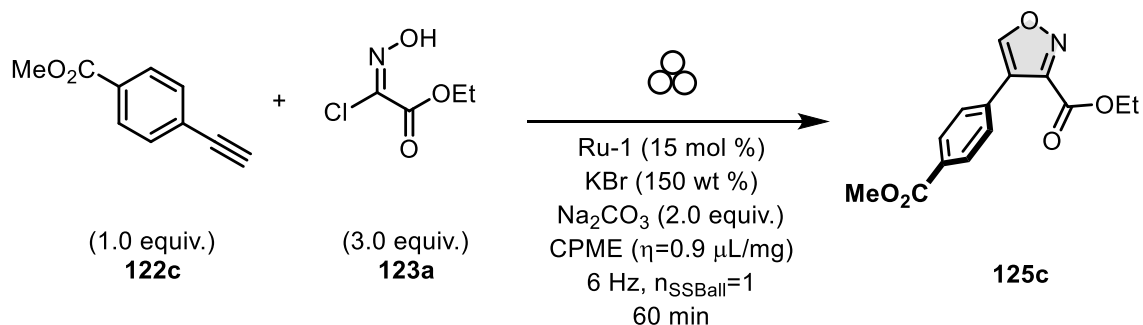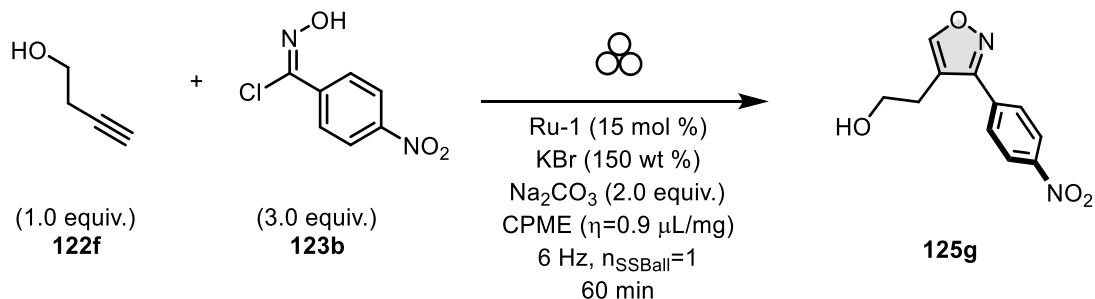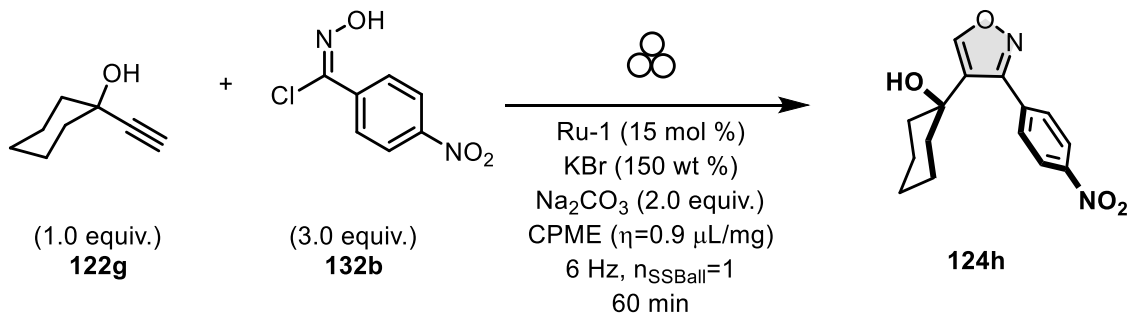
Synthesis of ethyl 4-(4-(methoxycarbonyl)phenyl)isoxazole-3-carboxylate (125c): 3,4-isoxazole **125c** was obtained following procedure PS2. **125c** was isolated by silica gel column chromatography using 9:1 Hex: EtOAc mixture as a white solid in 81 % yield (70 mg). R_f = 0.22, **^{1}H NMR** (500 MHz, CDCl$_3$) δ 8.62 (s, 1H), 8.08 (d, J = 8.4 Hz, 2H), 7.53 (d, J = 8.4 Hz, 2H), 4.41 (q, J = 7.1 Hz, 2H), 3.94 (s, 3H), 1.35 (t, J = 7.1 Hz, 3H). **^{13}C NMR** (125 MHz, CDCl$_3$) δ 166.5, 159.9, 157.7, 152.9, 131.9, 130.2, 129.7, 129.1, 121.4, 62.4, 52.3, 13.9. **HRMS** Calculated for C$_{14}$H$_{13}$NO$_5$ [M+H] 276.0866 found 276.0868.
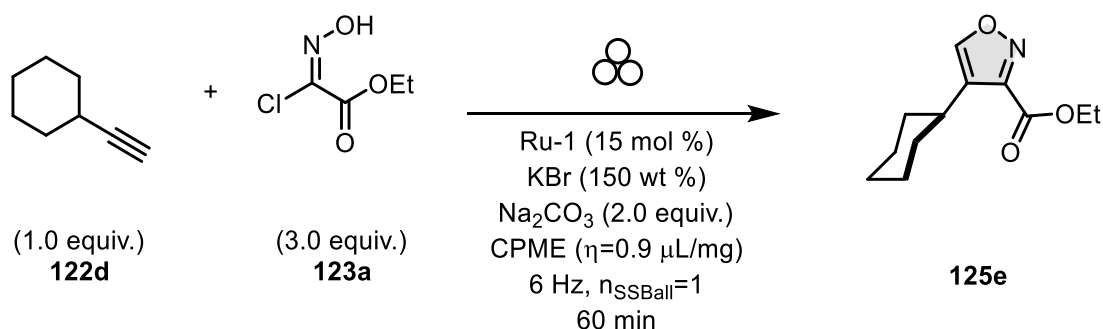
Synthesis of ethyl 4-cyclohexylisoxazole-3-carboxylate (125e): 3,4-isoxazole **125e** was obtained following procedure PS2. **125e** was isolated by silica gel column chromatography using 8:2 Hex: EtOAc mixture as a yellow oil in >99 % yield (105 mg). R_f = 0.65, **^{1}H NMR** (500 MHz, CDCl3) δ 8.25 (s, 1H), 4.44 (q, J = 7.1 Hz, 2H), 2.88 (tt, J = 11.8, 3.3 Hz, 1H), 2.04 – 1.97 (m, 2H), 1.83 – 1.77 (m, 2H), 1.42 (t, J = 7.1 Hz, 3H), 1.38 (dt, J = 5.9, 3.5 Hz,2H), 1.29 – 1.20 (m, 2H). **^{13}C NMR** (125 MHz, CDCl$_3$) δ 160.5, 155.9, 153.3, 127.4, 61.9, 33.7, 32.4, 26.4, 25.9, 14.1. **HRMS** Calculated for C$_{12}$H$_{17}$NO$_3$ [M+H] 224.1281 found 224.1282.
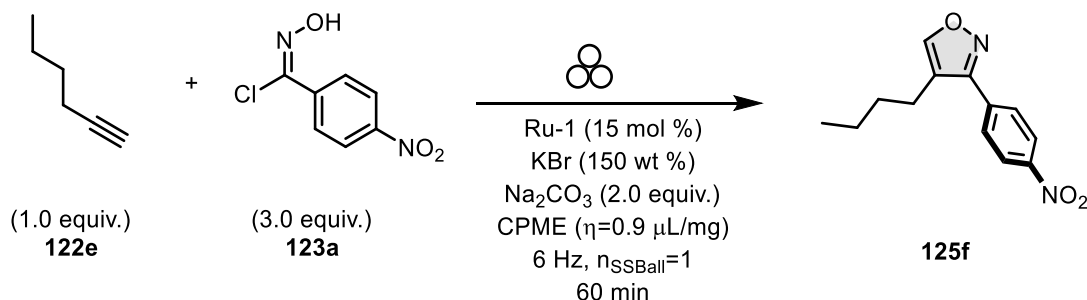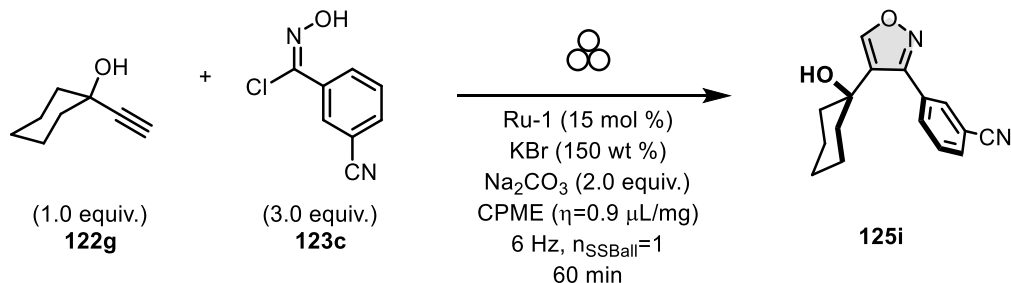
Synthesis of ethyl 4-butylisoxazole-3-carboxylate (125f): 3,4-isoxazole **125f** was obtained following procedure PS2. **125f** was isolated by silica gel column chromatography using 8:2 Hex: EtOAc mixture as a colourless oil in >99 % yield (120.7 mg). R_f = 0.8, **^{1}H NMR** (500 MHz, CDCl3) δ 8.28 (s, 1H), 4.44 (q, J = 7.1 Hz, 2H), 2.66 (t, 2H), 1.42 (t, J = 7.3 Hz, 3H), 1.40 − 1.36 (m, 2H), 0.94 (t, J = 7.3 Hz, 1H). **^{13}C NMR** (125 MHz, CDCl$_3$) δ 160.5, 157.0, 153.8, 121.4, 61.9, 31.6, 22.3, 21.8, 14.1, 13.7. **HRMS** Calculated for $C_{10}H_{15}NO_3$ [M+H] 198.1125 found 198.1125.

Synthesis of 2-(3-(4-nitrophenyl)isoxazol-4-yl)ethan-1-ol (125g): 3,4-isoxazole **125g** was obtained following procedure PS2. **125g** was isolated by silica gel column chromatography using 8:2 Hex: EtOAc mixture as a colourless oil in >99 % yield (120.7 mg). R_f = 0.43, **^{1}H NMR** (500 MHz, d^6-DMSO) δ 9.05 (s, 1H), 8.37 (d, J = 8.8 Hz, 2H), 7.96 (d, J = 8.8 Hz, 2H), 3.69 (t, J = 6.9 Hz, 2H), 3.16 (t, J = 6.9 Hz, 2H). **^{13}C NMR** (125 MHz, d^6-DMSO) δ 159.9, 159.5, 148.7, 135.3, 129.9, 124.6, 116.3, 32.9, 25.9. **HRMS** Calculated for $C_{11}H_{10}N_2O_4$ [M+H] 235.0713 found 235.0714.
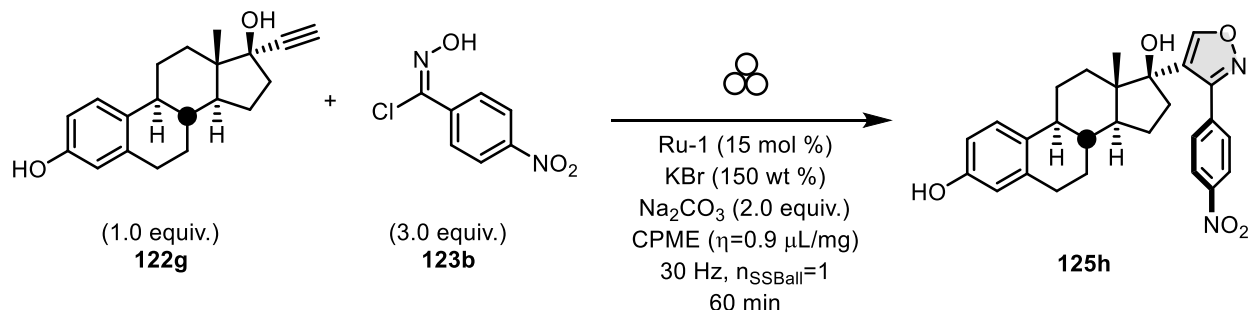

Synthesis of 1-(3-(4-nitrophenyl)isoxazol-4-yl)cyclohexan-1-ol (125h): 3,4-isoxazole **125h** was obtained following procedure PS2. **125h** was isolated by silica gel column chromatography using 8:2 Hex: EtOAc mixture as a white solid in >99 % yield (120.7 mg). R_f = 0.22, **^{1}H NMR** (500 MHz, d^6-DMSO) δ 8.99 (s, 1H), 8.33 (d, J = 8.8 Hz, 2H), 8.13 (d, J = 8.8 Hz, 2H), 5.23 (s, 1H), 1.77 − 1.67 (m, 2H), 1.65 − 1.53 (m, 4H), 1.50 − 1.40 (m, 1H), 1.36 − 1.27 (m, 2H), 1.23 − 1.12 (m, 1H).**^{13}C NMR** (125 MHz, d^6-DMSO) δ δ 160.3, 157.9, 148.4, 137.3, 131.5, 127.6 123.7, 67.1, 37.9, 25.5, 21.9. **HRMS** Calculated for $C_{15}H_{16}N_2O_4$ [M+H] 289.1183 found 289.1183.

Synthesis of 3-(4-(1-hydroxycyclohexyl)isoxazol-3-yl)benzonitrile (125i): 3,4-isoxazole **125i** was obtained following procedure PS2. **125i** was isolated by silica gel column chromatography using 8:2 Hex: EtOAc mixture as a yellow oil in 89 % yield (96 mg). R_f = 0.8, **^{1}H NMR** (500 MHz, CDCl$_3$) δ 8.38 (s, 1H), 8.16 (t, J = 1.5 Hz, 1H), 8.07 (dd, J = 7.8, 1.4 Hz, 1H), 7.73 (dt, J = 7.8, 1.3 Hz, 1H), 7.55 (t, J = 7.8 Hz, 1H), 2.00 (s, 1H), 1.84 – 1.77 (m, 2H), 1.72 – 1.54 (m, 6H), 1.47 (m, 2H).**^{13}C NMR** (125 MHz, CDCl$_3$) δ 159.9, 155.9, 134.2, 133.5, 132.8, 131.6, 129.1, 126.4, 118.4, 112.6, 68.5, 37.9, 25.2, 21.8. **HRMS** Calculated for C$_{16}$H$_{16}$N$_2$O$_2$ [M+H] 269.1285 found 269.1286.
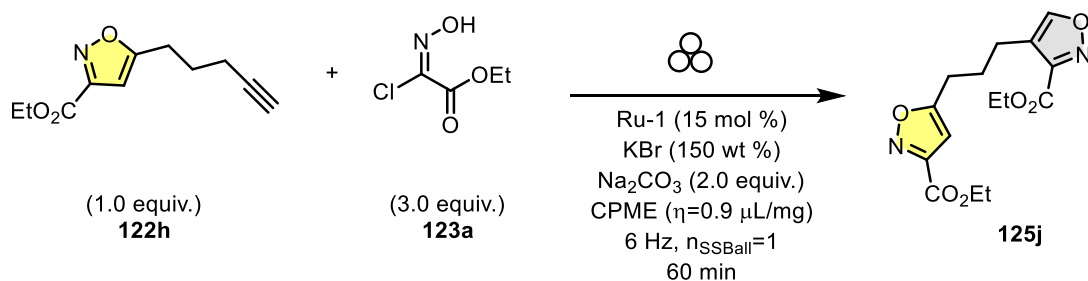
Synthesis of ethyl 5-(3-(3-(ethoxycarbonyl)isoxazol-4-yl)propyl)isoxazole-3-carboxylate (125j): 3,4-isoxazole **125j** was obtained following procedure PS2. **125j** was isolated by silica gel column chromatography using 7:3 Hex: EtOAc mixture as a white solid l in 88 % yield (96 mg). R_f = 0.48, **^{1}H NMR** (500 MHz, CDCl$_3$) δ 8.34 (s, 1H), 6.45 (s, 1H), 4.43 (p, J = 7.1 Hz, 4H), 2.87 (t, J = 7.5 Hz, 2H), 2.76 (t, J = 7.8 Hz, 2H), 2.04 (p, J = 7.6 Hz, 2H), 1.41 (q, J = 7.2 Hz, 6H).**^{13}C NMR** (125 MHz, CDCl$_3$) δ 174.34, 160.30, 160.05, 157.42, 156.44, 153.66, 119.90, 101.81, 62.09, 62.07, 27.28, 26.13, 21.38, 14.12, 14.10. **HRMS** Calculated for C$_{15}$H$_{18}$N$_2$O$_6$ [M+H] 323.1238 found 323.1235.

Synthesis of (9S,13R,14S,17S)-17-(3-(4-nitrophenyl)isoxazol-4-yl)-7,8,9,11,12,13,14,15,16,17-decahydro-6H-cyclopenta[a]phenanthrene-3,17-diol (125k): 3,4-isoxazole **125k** was obtained following procedure PS2 (using 30 Hz). **125k** was isolated by silica gel column chromatography using 100 % DCM to 9:1 MeOH:DCM mixture as a white solid in 91 % yield (72 mg). R_f = 0.1, **^{1}H NMR** ^{1}H NMR (500 MHz, d_6-DMSO) δ 8.94 (s, 1H), 8.29 (d, J = 8.9 Hz, 2H), 8.15 (d, J = 8.9 Hz, 2H), 6.89 (d, J = 8.5 Hz, 1H), 6.49 – 6.33 (m, 2H), 5.55 (s, 1H), 2.72 – 2.58 (m, 2H), 2.29 – 2.15 (m, 1H), 2.13 – 2.03 (m, 1H), 2.00 – 1.91 (m, 1H), 1.86 – 1.67 (m, 3H), 1.43 – 1.00 (m, 7H), 0.82 (s, 3H). **^{13}C NMR** ^{13}C NMR (126 MHz, d_6-DMSO) δ 161.2, 158.7, 155.3, 148.1, 146.4, 138.2, 137.5, 132.2, 130.6, 126.3, 125.8, 123.1, 115.3, 113.1, 81.0, 48.1, 47.4, 43.3, 33.9, 29.6, 27.4, 26.4, 23.0, 14.3. **HRMS** Calculated for C$_{27}$H$_{28}$N$_2$O$_5$ [M+H] 461.2071 found 461.2068.

4.7.4. Procedure S3 (PS3): Optimization of "Polung" synthesis of 3,4,5-isoxazoles.

This section describes a Ru(II)-free synthesis of 3,4,5-isoxazoles. Prior to the isolation, optimization control experiments were conducted with 50 mg of symmetrical internal alkyne **126a** to form 3,4,5-isoxazole **128.** All reported yields are ^{1}H-NMR yields obtained from the spectrum of the crude product.

Note: Prior to every reaction demonstrated in this section, the Teflon Jars were carefully washed with aqua regia, to remove leftovers of Ru(II) complex and avoid potential memory effects.

Table S4.4. *Effect of Frequency in the synthesis of 3,4,5-isoxazoles.*

Frequency (Hz)	Yield %
6 Hz	< 5
30 Hz	12
60 Hz	25

Table S4.5. *Effect of liquid additive in the synthesis of 3,4,5-isoxazoles.*

Liquid additive	η (μL/mg)	Yield %
CPME	0.9	12
CPME	0.5	< 5
DCE	0.9	15
IPA	0.9	< 5
DMF	0.9	< 5

Table S4.6. *Effect of the GAA in the synthesis of 3,4,5-isoxazoles.*

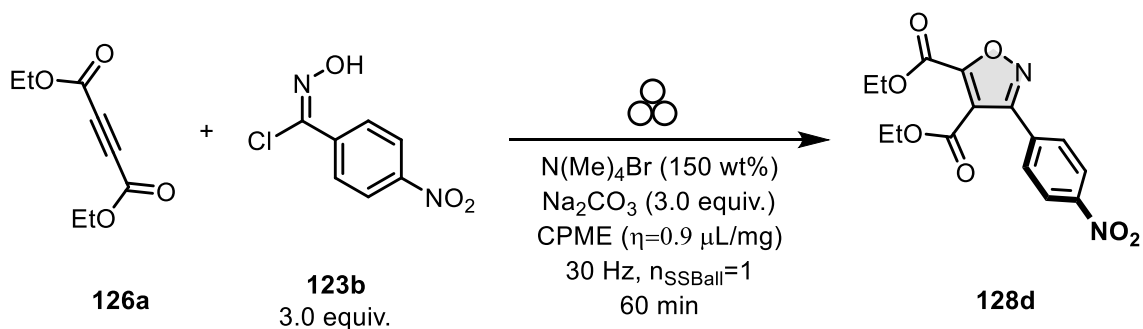| GAA	wt %	Yield %
KBr	150	12
ZnBr H_2O	150	< 5
NMe$_4$Br	150	50
NH$_4$(H$_2$W$_{12}$O$_{42}$) H$_2$O	150	< 5
CaBr$_2$ H$_2$O	150	< 5
NMe$_4$Br and Ru cat (5 mol %)	150	52
NMe$_4$Br No RuI	150	84
NMe$_4$Br No Ru-1 and 3.0 equiv of Na$_2$CO$_3$	150	84

It was continued using 3.0 equiv. of Na$_2$CO$_3$, since it provided more general conditions.

4.7.5. Procedure S4 (PS4): "Polung'' synthesis and isolation of 3,4,5-isoxazoles.

Note: Prior to every reaction demonstrated in this section, the Teflon Jars were carefully washed with aqua regia, to remove leftovers of Ru(II) complex and avoid potential memory effects.

126a 126b 126c

126d 126e
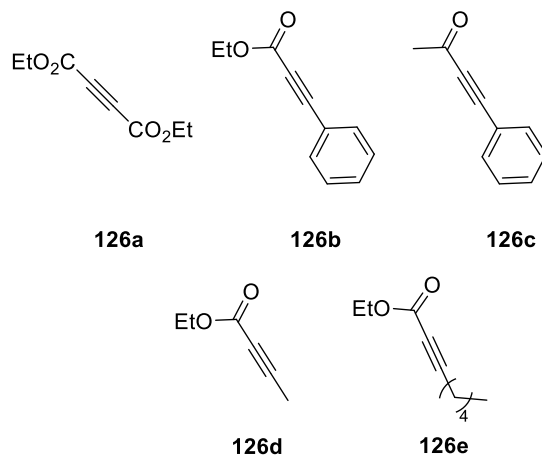
Figure S4.5. Internal Alkynes used for "Polung" synthesis of 3,4,5-isoxazoles.

123a 123b 123c 123d 123e

123f
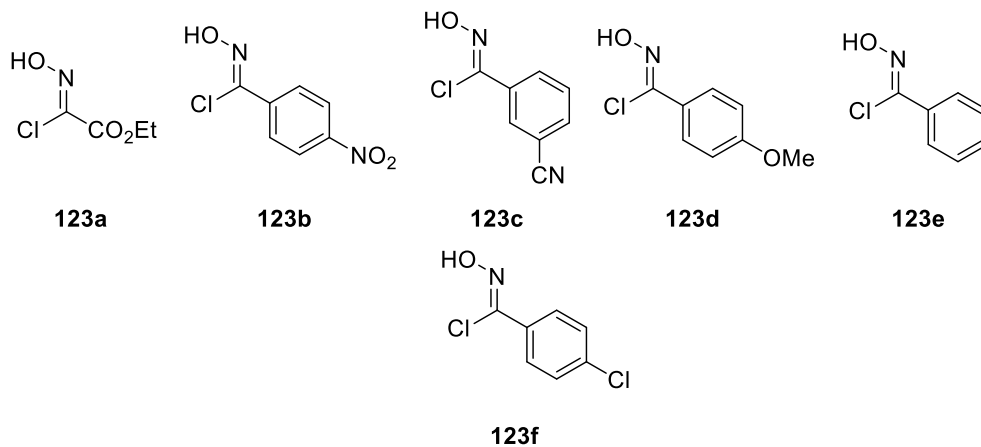
Figure S4.6. Hydroxyimidoyl chlorides used for the "Polung" synthesis of 3,4,5-isoxazoles.

Example procedure:

126a + **123b** (3.0 equiv.) → N(Me)₄Br (150 wt%), Na₂CO₃ (3.0 equiv.), CPME (η=0.9 μL/mg), 30 Hz, n_SSBall=1, 60 min → **128d**

Synthesis of diethyl 3-(4-nitrophenyl)isoxazole-4,5-dicarboxylate (128d): In a clear and dry Teflon Jar of 25 mL capacity and 1 SS ball of 1 cm diameter, it was directly weight **126a** (1.0 equiv., 0.586 mmol, 100 mg), hydroxyimidoyl chloride **123b** (3.0 equiv., 0.924 mmol, 140 mg), Na₂CO₃ (2.0 equiv., 0.612 mmol, 65 mg), KBr (150 wt%, 409 mg), CPME (η= 0.9μL/mg, 612 μL). The mixture was closed with the Teflon lit and recovered with parafilm. Then the reagents were milled for 60 minutes at 30 Hz. After 60 minutes, the jar was opened, and the mixture was passed over silica plug, using diethyl ether as an eluent. The desired isoxazole **128d** was isolated by silica gel column chromatography using 9:1 Hex: EtOAc mixture as a white solid in 70 % yield (138 mg). R_f= 0.10, **¹H NMR** (500 MHz, CDCl₃) δ ¹H NMR (500 MHz, CDCl₃) δ 8.33 (d, J = 7.9 Hz, 2H), 7.92 (d, J = 8.1 Hz, 2H), 4.49 (q, J = 7.1 Hz, 2H), 4.38 (q, J = 7.1 Hz, 2H), 1.44 (t, J = 7.1 Hz, 3H), 1.32 (t, J = 7.1 Hz, 3H). **¹³C NMR** (125 MHz, CDCl₃) δ 160.8, 160.7, 159.7, 155.9, 149.1, 133.2, 129.6, 123.9, 115.5, 63.2, 62.7, 14.0, 13.9. **HRMS** Calculated for $C_{15}H_{14}N_2O_7$ [M+H] 335.0874 found 335.0879.

126a + **123a** (3.0 equiv.) → N(Me)₄Br (150 wt%), Na₂CO₃ (3.0 equiv.), CPME (η=0.9 μL/mg), 30 Hz, n_SSBall=1, 60 min → **128a**
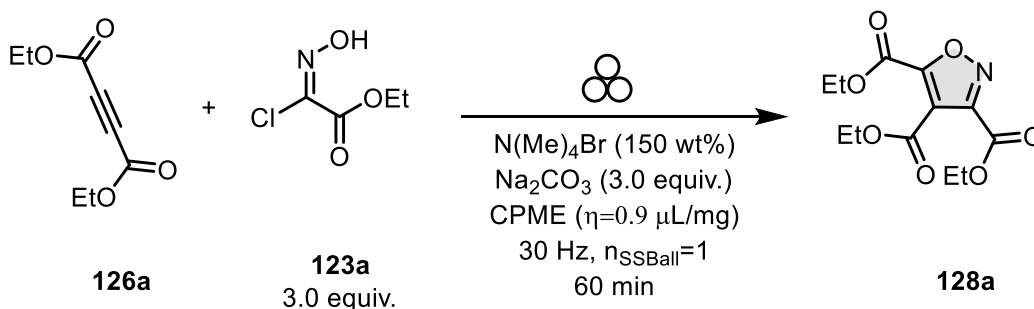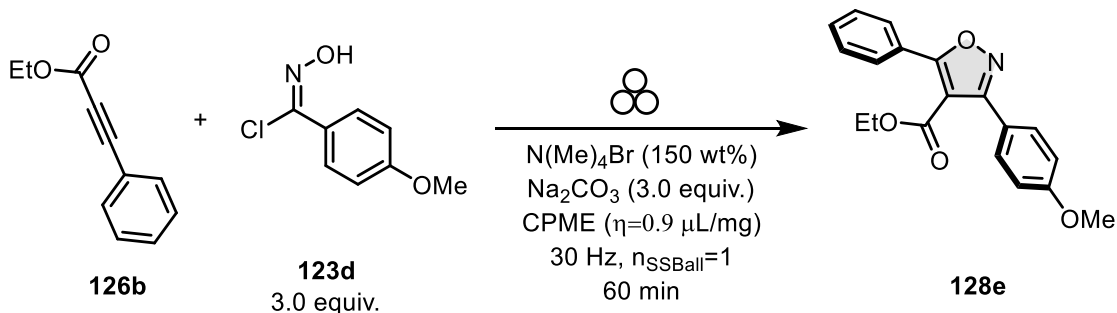
Synthesis of triethyl isoxazole-3,4,5-tricarboxylate (128a): 3,4,5-isoxazole **128a** was obtained following procedure PS4. **128a** was isolated by silica gel column chromatography using 9:1 Hex: EtOAc mixture as a colourless oil in >99 % yield (211 mg). R_f = 0.43, **¹H NMR** (500 MHz, CDCl₃) δ 4.46 (q, J = 7.2 Hz, 2H), 4.41 (q, J = 7.1 Hz, 2H), 4.26 (q, J = 7.1 Hz, 2H), 1.39 (t, J = 7.2 Hz, 3H), 1.35 (t, J = 7.1 Hz, 3H), 1.29 (t, J = 7.1 Hz, 3H). **¹³C NMR** (125 MHz, CDCl₃) δ 156.6, 155.6, 151.7, 148.35 (s), 106.7, 74.6, 63.6, 63.0, 13.9, 13.8. **HRMS** Calculated for $C_{12}H_{15}NO_7$ [M+H] 286.0921 found 286.0921.

126a + **123d** (3.0 equiv.) → N(Me)₄Br (150 wt%), Na₂CO₃ (3.0 equiv.), CPME (η=0.9 μL/mg), 30 Hz, n_SSBall=1, 60 min → **128b**
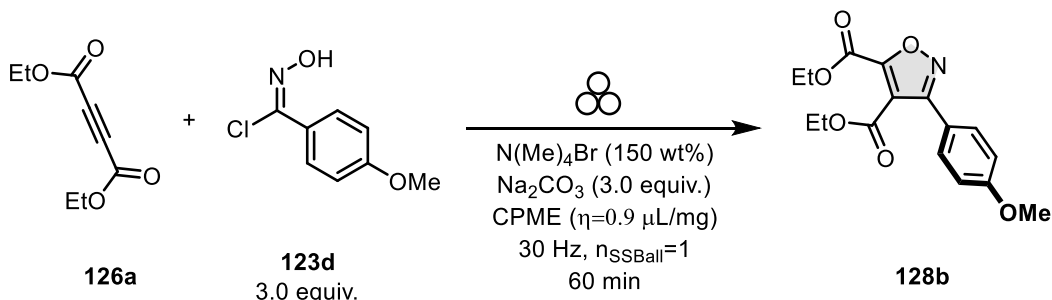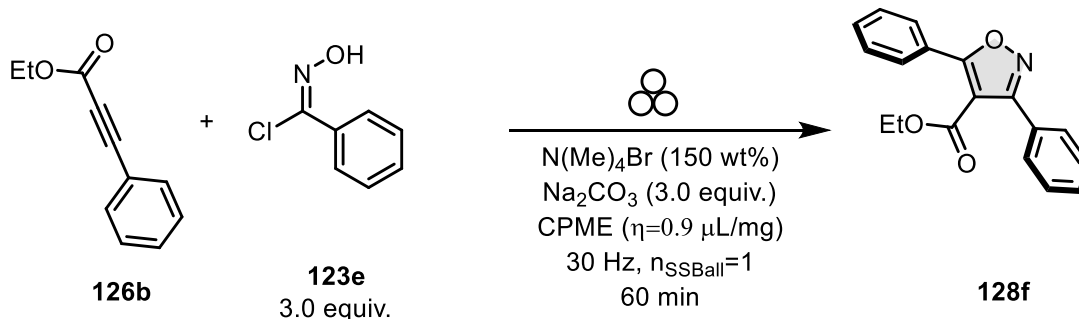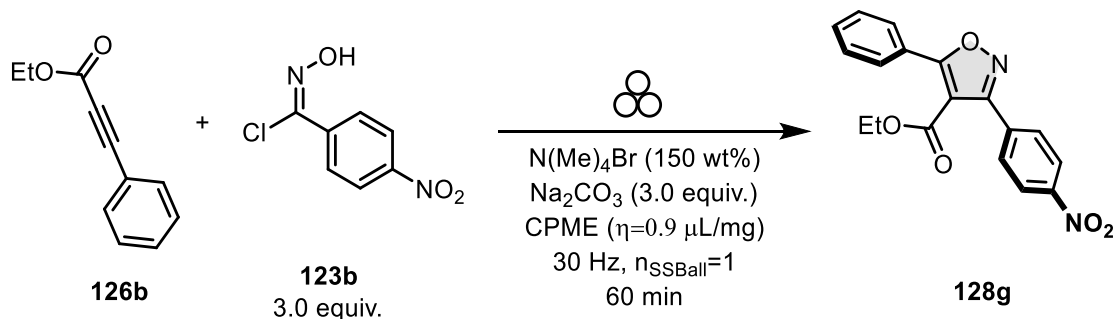
Synthesis of diethyl 3-(4-methoxyphenyl)isoxazole-4,5-dicarboxylate (128b): 3,4,5-isoxazole **128b** was obtained following procedure PS4. **128b** was isolated by silica gel column chromatography using 9:1 Hex: EtOAc mixture as a yellow oil in >99 % yield (196.7 mg). R_f = 0.23, **^{1}H NMR** (500 MHz, CDCl$_3$) δ 7.62 (d, J = 8.6 Hz, 2H), 6.93 (d, J = 8.7 Hz, 2H), 4.41 (q, J = 7.1 Hz, 2H), 4.34 (q, J = 7.1 Hz, 2H), 3.79 (s, 3H), 1.37 (t, J = 7.1 Hz, 3H), 1.29 (t, J = 7.1 Hz, 3H). **^{13}C NMR** (125 MHz, CDCl$_3$) δ 161.6, 161.5, 160.7, 159.3, 156.1, 129.6, 119.3, 115.9, 114.2, 62.8, 62.4, 55.3, 14.0, 13.9. **HRMS** Calculated for C$_{16}$H$_{17}$NO$_6$ [M+H] 320.1129 found 320.1129.

126a   **123e**
                 3.0 equiv.

N(Me)$_4$Br (150 wt%)
Na$_2$CO$_3$ (2.0 equiv.)
CPME (η=0.9 μL/mg)
30 Hz, n$_{SSBall}$=1
60 min
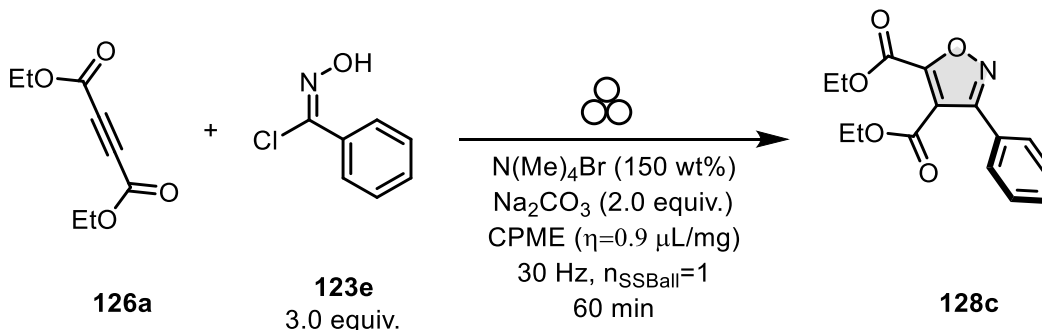
128c

Synthesis of diethyl 3-phenylisoxazole-4,5-dicarboxylate (128c): 3,4,5-isoxazole **128c** was obtained following procedure PS4. **128c** was isolated by silica gel column chromatography using 8.5:1.5 Hex: EtOAc mixture as a yellow oil in 87 % yield (147.4 mg). R_f = 0.23, **^{1}H NMR** (500 MHz, CDCl$_3$) δ 7.68 (dd, J = 8.0, 1.5 Hz, 2H), 7.49 – 7.40 (m, 3H), 4.44 (q, J = 7.1 Hz, 2H), 4.35 (q, J = 7.1 Hz, 2H), 1.39 (t, J = 7.1 Hz, 3H), 1.28 (t, J = 7.1 Hz, 3H). **^{13}C NMR** (125 MHz, CDCl$_3$) δ (125 MHz, CDCl$_3$) δ 161.36, 161.17, 159.50, 156.06, 130.60, 128.79, 128.15, 127.03, 116.12, 62.85, 62.39, 13.97, 13.82. **HRMS** Calculated for C$_{15}$H$_{15}$NO$_5$ [M+H] 290.1023 found 290.1023.

126b   **123d**
                 3.0 equiv.

N(Me)$_4$Br (150 wt%)
Na$_2$CO$_3$ (3.0 equiv.)
CPME (η=0.9 μL/mg)
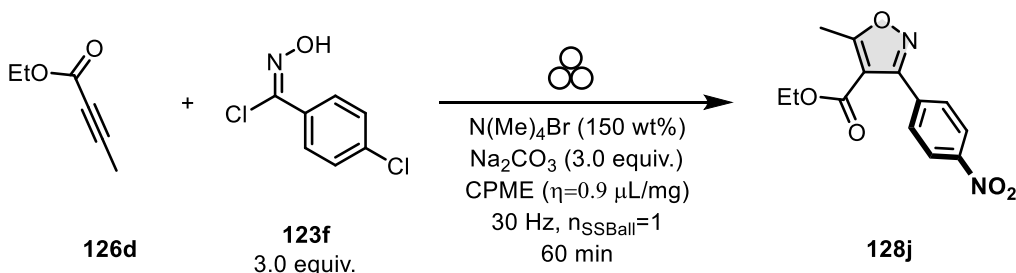30 Hz, n$_{SSBall}$=1
60 min

128e

Synthesis of ethyl 3-(4-methoxyphenyl)-5-phenylisoxazole-4-carboxylate (128e): 3,4,5-isoxazole **128e** was obtained following procedure PS4. **128e** was isolated by silica gel column chromatography using 93:7 Hex: EtOAc mixture as a white in 80 % yield (150.5 mg). R_f = 0.21, **^{1}H NMR** (500 MHz, CDCl$_3$) δ 7.90 (dd, J = 7.9, 1.6 Hz, 1H), 7.63 (d, J = 8.8 Hz, 1H), 7.55 – 7.47 (m, 1H), 6.99 (d, J = 8.8 Hz, 1H), 4.22 (q, J = 7.1 Hz, 1H), 3.85 (s, 1H), 1.14 (t, J = 7.2 Hz, 1H). **^{13}C NMR** (125 MHz, CDCl$_3$) δ 172.2, 162.6, 162.5, 160.9, 131.1, 130.4, 128.7, 128.5, 127.0, 120.8, 113.7, 108.2, 61.3, 55.3, 13.8. **HRMS** Calculated for C$_{19}$H$_{17}$NO$_4$ [M+H] 324.123 found 324.1233.

Synthesis of ethyl 3,5-diphenylisoxazole-4-carboxylate (128f): 3,4,5-isoxazole **128f** was obtained following procedure PS4. **128f** was 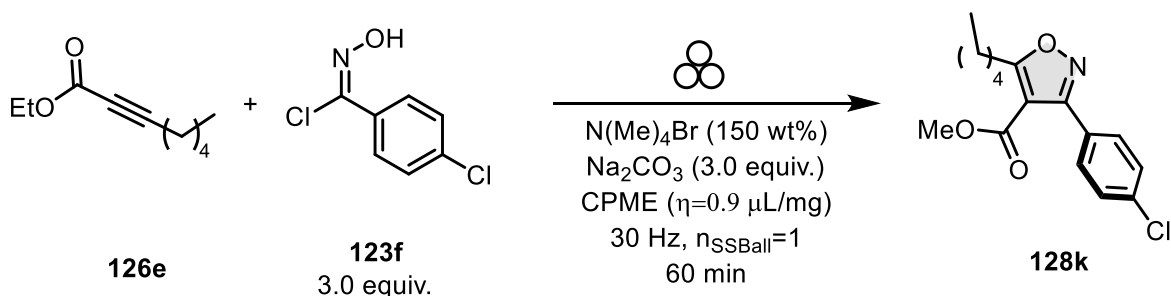isolated by silica gel column chromatography using 98:2 Hex: EtOAc mixture as a white solid in 93 % yield (156.5 mg). R_f = 0.15, **^{1}H NMR** (500 MHz, CDCl$_3$) δ 10.01 (s, 1H), 8.06 (d, J = 6.9 Hz, 2H), 7.78 (dd, J = 7.7, 1.8 Hz, 2H), 7.68 − 7.30 (m, 6H). **^{13}C NMR** (125 MHz, CDCl$_3$) 184.10, 175.39, 163.39, 132.40, 130.55, 129.40, 129.09, 129.06, 128.74, 127.24, 125.96, 114.40. **HRMS** Calculated for C$_{18}$H$_{15}$NO$_3$ [M+H] 294.1125 found 294.1125.

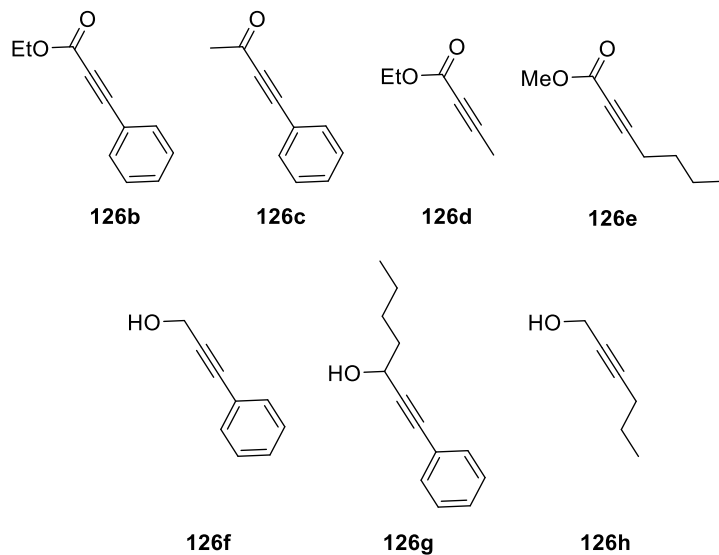

Synthesis of ethyl 3-(4-nitrophenyl)-5-phenylisoxazole-4-carboxylate (128g): 3,4,5-isoxazole **128g** was obtained following procedure PS4. **128g** was isolated by silica gel column chromatography using 95:5 Hex: EtOAc mixture as a yellow solid in 64 % yield (156.5 mg). R_f = 0.22, **^{1}H NMR** (500 MHz, CDCl$_3$) δ 8.37 − 8.30 (m, 2H), 7.95 − 7.91 (m, 2H), 7.89 − 7.85 (m, 2H), 7.60 − 7.51 (m, 3H), 4.22 (q, J = 7.1 Hz, 2H), 1.12 (t, J = 7.1 Hz, 3H). **^{13}C NMR** (125 MHz, CDCl$_3$) 173.53, 161.60, 161.59, 148.72, 135.10, 131.66, 130.32, 128.99, 128.55, 126.42, 123.35, 108.15, 61.51, 13.73. **HRMS** Calculated for C$_{18}$H$_{14}$N$_2$O$_5$ [M+H] 339.0975 found 339.0973.
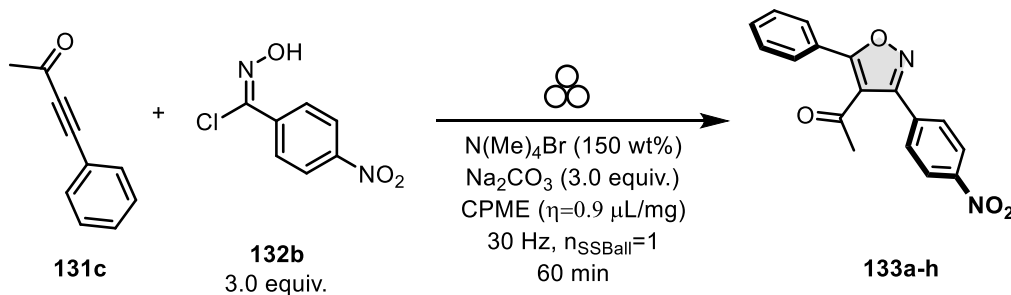
Synthesis of 1-(3-(4-nitrophenyl)-5-phenylisoxazol-4-yl)ethan-1-one (128h): 3,4,5-isoxazole **128h** was obtained following procedure PS4. **128h** was isolated by silica gel column chromatography using 95:5 Hex:

EtOAc mixture as a yellow solid in 61 % yield (122.1 mg). R_f = 0.13, **^{1}H NMR** (500 MHz, Acetone-d^6) δ 8.40 (d, J = 8.7 Hz, 2H), 7.98 (d, J = 8.7 Hz, 2H), 7.86 (d, J = 7.5 Hz, 2H), 7.71 – 7.60 (m, 3H), 2.25 (s, 3H). **^{13}C NMR** (125 MHz, Acetone-d^6) δ 193.4, 171.7, 160.8, 148.9, 135.1, 131.7, 130.3, 130.1, 129.1, 128.8, 126.9, 123.6, 30.4. **HRMS** Calculated for $C_{18}H_{14}N_2O_5$ [M+H] 309.0870 found 309.0870.

Synthesis of ethyl 5-methyl-3-(4-nitrophenyl)isoxazole-4-carboxylate (128i): 3,4,5-isoxazole **128i** was obtained following procedure PS4. **128i** was isolated by silica gel column chromatography using 9:1 Hex: EtOAc mixture as a yellow solid in 71 % yield (208 mg). R_f = 0.18 **^{1}H NMR** (500 MHz, CDCl$_3$) δ 8.36 – 8.25 (m, 2H), 7.90 – 7.77 (m, 2H), 4.26 (d, J = 7.1 Hz, 2H), 2.76 (s, 3H), 1.25 (t, J = 7.1 Hz, 3H) **^{13}C NMR** (125 MHz, CDCl3) δ 176.47, 161.45, 160.97, 148.66, 134.95, 130.59, 123.12, 108.48, 61.08, 14.03, 13.66. **HRMS** Calculated for $C_{13}H_{12}N_2O_5$ [M+H] 277.0819 found 277.082.
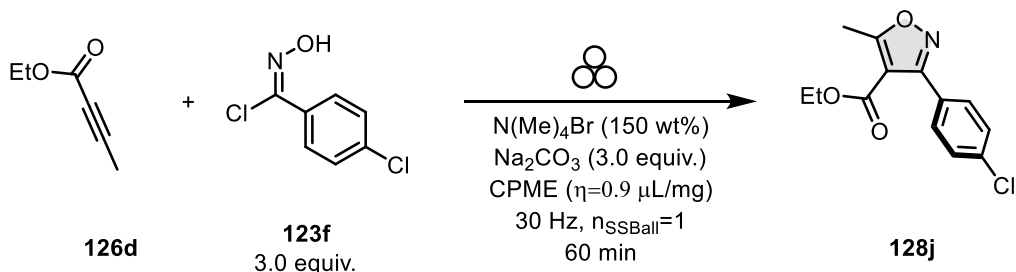
Synthesis of ethyl 3-(4-chlorophenyl)-5-methylisoxazole-4-carboxylate (128j): 3,4,5-isoxazole **128j** was obtained following procedure PS4. **128j** was isolated by silica gel column chromatography using 100 % Hex to 8:2 Hex: EtOAc mixture as a yellow oil in 70 % yield (80 mg). R_f = 0.50 **^{1}H NMR** (500 MHz, CDCl$_3$) 7.58 (d, J = 8.6 Hz, 2H), 7.41 (d, J = 8.6 Hz, 2H), 4.25 (q, J = 7.1 Hz, 2H), 2.73 (s, 3H), 1.25 (t, J = 7.1 Hz, 3H). **^{13}C NMR** (125 MHz, CDCl3) δ 176.0, 161.8, 161.7, 136.0, 130.8, 128.3, 126.9, 108.4, 60.8, 13.8, 13.6. **HRMS** Calculated for $C_{13}H_{12}NO_3Cl$ [M+H] 266.0578 found 266.0579.

Synthesis of ethyl 3-(4-chlorophenyl)-5-methylisoxazole-4-carboxylate (128k): 3,4,5-isoxazole **128k** was obtained following procedure PS4. **128k** was isolated by silica gel column chromatography using 100 % Hex to 8:2 Hex: EtOAc mixture as a colourless solid in 66 % yield (208 mg). R_f = 0.70 **^{1}H NMR** (500 MHz, CDCl$_3$) 7.57 (d, J = 8.5 Hz, 2H), 7.42 (d, J = 8.5 Hz, 2H), 3.78 (s, 3H), 3.18 – 3.02 (m, 2H), 1.85 – 1.69 (m, 2H), 1.43 – 1.30 (m, 4H), 0.92 (t, J = 6.9 Hz, 3H). **^{13}C NMR** (125 MHz, CDCl3) δ 179.9, 162.2, 161.6, 136.0, 130.7, 129.6, 128.3, 127.0, 51.7, 31.4, 27.5, 27.0, 22.2, 13.9. **HRMS** Calculated for C$_{16}$H$_{18}$NO$_3$Cl [M+H] 308.1048 found 308.1046.

4.7.6. Procedure S5 (PS5): "Umpolung'' synthesis and isolation of 3,4,5-isoxazoles.

Note: Prior to every reaction demonstrated in this section, the Teflon Jars were carefully washed with aqua regia, to remove leftovers of Ru(II) complex and avoid potential memory effects.

Figure S4.7. Internal Alkynes used for "umpolung" synthesis of 3,4,5-isoxazoles.
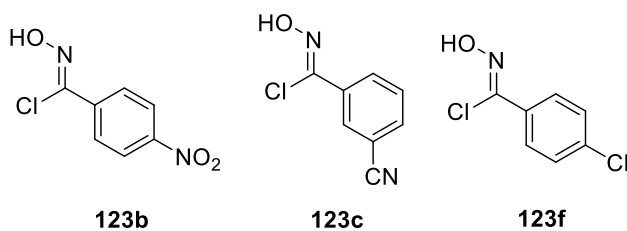
Figure S4.8. Hydroxyimidoyl chlorides used for the "umpolung" synthesis of 3,4,5-isoxazoles.

Example procedure for Ynones – PS5a:
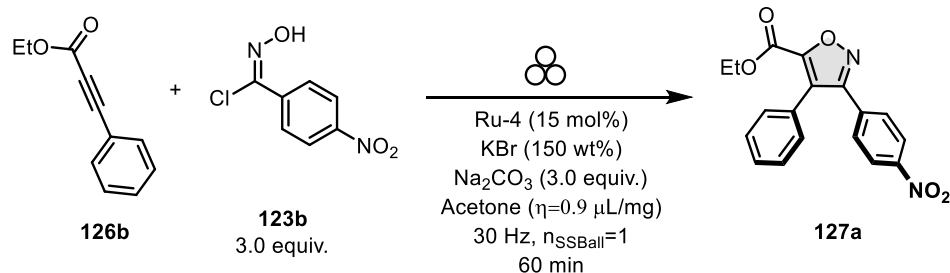
Synthesis of ethyl 3-(4-nitrophenyl)-4-phenylisoxazole-5-carboxylate (127a): In a clear and dry Teflon Jar of 25 mL capacity and 1 SS ball of 1 cm diameter, it was directly weight **126b** (1.0 equiv., 0.287 mmol, 50 mg, 47 µL), hydroxyimidoyl chloride **123b** (3.0 equiv., 0.861 mmol, 171 mg), Na$_2$CO$_3$ (3.0 equiv., 0.861 mmol, 91.2 mg), KBr (150 wt%, 499 mg), CPME (η= 0.9µL/mg, 831 µL), and **Ru-4** (15 mol%, 0.043 mmol, 18.6 mg). The mixture was closed with the Teflon lit and recovered with parafilm. Then the reagents were milled for 60 minutes at 30 Hz. After 60 minutes, the jar was opened, and the mixture was passed over silica plug, using diethyl ether as an eluent. The desired isoxazole **127a** was isolated by silica gel column chromatography using 99:1 Hex: EtOAc mixture as a yellow solid in 88 % yield (87 mg). R_f= 0.1, **^{1}H NMR** (500 MHz, CDCl$_3$) δ 8.39 − 8.31 (m, 1H), 8.17 (d, J = 8.7 Hz, 1H), 7.60 (d, J = 8.7 Hz, 1H), 7.47 − 7.38 (m, 1H), 7.27 (s, 1H), 4.35 (q, J = 7.1 Hz, 1H), 1.28 (t, J = 7.1 Hz, 1H). **^{13}C NMR** (125 MHz, CDCl$_3$) δ 160.6, 156.7, 156.7, 148.6, 134.1, 130.0, 129.4, 129.2, 128.6, 127.5, 124.1, 123.8, 62.2, 29.7, 13.9. **HRMS** Calculated for C$_{18}$H$_{14}$N$_2$O$_5$ [M+H] 339.0975 found 339.0974.
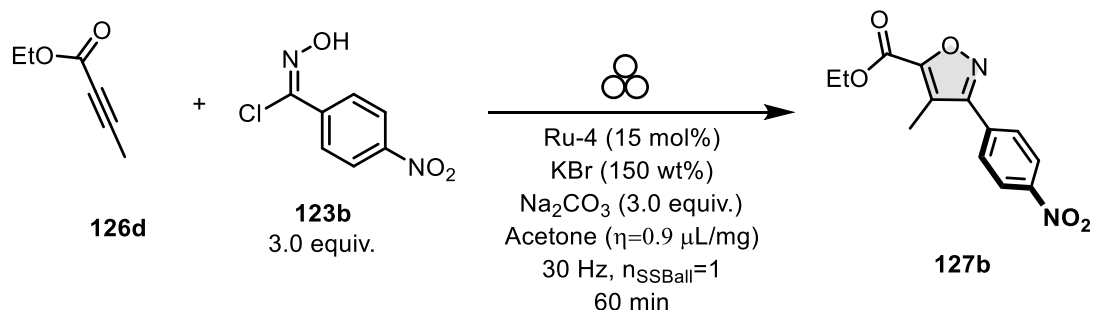
Synthesis of ethyl 4-methyl-3-(4-nitrophenyl)isoxazole-5-carboxylate (127b): 3,4,5-isoxazole **127b** was obtained following procedure PS5a. **127b** was isolated by silica gel column chromatography using 9:1 Hex: EtOAc mixture as a yellow solid in 81 % yield (100.30 mg). R_f = 0.15 **^{1}H NMR** (500 MHz, CDCl$_3$) δ 8.36 (d, J = 9.0 Hz, 2H), 7.86 (d, J = 9.0 Hz, 2H), 4.47 (q, J = 7.1 Hz, 2H), 2.45 (s, 3H), 1.45 (t, J = 7.1 Hz, 3H). **^{13}C NMR** (125 MHz, CDCl3) δ 161.9, 157.5, 156.8, 148.5, 134.7, 129.3, 124.1, 119.8, 62.1, 14.1, 8.9. **HRMS** Calculated for C$_{13}$H$_{12}$N$_2$O$_5$ [M+H] 277.0819 found 277.0819.
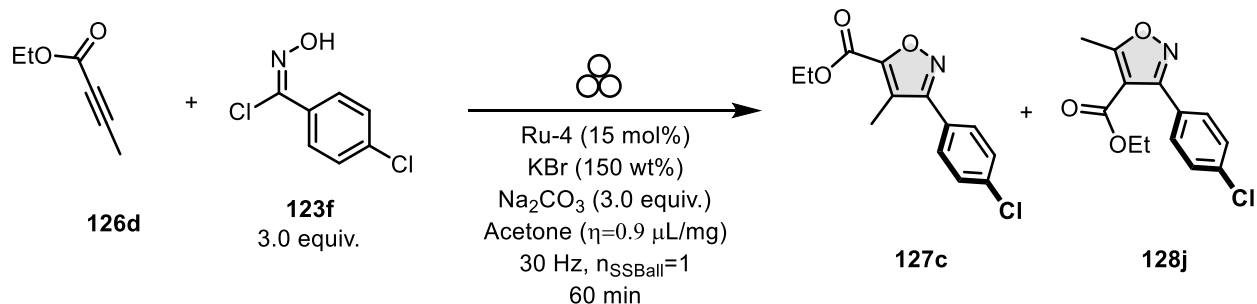
**Synthesis of ethyl 3-(4-chlorophenyl)-4-methylisoxazole-5-carboxylate (127c):** 3,4,5-isoxazole **127c** was obtained following procedure PS5a. **127c** was isolated as a mixture of isomers by prep-TLC using 9:1 heptane: EtOAc mixture as a yellow solid in >99 % yield (121 mg) with *rr*= 6:1. R_f = 0.26 (for the mixture) The NMR signals were deconvoluted using the signal from the ^{1}**H NMR** and ^{13}**C NMR** signals of isolated **133a-k.** ^{1}**H NMR of *127c*** (500 MHz, CDCl$_3$) δ 7.59 (d, *J* = 8.5 Hz, 2H), 7.47 (d, *J* = 8.5 Hz, 2H), 4.46 (q, *J* = 7.1 Hz, 2H), 2.40 (s, 3H), 1.44 (t, *J* = 7.1 Hz, 3H). ^{1}**H NMR of *128j (undesire)*** (500 MHz, CDCl$_3$) δ 7.57 (d, *J* = 2.0 Hz, 2H), 7.41 (d, *J* = 8.5 Hz, 2H), 4.25 (q, *J* = 7.1 Hz, 2H), 2.73 (s, 3H), 1.25 (t, *J* = 7.1 Hz, 3H).^{13}**C NMR of 133c-c** (125 MHz, CDCl$_3$) δ 162.8, 157.7, 156.1, 136.2, 129.6, 129.2, 126.9, 119.8, 61.9, 14.2, 8.9. ^{13}**C NMR of 133a-k** *(undesire)* (125 MHz, CDCl$_3$) δ 176.0, 161.8, 161.6, 136.0, 130.8, 128.2, 126.9, 108.3, 60.8, 14.0, 13.6. **HRMS** Calculated for C$_{13}$H$_{12}$NO$_3$Cl [M+H] 266.0578 found 266.0579.

126e   **123f** 3.0 equiv.   Ru-4 (15 mol%) KBr (150 wt%) Na$_2$CO$_3$ (3.0 equiv.) Acetone (η=0.9 µL/mg) 30 Hz, n$_{SSBall}$=1 60 min   **127d**   **128k**
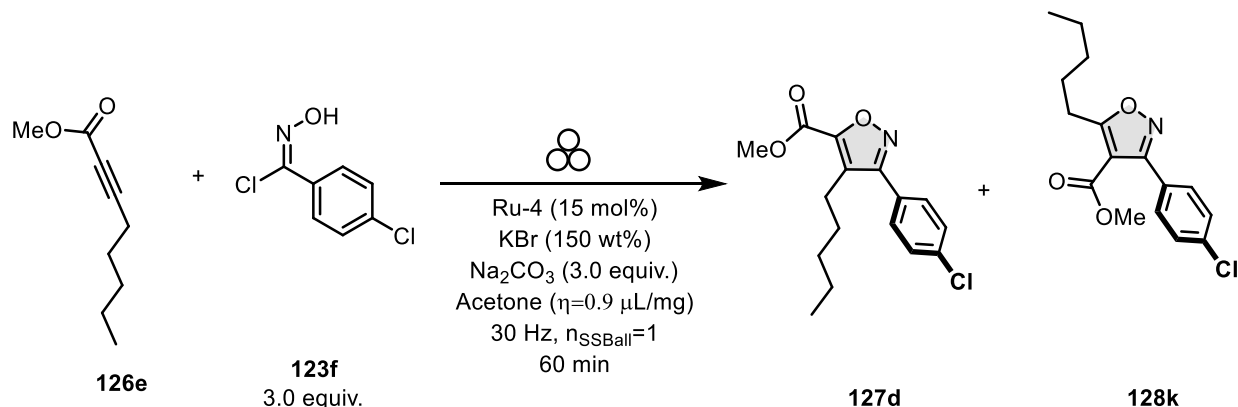
Synthesis of methyl 3-(4-chlorophenyl)-4-pentylisoxazole-5-carboxylate (127d): 3,4,5-isoxazole **127d** was obtained following procedure PS5a. **127d** was isolated as a mixture of isomers by prep-TLC using 9:1 hexane: EtOAc mixture as a colourless oil in >99 % yield (110 mg) with *rr*= 5.6:1. R_f = 0.50 (for the mixture) The NMR signals were deconvoluted using the signal from the ^{1}**H NMR** and ^{13}**C NMR** signals of isolated **128k.** ^{1}**H NMR of *127c*** (500 MHz, CDCl$_3$) δ 7.54 (d, *J* = 8.7 Hz, 2H), 7.47 (d, *J* = 8.7 Hz, 2H), 3.98 (s, 3H), 2.82 − 2.77 (m, 2H), 1.52 − 1.43 (m, 2H), 1.26 (m,4H), 0.83 (t, *J* = 7.1 Hz, 3H).^{1}**H NMR of *128k (undesire)*** (500 MHz, CDCl$_3$) δ 7.44 (d, *J* = 8.7 Hz, 1H), 7.41 (d, *J* = 8.7 Hz, 2H), 3.77 (s, 3H), 2.82 − 2.77 (m, 2H), 1.82 − 1.73 (m, 2H), 1.41 − 1.33 (m, 4H), 0.91 (t, *J* = 7.8 Hz, 3H).^{13}**C NMR of 127c** (125 MHz, CDCl$_3$) δ 162.7, 157.9, 155.7, 155.0, 129.9, 129.5, 129.2, 125.2, 52.5, 29.4, 22.5, 22.1, 13.9.^{13}**C NMR of 128k** *(undesire)* (125 MHz, CDCl$_3$) δ 179.8, 162.3, 161.6, 136.0, 130.7, 129.5, 128.3, 127.1, 51.6, 31.3, 27.4, 27.0, 22.2, 14.0. **HRMS** Calculated for C$_{16}$H$_{18}$NO$_3$Cl [M+H] 308.1048 found 308.1049.

126c   **123b** 3.0 equiv.   Ru-4 (15 mol%) KBr (150 wt%) Na$_2$CO$_3$ (3.0 equiv.) Acetone (η=0.9 µL/mg) 30 Hz, n$_{SSBall}$=1 60 min   **127e**
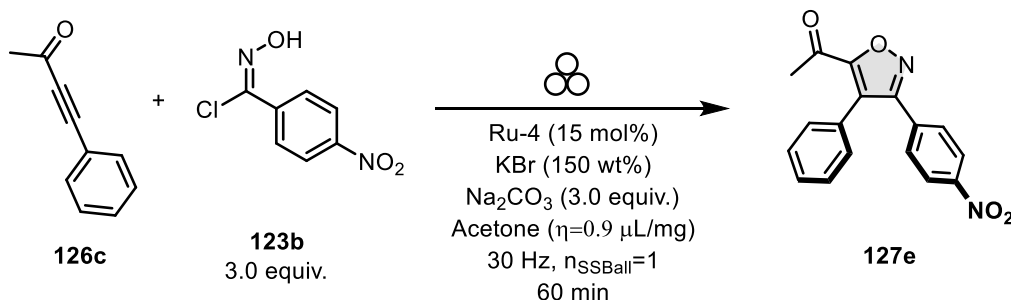
Synthesis of 1-(3-(4-nitrophenyl)-4-phenylisoxazol-5-yl)ethan-1-one (127e): 3,4,5-isoxazole **127e** was obtained following procedure PS5a. **127e** was isolated by prep-TLC using 9:1 Hex:EtOAc mixture as a white solid in 36 % yield (30 mg). R_f = 0.26 ^{1}**H NMR** (500 MHz, Acetone-*d⁶*) δ 8.25 (d, *J* = 9.0 Hz, 2H), 7.68 (d, *J* = 9.0 Hz, 2H), 7.50 − 7.42 (m, 3H), 7.39 (m, 2H), 2.51 (s, 3H). ^{13}**C NMR** (125 MHz, Acetone-*d⁶*) δ 186.5, 162.2,

161.1, 148.8, 134.5, 130.2, 129.7, 128.8, 128.6, 128.1, 123.7, 122.0, 27.6. **HRMS** Calculated for $C_{17}H_{12}N_2O_4$ [M+H] 309.0870 found 309.0873.

Example procedure for Ynols – PS5b:
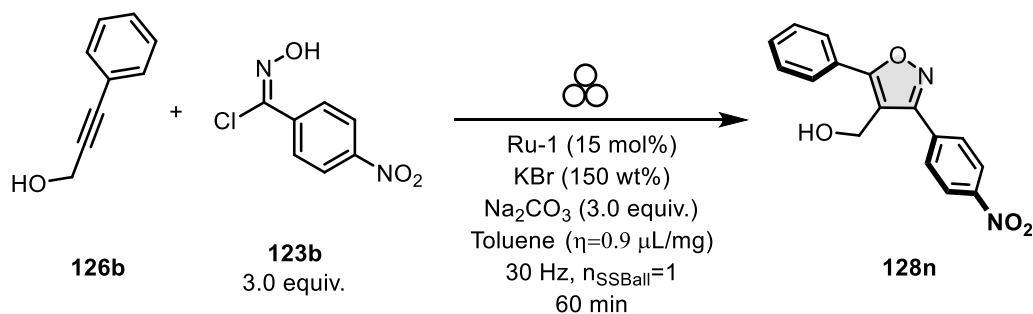
Synthesis of (3-(4-nitrophenyl)-5-phenylisoxazol-4-yl)methanol (128n): In a clear and dry Teflon Jar of 25 mL capacity and 1 SS ball of 1 cm diameter, it was directly weight **126f** (1.0 equiv., 0.378 mmol, 50 mg, 50 µL), hydroxyimidoyl chloride **123b** (3.0 equiv., 1.134 mmol, 227.38 mg), Na_2CO_3 (3.0 equiv., 1.134 mmol, 120.3 mg), KBr (150 wt%, 629 mg), CPME (η= 0.9µL/mg, 943 µL), and **Ru-1** (15 mol%, 0.043 mmol, 21.6 mg). The mixture was closed with the Teflon lit and recovered with parafilm. Then the reagents were milled for 60 minutes at 30 Hz. After 60 minutes, the jar was opened, and the mixture was passed over silica plug, using diethyl ether as an eluent. The desired isoxazole **128n** was isolated by silica gel column chromatography using 8:2 Hex: EtOAc mixture as a yellow solid in 88 % yield (100 mg). R_f= 0.20, **^{1}H NMR** (500 MHz, $CDCl_3$) δ 8.34 (d, J = 8.9 Hz, 2H), 8.10 (d, J = 8.9 Hz, 2H), 7.88 − 7.78 (m, 2H), 7.57 − 7.49 (m, 3H), 4.70 (s, 2H), 1.25 (s, 1H). **^{13}C NMR** (125 MHz, $CDCl_3$) δ 170.0, 162.0, 148.7, 135.1, 130.9, 129.5, 129.2, 127.6, 126.9, 124.1, 112.1, 53.8. **HRMS** Calculated for $C_{16}H_{12}N_2O_4$ [M+H] 297.0870 found 297.0870.

To determine the regioisomer obtained by the Ru catalyze reaction with the Ynols, we performed the reduction of 3,4,5-isoxazole **128g** with DIBAL-H**.**
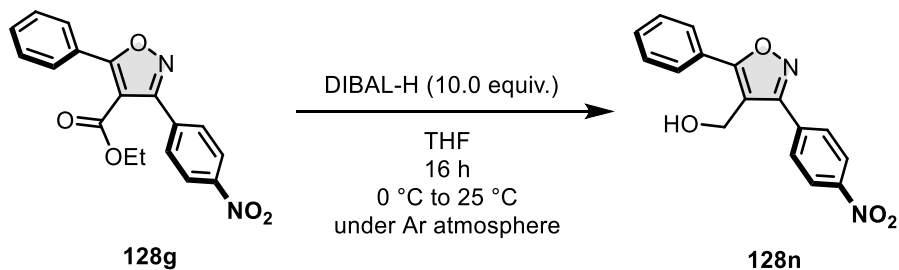
Synthesis of (3-(4-nitrophenyl)-5-phenylisoxazol-4-yl)methanol (128n) from ethyl 3-(4-nitrophenyl)-5-phenylisoxazole-4-carboxylate (128n). In a flamed dried 15 mL round-bottom flask equipped with a stir bar under Ar atmosphere, it was charged with solid 3,4,5-isoxazole **128g** (50 mg, 0.147 mmol, 1.0 equiv.). The solid was dissolved in 5.0 mL of dry THF. The isoxazole solution was cooled to 0 °C by submerging the in and ice-bath solution. Once reached 0 °C temperature, it was slowly added under constant stirring a (1.5 mL, 1.47 mmol, 1.0 equiv.) DIBAL-H solution in THF of approximately 1.0 M. Once all the DIBAL-H solution was added to the isoxazole solution, it was let to warm to 25 °C for a period of 16 h. After 16 h, the mixture was quenched with MeOH. The volume of the solution was reduced under reduced pressure, and the mixture was extracted with EtO_2 (20 mL), brine (2 X 30 mL), and water (2 X 30 mL). The organic layer was dried using Na_2SO_4, reduced under reduced pressure. Isoxazole **128n** was isolated in a silica column from 100 % Hex to 100 % EtOAc. Isoxazole **128n** was obtained in 80 % yield. **^{1}H NMR** (500 MHz, $CDCl_3$) δ 8.34 (d, J = 8.9 Hz, 2H), 8.10 (d, J = 8.9 Hz, 2H), 7.88 − 7.78 (m, 2H), 7.57 − 7.49 (m, 3H), 4.70 (s,

2H), 1.25 (s, 1H). ^{13}**C NMR** (125 MHz, CDCl$_3$) δ 170.0, 162.0, 148.7, 135.1, 130.9, 129.5, 129.2, 127.6, 126.9, 124.1, 112.1, 53.8. **HRMS** Calculated for C$_{16}$H$_{12}$N$_2$O$_4$ [M+H] 297.0870 found 297.0870.

The obtained analytical data matched with that of the isoxazole "128n" obtained by Ru catalysis.
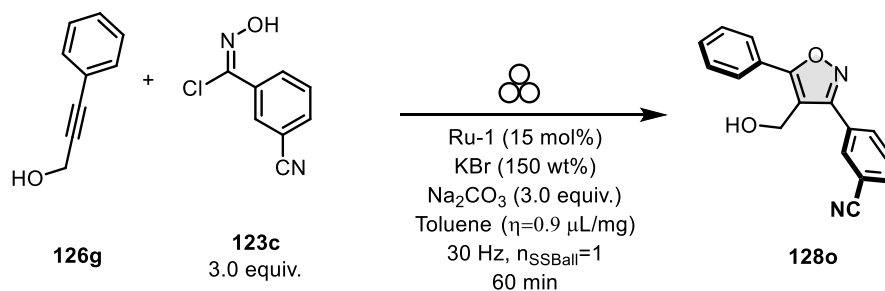
Synthesis of 3-(4-(hydroxymethyl)-5-phenylisoxazol-3-yl)benzonitrile (128o): 3,4,5-isoxazole **128o** was obtained following procedure PS5b. **128o** was isolated by silica column chromatography using 8:2 Hex:EtOAc mixture as a white solid in 88 % yield (92 mg). R_f = 0.12 **^{1}H NMR** (500 MHz, CDCl$_3$) δ 8.23 (s, 1H), 8.16 (d, J = 7.9 Hz, 1H), 7.88 − 7.82 (m, 1H), 7.79 (d, J = 7.8 Hz, 1H), 7.65 (t, J = 7.8 Hz, 1H), 4.70 (d, J = 3.7 Hz, 1H). **^{13}C NMR** (125 MHz, CDCl$_3$) δ 169.9, 162.0, 133.3, 132.8, 132.1, 130.8, 130.4, 129.8, 129.2, 127.6, 127.1, 118.3, 113.3, 111.9, 53.9. **HRMS** Calculated for C$_{17}$H$_{12}$N$_2$O$_2$ [M+H] 277.0972 found 277.0972.
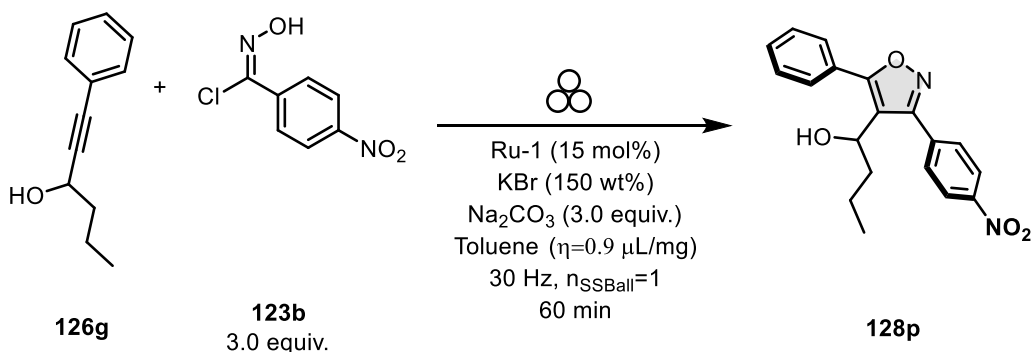
Synthesis of 1-(3-(4-nitrophenyl)-5-phenylisoxazol-4-yl)butan-1-ol (128p): 3,4,5-isoxazole **128p** was obtained following procedure PS5b. **128p** was isolated by silica column chromatography using 8:2 Hex:EtOAc mixture as a white solid in 94 % yield (89 mg). R_f = 0.26 **^{1}H NMR** (500 MHz, CDCl$_3$) δ 8.34 (d, J = 8.7 Hz, 1H), 8.10 (d, J = 8.6 Hz, 1H), 7.85 − 7.69 (m, 1H), 7.62 − 7.33 (m, 1H), 7.26 (s, 1H), 4.94 (t, J = 7.4 Hz, 1H), 1.76 − 1.66 (m, 1H), 1.59 (s, 1H), 1.56 − 1.45 (m, 1H), 1.32 − 1.20 (m, 1H), 1.17 − 1.02 (m, 1H), 0.73 (t, J = 7.4 Hz, 1H). **^{13}C NMR** (125 MHz, CDCl$_3$) δ 168.9, 161.8, 148.6, 136.3, 130.6, 130.5, 128.9, 128.4, 127.4, 123.7, 116.0, 65.5, 37.8, 30.9, 19.4, 13.5. **HRMS** Calculated for C$_{19}$H$_{18}$N$_2$O$_4$ [M+H] 339.1339 found 339.1337.
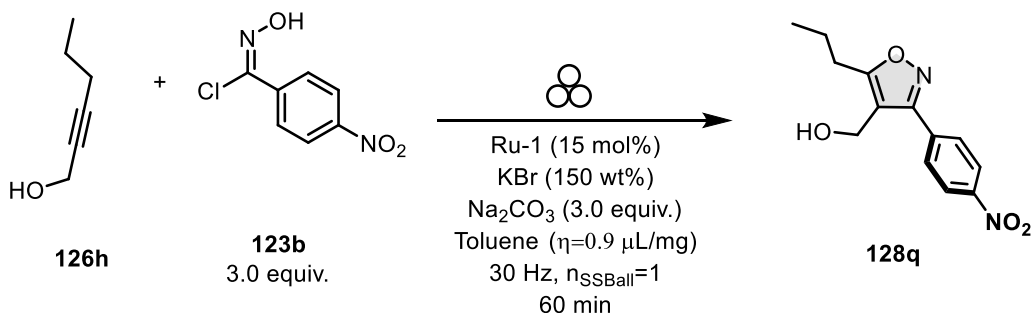
Synthesis of (3-(4-nitrophenyl)-5-propylisoxazol-4-yl)methanol (128q): 3,4,5-isoxazole **128q** was obtained following procedure PS5b. **128q** was isolated by prep-TLC using 7:3 Hex:EtOAc mixture as a yellow oil in 53 % yield (70 mg). R_f = 0.23 **^{1}H NMR** (500 MHz, CDCl$_3$) δ ^{1}H NMR (500 MHz, CDCl3) δ 8.33 (s, J = 7.6 Hz, 2H), 8.08 (d, J = 7.6 Hz, 2H), 4.58 (s, 2H), 2.84 (t, J = 7.0 Hz, 2H), 1.88 – 1.71 (m, 2H), 1.02 (t, J = 7.8 Hz, 3H).**^{13}C NMR** (125 MHz, CDCl$_3$) δ 173.0, 160.8, 148.6, 135.5, 129.3, 124.0, 112.7, 53.4, 27.5, 21.4, 13.8. **HRMS** Calculated for C$_{13}$H$_{14}$N$_2$O$_4$ [M+H] 263.1026 found 263.1027.

4.7.7. Procedure S6 (PS6): Transition Electron Microscope (TEM) Analysis

In this section, it is presented the procedure used to analyze by TEM the formation of Ru nanoparticles to determine the effect of the liquid additives.

The samples were prepared following the procedures outline from **PS2**, **PS5a**, and **PS5b**. From the supernatant obtained in the crude product and using a automated pipette, it was taken 10 µL of the supernatant and it was added to 800 µL of MeOH (The mixture was not sonicated). From the resulting solution, it was place a drop into a carbon-supported grid and it was let to evaporate, the support was studied by TEM.

Reaction Crude after Milling

Supernatant

Pipette 10 µL of the crude's supernatant in 800 µl of MeOH
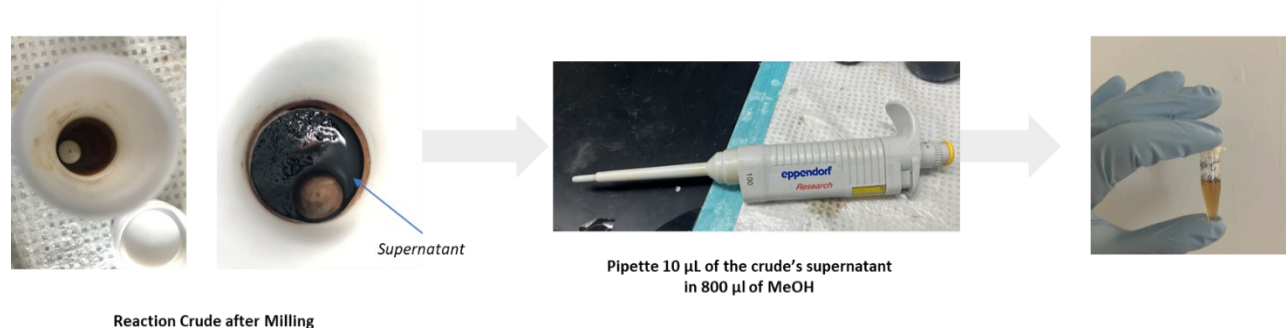
Figure s4.9. TEM sample preparation
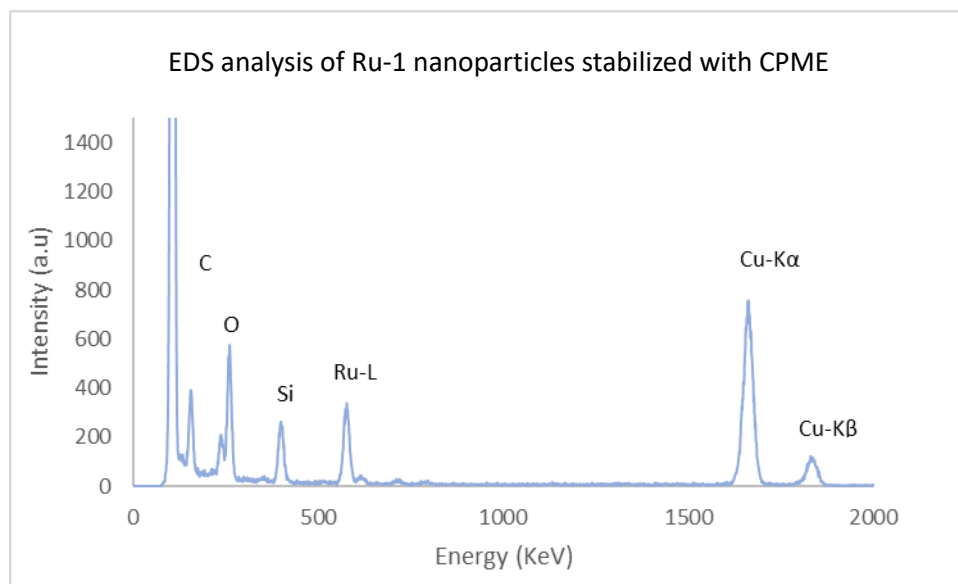
Figure S4.10. EDS elemental Analysis of **Ru-1** nanoparticles on 0.9 µL/mg of CPME
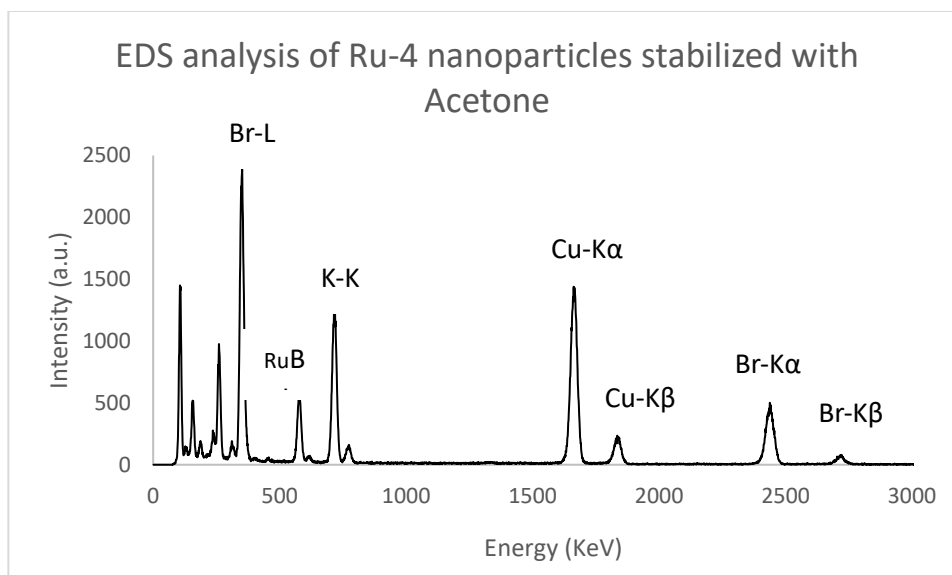
Figure S4.11. EDS elemental Analysis of **Ru-4** nanoparticles on 0.9 µL/mg of Acetone
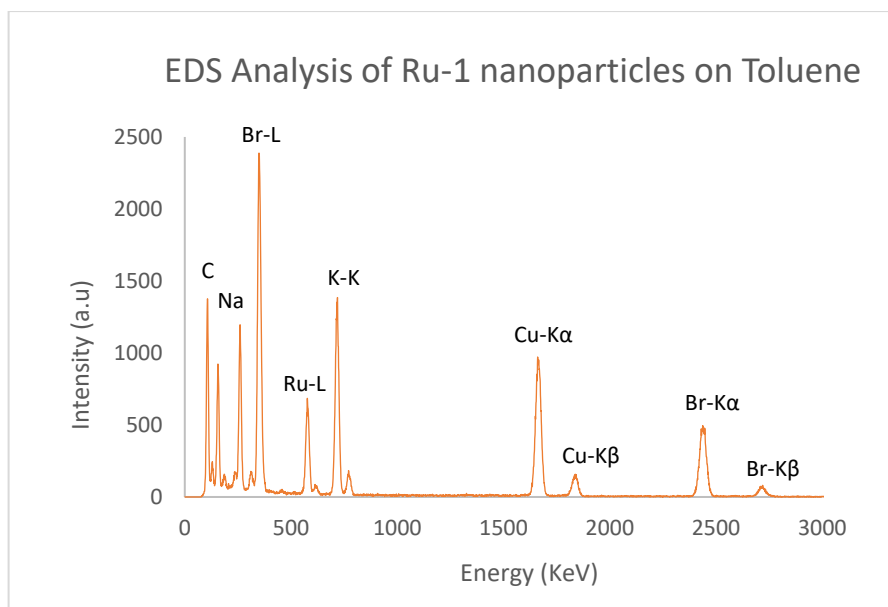
Figure S4.12. EDS elemental Analysis of **RuI** nanoparticles on 0.9 µL/mg of Toluene

4.7.8. Procedure S7 (PS7): Evaluation of Ru Catalyst by PXRD

It was evaluated the effects of LAG on the Ru catalysts (Ru-1 and Ru-4 complex) by milling the Ru catalyst, GAA, and liquid additive for a 60 min.
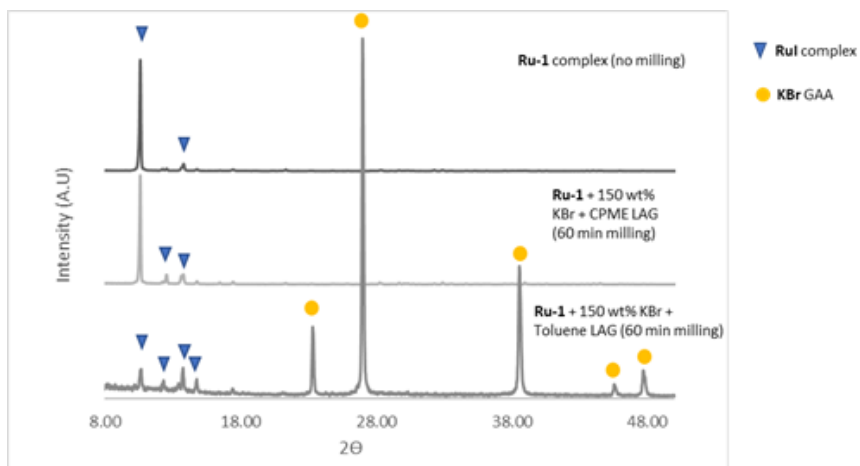
Figure S4.13. PXRD reflection of Ru-1 complex after milling with LAG
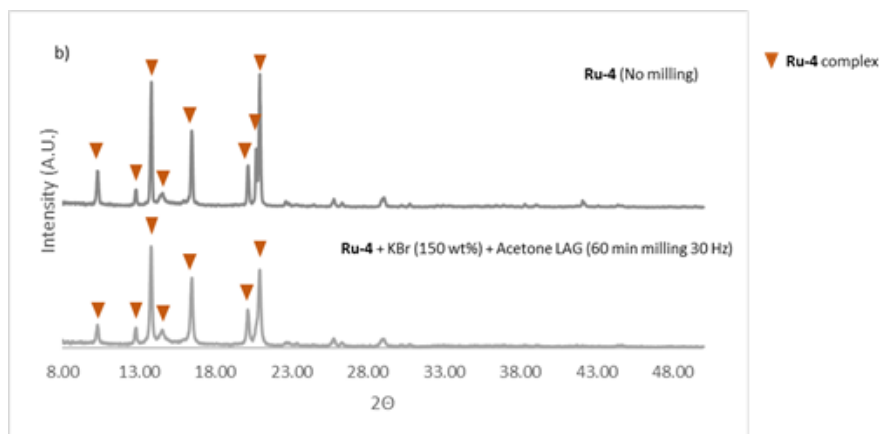
Figure S4.14. PXRD reflection of Ru-4 complex after milling with LAG.

4.7.8. NMR Spectra:

ethyl 4-(3,5-dimethoxyphenyl)isoxazole-3-carboxylate (125b):
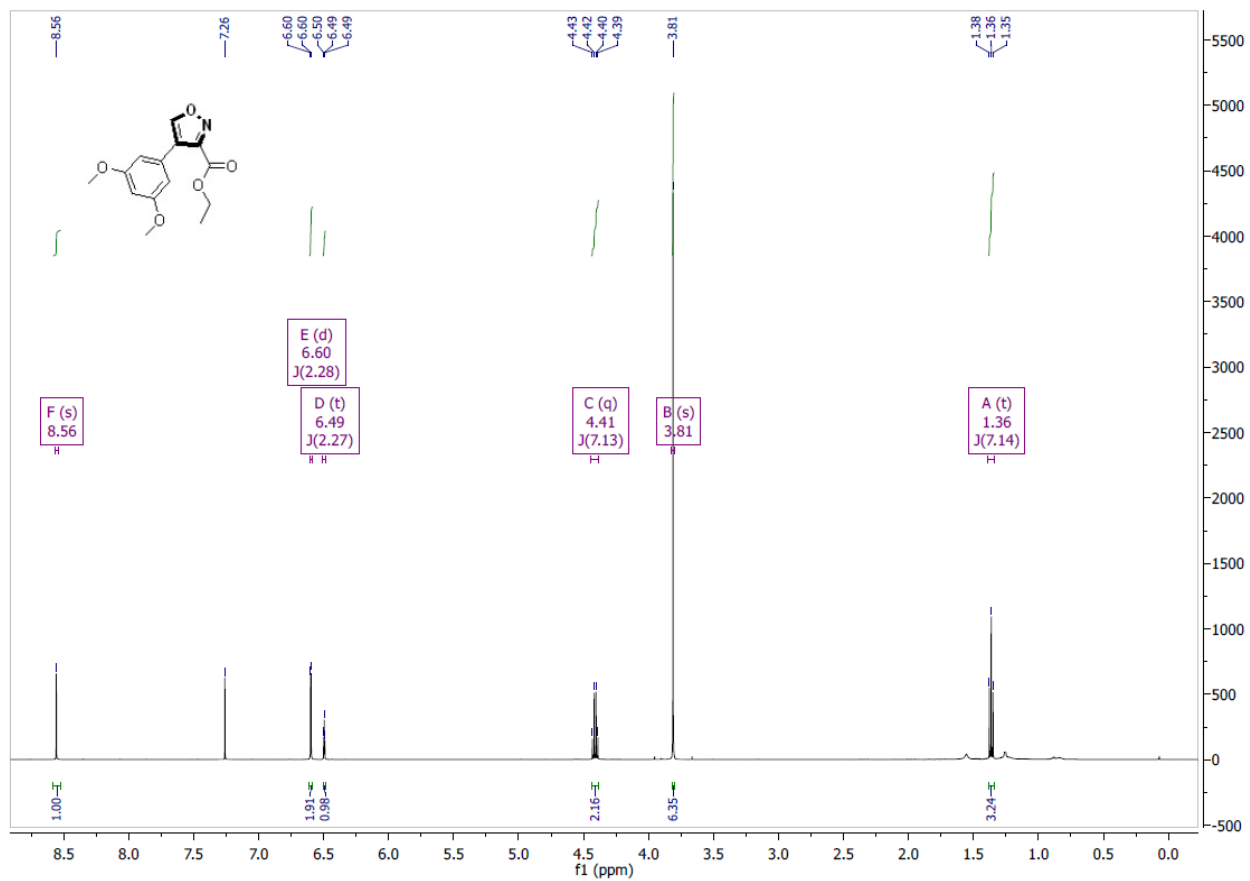
Figure S4.15. ^{1}H NMR of ethyl 4-(3,5-dimethoxyphenyl)isoxazole-3-carboxylate (124b):
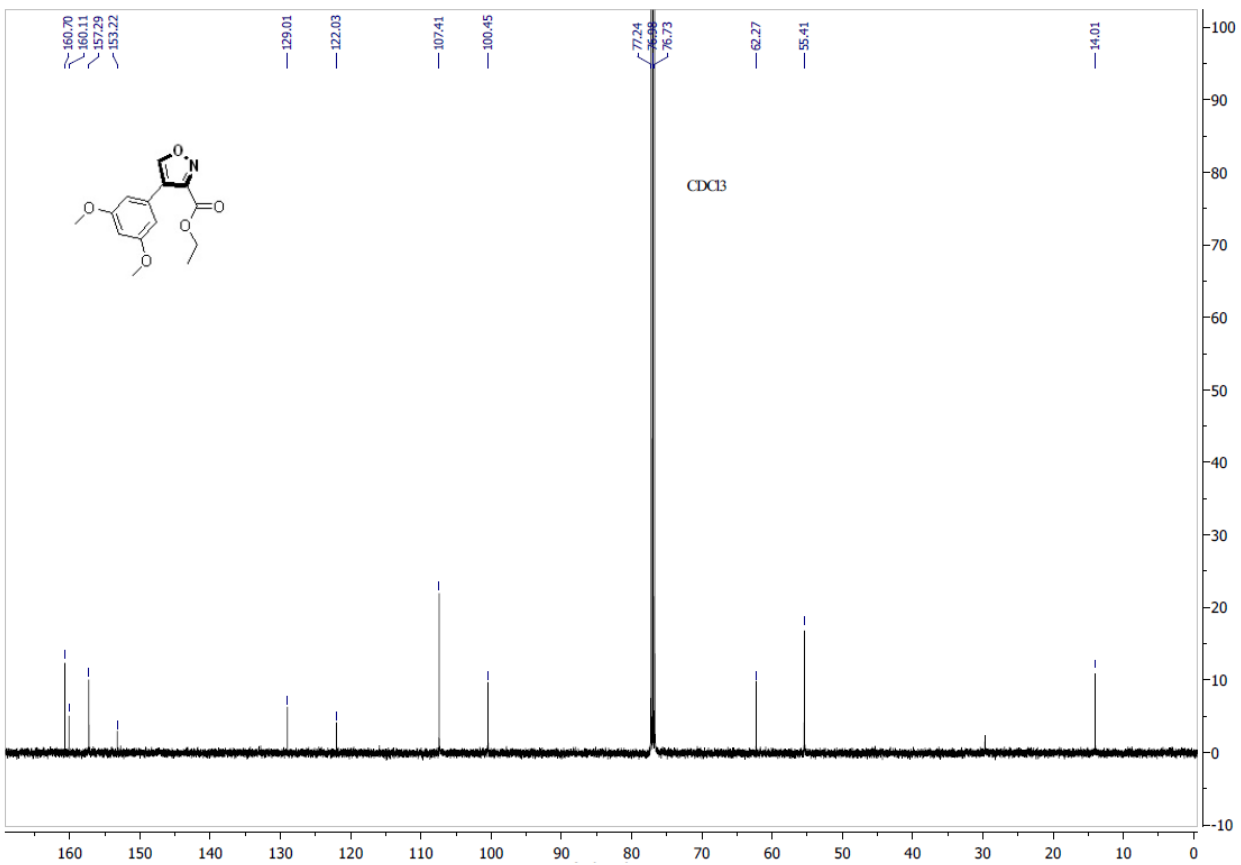
Figure S4.16. ^{13}C NMR of ethyl 4-(3,5-dimethoxyphenyl)isoxazole-3-carboxylate (125b)

ethyl 4-(4-(methoxycarbonyl)phenyl)isoxazole-3-carboxylate (125c):
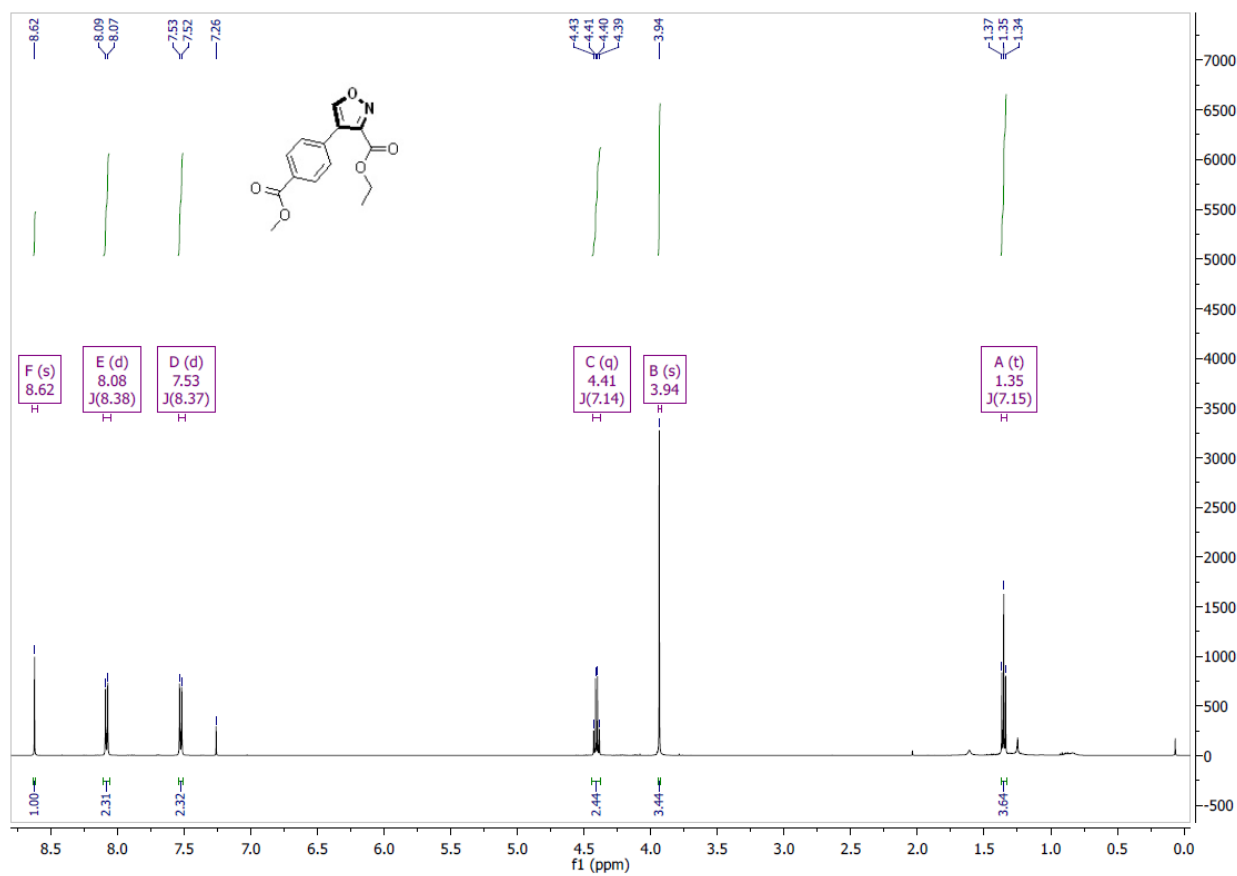
Figure S4.17. ^{1}H NMR of ethyl 4-(4-(methoxycarbonyl)phenyl)isoxazole-3-carboxylate (125c)
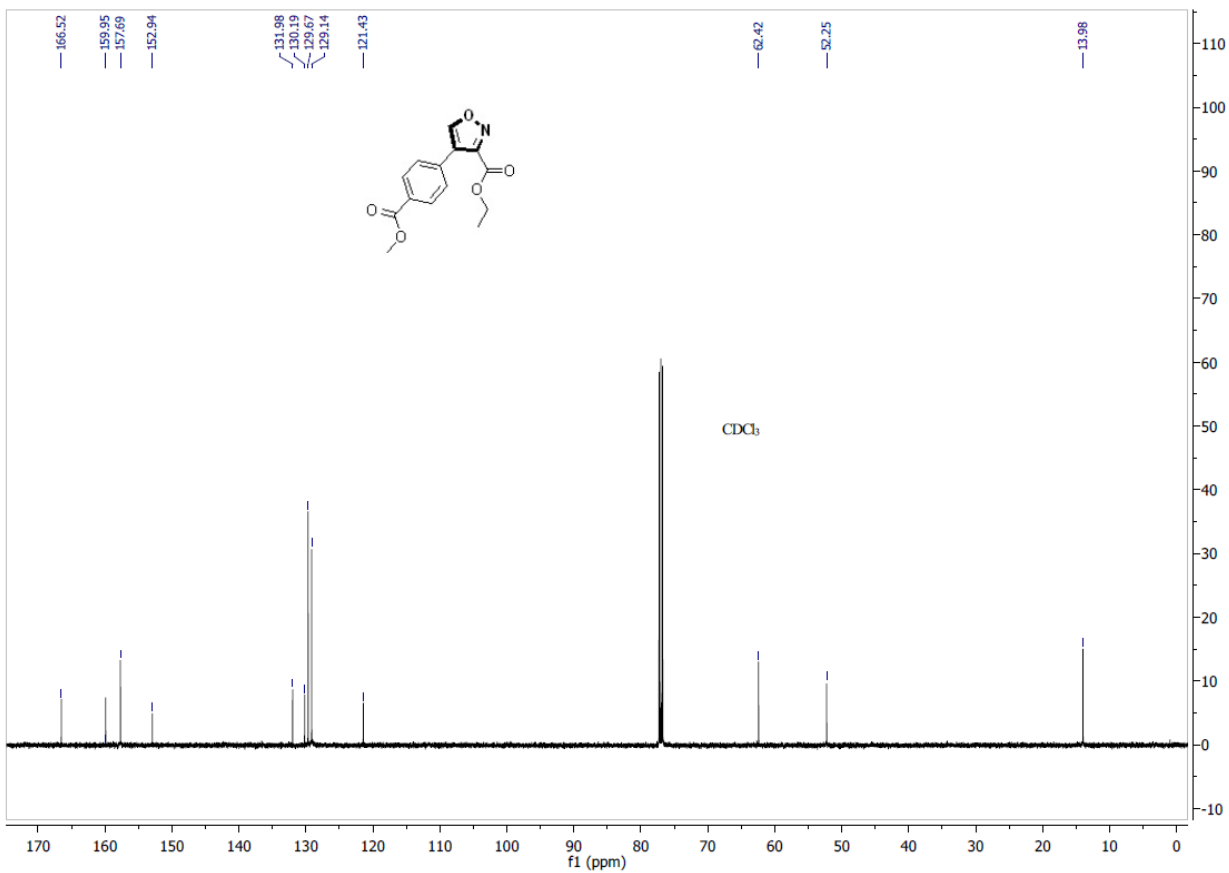
Figure S4.18. ^{13}C NMR of ethyl 4-(4-(methoxycarbonyl)phenyl)isoxazole-3-carboxylate (125c)

ethyl 4-cyclohexylisoxazole-3-carboxylate (125e):

Figure S4.19. ^{1}H NMR of ethyl 4-cyclohexylisoxazole-3-carboxylate (125e)
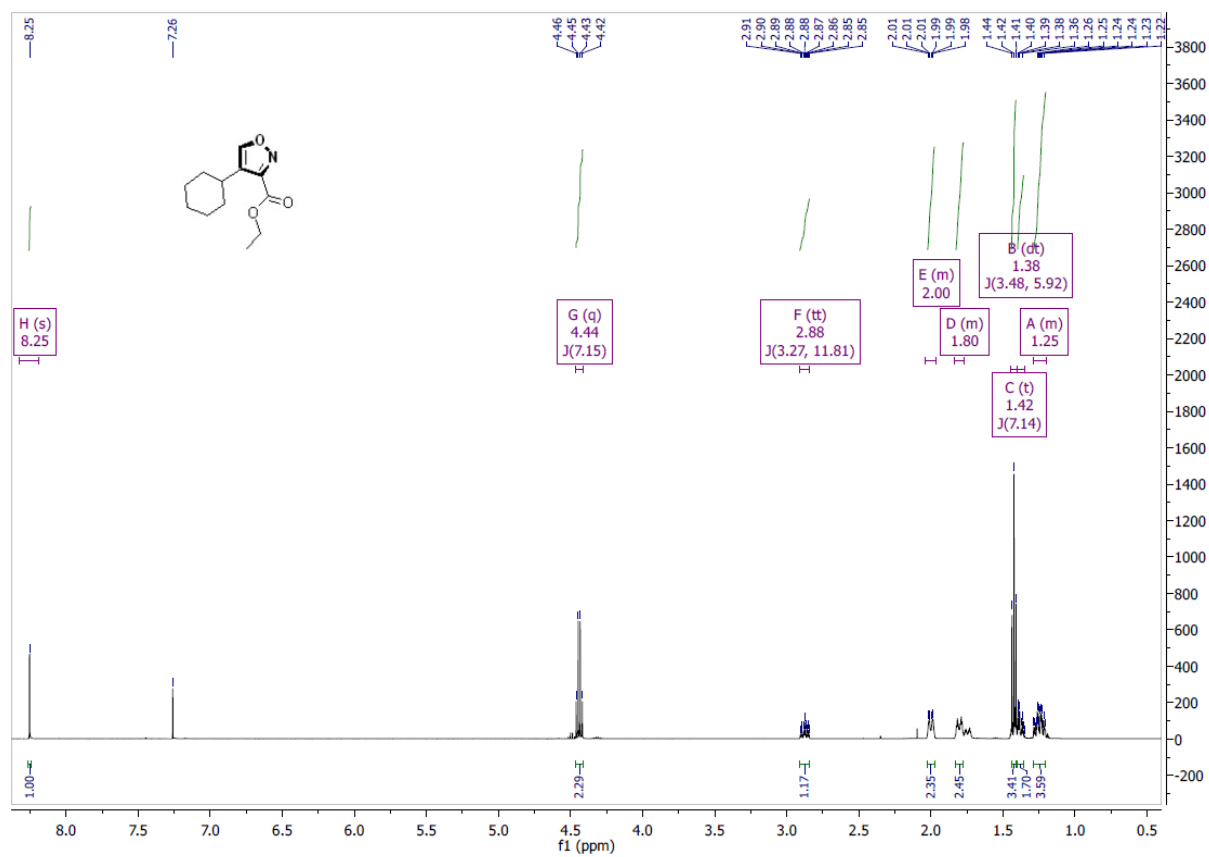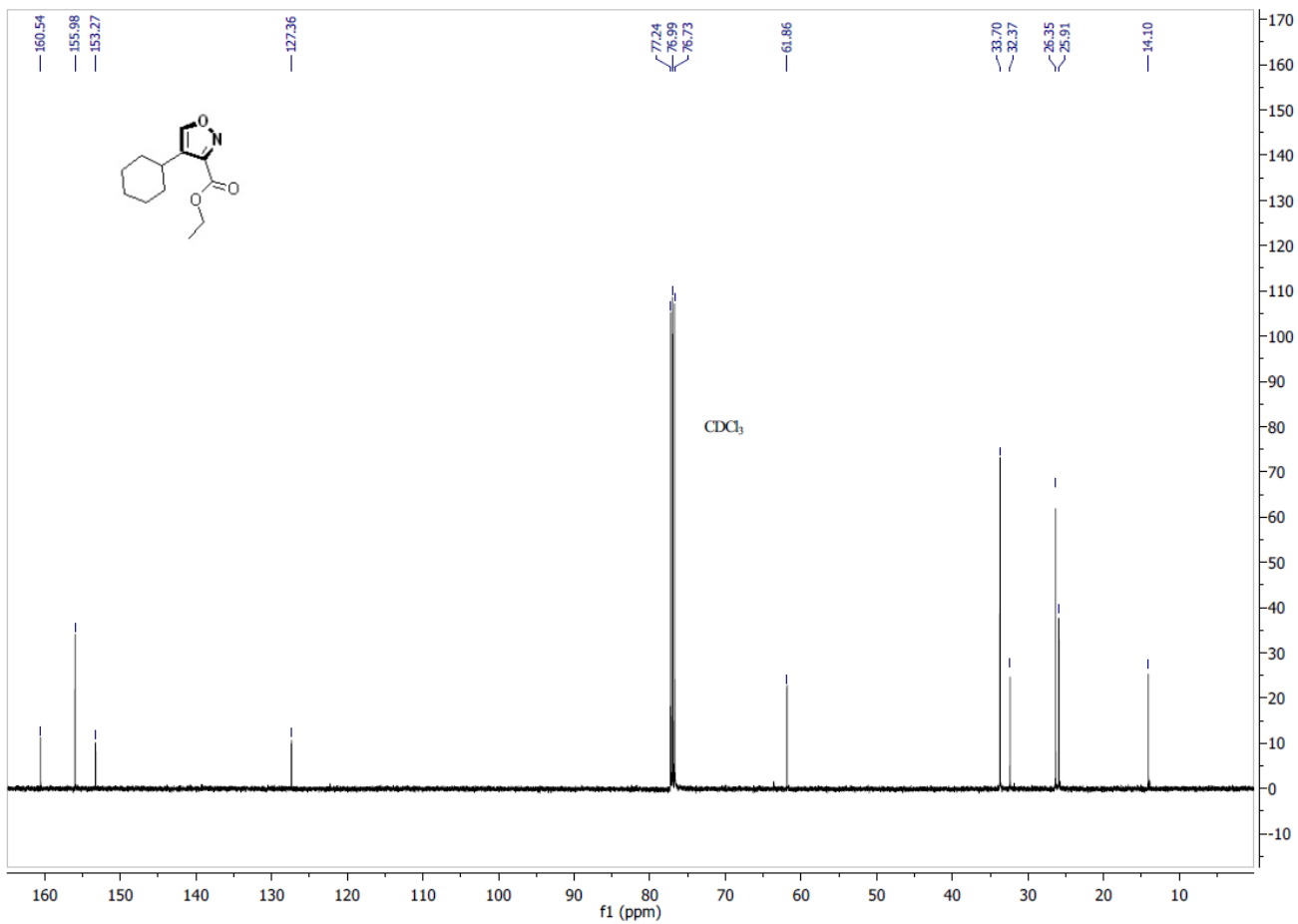
Figure S4.20. ^{13}C NMR of ethyl 4-cyclohexylisoxazole-3-carboxylate (125e)

ethyl 4-butylisoxazole-3-carboxylate (125f):
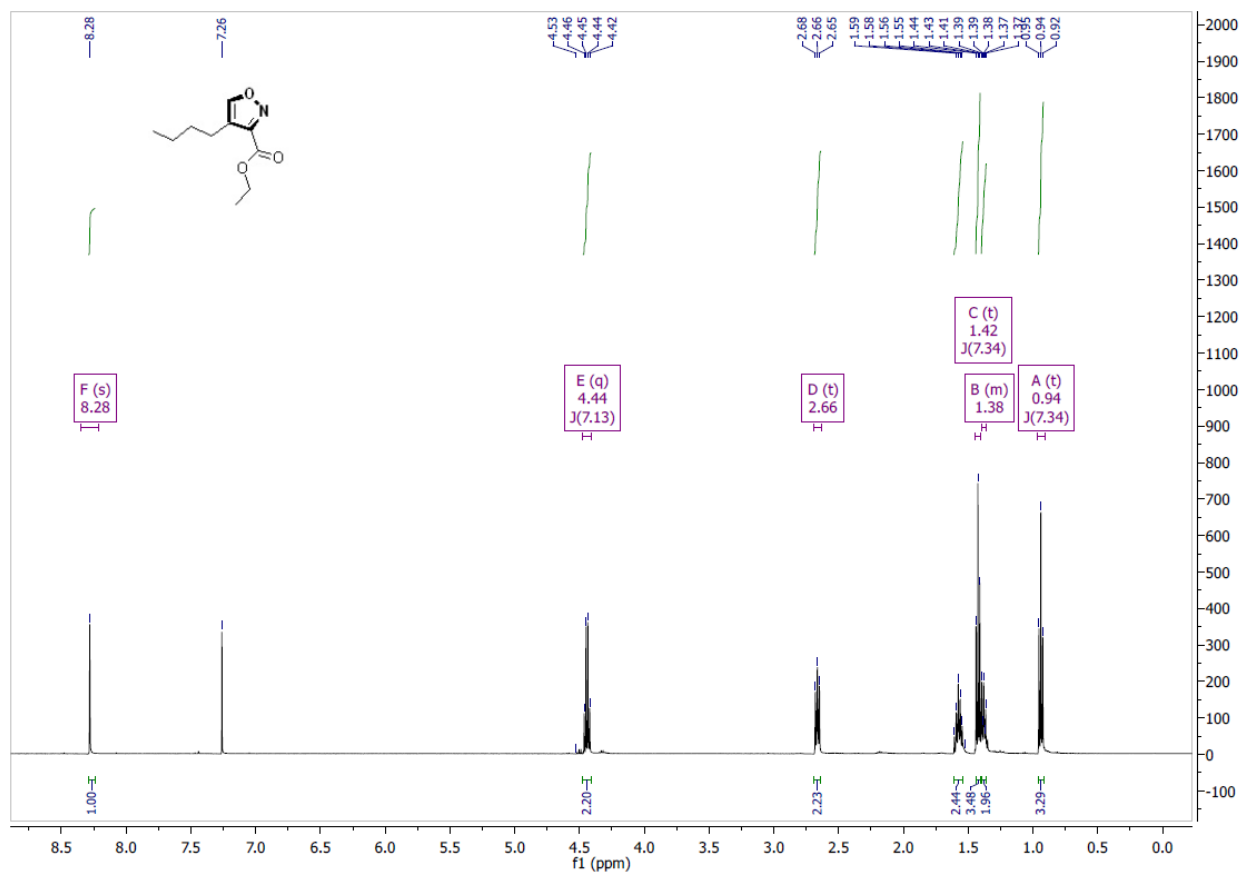
Figure S4.21. ¹H NMR of ethyl 4-butylisoxazole-3-carboxylate (125f)
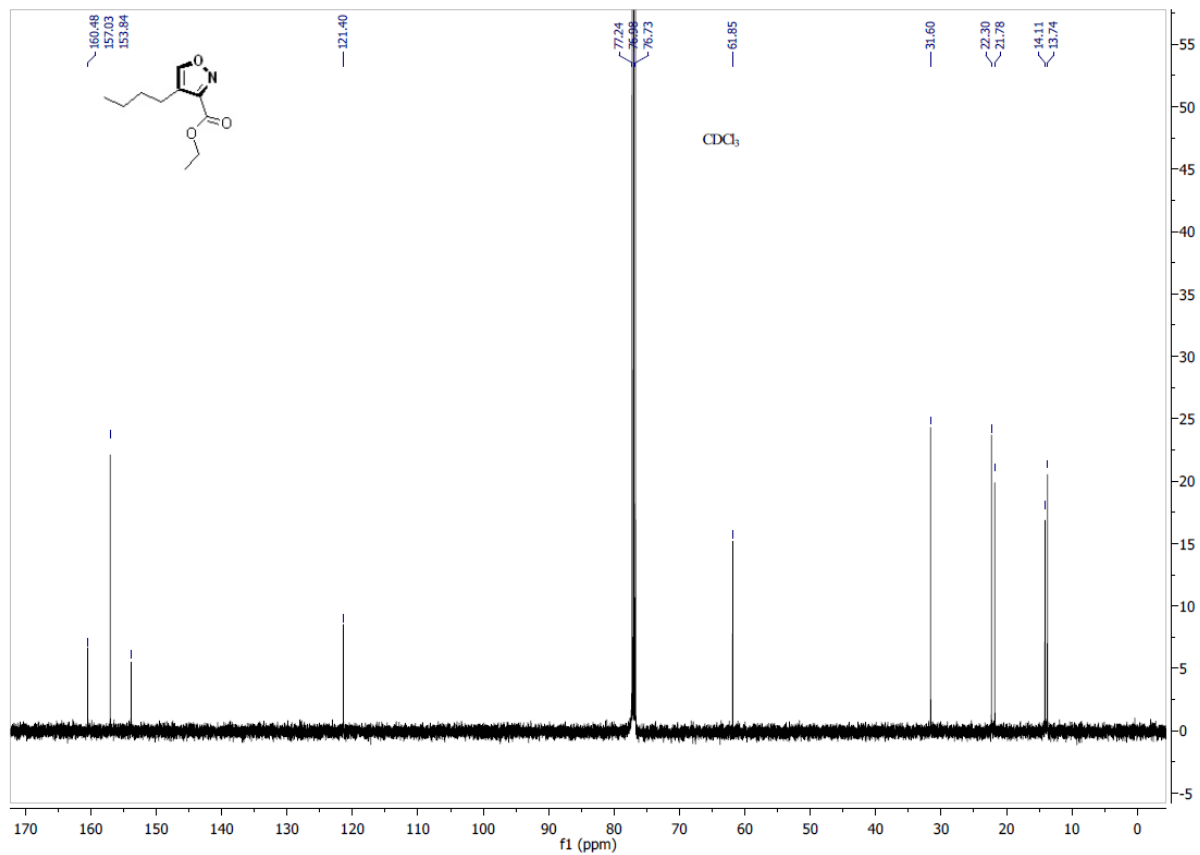
Figure S4.22. ^{13}C NMR of ethyl 4-butylisoxazole-3-carboxylate (125f)

2-(3-(4-nitrophenyl)isoxazol-4-yl)ethan-1-ol (125g):
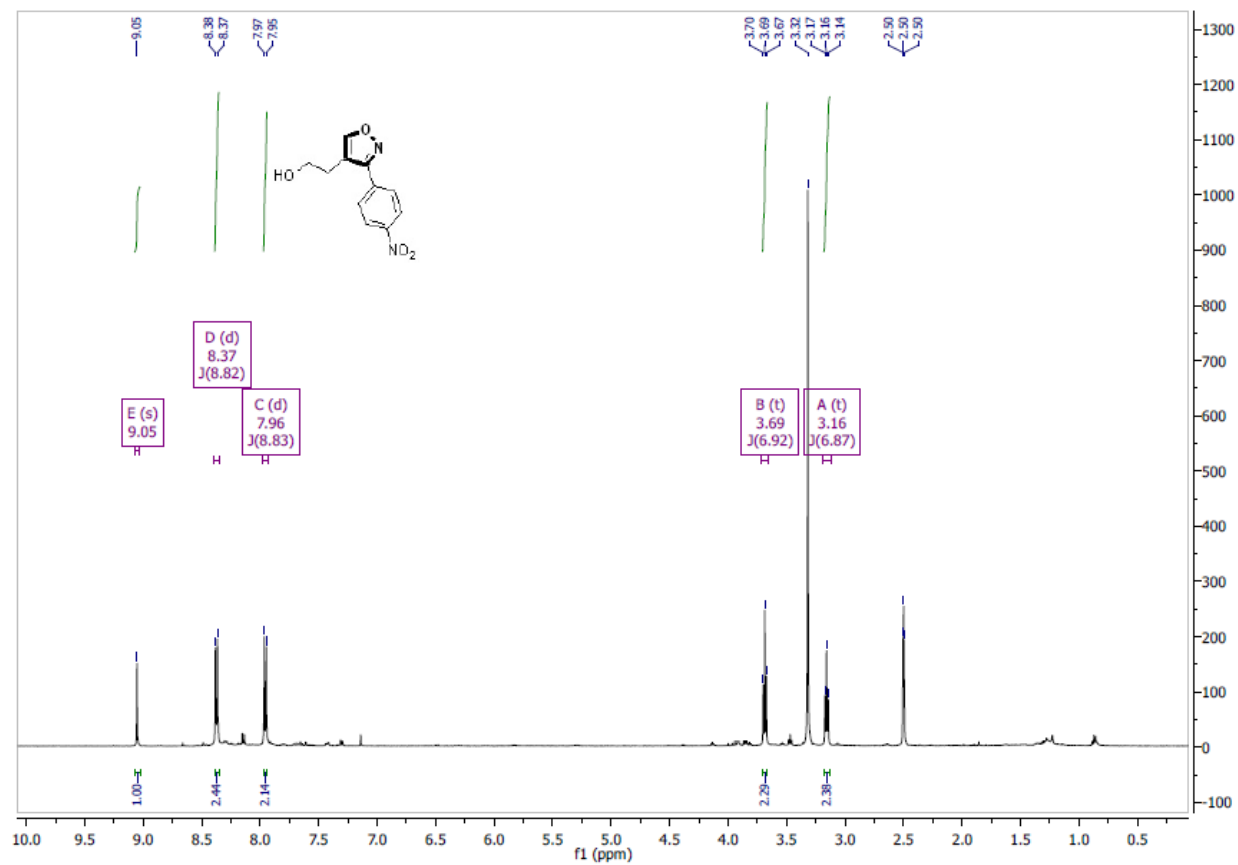
Figure S4.23. ¹H NMR of 2-(3-(4-nitrophenyl)isoxazol-4-yl)ethan-1-ol (125g)
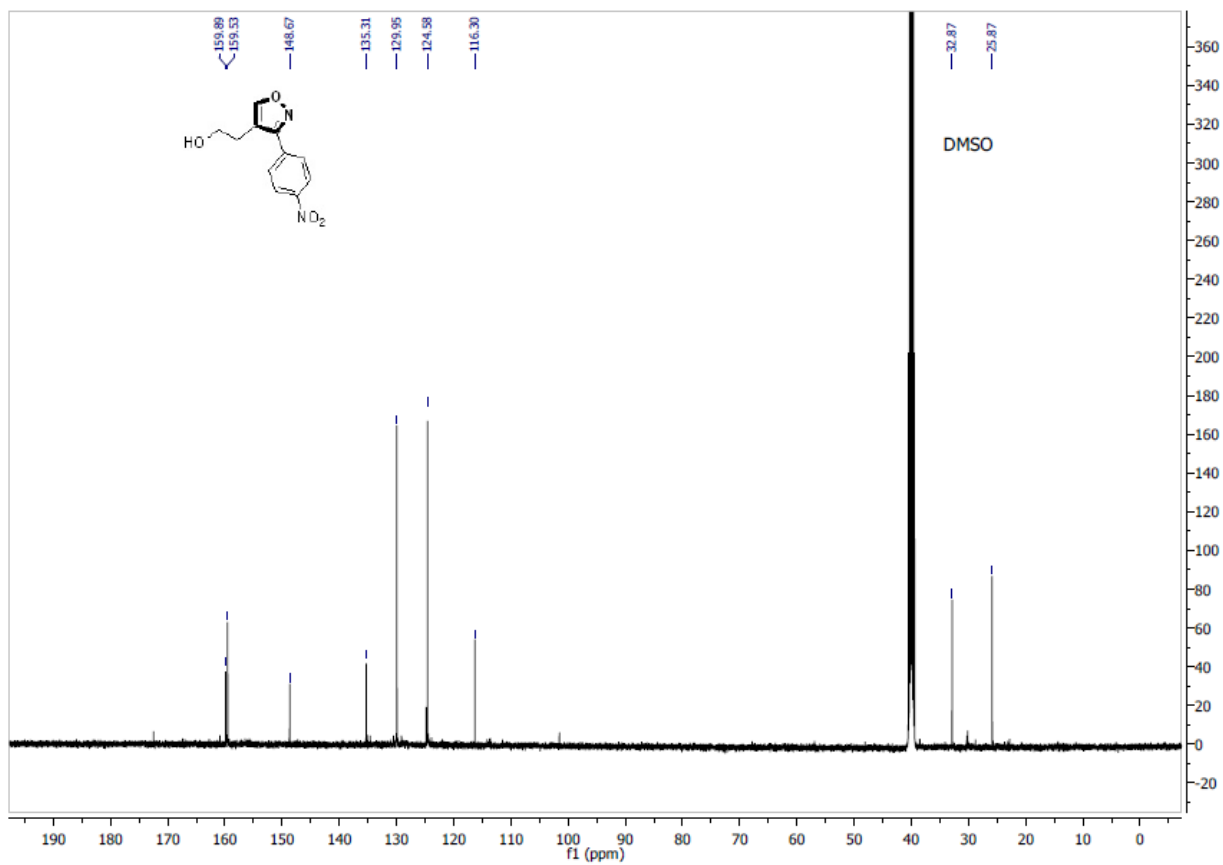
Figure S4.24. ^{13}C NMR of 2-(3-(4-nitrophenyl)isoxazol-4-yl)ethan-1-ol (125g)

1-(3-(4-nitrophenyl)isoxazol-4-yl)cyclohexan-1-ol (125h):
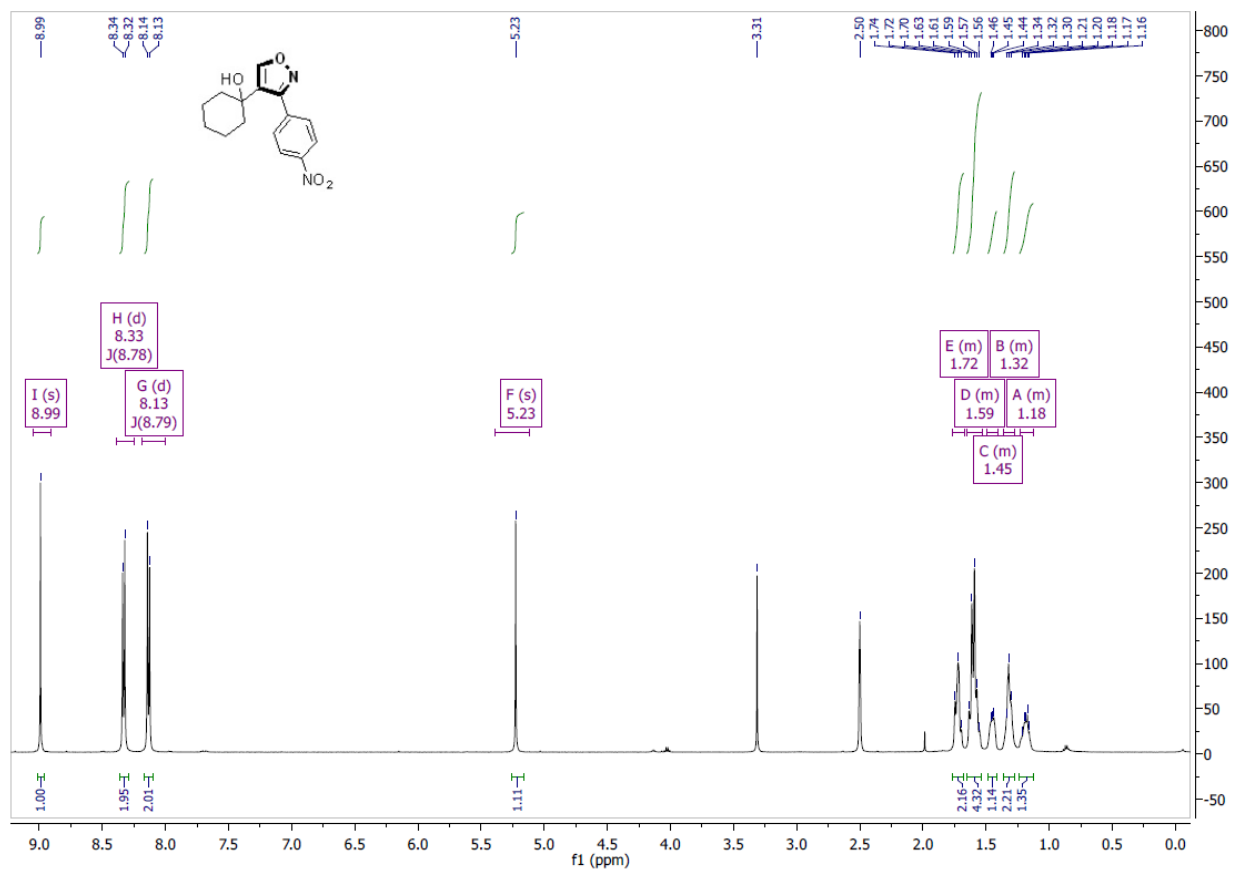
Figure S4.25. ¹H NMR of 1-(3-(4-nitrophenyl)isoxazol-4-yl)cyclohexan-1-ol (125h)
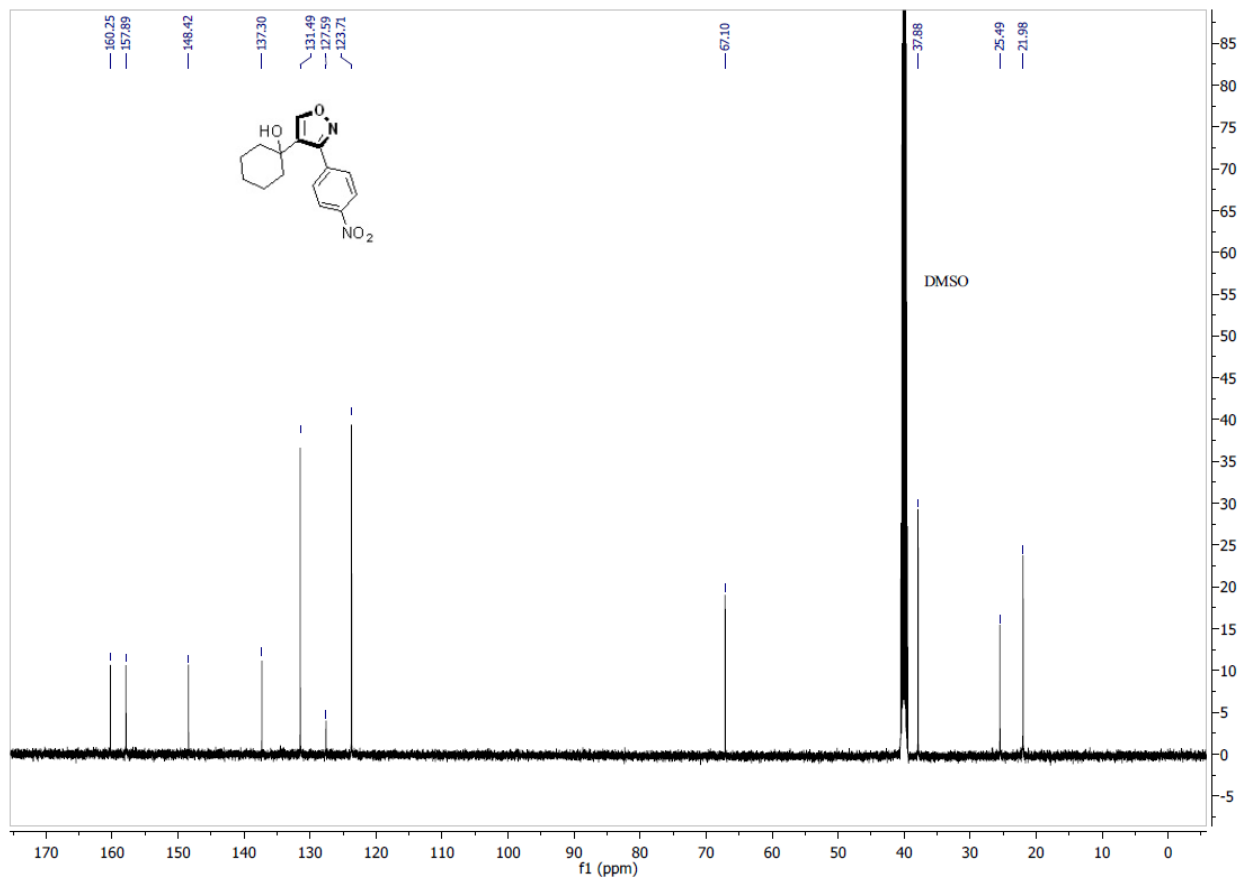
Figure S4.26. ^{13}C NMR of 1-(3-(4-nitrophenyl)isoxazol-4-yl)cyclohexan-1-ol (125h)

3-(4-(1-hydroxycyclohexyl)isoxazol-3-yl)benzonitrile (125i)
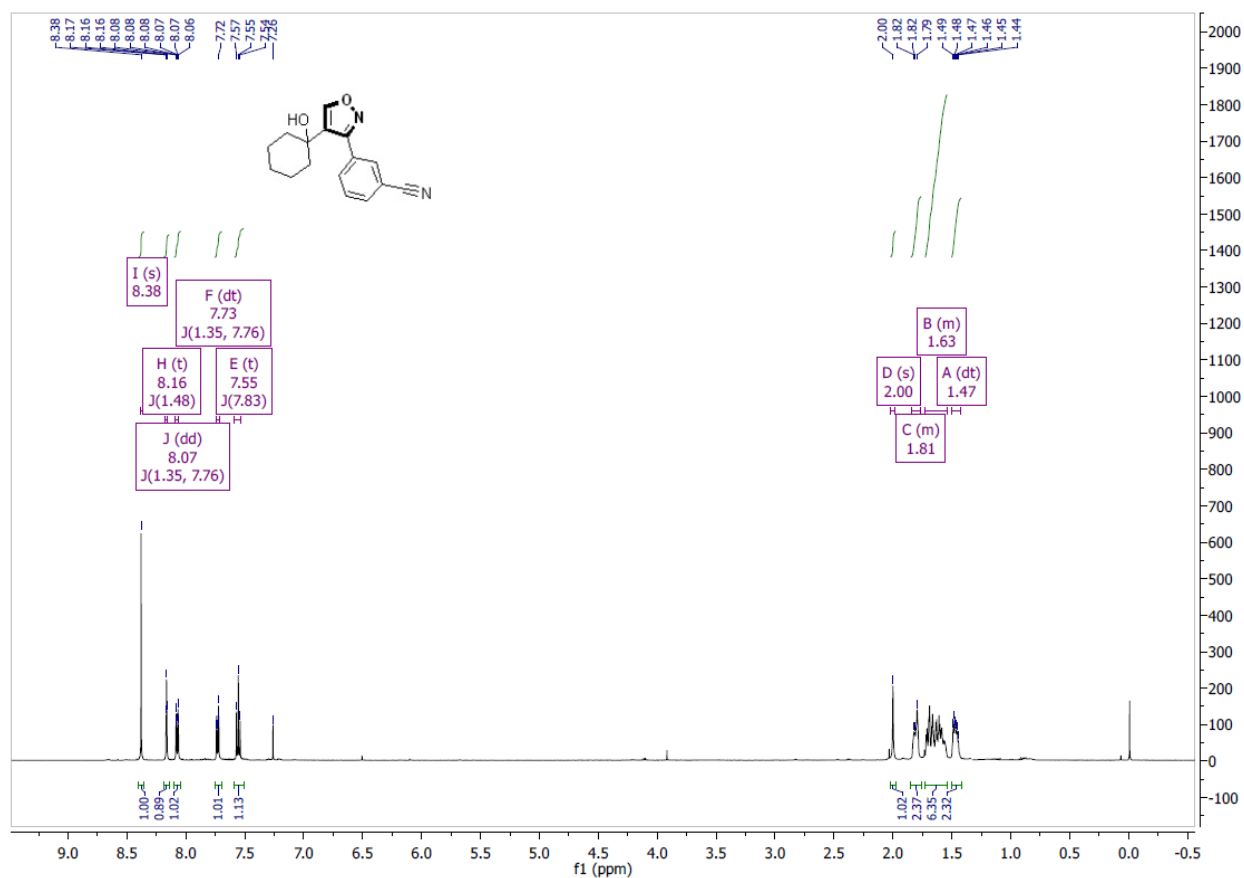
Figure S4.27. ^{1}H NMR of 3-(4-(1-hydroxycyclohexyl)isoxazol-3-yl)benzonitrile (125i)
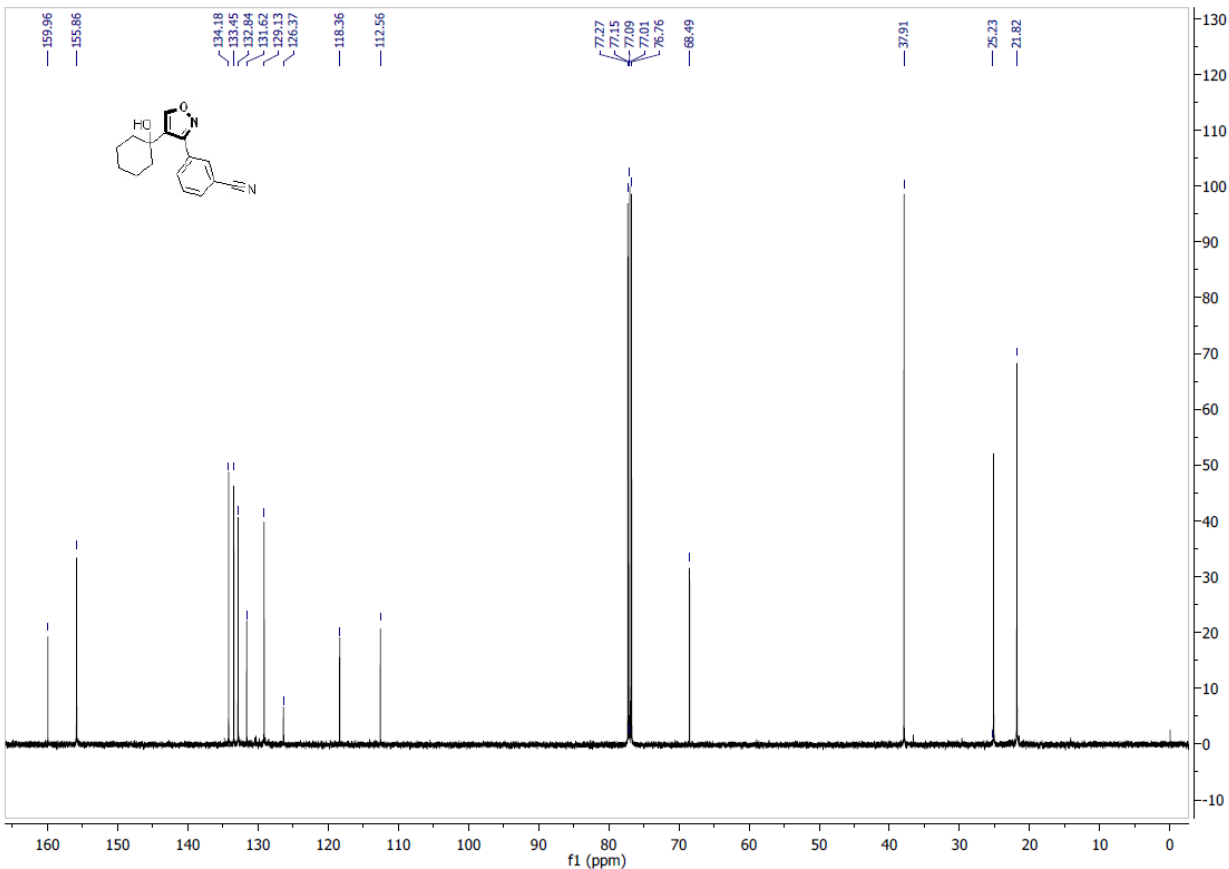
Figure S4.28. 13C NMR of 3-(4-(1-hydroxycyclohexyl)isoxazol-3-yl)benzonitrile (125i)

ethyl 5-(3-(3-(ethoxycarbonyl)isoxazol-4-yl)propyl)isoxazole-3-carboxylate (125j):
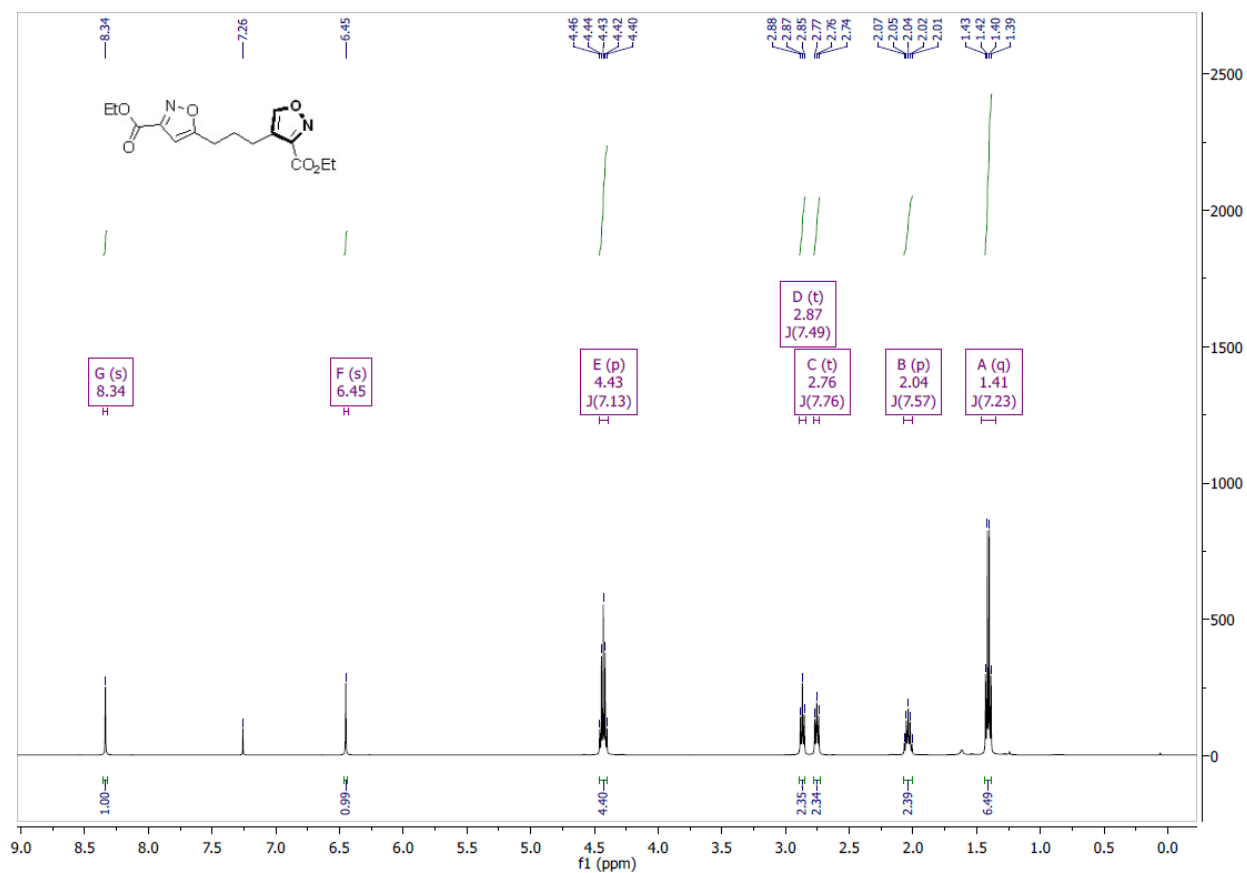
Figure S4.29. ^{1}H NMR of ethyl 5-(3-(3-(ethoxycarbonyl)isoxazol-4-yl)propyl)isoxazole-3-carboxylate (125j)
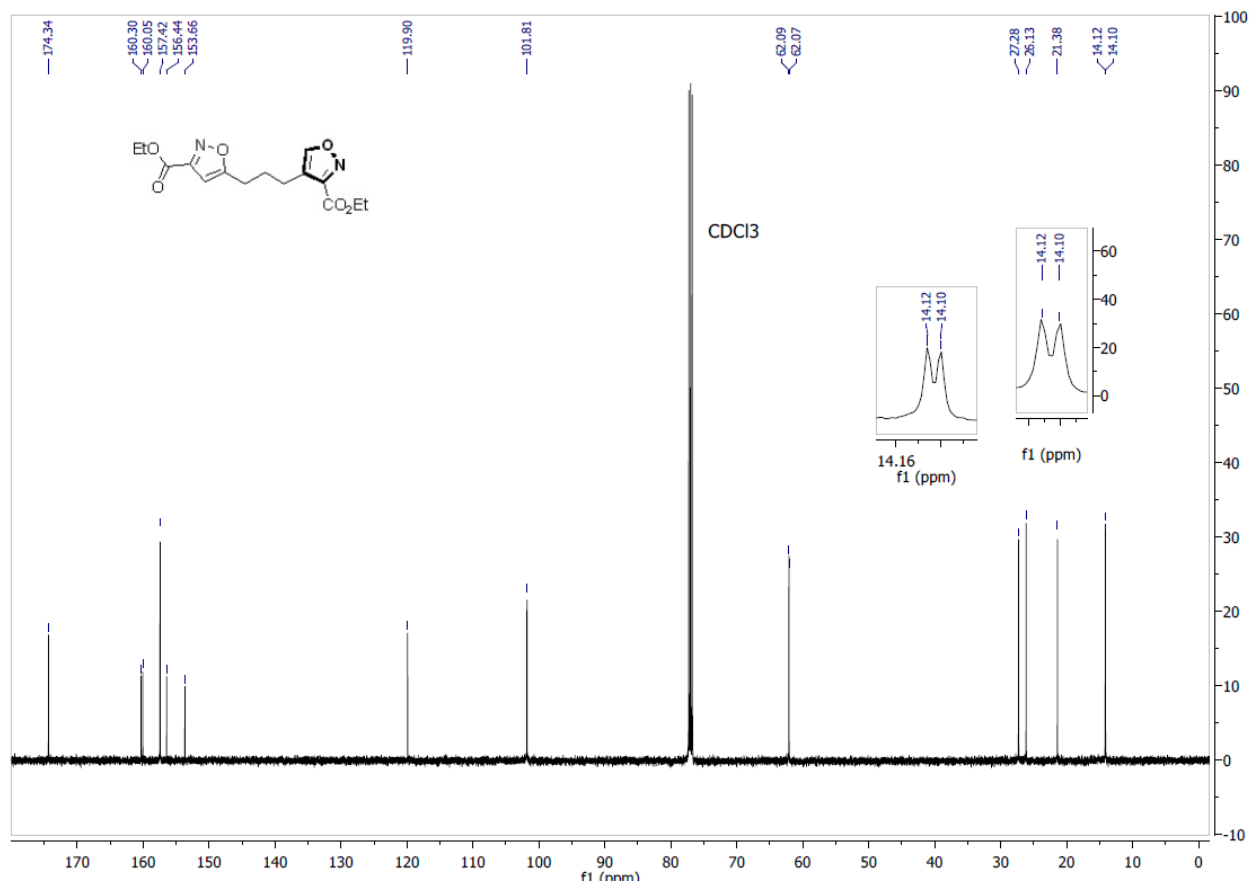
Figure S4.30. ^{13}C NMR of ethyl 5-(3-(3-(ethoxycarbonyl)isoxazol-4-yl)propyl)isoxazole-3-carboxylate (125j)

(9S,13R,14S,17S)-17-(3-(4-nitrophenyl)isoxazol-4-yl)-7,8,9,11,12,13,14,15,16,17-decahydro-6H-cyclopenta[a]phenanthrene-3,17-diol (125k):
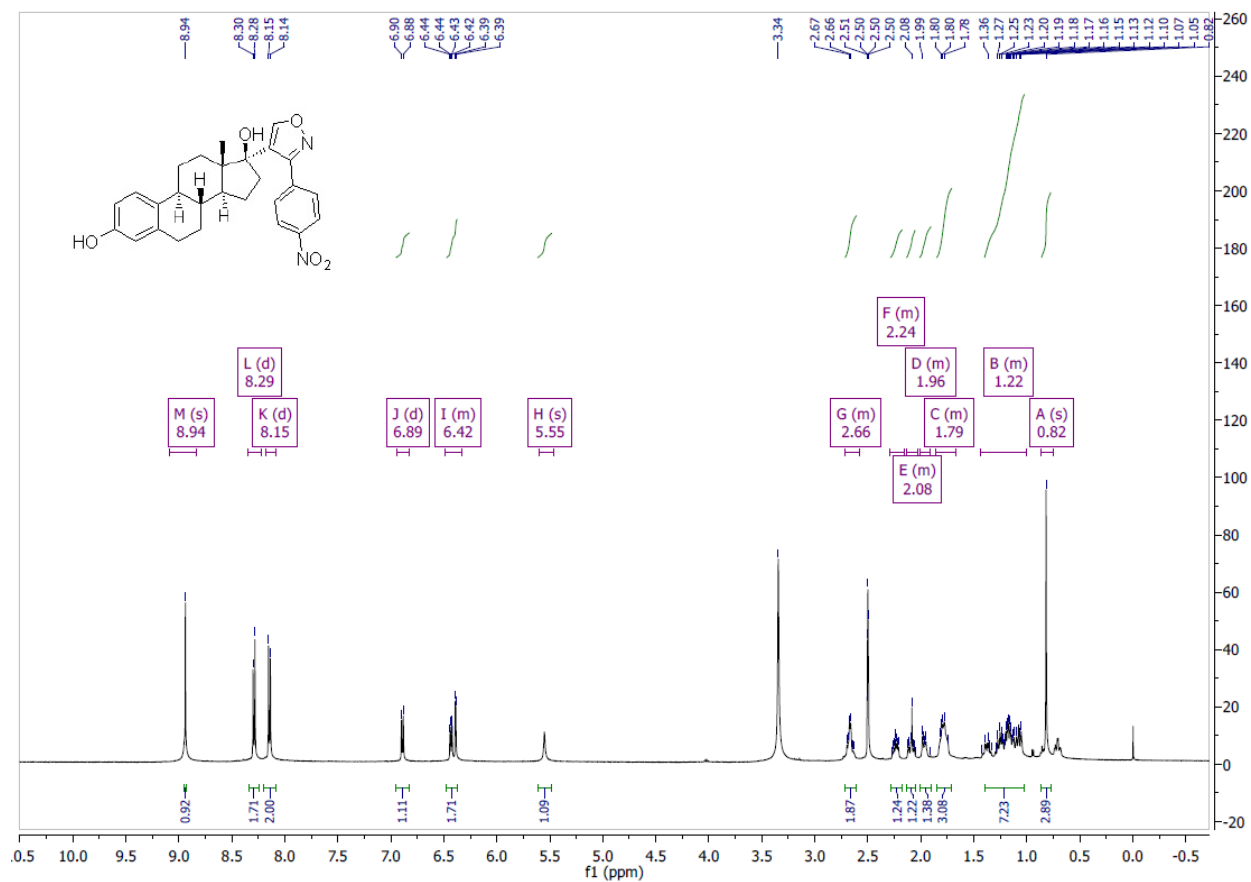
Figure S4.31. ^{1}H NMR of (9S,13R,14S,17S)-17-(3-(4-nitrophenyl)isoxazol-4-yl)-7,8,9,11,12,13,14,15,16,17-decahydro-6H-cyclopenta[a]phenanthrene-3,17-diol (125k)
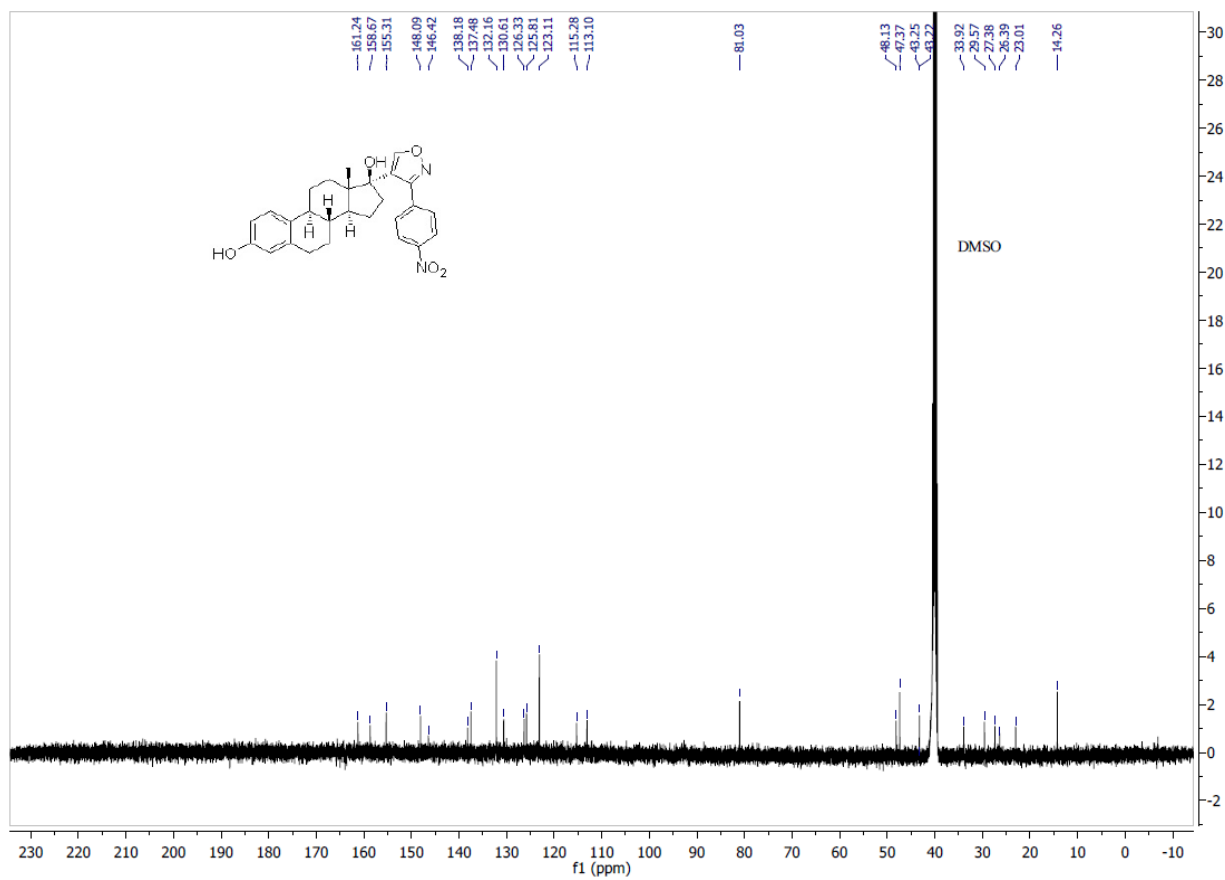
Figure S4.32. ^{13}C NMR of (9S,13R,14S,17S)-17-(3-(4-nitrophenyl)isoxazol-4-yl)-7,8,9,11,12,13,14,15,16,17-decahydro-6H-cyclopenta[a]phenanthrene-3,17-diol (125k)

triethyl isoxazole-3,4,5-tricarboxylate (128a):
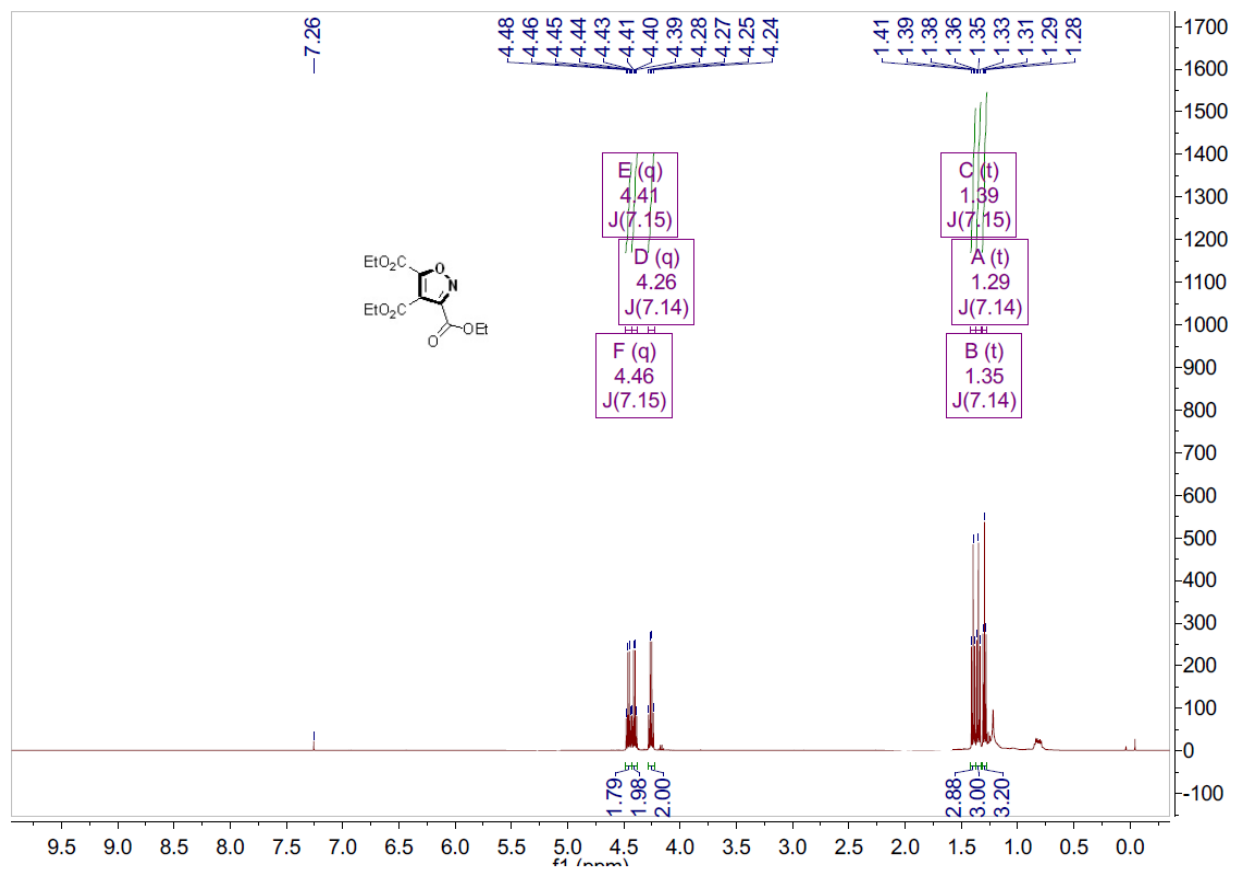
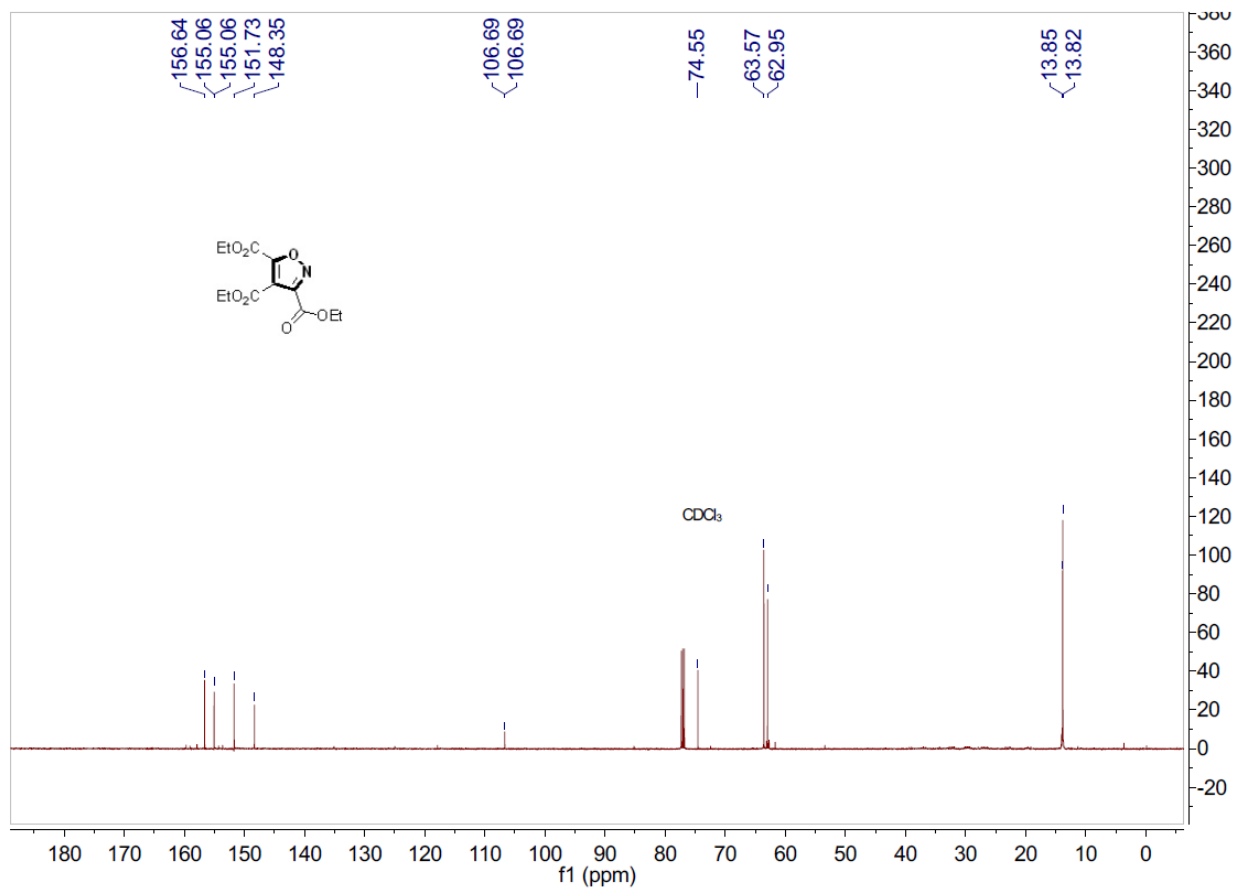**Figure S4.33**. ^{1}H NMR of triethyl isoxazole-3,4,5-tricarboxylate (128a)

Figure S4.34. ^{13}C NMR of triethyl isoxazole-3,4,5-tricarboxylate (128a)

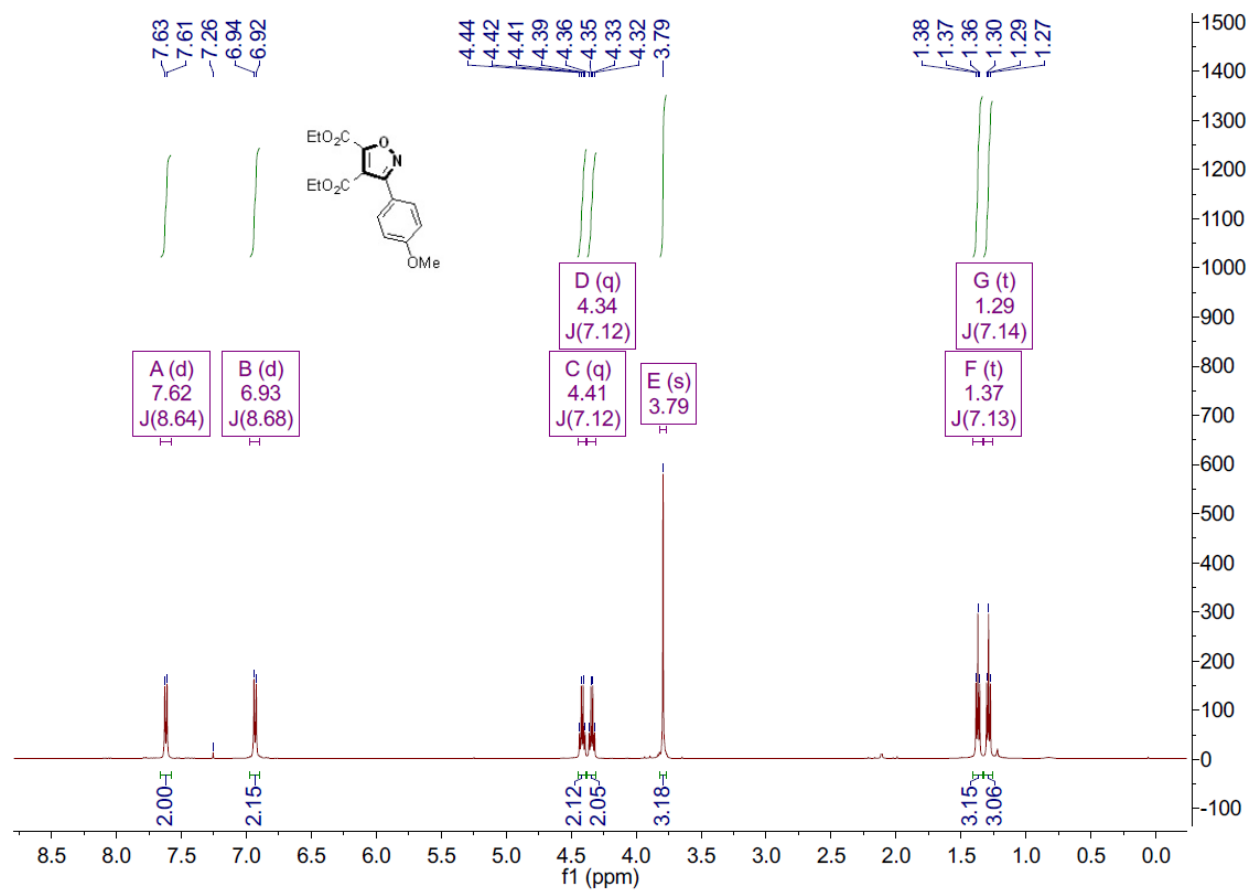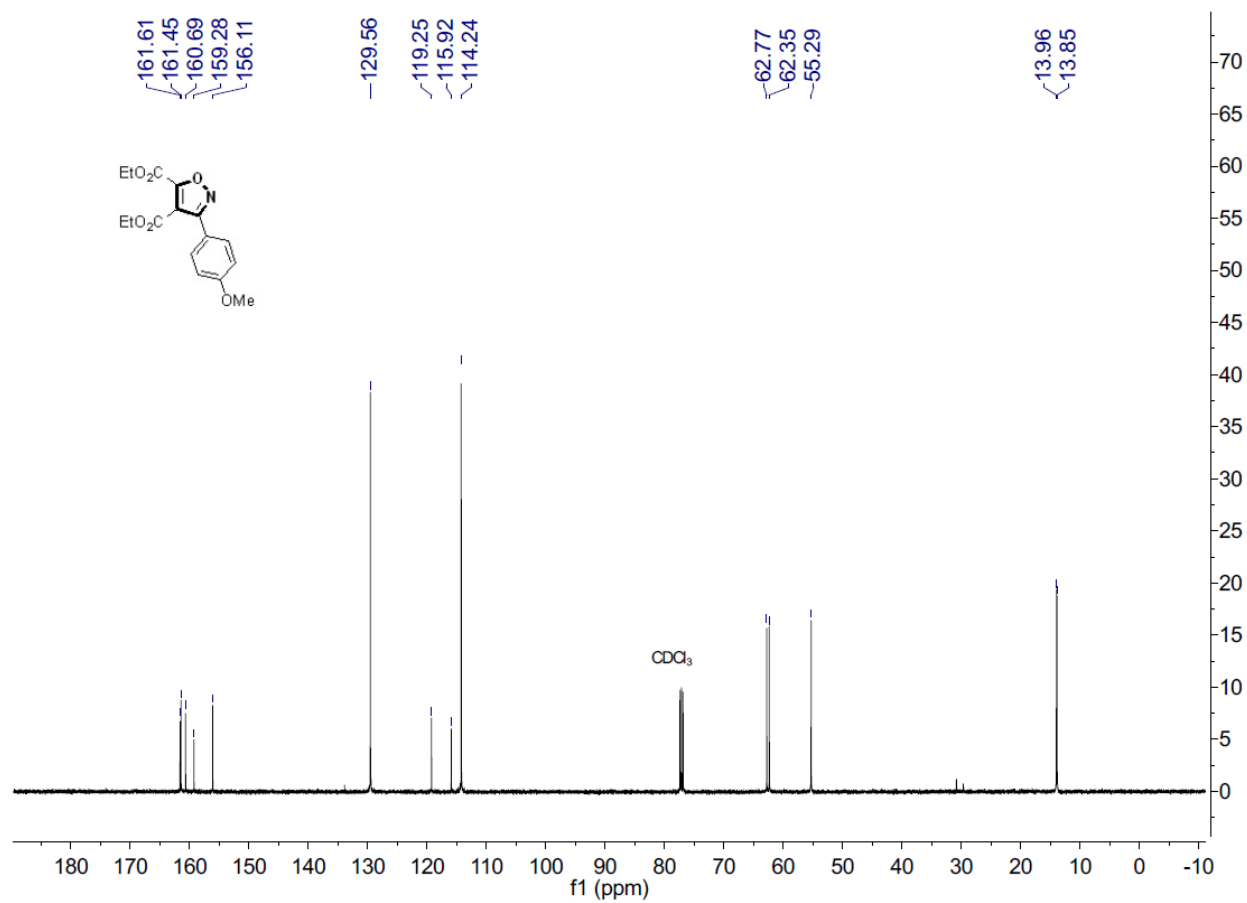*diethyl 3-(4-methoxyphenyl)isoxazole-4,5-dicarboxylate (128b):*

Figure S4.35. ^{1}H NMR of diethyl 3-(4-methoxyphenyl)isoxazole-4,5-dicarboxylate (128b)

Figure S4.36. ^{13}C NMR of diethyl 3-(4-methoxyphenyl)isoxazole-4,5-dicarboxylate (128b)

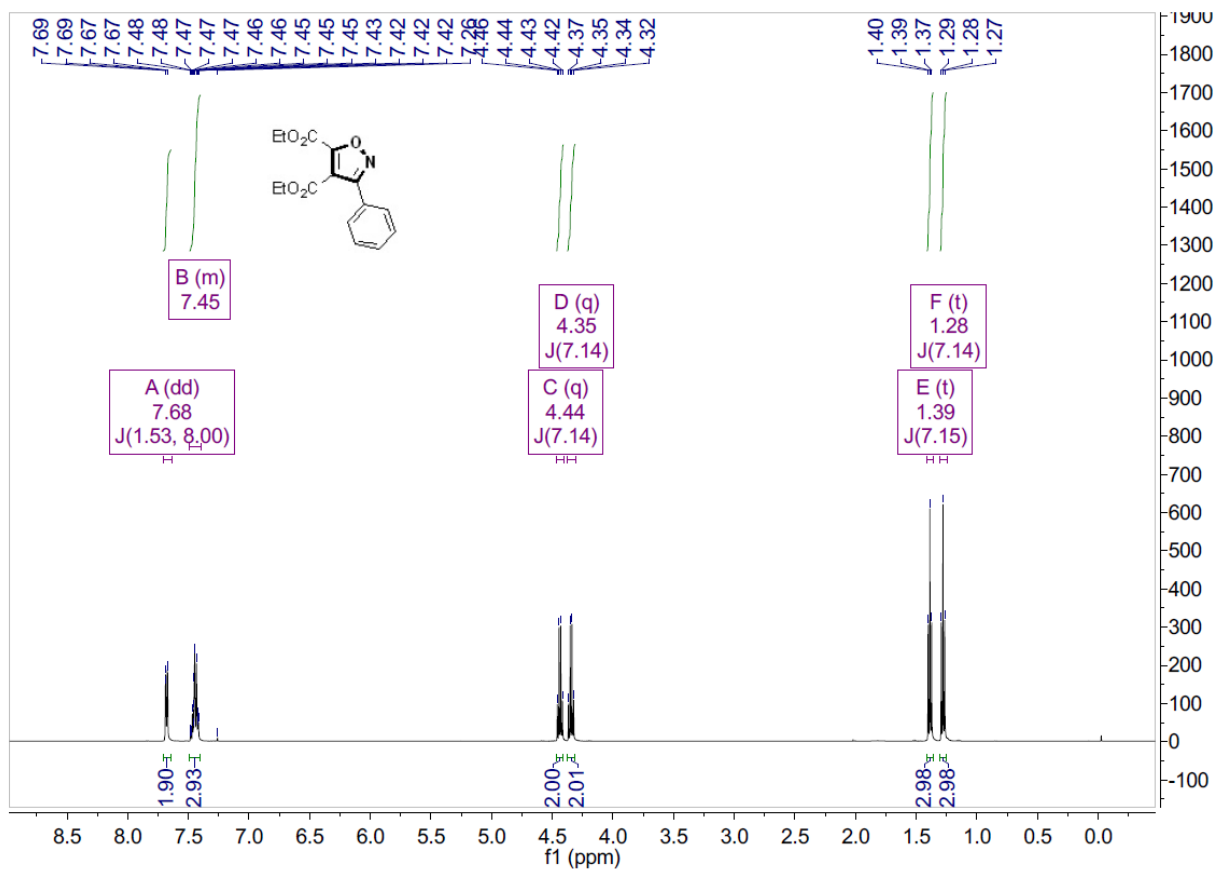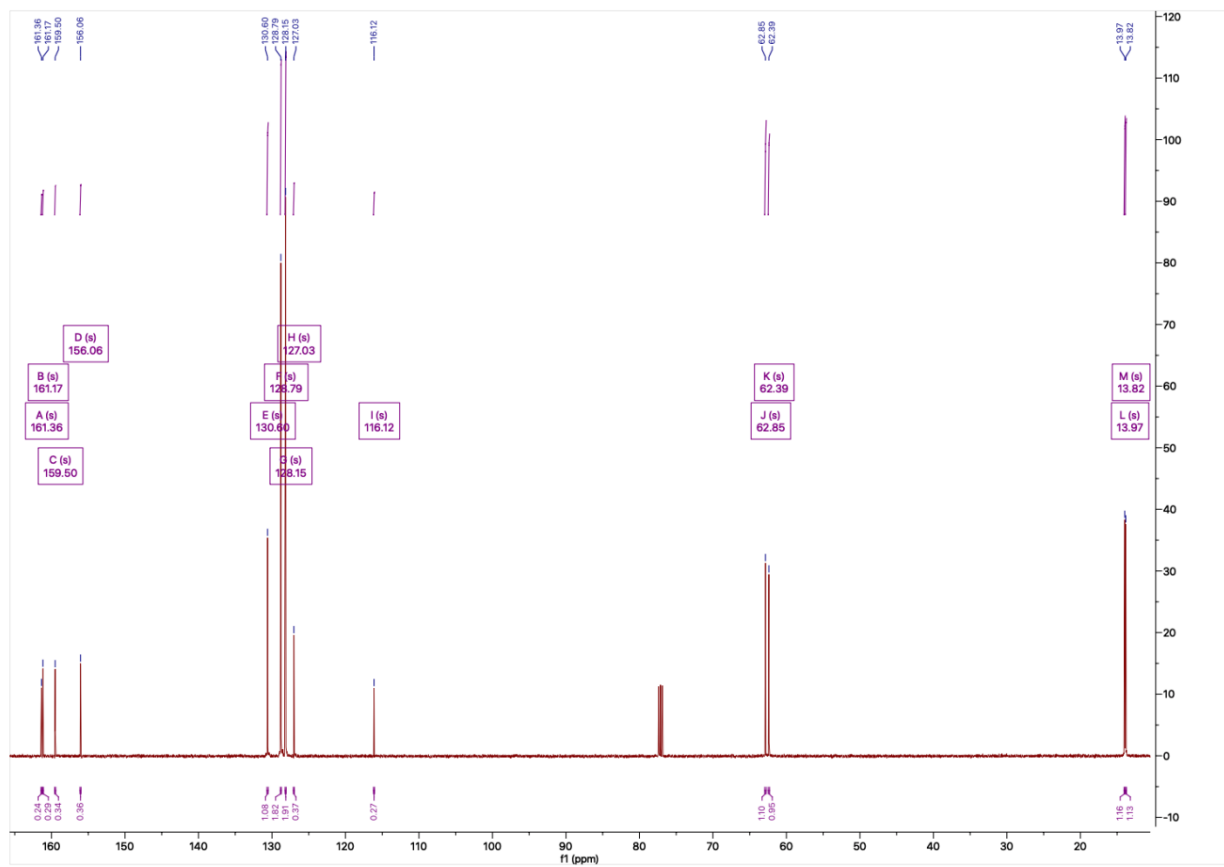*diethyl 3-phenylisoxazole-4,5-dicarboxylate (128c):*

Figure S4.37. ^{1}H NMR of diethyl 3-phenylisoxazole-4,5-dicarboxylate (128c)

Figure S4.38. ^{13}C NMR of diethyl 3-phenylisoxazole-4,5-dicarboxylate (128c)

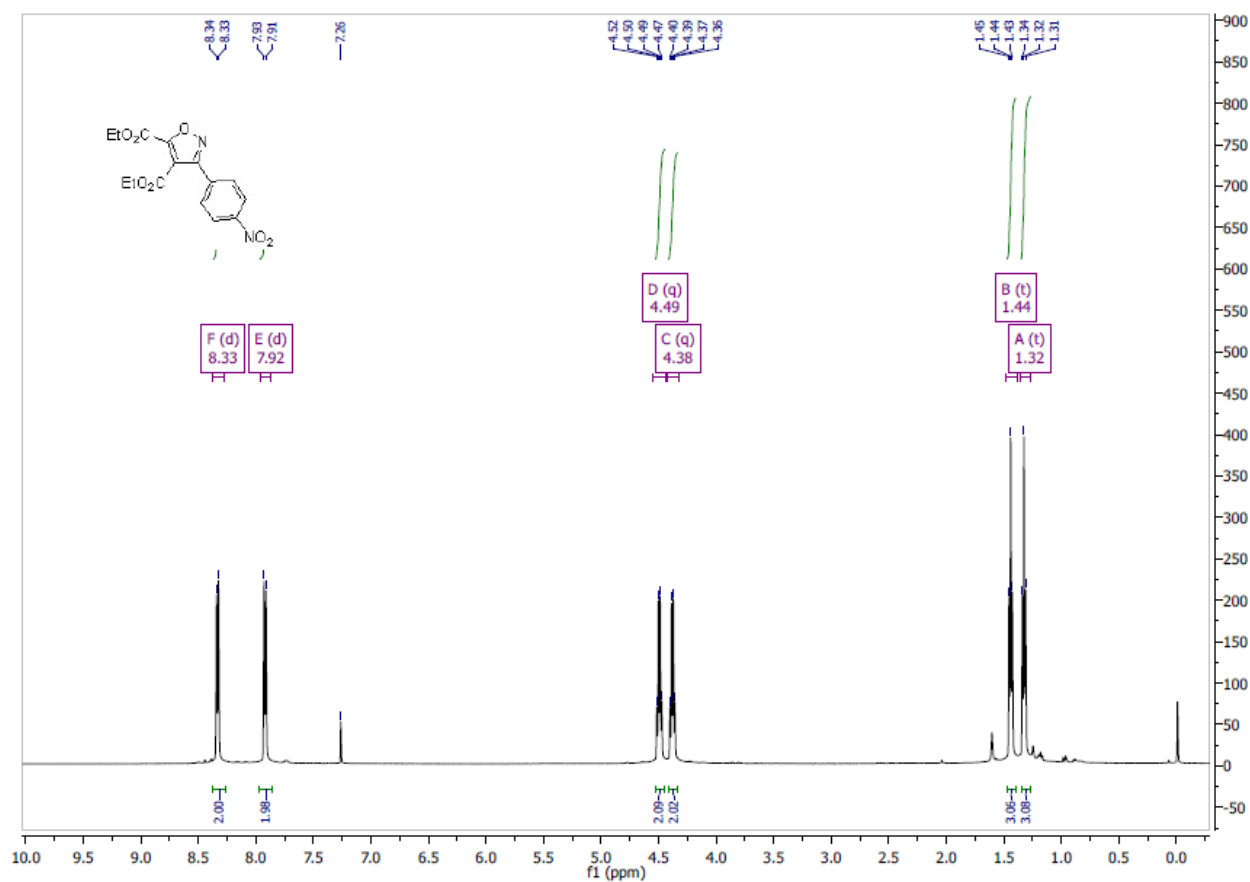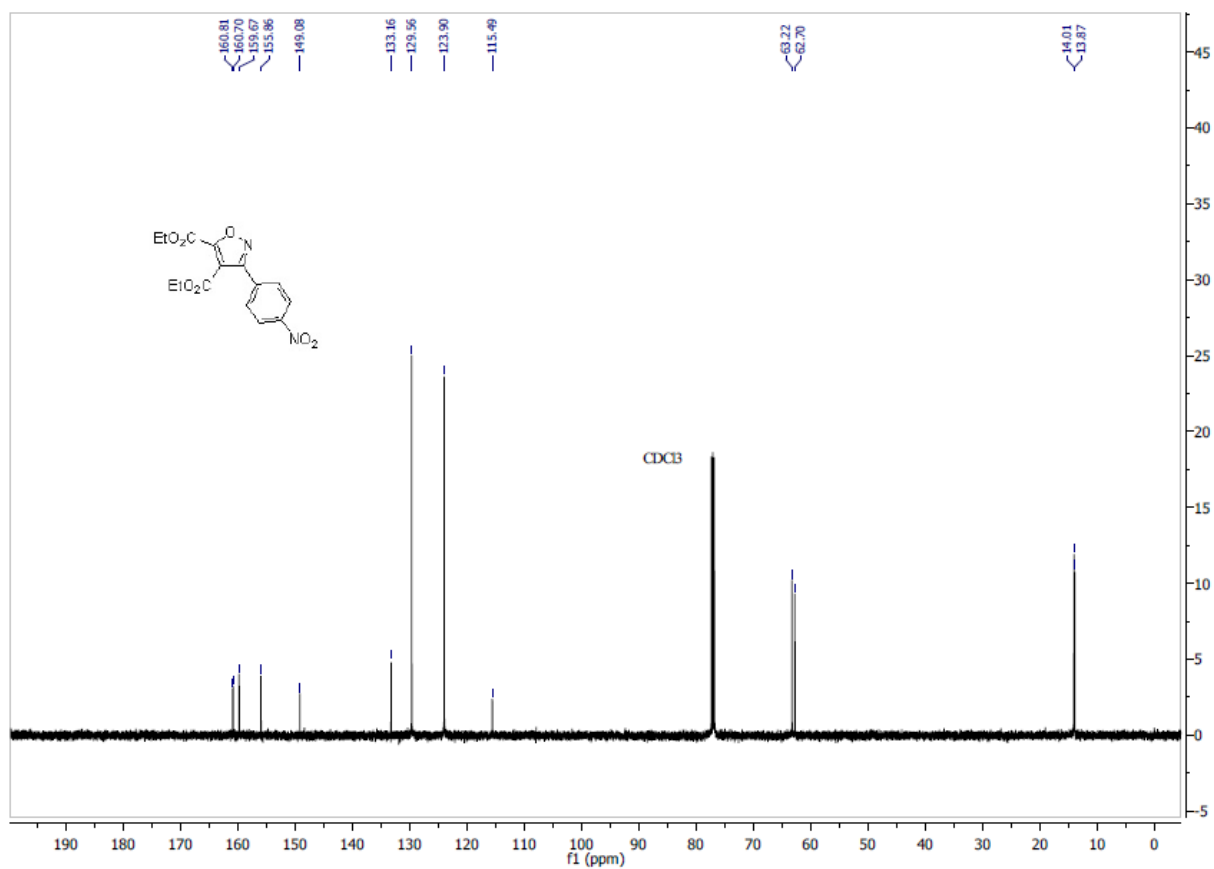*diethyl 3-(4-nitrophenyl)isoxazole-4,5-dicarboxylate (128d):*

Figure S4.39. ^{1}H NMR of diethyl 3-(4-nitrophenyl)isoxazole-4,5-dicarboxylate (128d).

Figure S4.40. ^{13}C NMR of diethyl 3-(4-nitrophenyl)isoxazole-4,5-dicarboxylate (128d).

ethyl 3-(4-methoxyphenyl)-5-phenylisoxazole-4-carboxylate (128e):

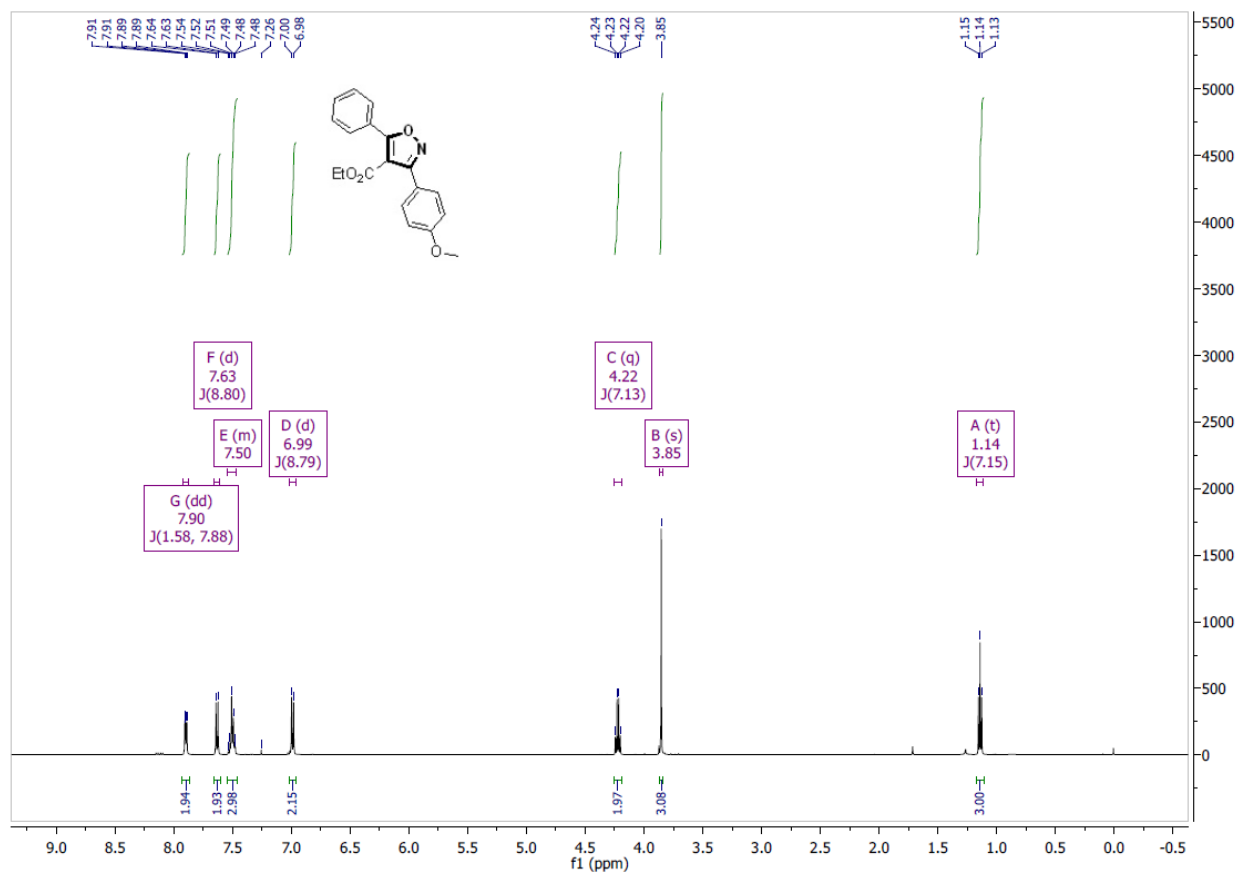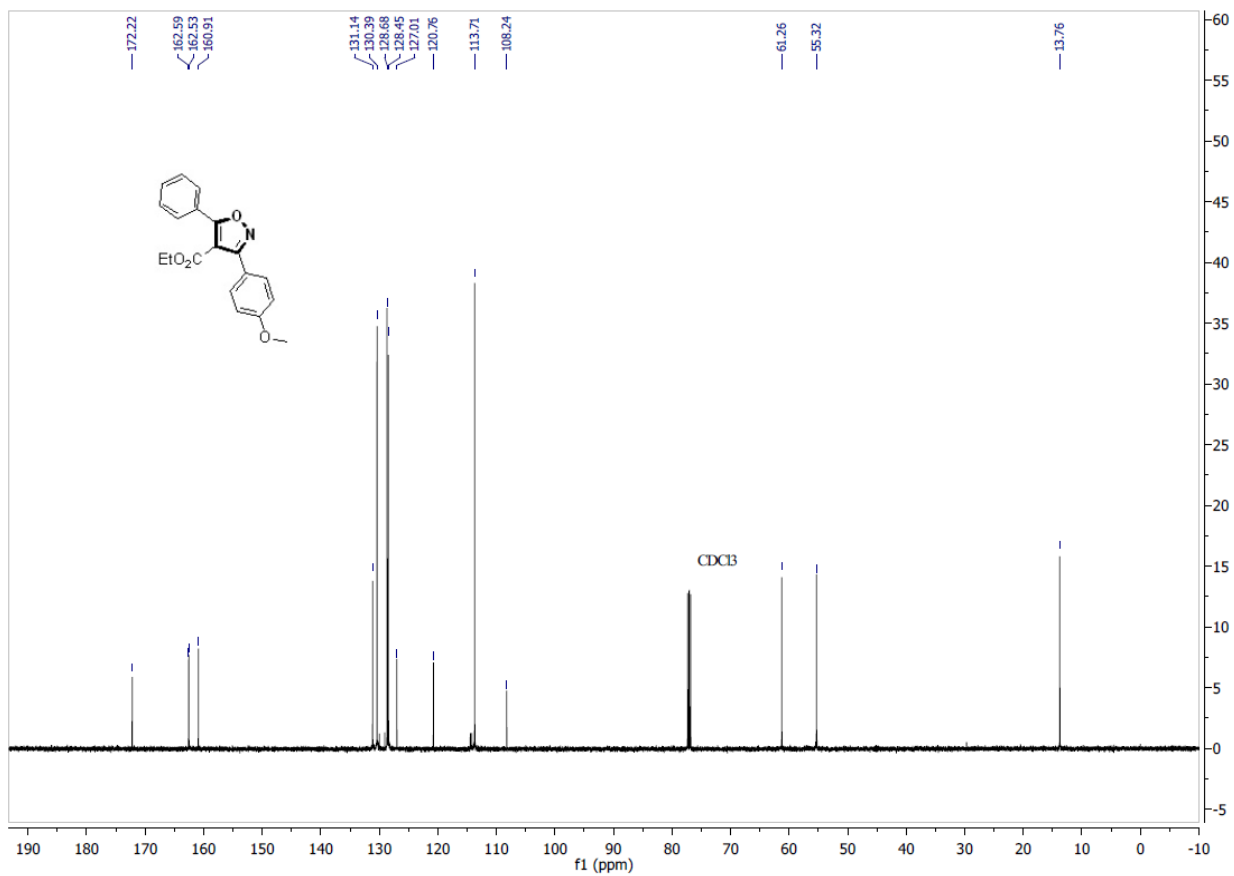**Figure S4.41**. ¹H NMR of ethyl 3-(4-methoxyphenyl)-5-phenylisoxazole-4-carboxylate (128e)

Figure S4.41. ^{13}C NMR of ethyl 3-(4-methoxyphenyl)-5-phenylisoxazole-4-carboxylate (128e)

ethyl 3,5-diphenylisoxazole-4-carboxylate (128f):
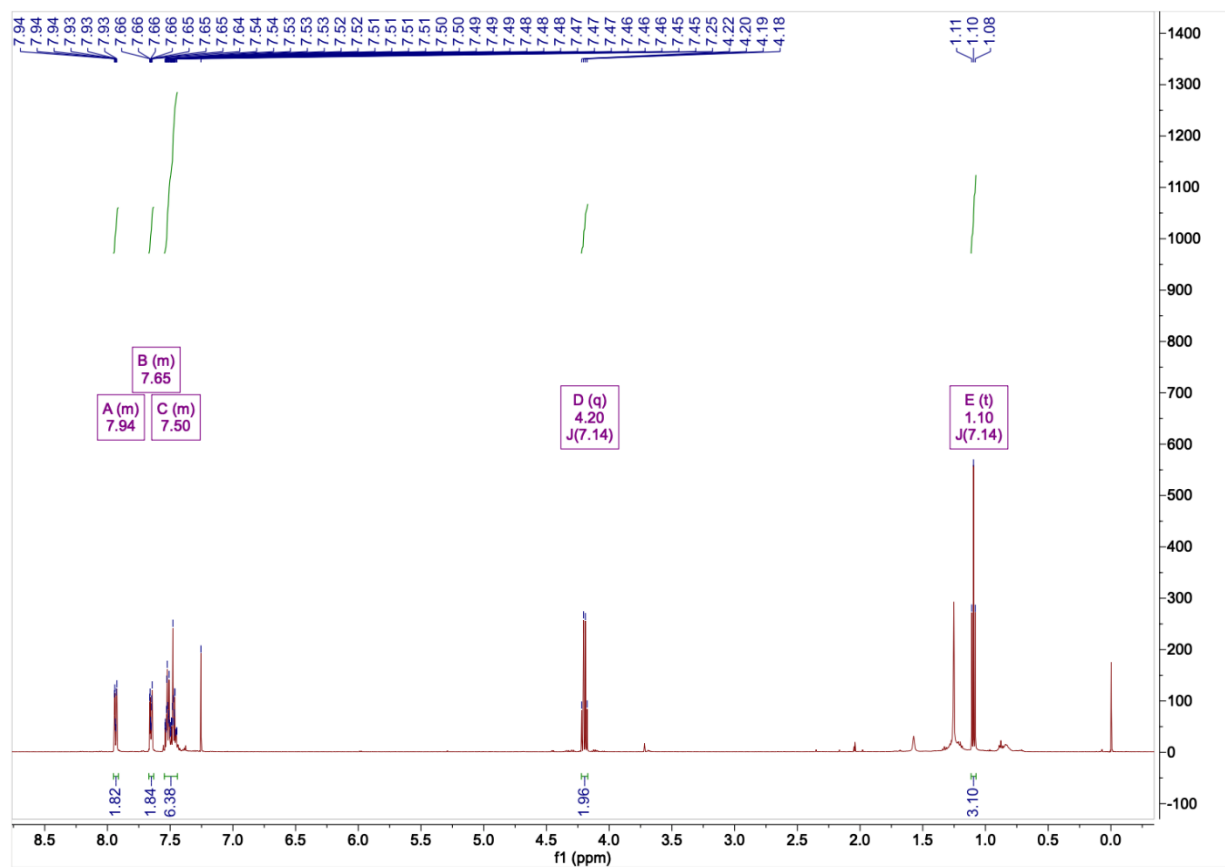
Figure S4.42. ¹H NMR of ethyl 3,5-diphenylisoxazole-4-carboxylate (128f)
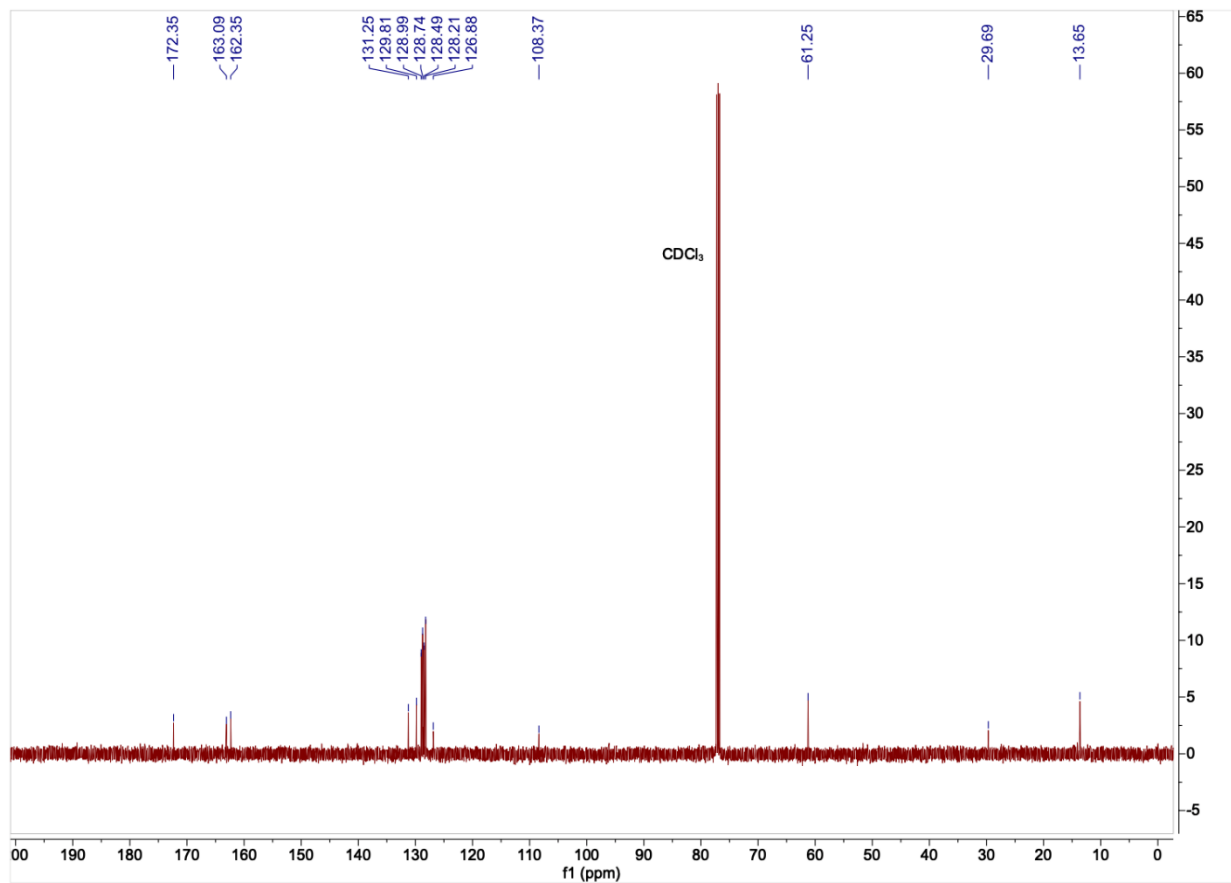
Figure S4.43. ^{13}C NMR of ethyl 3,5-diphenylisoxazole-4-carboxylate (128f)

ethyl 3-(4-nitrophenyl)-5-phenylisoxazole-4-carboxylate (128g):
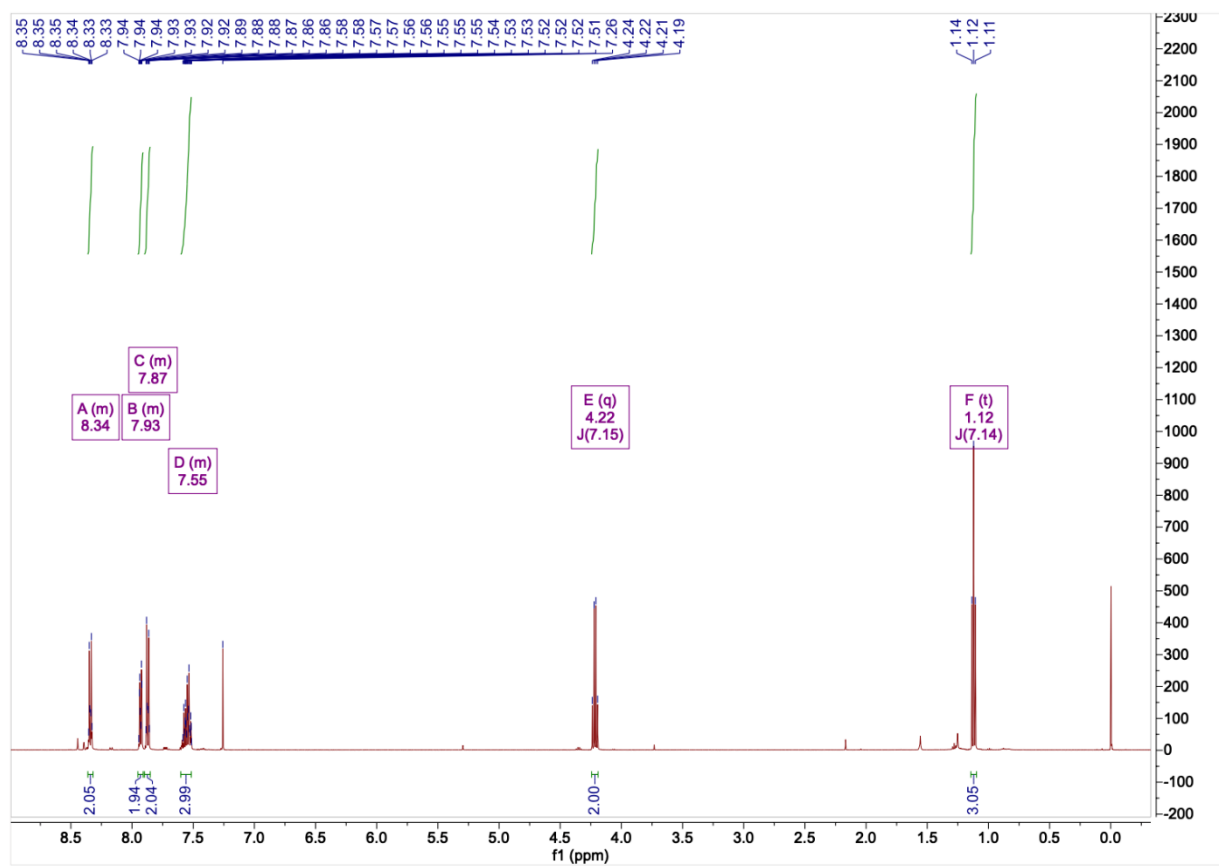
Figure S4.44. ^{1}H NMR of ethyl 3-(4-nitrophenyl)-5-phenylisoxazole-4-carboxylate (128g)
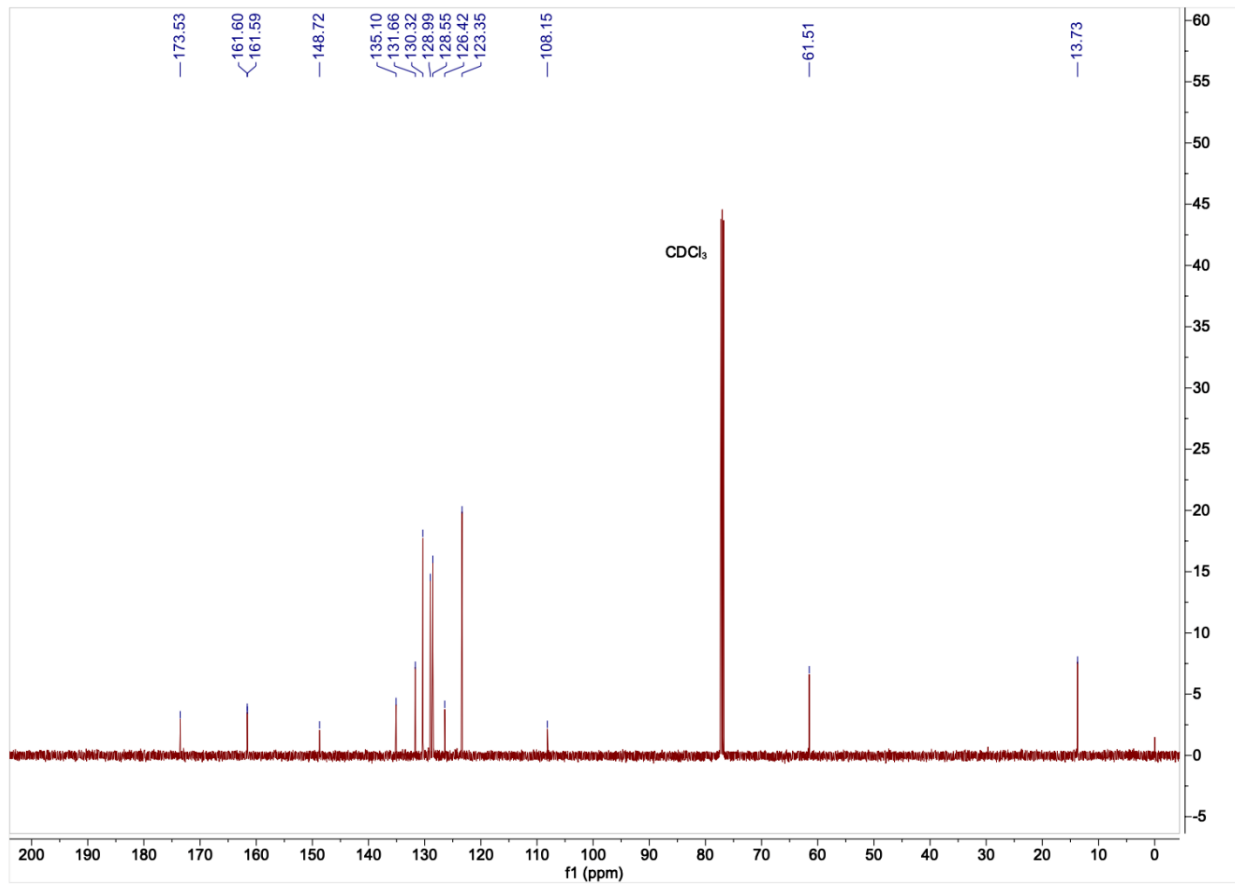
Figure S4.45. ^{13}C NMR of ethyl 3-(4-nitrophenyl)-5-phenylisoxazole-4-carboxylate (128g)

1-(3-(4-nitrophenyl)-5-phenylisoxazol-4-yl)ethan-1-one (128h):
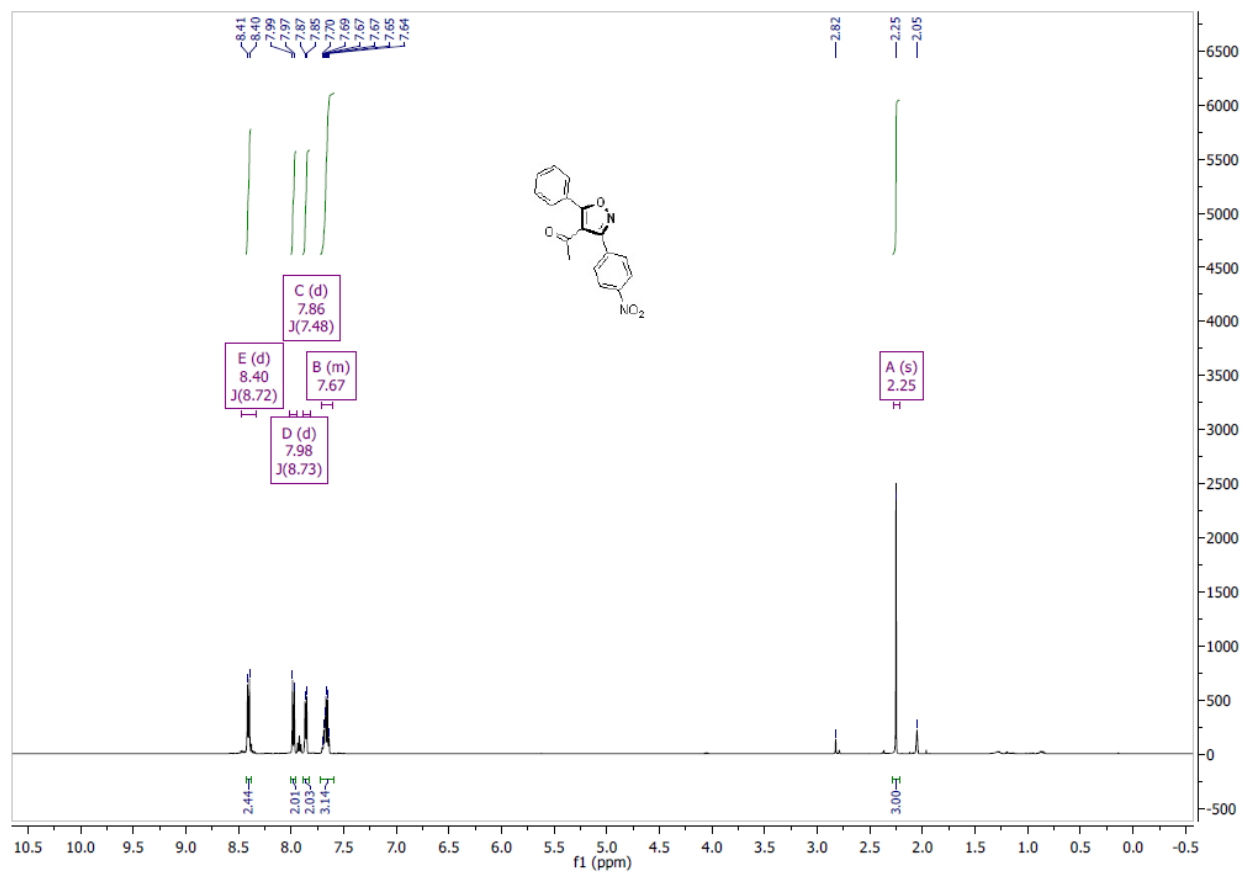
Figure S4.46. ^{1}H NMR of 1-(3-(4-nitrophenyl)-5-phenylisoxazol-4-yl)ethan-1-one (128h)
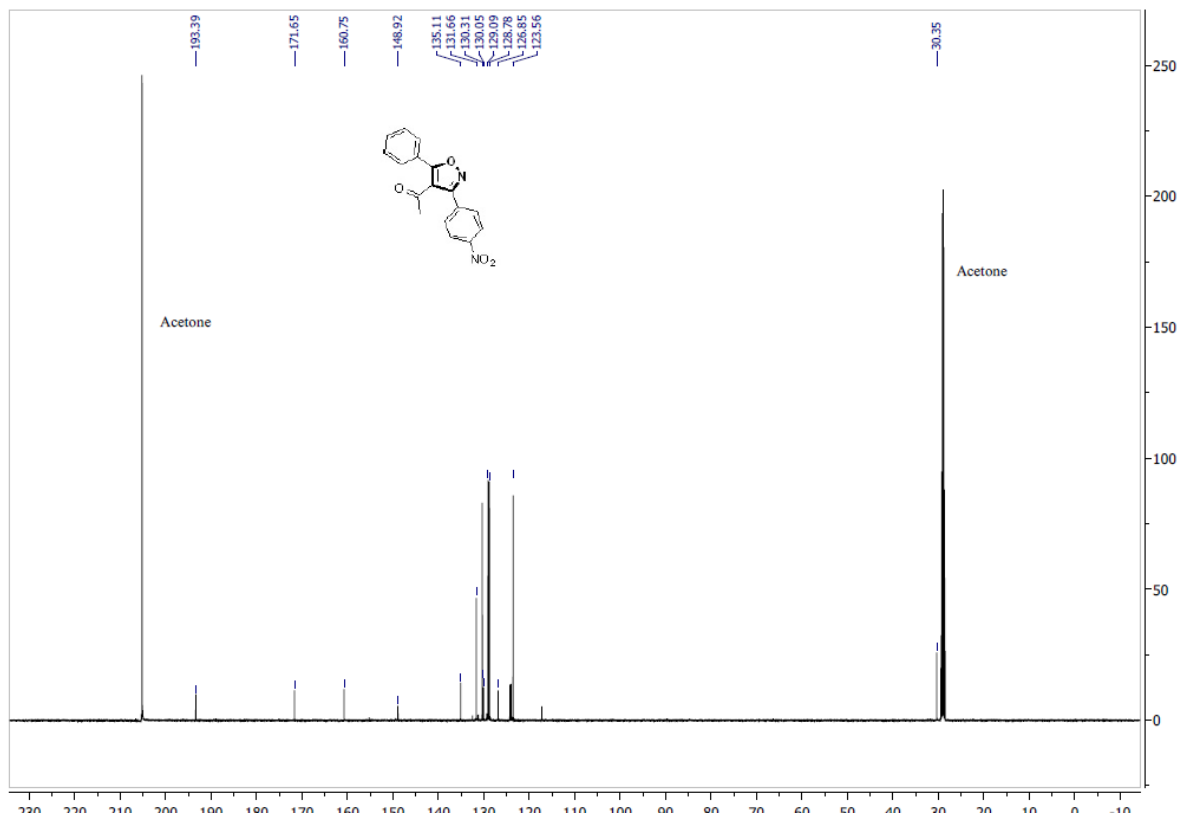
Figure S4.47. ^{13}C NMR of 1-(3-(4-nitrophenyl)-5-phenylisoxazol-4-yl)ethan-1-one (128h)

ethyl 5-methyl-3-(4-nitrophenyl)isoxazole-4-carboxylate (128i):

Figure S4.48. ^{1}H NMR of ethyl 5-methyl-3-(4-nitrophenyl)isoxazole-4-carboxylate (128i)

Figure S4.49. ^{13}C NMR of ethyl 5-methyl-3-(4-nitrophenyl)isoxazole-4-carboxylate (128i)

ethyl 3-(4-chlorophenyl)-5-methylisoxazole-4-carboxylate (128j):

Figure S4.50. ^{1}H NMR of ethyl 3-(4-chlorophenyl)-5-methylisoxazole-4-carboxylate (128j)

Figure S4.51. ^{13}C NMR of ethyl 3-(4-chlorophenyl)-5-methylisoxazole-4-carboxylate (128j)

ethyl 3-(4-chlorophenyl)-5-methylisoxazole-4-carboxylate (128k)

Figure S4.52. ^{1}H NMR of ethyl 3-(4-chlorophenyl)-5-methylisoxazole-4-carboxylate (128k)
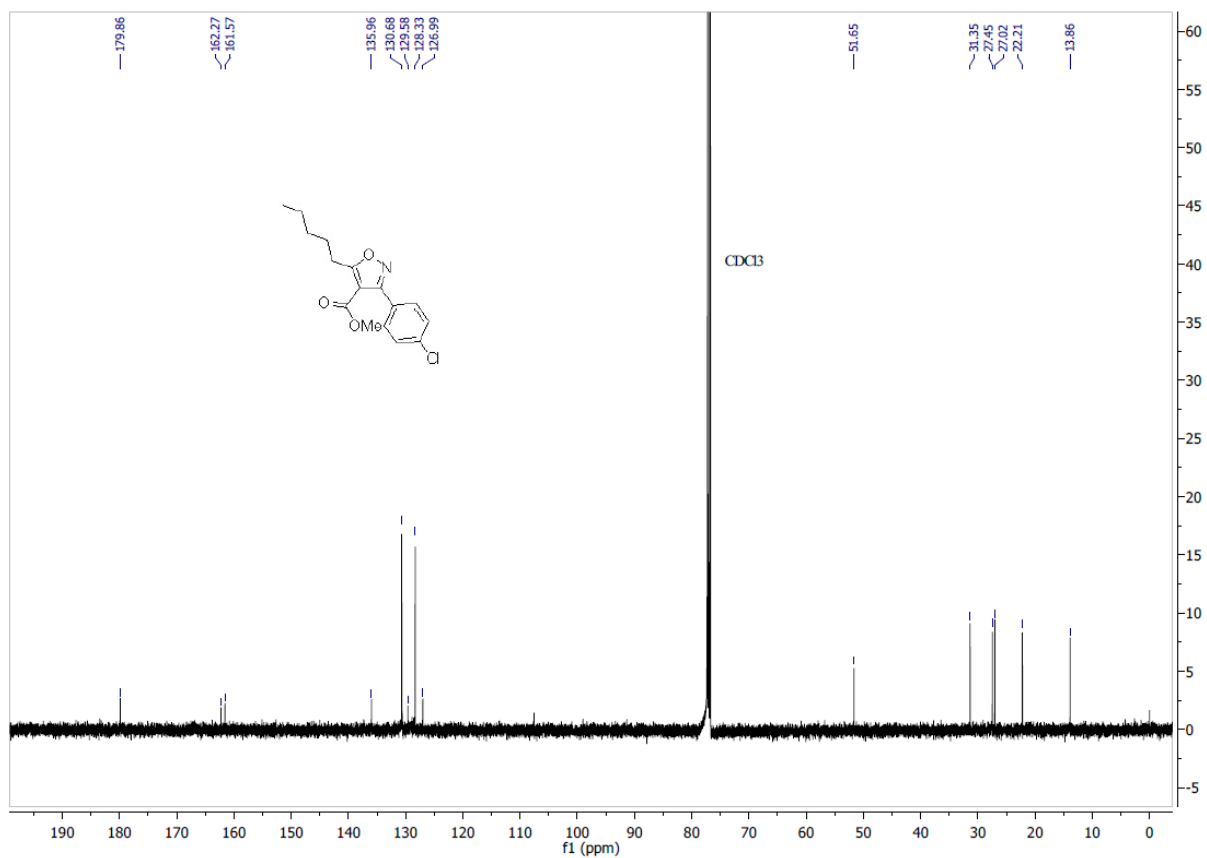
Figure S4.53. ^{13}C NMR of ethyl 3-(4-chlorophenyl)-5-methylisoxazole-4-carboxylate (128k)

ethyl 3-(4-nitrophenyl)-4-phenylisoxazole-5-carboxylate (127a):
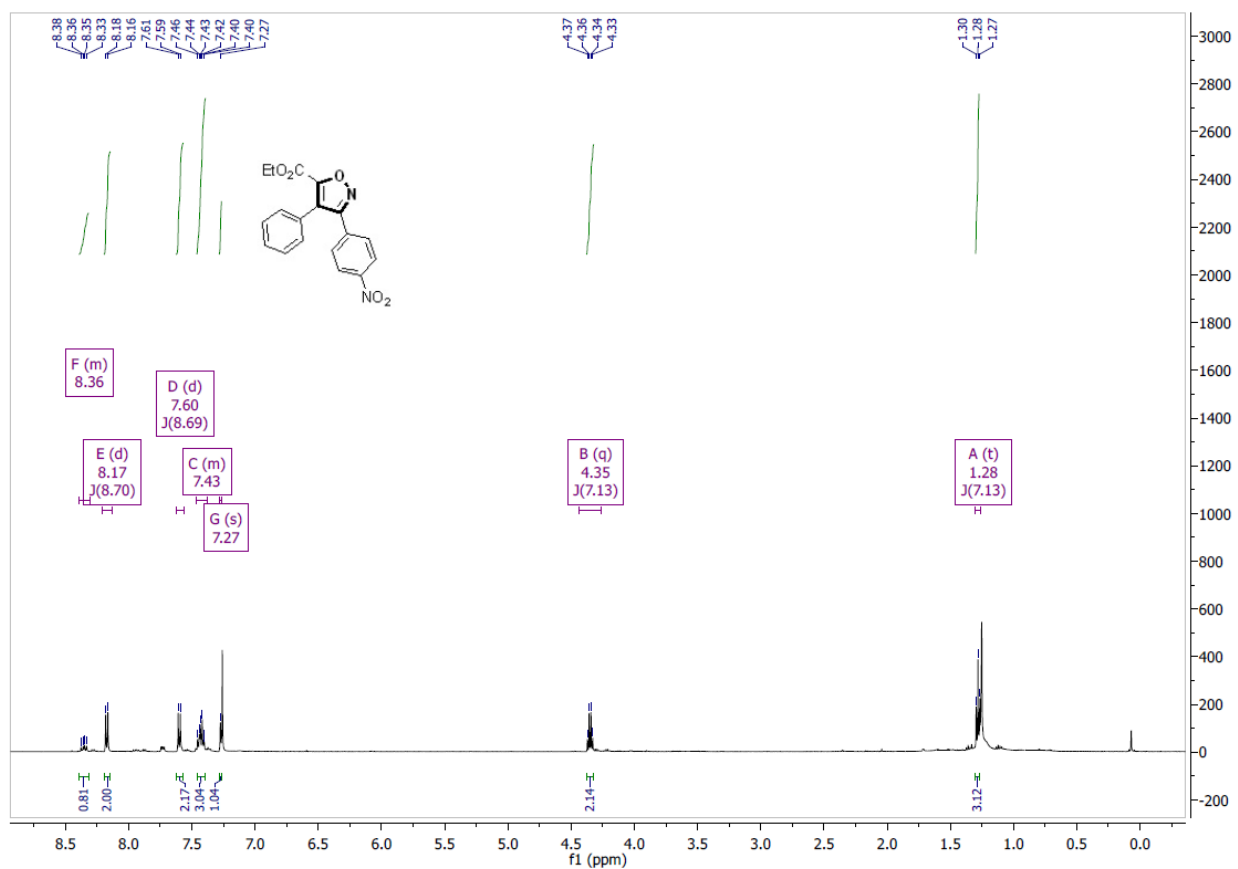
Figure S4.53. ¹H NMR of ethyl 3-(4-nitrophenyl)-4-phenylisoxazole-5-carboxylate (127a)
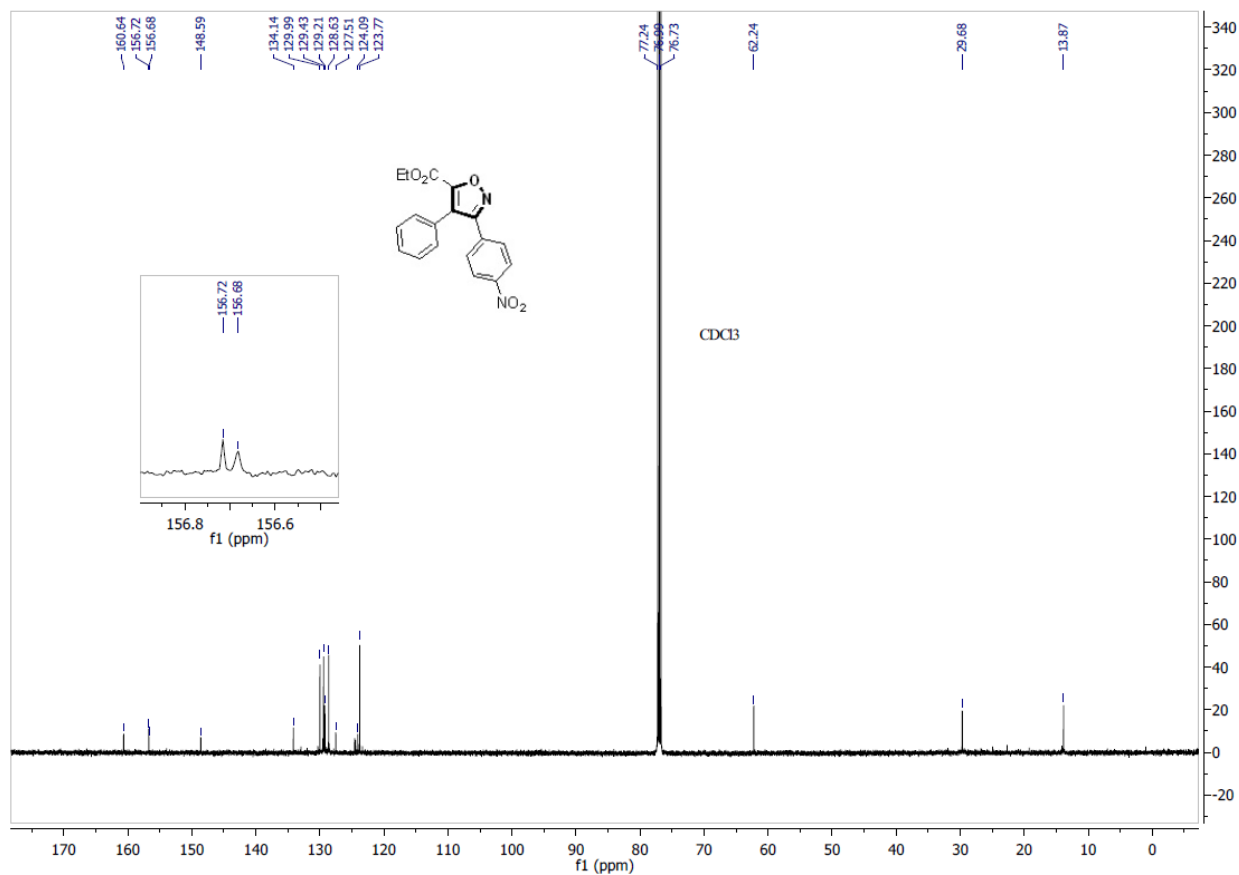
Figure S4.54. ^{13}C NMR of ethyl 3-(4-nitrophenyl)-4-phenylisoxazole-5-carboxylate (127a)

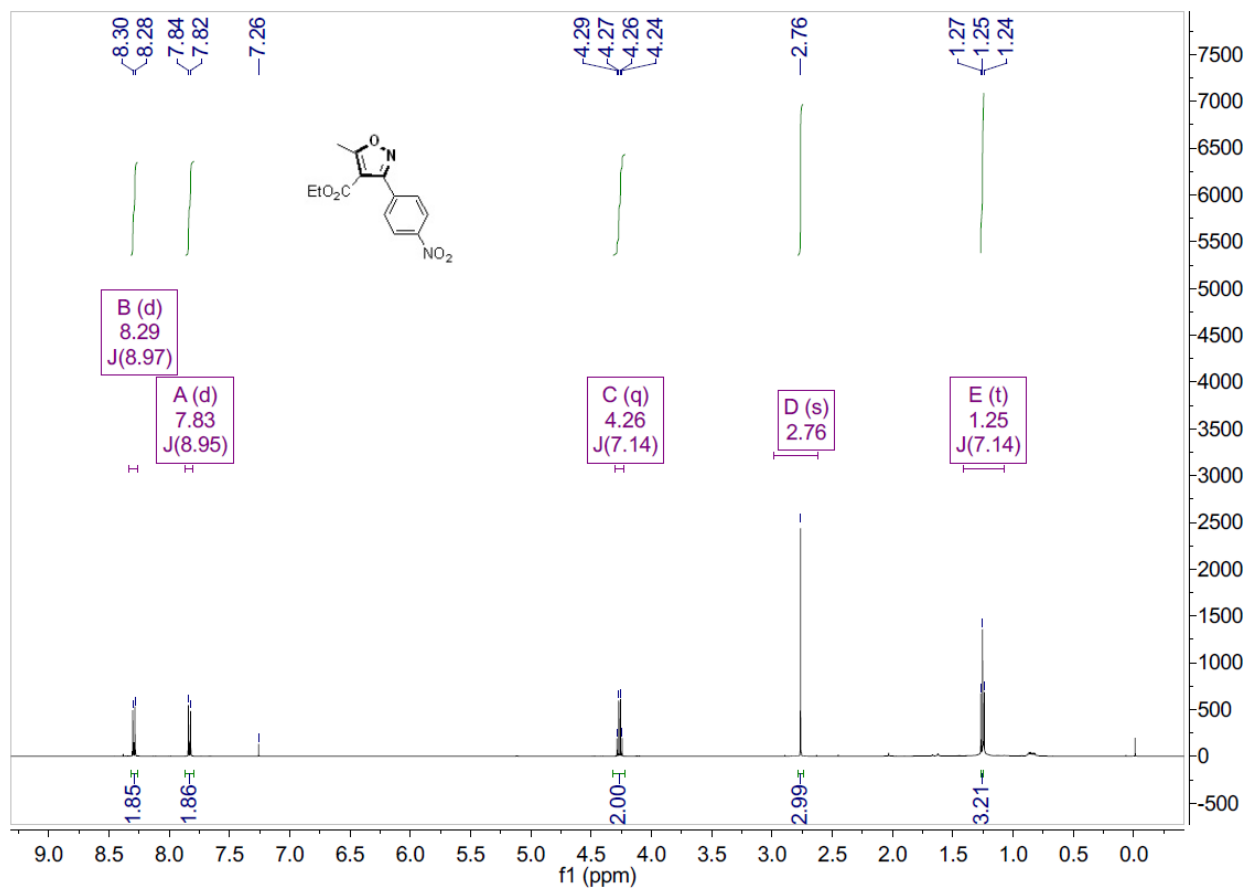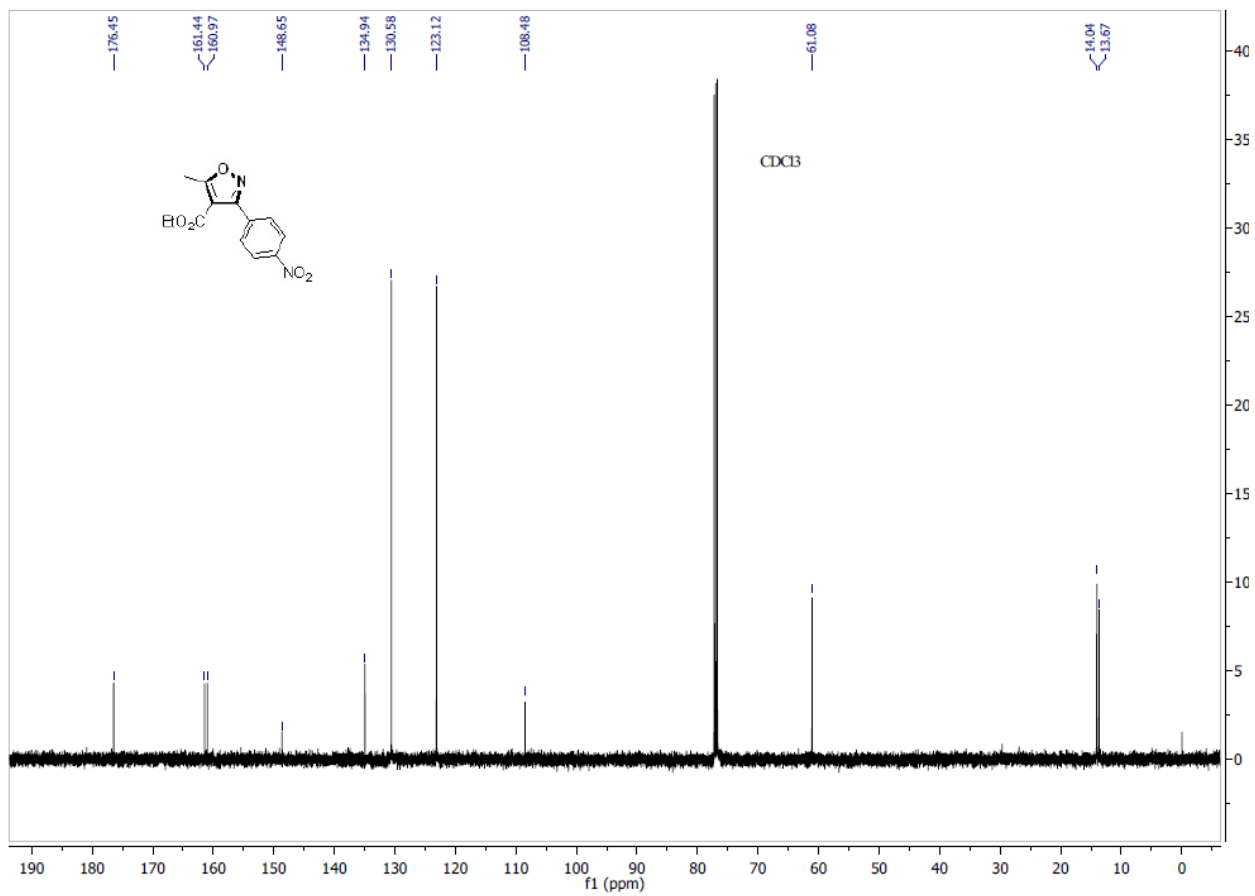*ethyl 4-methyl-3-(4-nitrophenyl)isoxazole-5-carboxylate (127b):*
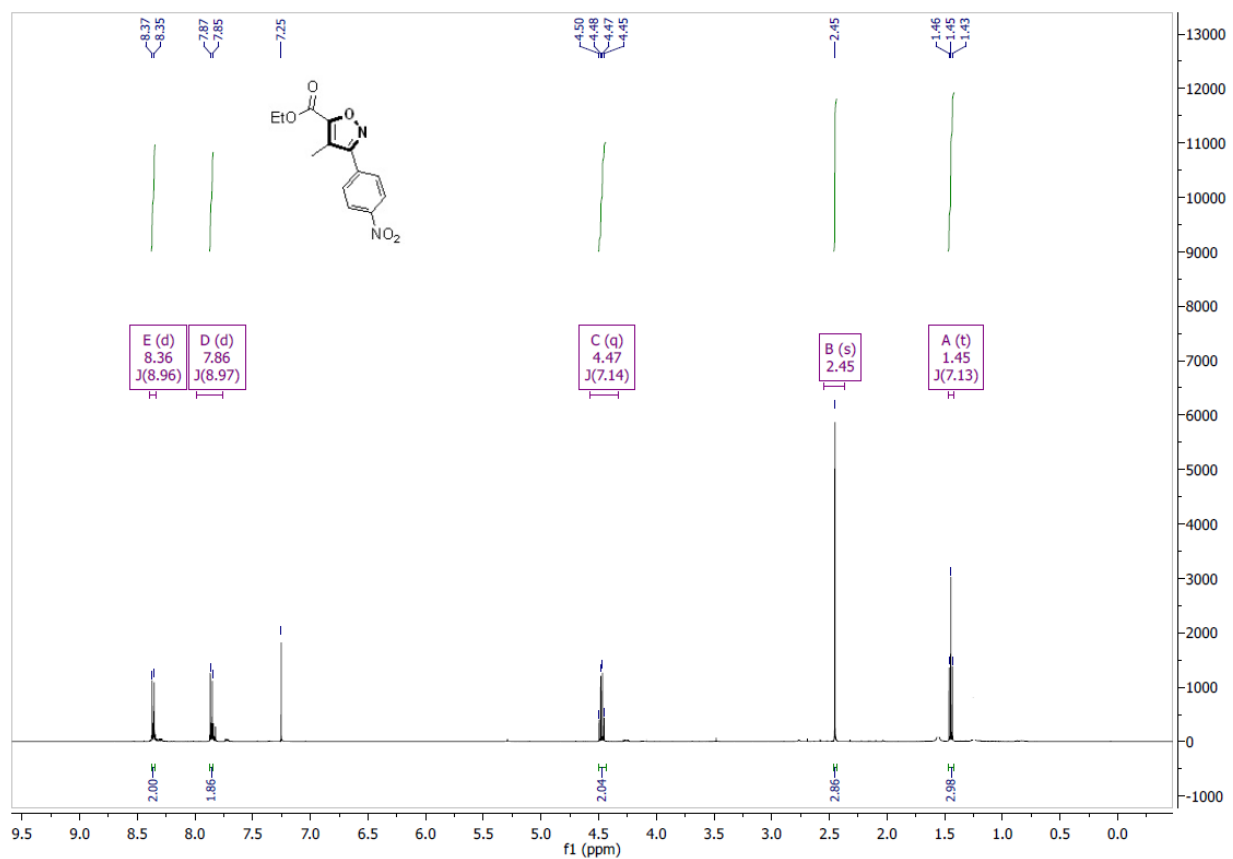
Figure S4.55. ^{1}H NMR of ethyl 4-methyl-3-(4-nitrophenyl)isoxazole-5-carboxylate (127b)
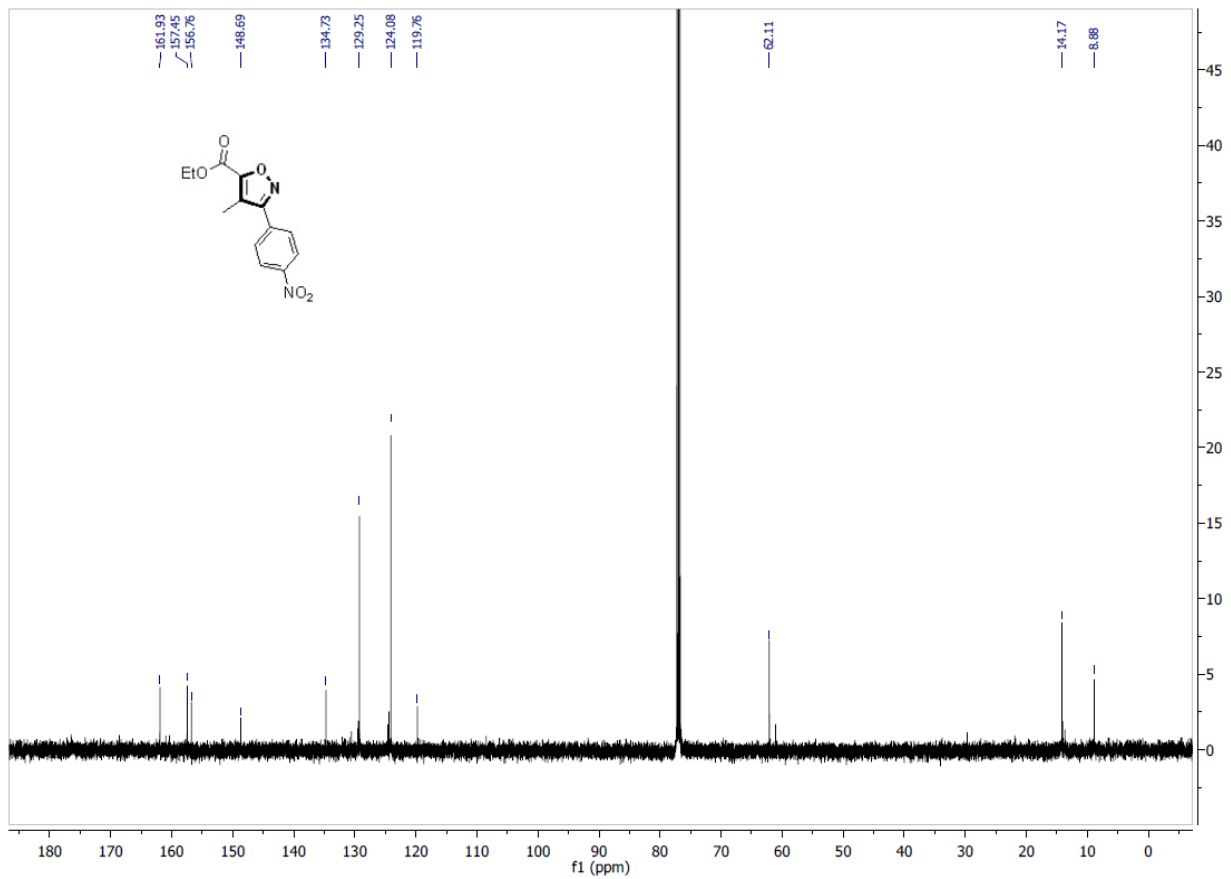
Figure S4.56. ^{1}H NMR of ethyl 4-methyl-3-(4-nitrophenyl)isoxazole-5-carboxylate (127b)

ethyl 3-(4-chlorophenyl)-4-methylisoxazole-5-carboxylate (133c-c):
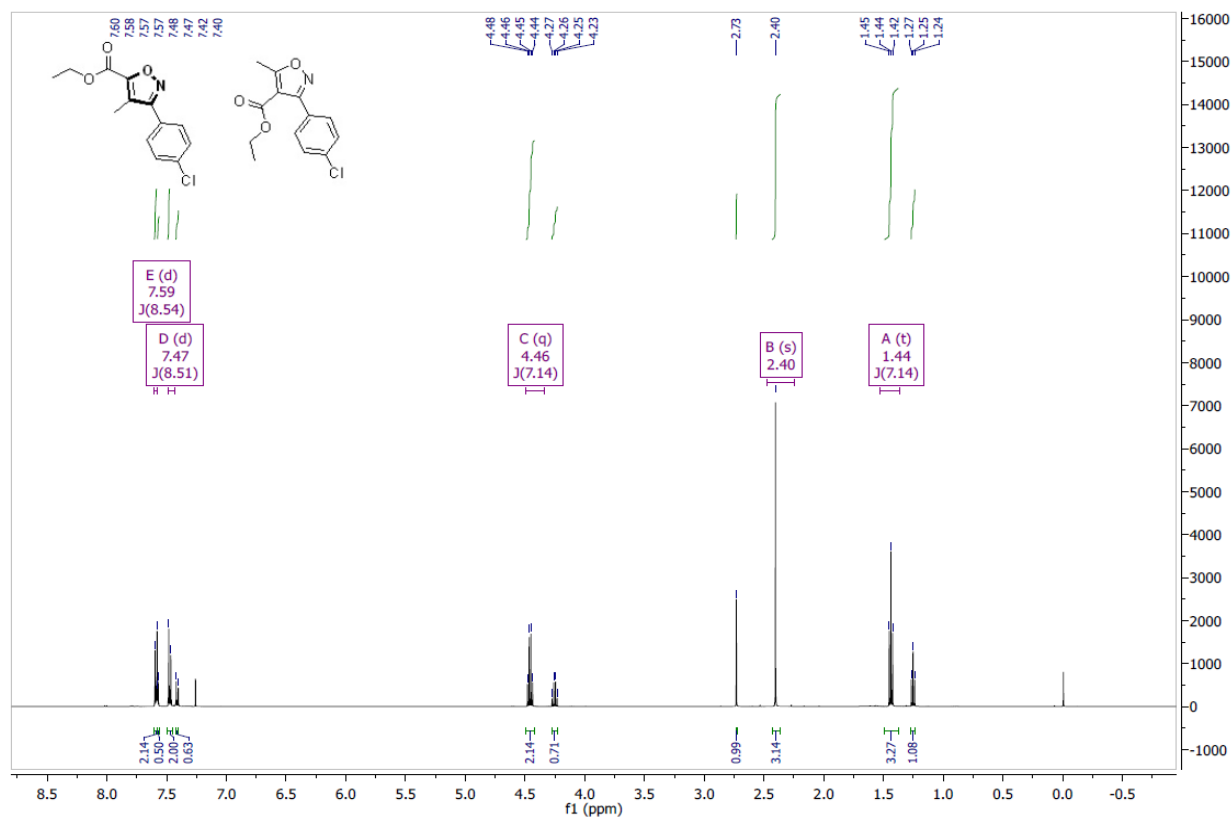
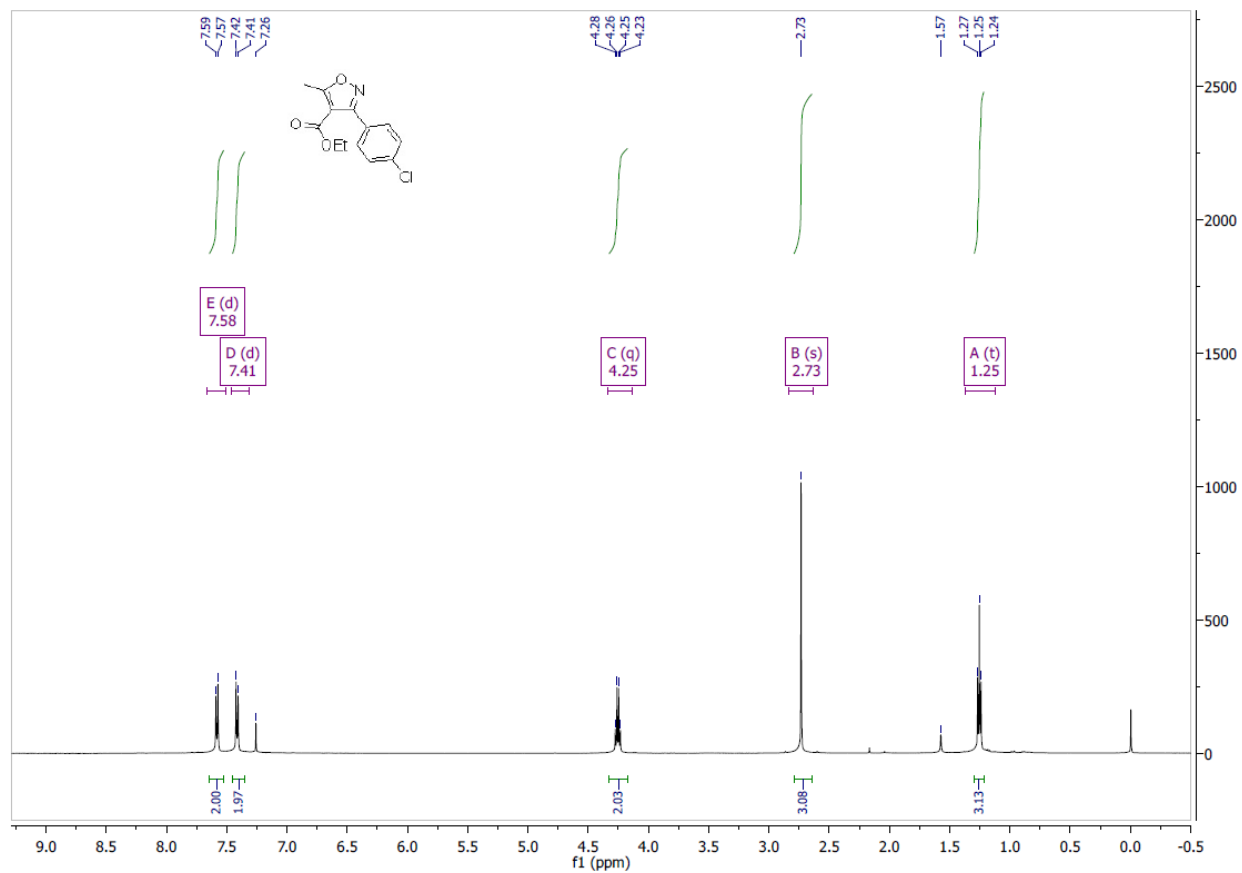**Figure S4.57.** 1H NMR of ethyl 3-(4-chlorophenyl)-4-methylisoxazole-5-carboxylate (127c)

Figure S4.58. ^{13}C NMR of ethyl 3-(4-chlorophenyl)-4-methylisoxazole-5-carboxylate (127c)

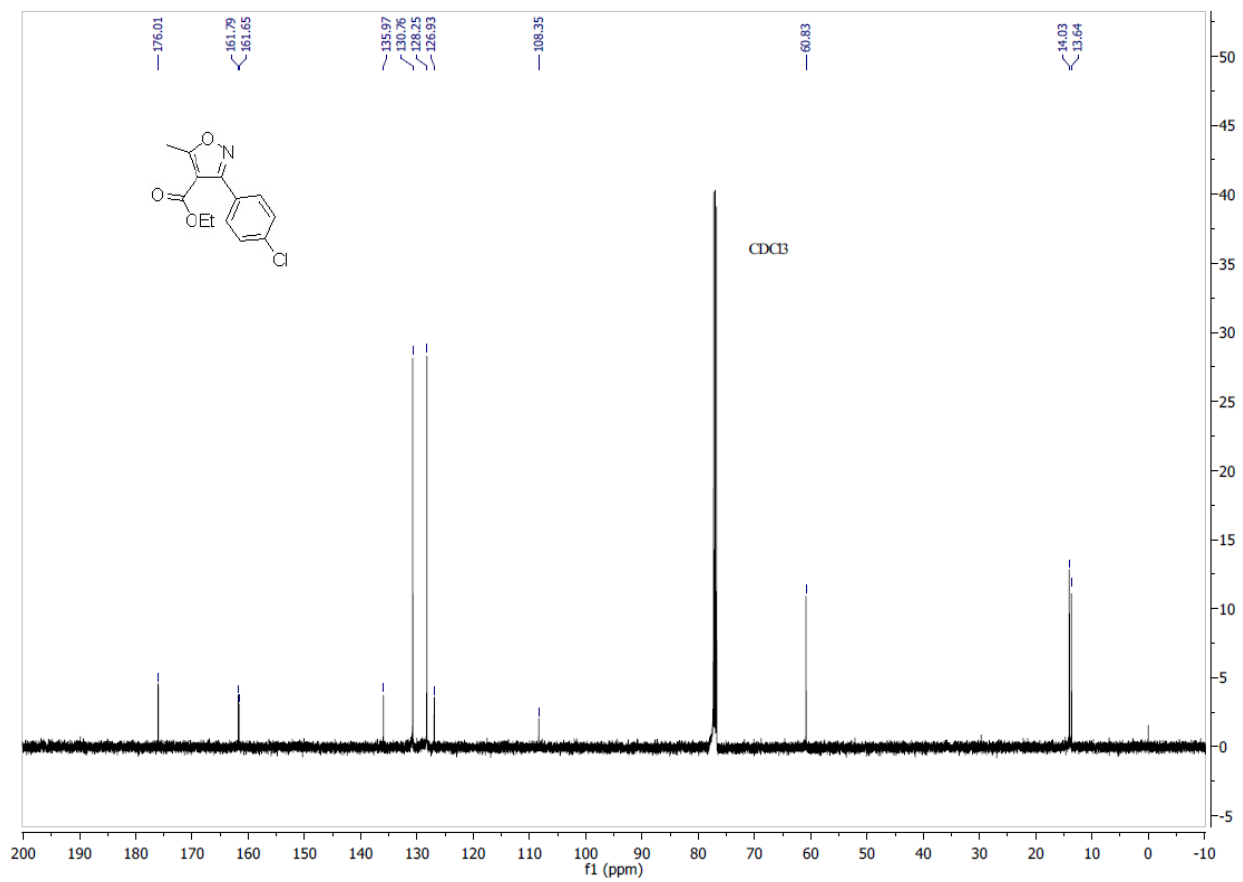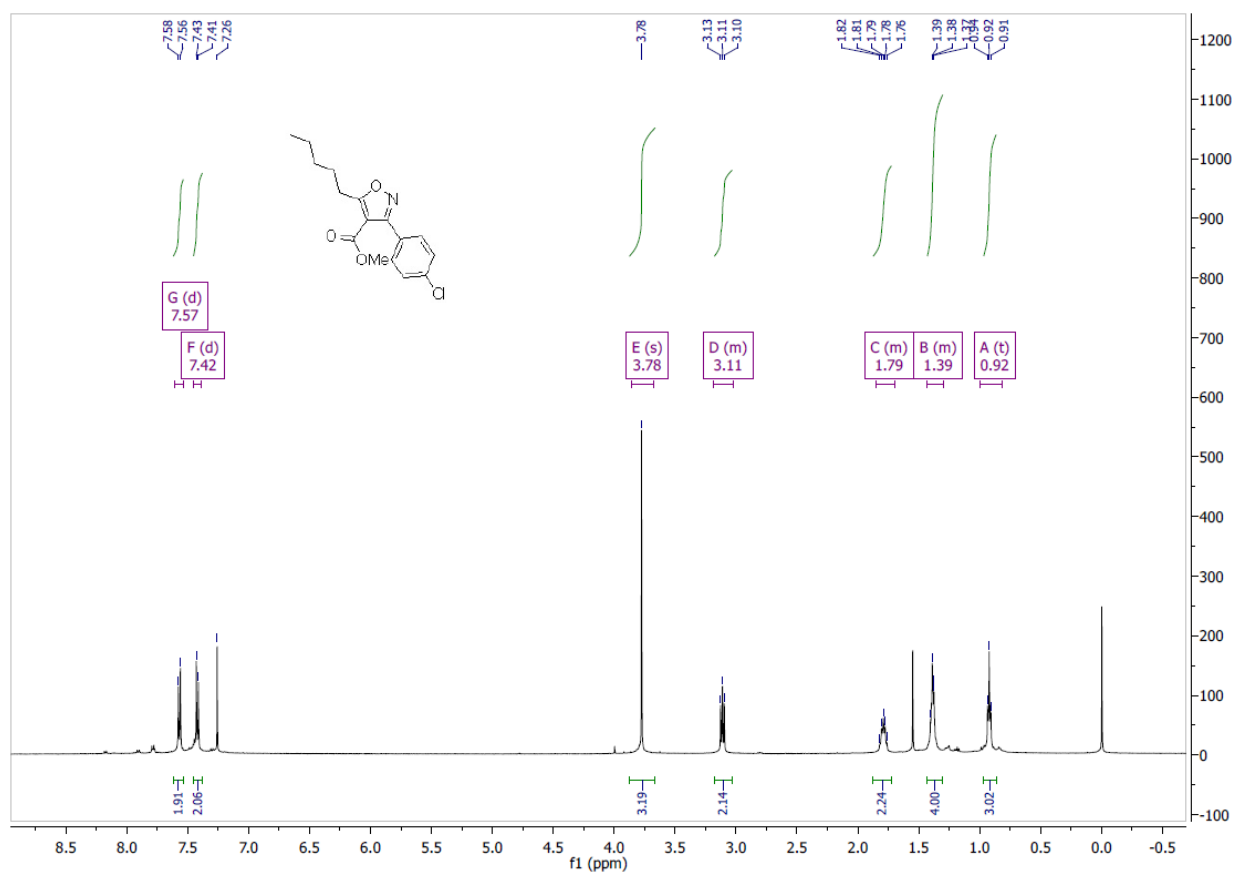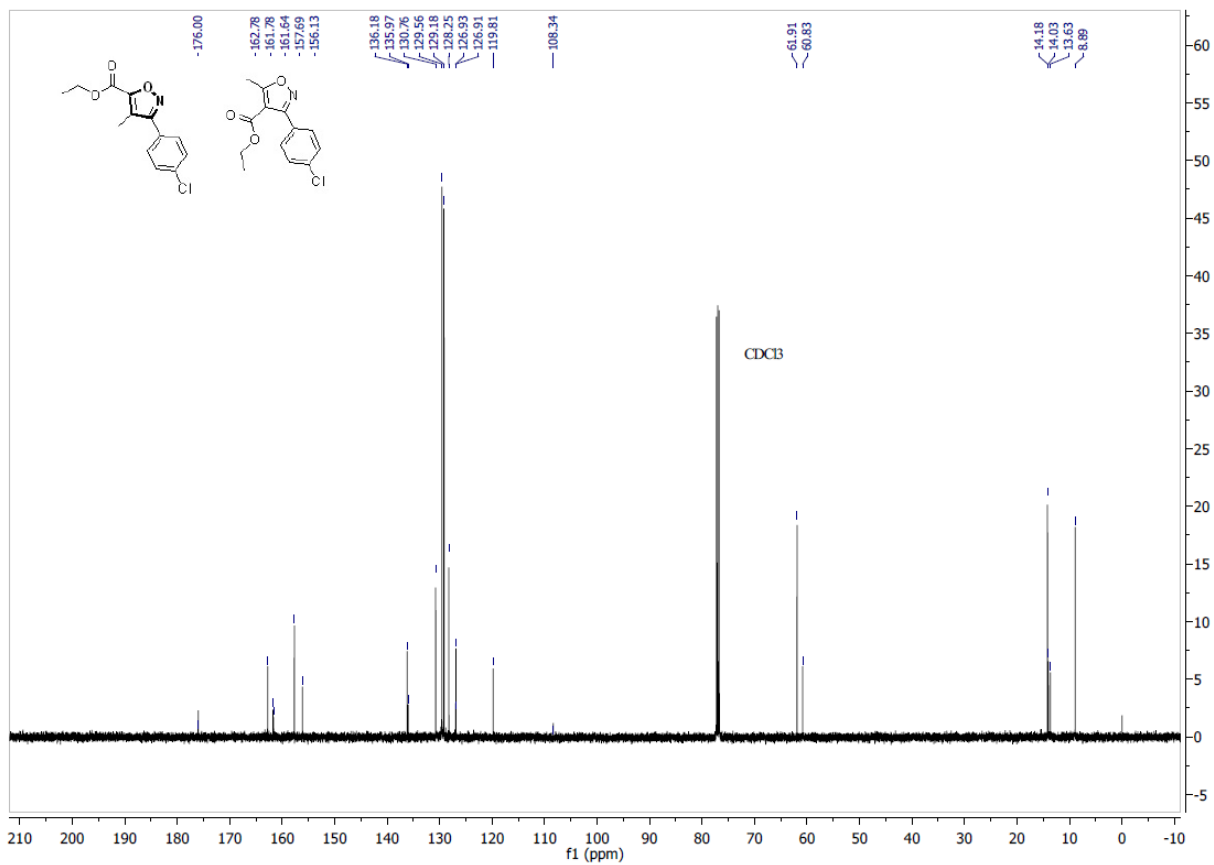*methyl 3-(4-chlorophenyl)-4-pentylisoxazole-5-carboxylate (127d):*
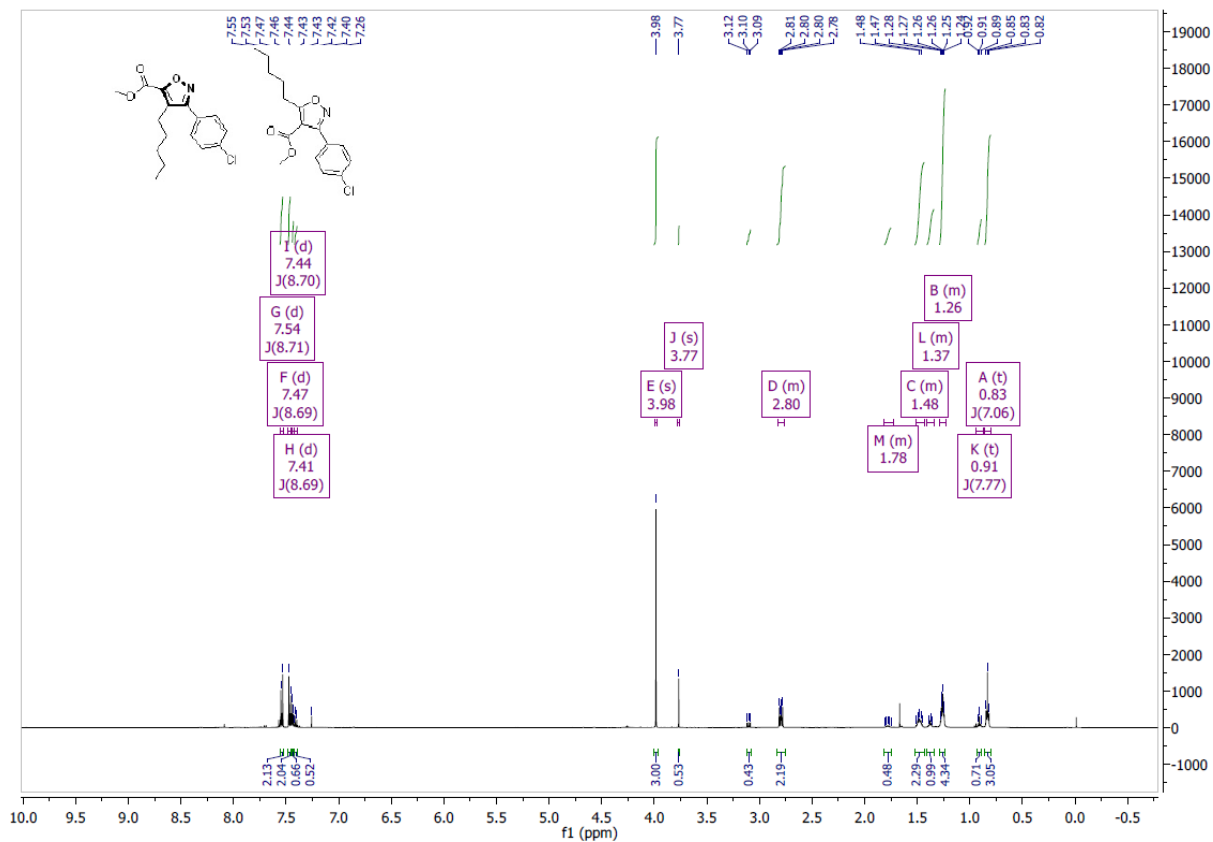
Figure S4.59. ^{1}H NMR of methyl 3-(4-chlorophenyl)-4-pentylisoxazole-5-carboxylate (127d)
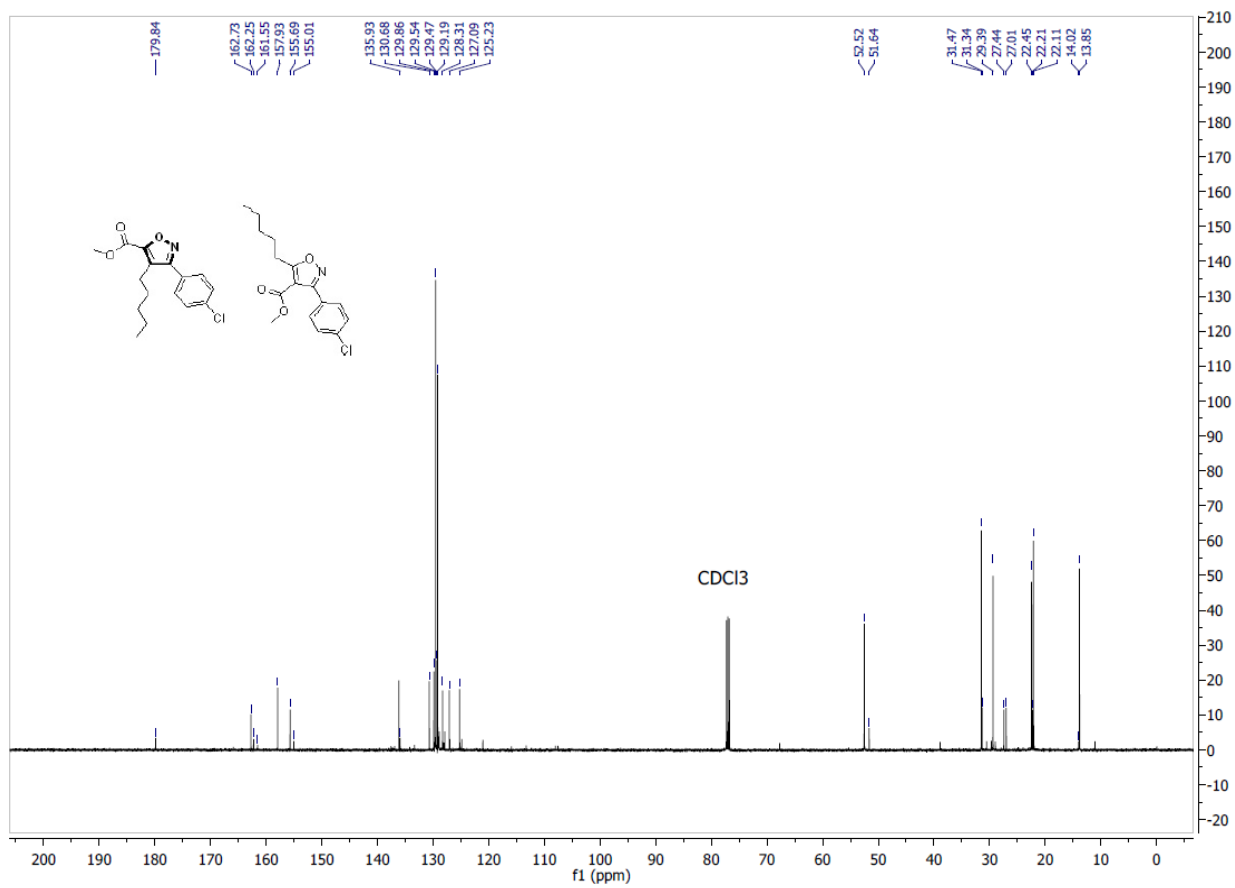
Figure S4.60. ^{13}C NMR of methyl 3-(4-chlorophenyl)-4-pentylisoxazole-5-carboxylate (127d)

1-(3-(4-nitrophenyl)-4-phenylisoxazol-5-yl)ethan-1-one (127e):
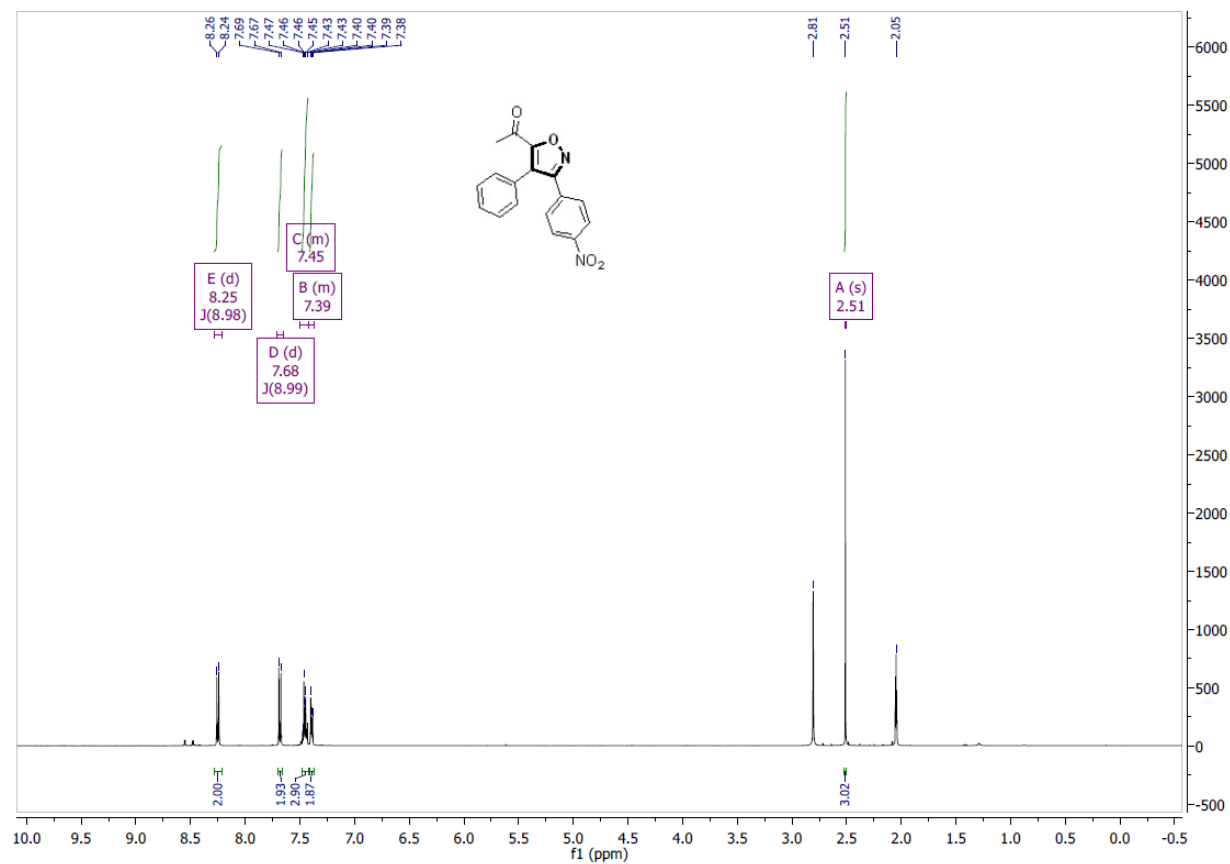
Figure S4.61. ¹H NMR of 1-(3-(4-nitrophenyl)-4-phenylisoxazol-5-yl)ethan-1-one (127e)
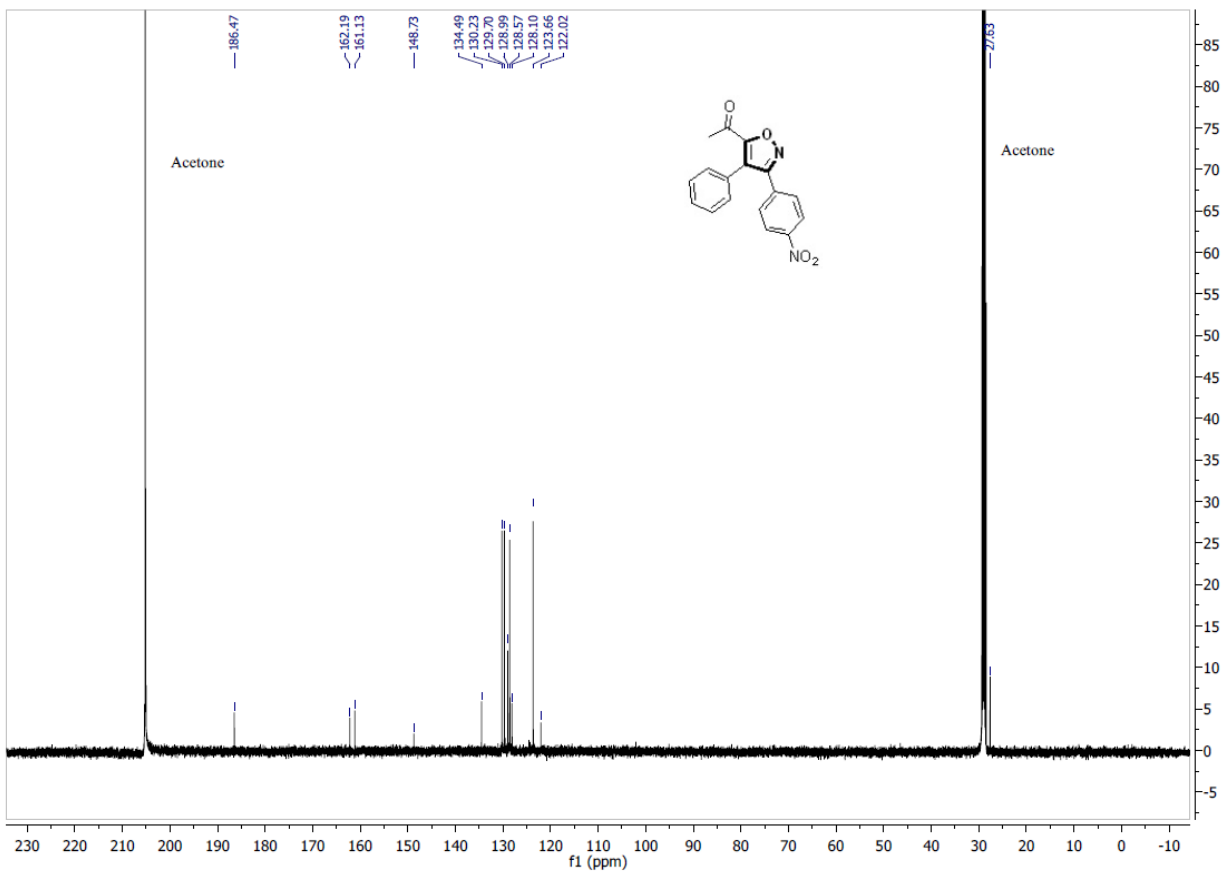
Figure S4.62. ^{13}C NMR of 1-(3-(4-nitrophenyl)-4-phenylisoxazol-5-yl)ethan-1-one (127e)

(3-(4-nitrophenyl)-5-phenylisoxazol-4-yl)methanol (128n):
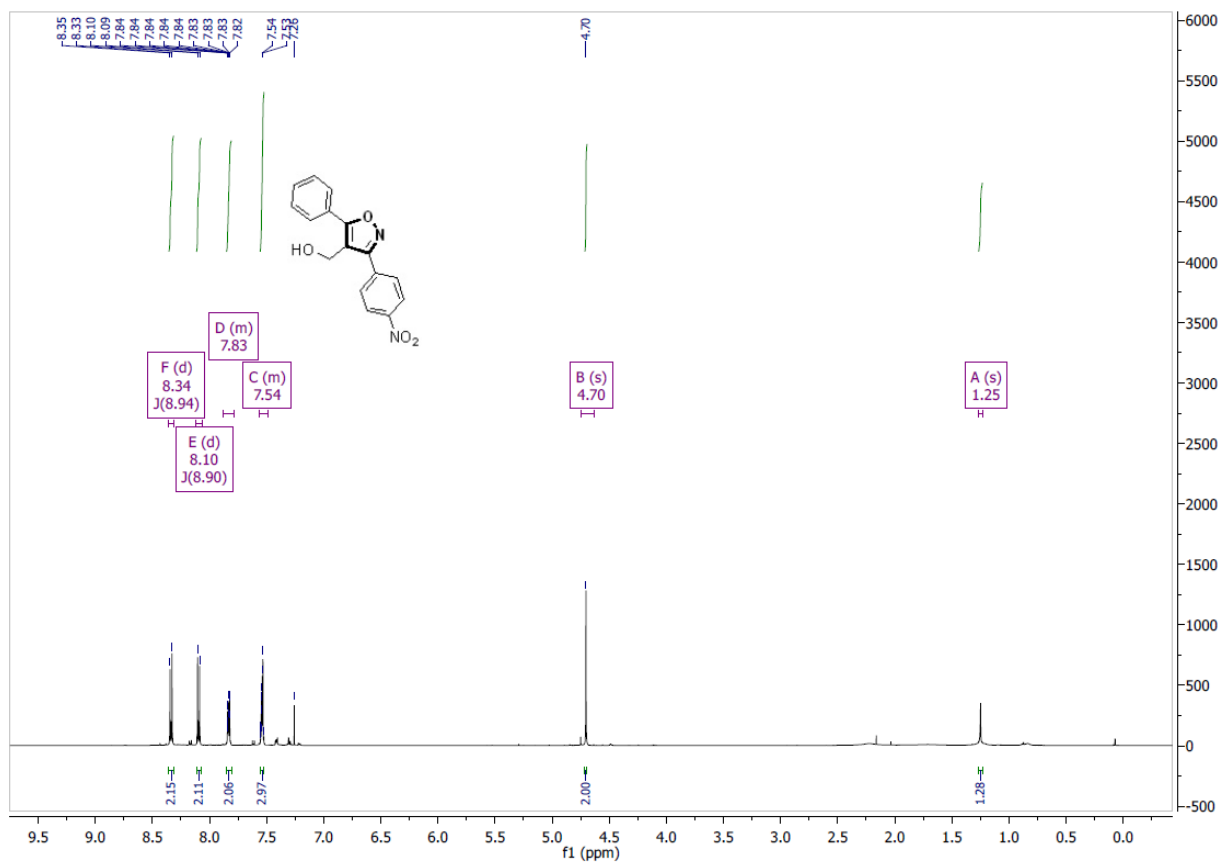
Figure S4.63. ^{1}H NMR of (3-(4-nitrophenyl)-5-phenylisoxazol-4-yl)methanol (128n)
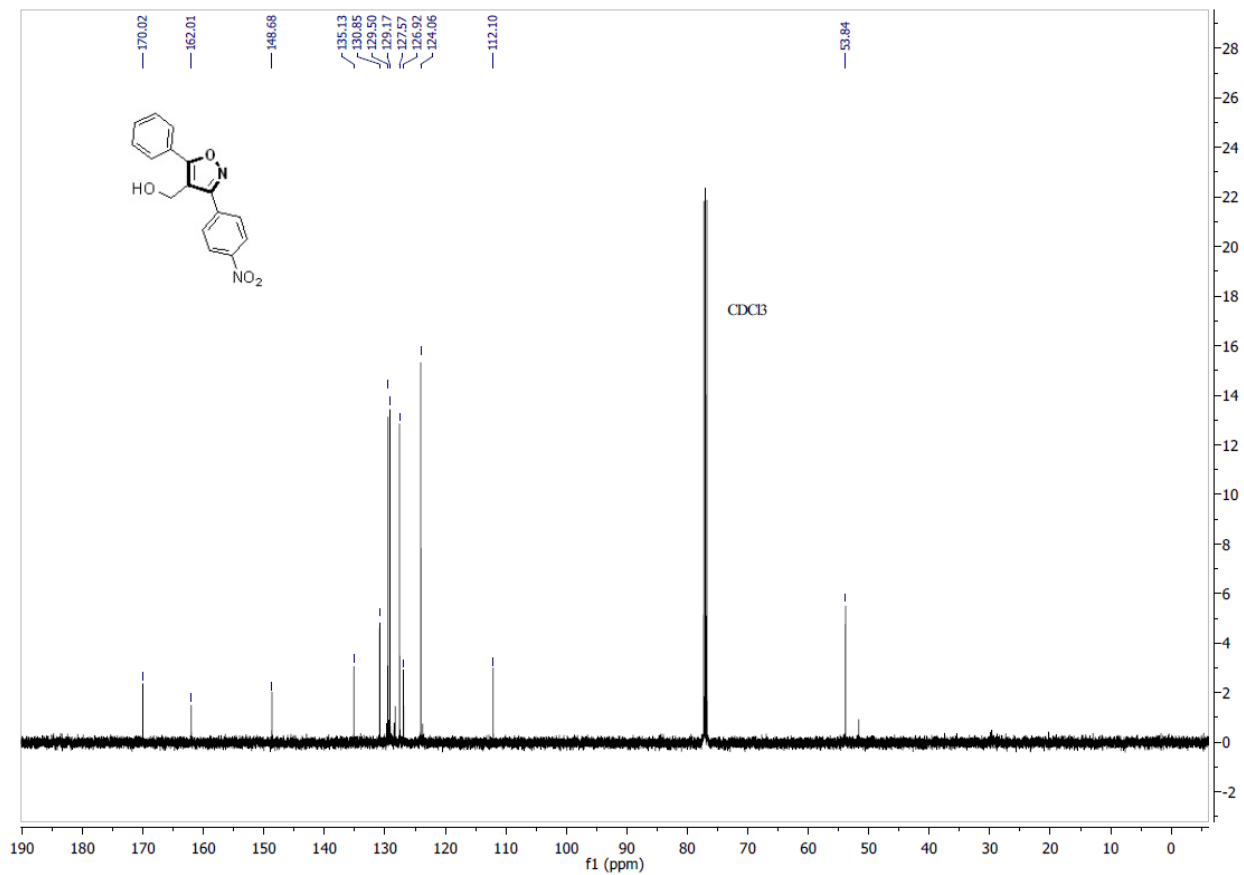
Figure S4.64. ^{13}C NMR of (3-(4-nitrophenyl)-5-phenylisoxazol-4-yl)methanol (128n)

3-(4-(hydroxymethyl)-5-phenylisoxazol-3-yl)benzonitrile (128o):
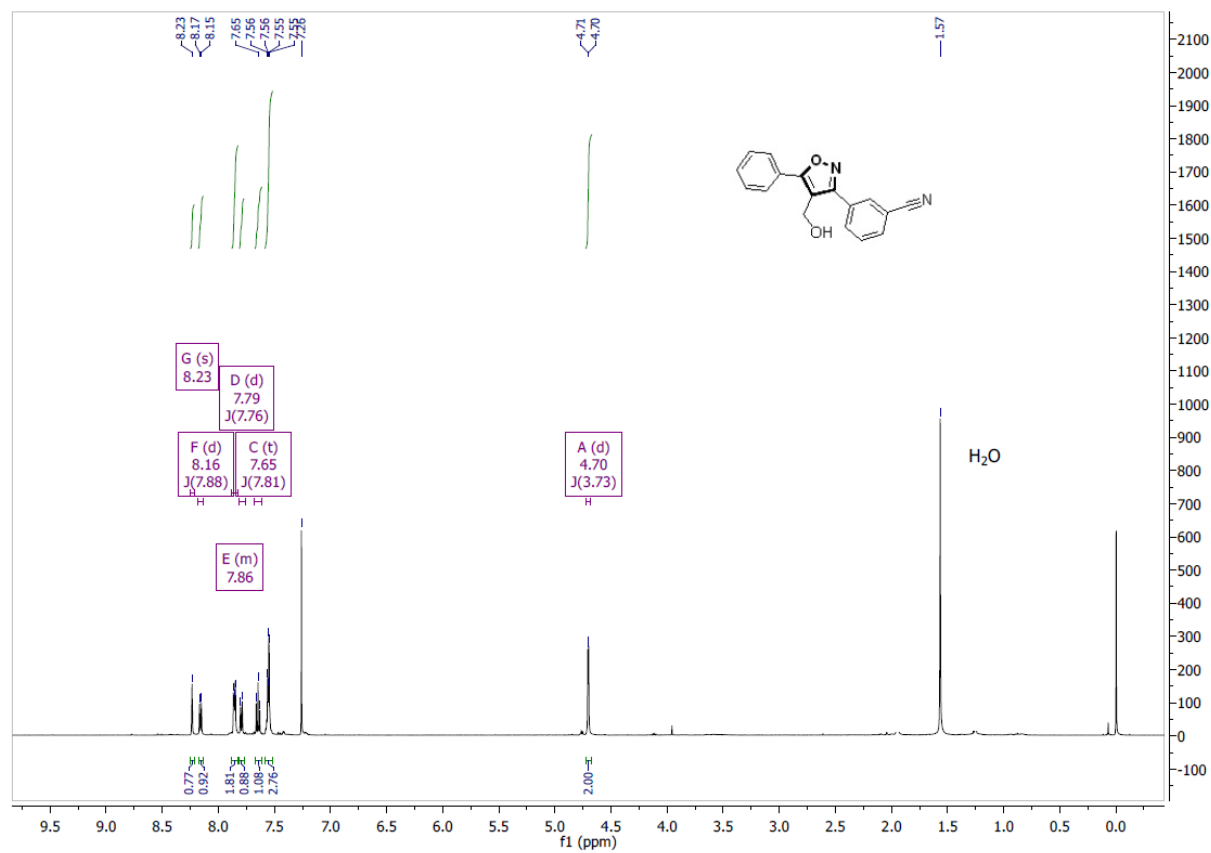
Figure S4.65. ¹H NMR of 3-(4-(hydroxymethyl)-5-phenylisoxazol-3-yl)benzonitrile (128o)
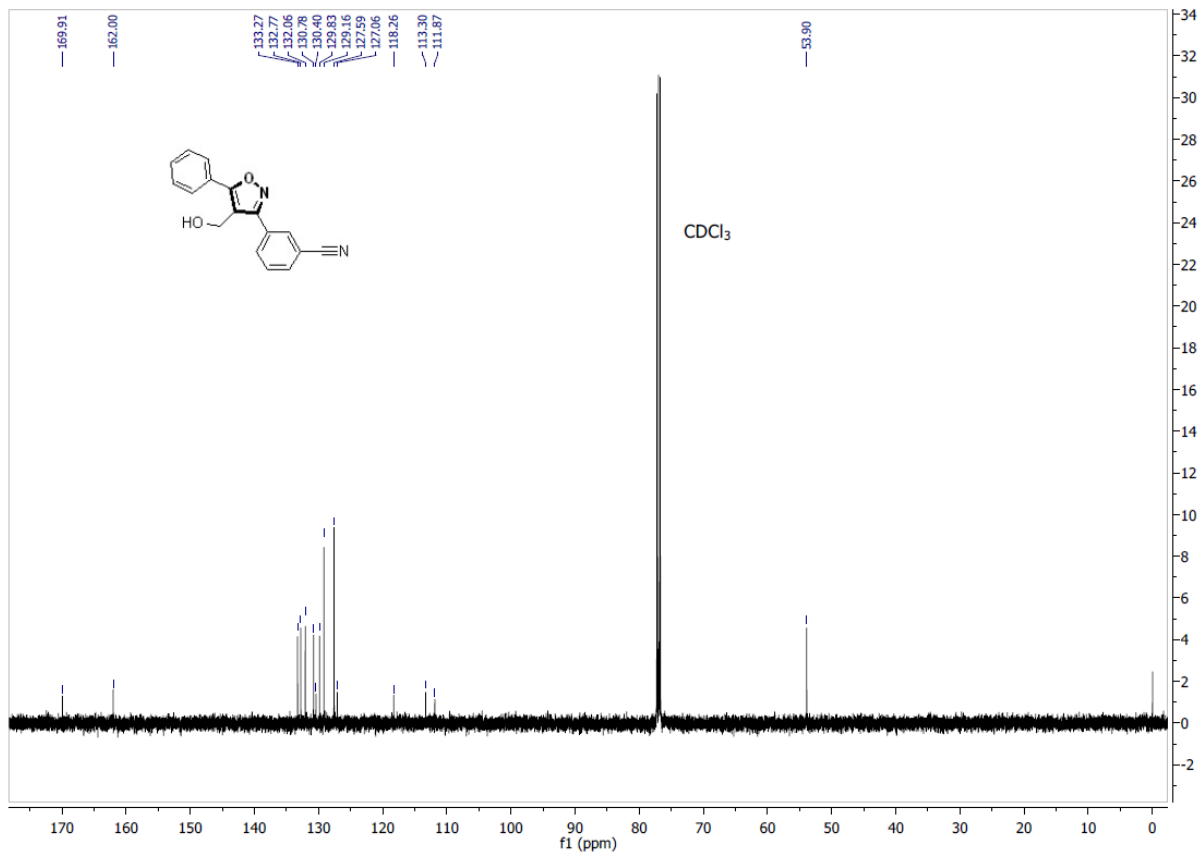
Figure S4.66. ^{13}H NMR of 3-(4-(hydroxymethyl)-5-phenylisoxazol-3-yl)benzonitrile (128o)

1-(3-(4-nitrophenyl)-5-phenylisoxazol-4-yl)butan-1-ol (128p)
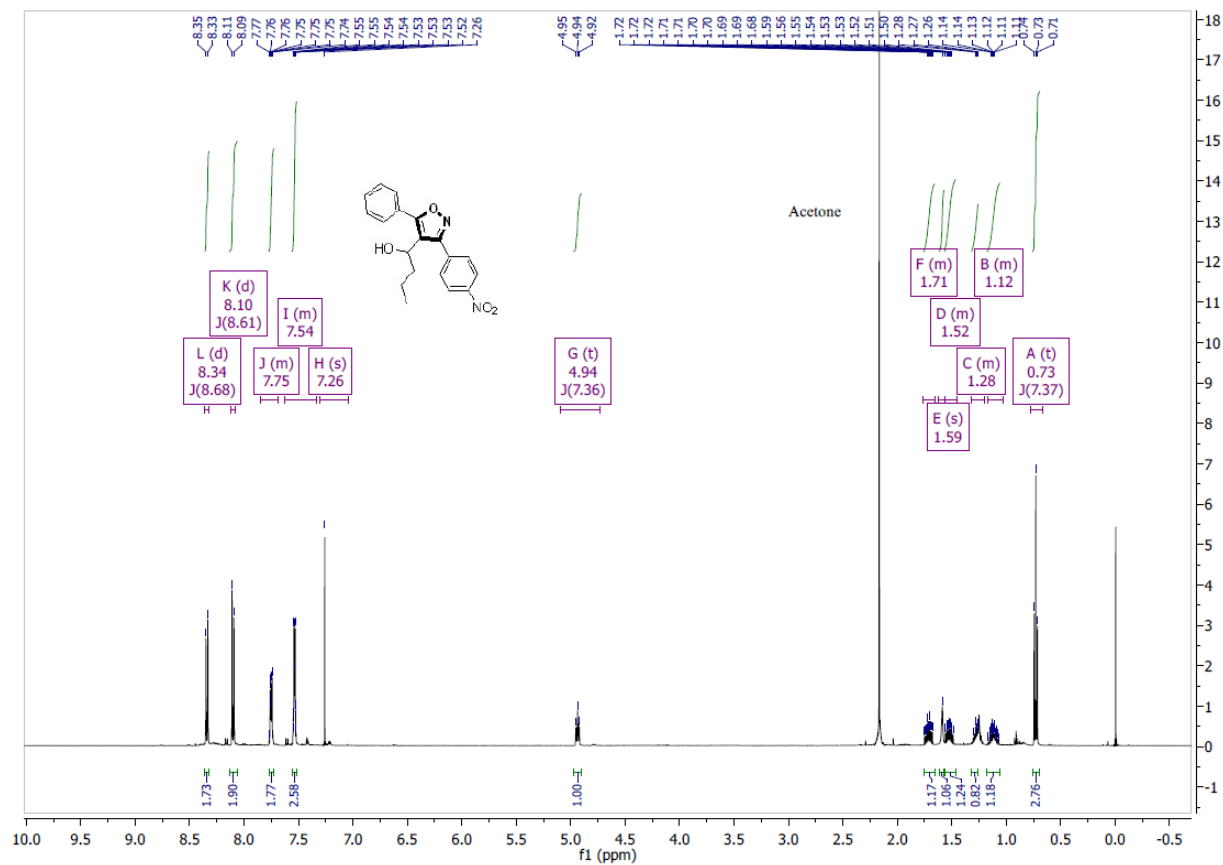
Figure S4.67. [^1]H NMR of 1-(3-(4-nitrophenyl)-5-phenylisoxazol-4-yl)butan-1-ol (128p)
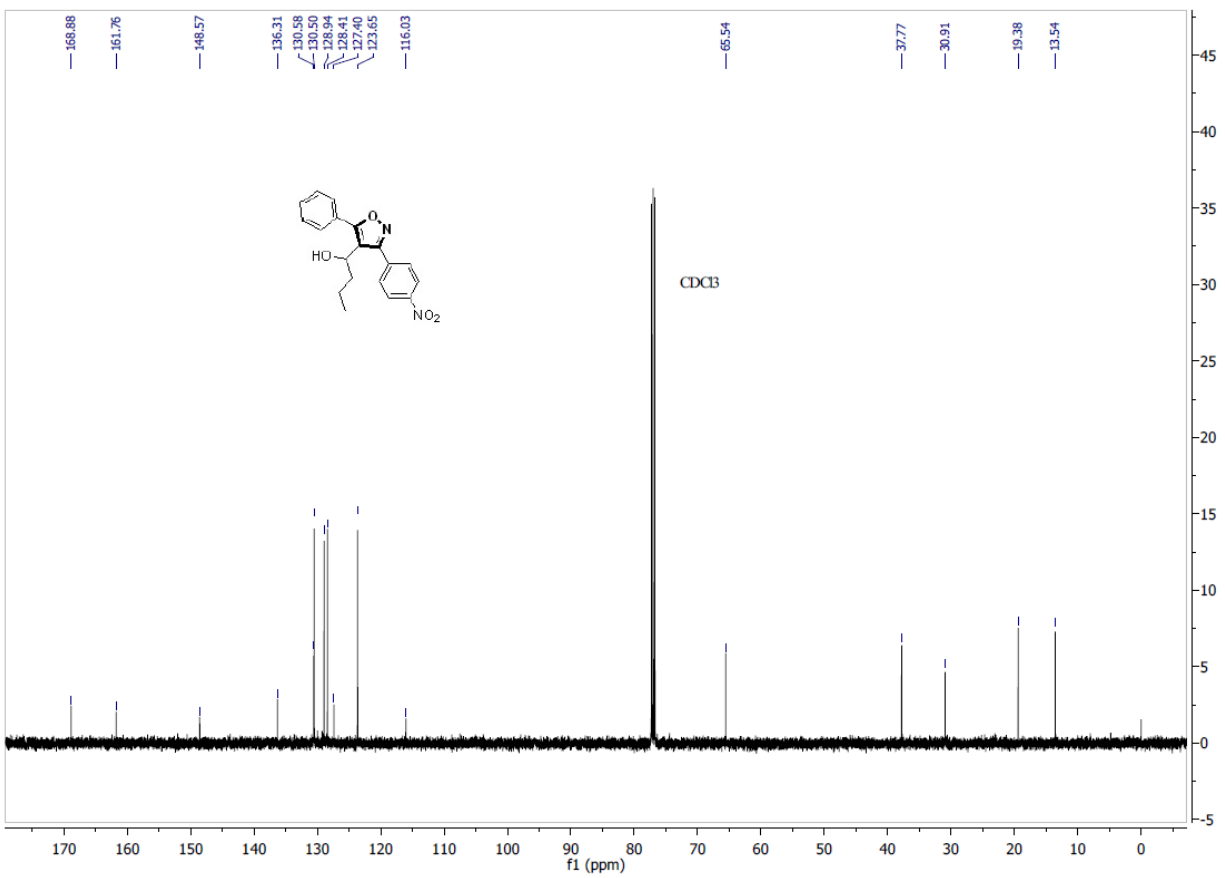
Figure S4.68. ^{13}C NMR of 1-(3-(4-nitrophenyl)-5-phenylisoxazol-4-yl)butan-1-ol (128p)

(3-(4-nitrophenyl)-5-propylisoxazol-4-yl)methanol (128q):
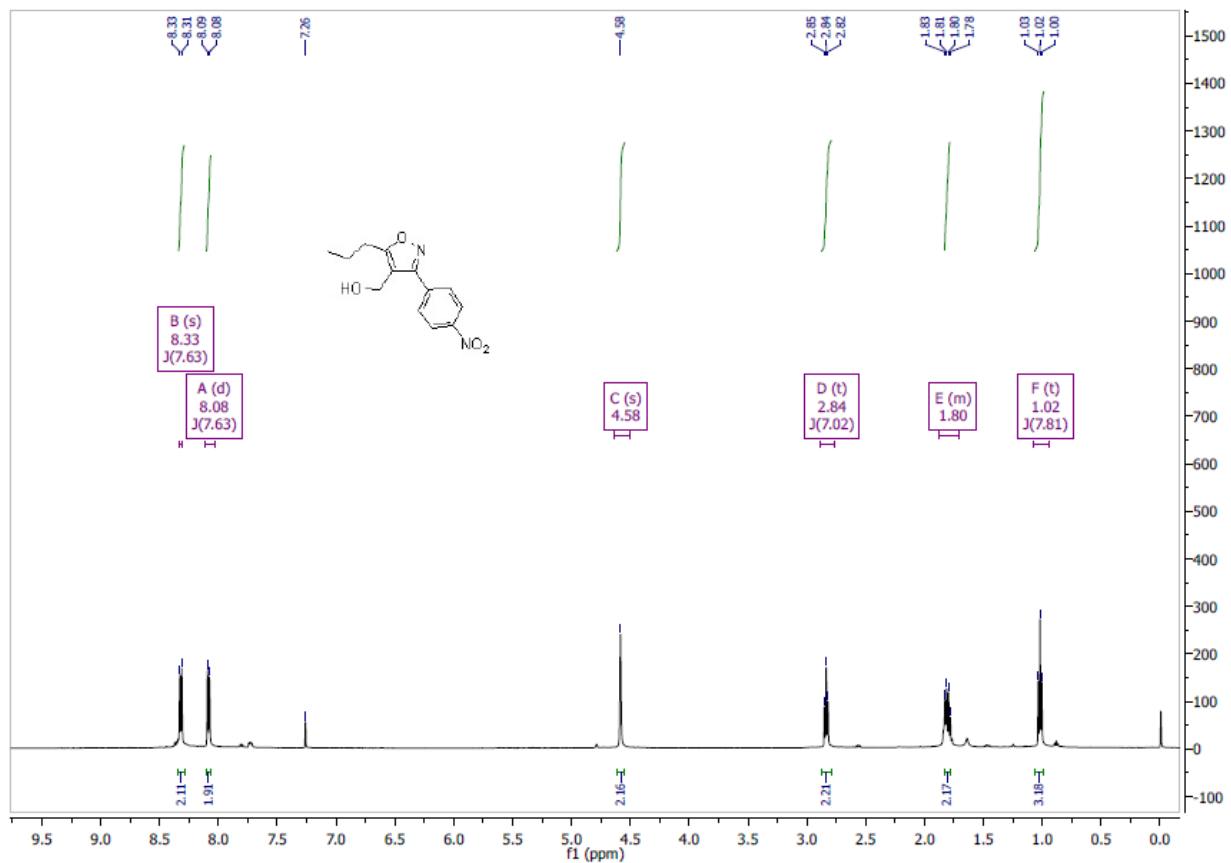
Figure S4.69. ^{1}H NMR of (3-(4-nitrophenyl)-5-propylisoxazol-4-yl)methanol (128q)
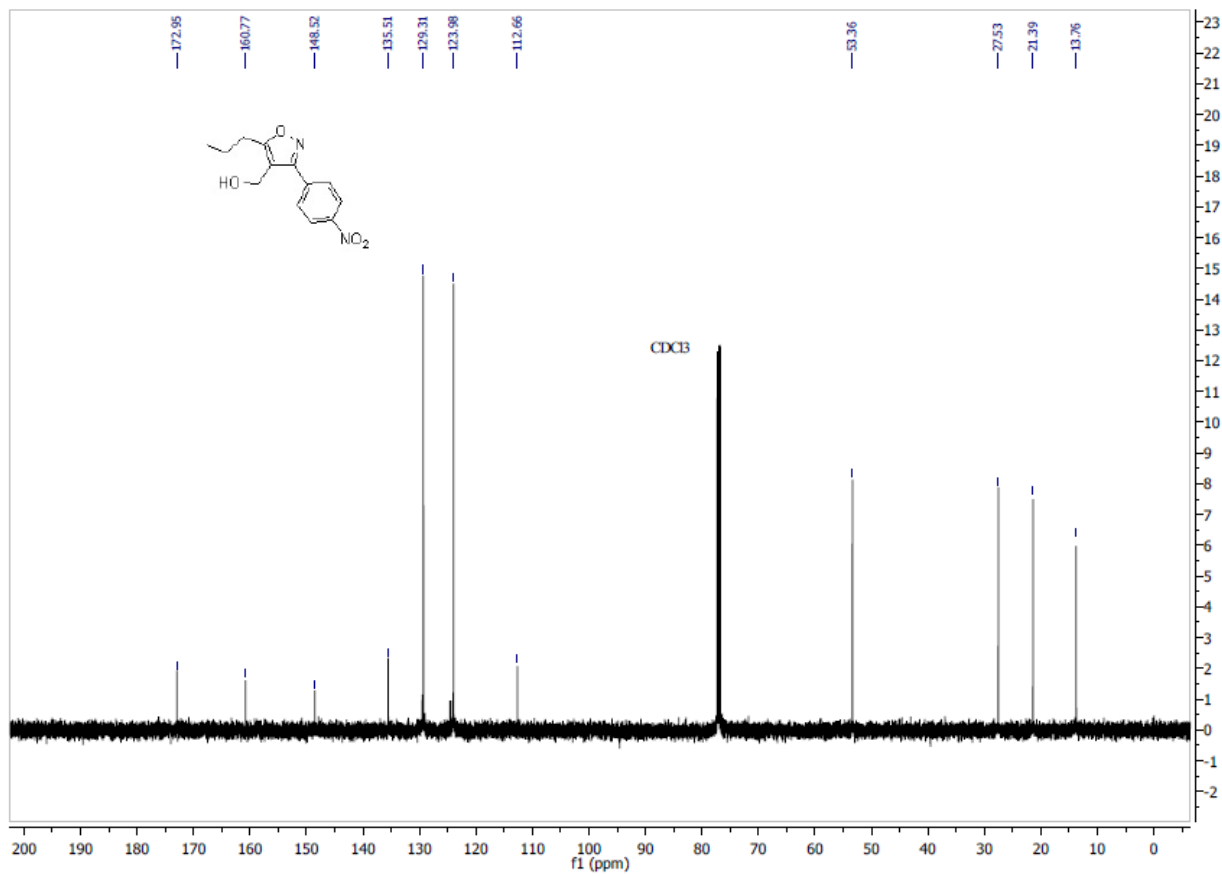
Figure S4.70. ^{13}C NMR of (3-(4-nitrophenyl)-5-propylisoxazol-4-yl)methanol (128q)

Chapter 5- Safety Concerns in Mechanochemical Reactions: Peroxide Handling, The Old New Problem

5.1. Abstract

Mechanochemical reactions represent a new avenue to perform reactions sustainably. As we progress rapidly in this field, new safety guidelines and protocols must be developed for reactions that occur under solvent-free conditions. Based on recent episodes, we discuss the hazards of using peroxides and safety pathway protocols for untested reaction mixtures.

5.2. Perspective

Mechanochemical reactions have proven to be a more sustainable and environmentally friendly technique for carrying out reactions without the need for large amounts of solvents, thereby improving the sustainability of organic reactions.[1] However, removing the solvent from the reaction conditions significantly affects the reaction profile and safety, as it is less effective in dissipating the heat generated in the reaction and providing a medium to homogenize the reaction mixtures to ensure reactivity. [2]

Based on this knowledge, there has been limited focus on reviewing and developing safety protocols and providing safety information to operational and research staff. It is essential to constantly consider that milling techniques such as mortar pestle, planetary ball milling, and mixer milling rely on media (balls or pestle), which facilitate the transfer of mass and energy to the reagents. [3,4,5] In addition, the reagents are in direct contact with the grinding media during the progress of the reaction, which can cause incompatibility between the milling material and the sample mixture due to the impurities produced by the leaching of the jar metal material. [6] This can result in unforeseen and sudden reactions that can harm research personnel. [7]

Among the most reported occupational risks and damage in research labs involve the use of peroxides. Peroxide reagents are frequently used in organic synthesis, as they facilitate the selective oxidation of organic compounds, and it has been demonstrated that the reactivity of peroxides stems from their ability to homolytically cleave the weak O-O bond, which is facilitated by the low dissociation energy.[8-10] Due to the low dissociation energy associated with peroxides, it is crucial to prioritize specific safety parameters, such as temperature control and careful addition, when handling peroxides.[7,11] These parameters are influential and vital given that most reported reactions are carried out using high dilution factors.

Despite the broad understanding and knowledge regarding the hazards of peroxides, several accidents have been reported in both academic and industrial settings, resulting in significant damage to equipment and personnel involved in the research. [12-14]

The use of peroxides under solvent-free conditions requires high precaution due to the limited heat dissipation and the increased rate of reactions observed for many mechanochemical conditions, which can lead to significantly larger consequences compared to solution-based processes, even when using lesser quantities of peroxide material. It is important to note that several peroxides, such as *m*-chloroperoxybenzoic acid, diacetyl peroxide, and acetyl benzoyl peroxide, are sensitive to mechanical shock or stress. [15] These are well documented in their material safety data sheet (MSDS). However, there is a number of peroxides reagents, which information regarding their shock sensitivity is not extensive.

Recently, we have witnessed an explosion of a reaction sample containing less than 300 mg potassium persulfate, an inorganic peroxide. The explosion caused by the mechanical stressed, occurred within 10 seconds of initiating the milling process in a ceramic jar, an inert and non-wearing material used to prevent contamination of the sample. The explosion was of such magnitude that it caused significant deformation to the right arm of the mixer milling equipment, which is surprising considering the strong and rigid

structure of the arm (**Figure 5.1a**). Additionally, it caused irreversible damage to the ceramics jars, leaving evidence of carbonization and emitting a sulphur like odour (**Figure 5.1b**). It is important to note that there were no physical injuries, but the magnitude of the explosion could have resulted in significant and even fatal damage, experiencing stress, anxiety, fear, and panic.
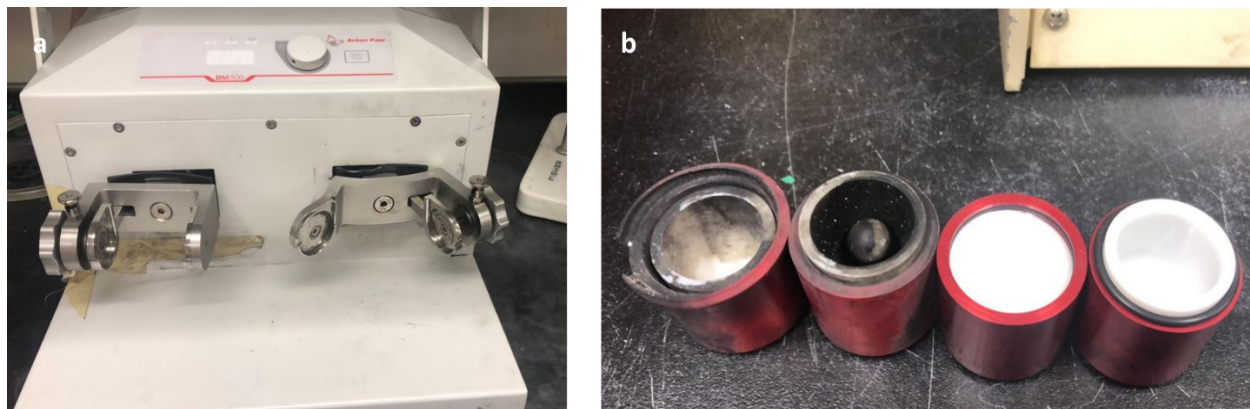
Figure 5.1. Damages to mixer mill and mixer mill capsules

Priestley *et al.* have suggested a security flow chart to determine for individual reaction components if milling is a safe options.[2] However, several researchers have shown that it is possible to mill peroxides, reporting successful and promising results.[16-18] We would like highlight that, although these reports showcase innovative research, replications of this research should be done carefully, with proper safety equipment, and performing the reaction on small scales.

Many reagents are effective for solution-based thermal conditions, but not all can be used for mechanochemical reactions in the solid-state. To date, there is no clear distinction between reagents specific to solvent-free conditions or solution-based thermal. Without specific information in the MSDS, we must be cautious to avoid unfortunate accidents that jeopardize safety. We recommend first examining the materials with high hazard, specifically those with an oxygen content > -200 units 2. Once this is done, we recommend doing a BAM Fallhammer test measures the materials sensitivity to mechanical shock. [15]

If the BAM Fallhammer test is successfully passed without detecting any type of explosion, a second BAM Fallhammer test should be conducted using all the reagent used for the reaction mixture. If this test is also successfully passed, a small-scale reaction can be carried out in a sealed stainless-steel (SS) milling jar, examining the reaction at low milling frequencies and evaluating its behaviours in short milling times (about 5- 10 min). The purpose of this test is to avoid potential risks due to the effect of the recurrent mechanical shock in the mixture.

In the case of using peroxides for mechanochemical reactions, we advise performing the above-mentioned tests and exercising extreme caution as the use of peroxides is associated with high risk. Additionally, we suggest adding the peroxide reagents just before the reaction begins, using a protective shield, and always using minimal amounts of peroxide.

In all cases, standardized safety precautions should be taken, such as using appropriate personal protective equipment (PPE) for each task you perform. Practice good workplace maintenance habits, personal hygiene, and equipment maintenance. Familiarize yourself with the FMSD safety data sheet (review section 7 and section 9 of the FMSD for information on impact sensitivity and perform the reaction within a fume hood). It is important to promote prevention not only of the physical and chemical risks associated

with severe harm to the involved researcher, but also to raise awareness about potential risks that may involve psychosocial and organizational hazards.

5.3. Conclusion

In summary, mechanochemical reactions are a new way of carrying out organic reactions. However, given the rapid evolution of protocols, it is necessary to evaluate and establish clear guidelines to ensure the safety of experienced and trainee researchers. Learning from recent experiences, we have realized the risks of working with peroxides and the importance of handling them with caution in a solvent-free environment. Although several successful cases have been reported using these oxidative reagents in mechanochemistry, we strongly recommend conducting preliminary tests using the BAM Fallhammer test for individual materials and mixtures. This should be followed by a small-scale reaction, using properly sealed screw-cap vials and grinding at low frequency for a short period of time. We insist on the need to take proper precautions to prevent incidents and accidents in the laboratory. In the event of being a victim of an unwanted incident, it is important to report, document, and participate in the implementation of precautionary measures for future similar research.

5.4. References

[1]   Ardila-Fierro, K. J.; Hernández, J. G. *ChemSusChem* **2021**, *14*, 2145–2162.

[2]   Priestley, I.; Battilocchio, C.; Iosub, A. V.; Barreteau, F.; Bluck, G. W.; Ling, K. B.; Ingram, K.; Ciaccia, M.; Leitch, J. A.; Browne, D. L. *Org. Process Res. Dev*. **2023**, *27*, 269–275.

[3]   Hwang, S.; Grätz, S.; Borchardt, L. *Chem. Commun*. **2022**, *58*, 1661–1671.

[4]   Effaty, F.; Gonnet, L.; Koenig, S. G.; Nagapudi, K.; Ottenwaelder, X.; Friščić, T. *Chem. Commun.* **2022**, *59*, 1010–1013.

[5]   Michalchuk, A. A. L.; Tumanov, I. A.; Boldyreva, E. V. *CrystEngComm* **2019**, *21*, 2174–2179.

[6]   Štefanić, G.; Krehula, S.; Štefanić, I. *Chem. Commun.* **2013**, *49*, 9245–9247.

[7]   Kelly, R. J. *ACS Chem. Heal. Safety Chemical* **1996**, *3*, 28–36.

[8]   ten Brink, G. J.; Arends, I. W. C. E.; Sheldon, R. *A. Chem. Rev.* **2004**, *104*, 4105–4123.

[9]   Targhan, H.; Evans, P.; Bahrami, K. J. *Ind. Eng. Chem*. **2021**, *104*, 295–332.

[10]   Bach, R. D.; Ayala, P. Y.; Schlegel, H. B. *J. Am. Chem. Soc.* **1996**, *118*, 12758–12765.

[11]   Clark, D. E. *Chem. Heal. Saf.* **2001**, *8*, 12–21.

[12]   Chappell, B. America (NY). 2017.

[13]   Office of Environmental Health & Safety. Peroxide Explosion Injures Campus Researcher.

[14]   Zhang, B.; Zhang, L.; Wang, H.; Wang, X. *ACS Chem. Heal. Saf.* **2021**, *28*, 244–249.

[15]   Noller, D. C.; Bolton, D. J. *Anal. Chem.* **1963**, *35*, 887–893.

[16]   Do, J.-L.; Tan, D.; Friščić, T. *Angew. Chemie* **2018**, *130*, 2697–2701.

[17]   Mkrtchyan, S.; Iaroshenko, V. O. *Chem. Commun.* **2021**, *57*, 11029–11032.

[18]   Kaiser, R. P.; Krake, E. F.; Backer, L.; Urlaub, J.; Baumann, W.; Handler, N.; Buschmann, H.; Beweries, T.; Holzgrabe, U.; Bolm, C. *Chem. Commun.* **2021**, *57*, 11956–11959.

Chapter 6- General Conclusion and Future Directions

6.1 General Conclusions

The general objective of this thesis was to evaluate the effect of mechanical stress generated through media-dependent techniques, specifically ball milling, in transition metal-mediated 1,3-dipolar cycloaddition reactions between nitrile oxides (NOs) and alkyne motif to form isoxazoles.

Initially, our investigation focused on developing a mechanochemical 1,3-dipolar cycloaddition to access 3,5-isoxazoles from terminal alkynes and nitrile oxides. Optimization and control experiments revealed that mechanical activation was insufficient to form the cycloadduct 3,5-isoxazole. Only a limited number of terminal alkynes dipolarophiles showed good reactivity. The use of a recyclable Cu/Al_2O_3 nanocomposite catalysts was found to enhance reactivity and broaden the scope of the reaction.

One limitation of many cycloaddition reactions is their poor selectivity when using substrates with two or more identical reactive sites, thereby restricting the use of symmetrical substrates. To address this issue, we conducted a study to evaluate the effect of mechanochemistry in stoichiometric desymmetrizations by 1,3-dipolar cycloadditions. Our comprehensive study demonstrated that mechanochemical reactions enable effective desymmetrization of various symmetrical dipolarophiles. However, the efficiency of the desymmetrization is influenced by the electronic compatibility between the dipole and dipolarophile. A direct comparison between solid-state and solution-based thermal processes clearly showed that the mechanochemistry conditions apply to a wide range of substrates, regardless of their aggregate state. In contrast, solution-based conditions are substrate-dependent and often yield limited selectivity. This newly opened chemical space offered a direct route to obtain unsymmetrical bis-3,5-isoxazoles through iterative 1,3-dipolar cycloadditions.

Although 3,5-isoxazoles are among the most common di-substituted isoxazoles, the 3,4-isomers are relatively rare. The control of regioselectivity in regio-divergent reactions remains a challenge. However, the investigation of Ru catalysis in solid-state and mechanochemistry demonstrated that 3,4-isoxazole can be obtained efficiently and regioselectively in excellent yields. Furthermore, this chemistry can be extended to internal alkyne systems, where mechanochemistry allows for the synthesis of both *polung* and *umpolung* 3,4,5-isoxazoles from internal alkynes and NOs.

It is worth noting that the reaction mechanism in mechanochemical conditions differs from those reported in solution-based conditions. Detailed mechanistic investigations revealed the importance of LAG in the catalyst performance, while the electronic properties of the NOs play a critical role in regioselectivity.

Mechanochemistry offers access to new types of selectivity and reactivity types that are either impossible or limited in traditional solution-based methods. Established protocols and concepts from solution-based chemistry have inspired rapid progress in this field. However, the reaction environment in the solution and solid state differ significantly. As a result, specific reagents and concepts cannot be directly translated. In such cases, careful monitoring and consideration of proper safety guidelines is essential.

Specifically, in the case of cycloadditions, mechanochemistry has proven to be a valuable technique for performing 1,3-dipolar cycloadditions. The use and benefit of this approach have been demonstrated through three protocols that enable access to all possible substitutions in the isoxazole motif while maintaining regioselectivity and promoting environmental sustainability.

6.2 Future Directions

This thesis highlights the benefits of mechanochemistry in cycloaddition reactions, specifically 1,3-DCs. While the advantages of pericyclic reactions in organic chemistry are well-known, limited studies demonstrate applications 1,3-DCs for the derivatization of pigments or dyes, substrates which are known to have limited solubility and reactivity. After having established the benefits of mechanochemistry for 1,3-DCs in small molecules, we propose to expand the reactivity of aromatic NOs **130*** by performing 1,3-DC between aromatic NOs **130*** and pigments with terminal alkynes **129** to form novel 3,5-isoxazoles pigments **131** and evaluate the novel photochemical properties of this compounds (**Figure 6.1**).
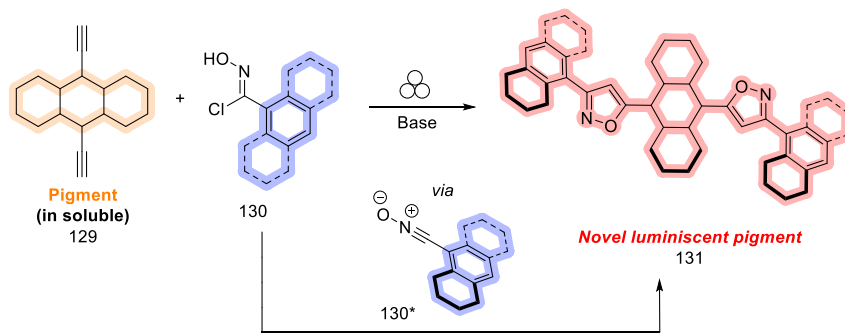
Figure 6.1. Synthesis of isoxazole containing pigments

Appendices

Appendix A: Copper Azide-Alkyne Cycloaddition (CuAAC)

The reaction conditions and stepwise mechanism that leads access to 1,4-triazoles.